

**Cenozoic palaeoenvironment of the Southern Ocean  
and East Antarctica:  
geological and palaeontological evidence from the Kerguelen  
Plateau, Vestfold Hills and Prince Charles Mountains.**

*Jason Matthew*

Jason Whitehead

B.Sc. (Grad. Dip. Hons. IASOS)

University of Tasmania

Submitted in fulfillment of the requirements for the degree of

Doctor of Philosophy

University of Tasmania

(July 2000)

*IASOS*

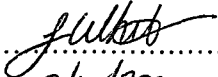
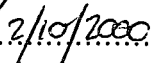
## Declaration

This thesis contains no material which has been accepted for a degree or diploma by the University or any other institution, except by way of background information and duly acknowledged in the Thesis, and to the best of the candidate's knowledge and belief no material previously published or written by another person except where due acknowledgment is made in the text of the Thesis.

Signed: .....  
Date: ..... 2/10/2000 .....

## Authority of Access

This thesis may be made available for loan. Copying of any part of this thesis is prohibited for two years from the date this statement was signed; after that time limited copying is permitted in accordance with the Copyright Act 1968.

Signed: .....  .....  
Date: .....  .....

## Abstract

Southern Ocean and Antarctic sediments from the Kerguelen Plateau, Vestfold Hills and Prince Charles Mountains contain evidence that suggest climatic conditions and ice sheet volume have fluctuated during the Cenozoic. Geological and palaeontological data show that at certain intervals the Antarctic climate was significantly warmer, and the East Antarctic Ice Sheet smaller, than today. Marine fossils are used to date these intervals of ice sheet reduction and to reconstruct the associated climatic conditions. The findings are compared with previous geological and ice sheet computer modeling studies, to help reconstruct Antarctica's climate history and test predictive models for ice sheet response to future global warming.

Fluctuating climatic conditions were identified in Quaternary and Pliocene marine sediments from the Southern Kerguelen Plateau. Unconformities formed during intense glacial intervals, when the velocity of the Antarctic Circumpolar Current increased. Deposition occurred during warmer climatic intervals. During the late Pliocene, 3.1 - 2.64 Ma and 3.2 - 3.1 Ma, the summer sea-surface temperature (SST) was 4.5 C° warmer than today at 62° S. This could have occurred only if the Antarctic Polar Front Zone was either ~1200 km further south or the temperature gradient across the associated fronts became significantly shallower.

Pliocene (4.5 - 4.1 Ma) marine sediments of the Sørødal Formation (Vestfold Hills) were also deposited when the summer SST was between 1.6° and 3.0 C° higher than today. When such temperatures are compared to glacial models, an increase in ice sheet volume would be expected due to increased snow accumulation versus ablation. Previous work suggests that the Sørødal Formation was deposited when the ice margin was ~50 km further inland. This suggests that a lower temperature than that proposed by earlier glacial models is required for ice sheet retreat. These findings may support more recent modeling studies that indicate ice sheet reduction can occur due to minor increases in water temperature.

The Pagodroma Group, in the northern Prince Charles Mountains, consists largely of diamict, and to a lesser degree, siltstone and sands deposited in the Lambert Graben during intervals of glacial retreat. *In situ* and glacially reworked marine diatoms on the Amery Oasis and Fisher Massif suggest that marine conditions occurred >250 km inland from the modern Amery Ice Shelf edge in the Plio-Pleistocene (3.1 - 1 Ma), Pliocene



(4.9 - 3.7 Ma) and middle Miocene (12.2 - 11.7 Ma), and >300 km inland in the Miocene (14.2 - 12.5 Ma and 14.2 - 6.2 Ma) and Oligocene (~36.6 - 30.2 Ma). Diatoms also provide an age control for three formations in the Pagodroma Group. Glacially reworked diatoms and stratigraphic relationships indicate that the Mt Johnston Formation, on Fisher Massif was deposited sometime between 36.3 - 12.5 Ma. *In situ* marine diatoms in Middle Miocene (14.2 - 12.5 Ma) siltstone from the Fisher Bench Formation, on Fisher Massif, suggest a summer SST of 3.5° to 5°C. An associated relative mean annual air temperature rise >15 C°, during ice shelf absence, caused deglaciation of the Lambert Graben, and is consistent with the predicted response from glacial models. The Bardin Bluffs Formation was deposited in the Amery Oasis 3.1 - 1 Ma. The lithostratigraphy of the formation indicates that the ice sheet volume varied greatly.

The Cenozoic geology of the central Menzies Range in the Southern Prince Charles Mountains is described. Glacial landforms and deposits formed more recently than 40 Ma during two climate phases. The first phase was warmer than today, and wet-based glacial conditions existed. Associated deposits consist of glacial diamict, lacustrine siltstone and sand deposited in a terrestrial alpine glacial environment. These deposits may be contemporaneous with the Pagodroma Group; however, age relationships are yet to be determined. The second climate phase was cold and similar to today's, and caused relatively minor glacial erosion and deposition.

Previous researchers have found controversial terrestrial higher plant fossils in the Transantarctic Mountains, which indicate a warmer Antarctic climate sometime in the late Neogene. The lack of a similar flora in the Vestfold Hills and Prince Charles Mountains may reflect earlier denudation of this vegetation during ice sheet development. However, biogeogeographical barriers may have prevented re-colonisation from the Transantarctic Mountains to other East Antarctic regions during later episodes of deglaciation in the Lambert Graben catchment identified in this study.

(Note: Dates in italics are calibrated to the Berggren *et al.* (1985a, b) geomagnetic time scales, other dates are revised to the Berggren *et al.* (1995) time scale)

## Acknowledgment

I wish to thank my advisors and colleagues Andrew McMinn, David Harwood, Patrick Quilty, and Barrie McKelvey. I am very grateful for the opportunities and advice you have given me. I feel very fortunate to have met and worked with such a good group of people and look forward to working with you in the future.

Andrew, thanks for introducing me to the world of diatoms, Antarctic research and, of course, smooth wines. To David and Barrie, thanks for opening the door to the Pagodroma Group. Dave, it was a great opportunity to work at UNL. Barrie, I enjoyed our PCM field season, the stratigraphic work on the Bardin Bluffs Formation and Menzies strata presented in this thesis is very much the fruits of both our efforts. What is the Guinness tally at now? Pat, thank you for the opportunity to work on the Sørsdal Formation. I feel lucky to have seen and worked on this with you.

This thesis was made possible through support from an Australian Postgraduate Award and Antarctic Cooperative Research Centre Scholarship. Various ASAC grants, including grant numbers 2086 and 1065, made this research possible. Further thanks to the Antarctic CRC, Institute of Antarctic and Southern Ocean Studies, University of Nebraska- Lincoln and Hamilton College, where much of this research was conducted.

The field work for part of this study was undertaken during the 1997/98 Australian National Antarctic Research Expedition (ANARE). I'd like to thank the Australian Antarctic Division for logistical support, especially that via the personnel of Davis Station, Helicopters Australia Ltd. and the crew of the *Aurora Australis*. Thanks to Field Training Officer Don Hudspeth for his alpine skills and my field colleagues, Mark Mabin, John Stone, and again Barrie McKelvey for their friendship, cooperation and support in the field.

Thanks also to other people who have sent me information and read drafts of my thesis: Fiona Taylor, Donna Roberts, Steven Bohaty, Michael Hambrey and Leanne Armand. Further thanks to Gene Domack, Amy Leventer, Peter Harris and Andrew McMinn who have provided unique experiences such as teaching, technical positions and cruise experience outside of my studies. Thanks also to David Harwood for supporting my travel expense to UNL. I'd like to say a very special thanks to Fiona, my family and friends.

# Table of Contents

1. Thesis Introduction	1
1.1 Aims	2
1.2 Southern Kerguelen Plateau	2
1.3 Vestfold Hills	3
1.4 Prince Charles Mountains	3
 <b>Section A: Background Review</b>	
2. Modern Antarctic and the Southern Ocean Environments	5
2.1 Terrestrial Environments	5
2.2 Marine Environments	8
2.2.1 Southern Ocean	8
– Ocean Circulation	8
– Ocean Fronts	11
– Water Bodies	11
Surface Waters	11
Subsurface and Intermediate Waters	12
Circumpolar Deep Water	12
Bottom Water	15
2.2.2 Sea Ice	15
2.2.3 Coastal	20
3. Antarctic Glacial Style and Stability	23
3.1 Glacial Style	23
3.1.1 Terrestrial Marine Deposits	24
3.1.2 Glacial Marine Deposits	29
3.1.3 Antarctic Glacial Style	31
3.2 Antarctic Ice Sheet Retreat and Ice Shelf Stability	31
4. Past Antarctic and Southern Environments	40
4.1 Terrestrial Environments	40
4.1.1 East Antarctica	40
4.1.2 West Antarctica	43
4.2 Marine Environments	46
4.2.1 Southern Ocean	46
4.2.2 Sea-ice	47
4.2.3 Coastal	48
5. Diatoms	50
5.1 Diatom Biology	50
5.2 Modern Antarctic and Southern Ocean Diatom Assemblages	51
5.3 Past Antarctic and Southern Ocean Diatoms	54
5.3.1 Diatom Evolution	54
5.3.2 Diatom Biostratigraphy	56
5.4 Diatom Taphonomy	57
5.4.1 Deposition: Marine, Glaciomarine and Lake	57
5.4.2 Preservation: Dissolution and Mechanical Breakage	59
5.4.3 Reworking	60
– Marine	60
– Aeolian	60
– Grounded Glaciers	63
– Sub-Iceshelf	63
– Meteorite	63

<b>Section B: Palaeoclimate Studies</b>	
6. Southern Kerguelen Plateau Quaternary-Pliocene Palaeoceanography	64
6.1 Introduction	64
6.1.1 Aims	64
6.1.2 Geological Setting	64
6.1.3 Phytoplankton Assemblages	65
6.1.4 Previous Work	66
6.2 Methods	70
6.2.1 Siliceous Microfossils	70
6.2.2 Statistical Analyses	72
6.2.3 X-Ray Imagery	74
6.2.4 Total Calcium Carbonate (TCC)	74
6.3 Results	91
6.3.1 Diatom Biostratigraphy	91
6.3.2 Statistical Analyses	92
6.3.3 Silicoflagellate Data	93
6.3.4 Lithological Data	93
6.4 Discussion	94
6.4.1 Deposition and Erosion on the Kerguelen Plateau	94
6.4.2 Sediment Composition	97
6.4.3 Oceanographic Changes	97
– Extant Diatom Assemblages	97
Assemblage I: Interglacial Antarctic Open Water	98
Assemblage II: Glacial and Pack-ice Associated	99
Assemblage III: Pliocene Interglacial Open Water	101
– Palaeoenvironmental Variations Amongst Extant Diatom Data	102
– Pliocene Palaeoceanography – Silicoflagellate Data	104
– Lithology and Carbonate Compensation Depth	105
6.4.4 Palaeoenvironmental Preference of Extinct Diatoms	105
6.4.5 Diatom Biostratigraphy	107
6.5 Summary	108
7. Palaeoenvironmental Interpretation of the Pliocene Sørødal Formation, Marine Plain, Vestfold Hill, East Antarctica	111
7.1 Introduction	111
7.1.1 Aims	111
7.1.2 Study Area	111
7.1.3 Previous Work	111
– The Sørødal Formation	111
– Age	113
– Ice Margin Position	113
– Sea-ice and SST	115
– Phytoplankton	115
7.2 Methods	116
7.3 Results	118
7.4 Discussion	118
7.4.1 Sea-ice	118
– Relative abundance of extant sea-ice diatoms	118
– Ecology of extant sea-ice diatoms	123
7.4.2 Sea surface temperature conditions	126
– Temperature Ranges of Extant Diatoms	126
– Absence of Microfossil Groups That Occur North of the Antarctic Polar Front	127
7.4.3 Palaeoenvironmental Interpretation of Extinct Diatoms	128
7.4.4 Future Climate Implications	128

7.5 Summary	131
8. Cenozoic Geology of the Northern Prince Charles Mountains, East Antarctica: Evidence from the Pagodroma Group	132
8.1 Introduction	132
8.1.1 Previous Work	134
8A. The Stratigraphy of the Pliocene – Early Pleistocene Bardin Bluffs Formation, Amery Oasis	136
8A.1 Introduction	136
8A.1.1 Aims	136
8A.1.2 Geological Setting	136
8A.1.3 Previous Work	138
8A.2 Stratigraphy	139
8A.3 Discussion	145
8A.4 Summary	147
8B. Diatom Biostratigraphy of the Pagodroma Group	149
8B.1 Introduction	149
8B.1.1 Aims	149
8B.1.2 Previous Work	149
8B.2 Methods	149
8B.3 Results and Discussion	152
8B.3.1 Diatom Taphonomy	152
8B.3.2 Pagodroma Group Biostratigraphic and Palaeoenvironmental Interpretation	155
– Mt Johnston Formation	155
– Fisher Bench Formation	155
– Battye Glacier Formation	158
– Bardin Bluffs Formation	158
– Member 1	158
– Member 2	160
8B.3.3 Palaeoenvironmental Significance of the Pagodroma Group and Correlations with Other Records	161
8B.4 Summary	164
8C. Palaeoenvironmental Conditions During Miocene Marine Deposition of the Fisher Bench Formation, Fisher Massif	166
8C.1 Introduction	166
8C.1.1 Aims	166
8C.1.2 Previous Work	166
8C.1.3 Geological Setting	166
8C.2 Methods	167
8C.3 Results	168
8C.4 Discussion	168
8C.4.1 Diatom Assemblage	168
8C.4.2 Diatom Palaeoecology	170
8C.4.3 Diatom Taphonomy	172
8C.4.4 Stability of the Amery Ice Shelf and the East Antarctic Ice Sheet	172
8C.5 Summary	175
9. Cenozoic glacial history of the Menzies Range, Southern Prince Charles Mountains, Antarctica	178
9.1 Introduction	178
9.1.1 Aims	178
9.1.2 Geological Setting	178
9.1.3 Previous Work	180
9.1.4 Glacial Sedimentology	180

9.2 Stratigraphy	181
– Pardoe Formation	181
– The Sub-Pardoe Formation Erosion Surface	186
– Trail diamict	186
– Amphitheatre diamict	187
– The Sub-Amphitheatre diamict Erosion Surface	188
– Quaternary Cobble-Boulder Gravels	188
9.3 Discussion	188
9.3.1 Regime 1: Warm Wet-Based Glaciation	189
– Phase 1. Development of sub-Pardoe Formation erosion surface	189
– Phase 2. Deposition of the Pardoe Formation	190
– Phase 3. Deposition of the Trail diamict	190
– Phase 4. The sub-Amphitheatre diamict erosion surface	191
– Phase 5. Deposition of the Amphitheatre diamict	191
9.3.2 Regime 2: Cold Dry-Based Glaciation	191
– Phase 6. Quaternary Dry-Based Cobble-Boulder Gravels	191
9.3.3 Palaeoclimate Considerations	191
9.3.4 The Age of the Menzies Range Landforms and Deposits	192
9.4 Summary	195
10. Past Biogeographical Barriers to Terrestrial Migration in Antarctica	197
10.1 Introduction	197
10.1.1 Aims	197
10.1.2 Previous Work	197
10.2 Methods	198
10.3 Results and Discussion	198
10.3.1 Palynology on the Pardoe Formation Lake Sediments	198
10.3.2 Biogeographical Barriers	198
10.4 Summary	203
11. Thesis Conclusion	204
11.1 Southern Kerguelen Plateau	204
11.2 Vestfold Hills	205
11.3 Prince Charles Mountains	206
11.4 Summary	209
12. References	210
Appendix 1: Map of Southern Ocean Locations in Thesis Text	
Appendix 2: Map of Antarctic Locations in Thesis Text	
Appendix 3: Kerguelen Plateau Diatom Data	
Appendix 4: Sørødal Formation Diatom Data	
Appendix 5: Pagodroma Group Diatom Data	
Appendix 6: Siliceous Microfossil Taxonomy and Plates	

---

**Section A:**  
**Background Review**

---

# 1. Thesis Introduction

The effects of future global warming on sea-level is of international concern (IPCC 1990; WCRP 1990; OECD / IEA 1994; SCCCS 1995). The potential for a major, global, sea-level rise in the future is held within the East Antarctic Ice Sheet (EAIS). If the EAIS were to melt global sea-level would rise ~66 m (calculated from Robin 1986). This greatly exceeds the ~15 m rise predicted from melting all other sources of ice on earth (Warrick and Oerlemans 1990; Hooke 1998). The large influence EAIS has on global sea-level brings into question, what is the stability of this feature?

Current climate data have been used to predict a 3° to 6.25 C° increase in global mean temperature over the next 100 years (IPCC 1990). Much of this warming may occur at high latitudes; for example, the Antarctic Peninsula has already undergone a 4° to 5 C° mean temperature rise in the last 50 years (Smith *et al.* 1996). Computer models of Antarctic glacial conditions predict that a temperature increase <5 C° could cause an increase in snow accumulation versus ablation, which may cause Antarctic ice sheet growth (Huybrechts 1993). However, an accompanying, albeit small, increase in water temperature may cause ice shelf melting, grounding line retreat and increased ice outflow that may result in ice sheet reduction (Warner and Budd 1998).

It is generally accepted that the current global warming trend has been caused, or enhanced, by an increase in anthropogenic greenhouse gases, notably CO<sub>2</sub> (IPCC 1990). The implication of global warming on sea-level can be determined through research into the extent and rate of natural climate change (McElroy and Mintzer 1993). Sediment records preserve past environmental information and enable natural climate change to be interpreted through palaeontological, sedimentological and geochemical analyses. The most recent analogue to the current climate trend, with elevated atmospheric CO<sub>2</sub>, may have existed in the late Pliocene (2.6-3 Ma) (Crowley 1996). During Pliocene warm intervals, atmospheric CO<sub>2</sub> concentrations were 30-50% higher than pre-industrial levels (Raymo *et al.* 1996). Significant warming intervals in the Pliocene, and Miocene, may be comparable to the future climate if greenhouse model predictions are correct. However, uncertainty exists over the extent, stability and style of Antarctic glaciation in the Neogene (Barrett 1992; Van der Wateren and Hindmarsh 1995). Two theories exist, both with very different implications for a greenhouse future (Stroeven *et al.* 1992).



Antarctic glaciation developed prior to the Miocene due to the continent's thermal isolation ~24 Ma (Mercer 1983; Barker *et al.* 1988; Kennett and Barker 1990; Robert and Maillott 1990). Although the exact time of ice sheet development is unclear, there is a general consensus that glacial conditions were unstable, and the glacial style was wet-based / polythermal until the middle Miocene (Flower and Kennett 1994). From this time on, conditions may have remained unstable and wet-based / polythermal through the Neogene, with terrestrial higher plants persisting in Antarctica until the late Pliocene (Webb and Harwood 1991, 1993; Harwood *et al.* 1991; 1992; Moriwaki *et al.*, 1992a; Wilson 1995). Alternatively, the ice sheet may have expanded, become stable and dry-based, and remained so through to today, eradicating Antarctica's terrestrial higher plants (Sugden 1992; Denton *et al.* 1993; Huybrechts 1993; Kennett and Hodell 1993; Marchant *et al.* 1993a, 1993b; Flower and Kennett 1994; Cowen 1995; Marchant *et al.* 1996; Sugden *et al.* 1995a, 1995b).

## 1.1 Aims

Antarctica's glacial history and ice sheet response to past climatic warming need to be resolved through geological evidence, if Antarctica's response to future global warming is to be predicted. Considering these issues, the aims of this thesis address the following questions:

- 1) How stable is the EAIS?
  - i) What was the Antarctic environment like during glacial retreat?
  - ii) Are computer models of Antarctic ice sheet response to global warming correct?
- 2) What were EAIS and Southern Ocean conditions like during the late Cenozoic?
 

In particular, after the Middle Miocene did:

  - i) the EAIS expand, become stable and dry-based,
  - ii) Southern Ocean conditions remain stable and relatively cold like today,
  - iii) terrestrial higher plants persist throughout Antarctica?

These questions are addressed through palaeontological and sedimentological analyses of sediment from three different regions of the Southern Ocean and Antarctica (Figure 1):

## 1.2 Southern Kerguelen Plateau

The Southern Kerguelen Plateau is positioned between a variety of oceanographic features in the Southern Ocean. Past migrations and changing environmental conditions across

these features are detected down marine gravity cores from lithological, diatom and silicoflagellate data, and can be related to climate change. The timing of these changes can be determined from diatom biostratigraphy.

### **1.3 Vestfold Hills**

*In situ* Pliocene marine sediments of the Sørsdal Formation outcrop on the Vestfold Hills. The formation is thought to have been deposited during warmer conditions when the EAIS margin was ~50 km further inland (Pickard *et al.* 1988). Detailed investigation of the diatoms in the formation enable comment on the environmental conditions during this interval.

### **1.4 Prince Charles Mountains**

Cenozoic glacial marine sediments of the Pagodroma Group and previously unrecorded terrestrial deposits, outcrop on the Prince Charles Mountains. These deposits contain direct and indirect evidence of major EAIS fluctuations. Some of these deposits can be dated using diatoms, and their lithostratigraphy and depositional environments described. Diatoms in marine sediments from the Pagodroma Group help determine marine conditions during glacial retreat. Lacustrine deposits from the Menzies Range were also investigated for palynological material and the results discussed in a larger biogeographical context.

The studies on the above areas have been organised as thesis chapters, and ultimately as separate papers for publication, as a result some of the laboratory procedures and literature review has been repeated within the chapters of this thesis.

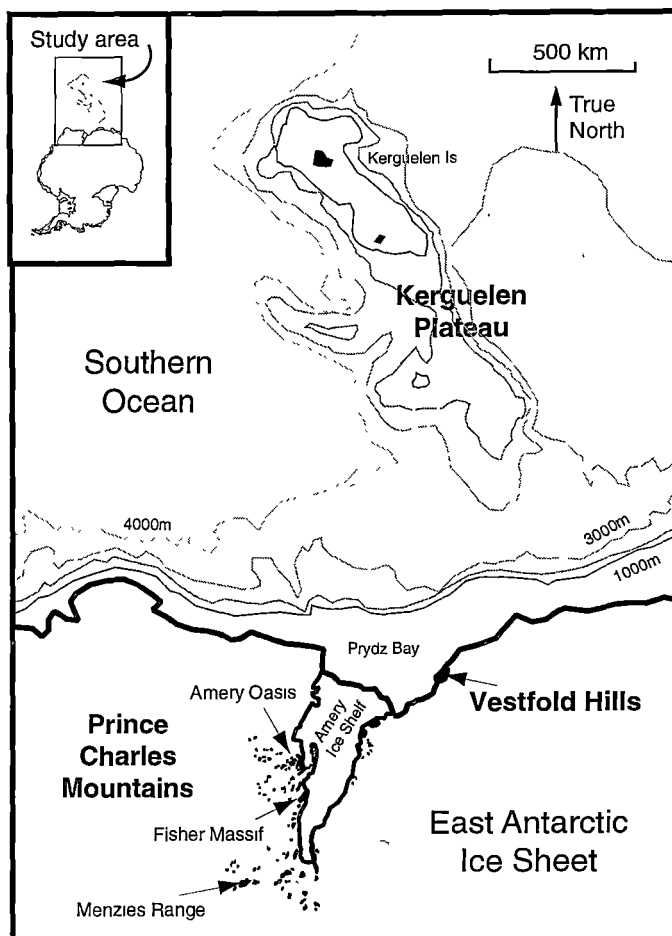


**Figure 1. Study areas:**

- 1) Kerguelen Plateau,
- 2) Vestfold Hills,
- 3) Prince Charles Mountains.

## 2. Modern Antarctic and the Southern Ocean Environments

### 2.1 Terrestrial Environments

Antarctica (Figure 2a), is the coldest, windiest and driest place on earth (Schwerdtfeger 1984). Around coastal East Antarctic, for example, the modern, mean annual air temperature is  $-15^{\circ}\text{C}$ , falling to  $-60^{\circ}\text{C}$  on the plateau (Huybrechts 1993). The cold conditions create a negative heat flux over the continent, which is balanced by cold air drainage in the form of katabatic winds (Davis and McNider 1997). The winds prevailing direction is from inland to the coast, although frequent cyclonic storms, originating offshore, may travel in the opposite direction (Barrett *et al.* 1997).

Ice sheets cover approximately 98% of Antarctica's surface (Fahnestock 1996), which contain ~90% of the world's ice and 70% of its fresh water (Key 1990). Much of the ice is in the form of two ice sheets: the East Antarctic Ice Sheet (EAIS) and the West Antarctic Ice Sheet (WAIS), which are divided partially by the Transantarctic Mountains (Colbeck 1980). The larger EAIS contains ~80% of the continent's ice volume (Bardin and Suyetova 1967), is up to 4776 m thick (Drewry 1983), and, in places, actually drains into the WAIS. However, much of the EAIS is dammed behind the Transantarctic Mountains (Denton 1995). The base of the EAIS is generally above sea-level, although substantial subglacial basins below sea-level do occur (Figures 2b and 3) (Drewry 1983; Kurinin and Aleshkova 1987). This is in contrast to the WAIS, which generally grounds below sea-level and covers large subglacial basins (Figure 2b) (Drewry 1983). The ice-free areas on Antarctica occur as exposed mountain ranges, dry valleys, isolated nunataks, coastal oases, and islands.

Antarctica is bordered by ice-shelves. The ice-shelves form up to 50% of its coastline (Fahnestock 1996), and are fed by the influx of outlet glaciers that flow from the surrounding ice sheets (Key 1990). Snow accumulating at the surface of the glaciers, and the freezing of sea-water at the base, also contributes to their formation (Heidelberg *et al.* 1991). Snow accumulation comes mainly from marine evaporation and decreases inland (Giovinetto and Bentley 1985). The flow of outlet glaciers, and the ice sheets themselves, is affected by the frigid Antarctic climate, creating dry-based and polythermal conditions beneath the ice. This is discussed further in Chapter 3.

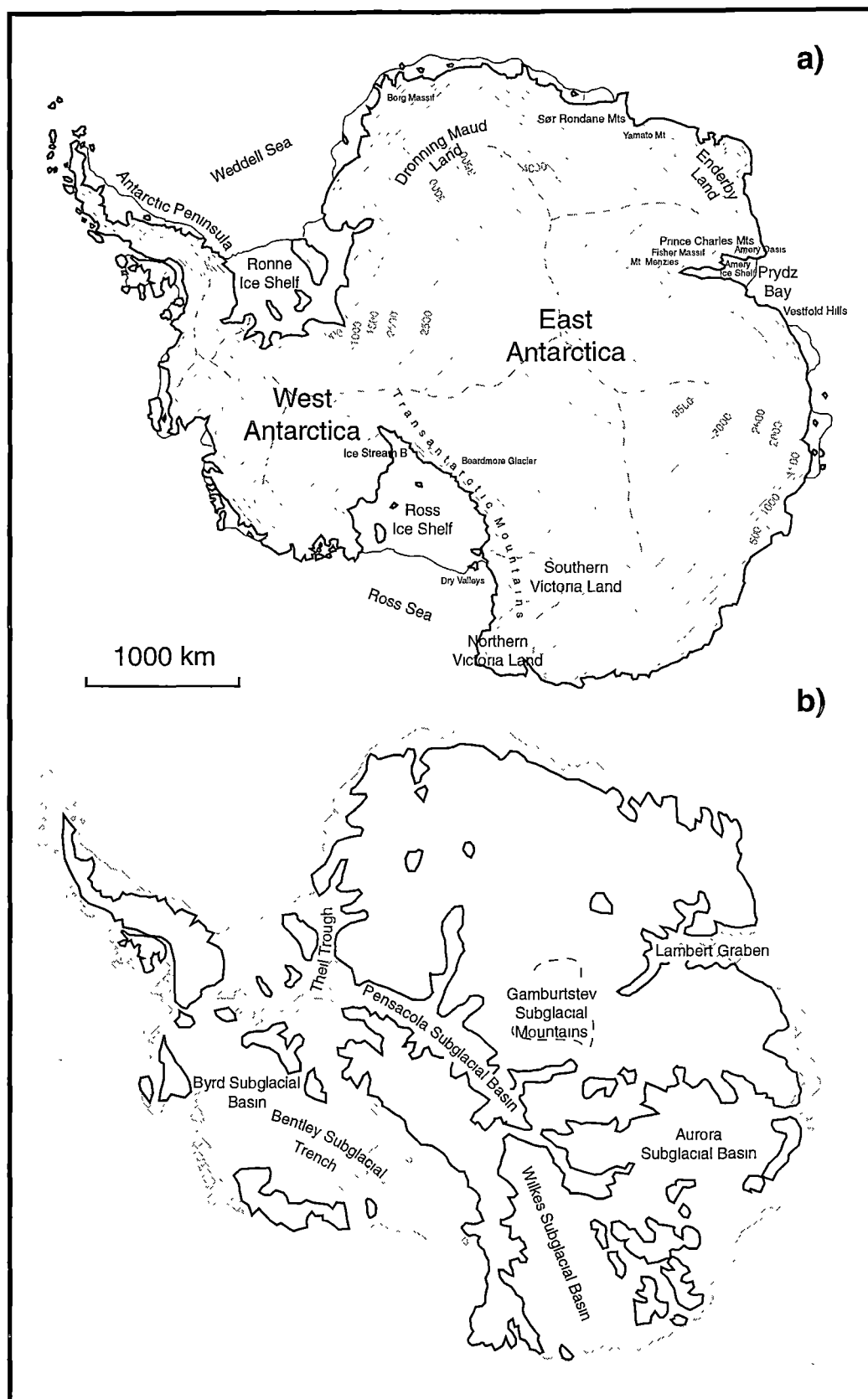


**Figure 2.** Antarctica's surface (a) and subglacial topography (b).

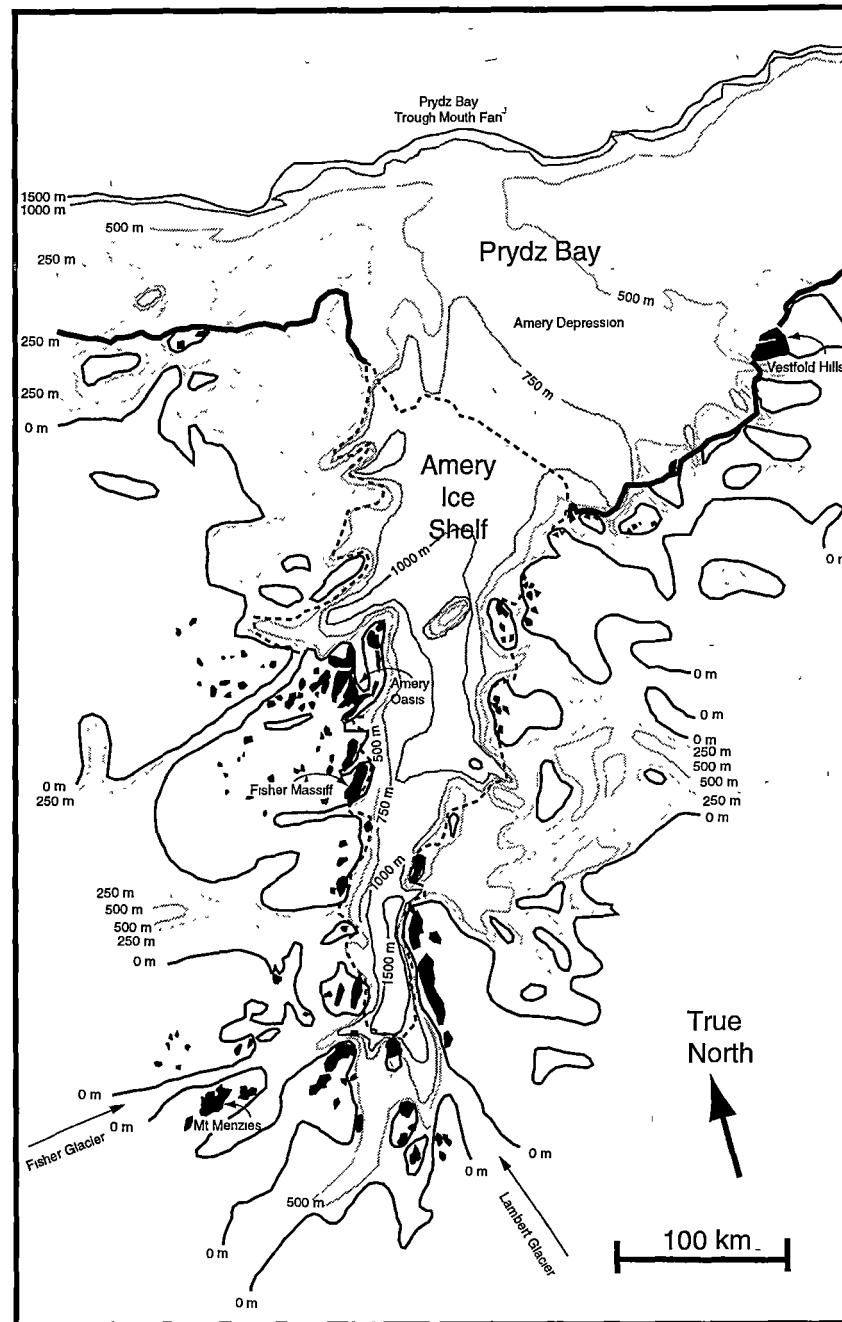


**Figure 3.** Lambert Graben subglacial topography and Prydz Bay bathymetry. (modified from Kurinin and Aleshkova 1987; Harris *et al.* 1997 and text in Phillips *et al.* 1996; Krebs 1997, 1998)

## 2.2 Marine environments

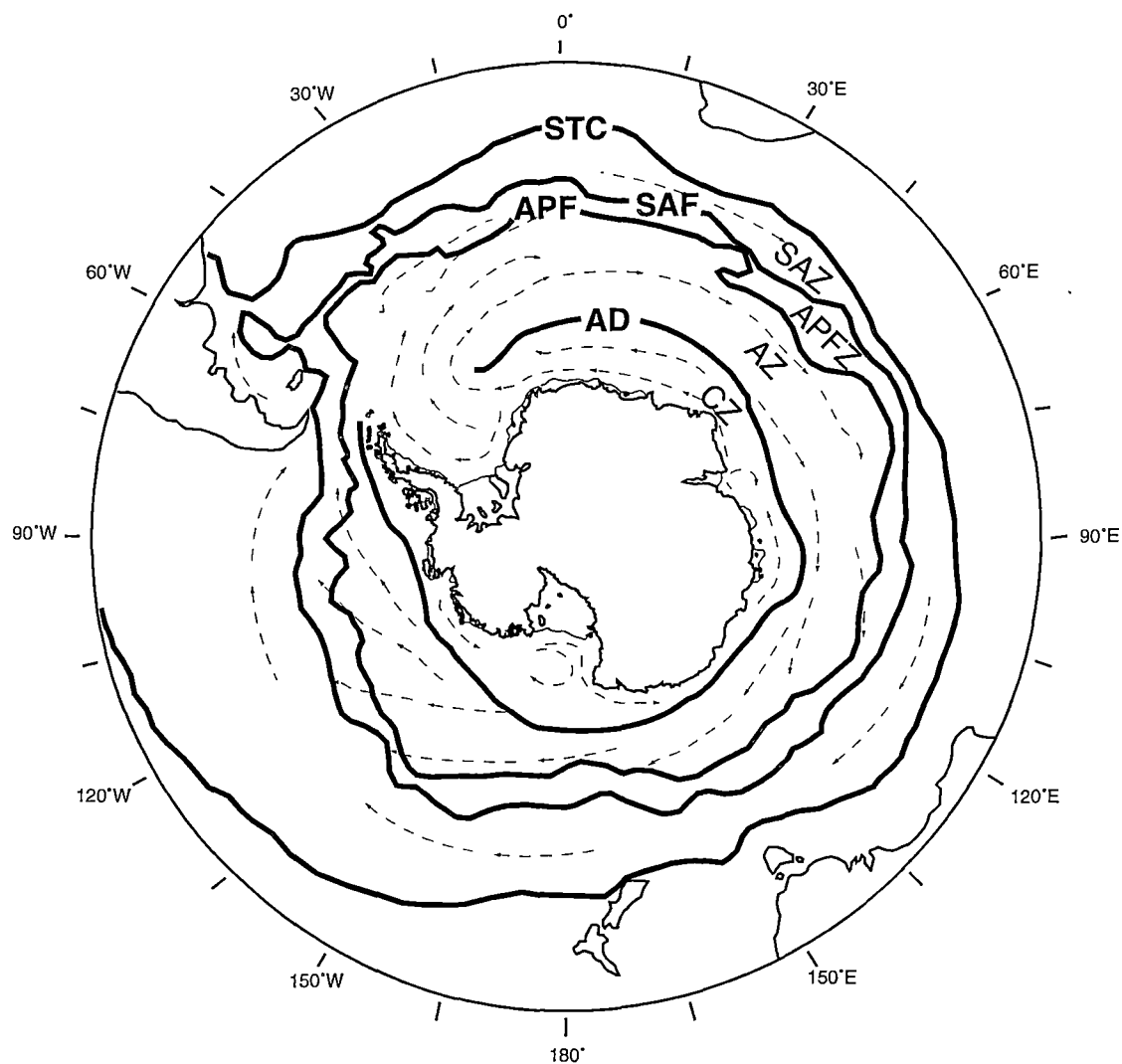
### 2.2.1 Southern Ocean

The Southern Ocean is generally considered to encompass the area south of the Subtropical Front (or Subtropical Convergence), between 38° S and 42° S (Tchernia 1980), and north of the Antarctic continent. The physical properties and circulation patterns of the Southern Ocean vary spatially, with latitude (Figures 4 and 5), depth (Figures 6 and 7), and temporally with season.

#### Ocean Circulation

The eastward flow of the Southern Ocean, between 35° S and 60° S, forms the Antarctic Circumpolar Current (ACC). The ACC is driven by the prevailing westerly winds of the West Wind Drift, which are created by cyclonic, low pressure systems that concentrate at Subantarctic latitudes (Patterson and Whitworth 1990). As a result, ~80% of ACC transport occurs between the Subantarctic and Polar Fronts (Rintoul and Church 1993; Orsi *et al.* 1995), discussed below. The width of the ACC is also constrained by the topography of the seafloor (Sverdrup *et al.* 1942). When it encounters deep water, its energy is spread vertically through the water column, diverting the current southward. In comparison, when the ACC flows over shallow regions its energy is spread horizontally and the current is diverted northwards (Gordon 1988; Whitworth 1988).

South of ~60 °S, the Southern Ocean flows to the west, forming the Antarctic Coastal Current. The coastal current is produced by Antarctic katabatic winds that are projected westwards at the coast by the Coriolis Effect (Davis and McNider 1997), and driven by the prevailing easterly winds of the East Wind Drift. Where the current is affected by the shape and bathymetry of the coastline, it also produces large cyclonic gyres, such as in the Ross and Weddell Seas, and, to a lesser degree, in Prydz Bay (Priddle 1990). Penetration of the ACC and coastal current through the water column to the seafloor (Priddle 1990) also affects sediment erosion and deposition processes. The horizontal circulation of waterbodies in the Southern Ocean, and over the Antarctic continental shelf, varies with vertical circulation.



#### Oceanographic Fronts

STC Subtropical convergence  
 SAF Subantarctic Front  
 APF Antarctic Polar Front  
 AD Antarctic Divergence

#### Oceanographic Zones

SAZ Subantarctic Zone  
 APFZ Antarctic Polar Front Zone  
 AZ Antarctic Zone  
 CZ Continental Zone

--- Surface Current Direction

**Figure 4.** Southern Ocean fronts and zones  
 (modified from Ackley 1996; Rintoul *et al.* 1997).



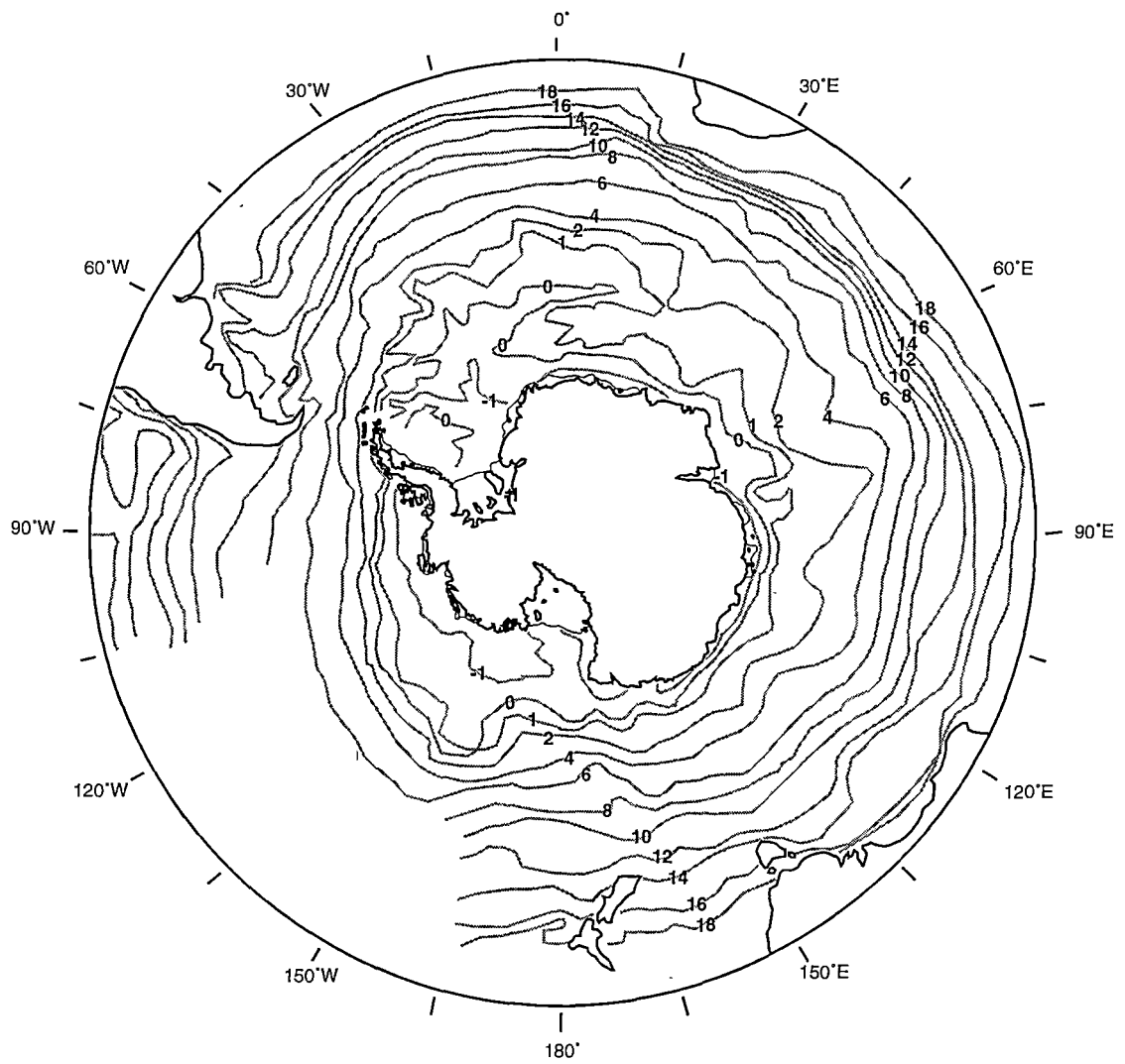


**Figure 5.** Summer (Jan-March) sea-surface temperature ( $^{\circ}\text{C}$ ) (after Gordon and Molinelli 1982).

## Ocean Fronts

Ocean fronts are complex zones created by the interaction between wind and the Coriolis Effect, forming areas of oceanic convergence and divergence (Pickard and Emery 1990). The sea-surface temperature and salinity at the fronts often have steep environmental gradients across a short latitude, but they are separated by larger zones with shallow environmental gradients (Figures 4 and 5) (Pickard and Emery 1990). Within the Southern Ocean, four distinct fronts are recognised: the Subtropical Front (STF), Subantarctic Front (SAF), Antarctic Polar Front (APF) or Antarctic Convergence (AC), and Antarctic Divergence (AD).

The APF is recognised as a region of convergence (down-welling), divergence (upwelling), or a combination of both (Gordon 1971) and is an area of high primary productivity (Knox 1994). The AD occurs between the ACC and the coastal current. Ekman Divergence between the two currents causes upwelling of nutrient-enriched Circumpolar Deep Water (Gordon 1988; Wong 1994). The enriched surface waters flow both north and south of the AD (Gordon 1971). The southerly flow is assisted by westerly katabatic wind stress, providing a broad region of onshore surface water transport, which possibly increases primary productivity on the Antarctic continental shelf (Davis and McNider 1997).

The fronts may also form “jet streams” that move with the ACC (Park *et al.* 1993). Surface eddies that often form in the ACC, for example, may accelerate its mean current flow velocity (Morrow *et al.* 1992) and occasionally spiral northwards off the APF (Pickard and Emery 1990).

## Water Bodies

The vertical structure of the Southern Ocean illustrates that it is part of a larger global system with water bodies entering at depth from other latitudes (Figure 6). The physical properties of Southern Ocean water bodies differ, as does their structure and position with latitude and depth (Figures 6 and 7).

### *Surface Waters*

There are two main surface water bodies south of the STF: Antarctic Surface Water (AASW) and Subantarctic Surface Water (SASW) (Gordon and Molinelli 1982) (Figure 6). AASW flows north and south from the AD (Gordon 1971). As it flows north, its temperature and salinity increase, and the AASW changes into SASW (Gordon 1971);

however, most of the northerly AASW is possibly subducted at the APF, where it becomes Antarctic Intermediate Water (Gordon 1971). On the continental shelf, and adjacent offshore areas, there is a lower salinity surface layer (Summer Surface Water (SSW)) created by seasonal sea-ice melting (Smith *et al.* 1984; Hosie 1994).

#### *Subsurface and Intermediate Waters*

North of the APF, two main water bodies form at subsurface and intermediate depths: Antarctic Intermediate Water (AAIW) and Ice Shelf Water (ISW). AAIW probably forms at the APF when AASW is subducted (Gordon 1971; Tomczak and Godfrey 1994). North of SAF, Subantarctic Mode Water (SAMW) probably is formed during the winter overturning of SASW (McCartney 1977). During summer on the continental shelf, Winter Water (WW) forms at intermediate depths, between SSW and Circumpolar Deep Water, as a remnant mixed layer (Smith and Tréguer 1994). Convection overturns WW on the shelf, causing it to form most of the water column here (Wong *et al.* 1998).

Cold, saline ISW is also present at intermediate water depths on the continental shelf (Wong 1994). It is formed when Low and High Salinity Shelf Water (LSSW and HSSW, respectively) come in contact with the base of ice shelves, causing ice melt and the production of very cold, less saline water (Carmack 1990; Wong *et al.* 1998). ISW is commonly produced in the Ross and Weddell Seas (Carmack 1990), and in Prydz Bay when LSSW comes in contact with the Amery Ice Shelf (e.g. Figure 7). The LSSW re-emerges into the bay at intermediate depths from beneath the western edge of the ice shelf (Wong 1994; Wong *et al.* 1998). The ISW becomes a less distinct water body as it moves further northwards and mixes with the surrounding shelf waters (Wong *et al.* 1998).

#### *Circumpolar Deep Water*

Circumpolar Deep Water (CDW) is the largest volume of water in the Southern Ocean. It is characterised by an upper layer (UCDW) that contains water from the Pacific and Indian Oceans, and a lower layer (LCDW) composed mostly of North Atlantic Deep Water (NADW) from the Norwegian Greenland Sea (Sarnthein *et al.* 1994; Smith and Tréguer 1994). South of the AD, UCDW and LCDW come together to form one modified layer (MCDW). The modified layer penetrates onto the continental shelf and mixes with other water bodies there (Middleton and Humphries 1989; Wong *et al.* 1998) to become colder, fresher and less saline than the more northerly CDW (Whitworth *et al.* 1998; Wong *et al.* 1998).

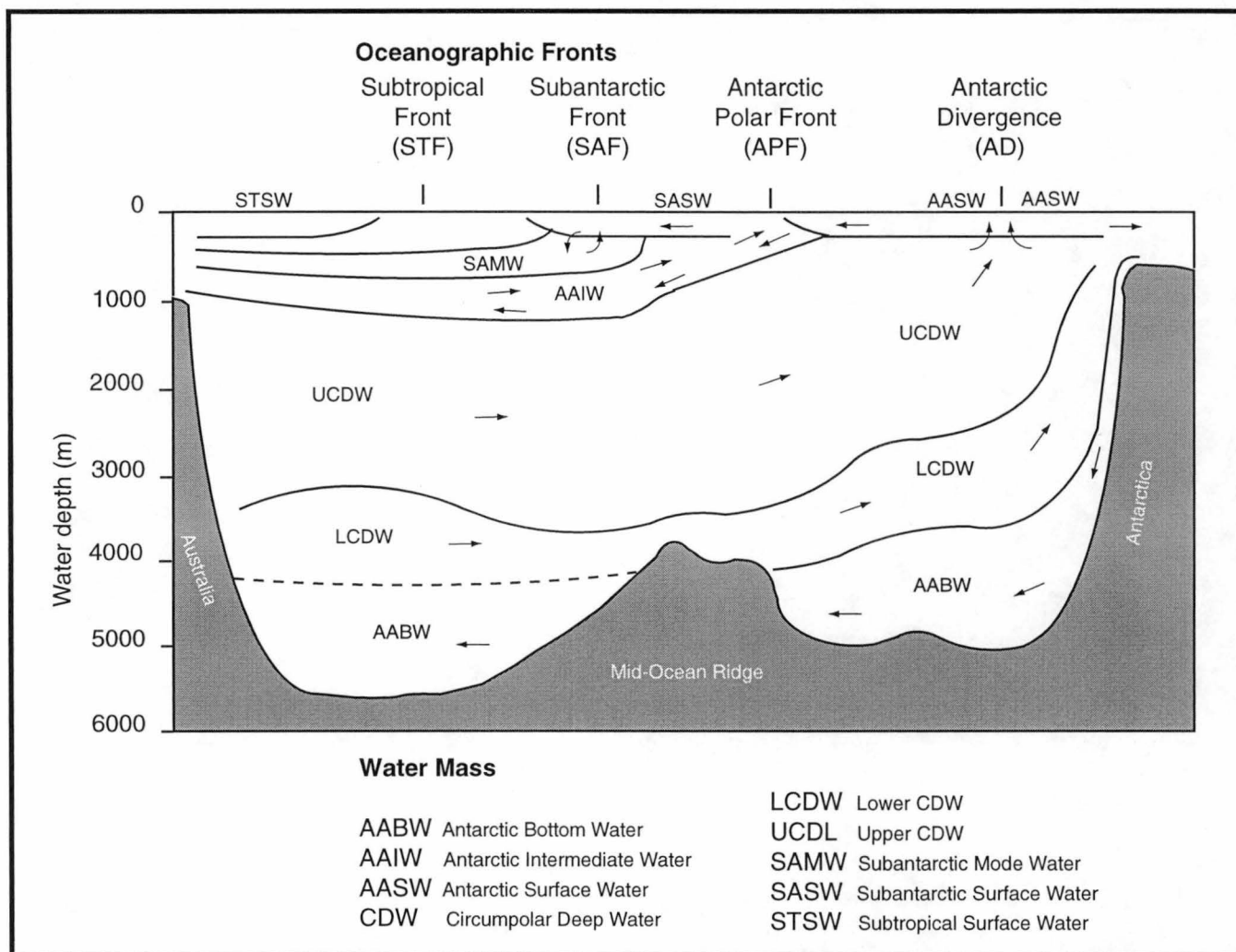


**Figure 6.** Southern Ocean water masses  
(Armand 1997, from Gordon and Molinelli 1982).

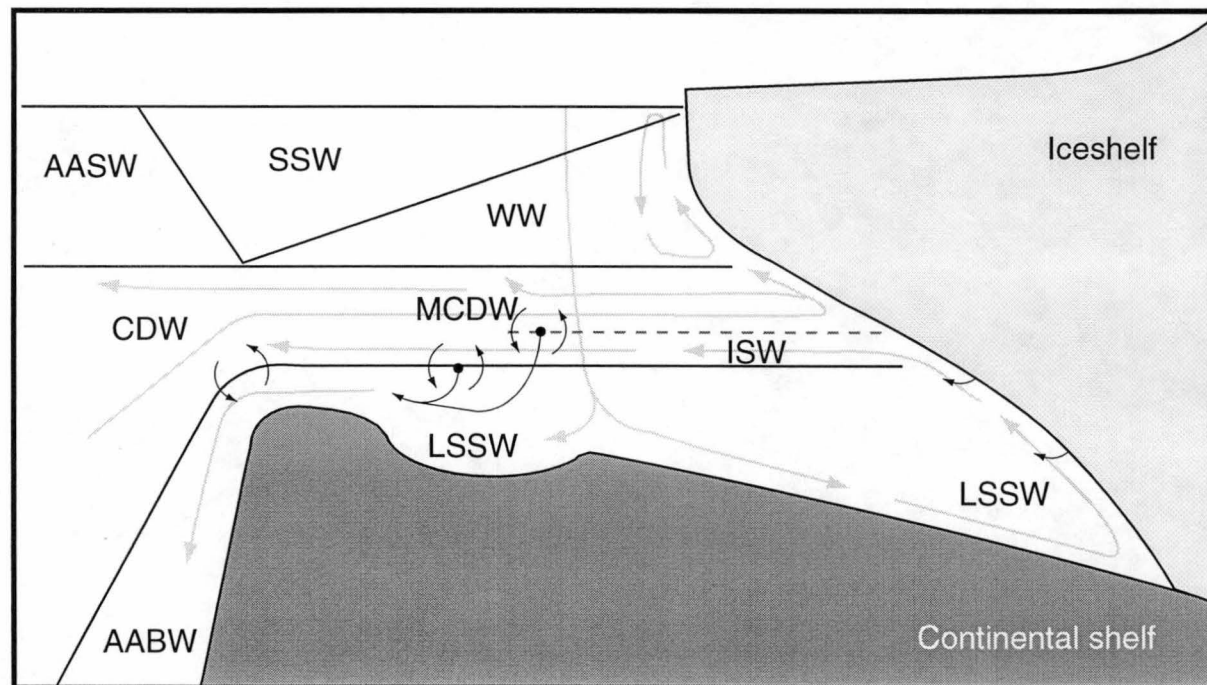


**Figure 7.** Southern Ocean water masses on the Antarctic continental shelf (from text in Wong 1994; Wong *et al.* 1998).

### *Bottom Water*

Antarctic bottom water (AABW) is the deepest water close to Antarctica. It is intrinsic to modern global ocean circulation, but its precise method of production is unknown. The formation of AABW has been linked to brine exclusion and the formation of LSSW and HSSW during the formation of sea-ice over the Antarctic continental shelf (Foster *et al.* 1987). These saline, dense waters mix with other water bodies and drain from the shelf slope to the abyssal seafloor as AABW (Jacobs *et al.* 1985). Most AABW is produced in the Weddell and Ross Seas (Foster *et al.* 1987; Jacobs *et al.* 1970) by the mixing of ISW and MCDW (Jacobs *et al.* 1970; Wong 1994). More recently, Wong *et al.* (1998) have suggested that a modified form of AABW is also formed in Prydz Bay, as Prydz Bay Bottom Water (PPBW) (Middleton and Humphries 1989). Here, sea-ice brine sinks as cold, dense LSSW and is thought to mix with CDW on the continental shelf slope and form saline shelf water, or modified AABW (Wong *et al.* 1998).

### **2.2.2 Sea-ice**

Antarctic sea-ice has a major influence on global climate. Sea-ice forms at  $-1.8^{\circ}\text{C}$  (Ackley 1996) and occurs just south of the  $-1.8^{\circ}\text{C}$  surface air temperature isotherm (Zwally *et al.* 1983). It affects ocean heat and momentum exchange to the atmosphere (Gow and Tucker 1990), global albedo, and ocean thermohaline circulation through the formation of Antarctic bottom water (Gordon and Comiso 1988). Locally, it increases light attenuation (Maykut 1985; Buckley and Trodahl 1987), scours shallow coastal areas within littoral depths (Clarke 1996a; 1996b), and reduces the effect of waves, the depth of the mixing layer, and surface water salinity as it melts (Smith and Nelson 1986; Knox 1994). The resulting surface layer is important to phytoplankton growth (Sullivan *et al.* 1993) in Antarctic, as well as in mid-latitude waters where some of it is transported (Zwally *et al.* 1983). The type of sea-ice formed and its concentration also vary considerably (Squire 1990), affecting light, nutrient levels and habitat structures within the ice, the surrounding water column and the seafloor in shallow areas.

The Southern Ocean has been zoned in terms of variations in physical parameters, nutrients and primary production (Tréguer and Jacques 1992; Jacques and Fukushi 1994), which are all closely related to sea-ice conditions (Figure 8). Moving north from the Antarctic Coast, these zonations are: the Permanent Ice Zones (PIZ), in the Weddell, Ross Seas and Prydz Bay; the Coastal and Continental Shelf Zone (CCSZ), which is sea-ice free 2-3 month of the year; the Seasonal Ice Zone (SIZ), where there is a major seasonal change in sea-ice coverage; and the Permanent Open Ocean Zone (POOZ), where there is

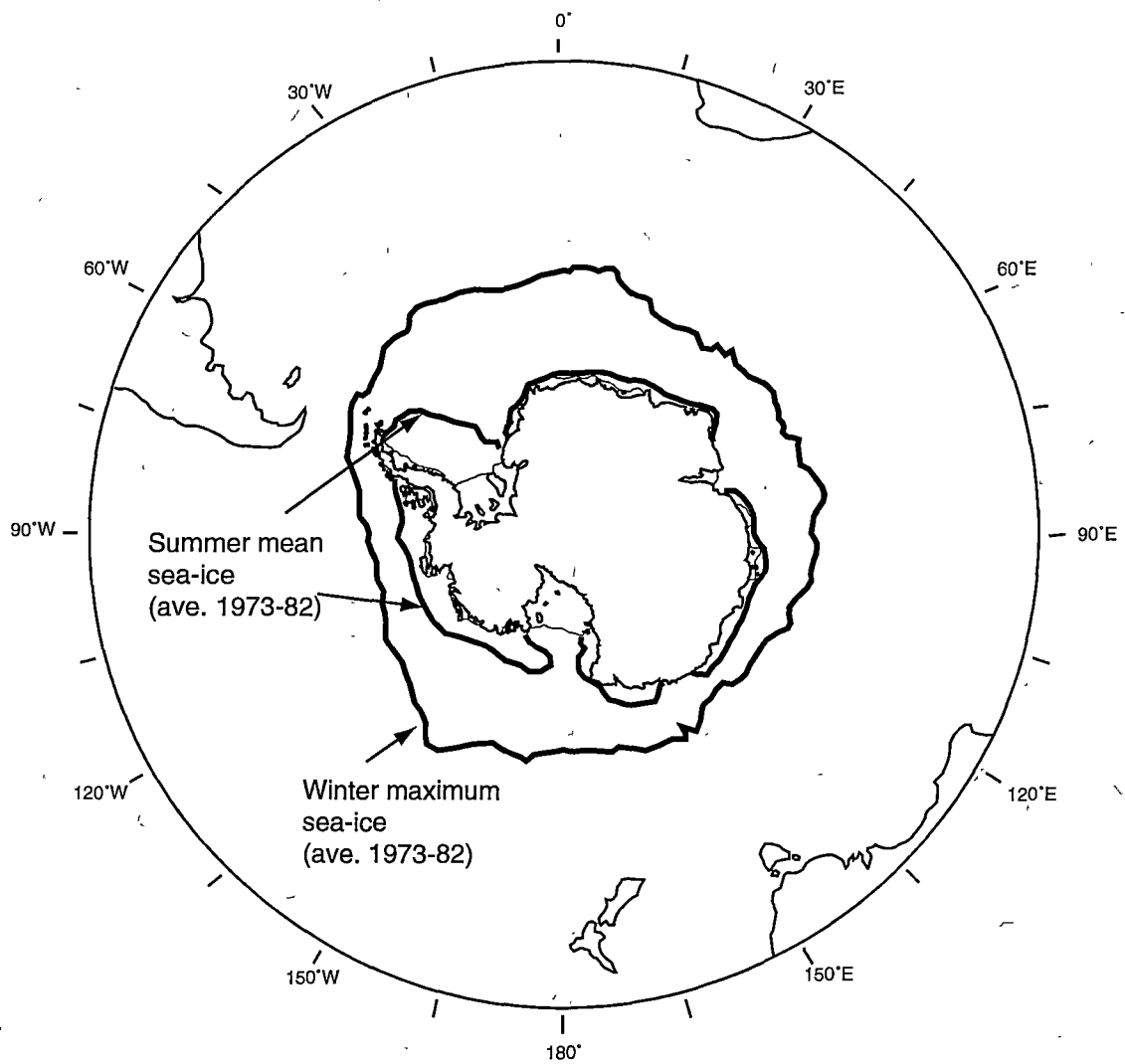
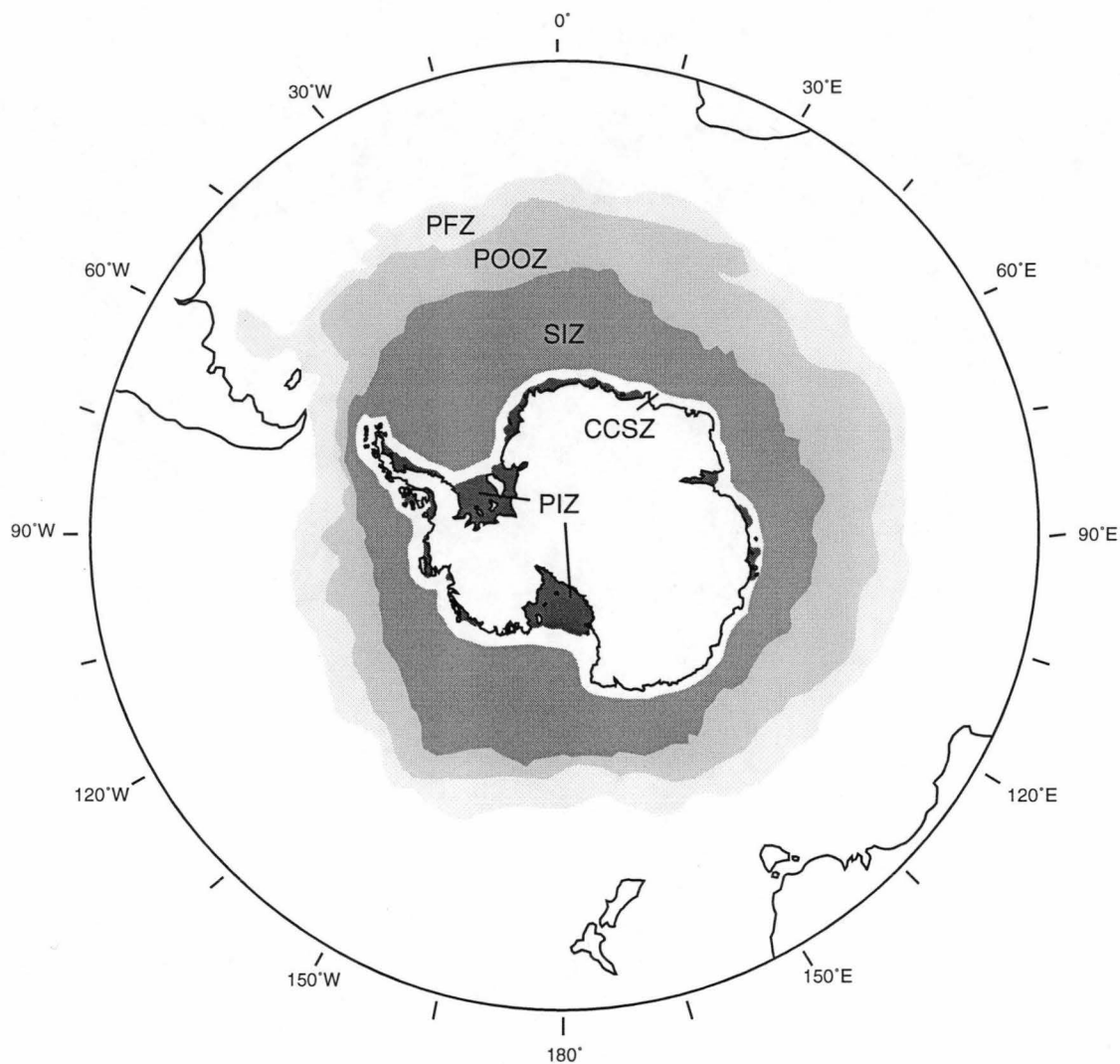


**Figure 8.** Seasonal sea-ice conditions in the Southern Ocean (modified from Bryan 1993).



### Oceanographic Zones

- PFZ Polar Front Zone
- POOZ Permanent Open Ocean Zone
- SIZ Seasonal Ice Zone
- CCSZ Coastal & Continental Shelf Zone
- PIZ Permanent Ice Zone

**Figure 9.** Zonation of the Southern Ocean, based largely on sea-ice conditions (modified from Tréguer and Jacques 1992)



no sea-ice (Figure 9). Beyond the POOZ is the Polar Front Zone (PFZ), which occurs between the APF and SAF as a sea-ice free, high productivity region associated with nutrient upwelling.

The annual growth and decay of Antarctic sea-ice is the most dramatic seasonal change experienced by the surface of any ocean on earth (Nicol and Allison 1997). At its maximum extent, during the austral winter (September) (Cavalieri and Parkinson 1981), it covers 20 million km<sup>2</sup> of the Southern Ocean (Squire 1990) (Figure 8). Following a four month period of retreat, from October to January (Parkinson and Cavalieri 1982), it is reduced to an area of only 4 million km<sup>2</sup> (Squire 1990) by the austral summer (February) (Zwally *et al.* 1983) (Figure 8). Most of the ice is reformed annually, during March to May, at a relatively slow rate (up to ~3 km per day). This contrasts to its rapid spring-summer retreat (up to ~20 km per day) (Comiso and Zwally 1984; Cavalieri and Parkinson 1981). In some areas perennial sea-ice may persist; this is found most commonly in the Weddell Sea where up to 50% of the sea-ice present in February is greater than 1 year old (Zwally *et al.* 1983).

Sea-ice first forms as randomly orientated crystals of frazil ice. These often give the water a grease-like appearance; hence it is commonly called “grease ice”. In general, the growth of frazil ice is the dominant mechanism for sea-ice formation in Antarctic waters (Worby *et al.* 1998). Once it reaches a coverage of ~ 30-40% over the water surface, the transition to a solid ice floe layer begins (Knox 1994). Beneath the floe, larger, vertically elongate, columnar, sea-ice crystals grow (Knox 1994). As the sea-water freezes, salt is excluded and some becomes caught in brine pockets between the ice crystals (Palmisano and Sullivan 1982). Further ice may form in the water column as small frazil ice crystals and platelets (10 - 15 cm in diameter and 0.2 - 0.3 cm in thickness) (Dayton *et al.* 1969), which can attach to the base of the floes (Knox 1990). If there is little wave or wind disturbance, large continuous sheets of sea-ice will form, which are generally <0.6 m in thickness (Worby *et al.* 1998). Beneath this, ice stalactites, up to 6 m long (Dayton and Martin 1971), and loose platelets layers, 1-5 m thick, may form due to brine drainage (Knox 1990). Sea-ice exceeding 15 cm in thickness is commonly overlain by snow (Knox 1994). The snow depth can vary greatly and depress the sea-ice below the surrounding water surface, allowing the infiltration of sea-water along the snow and sea-ice interface (Knox 1994). Pools can also form on the surface of the sea-ice through either surface melting (McConville and Wetherbee 1983) or flooding (Whitaker and Richardson 1980), or by a combination of both these processes. In coastal areas, shore fast-ice

anchored around the coast, by islands and embayments, forms perennial ice up to 10 m thick (Knox 1994). Perennial sea-ice often changes in structure, nutrients and optical properties due to brine drainage (Laws 1984).

Deformation of the sea-ice, due to water turbulence, water currents and wind, can create ice that contrasts highly in thickness and structure over a localised area. Wave turbulence can penetrate hundreds of kilometres into the sea-ice cover (Squire 1990; Worby *et al.* 1998), breaking up the sea-ice sheets into smaller floes (collectively called ice pack (Key 1990) and brash ice). Water turbulence in newly formed ice often forms circular “pancake-shaped” floes, which vary in diameter from 0.3 -3.0 m (Knox 1994) and generally have raised edges from bumping together (Squire 1990). Frazil ice can continue to form in the intervening water spaces and ultimately freeze the pancakes together, creating larger ice floes known as composite sea-ice sheets (Weeks and Ackley 1982; Squire 1990).

Compressive forces thrusting sea-ice sheets together can locally increase ice thickness (Weeks *et al.* 1989; Jefferies and Weeks 1992; Jefferies and Adolphs 1997; Worby *et al.* 1998). This affect also increases light attenuation and can produce sea-ice with alternating frazil and columnar ice layers (Squire 1990). Compressive forces can also produce large pressure ridges of broken sea-ice with up-thrusted blocks (Worby *et al.* 1998) that eventually decrease in salinity due to brine drainage (Squire 1990). In contrast, extensional forces can cause leads, or polynyas, to open in the sea-ice. Polynyas commonly form where katabatic winds drain from steep areas off the Antarctic continent, and blow the sea-ice offshore (Davis and McNider 1997). Synoptic winds along the coast have a similar influence, and sometimes exceed the effects of katabatic winds (such as along the Wilkes Land coast) (Cavalieri and Martin 1985). Polynyas also form due to warm deep water (or MCDW) upwelling on the continental shelf (as in the case of the Cosmonaut Sea polynya) (Comiso and Gordon 1996). Subsequent freezing of the exposed water, then transportation offshore by winds, causes up to ten times more sea-ice production in polynyas than in adjacent fast-ice areas (Cavalieri and Martin 1985). Therefore coastal polynyas are possibly areas of major AABW production (Gordon and Tchernia 1972; Zwally *et al.* 1985; Foster 1995).

In East Antarctica, the characteristics of the sea-ice pack are largely determined by the continual passage of synoptic weather systems through the region (Worby *et al.* 1998). Alternating compressive and extensional forces occur on the sea-ice pack with the passing

of the systems, changing the ice thickness and distribution (Worby *et al.* 1996). Cores collected through East Antarctic sea-ice indicate that it is predominantly frazil ice (~47%) formed in turbulent conditions, columnar ice (~39%), snow-ice (~13%); other ice types making up the remaining ~1% (Worby *et al.* 1998). The ice is highly mobile and constantly changes direction and speed. Ice cores indicate that ~40% of the floes are <0.1 m thick and rarely exceed 0.5 m in thickness without being deformed and rafted over each other (Worby *et al.* 1998). The thermodynamic and dynamic forcing parameters that determine East Antarctic sea-ice thickness and distribution are illustrated in Figure 10. Basal platelet ice formation has not been reported in the vicinity of many areas around the East Antarctic coast, such as near Syowa (69° S, 39° E) (Hoshiai 1977), Mawson (62° S, 62° E), Davis (68° S, 78° E) and Casey (66° S, 100° E) stations (McConville and Wetherbee 1983).

In Prydz Bay, sea-ice is present throughout autumn, winter and spring (Smith *et al.* 1984; Smith and Tréguer 1994), extending northwards to 58° - 60° S during the winter maximum (Jacka 1983). Polynyas occur west (MacKenzie Bay and Cape Darnley) and east (Amery and Prydz Bay) of the bay, and are probably associated with both synoptic and katabatic winds (Potter 1995; Worby *et al.* 1998). It has been suggested that they could also be associated with anomalously warm water in the centre of the bay (Smith and Tréguer 1994). Sea-ice breaks out of Prydz Bay in early summer, and open water predominates in January. Average sea-ice conditions in the region have been determined for the months October and February, when sea-ice is at its maximum and minimum extent (Gloersen *et al.* 1992).

### **2.2.3 Coastal**

Ice-shelves and ice-cliffs surround much of the Antarctic coastline (Anderson 1993). Around the ice-shelves, the marine environment is often deep, whilst ice-cliffs are usually associated with shallow areas and usually ground at sea-level (Anderson 1993). However, some ice-cliffs ground well below sea-level and the adjacent marine environment is deep due to isostatic depression (Anderson and Molnia 1989).

Rocky areas are rare around coastal Antarctica (Pickard 1986; Anderson 1993). Rocky coasts are generally surrounded by shallow marine environments that are often disturbed by ice-related processes, such as anchor ice development and sea-ice and iceberg scouring (Dayton 1969; Dayton *et al.* 1970; Richardson and Hedgpeth 1977; Laws 1984; Walton 1987; Clarke 1996a, 1996b). These regions are also influenced largely by the interplay of

isostatic and eustatic sea-level change. Where coastal marine embayments have become isostatically isolated from the marine environment, numerous lakes form (Pickard 1986).

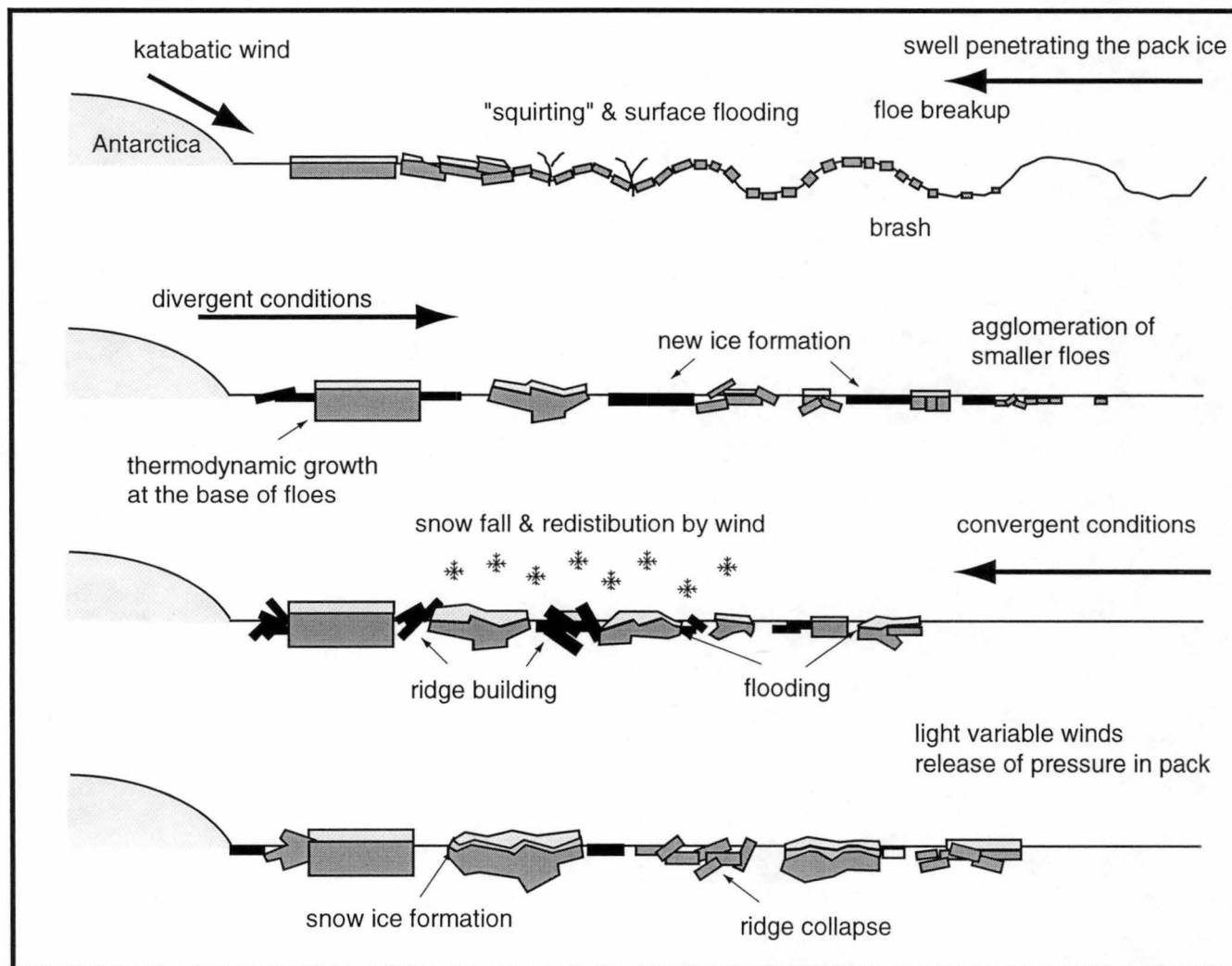


**Figure 10.** Sea-ice conditions off east Antarctica (from Worby *et al.* 1998).

### 3. Antarctic Glacial Style and Stability

#### 3.1 Glacial Style

Over 97% of Antarctica is covered by ice in the form of ice sheets (Chapter 2.1), which feed outlet glaciers on the coast. The thermal regime under which glaciers occur influence their style of glaciation: i.e. their shape, how they move and the erosional landscape and deposits they produce. Glacial style can be classified in many different ways.

Shape is commonly used to classify glaciers. Glaciers that are long, comparatively narrow and generally flowing in one direction down a valley are called valley glaciers (Hooke 1998). Where they reach the coast and interact with marine processes they become tide water glaciers. Short valley glaciers on mountains are called alpine glaciers, and where they occupy small basins on the mountain they are called cirque glaciers (Hooke 1998). Valley glaciers describe one end member of glacier shape, whilst the other extreme is an ice sheet. There is a continuum between these classifications where, for example, the EAIS feeds outlet glaciers, such as the Lambert and Fisher Glaciers. Although these both form part of the EAIS they are basically valley glaciers.

Glaciers are also classified by their thermal regime (Hooke 1998) and can be categorised as polar, subpolar or temperate, depending on their temperature. As with glacial shape, a continuum exists between these. The temperature of ice can be lowered below the freezing point of fresh water ( $0^{\circ}\text{C}$ ); however, increased pressure can cause the melting point of ice to be lower than  $0^{\circ}\text{C}$ . The point at which the ice to water phase change occurs is described as the “pressure melting point” (Benn and Evans 1998). The temperature of ice in polar glaciers is generally well below  $0^{\circ}\text{C}$  (except possibly near the base, as discussed below). Subpolar glaciers are sometimes referred to as polythermal, as they contain large volumes of ice that is both cold as well as at the pressure melting temperature (Hooke 1998). The cold ice generally occurs near the glacier’s surface and covers “warmer” ice at depth (Rabus and Echelmeyer 1997). Temperate glaciers are generally considered to be at the pressure melting temperature throughout (Hooke 1998), except perhaps near their surface (Hambrey 1994) which experiences seasonal changes (Benn and Evans 1998). It must be noted that this method of classification is highly simplistic as the thermal regime of individual glaciers may vary both spatially and temporally (Denton and Hughes 1981; Rabus and Echelmeyer 1997). In the following review, the term “wet-based ice” refers to

ice at the pressure melting point and “cold-based ice” to ice that is frozen at a temperature much below the pressure melting point.

Temperature largely determines the way glaciers move, how they erode the landscape and the types of sedimentary deposits that they form (Drewry 1986; Hambrey 1994; McLane 1995). Temperature affects the amount of ice melt beneath a glacier, so that warmer, temperate glaciers are wet-based and colder, polar glaciers are dry-based (Menzies 1995). Wet- and dry-based glaciers move differently (Hambrey 1994; Bennett and Glasser 1996). Wet-based glaciers move largely by sliding along their base (Menzies 1995) (Figure 11), assisted by meltwater, or meltwater combined with glacial debris, which lubricates the under surface (Lawson 1995; Menzies 1995). Slippage can also occur in unconsolidated sediment beneath the glacier (Alley 1989; Alley 1991). In contrast, dry-based glaciers move very little along their base. Instead they move largely through internal ice deformation (Menzies 1995; Bennett and Glasser 1996) (Figure 11). As a result, there is a smaller amount of erosion, and subsequently little deposition, associated with colder, dry-based glaciers in comparison with that beneath the warmer, wet-based glaciers (Hambrey 1994; Bennett and Glasser 1996). The erosional landforms associated with terrestrial temperate glaciation are illustrated in Figure 12. Wet-based alpine valley glaciers cause major U-shaped valley erosion (Benn and Evans 1998), whilst dry-based glaciers cause little modification to the previous landforms and deposits. The landforms beneath dry-based glaciers may even be well preserved, due to the absence of glaciofluvial processes and minimal basal sliding beneath the ice (Bennett and Glasser 1996).

### **3.1.1 Terrestrial Glacial Deposits**

Wet-based temperate glaciers and cold-based polar glaciers are the extremes in glacial style. The terrestrial depositional and erosional environments associated with these regimes are illustrated in Figure 13. Terrestrial glacial deposits can be divided into three facies zones: subglacial, supraglacial and proglacial (Figure 13) (Sugden and John 1976). In the subglacial zone, beneath the ice, lodgment till predominates after having been “plastered on” by pressure melting and / or other processes that release sediment from the ice’s basal debris layer (Shaw 1985; Dreimanis 1988). This can be deformed by ploughing, shearing and faulting to create deformation till, which assists the basal sliding of the ice (Alley 1989; Alley 1991) (Figure 11). Differential deformation (Boulton 1987), or sedimentation in subglacial cavities (Shaw 1983; Shaw and Kvill 1984), is thought to produce drumlin and rogen moraine hill-like deposits. Subglacial meltwater streams can also deposit fluvial sediments beneath the ice (Warren and Ashley 1994).

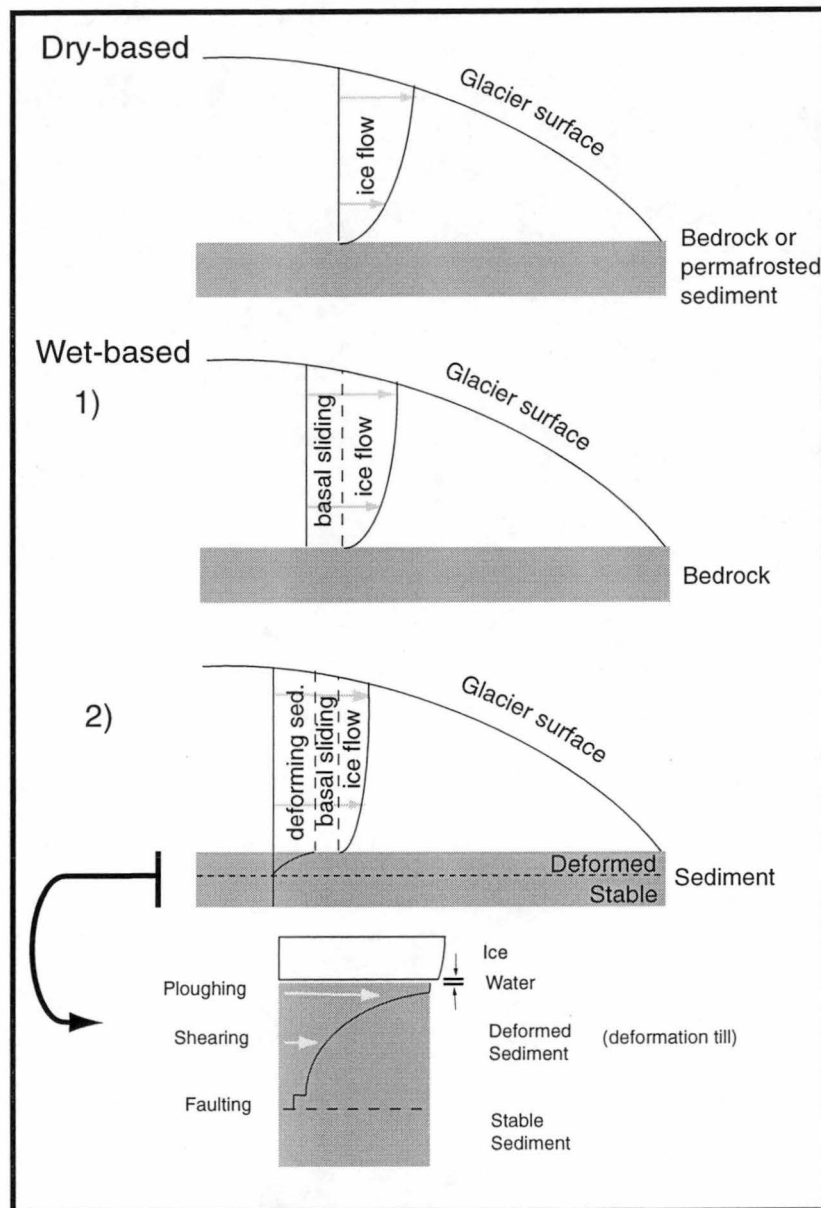


**Figure 11.** Glacial movement  
(modified from Bennett and Glasser 1996)



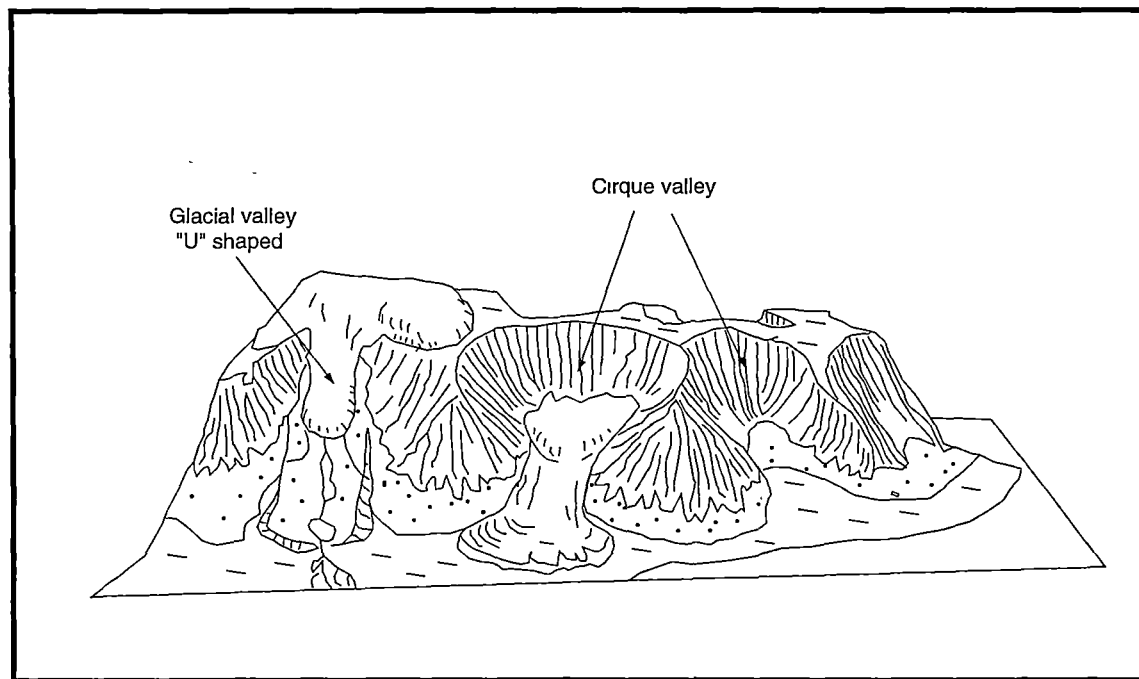


**Figure 12.** Wet-based glacial erosional landscape  
(modified from Humlum 1982)

The supraglacial facies zone consists of glacial margin (moraines) and glacial retreat deposits (sublimation till). Moraines can form at the margins of a glacier (end and lateral moraines), from passive non-advancing (ablation moraines) and actively advancing glacial ice (push and thrust moraines). This is a simplified use of the term “moraine”, however, as it is also applied to the description of numerous and varied subglacial and ice disintegration deposits (e.g. in Sugden and John 1976). Sublimation till is deposited through the ablation and release of glacial debris as the ice retreats. Other facies in the supraglacial zone include kettle lakes, which form in the depressions left from the ablation of stranded ice remnants (pingos), moraine lakes, which form behind moraines due to moraine damming, and braided river deposits from sediment laden glacial meltwater streams.

Lake, braided river and aeolian deposits occur in the proglacial zone and more distal areas (Sugden and John 1976; Edwards 1986; McLane 1995) (Figure 13).

Wet-based terrestrial glacier deposits differ greatly from dry-based terrestrial deposits. The wet-based deposits are generally thick and contain much glacial rock flour (terrigenous sand and silts) (Cowan and Powell 1991). Dry-based deposits are generally thinner, and contain less rock flour (Anderson *et al.* 1991; Anderson and Molnia 1989), due to the aridity and limited importance of ice melting in that environment (Benn and Evans 1998). Some minor basal sliding can occur, causing minor lodgment till deposition (Hasegawa *et al.* 1992). Most glacial debris is deposited as supraglacial ablation moraines and thrust moraines (at the ice margin), and hummocky and ice cored moraines due to ice disintegration (as the margin retreats) (Bennett and Glasser 1996; Benn and Evans 1998).

Generally these deposits are thinner and more clast supported, with angular clasts, in contrast with similar facies from wet-based glaciers. Glacial-fluvial meltwater streams tend not to be associated with cold-based glacial environments (Benn and Evans 1998). In the modern Antarctic environment, there is very little modification following deglaciation due to the extreme aridity (Benn and Evans 1998; Sugden *et al.* 1995a, 1995b; Sugden 1996). Strong winds winnow away the finer sediment fractions, however, producing gravel lags, and shaping the surfaces of clasts into faceted ventifacts; otherwise there is very little paraglacial activity (Benn and Evans 1998).

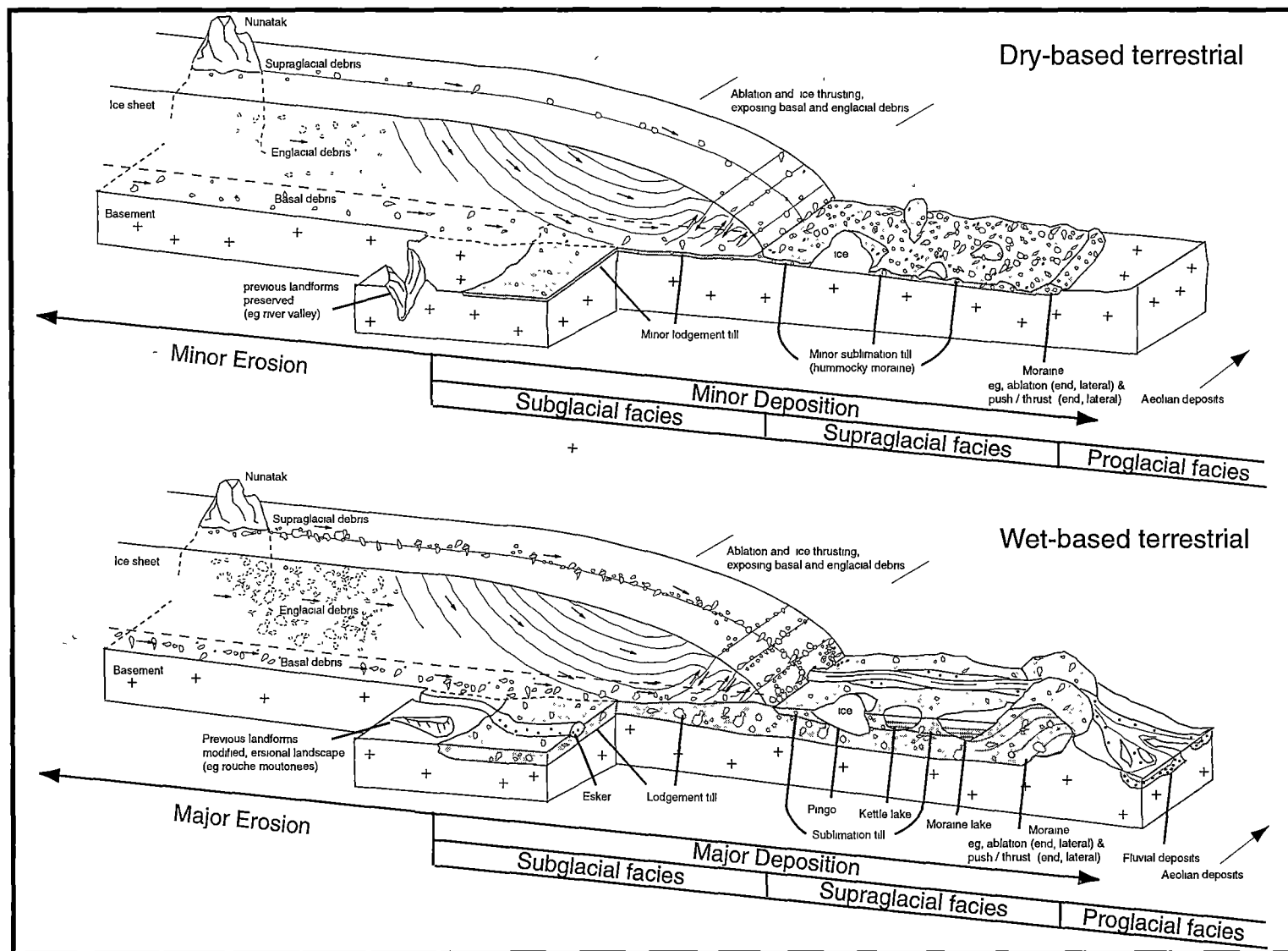


**Figure 13.** Terrestrial glacial facies (from information in Hambrey 1994; Menzies 1995; Benn and Evans 1998).

### 3.1.2 Glacial Marine Deposits

In this review, glacial marine deposits are categorised broadly as subglacial, sub-iceshelf and marine facies zones (Figure 14). Subglacial deposits are generally similar to those associated with terrestrial glaciation. As in the terrestrial setting, the wet-based glacial marine environment has higher terrigenous sediment input than dry-based glacial marine environments. For example, 200-2000 cm/yr of terrigenous sediment is deposited 1 km from the grounding line of a wet-based glacier in Alaska (Cowan and Powell 1991), whilst only ~2.1 mm/yr of terrigenous sediment is deposited Prydz Bay, 10 km from the Amery Ice Shelf edge (Domack *et al.* 1991). Meltwater streams in wet-based glacial marine environments deposit meltwater fans near the grounding line (Powell 1990), and the sediment laden meltwater plumes deposit sand and silts in more distal areas (Hambrey 1994). Coarse glacial debris is released as waterlain tills close to the grounding line and near ice cliff fronts through basal melting; frontal melting also occurs near the latter. If icebergs heavily influence the proximal marine environment, the release of ice rafted debris also deposits waterlain till here and the high terrigenous input dilutes the biogenic input.

The configuration of wet-based marine glaciers can differ from that illustrated in Figure 14. Meltwater streams may flow on the glacier's surface (Domack and Molnia 1983), and in some places the ice margins form a submarine wedge (in Domack and Molnia 1983) or restricted iceshelf (e.g. Glacier Bay, Alaska). The Alaskan example contrasts with Antarctica, where approximately 90% of the ice sheet flows into outlet glaciers (Sugden and John 1976), many of which flow into ice shelves that border approximately half of the continent's coastline (Fahnestock 1996). There is minor deposition beneath the ice shelves fed by cold-based glaciers (Domack and Harris 1998). Waterlain till, granulated sands and silts are deposited near the grounding line, due to basal melting of the ice shelf. Inland from the ice shelf edge, sediment is reworked beneath the shelf from the open marine environment by water current advection and gravity processes (Anderson *et al.* 1991; Domack and Harris 1998). However, the area between the grounding line deposits and reworked deposits near the ice shelf edge is starved of sediment (Kellogg and Kellogg 1988; Anderson *et al.* 1991; Domack and Harris 1998). Sediment deposition beyond the ice shelf edge is a mixture of terrigenous glacial sediment and biogenic ooze (10-60%) (Stockwell *et al.* 1991; Domack 1993; Harris *et al.* 1998). The terrigenous input comes largely from ice rafted debris (IRD) carried in icebergs (Goodell 1973) and there is a greater apparent concentration of IRD on and near the continental slope

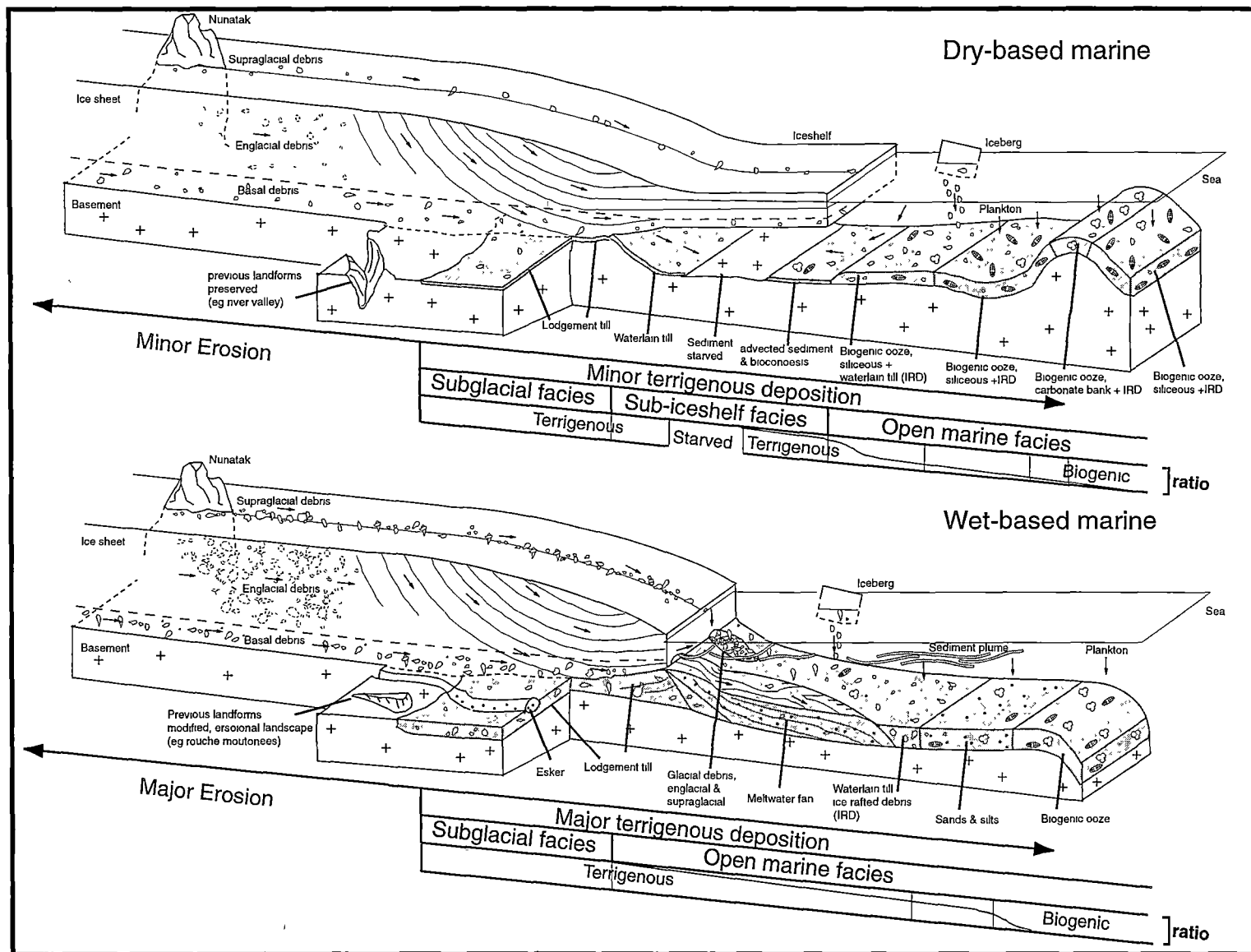


**Figure 14.** Marine glacial facies (from information in Anderson and Molnia 1989; Bryan 1993; Hambrey 1994; Menzies 1995; Benn and Evans 1998).

(Anderson *et al.* 1979; Leventer and Harwood 1993), which decreases markedly seaward of the shelf break (Anderson *et al.* 1980).

### **3.1.3 Antarctic Glacial Style**

Antarctica is the coldest place on earth, and one would expect all glaciers here to be dry-based. This is not always the case, however. The thickness of the ice and various basal heat sources can cause the base of the ice sheets to be at the pressure melting point. This can occur if the surface temperature is relatively high, snow accumulation is low, if there are geothermal heat sources, or if the ice flow velocities are high enough to produce frictional heat (Sugden and John 1976). Parts of the WAIS were found to be wet-based in ice cores from the Byrd Glacier (Gow *et al.* 1979), and a large lake ~14,000 km<sup>2</sup> has been found beneath the EAIS at Vostok (Ritz 1989; Muir 1996; Siegert and Ridley 1998). Areas of Antarctica where the basal ice is at melting point have been mapped by Budd *et al.* (1970, 1971) who identify basal ice melt beneath areas of the WAIS and EAIS. These results illustrate that basal melting occurs beneath the Amery Ice Shelf's tributary glaciers, suggesting that they are polythermal. The implications this has upon glacial erosion and deposition is not fully understood. Water at the base of the Amery Ice Shelf tributary glaciers could be causing basal slip, erosion and terrigenous sediment deposition, but terrigenous deposition rates in nearby Prydz Bay are low (Domack *et al.* 1991). This may reflect the large distance between the Amery Ice Shelf edge and the grounding zone, where deposition may be occurring; however, deposits associated with EAIS basal slip exposed in the Sør-Rondane Mountains are minor (Hasegawa *et al.* 1992). Polythermal-like glacial processes have also been described from recent glacial deposits in the Dry Valleys (Humphreys and Fitzsimons 1996). An alternative polythermal scenario can occur when the rocky areas around the Antarctic coast are heated by solar radiation, creating seasonal, partially wet-based conditions at shallow ice sheet depths, as observed in the Vestfold Hills (Fitzsimons 1990). This may have the potential to cause more erosion and deposition than characteristic Antarctic dry-based or cold-surfaced polythermal glaciers.

## **3.2 Antarctic Ice Sheet and Ice Shelf Stability**

Glaciers and ice sheets generally form at high elevations or in polar latitudes where snow accumulates and turns to ice at a faster rate than it is ablated (Bennett and Glasser 1996; Hooke 1998). Ablation describes all processes of ice removal, including melting, evaporation, sublimation, wind scouring, and iceberg calving (Benn and Evans 1998). Around Antarctica much ablation occurs through iceberg calving at ice shelf and ice cliff

edges (Benn and Evans 1998). Different areas of net ablation and accumulation divide glaciers and ice sheets into two zones: the accumulation zone and the ablation zone (Figure 15). The accumulation zone occurs over higher and colder regions of the ice sheet interior, where the rate of accumulation exceeds ablation, adding to the volume of ice. The ablation zone occurs at lower elevations near the ice sheet margin, where ablation exceeds accumulation (Benn and Evans 1998). The boundary between these, where accumulation equals ablation, is called the equilibrium line (Benn and Evans 1998). The size and shape of the ice sheet is dependent on the mass balance between accumulation and ablation, which is largely dependent on climate (Bennett and Glasser 1996).

Temperature is one of the major climate variables that affects glacial stability (Doake and Vaughan 1991). Temperature affects both the rates of accumulation and ablation through a combination of processes. The origin of Antarctica's ice is mostly snow from evaporation in the circum-antarctic marine environment. This is clearly visible in the accumulation rates over Antarctica, which decrease inland with distance from the marine source (Giovietto and Bentley 1985). Evaporation, and thus snow accumulation, increases with temperature (Huybrechts 1993). However, an increase in temperature also increases ablation, through melting and ice outflow as glacial stability declines (Warner and Budd 1998).

The effect of rising temperature on Antarctica's ice sheet mass balance has been modeled by numerous studies (e.g. Prentice *et al.* 1992; Huybrechts 1993; Warner and Budd 1998). If temperature were to increase continually, it would undoubtedly result in eventual ice sheet retreat and collapse. It has been estimated, however, that an initial increase  $<5^{\circ}\text{C}$  (Huybrechts 1993) could cause ice sheet growth, through increased marine evaporation and accumulation relative to ablation (Domack *et al.* 1991; Zwally 1994). As a result, sea-level can be lowered, initially, during warmer conditions, as may have occurred during past interglacials, due to increased snow accumulation on Antarctica (Kuijpers 1989). Further warming will cause ice sheet retreat and a global rise in sea-level, but increased accumulation would increase the relative height of the ice sheet (Huybrechts 1993). A rise of  $5^{\circ}$  to  $6^{\circ}\text{C}$  in mean air temperature may cause EAIS and WAIS reduction and grounding line retreat (Saari *et al.* 1987; Huybrechts and Oerlemans 1990; Huybrechts 1993). A global mean temperature rise of only  $3^{\circ}\text{C}$  (Warner and Budd 1998), and possibly a corresponding rise of  $10^{\circ}\text{C}$  in Antarctica, could cause WAIS collapse, whilst a rise of  $20^{\circ}\text{C}$  could cause complete EAIS disintegration (Huybrechts 1993). The effects of warming on Antarctic ice volume are illustrated in Figure 16.

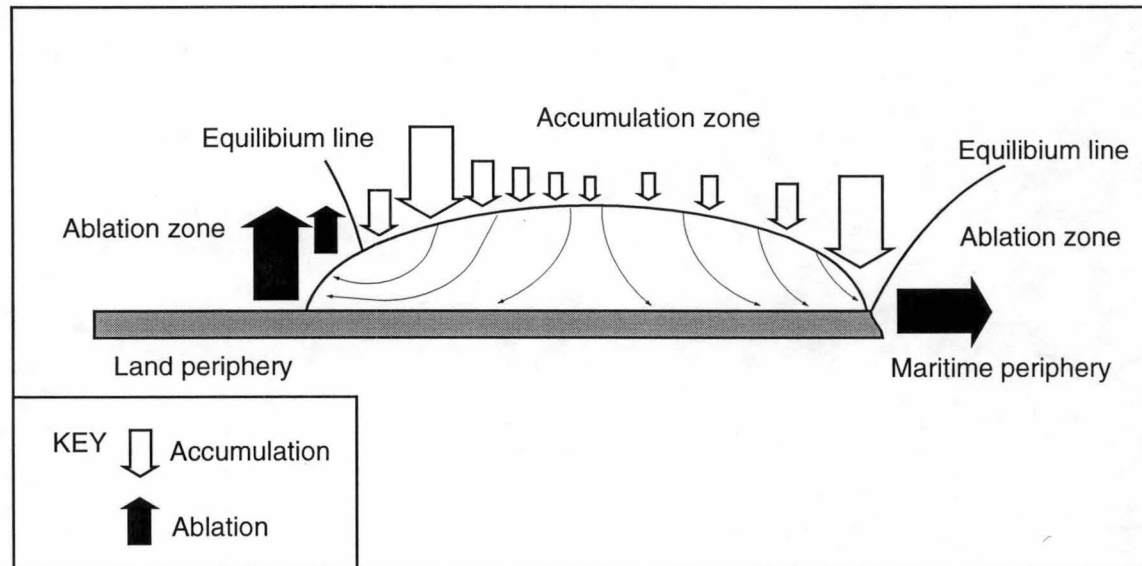


**Figure 15.** Ice sheet mass balance and variations in the position of the equilibrium line along land and sea peripheries (modified from Sugden and John 1976).



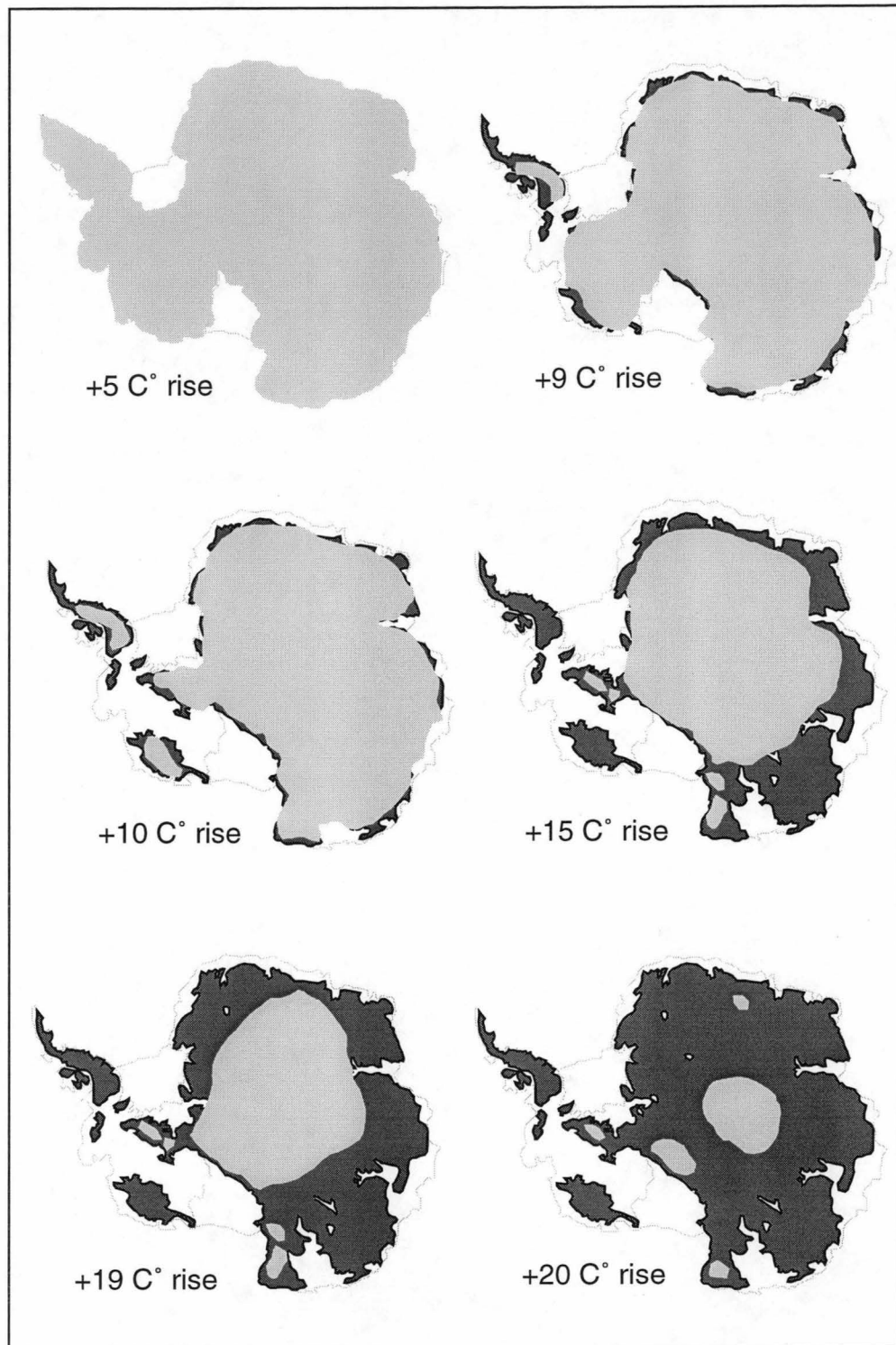


**Figure 16.** Ice sheet changes due to climatic warming  
(modified from Huybrechts 1993)

Temperature also affects ice shelf stability (Doake and Vaughan 1991). Although ice shelves border half of Antarctica, it is unclear what caused many of these to form and how stable they currently are (Fahnestock 1996). It appears that ice shelves do not occur where mean annual air temperature is  $>-4^{\circ}\text{C}$ , such as along the western side of the Antarctic Peninsula (Reynolds 1981; Fahnestock 1996). Temperature affects ice shelf stability, flow and structural integrity through varying input from tributary glaciers (Heidelberg *et al.* 1991), snow accumulation and ablation on their surface, and sea-water freezing and melting at their base and front (Thomas 1979). Warming causes extensive melting and fracturing (Fahnestock 1996), increased elasticity and reduced ice shelf thickness (Thomas 1979). Shear stress declines along the ice shelf margins (Huybrechts and Oerlemans 1990), and increases ice flow and ablation through iceberg calving (Thomas 1979). These affect the position of the ice shelf edge and can cause ice shelf collapse. Whilst the melting of ice shelves would not alter sea-level greatly, their collapse reduces the stability of tributary glaciers. The reduction in back-pressure, which the ice shelves exert upstream, increases the flow of ice from the continent and causes a larger sea-level rise (Thomas 1979). This process could cause rapid reduction of the WAIS if the Ross Ice Shelf collapsed and back-pressure was reduced on its tributary glaciers (Hooke 1998). The loss of tributary glacier stability is enhanced if the glacier grounds below sea-level (Alley and Whillans 1991), forming sea cliffs prone further to marine erosional processes (Anderson and Molnia 1989). Increased basal melting of ice shelves as they disappear, followed by increased strain rates in the thick floating ice near the grounding line, is considered the dominant process involved during the retreat of ice sheets grounding below sea-level (Warner and Budd 1998). Such considerations were neglected in earlier glacial models (e.g. Huybrechts 1993). It has been suggested that during a relatively small global mean temperature increase of  $3^{\circ}\text{C}$  an associated, albeit small, increase in sea-surface temperature could cause basal melting beneath Antarctic ice shelves (Warner and Budd 1998). This process may dominate the long-term response of the ice sheet, counteracting the effects of increased accumulation versus ablation, causing ice sheet retreat (Warner and Budd 1998).

The effect of temperature on sea-ice also influences ice shelf and ice cliff stability. It has been suggested that past EAIS reduction was assisted by the loss of sea-ice (Harwood *et al.* 1994) when SSST was between  $2^{\circ}$  and  $6^{\circ}\text{C}$  (Harwood 1986a). This is supported by modeling studies, which indicate that during an East Antarctic coastal mean air temperature of  $2^{\circ}\text{C}$ , there is a corresponding mean annual rise of  $17^{\circ}\text{C}$  over much of the continent, causing significant EAIS reduction (Prentice *et al.* 1992; Huybrechts 1993).

Temperature alone does not govern ice sheet stability and mass balance. It has been shown that Quaternary Antarctic ice volume has been influenced largely by global eustatic sea-level change (Clapperton and Sugden 1990; Huybrechts 1992), and less so by changes in accumulation and ablation (Huybrechts 1992). During the Quaternary, eustatic sea-level change was governed largely by glacial conditions in the Northern Hemisphere (Huybrechts 1990), causing Antarctic ice sheet grounding lines to move. A reduction in sea-level, for example, caused grounding lines to advance and ice to thicken in the peripheral areas of the ice sheet (Mabin 1990). In contrast, a sea-level rise caused grounding line retreat, but the amount of retreat depended on Antarctica's subglacial topography. A minor sea-level rise can easily float, or decouple, large areas of an ice sheet that grounds below sea-level, but has little affect on ice grounded above (Figure 17a) (Reading 1986; Menzies 1995). Ice sheet decoupling and grounding line retreat will essentially create an ice shelf that is less stable and more prone to marine erosion and basal melting. In response, ice volume declines as the ice sheet re-equilibrates to the new ice shelf conditions (Figure 17b) (Thomas 1979). This has considerable bearing on the WAIS, for example, which generally grounds 500-1200 m below sea-level. Furthermore, the subglacial topography beneath much of the WAIS slopes inland and forms basins (Key 1990). Catastrophic grounding line retreat can occur due to ice sheet decoupling over inland sloping basins, due to the lack of close areas within the new grounding line depths (Figure 17a) (Reading 1986; Menzies 1995).

The EAIS is considered more stable than the WAIS as it generally grounds above sea-level (Bentley 1997; Bindshadler and Bentley 1997) (Figure 2b), with a mean basal elevation of 15 m (Drewry *et al.* 1982). However, some areas, such as those below the Lambert Graben system, ground below sea-level (Figure 3). Part of the Lambert Graben slopes steeply inland and is covered by the Amery Ice Shelf. It is possible that interactions here, between sea-level and subglacial topography, since the Last Glacial Maximum (LGM) have caused catastrophic grounding line retreat. During the LGM, the Lambert Glacier grounded in Prydz Bay (Harris *et al.* 1997; Domack *et al.* 1998). Since the LGM, global mean air temperature has risen 4° to 5 C° (Tréguer 1994) and global sea-levels risen 150 m (Williams *et al.* 1998). The combined effects have probably decoupled the Lambert Glacier (Bindshadler 1998) and, combined with the inland, sloping subglacial topography, caused a dramatic grounding line retreat in excess of 500 km (calculated from Phillips *et al.* 1996; Krebs 1997, 1998) (Figure 18). In contrast, nearby areas of the East Antarctic coastal margin, where the EAIS does not cover deep subglacial

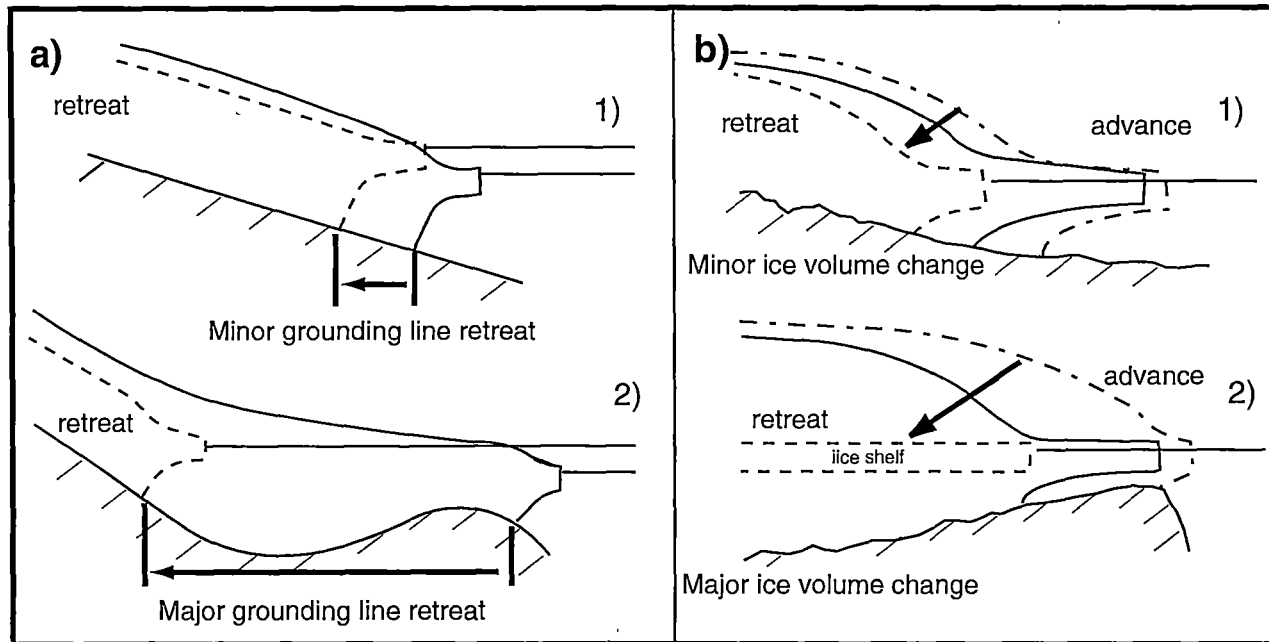


**Figure 17.** Minor and major (a) grounding line retreat and (b) ice volume changes due to the interaction of sea-level rise and subglacial topography (modified from Thomas 1979 and Reading 1986).

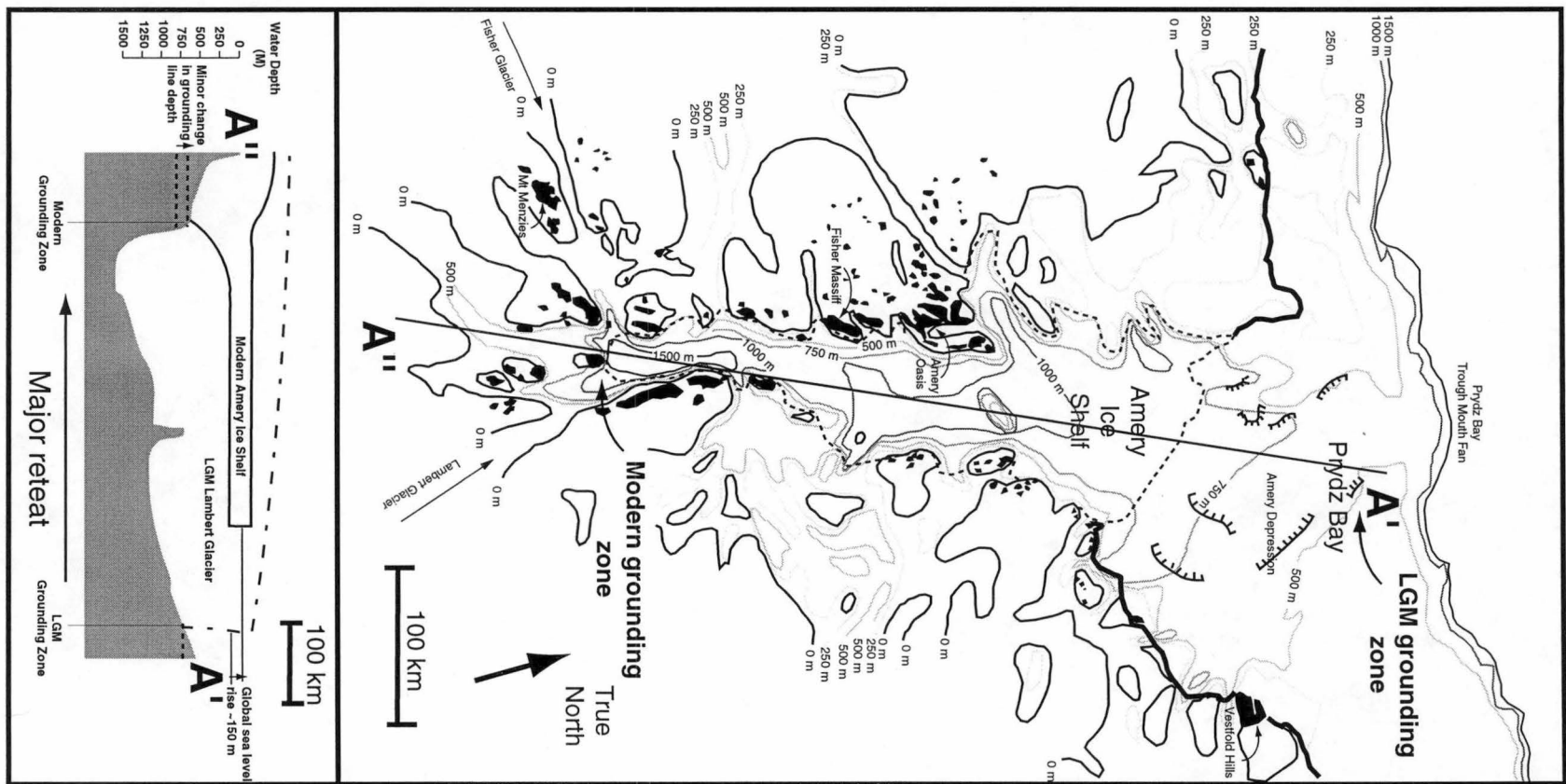


**Figure 18.** Catastrophic grounding line retreat in the Lambert Graben since the LGM, due to the interaction between the subglacial topography and eustatic sea-level rise (modified from Kurinin and Aleshkova 1987; Harris *et al.* 1997; and from text in Phillips *et al.* 1996; Krebs 1997, 1998; Williams *et al.* 1998).

embayments, have undergone smaller changes in grounding line position since the LGM. The coastal oases at Casey Station and the Vestfold Hills were ice covered during the LGM, beyond which the margin of the EAIS grounded at varying distances on the continental shelf (Colhoun 1991). However, parts of the Bunger Hills (Colhoun 1997) and the Larsemann Hills remained ice free (Burgess *et al.* 1994), and the ice margin has moved little since the LGM.

Northern Hemisphere glacial conditions have caused significant changes in Quaternary global sea-levels. If the current global warming trend were to melt all non-Antarctic glacial ice there would be a global sea-level rise of only 7.35 m (Warrick and Oerlemans 1990). This is considered sufficient, however, to decouple the WAIS and decrease its stability (Bindshadler 1998). If areas of the WAIS that ground below sea-level were to collapse, global sea-level would rise a further 5 m (IPCC 1990); complete WAIS collapse would cause yet another 2 m rise (calculated from Hooke 1998). Heating and expansion of the world's oceans would further increase sea-level (Meier 1984). Combined, these effects would result in a eustatic sea-level rise >14 m. A sea-level rise of ~50 m (Hooke 1998) to 66 m (calculated from Robin 1986) would occur if the EAIS were to collapse. During conditions warmer than the present, the influence of Northern Hemisphere glacial conditions on eustatic sea-level and Antarctic ice sheet grounding line position would decline. Changes in Antarctic ice volume, therefore, would be more dependent on local temperature, and its various effects on Antarctic accumulation and ablation.

## 4. Past Antarctic and Southern Environments

The Antarctic continent has not always been isolated geographically nor covered with an ice sheet. In the past, milder climatic conditions prevailed and the continent supported a variety of fauna and flora (Ashworth 1999). Numerous scientific techniques have been used to reconstruct Antarctica's palaeoenvironment. It is a complex history, however, as there are many alternative hypotheses consistent with the data. Numerous questions remain, for example, when did the first Cenozoic glaciers and ice sheets form? How stable were they? When did they change from wet-based to the prevailing dry-based glacial style? When did they become (if at all) relatively stable? The current views on Cenozoic climate are reviewed here, discussing the Antarctic (terrestrial) and Southern Ocean (ocean, sea-ice and coastal) environments.

### 4.1 Terrestrial Environments

Antarctic has remained close to the geographical south pole for the last 90 My, but a warmer climate prevailed for the first 60 My (Barrett 1996). The warmer climate was created by Antarctica's Gondwana connection, which caused the southerly circulation of warm equatorial waters to high southern latitudes (Robert and Maillott 1990). The southerly circulation was disrupted by continental drift, which opened the Drake Passage between Antarctica and South America, ~30 Ma (Oligocene). This altered the circulation of equatorial water (Mercer 1983; Kennett and Barker 1990; Robert and Maillott 1990) and caused climatic cooling. Cooling intensified as the Southern Ocean became larger and isolated Antarctica thermally ~24 Ma (Barker *et al.* 1988).

#### 4.1.1 East Antarctica

Cenozoic cooling of Antarctic climate may have caused glaciation in the middle Eocene (Wise *et al.* 1992). Early glaciers were probably restricted to mountainous regions of the Antarctic interior, where they are thought to have formed wet-based alpine glaciers (Drewry 1975; Wise *et al.* 1992; Huybrechts 1993).

Antarctic ice volume increased near the Eocene - Oligocene boundary. This is supported by a global shift in deep sea  $\delta^{18}\text{O}$  isotope data (Matthews and Poore 1980). The EAIS formed as alpine glaciers throughout East Antarctica joined progressively (Drewry 1975; Hambrey and Barrett 1993). The first ice sheet was considered to be thinner than that of today, and was temperate (wet-based) and capable of advancing easily across exposed

- areas of the East Antarctic craton and the shallow continental shelves (Anderson and Molnia 1989).

Early Oligocene tidewater glaciers flowed from the Transantarctic Mountains into the eastern Ross Sea, depositing glacial marine sediment evident in the CIROS-1 (Barrett 1989) and MSST-1 drill core sites (Harwood 1986a). In this region the early Oligocene glacial minimum was thought to have been restricted to tidewater - alpine glaciers on the Transantarctic Mountains. However, during glacial maxima the EAIS may have overridden the Transantarctic Mountains and grounded a short distance across the continental shelf in the Ross Sea (Hambrey and Barrett 1993). The EAIS also flowed down the Lambert Graben, into Prydz Bay, as the Lambert Glacier (Barker *et al.* 1998). The oldest glacial diamicts recovered from Prydz Bay were deposited between the middle Eocene to early Oligocene (ODP Site 739 and 742) (Hambrey *et al.* 1991, 1994). Seismic stratigraphy suggest that even older diamicts may be present, which could date back to the Cretaceous (Hambrey *et al.* 1994).

Throughout the late Oligocene – until the middle Miocene (36-14.8 Ma) the wet-based EAIS was highly variable and unstable (Barker *et al.* 1988; Flower and Kennett 1994). Across the Oligocene - Miocene boundary, deep sea  $\delta^{18}\text{O}$  isotope data suggest that Antarctic ice sheets fluctuated on a 40 kyr cycle, consistent with a Milankovitch orbital obliquity control on ice volume (Zachos *et al.* 1997). The EAIS remained unstable and wet-based until the middle Miocene (Barker *et al.* 1988; Flower and Kennett 1994), after which it expanded in a series of steps in the middle Miocene (14.5-14.1 Ma and 12.9-12.4 Ma). It is then thought to have become stable (Flower and Kennett 1994) with the development of arid polar desert and dry-based glacial conditions (Sugden 1992; Denton *et al.* 1993; Huybrechts 1993; Kennett and Hodell 1993). The ice sheet expanded again in the late Miocene (6.5-5 Ma), during which time it was thought to have exceeded its current size (Kennett 1978a; Kennett 1995). These interpretations are mostly based upon deep sea  $\delta^{18}\text{O}$  isotope data, and have been supported by other palaeoenvironmental evidence. For example, the subsequent cold conditions are thought to have preserved Miocene ice (>8.1 Ma) in the Transantarctic Mountains Dry Valleys (Cowen 1995; Sugden *et al.* 1995a). The landforms and deposits here are also thought to have experienced little erosion subsequent to the development of the current cold dry-based glacial and arid climatic conditions ~14 Ma (Sugden *et al.* 1995a, 1995b; Sugden 1996). This allowed the preservation of Miocene and Pliocene volcanic ash beds deposited throughout the region (Sugden 1992; Marchant *et al.* 1993a, 1993b, 1996). However, there have been problems



with K/Ar dating of some of these ash beds (Barrett *et al.* 1992) and it is possible that some of the beds are not *in situ* (Van der Wateren and Hindmarsh 1995). The lack of erosion in the Dry Valleys since the middle Miocene has also been questioned, as it fails to explain the source of Miocene and Pliocene glaciogenic sediment infilling the Dry Valleys and areas immediately offshore (Wilson 1995).

It is difficult to determine global and Antarctic ice volumes from pre-Pleistocene  $\delta^{18}\text{O}$  data (Prentice and Matthews 1991; Webb and Harwood 1991; Shackleton 1995; Bohaty and Harwood 1998). Global ice volume history from pre- 6 Ma deep sea  $\delta^{18}\text{O}$  data is poorly resolved as data sets are too few. The data suffer from low frequency artifacts (due to low frequency of sampling), low resolution in age constraint, distortion by higher frequency variations not considered in the low frequency of sampling, and errors created by dissolution and diagenesis (Denton *et al.* 1991). There are also problems separating ice volume from temperature signals during data interpretation (Kennett and Hodell 1995). These problems also affect Pliocene records to differing degrees. Early Pliocene shifts towards lower benthic  $\delta^{18}\text{O}$  values have been used to suggest reduced Antarctic ice volumes (Shackleton and Opdyke 1977). A similar change could also be explained by warmer deep waters (Shackleton 1995). It is expected, however, that deglaciation would be accompanied by warming of the deep water (Hodell and Venz 1992). Therefore, the  $\delta^{18}\text{O}$  signal would represent a combination of these influences and cannot be used to interpret both substantial Southern Ocean warming and major deglaciation (Kennett and Hodell 1995). In contrast, the ice sheet could remain stable, or even grow, through North Atlantic or Mediterranean warmer deep water flowing into the Southern Ocean (Shackleton 1995) increasing snow accumulation on Antarctica (Prentice and Matthews 1991).

Unconformities and sequence geometry on the Antarctic continental shelf suggest that major Miocene ice sheet expansion and retreat have occurred, through evidence from seismic data and sediment cores in Prydz Bay (Mackenson *et al.* 1992) and the Ross Sea (Anderson and Bartek 1992; Hambrey and Barrett 1993; Anderson 1994). More cores may be required to further validate the age of these unconformities in the Ross Sea (Barrett 1996). The EAIS may have remained unstable and wet-based / polythermal until the Plio-Pleistocene (Webb and Harwood 1991, 1993; Harwood *et al.* 1991; 1992; Moriwaki *et al.* 1992a; Wilson 1995). Some believe that during major Neogene EAIS retreat, East Antarctica subglacial basins were deglaciated and inundated by the sea. Marine sediments deposited in the Wilkes and Pensacola subglacial basins, during EAIS retreat, are thought by some (e.g. Harwood 1983; Harwood 1986a) to have been glacially eroded during later

wet-based EAIS advances. These advances deposited the Sirius Group throughout the Transantarctic Mountains and are thought to have transported marine sediment from the Wilkes and Pensacola Basins (Harwood 1983, 1986a, Harwood and Rose 1998; Harwood and Webb 1998). Furthermore, the Elephant Moraine in Southern Victoria Land has been found to contain debris from the Wilkes Basin, which has been recently aerally exposed on the ice sheet through ice thrusting and ablation (Faure and Harwood 1990). The Elephant Moraine and Sirius Group deposits contain diatoms and other microfossils of Lower Miocene, middle-Upper Miocene and Plio-Pleistocene age, suggesting that the EAIS retreated during these intervals (Webb *et al.* 1983, 1984; Faure and Harwood 1990; Harwood 1991).

Much debate surrounds the emplacement of the fossil diatoms from the Elephant Moraine and Sirius Group. It has been suggested that they are aeolian (Stroeve *et al.* 1996; Burckle *et al.* 1997), or resulted from a meteorite impact in the Southern Ocean, which deposited them over Antarctica as ejecta (Gersonde *et al.* 1997). Speculation therefore surrounds the age and palaeoenvironmental interpretation of these fossils, whilst their mode of emplacement continues to be the centre of debate (Harwood and Webb 1998; Stroeve *et al.* 1998). Nevertheless, *in situ* and glacially reworked diatoms and marine molluscs in siltstones and diamicts in the Pagodroma Group (Northern Prince Charles Mountains), indicate EAIS reduction during late Miocene and Pliocene marine incursions into the Lambert Graben, ~300 km and ~250 km inland from the current Amery Ice Shelf edge (Harwood in McKelvey and Stephenson 1990; Laiba and Pushina 1995, 1997). This suggests that the EAIS remained unstable after the Middle Miocene. The sedimentology of the Pagodroma Group also suggests that the glacial conditions were wet-based / polythermal (Hambrey and McKelvey 1995), in contrast with the dry-based glacial conditions suggested to have developed in the Dry Valleys during the middle Miocene (Sugden *et al.* 1995a, 1995b; Sugden 1996).

#### **4.1.2 West Antarctica**

Ice sheet models indicate that the WAIS developed under colder climatic conditions that followed the formation of the EAIS (Huybrechts 1993). It is widely accepted that the WAIS is a younger (Kerr 1981; Barrett 1982; Ciesielski *et al.* 1982; Flower and Kennett 1994), and less stable feature than the EAIS (Bentley 1997; Bindshadler and Bentley 1997), however, the timing of its development is unclear.

Research on the WAIS has been concentrated in the Ross Sea region, but here it is difficult to separate WAIS glacial evidence from localised glacial advance in the surrounding mountains. The WAIS may have formed in the earliest late Oligocene, when global ice volume, as interpreted from marine  $\delta^{18}\text{O}$  data, was 30% higher than today (Zachos *et al.* 1994). However, there are problems interpreting ice volume from such data, as discussed earlier. Grounding ice, identified from seismic data, occurred in the Ross Sea, during the mid to late Oligocene (Bartek *et al.* 1991; Anderson and Bartek 1992; Anderson 1994). It has been speculated, through the sedimentology of the CIROS-1 drillcore, that late Oligocene grounding ice in the Ross Sea originated from EAIS overriding the Transantarctic Mountains (Hambrey and Barrett 1993).

The Antarctic Peninsula was glaciated between the middle Eocene (~42 Ma) and mid Oligocene (~29.0 Ma to ~28.8 Ma) (Dingle *et al.* 1997). Outcrops on King George Island suggest that the climate began cooling dramatically in the late Oligocene to early Miocene (Birkenmajer 1987), with the development of a localised ice cap on the Antarctic Peninsula (Anderson and Molnia 1989). The ice cap eroded the surrounding continental shelf and deposited terrigenous turbidites on the adjacent continental rise (DSDP Site 325) (Tucholke *et al.* 1976). Seismic data from the Ross Sea suggest that the WAIS first formed in the early Miocene (Cooper *et al.* 1991; Anderson and Bartek 1992; Anderson 1994), and either reformed or expanded during intervals in the middle Miocene (Cooper *et al.* 1991; Anderson and Bartek 1992; Anderson 1994; Bartek *et al.* 1996; De Santis *et al.* 1997). These seismic ages have been extrapolated across the Ross Sea continental shelf from the few cores collected there, and the current age assignment may be inappropriate. For example, Miocene sediments recovered from the Ross Sea (CRP-1) were wrongly assigned an Oligocene (8 My older) age from seismic interpretation (Barrett *et al.* 1998), although the location was close to previous drill sites from which the age was extrapolated. Some claim the WAIS did not form until the late Miocene (Kerr 1981; Ciesielski *et al.* 1982; Barrett 1996) and therefore cores are required to validate the seismic interpretation of WAIS history (Barrett 1996).

Like the EAIS, the WAIS may have remained unstable during the Neogene. Glacially reworked fossils in sediment collected from beneath the modern Ross Ice Shelf identified that marine conditions occurred inland of the present ice shelf edge during the Miocene, 21-18 Ma, 16-14 Ma and 7.5-6 Ma (Brady and Martin 1979; Kellogg and Kellogg 1986; Scherer *et al.* 1988; Harwood *et al.* 1989). Further inland beneath the WAIS, at Upstream B, diatom evidence suggests middle and / or late Miocene and Pleistocene (~0.4 Ma)

marine deposition occurred during the absence of the WAIS (Scherer 1989; Scherer 1991; Scherer *et al.* 1998). Similar evidence for WAIS retreat occurs along the western margin of the ice sheet at Mount Murphy, where diatoms of early Miocene, middle Miocene, and possibly late Miocene and early Pliocene age occur in a siltstone outcrop thought to have been deposited during glacial reworking (LeMasurier *et al.* 1994).

Terrestrial higher plants possibly lived in Antarctica until, or during, the late Pliocene. Fossilised remains (leaves, wood and pollen) of *Nothofagus beardmorensis* Hill, Harwood *et al.* Webb have been found in the Sirius Group, Transantarctic Mountains (Carlquist 1987; Webb and Harwood 1987; Webb *et al.* 1987; Hill and Truswell 1993; Webb and Harwood 1993; Hill *et al.* 1996). *In situ* well-preserved leaves were found at Oliver Bluffs in the Transantarctic Mountains (Hill and Truswell 1993). The climatic implications of *Nothofagus* growing here depend upon the age interpretation of the Sirius Group deposits upon which they grew. If the diatoms in this deposit are glacially, as opposed to aeolian, reworked, they suggest that *Nothofagus* was growing here <3.8 Ma (Hill *et al.* 1996).

*Nothofagidites* pollen has also been found in reliably-dated Pliocene marine sediments in the Ross Sea (DSDP Site 274), in sufficient quantities to support strongly the hypothesis that *Nothofagus* was living in Antarctica during this time (Fleming and Barron 1994, 1996). The diversity and divergent forms of organisms (fish, insects and moss) found in association with this vegetation suggest that they are a remnant, as opposed to a reintroduced flora and fauna (Ashworth 1999). The possibility of this vegetation persisting in Antarctica until the Pliocene (Hill and Truswell 1993) raises questions about the likelihood of ice sheet expansion and the formation of cold, arid, climatic conditions in the middle Miocene. However, alternative evidence for global sea-level highstands suggest major Antarctic ice sheet fluctuations continued to occur in the Neogene (Haq *et al.* 1987; Krantz 1991; Wardlaw and Quinn 1991; Miller *et al.* 1996).

The interval 2.6 Ma is associated with a global change in climate and the onset of bipolar glaciation (Morrison and Kukla 1998). This climate change is thought to have altered dramatically Antarctic erosion and sedimentation by causing a change from warm, wet-based / polythermal to the colder, dry-based glacial conditions that now prevail (Webb and Harwood 1991, 1993; Harwood *et al.* 1991, 1992; Moriwaki *et al.* 1992a; Wilson 1995). This contrasts to the middle Miocene age given for this change in glacial style (e.g. Sugden *et al.* 1995a, 1995b; Sugden 1996). However, warmer Pleistocene episodes have

also been identified (Scherer 1991; Barrett *et al.* 1998; Scherer *et al.* 1998; Bohaty *et al.* 1998), during which Antarctica's glacial conditions may have been periodically warmer.

## **4.2 Marine Environments**

### **4.2.1 Southern Ocean**

The Southern Ocean first formed with the separation of Gondwana and opening of Drake Passage between Antarctica and South America, ~30 Ma (Mercer 1983). The formation of Drake Passage altered ocean circulation and caused Antarctic cooling (Kennett 1980). As continental drift continued to enlarge the Southern Ocean, the ACC and associated ocean fronts formed by 25-22 Ma (late Oligocene) and the Antarctic continent became thermally isolated by ~24 Ma (Kennett 1977; Kennett 1978b).

The ACC had intensified by the early Miocene developing into ocean fronts and zones comparable with those of today (Kennett 1978b). Climate changes during this time caused fluctuation in the ACC velocity, ocean front positions and environmental gradients (in salinity and temperature) across these fronts. During glacial intervals the ACC increased in velocity (Ciesielski *et al.* 1982), ocean fronts moved northwards, and / or the environmental gradient across these steepened (Bohaty and Harwood 1998). In contrast, during interglacials the ACC become slower, the ocean fronts migrated southwards and / or their environmental gradients weakened.

It is unclear whether oceanographic conditions in the Southern Ocean during the Neogene remained relatively stable or fluctuated. However, accumulating evidence indicates that the ACC velocity, ocean front and environmental gradients across the Southern Ocean have changed greatly during the Neogene. Changes in ACC velocity have altered deposition rates, creating hiatuses and drift deposits on the Maurice Ewing Bank (Ciesielski and Wise 1977; Ciesielski *et al.* 1982), Barker Ridge (Barker 1977) and the Kerguelen Plateau (Bohaty and Harwood 1998). The ACC velocity increased in the late Miocene (11 - 5.3 Ma), Pliocene (4 Ma) and Pleistocene (1 Ma), causing erosion on the Maurice Ewing Bank between intervals of lower ACC velocity and deposition (Ciesielski *et al.* 1982). Ocean fronts in the Southern Ocean have also moved, causing the migration of microfossil assemblages (Ciesielski and Grinstead 1986; Barron 1996) and biogenic facies (Ciesielski *et al.* 1982). For example, during the late Miocene (6.5 - 5 Ma) the Antarctic Polar Front Zone (APFZ) is interpreted to have migrated ~300 km north of its current position (Kennett 1978b). The decreasing water temperature around Antarctica

also caused a change in the dominant biogenic sedimentation, from calcareous coccoliths and foraminifera to siliceous diatom ooze (Kennett and Hodell 1993). In contrast, during the Pliocene the APFZ either migrated ~900 km south of its current position or the environmental gradient across the associated fronts weakened ~4.5 Ma, ~4.3 Ma and ~3.6 Ma, (Bohaty and Harwood 1998).

The onset of bipolar glaciation at 2.6 Ma (Morrison and Kukla 1998) greatly changed oceanographic conditions (Hodell and Ciesielski 1990). There have been intense cold periods during the Pleistocene. The high degree of erosion on the Maurice Ewing Bank at 1 Ma suggests that this is when the ACC attained its highest velocities (Ciesielski *et al.* 1982). Ocean front positions have also fluctuated throughout the Quaternary, during glacial and interglacials (Westall and Fenner 1990). There has been at least one interval of Pleistocene warming, during which the APFZ either migrated some distance south of its current position or the environmental gradient across the associated fronts significantly weakened (Abelmann *et al.* 1990; Westall and Fenner 1990; Barrett *et al.* 1998).

#### 4.2.2 Sea-ice

Like today, past sea-ice conditions were very sensitive to climate (Cooke and Hays 1982). Sea-ice may have first formed around Antarctica at 36.5 Ma (Eocene - Oligocene boundary) with the initial cooling of the Antarctic climate (Mackenson and Ehrmann 1992). Evidence for continued climatic cooling in the early Oligocene indirectly supports the presence of Antarctic sea-ice (Kennett and Stott 1990). Limited sea-ice formation at this time is thought to have produced a water mass similar to AABW (Benson 1975; Barker *et al.* 1988), as indicated in oxygen isotope data (Frakes and Crowell 1975).

Changing sea-ice conditions during the Cenozoic would have been greatly affected by climate change. Extant diatom assemblages deposited in the marine environment have been used to reconstruct past sea-ice conditions. Reduced sea-ice intervals in the Neogene have been identified from the low abundance of extant sea-ice associated diatoms (Abelmann *et al.* 1990; McMinn and Harwood 1995; Winter and Harwood 1997; Bohaty *et al.* 1998). Other studies have used the southerly migration of more northerly extant microfossils to illustrate warmer water (Ciesielski and Weaver 1974; Bohaty and Harwood 1998), and reduced sea-ice conditions around Antarctica (Abelmann *et al.* 1990). Other palaeotemperature proxies have been used to indicate past climatic warming and reduced sea-ice conditions. For example,  $\delta^{18}\text{O}$  measurement on an early Pliocene (~5.5 Ma) marine mollusc, *Chlamys tuftsensis* Turner, from the Dry Valleys indicate that the mean

annual sea-surface temperature was 3°C (Prentice *et al.* 1992). Similar measurements on early Pliocene (4.5-4.1 Ma) (Harwood *et al.* in press) samples from the Vestfold Hills, suggest that the mean annual sea-surface temperature could have been as high as 10.5°C (Quilty 1991). The absence of sea-ice here was supported by the general lack of ice rafted debris (Quilty 1993) and the occurrence of dolphin fossils that would have lived in a sea-ice free environment (Quilty 1992, 1993). Other fossil data from the Transantarctic Mountains also suggest reduced sea-ice conditions during intervals in the Neogene. The possible uninterrupted occurrence of *N. beardmorensis* vegetation in the Transantarctic Mountains until <3.8 Ma would have required temperatures as high as 5°C for at least 3 months of the year (Hill and Truswell 1993), which would have inhibited sea-ice formation.

#### 4.2.3 Coastal

Antarctic coastal and continental shelf environments are heavily influenced by glacial and climatic conditions. These influence water temperature, salinity, sea-ice, light, nutrient, and the style and rate of deposition and erosion. During extreme glacial advances in the past, grounding ice sheets covered coastal and continental shelf environments.

The history of Antarctica's coasts and continental shelves is incomplete and occasionally conflicting. Past EAIS expansions initially grounded at localised areas around the Antarctic continental shelf. This occurred in Prydz Bay during the Eocene-early Oligocene (Hambrey *et al.* 1991), in the Ross Sea during the mid to late Oligocene (Bartek *et al.* 1991), and the eastern Weddell Sea after the Oligocene (Barker *et al.* 1999).

During the late Oligocene and until the middle Miocene the EAIS advanced and retreated backward and forward across the continental shelf, eroding a rugged and fore-deepened topography (Anderson and Molnia 1989). Wherever the ice reached the shelf break eroded sediment was pushed over the slope, causing the seaward progradational of the continental shelf (Hambrey *et al.* 1991; Barker *et al.* in 1999). This process continued in the Lambert Graben and Prydz Bay, through much of the Neogene and Quaternary, forming the Prydz Bay Trough Mouth Fan on the shelf slope (Cooper *et al.* 1991; Hambrey *et al.* 1991; Leitchenkov *et al.* 1994; O'Brien and Harris 1995; Barker *et al.* 1998).

It is unclear when the first major Antarctic ice sheet grounded continuously around the continental shelf break. Grounding possibly occurred in the Middle Miocene (Kennett

1977, 1978a, 1978b, 1978c) or late Miocene (Flower and Kennett 1994; Kennett 1995; Zachos *et al.* 1997). It is even possible that it did not occur until after the late Pliocene, enabling the survival of *N. beardmorensis* in the Transantarctic Mountains. Nevertheless, there have been numerous times when the Antarctic ice sheets have grounded at the continental shelf edge around Antarctica (Anderson and Molnia 1989). Whenever this occurred, it completely covered shallow coastal areas beneath glacial ice, and severely disturbed Antarctic benthic communities. The most recent of these events occurred in the late Pleistocene (Anderson and Molnia 1989), but not during the Last Glacial Maximum (Burgess *et al.* 1994; Colhoun 1997; Domack *et al.* 1998).



## 5. Diatoms

### 5.1 Diatom Biology

Diatoms (Division: Bacillariophyceae) are unicellular, golden brown algae that live in the euphotic zone (generally <100 m) of almost all aquatic habitats. They have characteristic box-like cell walls (frustules), consisting of hydrated, amorphous silica, and range in size from 1 µm - 1000 µm (Barron 1985). The frustules are highly ornate and their taxonomy is based upon this and their shape (Medlin and Priddle 1990).

Diatoms have various modes of lifestyle, occurring as single cells or in colonies, and are either planktic or benthic (Round *et al.* 1990). Planktic diatoms are dispersed passively by ocean currents. They sometimes have adaptations that promote flotation, such as a lightly silicified frustules, extended strutted processes or spines, colony formation, or fat and oil stores in the cell (Barron 1993). Benthic diatoms grow on substrates within euphotic depths in streams, lakes and around coastal areas on rocks (epilithic), sand grains (epipsammic), silts (epipelagic), and plants (epiphytic) (Round 1981). Benthic diatoms can also live on animals (epizoic) (Round 1981), and sea-ice substrates (cryophilic).

Diatoms occur either as photosynthetic autotrophs, colourless heterotrophs or photosynthetic symbiotes (Schmaljohann and Röttger 1978). Most gain energy through photosynthesis, using sunlight, water and dissolved carbon dioxide (Lee 1989). Macro- and micro-nutrients are also essential for both diatom growth and function. Nutrients are obtained from the water column by active absorption through areolae (pores) into the cell (Harris 1986; Round *et al.* 1990). The macro-nutrients essential for plant growth are C, N, P, H, O, and S (Weier *et al.* 1982; Salisbury and Ross 1985; Raven *et al.* 1986). Diatoms also have a requirement for silica, which is used in the cell wall. Diatom cells take up silica actively in the form of monosilicic acid,  $\text{Si}(\text{OH})_3\text{O}^-$  (Riedel and Nelson 1985). When essential nutrients other than silica are limiting, diatoms cease to divide, but continue to uptake silica, creating heavily silicified frustules (Lewin 1957). When cell division rates are high, competition for silica decreases its availability and the frustules tend to be less silicified (Lewin 1957; Lee 1989). Micro-nutrients consist of the trace elements Cu, Zn, Mo, Mn, Mg, Co, Ca, Fe, B, Na, Cl, V, and vitamins that are required by plants in small quantities for successful growth (Tootill 1984). Most diatoms do not require vitamins (Laws 1984), and the trace element copper (Cu) adversely affects diatom silicon metabolism (Thomas *et al.* 1980). Nevertheless, the most productive regions in the

Southern Ocean are areas of upwelling, mixing in shallow waters, and divergent zones in deep water, where there is a large micro-nutrient supply (Laws 1984).

Traditionally Southern Ocean nutrient concentrations were not considered limiting to algal growth and function (Dieckmann *et al.* 1991; Nelson and Tréguer 1992). However, iron, which is used by algae in the production of chlorophyll, may be low enough to limit algal growth (Martin *et al.* 1991). Silica can also become limiting when depleted by diatom blooms, causing a shift in community structure from diatoms to non-siliceous phytoflagellates (McMinn and Hodgson 1993).

## **5.2 Modern Antarctic and Southern Ocean Diatom Assemblages**

Diatoms are the main primary producer throughout much of the Southern Ocean (Knox 1990). Their distribution is influenced by a variety of environmental variables, such as nutrient availability, light, temperature, salinity, sea-ice and water column stability (Smith and Nelson 1986). Only a small percentage of the living assemblage is preserved in the fossil record, due mostly to silica dissolution in the water column, as will be discussed in Chapter 5.4.2. Assemblages can be identified in surficial sediment studies throughout the Southern Ocean (Kozlova and Mukhina 1967; Abbott 1974; Truesdale and Kellogg 1979; DeFelice and Wise 1981; Pichon *et al.* 1987; Taylor *et al.* 1997).

Southern Ocean diatoms are mostly endemic circum-antarctic in distribution and, to a lesser degree, bipolar and cosmopolitan (Priddle 1990). From a review of the surficial sedimentary diatom distributions, four diatom assemblages can be identified in the Southern Ocean (Table 1). Three assemblages are oceanic (two are open water associated), and the other sea-ice associated. The fourth assemblage occurs in coastal regions and in Antarctic lakes.

**Table 1.** Abundant species and genera that characterise the four Southern Ocean diatom assemblages.

<b>Assemblage 1</b>	Citations	<b>Assemblage 2</b>	Citations
<b>Subantarctic</b>		<b>Antarctic Open Water</b>	
<i>Thalassionema nitzschioides</i> (group)	4, 5	<i>Fragilariopsis kerguelensis</i>	1, 2, 3, 4, 6, 8
<i>Roperia tessellata</i>	3, 4, 5	<i>Thalassiosira lentiginosa</i>	1, 2, 4, 6
<i>Roperia tessellata</i> var. <i>coscinodiscoides</i>	2	<i>Thalassiothrix</i> sp.	4
<i>Hemidiscus cuneiformis</i>	2, 3, 4, 5	<i>Thalassiothrix antarctica</i>	1, 2
<i>Fragilariopsis doliolus</i>	2, 3, 5	<i>Thalassiosira gracilis</i>	1, 4
<i>Nitzschia sicula</i> var. <i>rostrata</i>	2	<i>Thalassiosira gracilis</i> var. <i>expecta</i>	6
<i>Azpetia nodulifer</i>	2	<i>Eucampia antarctica</i>	2
<i>Azpetia tabularis</i>	4	<i>Trichotoxin reinboldii</i>	6
<i>Thalassiosira lentiginosa</i>	4		
<i>Eucampia antarctica</i> var. <i>antarctica</i>	9		
<b>Assemblage 3</b>	Citations	<b>Assemblage 4</b>	Citations
<b>Sea-ice</b>		<b>Coastal and lake</b>	
<i>Fragilariopsis curta</i>	1, 4, 5, 6, 7, 8	<i>Achnanthes</i> spp.	10, 11, 12, 13, 14, 15, 16, 17
<i>Eucampia antarctica</i>	1, 4	<i>Amphora</i> spp.	10, 11, 12, 13, 14, 15, 16, 17
<i>Eucampia antarctica</i> var. <i>recta</i>	9	<i>Anaulus</i> sp.	15
<i>Fragilariopsis sublineata</i>	4	<i>Cocconeis</i> spp.	10, 11, 12, 13, 14, 15, 16, 17
<i>Actinocyclus actinochilus</i>	4, 5	<i>Diploneis</i> spp.	11, 12, 15
<i>Fragilariopsis cylindrus</i>	4, 5, 6, 7, 8	<i>Fragilaria</i> spp.	10, 11, 12, 13, 14, 17
<i>Porosira gracilis</i>	5	<i>Hantzschia</i> sp.	10, 11, 13, 14
<i>Porosira turgiduloides</i>	5	<i>Gomphonema</i> sp.	17
<i>Simonseniella alata</i>	5	<i>Gomphonemopsis</i> spp.	11
<i>Stellarima microtrias</i>	5	<i>Gyrosigma</i> spp.	11, 12, 15, 17
<i>Porosira psuedodenticulata</i>	5	<i>Navicula</i> spp.	10, 11, 12, 13, 15, 16, 17
<i>Psuedo-nitzschia turgiduloides</i>	5, 6	<i>Pinnularia</i> spp.	10, 11, 12, 13, 14, 15, 17
<i>Fragilariopsis sublinearis</i>	5	<i>Pluerosigma</i> spp.	11, 12, 17
<i>Fragilariopsis obliquecostata</i>	5	<i>Porosira</i> sp.	11
<i>Fragilariopsis rhombica</i>	6	<i>Stauroforma</i> sp.	11, 13
		<i>Stauroneis</i> spp.	10, 11, 13, 17
		<i>Synedra</i> spp.	11, 12, 15, 16
		<i>Trachyneis</i> sp.	10, 11, 12, 13, 14, 15
		<i>Trigonium</i> sp.	12, 15
		<i>Tryblionella</i> sp.	10, 11, 12, 13, 14

#### References

- 1 (Kozlova and Mukhina 1967), 2 (Abbott 1974), 3 (DeFelice and Wise 1981), 4 (Pichon *et al.* 1987), 5 (Zielinski and Gersonde 1997), 6 (Taylor *et al.* 1997), 7 (Stockwell *et al.* 1991), 8 (Leventer 1992), 9 (Fryxell 1991), 10 (Roberts and McMinn 1996), 12 (Whitehead and McMinn 1997), 13 (Roberts and McMinn 1998), 14 (Roberts and McMinn 1997), 15 (Krebs 1977), 16 (Krebs 1983), 17 (Wasell and Håkansson 1992)

The three major oceanic diatom assemblages (Abbott 1974; Pichon *et al.* 1987) south of the STF these have been called:

- 1) Temperate (Kozlova and Mukhina 1967), Subtropical (Abbott 1974), assemblage C (DeFelice and Wise 1981), or the Subantarctic (Pichon *et al.* 1987) assemblage.
- 2) Subantarctic (Kozlova and Mukhina 1967; Abbott 1974), factor assemblage 4 (Truesdale and Kellogg 1979), assemblage A (DeFelice and Wise 1981), open ocean Antarctic (Pichon *et al.* 1987), or the oceanic (Taylor *et al.* 1997) assemblage.
- 3) Antarctic (Kozlova and Mukhina 1967; Abbott 1974), factor assemblage 1 (Truesdale and Kellogg 1979), assemblage B (DeFelice and Wise 1981), South Weddell (Pichon *et al.* 1987), or the shelf and coastal (Taylor *et al.* 1997) assemblage, which is sea-ice associated.

Given the inconsistencies in the nomenclature of these assemblages, they are hereafter referred to as: 1) Subantarctic, 2) Antarctic open water, 3) sea-ice associated, and 4) coastal assemblages. These are optimal within specific environmental ranges, and their biogeography is dependent on oceanographic and sea-ice conditions (Pichon *et al.* 1987).

The Subantarctic and Antarctic assemblages are separated by an ocean front. South of Australia the front is centered over the mid-oceanic ridge (Abbott 1974), where the summer sea-surface temperature is 7°C (Pichon *et al.* 1987), near the lower range of the SAF. Steep temperature and salinity gradients across the SAF separate lower and higher latitude diatoms into two distinctive open ocean assemblages. The APF also acts as a similar barrier, but physical changes across this front are not as steep as across the SAF (in Gordon and Molinelli 1982). However, the APF is often used to delineate a major change in sedimentary diatom assemblages (DeFelice and Wise 1981; Pichon *et al.* 1987). Therefore, it is unclear which oceanographic front corresponds with this change observed in sedimentological studies. The assemblage changes through ocean zones are more gradual where the environmental gradients are less steep (Pichon *et al.* 1987). The southern range of the Antarctic open ocean assemblage seasonally shifts with the sea-ice edge through the SIZ and CCSZ. This borders the third planktic Southern Ocean diatom assemblage, which is sea-ice associated.

The third Southern Ocean diatom assemblage consists of sea-ice associated species. Sea-ice supports cryophilic diatoms, which are often benthic in and upon the sea-ice substrate. Many are also planktic in the surrounding water column, being released as the sea-ice melts and contributing to algal blooms (Garrison and Buck 1985). Sea-ice is a complex

habitat that varies seasonally (Nicol and Allison 1997) and supports much variation in the cryophilic diatom assemblage (Whitaker and Richardson 1980; Cunningham 1997; Nicol and Allison 1997). Habitat and assemblage variations occur between coastal sea-ice ponds (Whitaker and Richardson 1980), fast-ice (Krebs 1983; Scott *et al.* 1994; McMinn 1994), perennial and annual sea-ice (Hasle and Syversten 1985), pack-ice (Scott *et al.* 1994), sea-ice edges (Kang and Fryxell 1992; Scharek *et al.* 1994), and differing sea-ice coverage, internal ice structure (Horner 1990) (Figure 19), stages of development (Scott *et al.* 1994) and decay (Horner 1990). Nevertheless, some diatoms occur in most sea-ice habitats, and characterise the sea-ice sediment assemblage.

The fourth Southern Ocean diatom assemblage occurs around rocky coastal areas and in Antarctic Lakes. Shallow aquatic habitats within euphotic water depths support sea-floor benthic diatoms (Krebs 1983; Whitehead and McMinn 1997; Roberts and McMinn 1996). These diatoms are benthic on rock, sediment, plant and animal substrates (Round *et al.* 1990). Although biogeographical differences in species around Antarctica have not been identified, recent speciation (during the last 10 000 years) may be occurring in isolated lake environments around the Antarctic margin, with the identification of new lake species (Roberts and McMinn 1999). In coastal marine areas the substrate type and light conditions cause assemblage variations (Whitehead and McMinn 1997). Assemblage variations also occur in lakes due to salinity differences (Roberts and McMinn 1996).

## **5.3 Past Antarctic and Southern Ocean Diatoms**

### **5.3.1 Diatom Evolution**

Climate changes in Antarctica and the Southern Ocean during the Cenozoic have had a major influence on diatom evolution (Burckle and Abrams 1986; Harwood 1991). These changes are identified in the diatom biostratigraphy of the Southern Ocean (Abbott 1974; McCollum 1975; Gombos 1977; Schrader 1976; Weaver and Gombos 1981; Ciesielski 1983; Gombos and Ciesielski 1983; Fenner 1984; Harwood 1986b; Gersonde *et al.* 1990; Gersonde and Burckle 1990; Baldauf and Barron 1991; Fenner 1991; Harwood and Maruyama 1992; Winter and Harwood 1997; Gersonde and Bárcena 1998; Bohaty *et al.* 1998). Whilst most biostratigraphic studies have not attempted to explain the evolutionary theory or processes driving Southern Ocean diatom evolution, Barron and Baldauf (1995) identified a general trend towards increasingly less-silicified frustules through the Cenozoic, which they link to silica competition.

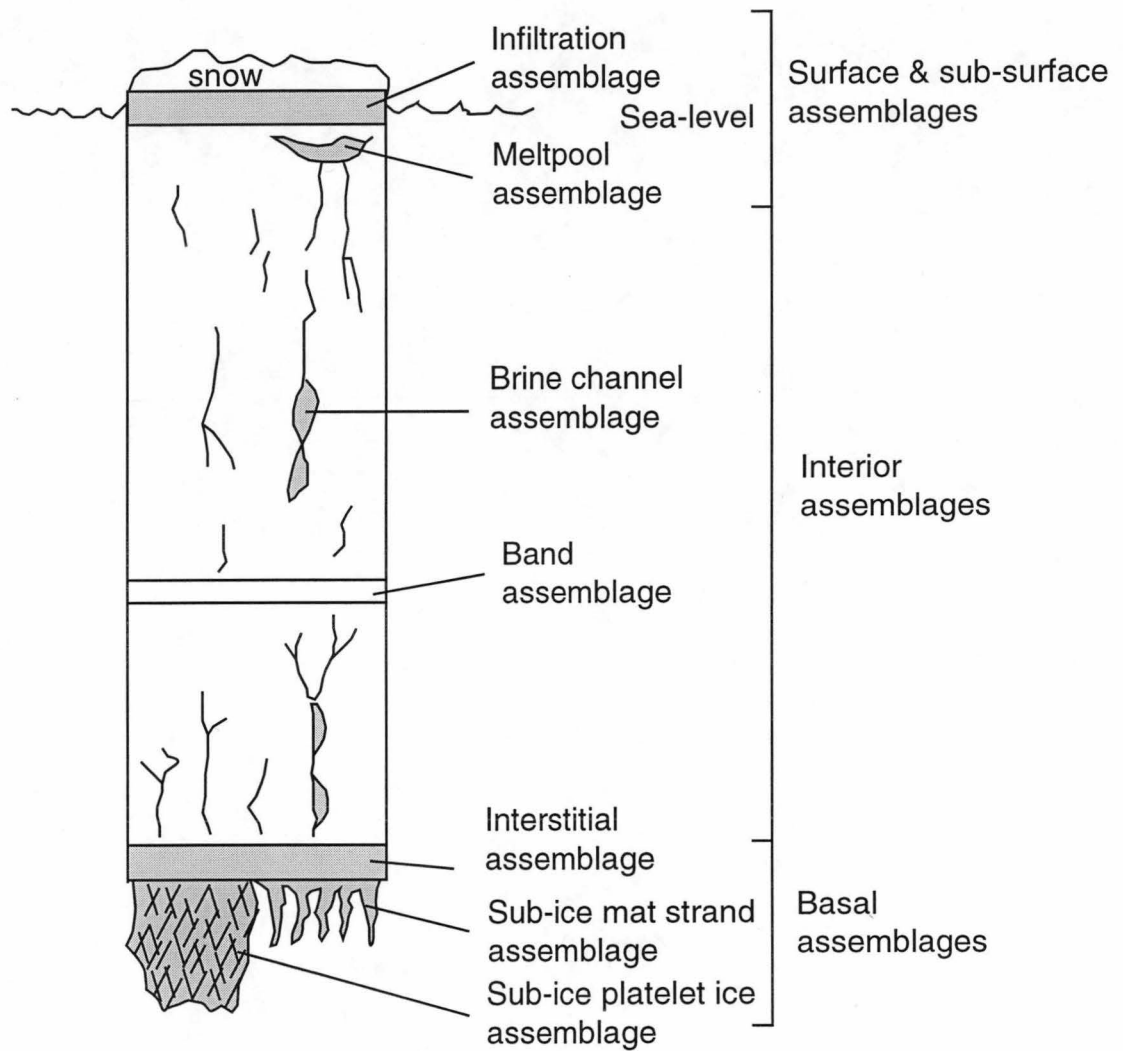


**Figure 19.** Diatom communities within sea-ice (modified from Knox 1994, after Horner *et al.* 1988).

There is no evidence for mass diatom extinction in the Cenozoic (Barron and Baldauf 1995). Episodes of rapid evolutionary change have been recognised, however, in the early Eocene - middle Eocene, at the Oligocene - Miocene boundary, early middle Miocene, late Miocene, and late Pliocene (Strelnikova 1990, 1991; Barron 1992; Baldauf 1993; Barron and Baldauf 1995). The changes are associated with periods of major, and rapid, climatic cooling at high latitudes, or with a major reorganisation of the ocean's surface water circulation due to changes in oceanic gateways (Barron and Baldauf 1995). During the Neogene, reduced glacial conditions may have also provided deglaciated, Antarctic inland marine basins with unique environmental conditions in which diatoms could have further evolved (Harwood 1991). A major Southern Ocean biostratigraphic change in the late Pliocene (2.6-2.4 Ma) has been associated with the onset of bipolar glaciation (Burckle and Abrams 1986; Harwood 1991; Barron 1992).

### **5.3.2 Diatom Biostratigraphy**

The most widespread Southern Ocean diatoms are planktic (Barron 1993) and cryophilic species. They are easily age constrained and their biostratigraphy is reasonably well established. This is not the case for more geographically restricted sea-floor benthics, however, which are generally limited to coastal sediments that have been poorly preserved around Antarctica.

The evolution and extinction of diatoms is identified by their first and last appearance in the geological record. The timing of these events is calculated from their association with other microfossil, magnetostratigraphic and isotope age controls from similar intervals within the record. A constant deposition rate is also generally assumed between the intervening dated intervals within the record, from which the diatom datums are extrapolated (e.g. Schrader 1976; Gersonde *et al.* 1990; Gersonde and Burckle 1990; Fenner 1991). Diachronous changes between the Southern Ocean and Antarctic shelf have been noted (Harwood and Maruyama 1992). These were identified by comparisons of Southern Ocean and Kerguelen Plateau cores (ODP Leg 120) (Harwood and Maruyama 1992) to coastal biostratigraphy from the eastern Ross Sea (DVDP 10, 11 and CIROS-2 cores) (Winter and Harwood 1997). These diatom datums were heavily linked to early magnetostratigraphic interpretations (Berggren *et al.* 1985a, 1985b) and have been since revised (Berggren *et al.* 1995) to provide some new datums (Bohaty *et al.* 1998).

## 5.4 Diatom Taphonomy

Taphonomy describes the processes that occur to an organism's remains following death. Different processes affect fossil preservation, transport and deposition. Understanding the taphonomy of diatoms is crucial for their biostratigraphic and palaeoenvironmental interpretation.

### 5.4.1 Deposition: Marine, Glacial marine and Lake

Siliceous diatom frustules dominate the biogenic sedimentation in the world's most productive ocean regions (Lisitzin 1971; Baldauf and Barron 1990). Biogenic silica deposition as diatom ooze often comprise up to 75% of the total sediment in the Southern Ocean (Jousé *et al.* 1971; DeMaster 1981; Gersonde and Wefer 1987). Most diatomaceous ooze is deposited in a circum-antarctic zone, 900 - 2000 km wide, called the Southern Belt (Lisitzin 1971) (Figure 20) and covers roughly the Antarctic Zone, between the APF and AD (Figures 4) (Hays 1967; Gordon 1971; Lisitzin 1971). South of the APF there is a zone of high diatom biogenic silica production, called the silica front, which results from nutrient upwelling (Van Bennekom *et al.* 1988). North of the Southern Belt, the sediment is a mixture of biogenic carbonates and silica (Howard and Prell 1994).

The area north of the Southern Belt is recognised as being rich in biogenic carbonate (Gordon 1971; Burckle and Cirilli 1987) from benthic and planktic foraminifera and planktic coccolithophorids. The proportion of carbonate south of the APF, where the cooler temperatures over the Antarctic Zone inhibit the growth of calcareous organisms, is reduced. The growth of coccolithophorids, for example, is severely limited at temperatures below 3°C (Burckle and Pokras 1991), and although they can still form coccoliths below this temperature, they are not abundant (Dmitriyenko 1989). Similar growth limitations occur amongst foraminifera, which together with the coccolithophorids, cause low CaCO<sub>3</sub> formation in surface waters south of the APF.

Carbonate produced in surface waters is readily dissolved, and at shallow depths the waters quickly become depleted and corrosive to solid CaCO<sub>3</sub>. The depth to which all solid carbonate is dissolved is called the Carbon Compensation Depth (CCD) (Bearman 1989). This is particularly shallow, ~500 m, immediately around Antarctica due to the low carbonate production (Domack 1988). As a result, the relative amount of biogenic silica deposition in the Southern Belt increases. This depositional pattern is disrupted, however, where carbonate is deposited at shallower depths below the CCD on the



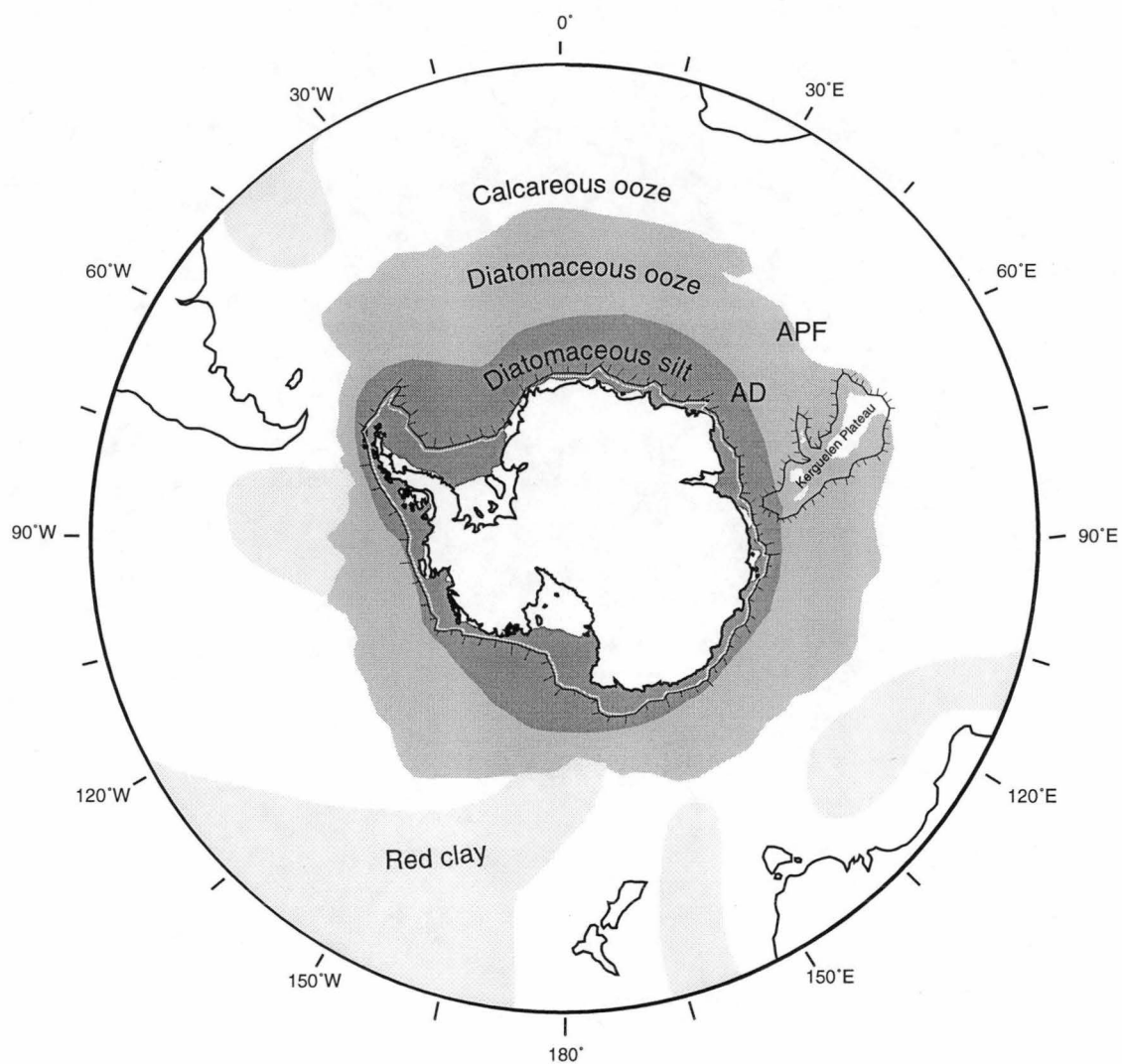


**Figure 20.** Southern Ocean sediment facies (modified from Hays (1967) and Goodell (1973)).

Antarctic continental shelf (Elverhøi 1984; Domack 1988) and the Kerguelen Plateau (Goodell 1973) (Figure 20). South of the Southern Belt, terrigenous, glacial, sediment input from the Antarctic continent dilutes the biogenic input, with the deposition of silty, diatomaceous clay (Hays 1967) (Figure 20). However, in sheltered Antarctic coastal fjords, with anoxic water conditions, biogenic silica may comprise more than 90% of the sediment (McMinn *et al.* 1998).

Diatomaceous sediment also accumulates in lakes on exposed rock regions in Antarctica (Roberts and McMinn 1996, 1997, 1998). Algal deposits also form in melt pool lakes that seasonally form on the ice shelves and Antarctic ice sheets (Kellogg and Kellogg 1987), but these have been understudied.

#### **5.4.2 Preservation: Dissolution and Mechanical Breakage**

Diatom preservation is dependent on the degree of mechanical breakage and dissolution. Dissolution is the chemical dissolving of diatom frustules, which increases with pH (Jorgensen 1955), temperature (Lewin 1961; Kamatani and Riley 1979), pressure (Lewin 1961; Barker *et al.* 1994) and salinity (Barker *et al.* 1994). Most dissolution occurs whilst a diatom is within the water column; therefore the time it takes for a frustule to sink to the sea-floor can influence its preservation. Diatoms generally experience less dissolution if they sink quickly, as is the case for larger, more heavily silicified species and diatomaceous aggregates. Aggregates form either as fecal pellets, during zooplankton grazing (Barron 1993), as clumps of marine snow (Honjo *et al.* 1982) from the binding of diatoms during increased mucous secretion (Smetacek 1985), or from entanglement during algal blooms (Leventer *et al.* 1996). Aggregates inhibit dissolution as they pass quickly through the surface water layer, where dissolution is most active (Hurd 1972). Active dissolution occurs in surface waters due to the relatively high water temperature here and low silicate concentrations due to phytoplankton use (diatoms, silicoflagellates and radiolarians) and zooplankton consumption (Kamatani and Riley 1979).

Once diatoms are deposited, dissolution continues at the sediment water interface and through interaction with sedimentary pore waters at depth below this interface (Heath 1974). Bioturbation and sediment reworking causes the mechanical breakage of diatoms, which increases their surface area to volume ratio and the effects of dissolution. Grazing in the water column causes little or no mechanical breakage (Dunbar *et al.* 1991; DeMaster *et al.* 1992).

Only 1 - 10% of biogenic silica fixed in the euphotic zone reaches the sea-floor (Lisitzin 1971; Calvert 1974; Heath 1974; Nelson and Goering 1977; Shemesh *et al.* 1989); only ~2% avoids post-depositional dissolution (Heath 1974). As a result, there is a preservational bias towards heavily silicified diatoms (Leventer and Harwood 1993). Increased surface area to volume ratio, in smaller and lightly silicified species increases the effects of dissolution. The amount of preservational bias is greatest in assemblages dominated by lightly silicified species. This includes sea-ice assemblages (Leventer and Harwood 1993; Leventer 1998) and assemblages in high productivity areas, where silicate competition during rapid growth causes the development of lightly silicified frustules (Lewin 1957; Lee 1989). There is also selective dissolution within assemblages with the loss of less silicified species (Shemesh *et al.* 1989; Pichon *et al.* 1992; Leventer 1998). Lightly silicified diatoms can be preserved in anoxic marine basins, with low pH and no bioturbators (McMinn 1995). However, such conditions are geographically restricted to sheltered Antarctic fjords (McMinn 1995). Nevertheless, regardless of the preservation biases, numerous studies have successfully demonstrated that fossil diatoms in Antarctic marine sediments can be used as proxies for past oceanographic and climatic conditions (e.g. Crosta *et al.* 1997).

### **5.4.3 Reworking**

#### Marine

Numerous processes can cause diatom reworking in the marine environment. On the Antarctic continental shelf, these are commonly water currents, associated with the Antarctic Coastal Current, Coastal Gyres, HSSW / LSSW drainage, and tides (Truesdale and Kellogg 1979; Taylor *et al.* 1997). Other significant causes of reworking in the marine environment include gravity flow processes, turbidity currents and slumping; ice related processes, such as iceberg and sea-ice scouring, anchor ice formation (Clarke 1996a, 1996b); and biological processes such as bioturbation.

#### Aeolian

Freshwater and marine diatoms have been collected from South Pole ice core samples, deposited <400 BP (Kellogg and Kellogg 1996). Similar diatoms were found in Holocene and LGM samples from the Vostok and Dome C ice cores (Burckle *et al.* 1988a, 1988b). Ninety-eight percent of the frustules found in Dome C are non-marine (Burckle *et al.* 1988a, 1988b), and the majority of those from the South Pole core are Antarctic species (Kellogg and Kellogg 1996). Non-marine and marine diatoms have also been found in the McMurdo Ice Shelf (Kellogg and Kellogg 1984; 1987). Some older extinct

Southern Ocean diatoms have also been found at these locations (Kellogg and Kellogg 1987, 1996).

It is suggested that non-marine diatoms on ice shelves near McMurdo Sound come from melt ponds that developed on the shelf surface during summer (Kellogg and Kellogg 1987). However, this process does not explain the presence of non-marine diatoms in the inland ice cores, especially during the LGM when it would have been too cold for meltwater ponds to form at these locations. The abundance of diatoms increases, with other aeolian material (dust and aerosols), during the LGM in Vostok and Dome C ice cores (Ram *et al.* 1988), suggesting that the diatoms are also aeolian in origin (Burckle *et al.* 1988a). Aeolian processes may also explain the occurrence of diatoms on Antarctic igneous and metamorphic terrain (Burckle and Potter 1996), meteorites (Burckle and Delaney 1999), and marine and glacial sediment exposures (Barrett *et al.* 1997; Harwood and Webb 1998).

Living diatoms in the Southern Ocean provide only a relatively minor aeolian source, through sea spray; air bubble popping (Harwood and Webb 1998), and sea-ice wind ablation. The most likely source of the diatoms in ice cores is the erosion of aeri ally exposed coastal marine and lake sediments.

Some diatoms found in Antarctic ice cores are endemic to areas outside Antarctica (Kellogg and Kellogg 1996). Non-Antarctic freshwater diatoms have also been found in surficial sediment and regolith samples from the Transantarctic Mountains (Barrett *et al.* 1998). These may have been transported by winds high in the atmosphere. Fresh water and marine diatoms have been found ~3000 m elevation above the Eastern Caribbean (Maynard 1968), and small empty valves of freshwater diatoms, <25 µm diameter or 60 µm long, are a common component in aerosol samples (Pye 1987). However, the atmospheric systems around Antarctica create an effective barrier to airborne diatoms from lower latitudes. The cyclonic circum-antarctic low pressure systems, over the APFZ, form a barrier of clouds and precipitation that extends several kilometres upwards (Shaw 1979). These weather systems rarely penetrate into the interior of Antarctica, instead they concentrate at Subantarctic latitudes and migrate clockwise around the continent (Shaw 1979). Precipitation here effectively removes airborne particles below the troposphere. The particles act as nucleation centres for water droplets and ice crystals in clouds, falling as rain and snow, which collect further particles during descent (Delmas and Legrand 1989).

The source of the aeolian diatoms in ice cores can be identified from isotopic analysis on dust particles also found in the cores. During glacial intervals most aeolian material found in Antarctica comes from Patagonia (Gaudichet *et al.* 1986, 1988; Grousset *et al.* 1992; Basile *et al.* 1997). This originated from South American continental shelf sediments that were aurally exposed during eustatic sea-level fall (Delmas and Petit 1994). The southern extreme of South America is far enough south to be influenced by Antarctic atmospheric systems. The northern migration of the APF around the Southern tip of South America causes the easy entrainment of dust off the continental shelf during storms and transports it to Antarctica (Burckle *et al.* 1988a). In turn, glacial expansion on Antarctica would cover rock areas and reduce the relative dust and diatom contribution from local sedimentary sources. During interglacial intervals, such as today, Antarctic aerosol composition is very similar to that identified from ice cores during glacial intervals (Delmas and Petit 1994). Interglacial Antarctic aerosols originate mainly from ice age aeolian deposits within South America's cold deserts (Delmas and Petit 1994). As a result, most dust found in Antarctic ice cores comes from South America, which is therefore the likely source regions for the majority of aeolian diatoms found in Antarctica (Harwood and Webb 1998).

Many of the diatoms found in Antarctic ice cores probably come from South America; however, diatoms identified in the South Pole ice core were called Antarctic species (in Kellogg and Kellogg 1996). Many of these are benthic genera such as: *Achnanthes*, *Cocconeis*, *Diploneis*, *Fragilaria*, *Navicula*, *Synedra*, *Rhabdonema* and *Trachyneis*. Benthic genera have been understudied in Antarctica, leading to past taxonomic inconsistencies. Whilst some of the species in Kellogg and Kellogg (1996) are described as non-marine species, they have also been documented in the Antarctic marine environment (Krebs 1977, 1983; Whitehead and McMinn 1997). Only recently have the Antarctic benthic diatoms been systematically described and illustrated (in Roberts and McMinn 1999). The majority of the South Pole ice core diatoms, previously described as Antarctic species, may be South American in origin. Therefore, it is possible that there are similarities between the South American and Antarctic benthic diatom assemblages, but this requires further investigation. It is possible that these species were deposited in shallow water depths during sea-level regression on the South American continental shelf. They could then have been aurally exposed and transported to Antarctica, and inland South American deserts. This suggestion is consistent with the results from isotope analysis. Nevertheless, local Antarctic diatom sources cannot be ignored, as many

Cenozoic deposits on the continent are actively eroding and can be used to explain the occurrence of some older extinct diatom species found in ice cores.

#### Grounded Glaciers

Erosion beneath grounded glacial ice can rework diatoms into glaciogenic deposits. The deposits can vary from lodgment till, such as beneath ice stream B (Scherer 1989, 1991; Scherer *et al.* 1998; Tulaczyk *et al.* 1998) and in the Sirius Group (Webb *et al.* 1983; Harwood 1983; Harwood 1985; Harwood 1986a), glacial marine waterlain till, as in the Pagodroma Group (Harwood in McKelvey and Stephenson 1990; Whitehead *et al.* 1996; McKelvey *et al.* 1997), and englacial moraines, like the Elephant Moraine (Faure and Harwood 1990).

#### Sub-iceshelf

At least four processes can rework diatoms beneath ice shelves. These are: 1) glacial erosion inland from the grounding line, 2) release of aeolian diatoms in the ice through basal melting (similar to process described in Burckle *et al.* 1997), 3) release from syndepositional lakes on the iceshelf surface (Bohaty *et al.* 1998), and 4) reworking and advection from the adjacent marine environments (living and sedimentary assemblages) beneath the ice shelf (Hambrey *et al.* 1992; Domack and Harris 1998).

#### Meteorite

Meteorite impact in the Southern Ocean could have dispersed marine sediment over Antarctica in the resulting impact ejecta. The Eltanin meteorite impact in the Southern Ocean ~2.15 Ma, is a possible example of this (Gersonde *et al.* 1997). This impact is thought to have disturbed Southern Ocean marine sediments spanning the last 50 My in age, depositing this over Antarctica in the resulting fallout.

---

**Section B:**  
**Palaeoclimate Studies**

---

## **6. Southern Kerguelen Plateau Quaternary-Pliocene Palaeoceanography.**

### **6.1 Introduction**

#### **6.1.1 Aims**

The aim of this study is to address whether oceanographic conditions in the Southern Ocean were stable or fluctuated during the Pliocene (discussed in Chapter 4). If climatic conditions were variable, this study aims to identify the magnitude of this variability using sedimentological and diatom fossil evidence. Diatom assemblages from the Pliocene and Quaternary (<3.2 Ma) are identified in five gravity cores from the Southern Kerguelen Plateau (Figure 21a), and compared to those in modern surface sediments from Prydz Bay (in Taylor 1999), the Indian sector of the Southern Ocean (e.g. Ciesielski and Weaver 1974; Pichon *et al.* 1987) and the Kerguelen Plateau (this study).

#### **6.1.2 Geological Setting**

The Kerguelen Plateau is ~2500 km long, between 200-600 km wide and rises 2-4 km above the adjacent marine basins (Barron *et al.* 1989a), making it the world's largest oceanic plateau (Ramsey *et al.* 1986; Domack and Domack 1991). The southern half of the Plateau is south of the Antarctic Polar Front (APF), but within the northern edge of the Seasonal Sea-Ice Zone (SIZ) (Goodell 1973; Tréguer and Jacques 1992; Bryan 1993) (Figure 21b).

Terrigenous sediment in the Southern Ocean is derived largely from Antarctic icebergs and is released as ice rafted debris (IRD) as the icebergs melt (Chapter 3.1.2). The majority of icebergs in the Indian sector of the Southern Ocean occur within 160 km of the Antarctic coast, where they remain under the influence of coastal currents (East Wind Drift) (Young *et al.* 1998). Near the south-eastern end of the Kerguelen Plateau, however, the coastal current projects into the southern margin of the Antarctic Circumpolar Current (ACC), and some icebergs are transported northward here (Young *et al.* 1998). Modern icebergs have been found well north of the Kerguelen Plateau, even as far as ~37° S (Goodell 1973), and it is quite possible that IRD could be deposited over the study region today. But generally few icebergs travel over the Kerguelen Plateau and the modern sediment here is almost completely biogenic (Goodell 1973) (Figure 22a).



Sediment deposited north of the APF consists largely of calcareous ooze (Gordon 1971; Burckle and Cirilli 1987), but the cold waters south of the APF inhibits calcium carbonate formation and preservation (Chapter 5.4.1). The shallow depth of the Kerguelen Plateau (<2000 m) is within the Carbonate Compensation Depth (CCD), enabling some carbonate preservation, which is deposited in a mixture of calcareous-siliceous ooze (Goodell 1973) (Figure 22a).

Environmental changes can cause north-south shifts in the APF and SIZ, as well as changes in ACC velocity and the amount of IRD deposition. During past glacial intervals the ACC has increased in velocity (Ciesielski *et al.* 1982), ocean fronts have moved northwards, and / or the temperature gradients across these have steepened (Bohaty and Harwood 1998). In contrast, during interglacials the ACC has been slower and ocean fronts have migrated southwards and / or their temperature gradients weakened. These oceanographic changes can cause changes in phytoplankton distribution, productivity and preservation, which in turn affects microfossil assemblage and sediment compositions (Burckle *et al.* 1996). The amount of IRD deposition on the Kerguelen Plateau can also reflect increases and decreases in Antarctic iceberg calving rates due to changes in Antarctic glacial conditions (Breza 1992). Increased velocity of the ACC during intense cold periods can prevent deposition, and cause erosion and the formation of IRD lag layers in some areas, as it has on the Maurice Ewing Bank (Ciesielski and Wise 1977; Ciesielski *et al.* 1982; Wise *et al.* 1992). Similar processes may also occur on the Kerguelen Plateau during intense glacial intervals.

### 6.1.3 Phytoplankton Assemblages

Southern Ocean phytoplankton assemblages have been identified from surface sediment assemblages (Chapter 5.2) (Figure 21c). Because the Southern Kerguelen Plateau is within the SIZ (Chapter 2.2.2) (Figure 23), Antarctic open water and sea-ice associated diatoms are deposited here (Chapter 5.2). Open water conditions during much of the summer cause Antarctic open water diatoms to dominate in surface sediments at similar latitudes to the study region (Pichon *et al.* 1987) (Figure 21d). However, the relative ratio of sea-ice associated diatoms increases further south, into Prydz Bay, where sea-ice persists longer during summer (Stockwell *et al.* 1991; Taylor *et al.* 1997; Taylor 1999).

North of the study area, at the APF, there is a distinct change in the relative abundance of the silicoflagellate genera *Dictyocha* and *Distephanus* in modern surface sediments (Ciesielski 1974; DeFelice and Wise 1981; Pichon *et al.* 1987). The ratio of *Dictyocha* to

*Distephanus* has been studied in surface sediments between Wilkes Land, Antarctica, and Australia (Ciesielski and Weaver 1974). *Dictyocha* were found to be dominant north of the APF (surface waters >5-6 °C), where the *Dictyocha* / *Distephanus* ratio in surface sediments is >0.5. In contrast, *Distephanus* is dominant south of the APF, where the ratio in surface sediments is <0.5 (Ciesielski and Weaver 1974). In surface sediments from the south-eastern Atlantic Ocean, *Dictyocha* is limited to sites north of the APF (DeFelice and Wise 1981). This has been also observed in surface sediments from the Atlantic and West Indian Ocean sectors of the Southern Ocean (Pichon *et al.* 1987).

#### 6.1.4 Previous Work

Ocean Drilling Program Legs 119 and 120 have collected extensive Cenozoic records from the Kerguelen Plateau (Barron *et al.* 1989a; Wise *et al.* 1992). Silicoflagellates and coccolithophorids in sediments from Sites 751A and 748B suggest that the climatic conditions fluctuated during the Pliocene (Barron 1996, Bohaty and Harwood 1998). During warm Pliocene intervals the Antarctic Polar Front Zone (APFZ) (Figure 21b) migrated ~900 km south, or the surface temperature gradient across associated fronts weakened, causing summer sea-surface temperatures (SST) 3° to 4 °C higher than today between 55° and 60° S (Barron 1996; Bohaty and Harwood 1998). The relative amount of biogenic carbonate deposition also increased (Mackenson *et al.* 1992). Diatoms in sediments from Sites 745B illustrate that winter sea-ice conditions fluctuated over the Kerguelen Plateau during the late Pleistocene (Kaczmarek *et al.* 1993). During the Last Glacial Maximum (LGM) sea-ice is thought to have remained over much of the Kerguelen Plateau throughout the year (Hays *et al.* 1976; CLIMAP 1981; Cooke and Hays 1982). This could also reflect the sea-ice conditions during earlier glacial intervals (Figures 23c and 23d). In a recent diatom study by Crosta *et al.* (1998), however, it has been suggested that the summer sea-ice cover in the Indian sector during the LGM differed little from today (Figure 23c).

In the present study, Quaternary and Pliocene sediments are dated using diatoms. Palaeoclimatic conditions are determined from the analysis of quantitative extant diatom and silicoflagellate data. The findings are compared to the lithology and sedimentary structures in the cores, identified from total percent carbonate analysis and x-ray imagery. These palaeoenvironmental proxies also enable comment on the ecology of some extinct diatoms. Because the Southern Kerguelen Plateau occurs within the northern edge of the SIJZ and south of the APFZ, it is an ideal place to investigate palaeoclimatic change.

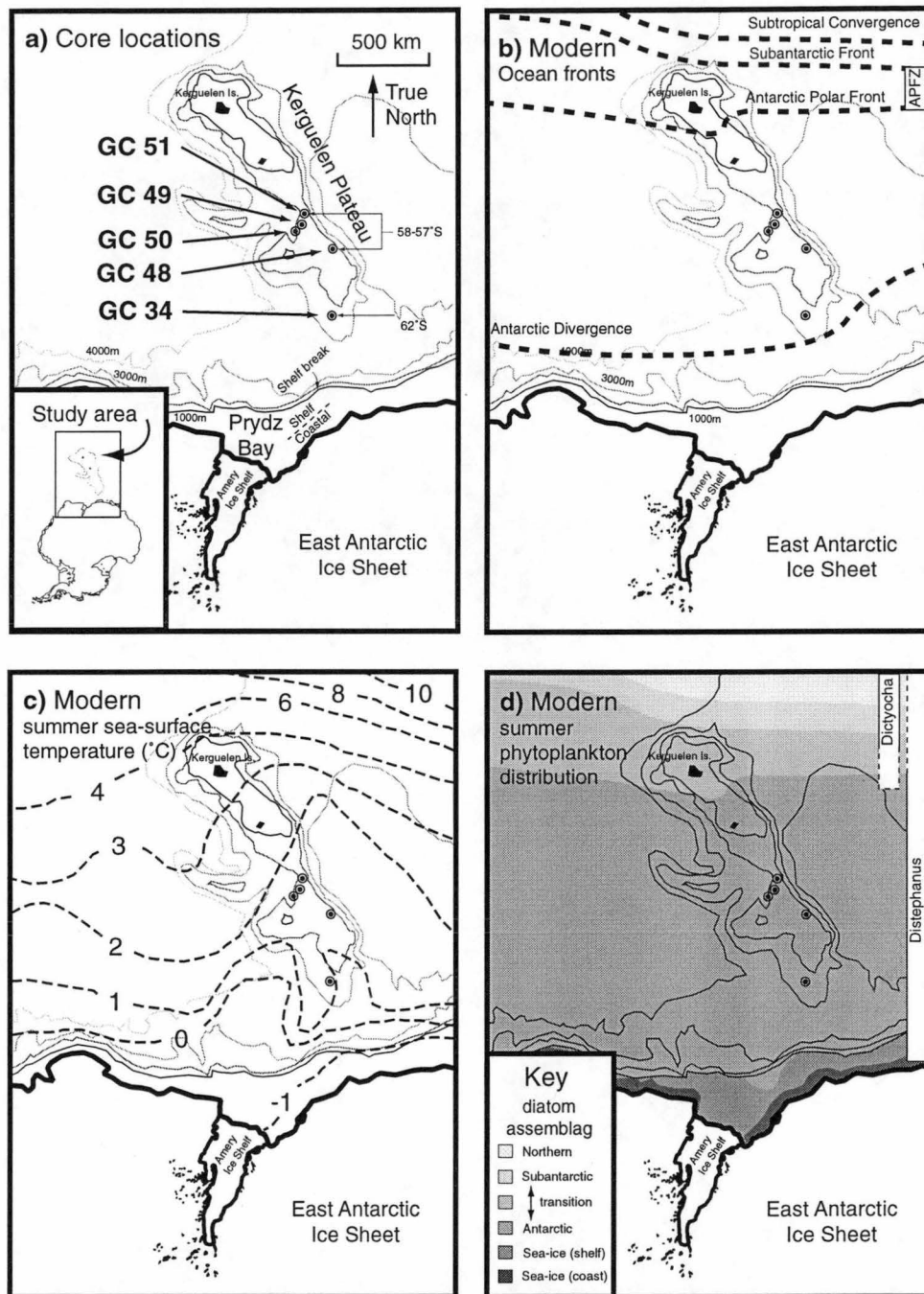


**Figure 21.** Gravity core locations from the Kerguelen Plateau, with sea-floor bathymetry (m below sea-level) (a). Approximate ocean front positions (b) (after Park *et al.* 1993; Rintoul *et al.* 1997), summer sea-surface temperatures (c) (after Gordon and Molinelli 1982), and summer phytoplankton distribution over the study region today (d) (modified from Abbott 1974; DeFelice and Wise 1981; Pichon *et al.* 1987; Taylor *et al.* 1997; Bohaty and Harwood 1998).

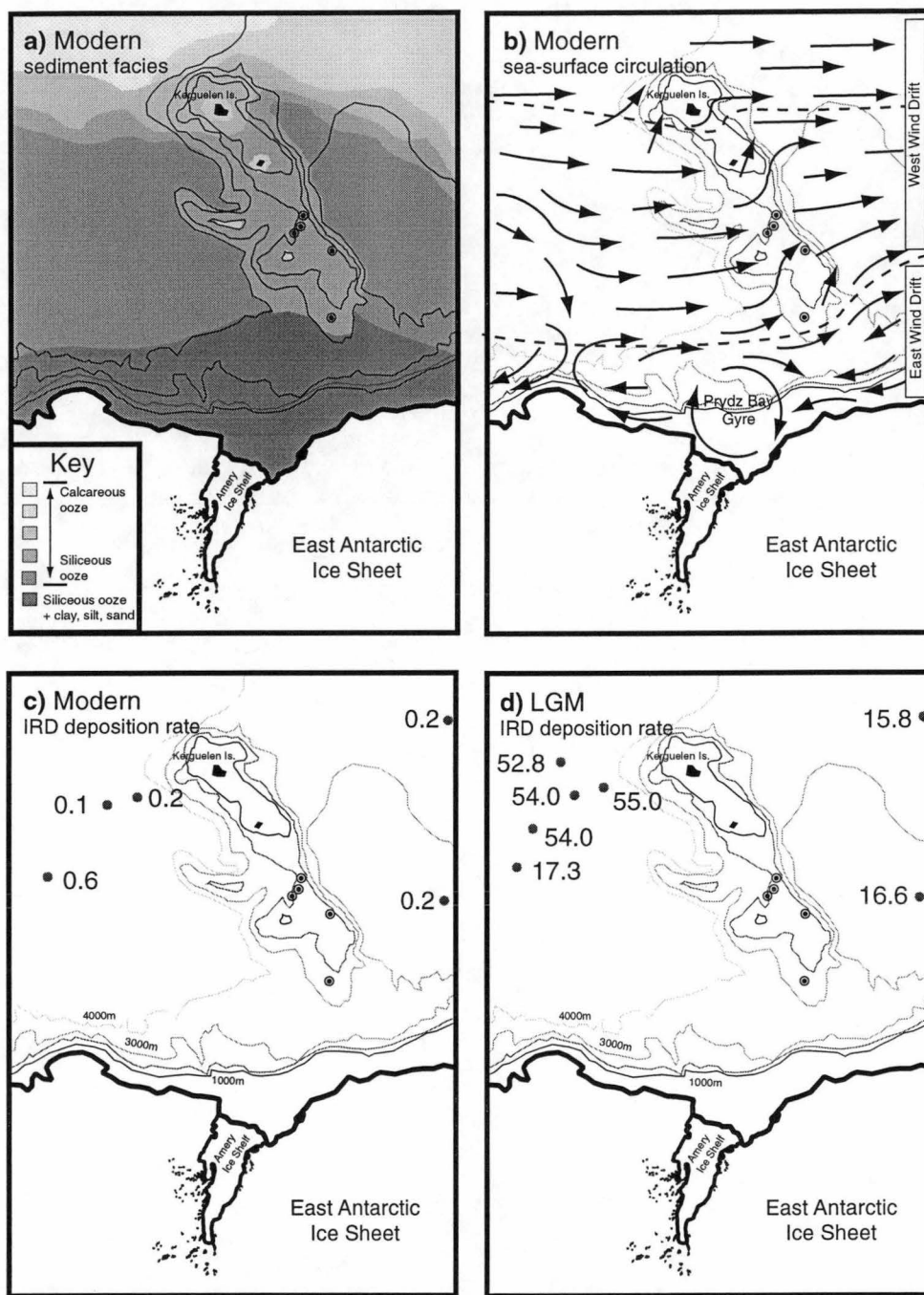


**Figure 22.** Sediment facies (a) (modified from Goodell 1973), sea-surface circulation (b) and IRD accumulation rate (mg/cm<sup>2</sup>/1000 yr) (c) (approximate data positions from Cooke and Hays 1982) over the study region today. During glacial intervals, such as the LGM, IRD accumulation rates were higher (d) (approximate data positions from Cooke and Hays 1982).

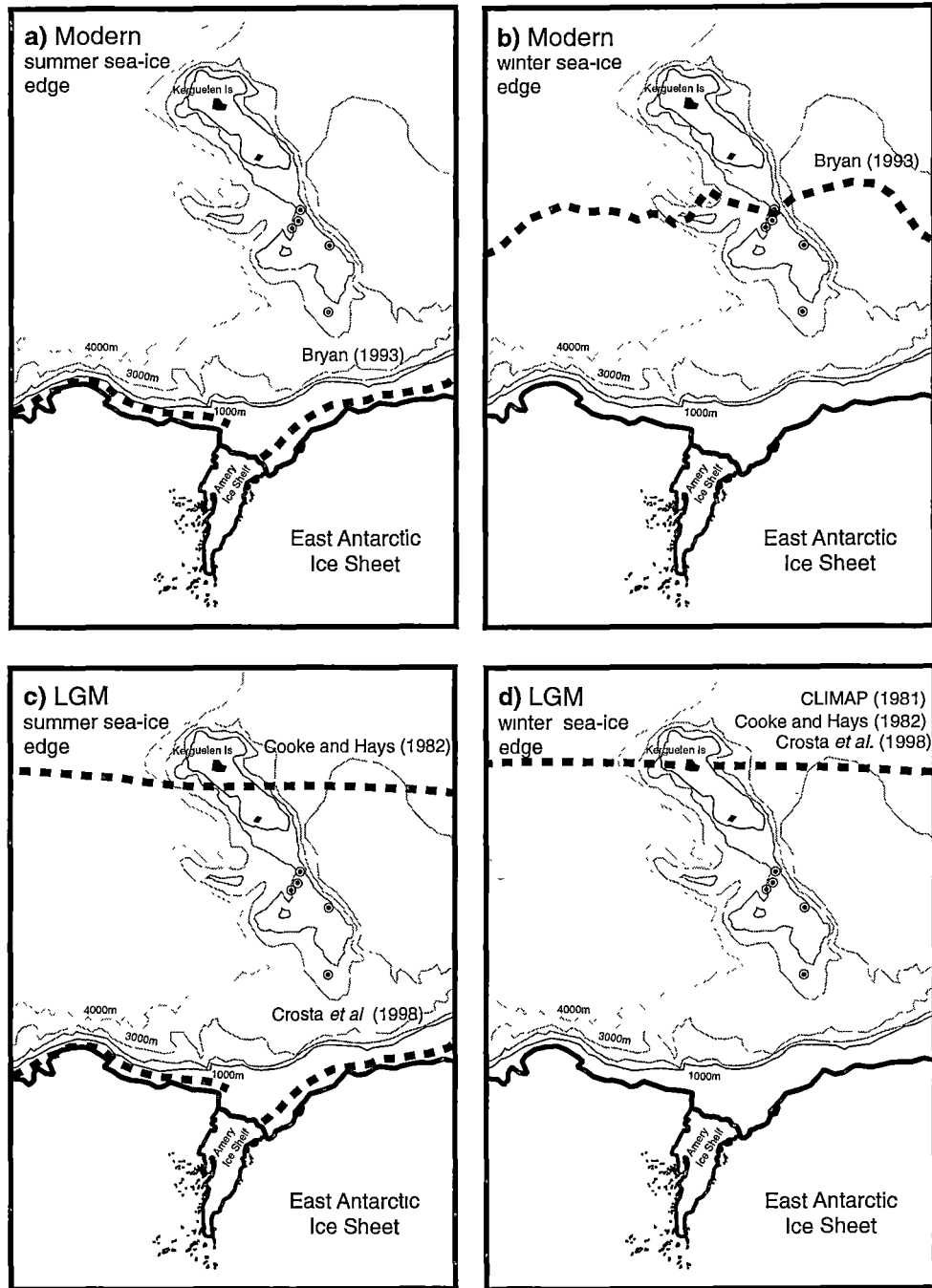


**Figure 23.** Approximate sea-ice edge position during modern and glacial (LGM), summer and winter, conditions.

## 6.2 Methods

Five sedimentary cores (Table 2) were collected using a gravity corer aboard the RSV *Aurora Australis* during two research programs: the 1993 Australian National Antarctic Research Expeditions (ANARE) Krill and Rock (KROCK) Survey, and the 1995 ANARE / Australian Geological Survey Organisation (AGSO) Survey AA 149. Shipboard personnel briefly described the lithology of the cores (Figures 24 to 28) and undertook preliminary diatom biostratigraphy (O'Brien *et al.* 1993, 1995).

### 6.2.1 Siliceous Microfossils

Siliceous microfossil sample preparation and microscopy were conducted at the Antarctic Co-operative Research Centre (CRC). The cores were sampled for siliceous microfossils at ~10 cm intervals. Samples were cleaned to remove carbonate by soaking for two days in dilute HCl. They were then centrifuged at 2500 revs. min<sup>-1</sup> for 5 minutes and rinsed with distilled water; the process was repeated three times to remove excess acid and residues. The washed samples were diluted (1-3 drops per 10 ml distilled water), pipetted onto glass cover-slips, and allowed to dry on a warm hot-plate (~50°C). Permanent slides were made by mounting the cover-slips with Norland Optical Adhesive 61 (refractive index = 1.56) and curing them under an UV light for 5 minutes. Diatoms were identified and counted using a Zeiss Standard 20 phase contrast light microscope, under 1000x magnification oil immersion. Approximately 400 diatom valves were counted per sample to establish their quantitative relative abundance (Appendix 3). Only intact valves, or broken specimens where more than half the valve remained, were counted. Exceptions to this were made for the fragile elongate genera, such as *Trichotoxon* and *Thalassiothrix*, which are rarely preserved intact and were counted from their distinctive end pieces. To calculate the total number of *Trichotoxon* and *Thalassiothrix* valves, the data was divided by two. The diatom *Dactyliosolen antarcticus* Castracane was counted from individual girdle bands identified in the samples, although it is unsure how many of these represent a single diatom. *Chaetoceros* cysts were recorded as individual valves, although they sometimes represent a complete diatom. Subsequent to counting, the slides were scanned to find any rare and biostratigraphically distinctive species.

The diatom biostratigraphic datums of Harwood and Maruyama (1992) have been applied in this study. This zonation was constructed using ODP cores also collected on the Kerguelen Plateau, and which readily apply to sediments collected from the same region in this study.

**Table 2.** Cores (name, location and length) used in this study.

<b>Core</b>	<b>Location</b>	<b>Length</b>
GC 34 (KROCK)	Lat. 62°20.4' S., Long. 81°14 9' E.	570 cm
GC 48 (AGSO AA 149)	Lat. 58°31.0' S., Long. 81°73.0' E.	490 cm
GC 49 (AGSO AA 149)	Lat. 57°36.2' S., Long. 78°18.1' E.	380 cm
GC 50 (AGSO AA 149)	Lat. 57°45.1' S., Long. 77°32.1' E.	440 cm
GC 51 (AGSO AA 149)	Lat. 57°07.2' S., Long. 78°27.2' E.	480 cm

Disconformities were identified by the absence of diatom zones, and specific age diagnostic diatom species in the cores. The datums were not revised from the Berggren *et al.* (1985a, 1985b) to the Berggren *et al.* (1995) timescale, as the findings were compared to other palaeoenvironmental studies, which were generally dated using older, unrevised timescales.

Subsequent to the diatom biostratigraphic interpretation, the Pliocene slides were re-scanned and silicoflagellates from the genera *Dictyocha* and *Distephanus* counted. The ratio of *Dictyocha* to *Distephanus* co-varies with sea-surface temperature and has been used to reconstruct past summer sea-surface temperatures (Mandra 1969; Mandra and Mandra 1970; Jendrzewski and Zarillo 1972; Ciesielski 1974; Ciesielski and Weaver 1973, 1974; Bohaty and Harwood 1998). The relationship between sea-surface temperature and the ratio of *Dictyocha* to *Distephanus*, identified in Ciesielski and Weaver (1974), has been applied to the Pliocene sediments in this study. The extinct species *Distephanus crux* (Ehrenberg) Haeckel has been excluded from the ratio, as in Bohaty and Harwood (1998), because the palaeoecology of this species is unknown.

### 6.2.2 Statistical Analyses

The diatom quantitative relative abundance data were converted to a percentage of the total number of cells in each sample. Rare species of biostratigraphic importance were recorded with an “r” in Appendix 3. Extinct species with restricted temporal distributions were removed from the analysis. Data containing extinct taxa can confuse analysis, making it difficult to identify environmentally related assemblage changes versus temporal, biostratigraphic changes. The bias this may cause to the remaining data is obvious in the relative ratio of extinct versus extant diatoms plotted for each core (Figures 24 to 28). The extant species data were re-percented and those species occurring >2%, in at least one of the samples, were used in the analysis. Species occurring <2% were removed as they are not sufficiently abundant to be adequately analysed with statistical techniques (Imbrie and Kipp 1971; Webb and Bryson 1972).

The resulting ‘species by sample’ data matrix (Q-mode) was analysed using Bray-Curtis cluster analysis in BioStat II (Pimentel 1993). Cluster analysis is a multivariate statistical technique that can be used to categorise large data sets, by forcing samples into discrete groups or clusters, which are illustrated on a two dimensional dendrogram (Shi 1995) (Figure 29). In this study samples are clustered depending on the similarity between their diatom assemblages. However, the cluster analysis does not illustrate the relationship



between these assemblages and the environment (Shi 1993). The cluster analysis was carried out using the Bray-Curtis dissimilarity index in association with unweighted pair group average linkage (UPMGA). The Bray-Curtis dissimilarity index allows effective analysis of data sets containing many zeros, (i.e. absence of species), whilst UPMGA joins two samples, at their average level of similarity between all the members of one cluster group and the other (Field *et al.* 1982).

Sample cluster groups identified from the cluster analysis were analysed further to identify the key indicator species within these groups. Those species with a statistically higher abundance in a group were identified using the student Newman-Keuls (SNK) multirange test (Zar 1984), in association with a single factor analysis of variance (ANOVA). The SNK compares a species' mean occurrence in different groups (Zar 1984). The SNK and ANOVA were performed using the multidimensional analysis (MDA) function in BioStat II. The indicator species have a statistically higher abundance within a group. These were checked against F- distribution tables for their corresponding degrees of freedom, with a cut off at the 0.05 probability level. Together with other such species they form the indicator assemblage for that group. Literature review has enabled comparisons of these assemblages to the dominant species in modern Antarctic assemblages (Table 3). The environmental conditions during their deposition could be described and the dominant assemblages plotted down core from the cluster analysis results.

Earlier studies have recognised a negative correlation between the dominant species from different environments, such as the sea-ice diatom *Fragilariopsis curta* (Van Heurck) Hustedt and the Antarctic open water diatom *Fragilariopsis kerguelensis* (O'Meara) Hustedt (Burckle *et al.* 1987; Won Hyung *et al.* 1991; Leventer 1992). The ratio of these two diatoms has been used as an environmental proxy for sea-ice versus open water conditions (Leventer 1992). However, other environmental factors may also affect their distribution and a more robust ratio would come from negatively correlated assemblages (Figure 30). A simple regression illustrates the strength of correlation between the indicator assemblages in this study. If  $R^2 = 0$  there is no relationship and if  $R^2 = 1$  there is a perfect relationship. A high negative correlation means that one assemblage occurs in the low abundance or absence of another. The ratio between these illustrates the degree to which one of the assemblages dominates, and provides a more realistic representation of the assemblages than the "present (dominant) / absent (not dominant)" result obtained from plotting cluster analysis results down core. The ratio plots have been compared to similar ratios calculated from the Kerguelen core tops (from this study) and surficial sediment data

from Prydz Bay (from ~100 samples in Taylor (1999)) (Table 4; Figures 31 to 35). This enables semi-quantification of the environmental conditions down core from their diatom assemblage ratios. The relative abundance of extinct taxa was also plotted down core to see if there were associations during temporal overlap with extant diatoms and silicoflagellates (Figures 31 to 35).

### **6.2.3 X-ray Imagery**

Archived core sections were x-ray photographed using a Siemens x-ray at the Hobart Repatriation Hospital, Tasmania. The x-ray was set at 63 kV, 6.3 mAs, 31.8 ms, and 0.0 min. The light was positioned at the 114 cm height setting. The film was developed automatically in a Curix capacity AGFA - Gevaert. The negatives were studied on a light table, and the sediment density and amount of ice rafted debris (IRD) noted (Figures 24 to 28). The density of the sediment has been described as low to high, relating to the sediment composition, and was determined partially through comparison with the percentage of  $\text{CaCO}_3$  in GC 50. X-ray imagery was used to illustrate the amount of IRD, described on a scale of 0 to 4. Zero represents IRD absent, 1 is at least some IRD, 2 is low IRD abundance (<20% of the x-ray image), 3 is moderately abundant IRD (<50% of the image), and 4 is IRD dominant (covering >50% of the image). The degree of clast support between the IRD was also noted. Disconformities were identified by the presence of IRD lag layers that were visible in the x-ray images.

### **6.2.4 Total Calcium Carbonate**

The total calcium carbonate ( $\text{CaCO}_3$ ) content was determined down the length of core GC 50 from samples collected at ~10 cm intervals. Biogenic carbonate was measured using a vacuum gasometric technique at the Antarctic CRC. Samples were dried in a 110°C oven, then crushed individually with a mortar and pestle to a fine powder <63  $\mu\text{m}$ . Between 300-700 mg of the crushed sample was weighed accurately and placed in a reaction vessel with an attaching side arm, in which 5 ml of concentrated phosphoric acid was placed. The reaction vessel was clamped shut and made air tight. The vessel was attached to an air compressor and the air pressure within the vessel set, and recorded accurately. The acid was then tipped from the side arm into the body of the reaction vessel containing the crushed sample. The reaction between these was allowed to continue for 1.25 hours and the sample agitated by hand every 20 minutes. On completion of the reaction, the change in pressure within the reaction vessel was measured. This value, combined with the known weight of sample, was used to determine the total abundance of  $\text{CaCO}_3$ , and expressed as a percent total calcium carbonate.

**Figures 24-28.** Sediment and diatom data from gravity cores (GC 34, 48, 49, 50, 51) collected from the Southern Kerguelen Plateau. The figures illustrate:

- depth down core (metres),
- ship log (Munsell chart colour number and sedimentary structures),
- core x-ray imagery (indicating sediment density, structures)
- amount of ice rafted debris (from x-ray imagery),
- diatom biostratigraphic zones and the position of key datums,
- relative abundance (%) of extant species within the samples.

Figure 26 also illustrates the total carbonate content as a percentage of total sediment.

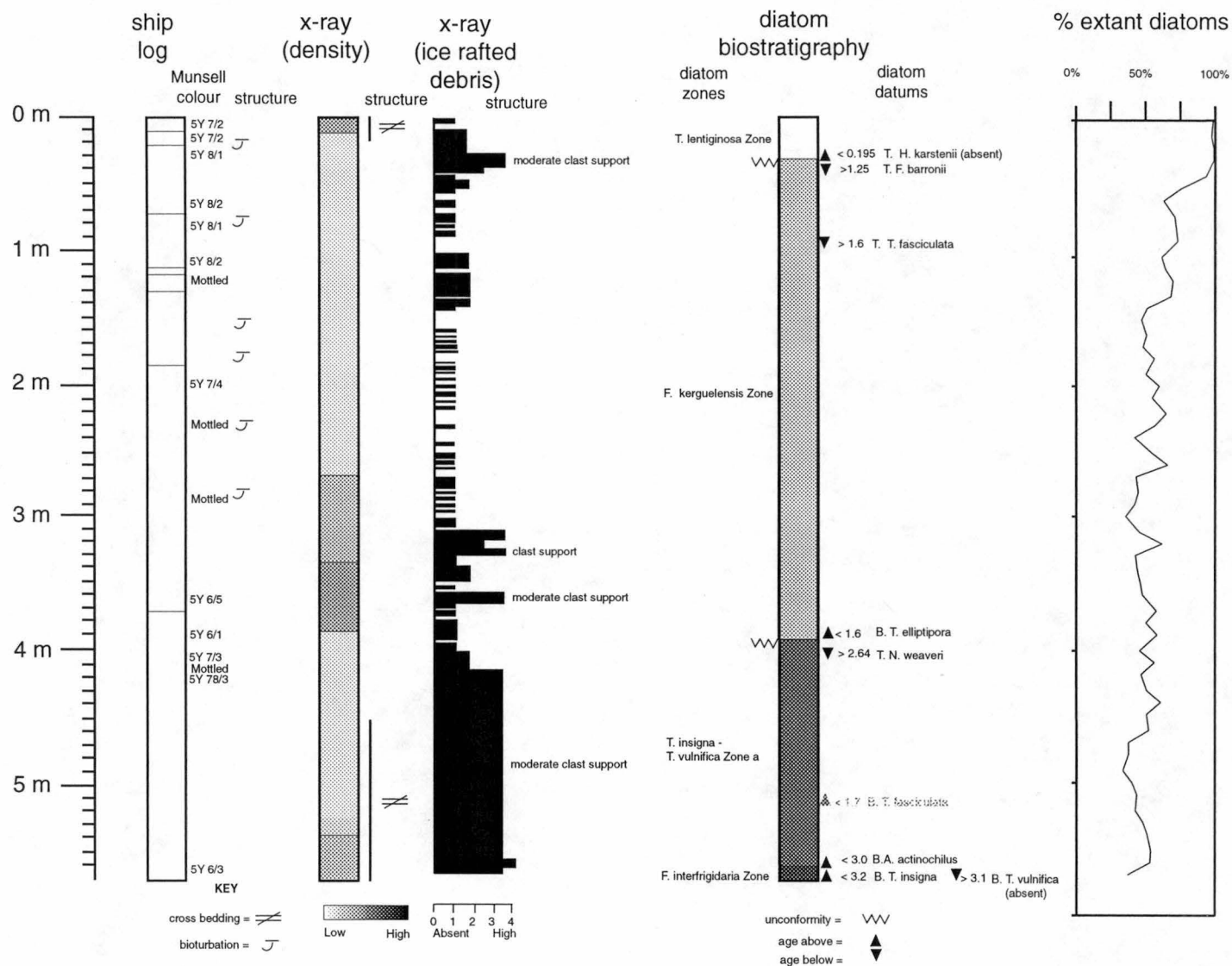


Figure 24. GC 34 (KROCK), Lat. 62°20.4' S., Long. 81°14.9' E.

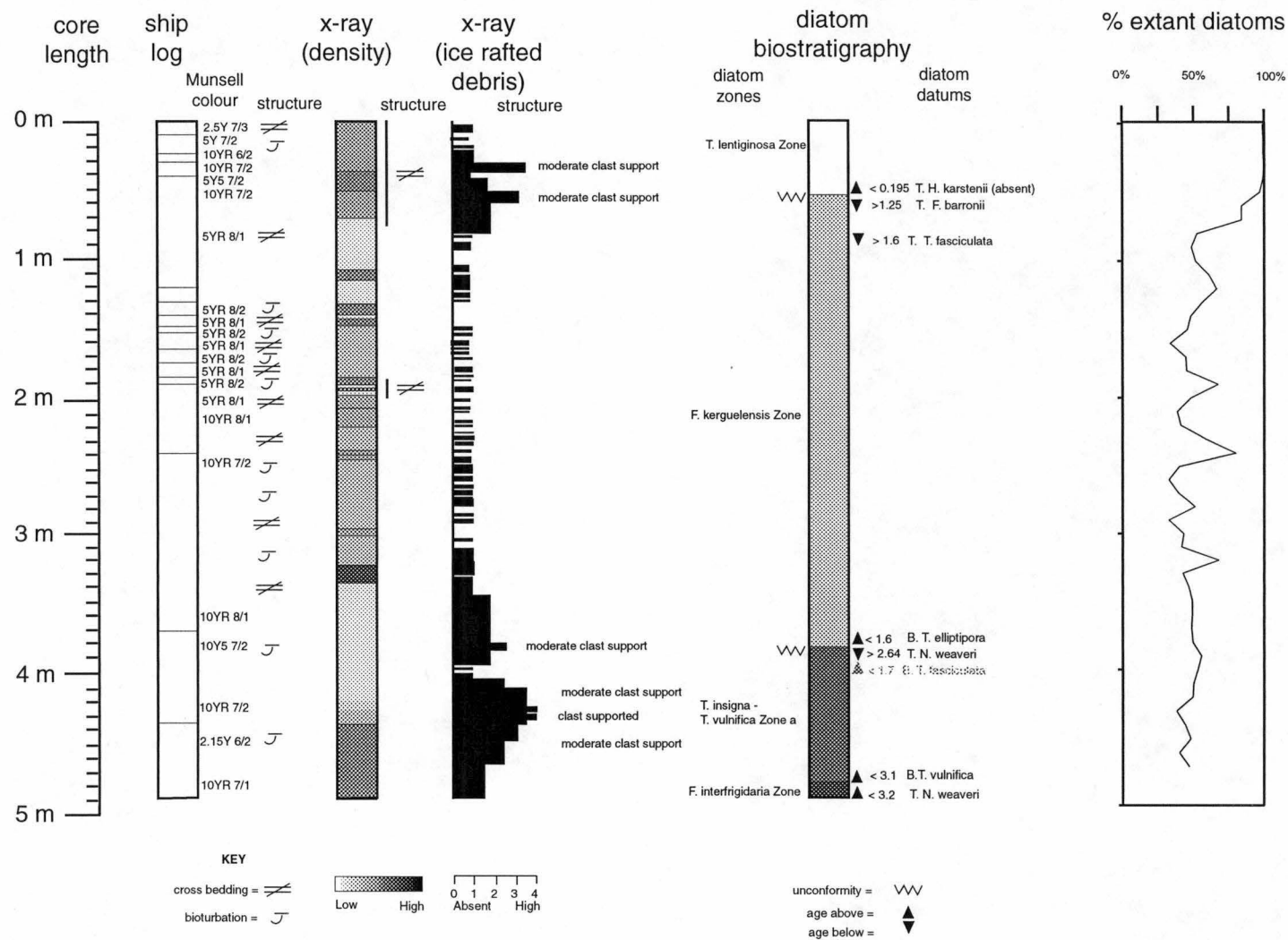


Figure 25. GC 48(AGSO AA 149), Lat. 58°31.0' S., Long. 81°73.0' E.

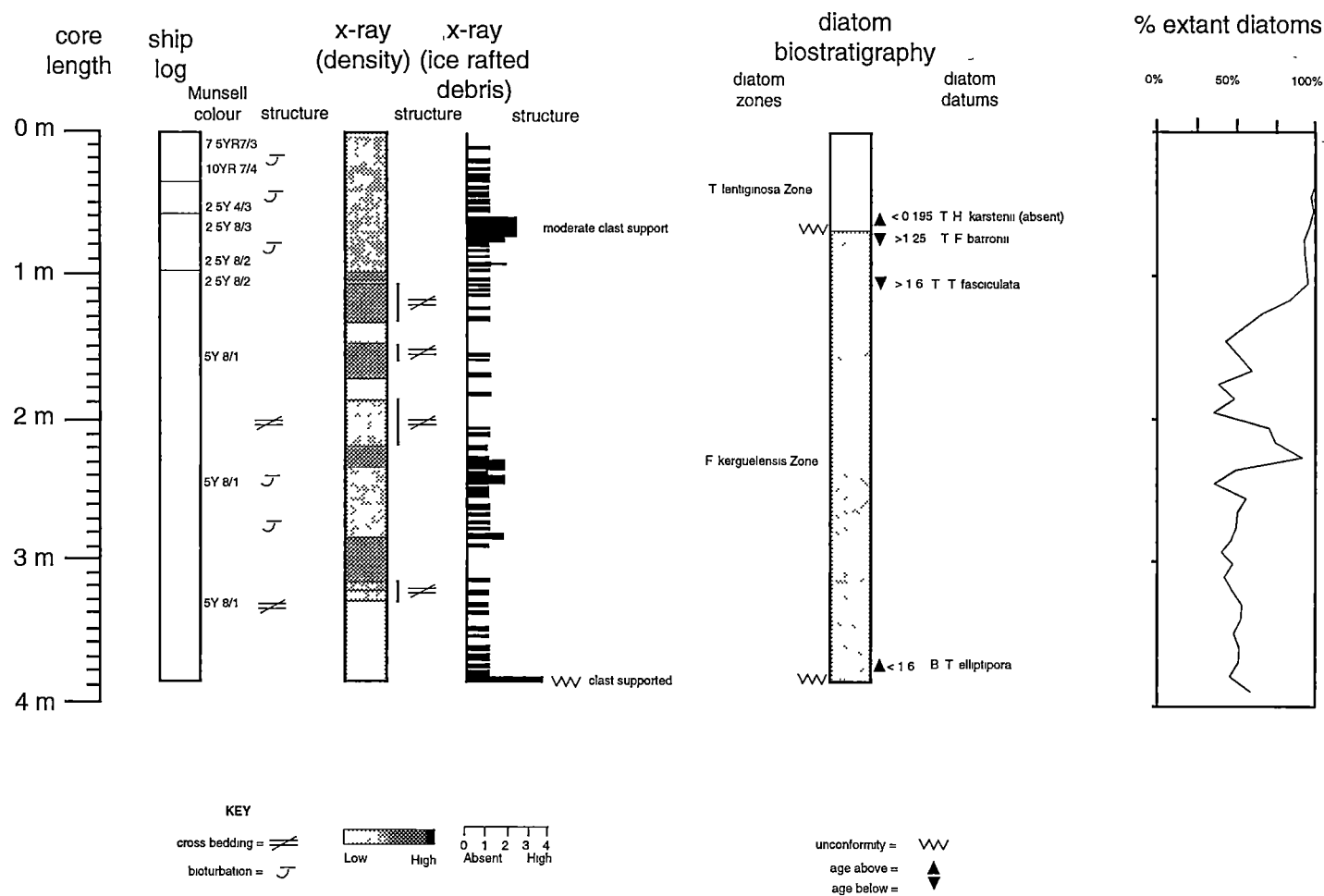
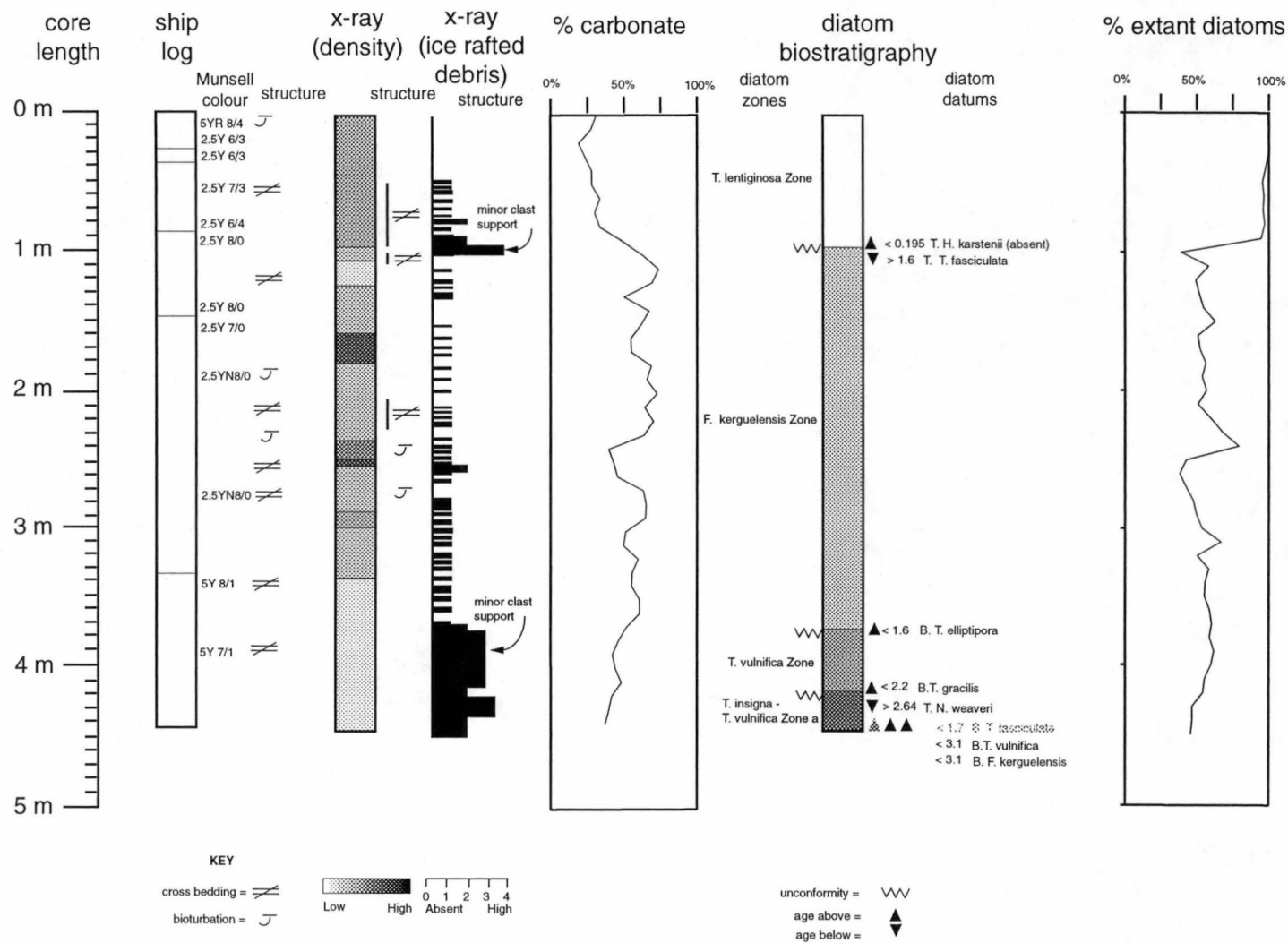
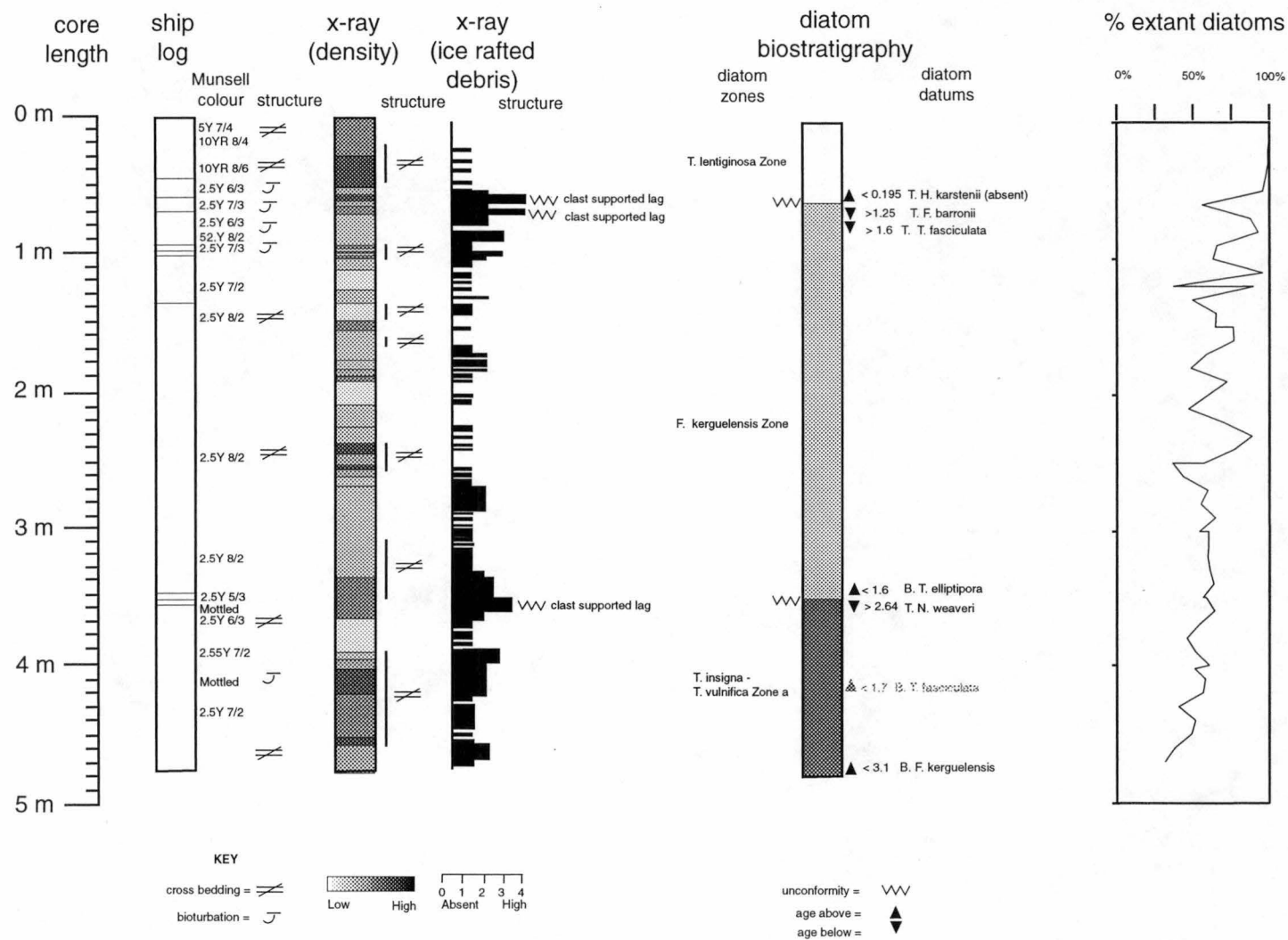


Figure 26. GC 49 (AGSO AA 149), Lat. 57°36.2' S., Long 78°18.1' E.



**Figure 27.** GC 50 (AGSO AA 149), Lat. 57°45.1' S., Long. 77°32.1' E.



**Figure 28.** GC 51(AGSO AA 149), Lat. 57°07.2' S., Long. 78°27.2' E.



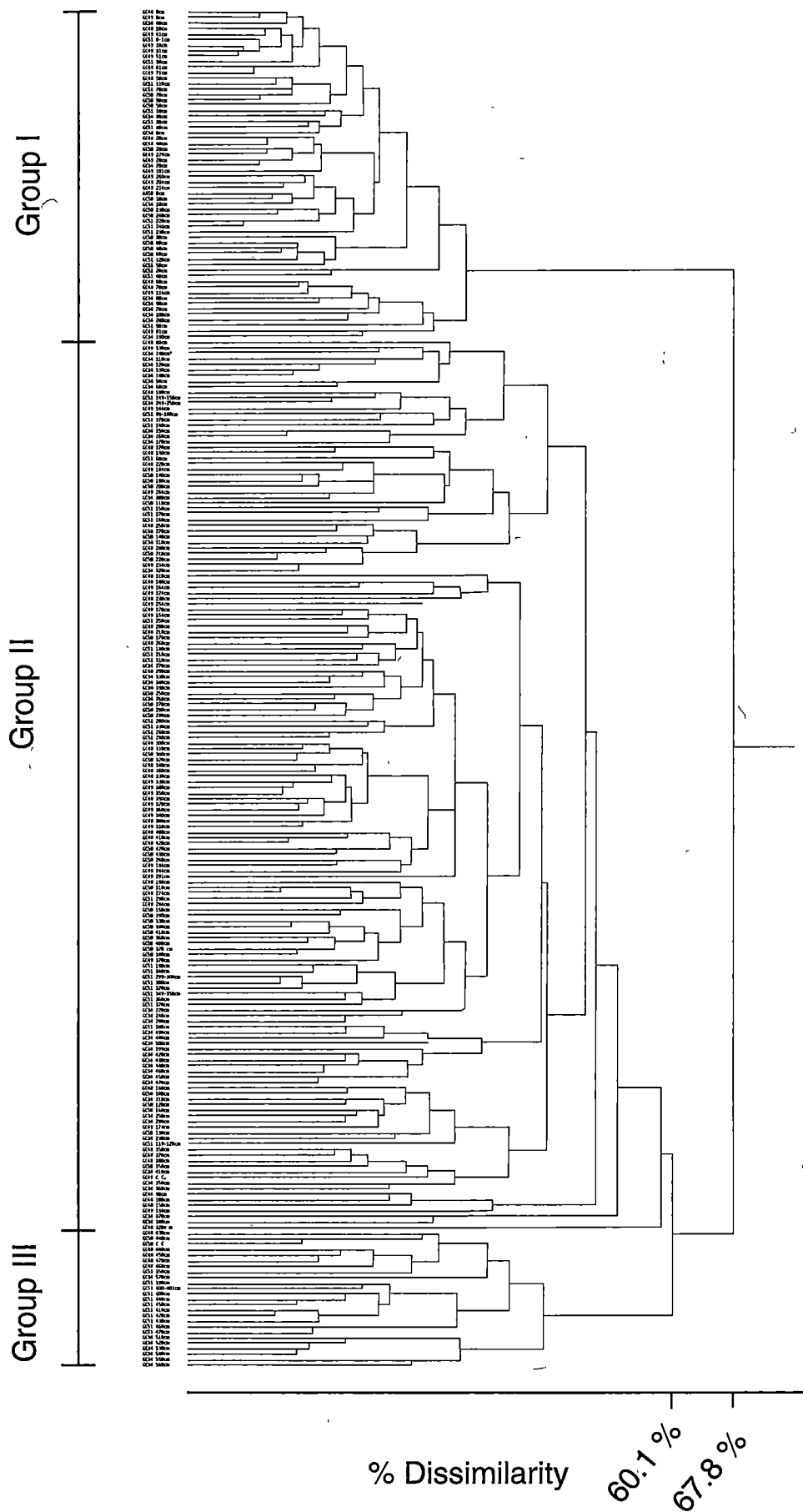


**Figure 29.** Bray-Curtis cluster analysis results. Three sample groups were identified. The diatom assemblages in the Group I samples are 67.8% dissimilar from the assemblages in the Group II and III samples. The assemblages in Groups II and III are 60.1% dissimilar.

**Table 3.** Indicator species indentified from SNK and ANOVA, with a literature review of their assemblage associations.

Species	Group mean value (%)			Assemblage	Citations
	I	II	III		
<b>Group I</b>					
<i>Fragilaropsis kerguelensis</i>	<u>58.06</u>	11.14	0.22	Ant. open water	1, 2, 3, 4, 6, 8
<i>Fragilaropsis separanda</i>	<u>8.13</u>	1.93	0.01	Ant. open water	2, 3, 4, 6, 9
<i>Thalassiosira gracilis</i>	<u>1.59</u>	0.50	0.12	Ant. open water	1, 4, 5
<i>Actinocyclus actinochilus</i>	<u>0.84</u>	0.30	0.02	Sea-ice assoc. & Ant. open water	Discussed in text
<i>Azpeitia tabularis</i>	<u>0.14</u>	0.02	0.04	Subant. & Ant. open water	Discussed in text
<i>Navicula directa</i>	<u>0.11</u>	0.02	0.02	? - sea-floor benthic species	Discussed in text
<b>Group II</b>					
<i>Fragilaropsis curta</i>	5.18	<u>21.86</u>	9.97	Sea-ice assoc.	1, 4, 5, 6, 7, 8
<i>Thalassiosira lentiginosa</i>	5.24	<u>18.24</u>	4.18	Ant. open water	1, 2, 4, 6
<i>Thalassiosira oliverana</i> (coarse)	0.01	<u>1.72</u>	0.37	(Ant. open water) ?	(3, 5, 17)?
<i>Coscinodiscus</i> sp.	0.11	<u>1.03</u>	0.24	?	
<i>Thalassiosira gracilis</i> var. <i>expecta</i>	0.46	<u>0.97</u>	0.22	Ant. open water & sea-ice edge	6, 19
<i>Nitzschia peragalli</i>	0.04	<u>0.88</u>	0.07	Sea-ice assoc.	11
<i>Fragilaropsis sublinearis</i>	0.16	<u>0.82</u>	0.25	Sea-ice assoc.	5
<i>Fragilaropsis rhombica</i>	1.81	<u>0.63</u>	2.91	Sea-ice assoc.	5, 6, 7, 9, 10, 12, 13, 14
<i>Thalassiosira gravida</i>	0.04	<u>0.38</u>	0.05	Sea-ice edge	18, 20
<b>Group III</b>					
<i>Dactylosolen antarcticus</i>	3.93	7.80	<u>29.43</u>	Ant. open water	9, 6, 7
<i>Thalassiosira oestrupii</i>	1.97	6.34	<u>14.38</u>	Ant. open water & sea-ice edge	15, 16, 17
<i>Fragilaropsis ritscheri</i>	3.02	4.90	<u>7.23</u>	Subant., Ant. open water/sea-ice edge	20 / 17
<i>Trichotoxon reinboldii</i>	0.33	2.93	<u>6.69</u>	Ant. open water	6, 7
<i>Chaetoceros</i> cysts	0.72	0.40	<u>2.58</u>	?	
<i>Cortheron</i>	0.01	0.08	<u>2.57</u>	?	
<i>Thalassiosira maculata</i>	0.55	1.68	<u>2.53</u>	Ant. open water	20
<i>Thalassionema</i> spp	0.15	0.12	<u>0.98</u>	Ant. open water	5

#### References

1 (Kozlova and Mukhina 1967), 2 (Abbott 1974), 3 (DeFelice and Wise 1981), 4 (Pichon *et al.* 1987), 5 (Zielinski and Gersonde 1997), 6 (Taylor *et al.* 1997), 7 (Stockwell *et al.* 1991), 8 (Leventer 1992), 9 (Kozlova 1966), 10 (Abbott 1973), 11 (Medlin and Priddle 1990), 12 (Tanimura 1992), 13 (Leventer 1992), 14 (Gersonde and Wefer 1987), 15 (Garrison *et al.* 1987), 16 (Horner 1985), 17 (Armand 1997), 18 (Moisan and Fryxell 1993), 19 (Fryxell and Kendrick 1988), 20 (Johansen and Fryxell 1985).

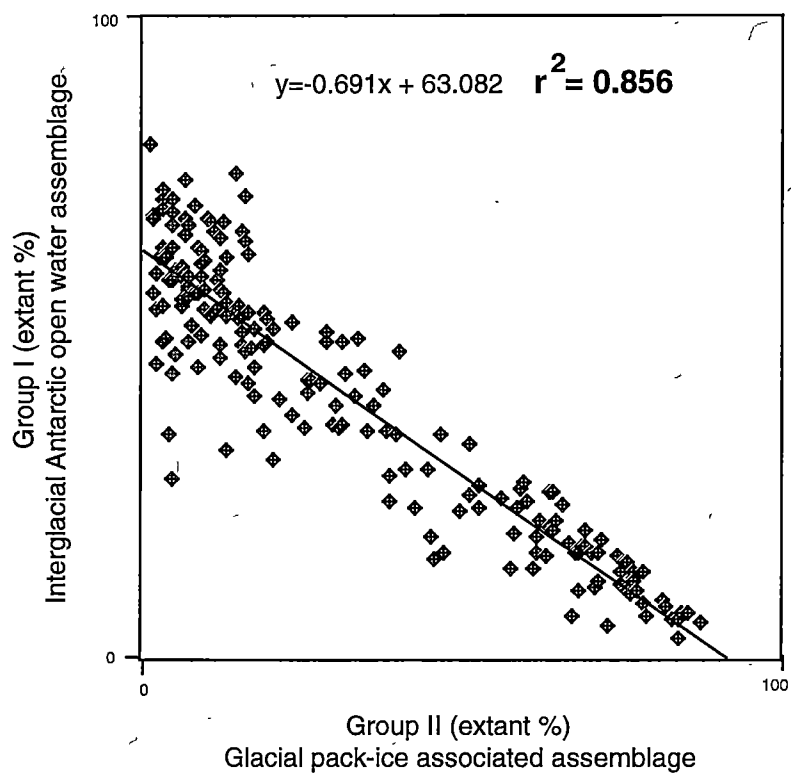


**Figure 30.** Strong negative correlation between the cluster analysis diatom assemblages in Groups I and II in the Quaternary sediment samples.

**Table 4.** Ratio between modern surficial sediment Group I and II assemblages, and corresponding modern environmental conditions.

Location		Coastal	Shelf	Shelf break	Kerguelen Plateau	
Latitude		~69° S	69-67° S	67° S	62° S	58 - 57° S
<u>Ratio</u>		<u>0.03</u>	<u>0.06</u>	<u>0.36</u>	<u>0.98</u>	<u>0.99</u>
Temp. (°C) (Jan-Feb)		-1.1 to -0.6	-1.1 to -0.6	-1.1 to -0.6	0.5 to 1	1 to 2
Salinity (ppt) (Jan-Feb)		33.6 to 33.8	33.6 to 33.8	33.8 to 34.0	approx. 33.8	approx 33.8
Sea-ice cover (%) 1978-1991	January	35	18	11	-	-
	February	26	11	6	-	-

Coastal, Shelf and Shelf Break ratios calculated from data in Taylor (1999), water temp and salinity information from FIBEX (Kerry et al. 1987a) and SIBEX II (Kerry et al. 1987b) data, and sea-ice information from SMMR and SSM/I passive microwave records (US National Climate Data Centre).

Kerguelen Plateau ratios calculated from core tops, this study.  
Kerguelen environmental information from Gordon and Molinelli (1986)

**Figures 31-35.** Diatom and silicoflagellate data from gravity cores (GC 34, 48, 49, 50, 51) collected from the Southern Kerguelen Plateau. The figures illustrate:

- depth down core (metres),
- stratigraphic position of key diatom datums,
- stratigraphic position of significantly dominant cluster analysis groups (from extant diatom data). The boundaries between the groups are projected across other core data (solid grey line),
- ratio between Group I (sea-ice associated diatoms) and Group II (open water diatoms), indicating the degree to which either of these conditions dominated during different intervals in the cores. Warming intervals (more Group II diatoms), that were not statistically significant over cooler intervals, are projected across other core data (dashed grey line),
- changing relative abundance of extinct diatom species are plotted, enabling comparison to extant diatoms assemblages in cluster Groups I, II and III,
- the relative abundance of silicoflagellates (*Dictyocha* and *Distephanus*) are plotted for the Pliocene core intervals.

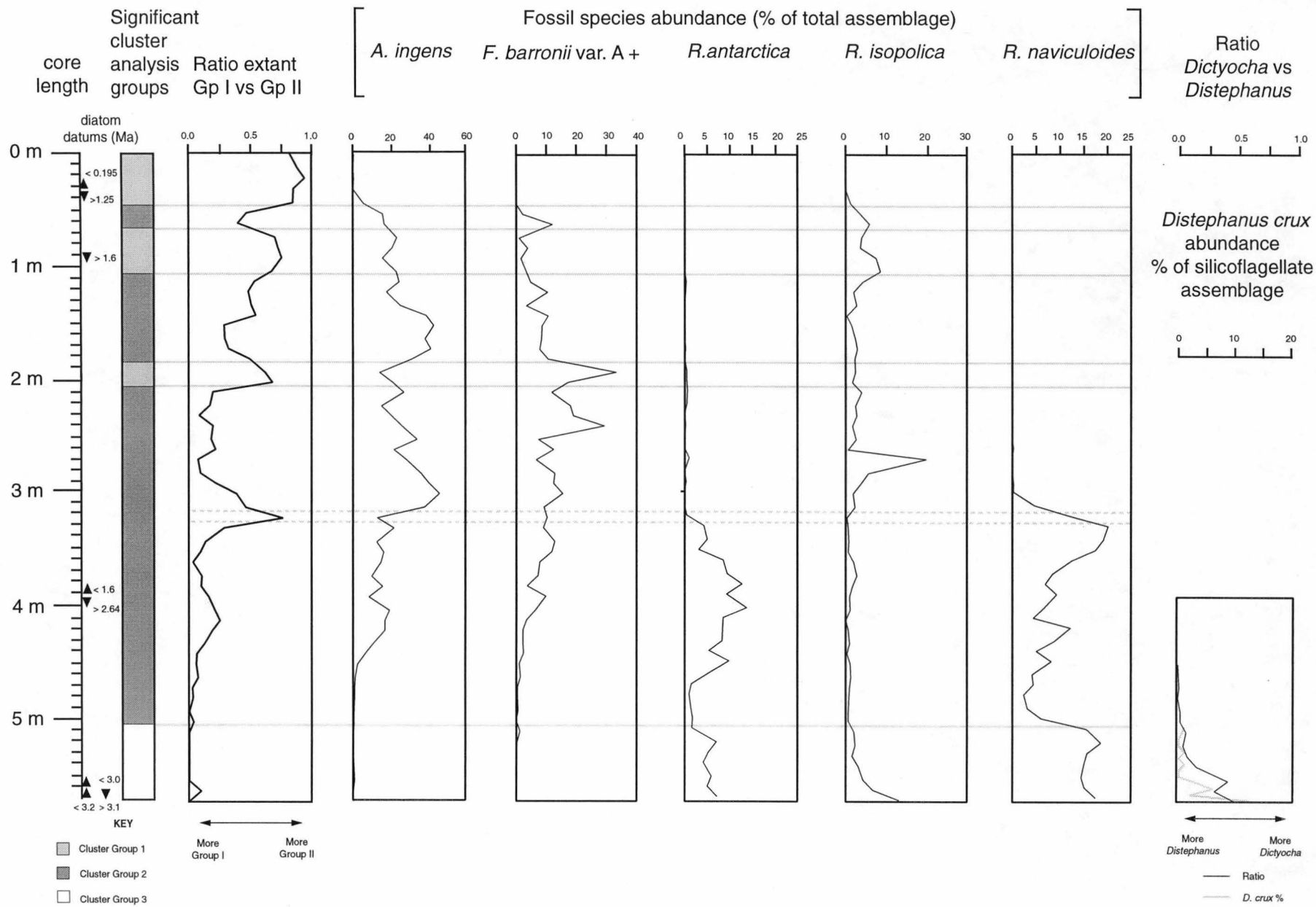


Figure 31. GC 34



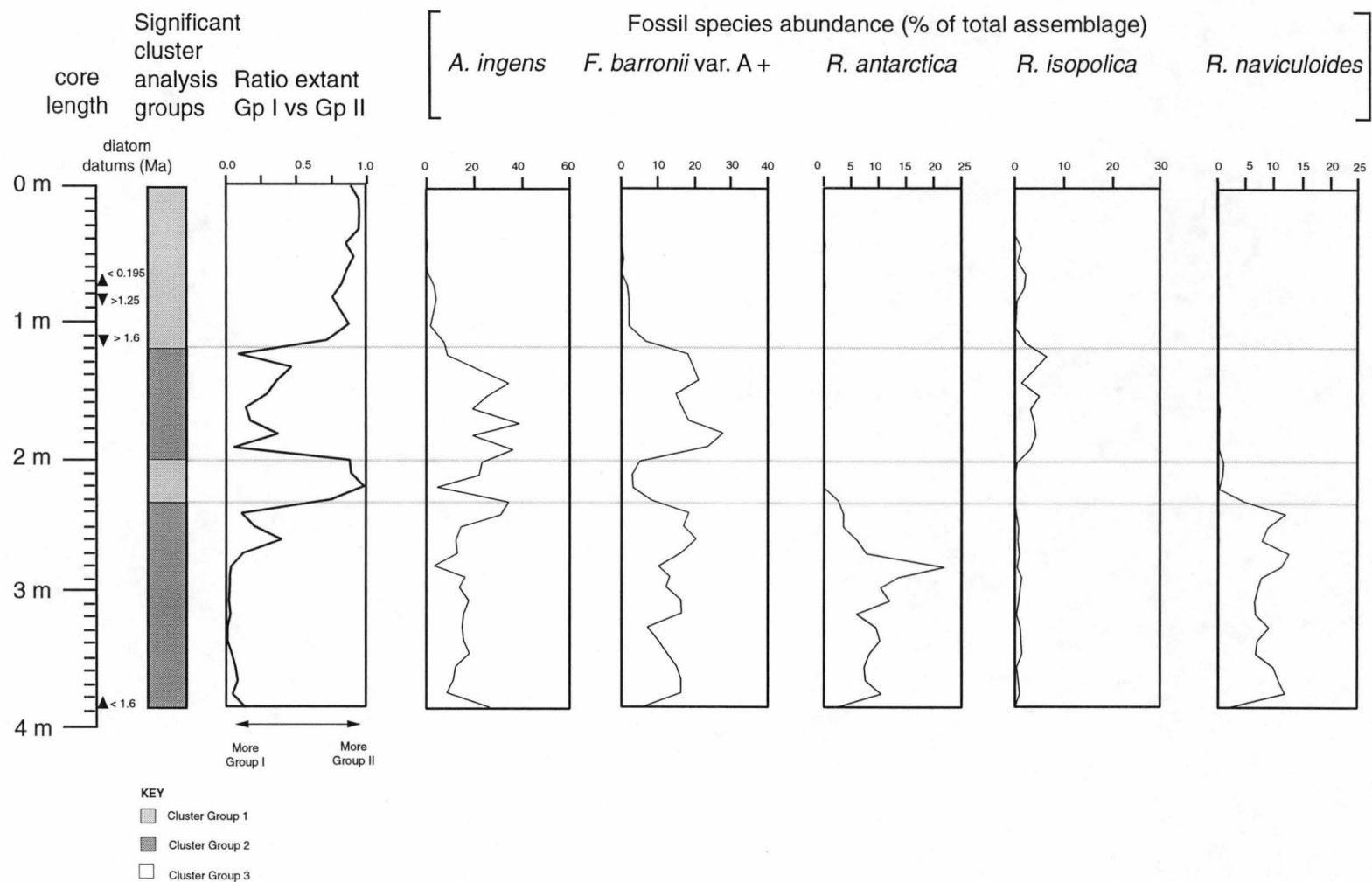


Figure 33. GC 49





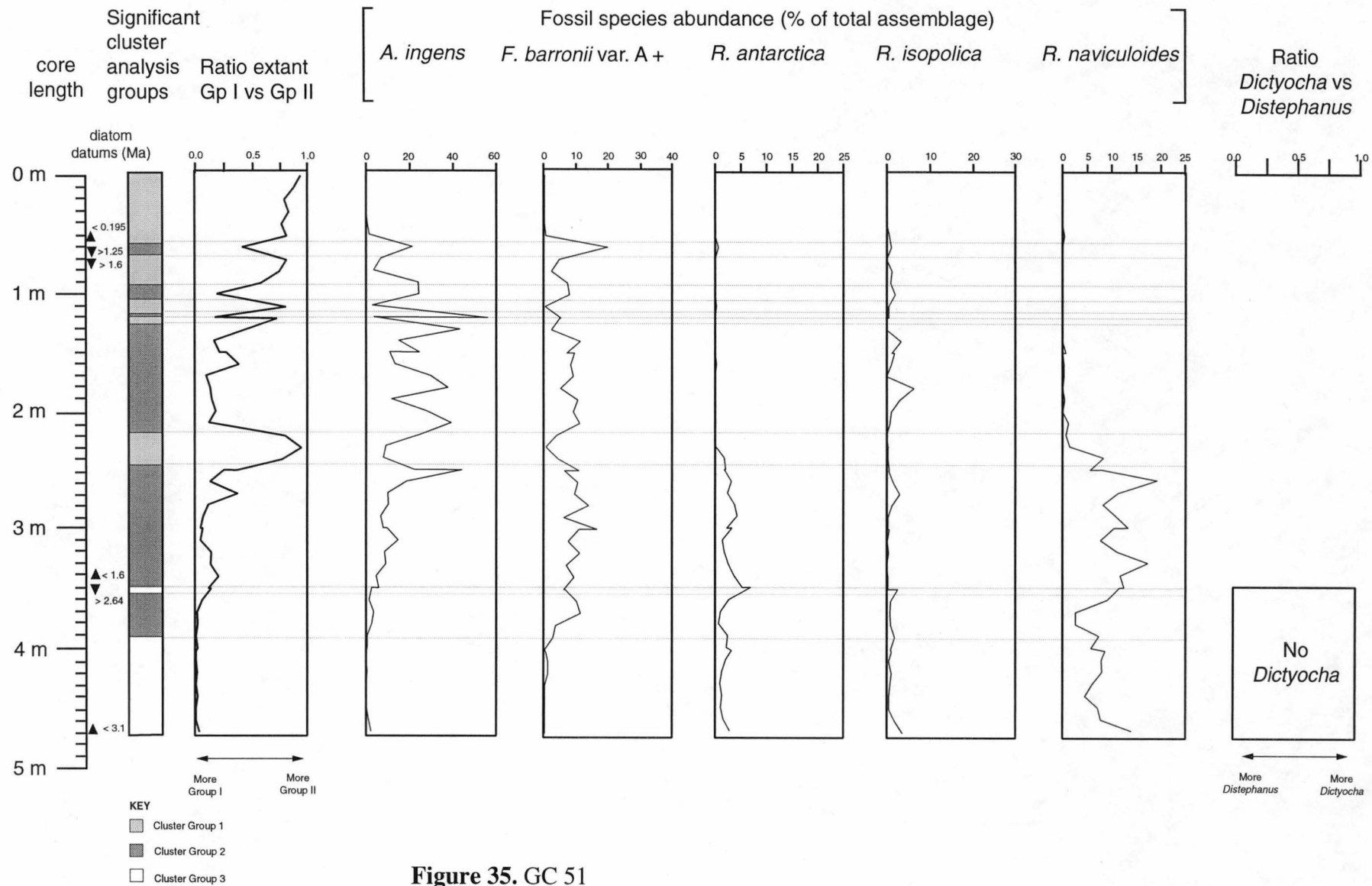


Figure 35. GC 51

## 6.3 Results

### 6.3.1 Diatom Biostratigraphy

Five diatom zones were identified in the Kerguelen gravity cores using the diatom biostratigraphic zonation defined by Harwood and Maruyama (1992). The records span minor intervals of deposition that occurred more recently than 3.2 Ma. Two diatom zones occur within the Quaternary interval: the *Fragilariopsis kerguelensis* (O'Meara) Hasle Zone and the *Thalassiosira lentiginosa* (Janisch) Fryxell Zone. A disconformity occurs between the zones, as the *T. lentiginosa* Zone was deposited <0.195 Ma, indicated by the absence of *Hemidiscus karstenii* Jousé (LAD 0.195 Ma). The underlying *F. kerguelensis* Zone was deposited >1.25 Ma, indicated by the presence of *Fragilariopsis barronii* (Gersonde) Gersonde *et* Barcena (LAD 1.25 Ma). The Quaternary / Pleistocene *F. kerguelensis* Zone spans much of the core lengths (Figures 24 to 28) and was deposited <1.25 Ma; however, the presence of *Thalassiosira fasciculata* Harwood and Maruyama (LAD 1.6 Ma), near the top of these intervals, indicates that much of the *F. kerguelensis* Zone was deposited >1.6 Ma. The bottom of these intervals is also often marked by the first appearance of *Thalassiosira elliptipora* (Donahue) Fenner (FAD 1.6 Ma), indicating that the *F. kerguelensis* Zone was deposited <1.6 Ma. These findings suggest that much of the *F. kerguelensis* Zone in the cores was deposited ~1.6 Ma. Other diatoms (e.g. *Rouxia antarctica* Heiden, *Rouxia isopolica* Schrader and *Rouxia naviculoides* Schrader) have their last appearance in the *F. kerguelensis* Zone.

Quaternary sediment disconformably overlies Pliocene sediments in all the cores except GC 49. The disconformity was evident through the absence of the Pleistocene *Thalassiosira kolbei* (Jousé) Gersonde Zone. A small interval from the *Thalassiosira vulnifica* (Gombos) Fenner Zone occurs in GC 50, but was absent from the other cores. The *T. vulnifica* Zone in GC 50 was deposited ~2.2 Ma, indicated by the presence of *T. vulnifica* (LAD 2.2 Ma) and *Thalassiosira gracilis* var. *gracilis* (Karsten) Hustedt (FAD 2.2 Ma). In GC 50, this zone overlies the *Thalassiosira insigna* (Jousé) Harwood *et* Maruyama - *T. vulnifica* Zone "a". In the other cores, the *F. kerguelensis* Zone overlies the *T. insigna* - *T. vulnifica* Zone "a". The *T. insigna* - *T. vulnifica* Zone "a" was deposited <3.1- >2.64 Ma in GC 48, GC 50 and GC 51. This is indicated by the presence of *Fragilariopsis weaveri* (Ciesielski) Gersonde *et* Bárcena (LAD 2.64 Ma) and *T. vulnifica* (FAD 3.1 Ma) in GC 48; the presence of *F. weaveri* (LAD 2.64 Ma), *T. vulnifica* (FAD 3.1 Ma) and *F. kerguelensis* (FAD 3.1) in GC 50; and the presence of *F. weaveri* (LAD 2.64 Ma) and *F. kerguelensis* (FAD 3.1) in GC 51. In GC 34, the

*T. insigna* - *T. vulnifica* Zone “a” was deposited between 3.0 - 2.64 Ma, indicated by the presence of *F. weaveri* (LAD 2.64 Ma) and *Actinocyclus actinochilus* (Ehrenberg) Simonsen (FAD 3.0 Ma). The diatom *T. fasciculata* has a documented FAD at 1.7 Ma (Harwood and Maruyama 1992); however, in this study it consistently has a first appearance in the *T. insigna* - *T. vulnifica* Zone “a”. In GC 48 and GC 34, the *T. insigna* - *T. vulnifica* Zone “a” overlies the *Fragilariopsis interfrigidaria* (McCollum) Gersonde *et* Bárcena Zone. The *F. interfrigidaria* Zone was deposited between 3.2 - 3.1 Ma, as indicated by the absence of *T. vulnifica* (FAD 3.1 Ma) and presence of *F. weaveri* (FAD 3.2 Ma) and *T. insigna* (FAD 3.2 Ma) in GC 48; and the absence of *T. vulnifica* (FAD 3.1 Ma) and presence of *T. insigna* (FAD 3.2 Ma) in GC 34.

There is considerable evidence for reworking in many of the cores. As a result, FADs are the most reliable datums. Sediment deposited during the *F. kerguelensis* Zone contains many older reworked diatoms. In GC 51 these are: *Thalassiosira torokina* Brady, *Rouxia heteropolara* Gombos, *T. kolbei*, *Thalassiosira webbi* Harwood and Maruyama, *Fragilariopsis aurica* (Gersonde) Gersonde *et* Bárcena, *Fragilariopsis praeurta* (Gersonde) Gersonde *et* Bárcena, and *T. insigna* and *Fragilariopsis praeinterfrigidaria* (McCollum) Gersonde *et* Bárcena near the Pliocene-Pleistocene disconformity. In GC 50 the reworked species are: *F. praeurta*, *F. praeinterfrigidaria*, *T. kolbei*, *T. insigna* and restricted reworking *Thalassiosira striata* Harwood and Maruyama near the Pliocene-Pleistocene disconformity. In GC 49 reworked species are: *F. praeurta*, *F. barronii*, *F. interfrigidaria*, *T. vulnifica* and *T. webbi*. In GC 48 reworked species are: *F. praeurta*, *F. praeinterfrigidaria*, *T. inura*, *Thalassiosira inura* - *insigna* (transition) Harwood *et* Maruyama, *T. kolbei*, *F. interfrigidaria*. In GC 34 reworked species are *F. aurica*, *F. barronii*, *T. insigna* and *T. inura*. Reworking has also occurred within the Pliocene, with appreciable amounts of *F. praeurta*, *F. praeinterfrigidaria* and *F. aurica* being found in younger Pliocene intervals.

### 6.3.2 Statistical Analyses

A cluster analysis dendrogram illustrating sample affinity, based upon relative abundance of extant diatoms, is illustrated in Figure 29. This dendrogram fits the data well, having a cophenetic correlation coefficient of 0.76. Three sample groups were identified, in which Group I is separated from Groups II and III, by 67.8% dissimilarity between the diatom assemblages. Group II is separated from Group III at 60.1% dissimilarity. The positions of these groups were recorded down core (Figures 31 to 35).

Indicator species abundant within these groups were identified from SNK and ANOVA, where they form distinctive assemblages (Table 3). A strong relationship exists between the assemblages in Groups I and II, which are negatively correlated ( $R^2 = -0.86$ ) through the Quaternary core intervals (Figure 30). The ratios between these assemblages were plotted down core (Figures 31 to 35). However, the temporal absence of some indicator species in the Pliocene, in particular those from Group I, causes this ratio to be less applicable to Pliocene time intervals. The Group III assemblage dominates some Pliocene intervals. Environmental information associated with the assemblage ratios was calculated from the core tops and modern Prydz Bay data in Taylor (1999), and was tabulated (Table 4).

The extinct species *Actinocyclus ingens* Rattray, *F. barronii* var. A+B, *R. antarctica*, *R. isopolica* and *R. naviculoides* had a high abundance in the Pleistocene, and their percentage relative abundance was plotted down core (Figures 31 to 35).

### 6.3.3 Silicoflagellate Data

The genus *Dictyocha* was found in Pliocene sediments from GC 48 and GC 34. It is rare in the GC 48 intervals >2.64-3.1 Ma and >3.1-3.2 Ma (maximum = 0.01%), but more abundant in the GC 34 intervals >2.64-3.0 Ma (maximum = 46%) and >3.1-3.2 Ma (maximum = 49%) (Figures 31 and 32). *Distephanus crux* also occurred in both cores, reaching its highest abundance towards the base of GC 34, where it comprised up to 13% of the silicoflagellate assemblage (Figure 31).

### 6.3.4 Lithological data

In the ship-based logs all the cores are described as being carbonate rich (O'Brien *et al.* 1993, 1995), but the percent carbonate calculated from GC 50 indicates that the lithology varies (Figure 27). The upper Quaternary interval (<0.195 Ma) contained between 19-49% total carbonate content, with a mean value of 31%. The lower Quaternary interval (between 1.25 - 1.6 Ma) contained 39-73% carbonate, with a mean value of 59%. Collectively, the Pliocene intervals (between ~2.2 - 3.1 Ma) contained 37-48% total carbonate content, with a mean value of 42%. The Pliocene intervals, however, contained a high amount of IRD, which probably decreased the total percent of carbonate.

The grain size has generally been described as clay-silt (O'Brien *et al.* 1993, 1995), and the cores contained occasional IRD (Figures 24 to 28). Indistinct bedding was identified where the sediment changed colour. The colour was also mottled in many places. The

sediment varied in structure from massive, cross bedded, to bioturbated (Figures 24 to 28). X-ray images of the cores identified more subtle lithological changes, represented by changes in sediment density (Figures 24 to 28). Considerable variation in IRD was also identified, but in general the Pliocene intervals contained a high amount of IRD. The IRD formed clast-supported layers in some cores (Figures 24 to 28). These layers often correspond with changes in biostratigraphic diatom zonations, between the Quaternary *T. lentiginosa* and *F. kerguelensis* Zones, and the Pleistocene *F. kerguelensis* and Pliocene Zones (Figures 24 to 28).

## 6.4 Discussion

### 6.4.1 Deposition and Erosion on the Kerguelen Plateau

The velocity of the ACC probably influences deposition and erosion on the Kerguelen Plateau. Biogenic deposits have accumulated on the Southern Kerguelen Plateau during interglacial and glacial intervals. During intense glacial intervals an increase in ACC velocity, due to increased winds speeds, may have created the disconformities identified in the Southern Kerguelen Plateau cores, and probably explains the fragmentary nature of the Quaternary – Pliocene sequences recovered. There are many similarities between the thickness of the sediment in the gravity cores, from the diatom zones identified in this study, to that recovered during Kerguelen Plateau Ocean Drilling Program Legs 119 and 120 (Figure 36).

The absence of diatom zones and age-diagnostic diatom species, and the formation of IRD lags visible in the core's x-ray images (Figs. 24 to 28) allow three disconformities to be identified. The disconformities formed between: 1) 1.6 - 0.195 Ma, 2) 2.2 - 1.6 Ma and 3) 3.1 - 2.2 Ma. Lags formed along some of the disconformities when high ACC velocities winnowed away the finer biogenic sediment. Cross bedding structures visible in the core logs and x-ray images indicate directional water flow, where sediment was redistributed by the ACC. This is consistent with the low, but pervasive, amount of biostratigraphic mixing identified in the cores and described in the results.

In all the cores the Quaternary can be divided into two intervals, separated by a disconformity (Figures 24 to 28). The upper interval was deposited <0.195 Ma, and the lower interval deposited between 1.6 - 1.25 Ma. The upper Quaternary member may represent deposition since the LGM, during which increased ACC velocities may have removed earlier Pleistocene deposits and contributed to lag formation.

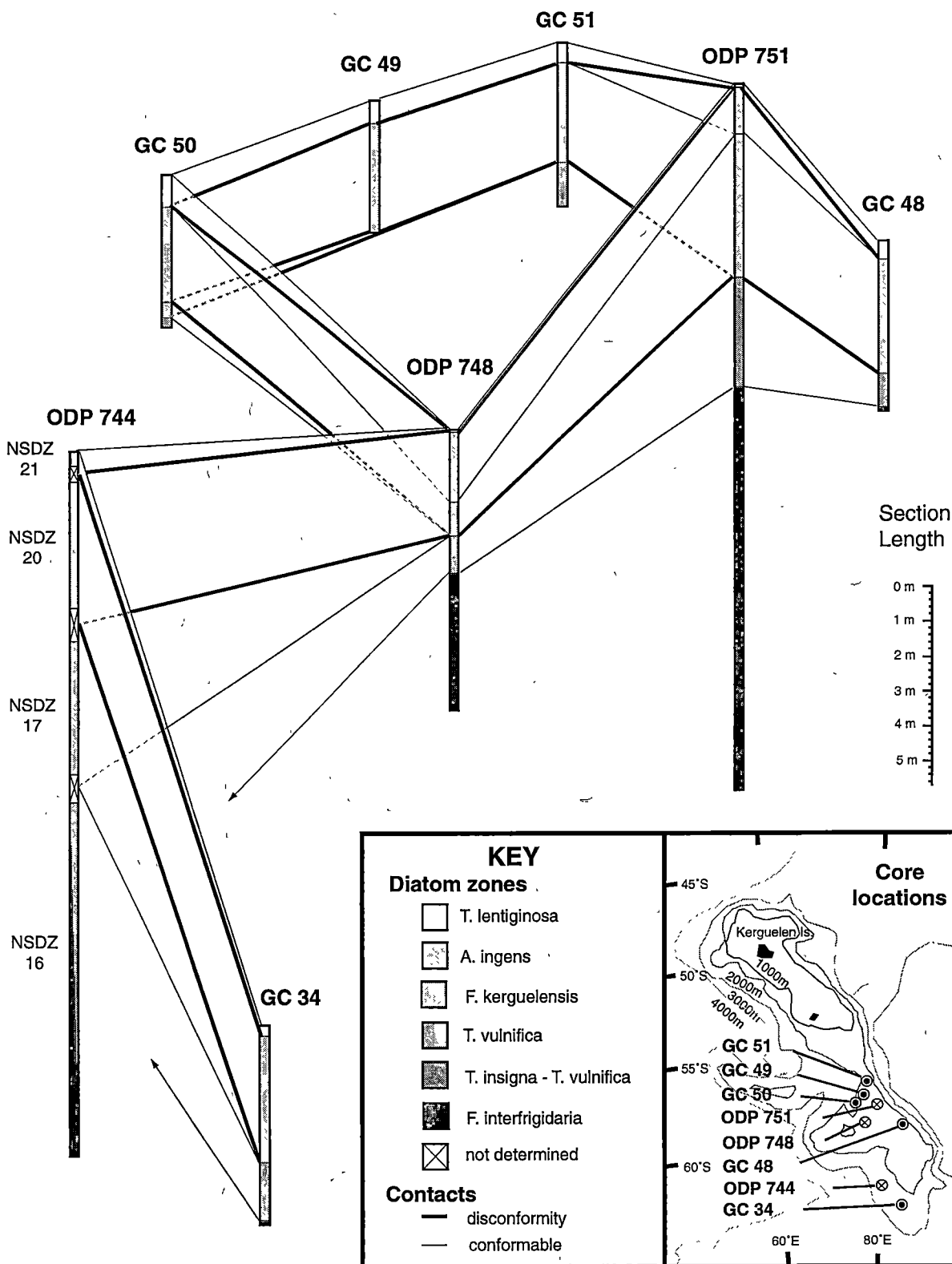


**Figure 36.** Fence diagram illustrating variation in thickness of sediment over the Southern Kerguelen Plateau. The thickness of the diatom zones in this study can be compared to those in Harwood and Maruyama (1992) (ODP Sites 751 and 748), and similar zones in Bauldauf and Barron (1991) (ODP Site 744).

However,  $^{14}\text{C}$  dating is required to verify this. Well developed lags may have formed a protective barrier, preventing the erosion of the underlying sediments.

A lag deposit formed on top of much of the Pliocene sequence, protecting it from erosion during the Pleistocene. In GC 50, this disconformity is between 2.2 - 1.6 Ma in age. It may have also been identified in ODP Site 751, where a disconformity is dated as forming 2.2 - 1.9 Ma (Rack and Palmer-Julson 1992). During the period 2.7 - 1.0 Ma, there was an increase in Antarctic Bottom Water (AABW) production, and an intensification in Circumpolar Deep Water (CPDW) and ACC velocity, creating hiatuses at deep and shallow depths throughout the Southern Ocean (Ciesielski and Grinstead 1986; Ledbetter and Ciesielski 1986). On the Maurice Ewing Bank, increased ACC velocity caused regional disconformities and removed sediments between 2.0 - 1.0 Ma in age (Ciesielski *et al.* 1982). This has been associated with glacial conditions that peaked 1.2 - 1.0 Ma (Ciesielski *et al.* 1982). The degree of erosion on the Maurice Ewing Bank suggests that this is when the ACC obtained its highest velocities (Ciesielski *et al.* 1982), creating a thick IRD lag that protected the underlying sediment from further erosion (Ciesielski and Wise 1977; Ciesielski *et al.* 1982; Wise *et al.* 1992). The formation of this lag has been also tentatively correlated with the age of the greatest glaciation that has occurred in Patagonia ~1.0 - 0.7 Ma (Ciesielski *et al.* 1982), and may correlate with the Pliocene-Pleistocene disconformity found throughout the Southern Kerguelen Plateau.

Clast-supported, lag-like layers in the Pliocene intervals from GC 34, GC 48 and GC 50 provide evidence that the ACC velocity fluctuated throughout the Pliocene. This is supported by the absence of the *T. insigna* - *T. vulnifica* Zone “b” in GC 50, where the disconformity formed between 2.2-3.1 Ma. It may correspond with a disconformity that formed nearby in the South Indian Ocean due to changes in the ACC or Circumpolar Deep Water (CDW) 2.0-3.4 Ma (Osborn *et al.* 1983). High IRD concentrations throughout the Pliocene intervals recovered from the Southern Kerguelen Plateau may also represent hiatuses or reduced deposition rates. This could explain the small amount of sediment identified in the Pliocene diatom zones. High amounts of IRD could also represent a greater presence of icebergs over the Kerguelen Plateau at these times. Antarctica may have had a more temperate glacial environment >2.6 Ma (Webb and Harwood 1991, 1993; Harwood *et al.* 1991, 1992; Moriwaki *et al.* 1992a; Wilson 1995), which would have caused higher ice flow rates and erosion, and produced more sediment-laden icebergs, than during later colder conditions <2.6 Ma. High IRD deposition at the Kerguelen Plateau would require that the ice shelf grounding line be situated close to the shelf break



to prevent the loss of basal debris by basal melting processes before calving (Ehrmann *et al.* 1992). This may suggest that East Antarctic ice shelves, such as the Amery Ice Shelf, were reduced in extent during the Pliocene. Reduced Amery Ice Shelf conditions in the Pliocene is supported by direct evidence from the Pagodroma Group, in the Prince Charles Mountains (Chapter 8).

#### **6.4.2 Sediment Composition**

The cores consist mostly of calcareous-siliceous ooze. Variations in total calcium carbonate were measured down GC 50; the variation is also reflected in down core density changes. Darker intervals of sediment identified from x-ray imagery correspond with denser sediment, which are generally intervals with lower carbonate content. The relative amount of terrigenous sediment, which also depresses carbonate values, is reflected in the amount of IRD in the x-ray images (Figures 24 to 28). It is therefore reasonable to assume that low carbonate and low IRD intervals probably contain higher amounts of biogenic silica.

The density changes seen in the core x-ray images reflect fluctuation in the amount of biogenic silica versus carbonate deposition. The latitudinal change, from southern siliceous sedimentation to more northern calcareous sedimentation, and the deposition of calcareous sediments at shallow depths above the CCD have been discussed earlier (Chapter 6.1.2). The fluctuation in the relative amount of these biogenic sediments has been used to illustrate front movements and / or changing environmental gradients across the APFZ (Burckle *et al.* 1996). Evidence for oceanographic changes over the Kerguelen Plateau based on sediment composition will be discussed in the following section with the diatom evidence for similar changes.

#### **6.4.3 Oceanographic Changes**

##### Extant Diatom Assemblages

Only a small fraction of the living diatom assemblage is preserved in the fossil record due to dissolution (Chapter 5.4.2). Across the Southern Ocean there is a large dissolution gradient (Pichon *et al.* 1992), which is lowest (~20%) in the productive waters of the APFZ but increases greatly to both the north and south (Pichon *et al.* 1992). That portion of the living assemblage that does become preserved in the sedimentary record can be analysed statistically to identify past oceanographic conditions (Martinez-Macchiavello *et al.* 1996; Pichon *et al.* 1987; Cunningham *et al.* 1999). In this study, diatom assemblages have been identified from SNK and ANOVA, based on the Bray-Curtis cluster analysis

groups. The environmental conditions that they represent have been identified through literature review (Table 3). The modern ecology and distribution of the indicator species in Groups I, II and III suggest that they belong to the assemblages below.

*Assemblage I: Interglacial Antarctic open water assemblage.*

Assemblage I contains abundant *Fragilariopsis kerguelensis*, *F. separanda* Hustedt and *Thalassiosira gracilis* var. *gracilis* (Karsten) Hustedt, which are abundant in the modern Antarctic open water assemblage (Table 3). Some species identified in assemblage 1 have not been recorded previously as indicative of modern, Antarctic open water conditions. These include *Azpeitia tabularis* (Grunow) Fryxell *et al.* Sims, which is generally more abundant in Subantarctic assemblages (Pichon *et al.* 1987), *Navicula directa* (Smith) Ralfs in Pritchard, which generally occurs in coastal benthic assemblages (Whitehead and McMinn 1997) and in high abundance in saline lakes (Roberts and McMinn 1999), and *Actinocyclus actinochilus* (Ehrenberg) Simonsen, which has been called both a sea-ice (Pichon *et al.* 1987) and an Antarctic open water species (Taylor *et al.* 1997).

It is likely that *A. tabularis* has been identified as part of the Antarctic open water assemblage in the present analysis because the Subantarctic assemblage is not represented (Table 3). The abundance of *N. directa* is low in all of the study groups, and although it is statistically more abundant in the Antarctic open water assemblage, it is not a good indicator species. *Navicula directa* has been found in both modern sea-ice and water samples (near ice and in open water areas) (Hsiao 1980; Ligowski 1987; Ligowski *et al.* 1988; Tanimura *et al.* 1990; Kang and Fryxell 1993; McMinn and Hodgson 1993). The distribution of *A. actinochilus* spans both sea-ice and open water habitats, where summer sea-surface temperatures range between -2°C and 2°C (Zielinski and Gersonde 1997). Its maximum abundance occurs where summer sea-surface temperatures are between -1.0°C and 0.5°C (Zielinski and Gersonde 1997), and it is possibly a cool water species (Armand 1997) associated with the sea-ice edge (Medlin and Priddle 1990). It has been found in newly formed sea-ice (Tanimura *et al.* 1990; Garrison and Close 1993), fast-ice and pack-ice (Horner 1985; Krebs *et al.* 1987; Garrison and Buck 1989; Garrison 1991). The sedimentary distribution of *A. actinochilus* suggests that it is a sea-ice species (Pichon *et al.* 1987); however, in surface sediment assemblages it has been shown to increase seaward of Prydz Bay (Stockwell *et al.* 1991), where it has been identified as part of the Antarctic open water assemblage (Taylor *et al.* 1997). These latter observations are consistent with its occurrence here with other Antarctic open water species.

*Assemblage II: Glacial pack-ice associated assemblage.*

The most abundant species in assemblage II, *F. curta*, is characteristic of the modern sea-ice assemblages (Kozlova and Mukhina 1967; Pichon *et al.* 1987; Stockwell *et al.* 1991; Leventer 1992; Taylor *et al.* 1997; Zielinski and Gersonde 1997). Although *F. curta* can be locally abundant near the seasonal sea-ice edge (Garrison *et al.* 1982; Fryxell 1989; Kang and Fryxell 1993), it is generally most abundant in sediments beneath areas with high summer sea-ice concentrations (Kozlova 1966; Truesdale and Kellogg 1979; DeFelice and Wise 1981; Taylor *et al.* 1997). Other species in assemblage II also occur in the modern sea-ice assemblages, such as *Fragilariopsis sublinearis* Hustedt and *Nitzschia peragallii* Hasle (Table 3).

The second most abundant species in assemblage II is *T. lentiginosa*, which has its highest abundance in modern Antarctic open water assemblages (Kozlova and Mukhina 1967; Abbott 1974; Pichon *et al.* 1987; Taylor *et al.* 1997). Other *Thalassiosira* spp. are also abundant in assemblage II (Table 3). The genus is generally associated with open water (Hasle and Heimdal 1968; El-Sayed 1971; Kellogg and Kellogg 1987; Leventer and Dunbar 1987, 1988; Fryxell and Kendrick 1988; Leventer 1992, 1998; Kang and Fryxell 1993). It is uncommon in sea-ice (Garrison and Buck 1985; Fryxell and Kendrick 1988; Leventer and Dunbar 1988, 1996; Dunbar *et al.* 1989; Zielinski and Gersonde 1997), as a maximum abundance of only 0.5% has been observed in sea-ice samples from McMurdo Sound (Leventer and Dunbar 1987). In general, *Thalassiosira* are open water diatoms, with the exception of *Thalassiosira australis* Peragallo, which is a dominant species beneath areas of snow-free fast-ice (McMinn 1996).

It has been suggested that *Thalassiosira* spp. are generally absent in and beneath sea-ice because they are inhibited by low light (Fryxell *et al.* 1987; Leventer 1998). *Thalassiosira scotia* Fryxell *et* Hoban, for example, has a high saturation irradiance and does not develop photoinhibition in high light conditions (Rivikin and Putt 1987). Blooms of *Thalassiosira* in the open waters of the Terra Nova Bay polynya are consistent with this. The polynya has a shallow mixing layer that can maintain diatoms in the shallow, high light, environment (Arrigo, pers. comm. 1998). In contrast, deeper mixing in the Ross Sea Polynya may be the cause of *Thalassiosira* being absent from here, and *Phaeocystis* sp. dominating (Arrigo, pers. comm. 1998). *Thalassiosira*, and *Phaeocystis*, have been described as opportunistic in open water areas, decreasing the relative abundance of sea-ice associated *Nitzschia* and *Fragilariopsis* spp., which may prefer low light conditions (Garrison and Buck 1985).

The mixture of sea-ice and open water species in assemblage II may reflect the sea-ice assemblage under which it formed. Today, mixed assemblages occur in sediments deposited beneath the SIZ, where the seasonal change from sea-ice to open water creates a succession in the diatom assemblages. The dominant diatoms (*F. kerguelensis* and *F. curta*) from assemblages I and II are negatively correlated in the modern environment (Burckle *et al.* 1987; Won Hyung *et al.* 1991; Leventer 1992). However, assemblage II contains a mixed assemblage of species that co-vary in abundance opposite to that which would be expected in modern plankton and surface sediment assemblages. Assemblage II is dominated by sea-ice associated *F. curta*, and contains a lesser amount of the sea-ice species *F. sublinearis* and *F. peragallii*. However, the assemblage contains a high abundance of Antarctic open water diatoms such as *T. lentiginosa* and other *Thalassiosira* spp., which co-vary unexpectedly with the sea-ice species.

The high abundance of sea-ice diatoms in assemblage II from the Southern Kerguelen Plateau may represent deposition during glacial intervals. Sea-ice diatoms are currently rare in abundance over the plateau, as indicated by the core top data (Appendix 3). During glacial intervals, such as the Last Glacial Maximum (LGM), sea-ice may have extended out to lower latitudes (Hays *et al.* 1976; CLIMAP 1981; Cooke and Hays 1982) and covered the Southern Kerguelen Plateau. As a result, the proportion of sea-ice diatoms in the underlying sediments at these, and more northern latitudes, increased (Armand 1997). Previous studies (Hays *et al.* 1976; CLIMAP 1981; Cooke and Hays 1982) have not commented in detail on the structure of the sea-ice habitat beyond the Antarctic continental margin during such intervals. Near the continental margin, a closed cover of multiyear sea-ice may have developed, reducing light penetration and decreasing diatom productivity (Grobe and Mackenson 1992). Today in areas where there is a closed cover of multiyear sea-ice a fast-ice diatom assemblage develops, and the underlying sediment is dominated by *F. curta* (e.g. Stockwell *et al.* 1991; Taylor *et al.* 1997).

During glacial intervals, both the diatom assemblages and summer sea-ice habitat over the Southern Kerguelen Plateau may have differed from those around the Antarctic margin today. Modern phytoplankton are most active during the spring-summer (Medlin and Priddle 1990) when modern sea-ice is south of the Antarctic Divergence (AD) (Bryan 1993). Ekman divergence and surface water currents cause convergent sea-ice drift, which creates congested pack-ice conditions around the Antarctic coast (Davis and McNider 1997; Watkins and Simmonds 1998). During glacial intervals, summer sea-ice

cover may have remained north of the AD (and the Kerguelen Plateau) (Hays *et al.* 1976; CLIMAP 1981; Cooke and Hays 1982). The structure of the summer sea-ice habitat here may have been analogous to today's winter sea-ice maximum. Modern winter sea-ice extends further north, beyond the AD, where it is affected by eastward wind stress (Watkins and Simmonds 1998). Strong circum-antarctic wind and wave activity facilitates sea-ice breakup causing pack-ice to form around the northern edge of the sea-ice zone above the AD. Here the surface water currents push the pack-ice further northward, causing it to become less concentrated with dispersion and melting, creating open pack-ice conditions (Watkins and Simmonds 1998). The open pack-ice is also more susceptible to atmospheric and oceanic forcing (Watkins and Simmonds 1998).

If the sea-ice edge was north of the AD during glacial intervals, summer pack-ice at the northern ice-edge could have been less concentrated than that around the Antarctic coastline in summer today. A habitat with less concentrated pack-ice could have supported a mixed diatom assemblage similar to assemblage II. The loose pack-ice would support sea-ice diatoms (e.g. *F. curta*), with open water species (e.g. *Thalassiosira*) in the intervening shallow-mixed, open-water areas. These findings are important for sea-ice reconstruction north of the AD based on diatoms. The formation of mixed assemblages north of this region during past sea-ice conditions suggest that modern analogues do not directly apply to records north of the AD.

----- Different sea-ice conditions may largely explain the presence of different open water species observed between assemblages I and II. Due to its high light preference, it is possible that *Thalassiosira* out competes other open water species in the shallow-mixed surface waters produced by melting pack-ice. Such conditions probably formed in an open pack-ice habitat during the deposition of assemblage II. It is possible the open water species abundant in assemblage I (e.g. *F. kerguelensis*, *F. separanda*, and *T. gracilis*), may have a lower light requirement, giving them a competitive advantage over *Thalassiosira* in ice free areas where the mixing layer is deeper. Open water, deep-mixing probably occurred during the deposition of assemblage I.

### *Assemblage III: Pliocene interglacial Antarctic open water assemblage.*

Many of the indicator species in assemblage III, such as *D. antarcticus*, *Thalassiosira maculata* Fryxell *et* Johansen, *Thalassiosira oestrupii* (Ostenfeld) Hasle, *Trichotoxon reinboldii* (Van Heurck) Reid *et* Round, and *Thalassionema* spp., are abundant in the modern Antarctic open water assemblage (Table 3). The habitat preference of

*Fragilariopsis ritscheri* Hustedt is unclear, but a review of previous work on this species suggests that it is generally found in the Antarctic zone (Armand 1997) in sediment beneath areas where the summer sea-surface temperature is  $<5^{\circ}\text{C}$  (Zielinski and Gersonde 1997) (Figure 21c). This zone is covered by seasonal sea-ice and permanent open water, and is within the region where the Antarctic open water assemblage occurs.

Assemblage III is exclusive to the Pliocene interval in the cores. It is possibly a temporal assemblage that has formed in the absence, or low abundance, of assemblage I indicator species in the Pliocene. These include: *F. kerguelensis* (FAD 3.1 Ma), *A. actinochilus* (FAD 3.0 Ma) and *T. gracilis* (FAD 2.2 Ma) (Harwood and Maruyama 1992). It is most likely that assemblage III is the extant part of the Antarctic open water assemblage that existed before the assemblage I species evolved or became abundant.

#### Palaeoenvironmental Variations amongst Extant Diatom Data

The cluster analysis sample groups were plotted down core to illustrate palaeoenvironmental variations (Figures 31 to 35). Quaternary intervals deposited  $<0.195$  Ma, or possibly after the LGM, were dominated by open water conditions similar to that over the Kerguelen Plateau today (assemblage I). The intervals deposited between 1.6 - 1.25 Ma were influenced largely by sea-ice (assemblage II); however, brief, warmer open water intervals also occurred. The ratio between assemblages I and II down core assist in quantifying Quaternary summer sea-surface temperature, salinity and sea-ice concentrations. Oceanographic conditions in the late Quaternary interval ( $<0.195$  Ma) appear similar to today.

During the earlier Quaternary interval (between 1.6 - 1.25 Ma) the dominance of assemblage II (Group II intervals in Figures 31 to 35) provides evidence for glacial conditions. In these intervals, the ratio between assemblages I and II are comparable to modern shelf (0.06) and shelf break (0.36) values (Table 4). The results suggest that summer (January-February) sea-surface temperatures ranged between  $-0.6^{\circ}$  and  $-1.1^{\circ}\text{C}$ , salinity between 33.6-34.0‰, and pack-ice concentrations between 6-18%. As discussed above, modern analogues may not apply to sea-ice reconstruction north of the AD. However, the ratio between assemblage I and II in the Kerguelen cores (in the intervals dominated by assemblage II), occurs between modern Prydz Bay continental shelf and shelf break ratios. Sea-ice diatoms and Antarctic open water diatoms dominate the continental shelf and shelf break of Prydz Bay, respectively, today (Taylor *et al.*, 1997).

Therefore, the intermediate ratios obtained on the Kerguelen Plateau may reflect open pack-ice conditions, which could have created assemblage II.

The diatoms *R. antarctica* and *R. naviculoides* became extinct during a warm period recorded ~1.6 Ma in each of the cores. The similar time suggests that the Quaternary records in all of the cores can be correlated, and their palaeoclimatic records can be compared. Latitudinal differences in the study region's environment must be considered though. The effect that warming had ~1.6 Ma at each core location declines southward. This is visible in all the cores during the warming interval associated with the decline in *R. antarctica* and *R. naviculoides* (Figures 31 to 35). There is a reduction in the warm, open-water assemblage I versus the sea-ice associated assemblage II in this interval with increasing latitude. Throughout this distinct interval warmer open-water conditions were statistically dominant (in the cluster analysis results) over pack-ice conditions, with the exception of the most southern and coldest site (GC 34). Much of the interval between 1.6 – 1.25 Ma, on the Kerguelen Plateau, was dominated by sea-ice conditions and climate cyclicity. This is consistent with conditions in the Weddell Sea (1.6 - 0.7 Ma), characterised by cooling conditions and the dominance of sea-ice, but with a pronounced climatic cyclicity (Abelmann *et al.* 1990). The Quaternary intervals between 1.6 - 1.25 Ma correlate over a north-south distance ~770 km, along the Southern Kerguelen Plateau. Although the interval is only a few metres thick, the formation of an IRD lag formed a protective barrier on top of the deposit, preventing erosion.

The Pliocene cluster analysis Groups II and III identify pack-ice and open-water conditions respectively. In GC 50, assemblage II dominated ~2.2 Ma, suggesting that pack-ice was present during summer. Intermittent open-water and pack-ice during summer 3.1 - 2.64 Ma is inferred from all sites, except GC 49. At the most northern location, GC 51, the top of the interval between 3.1 - 2.64 Ma is dominated by assemblage III, suggesting that in summer open-water dominated. The oldest part of this interval, further down GC 51 is dominated by assemblage III, suggesting predominately open water conditions during summer. Similar trends are visible further south, in intervals deposited 3.1 - 2.64 Ma (GC 50 and GC 48) and 3.0 - 2.64 Ma (GC 34). However, the upper warm interval from GC 51 is lacking. In GC 50, GC 48 and GC 34 the later part of this interval is dominated by summer pack-ice, but earlier open-water conditions are evident with the dominance of assemblage III. Open water could have also occurred between 3.2 - 3.1 Ma, as assemblage III is dominant during this interval in GC 34 and GC 48.

### Pliocene Palaeoceanography - Silicoflagellate Data

Silicoflagellate data indicate that significant warming accompanied some of the Pliocene open water intervals. During these intervals the APFZ either moved southward or the temperature gradients across associated ocean fronts became shallower.

The open water interval >2.64- <3.0 Ma in GC 34 contains appreciable amounts of *Dictyocha* (Figure 31). The occurrence of *Dictyocha* spp in GC 34, at 62° S, could have only occurred if the APFZ was either ~1200 km further south or the temperature gradients across associated ocean fronts became significantly shallower. Only rare amounts of *Dictyocha* were found 3.1 - 2.64 Ma in GC 48, which probably represents a different interval to that preserved in GC 34. The maximum abundance of *Dictyocha*, 3.0 - 2.64 Ma, in GC 34 (46%) suggest that the summer sea-surface temperature was 5°C, which is 4.5°C warmer than today.

Warmer conditions also occurred on the Kerguelen Plateau 3.0-3.1 Ma, evident from diatom (Barron 1996) and coccolithophorid (Barron 1996; Bohaty and Harwood 1998) data from Site 751, which suggest that the summer sea-surface temperature was 3° to 4°C warmer than today (Barron 1996). Similar data obtained through out the Southern Ocean (DSDP 266, ODP 699A, ODP 747A and *Eltanin* Core 50-28), suggest that a 1.2° to 4.0°C warming occurred between 3.1 - 2.9 Ma (Barron 1996). Furthermore, it has been proposed that major warming <3.1 Ma caused East-Antarctic Ice Sheet reduction to a third of its present size (Harwood 1983; Webb *et al.* 1983, 1984; Harwood 1986a; Webb and Harwood 1991). This event may be contemporaneous with summer sea-surface temperatures 4.5°C warmer than today, 3.0 - 2.64 Ma at 62° S, evident in GC 34.

Evidence for late Pliocene warming, like that in GC 34, could be largely absent from other Southern Ocean records due to erosion from AABW and ACC flow during later glacial intervals. Disconformities could exist in GC 34, 48 and 50, removing all or some of the sediments deposited between 3.1 - 2.64 Ma (as mentioned above). Deep sea  $\delta^{18}\text{O}$  evidence from the South Atlantic (ODP 704 and 701) indicates that cool conditions peaked at 2.63 Ma and ~2.9 Ma (Hodell and Warnke 1991) and may have caused erosion on the Kerguelen Plateau. It is also likely that erosion accompanied the onset of bipolar glaciation 2.6 - 2.4 Ma, as noted from disconformities in the Weddell Sea (Abelmann *et al.* 1990). Erosion could explain why the late Pliocene sections recovered from the Southern



Kerguelen Plateau are so short (e.g. <1.7 m thick in GC 34), but sometimes span large time intervals (e.g. ~600 000 years in duration in GC 34).

High abundance of *Dictyocha* was also found in the GC 34 interval between 3.2 - 3.1 Ma. The *Dictyocha* to *Distephanus* ratio in GC 34 indicates that summer sea-surface temperatures peaked at around 5°C, causing an approximately 4.5 C° warming relative to today. This warming coincides with a high amount of *D. crux* (13%), which reaches similar percentages in ODP 751 during an older warming interval ~4.3 Ma (Bohaty and Harwood 1998). However, diatom biostratigraphy suggests that these warming events are unrelated to each other.

#### Lithology and Carbonate Compensation Depth

The Quaternary diatom assemblage changes within GC 50 do not correspond with the observed lithology changes (Figure 27); the interglacial, Antarctic open water assemblage (assemblage I) dominates the upper Quaternary intervals (<0.195 Ma). The total percentage of carbonate measured at intervals within GC 50 indicates that less carbonate was deposited during this interval than in those associated with pack-ice conditions between 1.6 - 1.25 Ma (Figure 27). This is assumed to be the case in all cores, based on sediment density determined by x-ray analysis, as discussed above. Results indicate that the CCD was deeper in the early Quaternary (between 1.6 - 1.25 Ma), resulting in higher carbonate deposition. Alternatively, the physiology of calcareous organisms may have differed from today during this interval, enabling them to produce carbonate at colder temperatures. The atmospheric CO<sub>2</sub> concentrations could also have been different, altering the amount of carbonate production in the surface waters. The ability to change CCD depth, independent of temperature, complicates palaeoenvironmental interpretations based on the relative total percentage of carbonate and requires further investigation.

#### **6.4.4 Palaeoenvironmental Preference of Extinct Diatoms**

The ecology of extinct Southern Ocean diatoms is poorly understood, due to the obvious lack of living material and the inability to reconstruct past surface distributions from their patchy temporal and spatial records. The lack of data makes the interpretation of old palaeoenvironmental records difficult as they become dominated increasingly by extinct species. Where the temporal distribution of extinct species overlaps with those living today, however, the ecology of the extinct species can be estimated. The findings can then be applied to older records that do not contain many, if any, extant species.

Where extinct Southern Ocean diatoms extend into the Pleistocene interval dominated by extant species, it is possible to compare the two. The relative abundance of extinct taxa (*A. ingens*, *F. barronii* var. A+B, *R. isopolica*, *R. antarctica*, and *R. naviculoides*) is compared to the ratio of extant diatoms between assemblages I and II, and to the ratio of *Dictyocha* to *Distephanus* from the Pliocene interval (Figures 31 and 32). The relative abundance of *A. ingens* and *F. barronii* var. A+ B fluctuate throughout the Pleistocene (Figures 31 and 35), but neither appear to correlate with fluctuations in the extant Antarctic open water nor pack-ice associated assemblages. Other factors may influence their abundance. The result may reflect preferential preservation of *A. ingens*, due to its heavy silicification, or it may be an artifact of the data, due to loss of *R. antarctica* and *R. naviculoides* from the upper part of the record altering the relative abundance of the remaining species. This latter point may also have affected the relative abundance of *R. isopolica*, which tends to be more abundant in colder intervals where *R. antarctica* and *R. naviculoides* are absent. The abundance of *R. antarctica* and *R. naviculoides* is high during the lower cold, pack-ice associated, Pleistocene intervals across all the cores. Both decline during the first warmer Pleistocene open water interval and do not return during later Pleistocene cold intervals. This probably represents the localised extinction of these species from the Southern Kerguelen Plateau.

*Rouxia antarctica* and *R. naviculoides* have been described as having a Southern Ocean distribution, becoming more abundant in the late Pliocene and preferring waters south of the APF (Abelmann *et al.* 1990). Their high abundance with extant diatoms in assemblage II, during the lower Pleistocene core intervals, suggests that they were associated with low concentrations of pack-ice. However, during warm Pliocene intervals when the summer SST at GC 34 was approximately 5°C (indicated by the ratio of *Dictyocha* to *Distephanus*), their abundance increased. The opposing response of these species to warm and cold temperature proxies suggests that factors other than temperature greatly affected their distribution. Two hypotheses are discussed below to offer an explanation for the variation in *R. antarctica* and *R. naviculoides*:

- 1) *Rouxia antarctica* and *R. naviculoides* abundance may have been higher where salinity was low. Low salinity is associated with summer pack-ice melt (Smith and Nelson 1986; Knox 1994) and may explain the high abundance of *R. antarctica* and *R. naviculoides* with the Pleistocene pack-ice associated diatoms in assemblage II. However, low surface water salinity could have also occurred in open water areas during Pliocene warming. The salinity may have been lowered by warmer glacial conditions in Antarctica, during which

there would have been increased ice sheet melt and a greater iceberg influence in the surrounding marine environment. The high amount of IRD over the Southern Kerguelen Plateau during the Pliocene supports the enhanced presence of melting icebergs during these warm intervals. This may have lowered surface water salinity and caused an increase in *R. antarctica* and *R. naviculoides*. If the abundance of *R. antarctica* and *R. naviculoides* was salinity dependent, they could have occurred over the Kerguelen Plateau during warm (Antarctic, wet-based glacial conditions and increases iceberg release) and cold (sea-ice influenced) conditions.

2) *Rouxia antarctica* and *R. naviculoides* are both raphid pennate diatoms. Raphid valves in some extant diatoms are associated with motility on a benthic substrate (Hopkins 1966; Drum 1969; Pickett-Heaps *et al.* 1986; Lee 1989). Sea-ice and icebergs are thought to provide a substrate for some modern benthic diatoms found in sea-ice (e.g. *Pinnularia quadratarea* (Østrup) Heiden) (Krebs *et al.* 1987; Tanimura *et al.* 1990), and could have therefore provided a substrate for *R. antarctica* and *R. naviculoides*. The presence of sea-ice is related directly to sea-surface temperature, but icebergs can indicate a variety of climatic conditions (Mikhail and Saltzman 1994); one of these being warmer than today with greater Antarctic ice outflow and iceberg formation. If *R. antarctica* and *R. naviculoides* were benthic on ice, they could have occurred over the Kerguelen Plateau during warm (Antarctic, wet-based glacial conditions and increases iceberg release) and cold (sea-ice influenced) conditions.

---

#### 6.4.5 Diatom Biostratigraphy

Difficulties were encountered in this study with the application of the diatom zonations of Harwood and Maruyama (1992). They place the FAD of *T. fasciculata* at 1.7 Ma; however, it appears 6.0 - 5.1 Ma in their data from ODP Site 751A. Due to this uncertainty, the FAD for this species has not been used as a biostratigraphic marker in the present study.

*Fragilariopsis praecurta* has a LAD of ~1.6 Ma and appears consistently throughout part of the Pliocene, <3.2 Ma, and the lower part of the Pleistocene (*F. kerguelensis* Zone), ~1.6 Ma. This contrasts with Harwood and Maruyama's (1992) LAD of 3.6 Ma for *F. praecurta*. It is possible that this species has been reworked into the Kerguelen Plateau sediment; however, its abundance as a reworked fossil would be expected to decline through the record with time. Instead, its abundance fluctuates at times up to 6%. It may

be possible, however, that *F. praecurta* has been misidentified with some specimens of *Fragilariopsis separanda* var. A in the present study.

*Fragilariopsis praeinterfrigidaria* occurs consistently within the *T. insigna* - *T. vulnifica* Zone “a”, with a LAD 3.0 - 2.64 Ma. This contrasts with its published LAD of 3.5 Ma (Harwood and Maruyama 1992). In the present study, *F. praeinterfrigidaria* may have been reworked. As observed with *F. praecurta*, the abundance of *F. praeinterfrigidaria* fluctuates and formed up to 12% of the total diatom assemblage in some samples. It is possible that the LAD of *F. praeinterfrigidaria* is less than the published 3.5 Ma in Harwood and Maruyama (1992), but further investigation will be required to confirm this.

*Rouxia antarctica*, *R. isopolica* and *R. naviculoides* have their last appearance in the *F. kerguelensis* Zone ~1.6 Ma. In all cores studied here, the LAD of *R. antarctica* and *R. naviculoides* occurs within the interval dated at ~1.6 Ma. In GC 51, GC 49, GC 48, and GC 34, the LAD of *R. isopolica* is 1.25-1.6 Ma. Abbott (1974) identified *Rouxia* spp. in the *T. lentiginosa* Zone (Harwood and Maruyama 1992). *Rouxia leventerae* Bohaty *et al.* has also been identified in the *T. lentiginosa* Zone of CRP-1, with *R. antarctica* having a last appearance in the *T. ingens* Zone (Bohaty *et al.* 1998). It is proposed here that the LAD of *R. antarctica* and *R. naviculoides*, at ~1.6 Ma, and *R. isopolica*, between 1.6 - 1.25 Ma, on the Kerguelen Plateau represents the localised extinction of these species from the northern region of the Southern Ocean. Given the persistence of *R. antarctica* closer to Antarctica <1.6 Ma (in Bohaty *et al.* 1998), further work is required to refine the Southern Ocean diatom biostratigraphic framework and to separate temporal and biogeographical influences.

## 6.5 Summary

Quaternary and Pliocene palaeoclimatic conditions have been studied using five gravity cores from the Southern Kerguelen Plateau. They have been dated by diatom biostratigraphy, and the palaeoclimate reconstructed. Results indicate that two Quaternary intervals and three Pliocene intervals are present, and at least three disconformities have formed <3.2 My ago. Three extant diatom assemblages are identified: assemblage I (an interglacial Antarctic open water assemblage), assemblage II (a glacial pack-ice associated assemblage), and assemblage III (a Pliocene interglacial Antarctic open water assemblage). There is a strong negative correlation between assemblages I and II during the Quaternary.

The Upper Quaternary interval, deposited <0.195 Ma, may represent deposition since the LGM. The diatom assemblages suggest that summer sea-ice, salinity and sea-surface temperatures varied little from today. The upper and lower Quaternary intervals are separated by a disconformity, which is associated with an IRD lag. The lower Quaternary intervals were deposited between 1.6 - 1.25 Ma. They contain evidence for changes in sea-ice and open-water conditions, which may relate to glacial and interglacial cycles. The diatoms *R. antarctica* and *R. naviculoides* have their last appearance during the lowest interglacial intervals, ~1.6 Ma. The intervals correlate across the Southern Kerguelen Plateau from north to south, a distance of ~770 km. The formation of an armoring lag layer on top of this interval may have allowed its preservation, protecting it from erosion during periods of high ACC velocity caused by later intense glaciation.

Summer sea-surface temperature and salinity were -0.6° to -1.1°C and 33.6-34.0‰, respectively, during glacial cycles in the Lower Quaternary interval. Open pack-ice dominated, with a summer sea-ice concentration between 6-18%. This created a co-varying, mixed assemblage of Antarctic open water diatoms (*Thalassiosira* spp.) and cryophilic diatoms (e.g. *Fragilariopsis curta*), which differs from most modern diatom assemblages. During interglacials, the summer sea-surface temperature was similar, or cooler, than today (approximately 0.5° to 1.5°C). The total percentage of carbonate during glacial intervals, 1.6 - 1.25 Ma, was greater than in warmer conditions <0.195 Ma, suggesting that the CCD was deeper in the past. Factors other than temperature and depth (e.g. atmospheric CO<sub>2</sub> concentration) therefore appear able to affect carbonate deposition and require further investigation.

The Quaternary and Pliocene sediment is separated by a disconformity that formed 2.2 - 1.6 Ma, and is generally associated with an IRD lag. In the Pliocene (~2.2 Ma), summer pack-ice dominated. An intense cold interval may have created a disconformity, due to increased ACC velocity, 3.1 - ~2.2 Ma. Prior to this, 3.0 - 2.64 Ma, intermittent summer pack-ice / open-water conditions dominated. In the later and earlier parts of this interval, open-water dominated in summer at the most northerly site studied at GC 51 (57° S), but was separated by an interval when summer pack-ice prevailed. During the later open-water episode the summer sea-surface temperature was <5°C.

Warmer water conditions than today occurred during the open-water intervals 3.0 - 2.64 Ma and 3.2 - 3.1 Ma, evident in GC 48 (58° S) and GC 34 (62° S). During the warmest conditions, evident in GC 34, the summer sea-surface temperature was

approximately 5°C, which was 4.5 C° warmer than today. A 4.5 C° warming at GC 34 (62° S) could have occurred only if the APFZ was either ~1200 km further south than today, or if the temperature gradient across the associated ocean fronts became significantly shallower.

The Pliocene intervals contain much IRD. This may reflect a heavy iceberg influence due to warmer glacial conditions in Antarctica, which may have caused increased sediment discharge and iceberg calving.

## **7. Palaeoenvironmental Interpretation of the Pliocene Sørsdal Formation, Marine Plain, Vestfold Hills, East Antarctica**

### **7.1 Introduction**

#### **7.1.1 Aims**

The aim of this study is to reconstruct the palaeoenvironmental conditions of the Sørsdal Formation, marine sediments deposited in the Vestfold Hills, Antarctica, during Pliocene (4.5-4.1 Ma) climate warming and glacial retreat (Pickard *et al.* 1988; Harwood *et al.* in press; Quilty *et al.* in press) (Figure 37). This study will reconstruct the summer sea-surface temperature and sea-ice conditions through the use of diatom microfossils. These findings will be used to 1) comment on Pliocene palaeoclimate and 2) test computer model predictions (eg Huybrechts 1993) for the position of the ice-sheet margin during climatic warming. This study provides an opportunity to test hypothetical models of ice sheet behavior against real evidence from the geological record, and will aid our understanding of Antarctic ice sheets' response to future global warming.

#### **7.1.2 Study Area**

Today, the Vestfold Hills are flanked by the East Antarctic Ice Sheet to the east and the Sørsdal Glacier to the south (Figure 37). This places the Sørsdal Formation only 2 km from the Sørsdal Glacier, and 15 km from the ice sheet margin. Coastal summer sea surface temperatures (SST) around Prydz Bay are generally between -1.1°C and -0.6 °C (Kerry *et al.* 1987a, 1987b), but values as high as 1.39°C have been recorded near the Vestfold Hills (Gibson 1998). Modern fast ice develops around the Vestfold Hills in early winter. During summer it is occasionally trapped in coastal areas, where it becomes multiyear ice if complete melting does not occur.

#### **7.1.3 Previous Work**

##### The Sørsdal Formation

The Sørsdal Formation (Quilty *et al.* in press) is aerially exposed in the Vestfold Hills and covers ~10 km<sup>2</sup> of Marine Plain, where it unconformably infills broad valleys between hills of Precambrian metamorphic basement rock (Adamson and Pickard 1983) (Figure 37). The formation comprises ~7 m of sandy diatomite and diatomaceous sand, and a minor amount of lithified sandstone and sandy diamicton (Adamson and Pickard 1983; Zhang *et al.* 1983; Zhang and Peterson 1984; Adamson and Pickard 1986; Pickard *et al.* 1986, 1988; Zhang 1989; Quilty *et al.* in press).

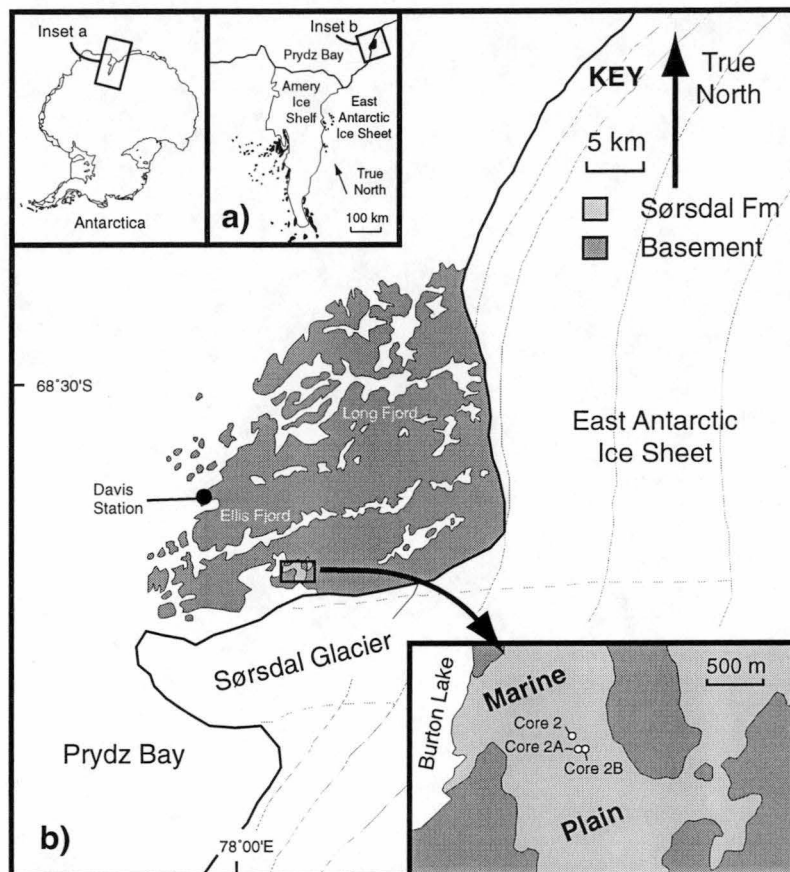


**Figure 37.** Sørdsdal Formation precussion core sites, in the Vestfold Hills, East Antarctica.



The lithified sandstone has been referred to as the Graveyard Sandstone Member (Quilty *et al.* in press) (Figure 38). Palaeoenvironmental data inferred from the diatom data and field observations suggest that the Sørødal Formation was deposited in a shallow coastal marine embayment <25 m deep (Harwood *et al.* in press), with elevated basement areas around the embayment forming islands (Quilty *et al.* in press). The lithology of the formation tends to coarsen upward, indicating that the water depth became progressively shallower with time (Zhang 1983; Zhang and Peterson 1984; Pickard *et al.* 1988).

### Age

Diatom biostratigraphy provides a Lower Pliocene age constraint of 4.5 to 4.1 Ma for the Sørødal Formation (Harwood *et al.* in press). Diatoms here correlate to the *Fragilariopsis barronii* Zone in reference sections from the Kerguelen Plateau (Harwood and Maruyama 1992) and the Ross Sea (Winter and Harwood 1997). The presence of *Fragilariopsis barronii* (Gersonde) Gersonde *et* Bárcena, *Thalassiosira fasciculata* Harwood and Maruyama, *Thalassiosira striata* Harwood and Maruyama and *Rouxia diploneides* Schrader, which all have first appearance datums (FADs) younger than 4.5 Ma, supports the *F. barronii* Zone age assignment (Harwood *et al.* in press). The FAD of *T. kolbei* has been used to define the top of the *F. barronii* Zone on the Antarctic shelf (Winter and Harwood 1997). The absence of *Thalassiosira kolbei* (Jousé) Gersonde (FAD 4.1 Ma), as well as *Thalassiosira lentiginosa* (Janisch) Fryxell (FAD 4.2 Ma) and *Fragilariopsis ritscheri* Hustedt (FAD 4.9 Ma) suggests that the Sørødal Formation is older than ~4.1 Ma and within the *F. barronii* Zone (Harwood *et al.* in press).

### Ice Margin Position

It is assumed that the ice-sheet margin was at least 50 km inland of its current position during deposition of the Sørødal Formation (Pickard *et al.* 1988). Justification for this assumption comes from the large amount of aeolian sand grains in the formation (Pickard *et al.* 1988). At that time the Vestfold Hills would have been largely below sea-level and unable to provide the source for this aeolian sediment, which then would have had to come from aerially exposed rocks that were further inland during ice margin retreat. The current sub-glacial topography indicates that the closest region where the ice sheet margin could have grounded at that time is ~50 km inland (Pickard *et al.* 1988).

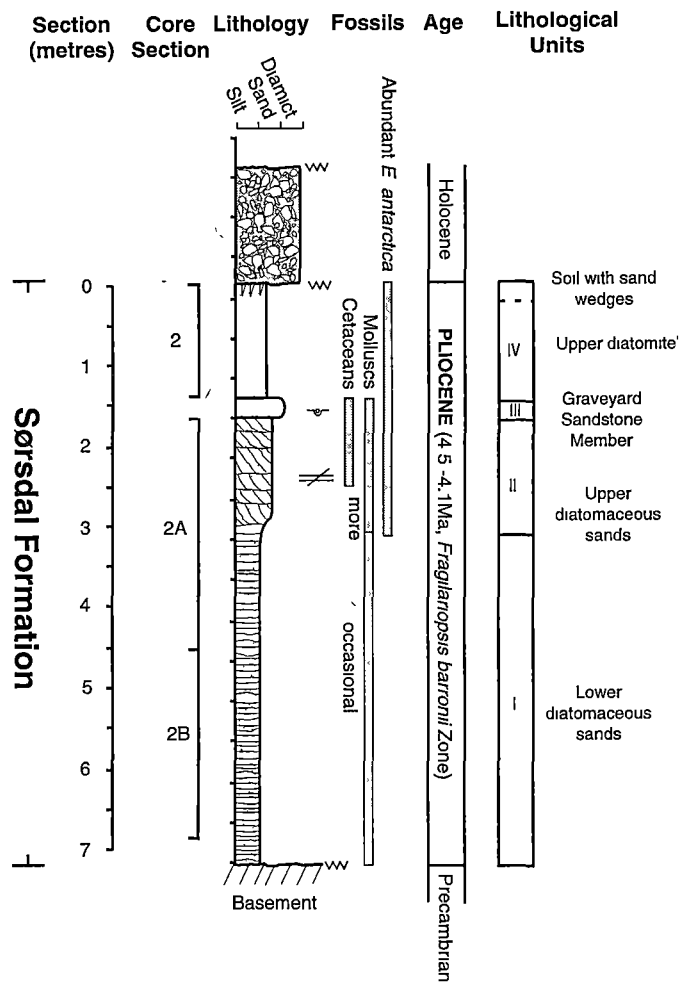


**Figure 38.** The Sørsdal Formation Type Section, previous lithological (Quilty *et al.* in press) and fossil age data (Harwood *et al.* in press).

### Sea-ice and SST

The palaeoclimate at the time of deposition of the Sørsdal Formation was thought to be warmer than today, with elevated marine temperatures and the absence, or significant reduction, of sea-ice (Harwood 1986; Pickard *et al.* 1986, 1988; Quilty 1991, 1992, 1993; Fordyce and Quilty 1994). Reduced sea-ice conditions are evident from the generally low abundance of extant sea-ice diatoms (Harwood 1986; Pickard *et al.* 1986, 1988) and the lack of ice rafted debris (from sea-ice or icebergs) through all but the upper most part of the formation (Quilty 1993; Quilty *et al.* in press). Other palaeotemperature data support the inferred warmer temperatures (Quilty 1991, 1992, 1993; Fordyce and Quilty 1994). Preliminary, but tentative, water temperatures up to 10.5°C were obtained from  $^{18}\text{O}$  measurement on the fossil mollusc, *Chlamys tuftsensis* Turner (Quilty 1991, 1992). Dolphin and small whale fossils are also present (Adamson & Pickard 1986; Colbert 1991; Pickard 1986; Daniels 1996). Their modern relatives do not live in sea-ice habitats, but occur near the Antarctic Polar Front (APF) (Fordyce, in Quilty 1993; Fordyce and Quilty 1994) where summer sea-surface temperatures are 4° to 5°C (Quilty 1992, 1993). Only one interval in the Sørsdal Formation, the Graveyard Sandstone Member (Quilty *et al.* in press), appears to be influenced by glacial deposition. This unit contains diamicts (Quilty 1994), ice rafted debris and a relative increase in diatoms associated with the sea-ice environment (Harwood 1986; Pickard *et al.* 1986, 1988).

### Phytoplankton

The palaeoenvironmental interpretation of the Sørsdal Formation presented here, is based largely upon fossil diatom evidence. Diatoms (Division: Bacillariophyceae) are unicellular, golden brown algae that live in the euphotic zone (generally <100 m) of almost all aquatic habitats (Round *et al.* 1990). The Sørsdal Formation sea-ice diatom assemblage will be compared, using Chi-square tests, to modern diatom data from Prydz Bay (in Taylor 1999) and the southern Kerguelen Plateau (Whitehead, unpublished) surface sediment samples.

These regions span much of the modern season sea-ice zone, where surface sediment diatom assemblages reflect the latitudinal gradient in summer (January-February) sea-ice concentration. For example, the relative ratio of sea-ice associated diatoms increases towards Prydz Bay, where sea-ice persists longer during summer (Stockwell *et al.* 1991; Taylor *et al.* 1997). Summer sea-ice concentration also co-varies with SST.

The presence and absence of various extant phytoplankton species (diatoms, silicoflagellates and coccolithophorids) of known temperature range (in Ciesielski and Weaver 1974; Dmitriyenko 1989; Armand 1997; Zielinski and Gersonde 1997) will also be used to constrain early Pliocene SST in the Sørøsdal Formation. At the Antarctic Polar Front (APF) there is a distinct change in the relative abundance of the silicoflagellate genera *Dictyocha* and *Distephanus* in modern surface sediments (Ciesielski 1974; DeFelice and Wise 1981; Pichon *et al.* 1987). The ratio of *Dictyocha* to *Distephanus* in surface sediments between Wilkes Land, Antarctica, and Australia, indicates that *Dictyocha* occurs north of the APF (where surface waters are  $>5^{\circ}$  or  $6^{\circ}\text{C}$ ). Sediment deposited north of the APF also consists largely of calcareous ooze (Gordon 1971; Burckle and Cirilli 1987), due to the deposition of calcareous coccolithophorids (Burckle and Cirilli 1987). The presence of *Dictyocha* and coccolithophorids further south, in Sites 751 and 748, on the southern Kerguelen Plateau, has been used to interpret warmer climatic intervals in the Pliocene (Bohaty and Harwood 1998), and a similar approach will be undertaken on the Sørøsdal Formation.

This study differs from all previous diatom studies of the Sørøsdal Formation, which have concentrated primarily on the age interpretation. Previous diatom interpretations of SST and sea-ice concentration have used qualitative data and less rigorous reviews of diatom ecology, and as a result, no SST or sea-ice concentrations were given. This study, therefore, aims to reconstruct the SST and sea-ice concentration of the Sørøsdal Formation using quantitative diatom data and a more detailed review of diatom ecology.

## 7.2 Methods

Sediment samples from the Sørøsdal Formation were collected during an Australian National Antarctic Research Expedition (ANARE) in 1993/94. The Sørøsdal Formation strata are generally horizontally bedded. They were cored with a percussion-corer at three closely spaced locations (2, 2A and 2B) down slope (Figure 37), to sample a composite section (Quilty 1994; Quilty *et al.* in press).

Siliceous microfossils were analyzed from 36 samples from the Sørøsdal Formation. Microfossil preparation and microscopy were conducted at the Antarctic CRC, Hobart. The Sørøsdal Formation samples were soaked in very dilute  $\text{H}_2\text{O}_2$  to clean the samples and then centrifuged at 2500 rpm for 5 minutes and rinsed at least three times with distilled water to remove excess residues. Sub-samples from the cleaned samples were suspended

in distilled water (1-3 drops per 10 ml distilled water). The suspension was pipetted onto glass coverslips, dried on a hot plate (~50°C), and mounted on glass slides using Norland Optical Adhesive # 61 (refractive index = 1.56) and cured under an UV light for 5 minutes.

Slides were examined using a Zeiss Standard 20 phase contrast light microscope, with a 100x objective. Approximately 400 valves and cysts were counted per sample. Only intact valves, or broken specimens where more than half the valve remained, were counted. Exceptions to this were made for the fragile elongate genera, such as *Trichotoxon* and *Thalassiothrix*, which are rarely preserved intact and were counted from their distinctive end pieces and the total divided by two. Diatom *Dactyliosolen antarcticus* Castracane was counted from individual girdle bands identified in the samples, although many represent a single diatom. *Chaetoceros* resting spores were recorded as individual valves.

Quantitative relative abundance data were collected for individual species in the Sørødal Formation samples. All diatom data were converted to relative percentage abundance. The diatom data were compared to previously collected data (Harwood 1986; Pickard *et al.* 1986, 1988; Harwood *et al.* in press). Species not identified in this study, but identified in Harwood *et al.* (in press), are included in the data with a symbol “r”, indicating their rare occurrence (Appendix 1).

Benthic diatoms were excluded from sea-ice and water temperature interpretations, as their ecology is less well-known than that of planktic diatoms (Laws 1984; Round *et al.* 1990). The remaining planktic assemblage is more diagnostic of these environmental changes. Counts of *Chaetoceros* occurrence were also removed from the calculation, because their overwhelming abundance in some assemblages often masks the presence of less abundant, but ecologically important taxa (Leventer *et al.* 1996). In the remaining planktic data, extant diatoms of known environmental preference were identified through literature review (Table 5). The ecology of useful extant taxa observed here, and in earlier studies of the Sørødal Formation, is included in the palaeoenvironmental discussion.

The cumulative abundance of sea-ice diatoms, relative to the total number of extant taxa of known ecological preference, was plotted stratigraphically for the Sørødal Formation (Figure 39). These data were compared through Chi-squared tests to similar data from modern sediments along the Antarctic coast (12 samples), continental shelf (44 samples), shelf break (37 samples) (in Taylor 1999) and southern Kerguelen Plateau (4 samples)

(Whitehead, unpublished data) (Table 6). Corresponding sea-ice and surface water temperatures were reconstructed for the Sørsdal Formation by comparison with the modern data.

### 7.3 Results

Extant planktic diatoms comprise 32-81% of the total assemblage encountered in the Sørsdal Formation samples. The planktic component of the assemblage (including extinct species) is dominated by *Chaetoceros*, which forms between 65-94% of the assemblage. Most of the *Chaetoceros* species observed appear to be extant and occur as resting spores, of which <18% are vegetative cells.

Non-*Chaetoceros* planktic diatoms comprise 3-20% of the planktic assemblage; 56-92% of these are extant, and the ecology of 33-83% of them is reasonably well understood. Studies that provide ecological information about these species were tabulated (Table 5). Of the extant taxa of known ecological preference in the Sørsdal Formation, 4-51% of the assemblage are sea-ice diatoms (Figure 39). Chi-squared tests indicate that there are significantly fewer sea-ice diatoms in the Sørsdal Formation than in modern coastal sediments (Table 7).

Chi-square test results (Table 7) illustrate no significant difference (at 5% level of significance), between the percentage that sea-ice diatoms are of the extant taxa of known ecology (excluding *Chaetoceros*), in modern Kerguelen Plateau and numerous Sørsdal Formation samples (from the following sample depths (cm) below the top of the formation: 10, 195, 205, 255, 285, 315, 335, 245, 375, 420, 435, 445, 510, 560, 570 and 670).

### 7.4 Discussion

#### 7.4.1 Sea-ice

##### Relative abundance of extant sea-ice diatoms

The quantitative relative abundance of extant sea-ice diatoms in the Sørsdal Formation has been compared with that in modern sediments. The comparison of absolute diatom abundance is not applicable for sea-ice reconstruction of the Sørsdal Formation, as these sediments were deposited in a coastal setting, where the amount of biogenic sediment is highly variable due to differences in diatom preservation and sediment reworking

**Table 5.** Environmental association of extant diatoms in the Sørsdal Formation, as identified through literature review.

Extant species	Environment	Citations
<i>Eucampia antarctica</i> var. <i>recta</i>	sea-ice associated	9
<i>Fragilariopsis curta</i>	sea-ice associated	1, 4, 5, 6, 7, 8
<i>Fragilariopsis</i> sp. cf. <i>obliquecostata</i>	sea-ice associated	(16, 17, 25) ?
<i>Fragilariopsis sublinearis</i>	sea-ice associated	5, 25
<i>Odontella weissflogii</i> *	sea-ice associated	22, 23
<i>Pseudo-nitzschia turgiduloides</i> *	sea-ice associated	5, 6, 17, 18
<i>Stellarima microtrias</i>	sea-ice associated	19
<i>Fragilariopsis ritscheri</i>	Sea-ice edge and / or open water	11, 14
<i>Thalassiosira antarctica</i>	Sea-ice edge and / or open water	16, 20,
<i>Thalassiosira gracilis</i> var. <i>expecta</i>	Sea-ice edge and / or open water	6
<i>Thalassiosira gravida</i>	Sea-ice edge and / or open water	11, 15, 21
<i>Thalassiosira oestrupii</i>	Sea-ice edge and / or open water	12, 13, 14
<i>Dactyliosolen antarcticus</i>	open water	6, 7, 10
<i>Fragilariopsis separanda</i>	open water	2, 3, 4, 5, 6, 10
<i>Stellarima stellaris</i>	open water	5
<i>Thalassiosira gracilis</i> var. <i>gracilis</i>	open water	1, 4, 5
<i>Thalassiosira maculata</i>	open water	11
<i>Thalassiosira oliverana</i>	open water	14, 16
<i>Thalassiothrix</i> sp.	open water	4
<i>Thalassionema nitzschioides</i> (group)	open water	4, 5
<i>Trichotoxon</i> sp.	open water	6,7
<i>Chaetoceros</i> spp.	?	
<i>Coscinodiscus oculoides</i>	?	
<i>Coscinodiscus oculus-iridus</i>	?	
<i>Croophilum</i> sp.	?	
<i>Paralia</i> spp.	?	
<i>Rhizosolenia hebetata</i> (group)	?	
<i>Rhizosolenia styliformis</i> (group)	?	

#### References

- 1 (Kozlova and Mukhina 1967), 2 (Abbott 1974), 3 (DeFelice and Wise 1981),
- 4 (Pichon *et al.* 1987), 5 (Zielinski and Gersonde 1997), 6 (Taylor *et al.* 1997),
- 7 (Stockwell *et al.* 1991), 8 (Leventer 1992), 9 (Fryxell 1991), 10 (Kozlova 1966),
- 11 (Johansen and Fryxell 1985), 12 (Garrison *et al.* 1987), 13 (Horner 1985),
- 14 (Armand 1997), 15 (Moisan and Fryxell 1993), 16 (Medlin and Priddle 1990),
- 17 (Watanabe 1988), 18 (Scott *et al.* 1994), 19 (Hasle *et al.* 1988),
- 20 (Hasle and Heimdal 1968), 21 (Fryxell and Kendrick 1998), 22 (Garrison and Buck 1989),
- 23 (Garrison 1991).

(\* denotes species identified in Harwood *et al.* in press, but not seen in this study)

**Table 6.** Modern diatom relative abundance in surficial sediments, expressed as a relative amount of i) extant taxa found in the Sørsdal Formation of known ecology (excluding *Chaetoceros* ), ii) of the extant taxa that are sea-ice associated, a iii) how much *Thalassiosira* spp. comprise the total of all the planktic diatoms present. Values are from surface sediments from Prydz Bay coastal and shelf areas (calculated from Taylor 1999) and the Kerguelen Plateau (core tops in Chapter 6

Location	Coastal	Shelf	Shelf break	Kerguelen
Latitude	~69° S	69-67° S	67° S	58 - 57° S
i) % extants of known ecology (excl. <i>Chaetoceros</i> )	<u>58.6</u>	<u>58.0</u>	<u>47.0</u>	<u>25.5</u>
ii) % of above that are sea-ice spp.	<u>96.9</u>	<u>88.6</u>	<u>68.3</u>	<u>13.5</u>
iii) % <i>Thalassiosira</i> (of all the planktics)	<u>3.1</u>	<u>9.0</u>	<u>13.8</u>	<u>9.7</u>
Temp. (°C) (Jan-Feb)	-1.1 to -0.6	-1.1 to -0.6	-1.1 to -0.6	1 to 2
Sea-ice cover (%) 1978-1991				
January	35	18	11	absent
February	26	11	6	absent

water temp and salinity information from FIBEX (Kerry *et al.* 1987a) and SIBEX II (Kerry *et al.* 1987b) data, and

sea-ice information from SMMR and SSM/I passive microwave records (US National Climate Data Centre).

Kerguelen environmental information from Gordon and Molinelli (1986)



**Table 7.** Chi-square distributions illustrate no significant difference (at 5% level of significance, as underlined and in bold), between the percentage that sea-ice diatoms are of the extant taxa of known ecology (excluding *Chaetoceros* ), in modern Kerguelen Plateau (Table 6 data row ii) and numerous Sørødal Formation samples. Sørødal Formation intervals, of no significant difference from modern Kerguelen Plateau samples, may have experienced similar SST and sea-ice conditions from those on the southern Kerguelen Plateau today.

Sample	2(0-10)	2A(10-20)	2A(20-30)	2A(30-40)	2A(40-50)	2A(80-90)	2A(90-100)	2A(120-130)	2A(130-140)
Core depth (cm)	10	175	185	195	205	245	255	285	295
coastal ~69° S	2143.01	1720.97	690.66	2450.06	1968.64	1095.49	2053.12	2502.14	1136.87
shelf 69-67° S	512.30	400.48	137.37	594.48	465.92	238.35	488.36	608.48	248.89
shelf break 67° S	123.13	86.60	13.27	151.06	107.75	38.22	115.16	155.89	41.12
Kerg 58-57° S	<u>0.86</u>	11.33	122.69	<u>0.49</u>	<u>3.62</u>	58.04	<u>2.03</u>	<u>0.93</u>	53.36

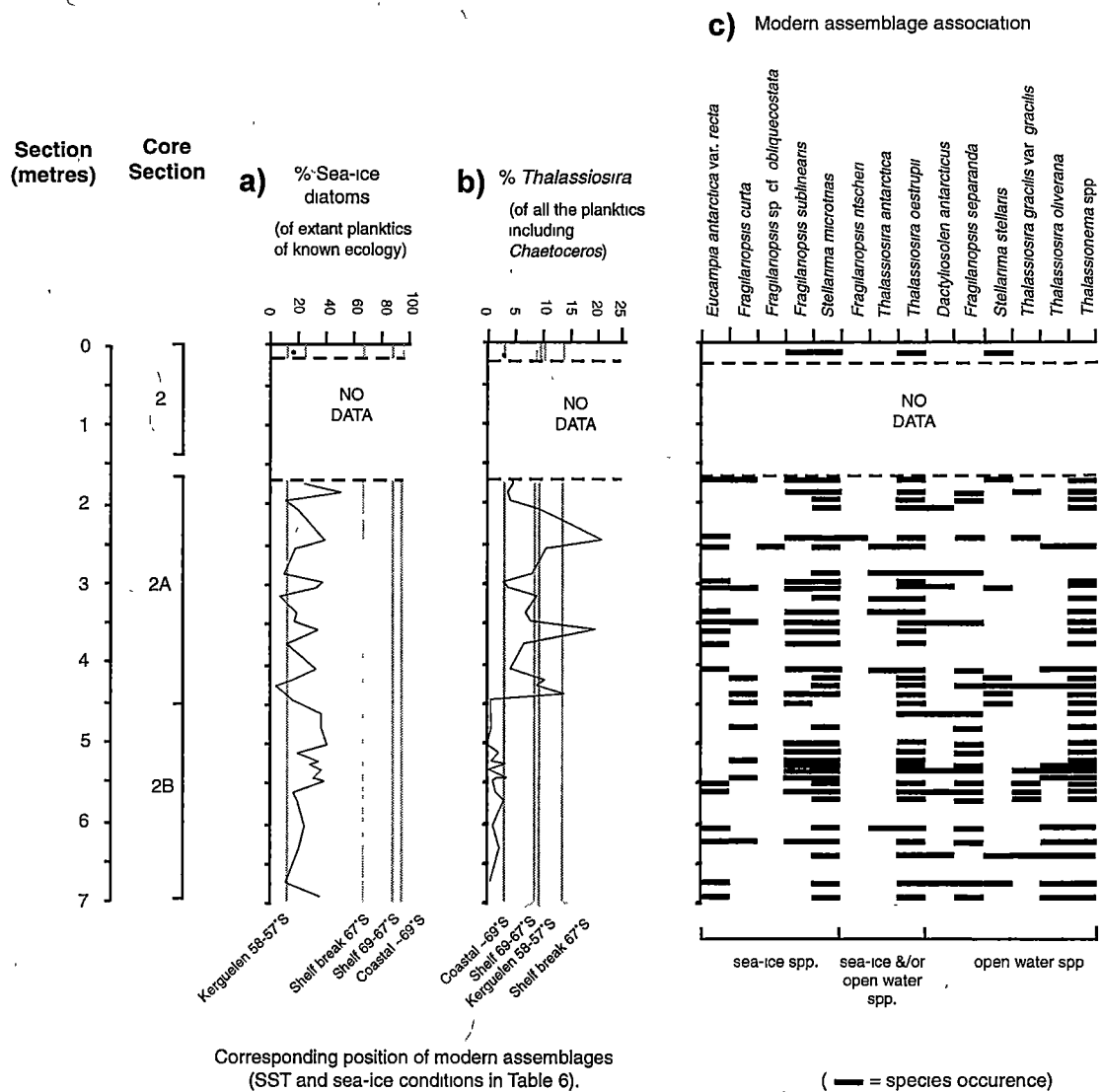
Sample	2A(140-150)	2A(150-160)	2A(170-180)	2A(180-190)	2A(190-200)	2A(210-220)	2A(240-250)	2A(260-265)	2A(265-270)
Core depth (cm)	305	315	335	345	355	375	405	420	425
coastal ~69° S	1345.16	2681.96	2001.81	2090.96	1291.45	2390.39	1345.16	2190.13	2862.77
shelf 69-67° S	302.40	656.93	474.72	498.43	288.54	578.47	302.40	524.87	705.81
shelf break 67° S	56.47	172.75	110.65	118.50	52.41	145.56	56.47	127.35	189.97
Kerg 58-57° S	33.69	<u>3.46</u>	<u>2.94</u>	<u>1.47</u>	38.18	<u>0.15</u>	33.69	<u>0.45</u>	7.46

Sample	2A(270-280)	2A(280-290)	2B(0-10)	2B(20-30)	2B(40-50)	2B(50-60)	2B(60-70)	2B(75)	2B(70-80)
Core depth (cm)	435	445	460	480	500	510	520	525	530
coastal ~69° S	2404.94	2161.22	1174.59	1174.59	1033.69	1968.64	1263.45	1554.24	1174.59
shelf 69-67° S	582.37	517.15	258.53	258.53	222.66	465.92	281.33	356.76	258.53
shelf break 67° S	146.89	124.76	43.81	43.81	33.98	107.75	50.32	72.90	43.81
Kerg 58-57° S	<u>0.22</u>	<u>0.68</u>	49.33	49.33	65.60	<u>3.62</u>	40.68	19.45	49.33

Sample	2B(85-90)	2B(80-90)	2B(90-95)	2B(100-110)	2B(110-120)	2B(140-150)	2B(170-180)	2B(210-220)	2B(235-237)
Core depth (cm)	540	540	545	560	570	600	630	670	687
coastal ~69° S	1434.78	1345.16	1100.88	2143.01	1968.64	1720.97	1926.21	2450.06	1219.96
shelf 69-67° S	325.63	302.40	239.72	512.30	465.92	400.48	454.67	594.48	270.15
shelf break 67° S	63.40	56.47	38.59	123.13	107.75	86.60	104.06	151.06	47.11
Kerg 58-57° S	26.98	33.69	57.42	<u>0.86</u>	<u>3.62</u>	11.33	<u>4.61</u>	<u>0.49</u>	44.77



**Figure 39.** The Sørsdal Formation diatom data. (a) Cumulative percentage of sea-ice diatoms expressed as a relative amount of the extant planktic diatoms of known ecology. (b) Cumulative percentage of all *Thalassiosira* spp. expressed as a relative amount of all planktic diatoms. In (a) and (b) corresponding values (from Table 6) calculated from modern PrydzBay (Taylor 1999) and Kerguelen Plateau (Whitehead, unpublished) data are illustrated. (c) The stratigraphic position of extant diatoms of known ecological preference are illustrated.

(Franklin 1997; McMinn *et al.* 1998). As a result, the absolute abundance of diatoms would fluctuate greatly in response to variables other than sea-ice concentration and SST.

Comparison of relative abundance of planktic extant diatoms, of known ecological preference, in modern surface sediments and the Sørødal Formation indicate that extant sea-ice diatoms comprise a significantly smaller proportion of this assemblage in the Sørødal Formation than on the modern Antarctic continental shelf in Prydz Bay. Chi squared analysis indicates that in many intervals of the Sørødal Formation their abundance is not significantly different from that on the southern Kerguelen Plateau (Table 7). Therefore, comparison with the modern assemblage (Table 6) suggests that during the warmest intervals, summer (January-February) sea-ice was absent and the SSTs were around 1° to 2.0°C, which is higher than the conditions that generally occur today around the coast (Figure 39). Relative diatom abundance can also be partially controlled by the abundance and preservation of other taxa. For example, a major difference between modern and Pliocene samples is the presence of extinct taxa of unknown ecological preference in the older material. Some extinct taxa may have been sea-ice associated, and therefore the interpreted Sørødal Formation summer sea-ice concentration could have been higher, and SST lower than calculated. Conservative abundance estimates calculated from the extant sea-ice diatoms suggest that the conditions in the Vestfold Hills would have been comparable to, or cooler than, that now over the southern Kerguelen Plateau. Significantly warmer conditions than those existing over the southern Kerguelen Plateau are unlikely, especially if some of the extinct taxa were sea-ice associated.

#### Ecology of extant sea-ice diatoms

The occurrence of extant sea-ice associated diatoms in the Sørødal Formation provides compelling evidence for the presence of sea-ice in some intervals of the Sørødal Formation.

The occurrence of *Eucampia antarctica* (Castracane) Mangin has been used as evidence for the presence of sea-ice in the Sørødal Formation (Harwood 1986; Harwood, in Pickard and Adamson 1986a; Pickard *et al.* 1986, 1988) or open water ice-edge conditions (Harwood *et al.* in press). The current study has found *Eucampia antarctica* var. *recta* (Mangin) Fryxell *et* Prasad winter valves through various intervals in the section (Figure 39). This taxon has been previously grouped with *Eucampia antarctica* (Castracane) Mangin var. *antarctica* and called *Eucampia antarctica* (Castracane) Mangin. *Eucampia antarctica* var. *recta* can be differentiated from *E. antarctica* var. *antarctica*, due to its

symmetrical shape in broad girdle view (Fryxell 1991) seen under the light microscope. The ecology of the two varieties also differs; *E. antarctica* var. *antarctica* generally occurs in open water and *E. antarctica* var. *recta* in association with sea-ice (Fryxell and Prasad 1990; Fryxell 1991). *Eucampia antarctica* var. *recta* winter valves develop during unfavorable conditions (eg low light levels) during winter (Fryxell and Prasad 1990), often associated with winter sea-ice. The presence of *E. antarctica* var. *recta* winter valves in the Sørsdal Formation indicates that winter sea-ice may have been present. Their abundance through much of the formation is low, comprising <4% of the planktic assemblage studied here. Other studies documented an increase in the abundance of *E. antarctica*, (possibly *E. antarctica* var. *recta*) to >25% (of the total diatom assemblage), within the upper three meters of the formation (Harwood 1986; Pickard *et al.* 1986, 1988).

Other sea-ice taxa occur in the Sørsdal Formation (Table 5) and, surprisingly, these sometimes occur in intervals lacking *E. antarctica* var. *recta*. (Figure 39). It is possible that this reflects differences in the structure of the sea-ice community. The Sørsdal Formation is thought to have been deposited in an inshore environment (Adamson and Pickard 1986) and *Eucampia antarctica* var. *recta* is generally low in abundance in coastal areas (Gersonde and Wefer 1987; Stockwell *et al.* 1991; Fryxell 1991; Leventer 1992; McMinn and Hodgson 1993).

Sea-ice reconstruction is complicated by the limited information on modern diatom physiology and ecology. The presence of extant sea-ice diatoms provides compelling, but not definitive, evidence for the presence of sea-ice. In the past the Antarctic environment may have differed from today. Prior to 2.6 Ma, Antarctica's climate and glacial style is considered to have been warmer (Webb and Harwood 1991, 1993; Harwood *et al.* 1991; 1992; Moriwaki *et al.* 1992; Wilson 1995) and conditions may have existed that have no modern analogue in Antarctica, such as the release of turbid glacial melt water into the marine environment. Sea-ice associated diatoms such as *E. antarctica* var. *recta* and *Fragilariopsis curta* (Van Heurck) (Garrison *et al.* 1982, 1983; Fryxell 1989; Bianchi *et al.* 1992; Kang and Fryxell 1993; Leventer and Dunbar 1996) could have been maintained during deposition of the Sørsdal Formation in the absence of sea-ice, due to the presence of turbid glacial melt waters with low salinity and light conditions.

Lightly-silicified, extant sea-ice diatoms, such as *Thalassiosira australis* Peragallo and *Navicula glaciei* Van Heurck, are notably absent from the Sørsdal Formation (Harwood *et*

*al.* in press), but this does not prove that sea-ice was absent. In modern coastal deposits, where such taxa occur in low abundance <4% (McMinn 1995), they are rarely preserved as fossils (Leventer 1998), except in anoxic waters where enhanced preservation of lightly silicified frustules (up to 50%) is attributed to low pH and the absence of benthic fauna (McMinn 1995). the presence of a benthic fauna in the Sørsdal Formation, with the preservation of molluscs fossils, could have inhibited the preservation of lightly silicified diatoms; or their absence could be temporal. It is possible that some extant sea-ice species not identified in the formation (eg *T. australis* and *N. glaciei*), had not yet evolved. The absence of certain extant sea-ice species from the Sørsdal Formation, therefore, cannot be used to support the absence of sea-ice. Some sea-ice associated diatoms occur in much older geological records. For example, *Stellarima microtrias* (Ehrenberg) Hasle *et* Sims and *E. antarctica* var. *recta* have been recovered from Middle Miocene sediments in the Pagodroma Group, Prince Charles Mountains (Whitehead, unpublished), and a precursor to *F. curta* may have existed in the early-late Miocene, and was recovered from erratics deposited in the Transantarctic Mountains (Harwood and Bohaty 2000).

*Chaetoceros* resting spores, similar to those from extant species, are abundant in the Sørsdal Formation. Their abundance is similar to that observed in some modern coastal sediments (~90%) (Leventer 1991; Stockwell 1991; Taylor 1999). Vegetative *Chaetoceros* cells are more common in pack-ice than fast-ice (Scott 1992), but tend to bloom in stratified open water areas (Crosta *et al.* 1997). Stratified open water conditions form where there is glacial runoff, sea-ice melt (Crosta *et al.* 1997), and in coastal areas protected from storms (Niiler *et al.* 1991). Sea-ice concentration appears to have been low in the Sørsdal Formation intervals studied. Low sea-ice concentration would have supported low numbers of *Chaetoceros* and provided a negligible contribution to water stratification, which would have otherwise been favorable for algal blooms. The high abundance of *Chaetoceros* spores in the Sørsdal Formation probably reflects seasonally stratified open water conditions caused by increased glacial melt-water, during warmer climatic conditions in the Pliocene. Water stratification would have been enhanced by the depositional setting, which was a sheltered embayment between islands, that would have reduced wave effects and mixing.

#### 7.4.2 Sea Surface Temperature Conditions

##### Temperature ranges of extant diatoms

The temperature ranges of many extant diatoms in the modern environment have been studied (eg Zielinski and Gersonde 1997). The presence of these diatoms in the Sørødal Formation can be used to discuss SST (Figure 40).

The presence of *Thalassionema* spp. and *D. antarcticus* suggest that the summer SST was  $>0^{\circ}\text{C}$  through much of the Sørødal Formation (Armand 1997; Zielinski and Gersonde 1997). The presence of *Stellarima stellaris* (Roper) Hasle et Sims in some intervals of the Sørødal Formation (Figure 39), suggests that the summer SST was  $>3^{\circ}\text{C}$ . Although *S. stellaris* has rarely been differentiated from *S. microtrias* in Southern Ocean studies, data from 97 Southern Ocean core top samples indicated that *S. stellaris* occurs in surficial sediments beneath areas where the February SST is  $>3^{\circ}\text{C}$  (Armand 1997). The maximum summer SST is, however, more difficult to constrain. Some extant species present in the Sørødal Formation do not tolerate high temperatures, but can form evasive resting spores. *Stellarima microtrias*, *Odontella weissflogii* (Janisch) Grunow and *Thalassiosira antarctica* Comber, for example, occur in waters  $<1^{\circ}\text{C}$ ,  $<9^{\circ}\text{C}$  and  $<9.5^{\circ}\text{C}$  respectively (Zielinski and Gersonde 1997), but could have formed resting spores to evade higher summer SST. As a result, their upper temperature tolerance limits cannot necessarily be used to constrain the maximum temperature.

A number of extant species present in the Sørødal Formation are unable to form resting spores. Resting spore formation has not been observed in *Fragilariopsis curta*, *F. ritscheri*, *F. sublinearis* (Van Heurck) Heiden, *Pseudo-nitzschia turgiduloides* (Hasle) Hasle, *Thalassiosira oliverana* (O'Meara) Makarova et Nikolaev, and *E. antarctica* var. *recta*. These species occur in waters  $<2^{\circ}\text{C}$ ,  $<5^{\circ}\text{C}$ ,  $<1^{\circ}\text{C}$ ,  $<1^{\circ}\text{C}$ ,  $<5^{\circ}\text{C}$  and  $<5^{\circ}\text{C}$ , respectively (Zielinski and Gersonde 1997). Some sea-ice diatoms can lower their metabolic rate during unfavorable conditions (Palmisano and Sullivan 1982), but are unable to avoid them completely. Therefore the occurrence of *F. sublinearis* and *P. turgiduloides* in the Sørødal Formation may indicate that the SST remained  $<1^{\circ}\text{C}$  somewhere around the Antarctic coast during the warmest Sørødal Formation intervals.

Warmer conditions in the past may have caused partial deglaciation of the Lambert Graben. During such intervals, the SST in the graben was possibly cooler ( $<1^{\circ}\text{C}$ ) than that further north in the Vestfold Hills (sometimes  $>3^{\circ}\text{C}$  as indicated by *S. stellaris*). This difference may have enabled the maintenance of some species, such as *F. sublinearis* and

*P. turgiduloides*, during the warmer intervals evident in the Sørsdal Formation. Species changes in the Sørsdal Formation could represent changing diatom distribution in and out of the Lambert Graben, in response to seasonal and longer term climate change.

*Fragilariopsis praeinterfrigidaria* (McCollum) Gersonde *et* Bárcena has been recently recovered from the Bardin Bluffs Formation, Prince Charles Mountains, and provides the first evidence of glacial retreat in the Lambert Graben, which may be contemporaneous with the deposition of the Sørsdal Formation (Whitehead, unpublished).

The presence of *E. antarctica* var. *recta* winter valves may suggest that winter (September) sea-ice was present during the deposition of the Sørsdal Formation. The development of sea-ice occurs when the SST reaches  $-1.8^{\circ}\text{C}$  (Ackley 1996). Sea-surface temperature is reduced by cooling air temperatures, as is visible along the modern maximum sea-ice extent, which occurs just south of the  $-1.8^{\circ}\text{C}$  surface air temperature isotherm (Zwally *et al.* 1983). If sea-ice formed during deposition of the Sørsdal Formation, this would indicate that the winter air temperatures were  $-1.8^{\circ}\text{C}$  or lower. The Sørsdal Formation temperature interpretation is limited, however, by the current degree of knowledge about extant diatoms. Environmental factors, other than sea-ice and SST may also affect Southern Ocean diatom distribution (eg salinity), and not until these factors are understood will the palaeoenvironmental interpretation of diatoms be totally reliable.

#### Absence of microfossil groups that occur north of the Antarctic Polar Front

Calcareous coccoliths were notably absent from the Sørsdal Formation samples, either due to ecological or preservational reasons. Minor amounts of biogenic carbonate, deposited as molluscs and very rare foraminifera throughout the formation indicate that deposition occurred above the carbonate compensation depth (Quilty 1988). It is possible that some carbonate dissolution has occurred, with the formation of calcareous concretions that may have destroyed any coccoliths that were present. The inshore depositional setting of the Sørsdal Formation may also explain their absence, as coccoliths are generally uncommon in coastal areas because of their intolerance to high light levels (Siesser 1993). In tropical areas they reach a maximum abundance at 50 m water depth and between 10-20 m water depths in cooler temperate environments (Siesser 1993). The latter is within the depth range interpreted for the Sørsdal Formation (Harwood *et al.* in press). Most coccolithophorids prefer normal marine salinities ( $\sim 36\text{‰}$ ); however many can tolerate a range of salinities. For example, the extant species *Emiliana huxleyi* (Lohmann) Hay and Mohler has been found in salinities between  $11\text{‰}$  and  $41\text{‰}$  (Siesser 1993). It is unclear, however, if Pliocene coccolithophorids also had a broad salinity tolerance. It is likely that

temperature was a limiting factor that caused the absence of coccoliths from the Sørsdal Formation.

The absence of coccoliths in the formation may help constrain the maximum SST. A similar approach has been used elsewhere to indicate cool water conditions in other Pliocene deposits in the Southern Ocean (Wei and Thierstein 1991; Burckle *et al.* 1996). Whilst some coccolithophorids occur in waters as cold as  $-1.7^{\circ}\text{C}$  (Braarud 1979; Honjo 1990), their growth is severely limited at temperatures  $<3^{\circ}\text{C}$  (Burckle and Pokras 1991), and their abundance is low in water temperatures  $<5^{\circ}\text{C}$  (Dmitriyenko 1989). The absence of coccoliths from the Sørsdal Formation may suggest that the summer SST remained  $<5^{\circ}\text{C}$ . The absence contrasts with deposits in warmer water areas ( $>5^{\circ}\text{C}$ ), which contain abundant calcareous coccolithophorids (Goodell 1973; Burckle *et al.* 1996). The temperature interpretation of the Sørsdal Formation may also be supported by the absence of other warm water fossils, such as the silicoflagellate genus *Dictyocha* that lived in the Pliocene and occurs today in waters  $>5^{\circ}\text{C}$  (Bohaty and Harwood 1998). No silicoflagellates have yet been recovered from the formation. The absence of warm water fossils and the presence of cooler water diatoms, such as *F. sublinearis* and *P. turgiduloides*, *T. oliverana* and *E. antarctica* var. *recta*, in the Sørsdal Formation, also suggest that the water temperature was  $<5^{\circ}\text{C}$ .

#### 7.4.3 Palaeoenvironmental Interpretation of Extinct Diatoms

There are numerous extinct *Thalassiosira* species in the Sørsdal Formation (Appendix 1). Modern *Thalassiosira* spp., with the exception of *T. australis* (McMinn 1996), are generally associated with open water conditions (Hasle and Heimdal 1968; Leventer 1992, 1998) and are uncommon in sea-ice (Leventer and Dunbar 1996; Zielinski and Gersonde 1997). The combined abundance of *Thalassiosira* in the Sørsdal Formation exceeds that observed in modern Antarctic coastal sediments through 175 – 445 cm below the top of the formation (Figure 39). If the extinct *Thalassiosira* species in the Sørsdal Formation were open water diatoms, their high abundance suggests that open water dominated this interval of the formation. This interpretation is uncertain, however, until further research can test this assumption.

#### 7.4.4 Future Climate Implications

The argument above suggests that the Sørsdal Formation was deposited in a warmer climate than exists along the Antarctic coast today. The summer SST was probably  $>0^{\circ}\text{C}$ , in many intervals, and  $>3^{\circ}\text{C}$  in others. It is likely the summer SST remained  $<5^{\circ}\text{C}$ .



Today's summer SST around coastal regions of Prydz Bay are between  $-1.1^{\circ}\text{C}$  to  $-0.6^{\circ}\text{C}$  (Kerry *et al.* 1987a, b); however, values as high as  $1.39^{\circ}\text{C}$  have been recorded near the Vestfold Hills (Gibson 1998). At its warmest, the rise in summer SST in the Sørødal Formation was approximately  $3^{\circ}\text{C}$ , relative to today. However, it is likely that the temperature rise through much of the Sørødal Formation was lower than this. For example, the warmer water *S. stellaris* occurs only in some intervals of the formation when the SST was  $>3^{\circ}\text{C}$ , which represents a relative rise approximately  $>1.6^{\circ}\text{C}$ . It is likely that in other intervals, lacking *S. stellaris*, the conditions were cooler than this.

The effects of rising temperature on Antarctica's ice sheet mass balance have been modeled by numerous workers (eg Huybrechts 1993; Prentice *et al.* 1992; Warner and Budd 1998). It was found that a mean annual air temperature rise of  $<5^{\circ}\text{C}$  could cause ice sheet growth (Huybrechts 1993); caused by an increase in marine evaporation and snow accumulation on Antarctica, relative to ablation (Domack *et al.* 1991; Zwally 1994). The relative increase in summer SST through the Sørødal Formation was probably  $<3^{\circ}\text{C}$ . In turn, this may represent a mean annual temperature rise approximately  $3^{\circ}\text{C}$ . It is likely, as mentioned above, that the temperature rise through much of the Sørødal Formation was less than this. When compared to modeling results, the maximum temperature rise that could have occurred in the Sørødal Formation would cause an increase in ice-sheet volume. In contrast, the Sørødal Formation is thought to have been deposited during an  $\sim 50$  km ice margin retreat (Pickard *et al.* 1988). A lower temperature requirement for ice sheet retreat, evident here, is less than that proposed from glacial models and could have implications for the effects of future global warming.

The Sørødal Formation findings may be consistent with more recent glacial modeling studies (eg Warner and Budd 1998). Their study suggests a relatively minor increase in water temperature can out-weigh the effects of increased accumulation. Although an initial increase in accumulation could offset the loss of grounded ice to the sea, eventually the ice shelves would retreat and the ice flow rates increase, causing the ice sheet volume to decline (Warner and Budd 1998). Many of these changes can occur in the early stages of climatic warming, causing rapid Antarctic ice sheet retreat (Warner and Budd 1998).

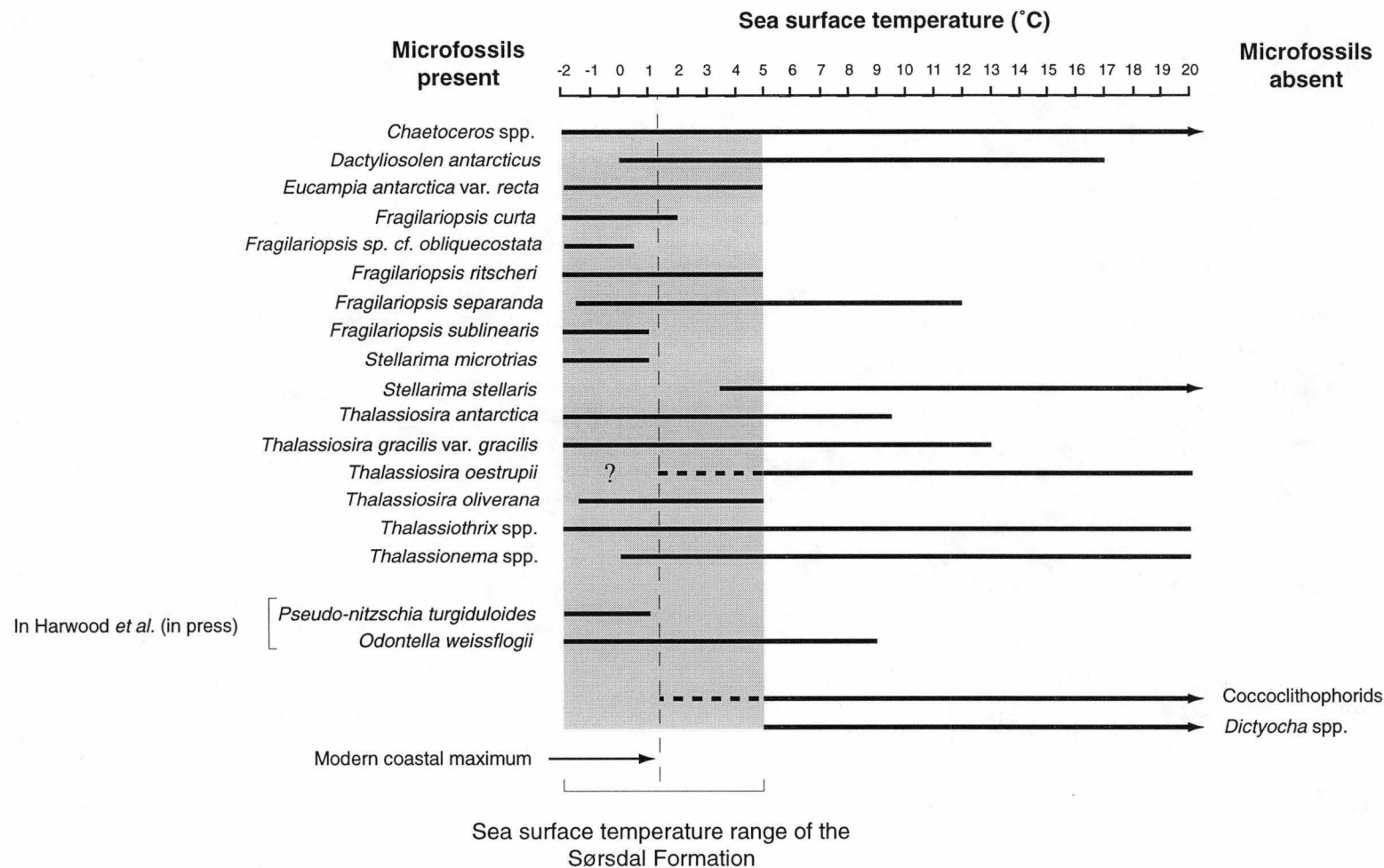


**Figure 40.** Temperature range of extant microfossils present in, and absent from, the Sørsdal Formation. based on DeFelice and Wise (1981), Dmitriyenko (1989), Honjo (1990), Leventer (1992); Armand (1997), Zielinski and Gersonde (1997).

## 7.5 Summary

Pliocene (4.5-4.1 Ma) marine sediments of the Sørødal Formation (Vestfold Hills, Antarctica) were deposited in a shallow coastal marine embayment. Melt-water stratification may have created a productive, open water environment, in which *Chaetoceros* bloomed. Extant sea-ice associated diatoms in the formation provide compelling, but not definitive, evidence for seasonal sea-ice. Their relatively low abundance in the intervals studied suggests that the sea-ice concentration and duration of seasonal cover were reduced, relative to today. The extant diatom *S. stellaris* in some intervals of the formation, suggests that the summer SST was  $>3^{\circ}\text{C}$ . The lack of coccolithophorids, the silicoflagellate *Dictyocha*, and the presence of cooler water diatoms, *T. oliverana*, *E. antarctica* var. *recta*, *F. sublinearis* and *P. turgiduloides*, suggests that the summer SST remained  $<5^{\circ}\text{C}$ . This is consistent with the presence of non-cryophilic cetacean fossils that suggests the summer SST was at times  $4^{\circ}$  to  $5^{\circ}\text{C}$  (Quilty 1992, 1993). It is likely that non-cryophilic cetaceans occurred around the Vestfold Hills during seasonal sea-ice absence or open water conditions during more sustained warm periods. Relative to today, these intervals represents a minimum SST rise of approximately  $1.6^{\circ}\text{C}$ . The maximum relative rise in SST was approximately  $3^{\circ}\text{C}$ . However, these interpretations are limited by the current state of knowledge about modern diatom ecology. During deposition, the ice margin is thought to have been  $\sim 50$  km further inland (Pickard *et al.* 1988). This contrasts with the expected ice sheet response from earlier glacial models (eg Huybrechts 1993), which predict ice sheet expansion due to increased evaporation and accumulation when temperatures rise  $<5^{\circ}\text{C}$ . The findings from the Sørødal Formation support more recent glacial models (eg Warner and Budd 1998), which explain how glacial retreat can occur due to minor increases in water temperature. A lower temperature requirement for ice sheet retreat, evident in the Sørødal Formation, could have implications concerning the effects of future global warming.

## **8. Cenozoic Geology of the Northern Prince Charles Mountains, East Antarctica: Evidence from the Pagodroma Group**

### **8.1 Introduction**

The potential for a major sea-level rise in the future is held within the East Antarctic Ice Sheet (EAIS) (Chapter 3). Given the large sea-level rise that would result from EAIS collapse, this study focuses on the stability of this feature through research into its past variability.

The largest catchment area in East Antarctica (~13% of the East Antarctic Ice Sheet) drains through the Lambert Graben (Brown et al. 1995). Glaciers converge here, forming the Amery Ice Shelf that grounds 400 km inland (Phillips et al. 1996; Krebs 1997, 1998) (Figure 41). The Prince Charles Mountains (PCMs) flank the sides of the graben and are partially covered with glacial marine sediment of the Pagodroma Group (Hambrey and McKelvey 1995; McKelvey et al. 1995, 1997). These contain a record of changing glacial conditions in the Lambert Graben that reflect larger Cenozoic EAIS variations.

Pagodroma Group deposits have been identified through much of the northern Prince Charles Mountains (Bardin 1982; Hambrey and McKelvey in press; McKelvey et al. in press). The group was deposited in a glacial marine, fjordal, environment in the Lambert Graben (Hambrey and McKelvey in press). The lithology is predominately waterlain diamicts deposited under a proximal, heavy ice-berg influence (Hambrey and McKelvey in press). However, more distal, rarer fossiliferous siltstone deposits also occur (Bardin and Belevich 1985; McKelvey et al. 1997; Hambrey and McKelvey in press). These sediments, which are thought to have been deposited in a warmer glacial setting, during reduced EAIS conditions (Hambrey and McKelvey in press), partially infilled the Lambert Graben but have since been largely removed by glacial erosion. The Pagodroma Group represents the remnants of these infilling deposits, preserved on the Prince Charles Mountains that were once part of the Lambert Graben, fjord, walls and floor. Pagodroma Group deposits on the Amery Oasis and Fisher Massif have been divided into four formations (Hambrey and McKelvey in press; McKelvey et al. in press). The Mt Johnston and Fisher Bench Formations occur on Fisher Massif, and the Battye Glacier and Bardin Bluffs formations occur on the Amery Oasis (Figure 41). These formations occur at progressively lower elevations and comprise a composite record >1200 m thick

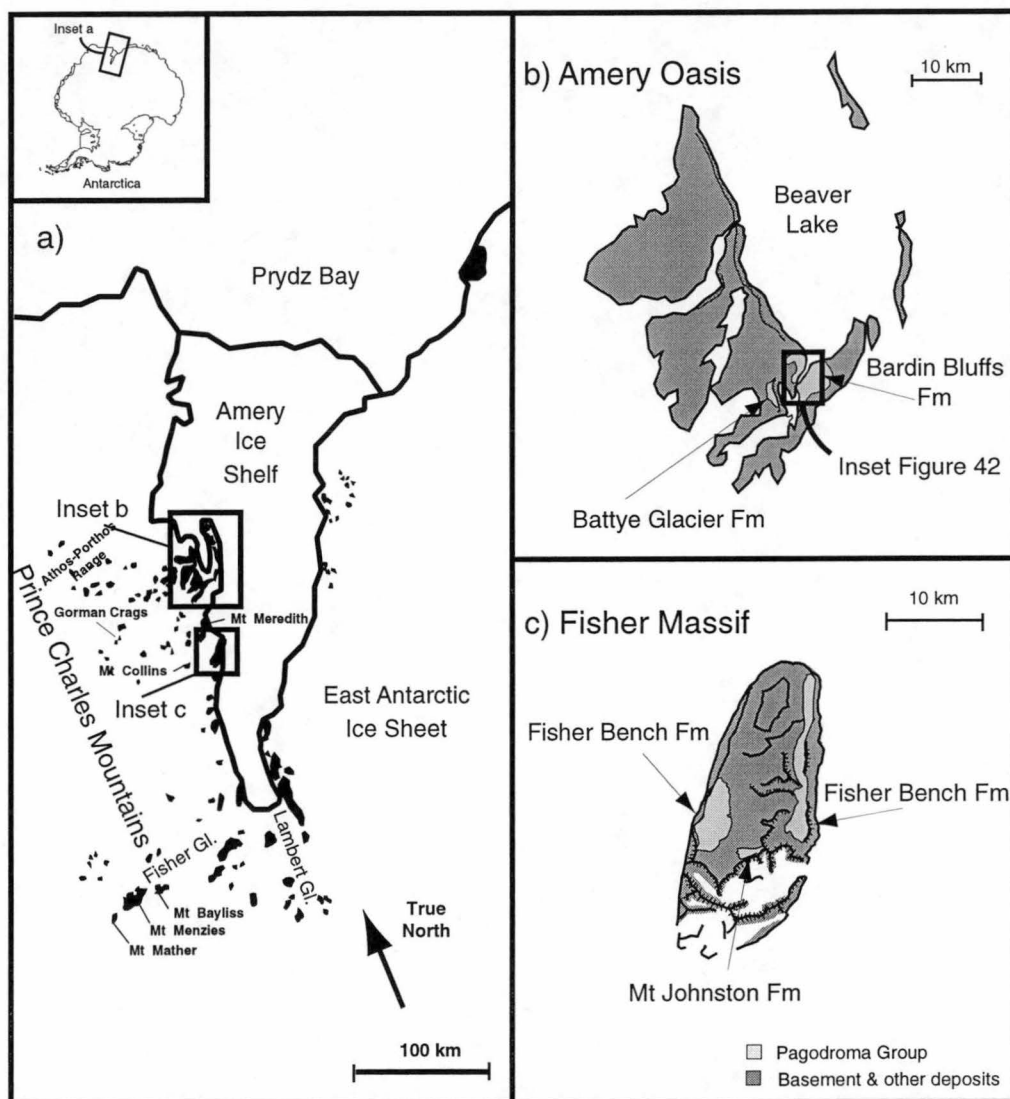


**Figure 41.** Pagodroma Group on the Amery Oasis and Fisher Massif (information Laiba and Pushina 1997; McKelvey *et al.* in press)

(McKelvey et al. 1995). The older formations occur at higher elevations, and have been sectioned by later glacial erosion. Younger formations have been deposited on the resulting, lower, erosion surfaces (Hambrey and McKelvey in press). The relative influence of down cutting versus uplift is unknown, however, this landscape succession has been illustrated by McKelvey et al. (in press). The massive quantity of eroded sediment from the Pagodroma Group has been redeposited on the Prydz Bay continental shelf during glacial advance. During extreme advances, this processes has contributed to the seaward accretion of the shelf at the Prydz Bay Trough Mouth Fan (Cooper et al. 1991; Hambrey et al. 1991; Leitchenkov et al. 1994; O'Brien and Harris 1995; Barker et al. 1998).

This is a three part study that describes the stratigraphy of the Bardin Bluffs Formation (Chapter 8A), biostratigraphically dates the formations within the Pagodroma Group, identifies past marine intervals in the Lambert Graben (Chapter 8B), and identifies the environmental conditions during marine deposition in the Fisher Bench Formation (Chapter 8C).

### **8.1.1 Previous Work**

The Pagodroma Group was discovered during an Australian National Antarctic Research Expedition (ANARE) in the Amery Oasis, in 1958, with McLeod (1958) commenting on the exposures of the current Battye Glacier Formation. Later, Russian researchers discovered the Bardin Bluffs Formation (Bardin 1975), who called it an early glaciogenic deposit. They later commented on its mineralogy (Bardin 1982), micropalaeontology (Bardin and Belevich 1985), lithology (Bardin and Kolosova 1988) and mollusc fossils (Bardin and Chepalyga 1989). They interpreted this deposit as being between Miocene and Pliocene in age. Russian researchers also commented on similar deposits on Mt Meredith, Fisher Massif and Mt Collins (Bardin 1982), and described the mineralogy and lithology of the current Battye Glacier Formation (Bardin and Kolosova 1988). In review of the Russian research, Drewry (1983) called the current Bardin Bluffs Formation the Pagodroma Tillite. ANARE researchers mapped the local extent of this deposit (McKelvey and Stephenson 1990), and dated it as Pliocene in age based on amino acid racemisation on *in situ* molluscs that lived here during glacial retreat (Hart and McKelvey 1991; Hart 1994). Miocene-Pliocene marine diatoms (Harwood, in McKelvey and Stephenson 1990; Whitehead *et al.* 1996) and lake diatoms (Harper and Harwood 1992; Whitehead *et al.* 1996) were identified in the waterlain diamicts, and are thought to have been glacially reworked from *in situ* marine and lake sediments deposited in the Lambert

Graben during glacial retreat. ANARE field researchers also discovered reworked molluscs in the tills (Adamson and Darragh 1991) and used geomorphological features to comment on the extent and antiquity of the deposit (Mabin 1990; Adamson and Darragh 1991), identifying a pre-existing alpine erosional landscape (Adamson *et al.* 1997). Similar deposits were described on Fisher Massif (McKelvey 1994) and the term Pagodroma Group was used to describe these and other similar deposits in the northern Prince Charles Mountains (McKelvey *et al.* 1995; Hambrey and McKelvey 1995). Russian researchers discovered *in situ* diatoms in the current Fisher Bench Formation, on Fisher Massif (Laiba and Pushina 1995); they also briefly described this deposit and identified the diatoms as Miocene in age (Laiba and Pushina 1997).

Formation names were given to the different aged deposits within the group, their stratigraphy largely determined (McKelvey *et al.* in press), and lithology described (Hambrey and McKelvey in press). *In situ* mollusc bearing intervals have also been found in the Battye Glacier Formation (Hambrey and McKelvey in press; McKelvey *et al.* in press). Further units correlative with the Pagodroma Group were identified at Gorman Crag, and in the far northern Prince Charles Mountains, Athos-Pothos Ranges (Bardin 1982; McKelvey *et al.* in press) (Figure 41a).

Considering the Neogene climate questions in this thesis, the Pagodroma Group makes the Prince Charles Mountains a unique and ideal location for studying Neogene, and in particular Pliocene, East Antarctic glacial history. The lack of *in situ* Pliocene marine sediments in the Sirius Group, Transantarctic Mountains (Harwood 1986a; McKelvey *et al.* 1991; Webb *et al.* 1996), and the general lack of good sections of this age around the Antarctic continental margin (Barron *et al.* 1989b; Barrett 1989) highlight this. Thick, *in situ*, Cenozoic deposits like those in the Pagodroma Group have only been obtained elsewhere through international drilling operations, such as the Deep Sea Drilling Program (DSDP), Ocean Drilling Program (ODP), Dry Valley Drilling Project (DVDP), and various McMurdo sound drilling programs (MSSTS, CIROS and CRP). These drilling operations have concentrated on the periphery of Antarctica, whilst the Pagodroma Group provides the only direct and *in situ* evidence of changing glacial conditions deep inland. Evidence for glacial advance and retreat in the Lambert Graben, from the Pagodroma Group, can be compared to Cenozoic data from Prydz Bay (ODP 119 and 120). Together they provide a land to sea transect that can help to spatially and temporally constrain the degree of past EAIS variability.

## **8A. The stratigraphy of the Pliocene - early Pleistocene Bardin Bluffs Formation, Amery Oasis.**

### **8A.1 Introduction**

#### **8A.1.1 Aims**

This study details the basal stratigraphy of the Bardin Bluffs Formation, the youngest formation of the glaciogene Neogene to Early Pleistocene Pagodroma Group (McKelvey *et al.* in press) (Figure 41b). As well as refining the stratigraphy of the Bardin Bluffs Formation, an effort has been made to establish the stratigraphic relationship between two horizons from which a benthic diatom flora (sample 20-12 of Bardin and Belevich 1985) and an open marine foraminiferal fauna (sample 90-7 of Webb, pers. comm. 1999) have been described. Similarly, the stratigraphic position of mollusc-bearing outcrops alongside Beaver Lake (Bardin and Chepalyga 1989) have been integrated into the Bardin Bluffs Formation. The age of the formation has also been revised.

#### **8A.1.2 Geological Setting**

Pagodroma Gorge links Beaver Lake to Radok Lake, in the southern part of Amery Oasis (Figure 42). The extensively deglaciated Amery Oasis covers an area of about 1800 km<sup>2</sup> and borders the western side of the Amery Ice Shelf.

Pagodroma Gorge trends approximately 045° and is cut into gently dipping Permo-Triassic fluvial strata of the 2500 m thick Amery Group (McLoughlan and Drinnan 1997; Fielding and Webb 1995). The northeastern 4 km of the gorge is essentially straight, whereas the 3 km long southwestern portion that connects to Bainmedart Cove, winds between interlocking spurs.

In general, the exposure of the semi-lithified Bardin Bluffs Formation is poor. The Bardin Bluffs Formation is widespread in the Radok Lake-Beaver Lake region of the Amery Oasis (Figure 41b), but good to moderate exposure exists at only (i) along Pagodroma Gorge, (ii) on the northern side of Quike Gully, which enters the mouth of Pagodroma Gorge, and (iii) overlooking the southeastern shores of Radok Lake. The study largely centres on Bardin Bluffs in Pagodroma Gorge, which contain the type section of the Bardin Bluffs Formation. These bluffs are close to the mouth of the gorge, near where it enters Beaver Lake in the Amery Oasis (Figure 42).



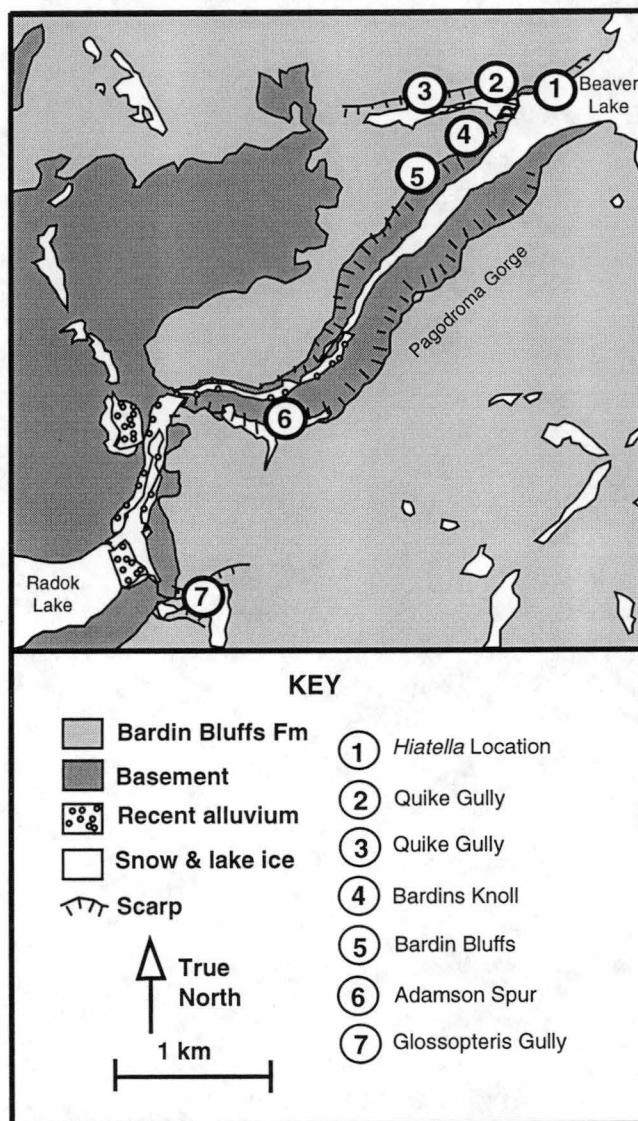


**Figure 42.** Geological map of the Bardin Bluffs Formation (modified from McKelvey and Stephenson 1990), with study locations numbered.

On either side of the gorge, whose walls rise to 180 m in elevation, the Bardin Bluffs Formation rests unconformably as a blanket (<50 m thick) upon the Amery Group. The regional topography of the unconformity surface appears to be that of a gently undulating slope. Over a distance of 6 km it falls eastwards, from 180 m in elevation near Radok Lake, to near sea-level, along the western shore of Beaver Lake. The sloping erosion surface is a composite one that is dissected locally by the remnants of several steep sided, older, valley profiles, which individually are up to ~50 m deep. A cross section of one of these valleys is exposed near the base of Bardin Bluffs. The valley appears to have been once contiguous with the similar, but less well exposed, profiles occurring nearby at Adamson Spur and Glossopteris Gully (Figure 42).

### **8A.1.3 Previous Work**

Drewry (1981) applied the name Pagodroma Tillite to the glaciogene strata in Pagodroma Gorge that had been reported by Bardin (1980). He summarized the sequence as "two clearly different till units separated by a transitional horizon of fluvioglacial deposits". He cites Bardin's age estimates, which were based largely on the abundance of authigenic minerals that were compared to similar abundances in East Siberian tills, of mid-Pliocene (lower till) and Upper Pliocene (upper till) age. Drewry (1981) considered the two tills to indicate thicker ice and, therefore, an expanded ice sheet at those times.

Bardin (1982) described and also illustrated the Bardin Bluffs exposures considered in this study. He recognised a lower 15 to 20 m thick, grey-coloured, sequence of glaciogene strata (denoted by Bardin as Mc) overlain by >40 m of diamicts (denoted by Bardin as Mk), with a brown surface-weathering patina. Bardin (1982) suggested an "interruption of glacial sedimentation" separated the two sequences. The older grey sequence (Mc) he noted contains a predominance of Amery Group clasts, and its overall grey colour he attributed to carbonaceous materials from the underlying Permian coal measures (in the Amery Group). Based upon their respective degrees of diagenesis, Bardin (1982) suggested the older unit to be of Miocene - Pliocene age, and the younger to be late Pliocene. Bardin and Kolosova (1983) emphasized the abundance of fine grained sediment in the lower part of the section, which they considered to be no older than early Miocene. In addition, they described an equivalent fossiliferous sequence, which is referred to herein as the *Hiatella* Location. This occurs on the western shore of Beaver Lake about 1 km northeast of Bardin Bluffs (Figure 42).

Bardin and Belevich (1985) described a brackish cold water (<5°C) benthic diatom flora, dominated by extant species, which was recovered from about 1 m above the base of the grey sequence at Bardin Bluffs. However, no diatoms were recovered from three younger samples also collected from the grey sequence. Bardin and Belevich (1985) suggested a post-early Miocene age for the flora, which they considered to represent an environment similar to that of today.

Bardin and Chepalyga (1989) identified the marine mollusc *Hiatella* cf. *H. arctica* (Linnaeus 1769) from the *Hiatella* Location (Figure 42), which occurs in abundance (albeit crushed or fragmented) between about 2 and 4 m above the base of the grey sequence. These authors considered the sequence to be of Miocene age and the molluscs to record water temperatures between 5° and 7°C warmer than that of Beaver Lake today.

The name Pagodroma Tillite was also applied to the glaciogene strata at Bardin Bluffs, along Pagodroma Gorge, and to similar strata distributed east and west of Radok Lake by McKelvey and Stephenson (1990). They considered the cutting of Pagodroma Gorge to post-date the Pagodroma Tillite. Reworked diatom floras recovered from their Pagodroma Gorge samples were identified as late Miocene and middle Pliocene in age (Harwood in McKelvey and Stephenson 1990).

Adamson and Darragh (1991) and Adamson *et. al.* (1997) demonstrated that there was considerable local relief, in the form of a palaeovalley, on the sub-Pagodroma Tillite erosion surface exposed in Pagodroma Gorge. They clearly showed the Pagodroma Tillite infilled this valley form, some of which is coincident with the present day gorge.

McKelvey *et. al.* (1995, 1997) introduced the term Pagodroma Group to incorporate all Cenozoic pre-Pleistocene glaciogene strata in the northern Prince Charles Mountains. Hambrey and McKelvey (in press) interpreted the deposition of the Pagodroma group to have been fjordal, in an environment warmer than that of today. They considered the Pagodroma Group strata occurring east of Radok Lake to be Pliocene in age, and defined this as the Bardin Bluffs Formation, but no internal subdivision of the formation was attempted. Microfossil assemblages including foraminifera, a single radiolarian species and diatoms placed deposition of the older part of the Bardin Bluffs Formation as occurring at some time between 5 - 1 Ma (Webb, pers. comm. 1999).

## 8A.2 Stratigraphy

All accessible outcrops of the Bardin Bluffs Formation were closely examined at the type locality (Figures 43 and 44). Similar, but less well exposed, sequences were also examined nearby at Bardin Knoll and on the northern side of Quike Gully (Figures 42 and 45). Two other sections were examined at Adamson Spur and the *Hiatella* Location (Figure 43 and 45), approximately 2 km southwest and 2 km northeast of Bardin Bluffs respectively (Figure 42).

Several features of the sequence exposed at Bardin Bluffs merit comment.

- 1) Two lithological Members were identified (Figures 43, 44 and 45). The lower Member 1 type section was subdivided into three lithological units (Figure 44).
- 2) The basal Member 1 occupies a valley incised into the Permo-Triassic fluvial basement rocks of the Amery Group. The axis of the palaeovalley trends approximately north - northwest. The eastern wall of this palaeovalley is moderately well exposed and the Member 1 strata which abut it contain an abundance of angular sandstone clasts. These constitute a talus that mantles the steep unconformity surface. Further away from the palaeovalley wall, such clasts within Member 1 are few. Similar talus breccias also occur at the base of both the Bardin Knoll and *Hiatella* Location sections (Figure 45).
- 3) Although the basal contact between Member 1 and the Amery Group was not exposed in the section measured at Bardin Bluffs, in several adjacent outcrops, and within 20 m of the Bardin Knoll section, the unconformity surface is friable and clearly chemically weathered to depths of up to 1.5 m.
- 4) The disconformity, or erosional surface, that separates Member 1 from Member 2 gently undulates over a lateral distance of several tens of metres. Furthermore, about 150 m west of the Bardin Bluffs section, soft-sediment deformed muddy siltstone clasts up to 50 cm across, and apparently derived from Member 1, are present within Member 2.
- 5) Comparison of the Bardin Bluffs section measured (Figure 44) with that illustrated in Bardin and Belevich (1985, Figure 2A), indicates that their sample 20-12, containing benthic diatoms, was recovered from within Unit 1 of Member 1.

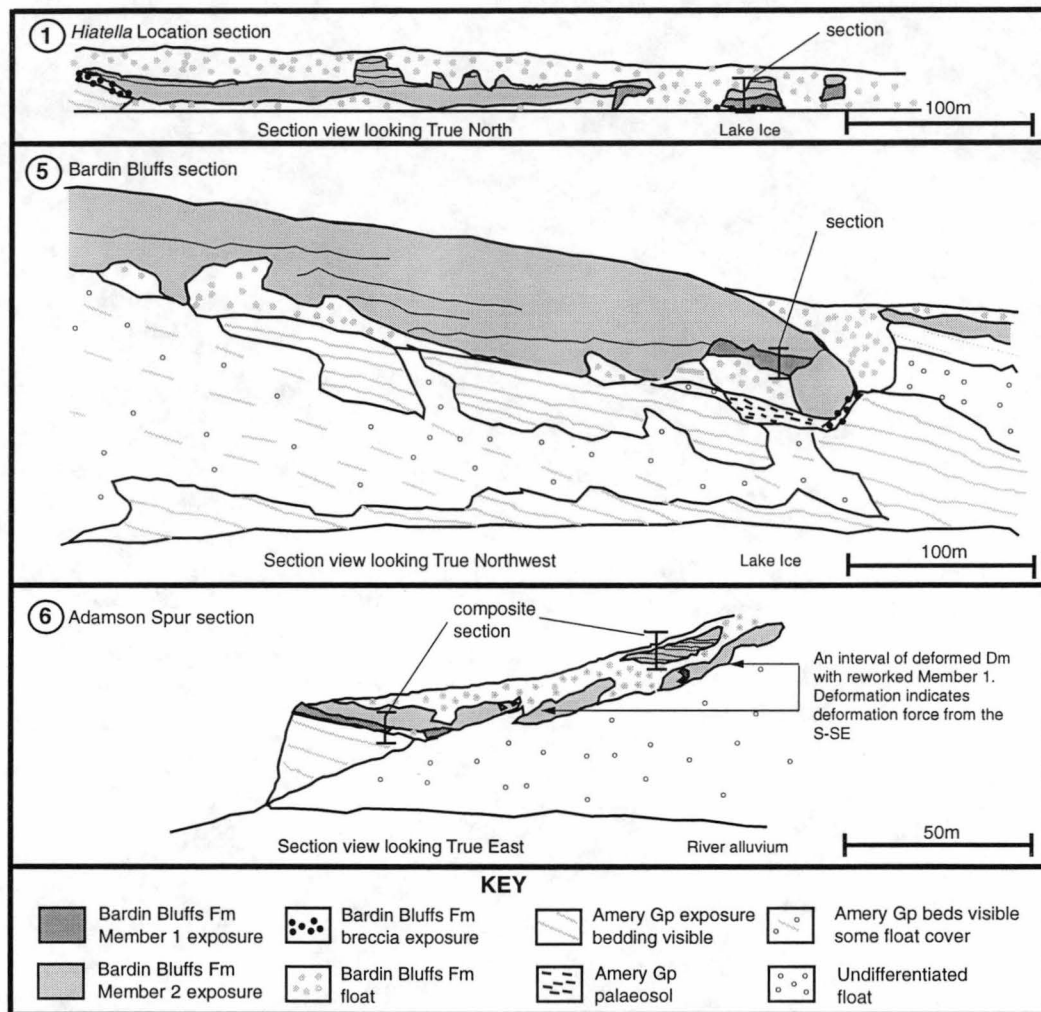


**Figure 43.** Outcrop sections through the Bardin Bluffs Formation at the *Hiattella* Location, Bardin Bluffs and Adamson Spur.

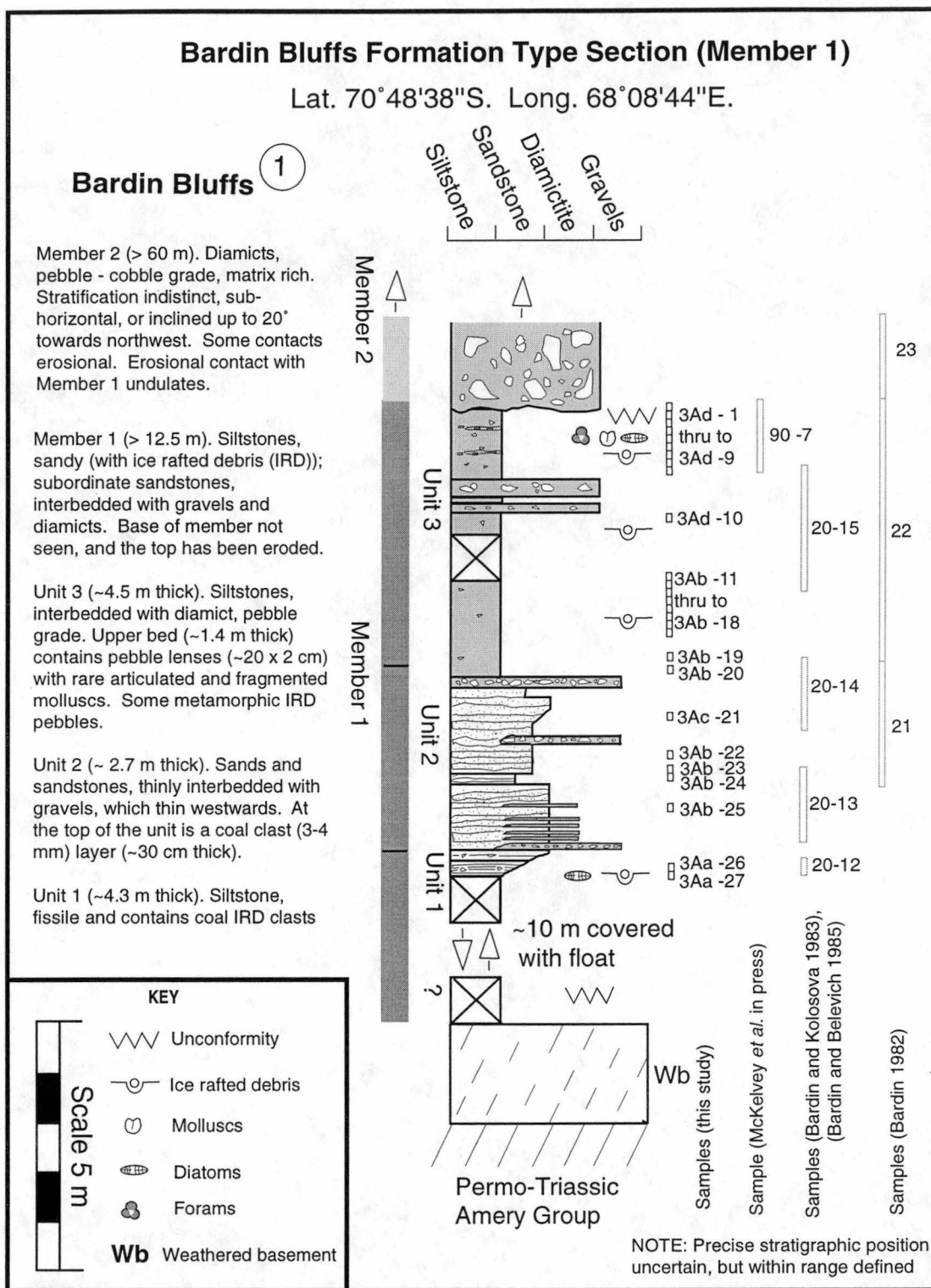


**Figure 44.** Lithological log of the Bardin Bluffs Formation type section (Member 1) at Bardin Bluffs. Previous and current sample intervals are illustrated, including the fossiliferous samples 20-12 and 90-7.

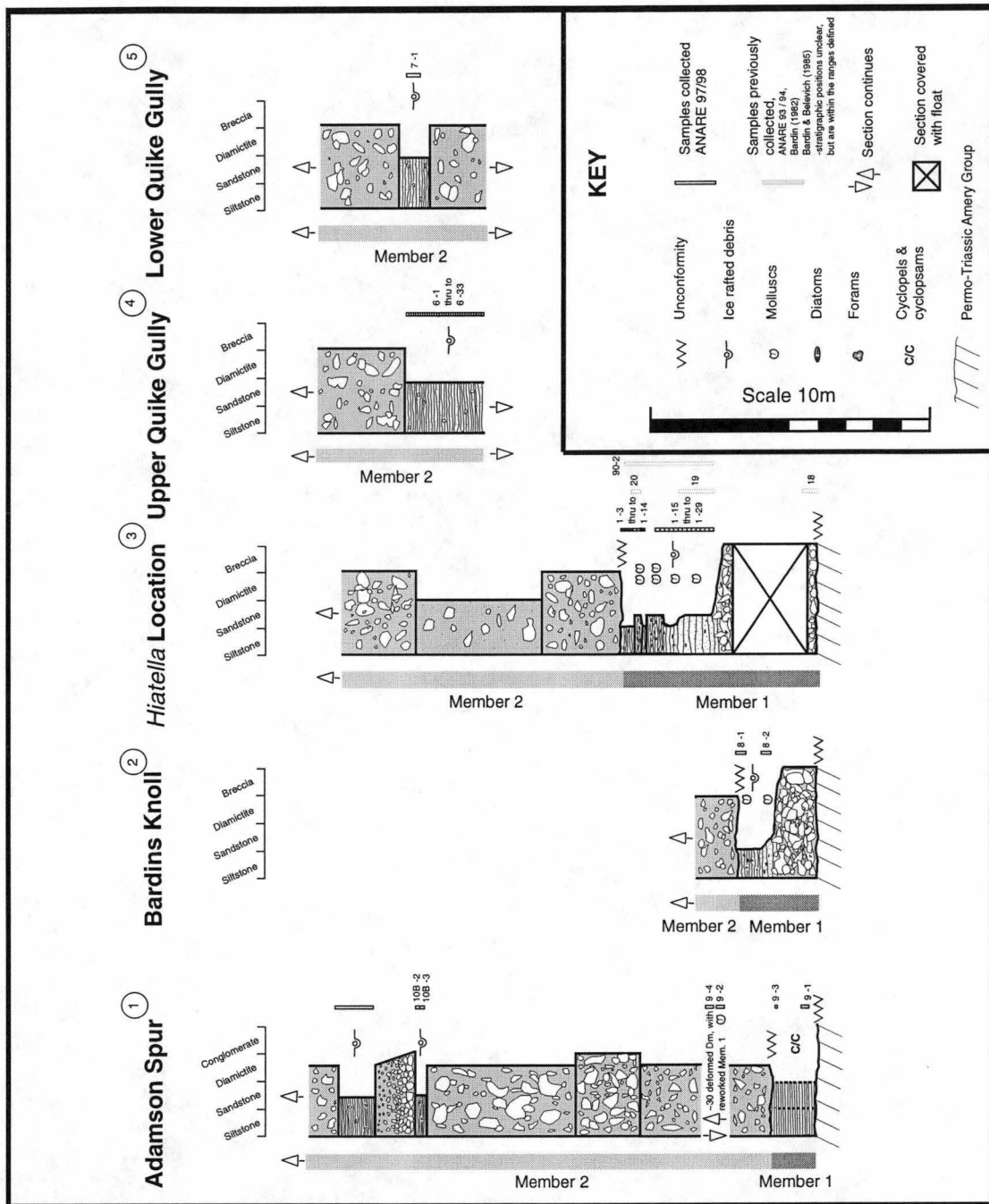


**Figure 45.** Bardin Bluffs Formation lithological logs from numbered study locations. The position of previous and current sample intervals are illustrated.

The foraminifera and radiolarian assemblage, in sample 90-7, identified by Webb (pers. comm. 1999), comes from Unit 3 of Member 1 (Figure 44).

6) The depositional age of Member 1 can be relatively well constrained from its diatom (Bardin and Belevich 1985), foraminifera and radiolarian assemblages (McKelvey *et al.* in press; Webb, pers. comm. 1999). Taxonomic revision of the diatoms illustrated in Bardin and Belevich (1985) has identified *Actinocyclus actinochilus* (Ehrenberg) Simonsen in their Plate 1, figure 4 (Harwood, pers. comm. 1998). This is an extant species that first appeared in the late Pliocene 3.1 Ma (Bohaty *et al.* 1998). The stratigraphically higher foraminifera and radiolarian fossils constrains a depositional age between 5 and 1 Ma (Webb, pers. comm. 1999). Thus an age of late Pliocene (3.1 Ma) to early Pleistocene (1 Ma) seems appropriate for Member 1.

The depositional style of Member 2 offers some further age constraint for the whole formation. The global Pliocene-Pleistocene boundary placed at 2.6 Ma by Morrison and Kukla (1998) relates to a marked change in climate and the onset of bipolar glaciation. It is thought that this resulted in a dramatic change in Antarctic sedimentation, with a transition from warm, wet-based / polythermal glaciation to cold, dry-based glaciation (Webb and Harwood 1991; Harwood *et al.* 1992; Moriwaki *et al.* 1992a; Wilson 1995). The depositional style of Member 2 is clearly wet-based or polythermal (Hambrey and McKelvey in press), and therefore could be assumed to predate the onset of cold dry-based glaciation at ~2.6 Ma. The age of the whole formation, including Member 2, could thus be placed between 2.6 Ma and 3.1 Ma. However, warmer Antarctic Pleistocene episodes have been identified (Scherer 1991; Barrett *et al.* 1998; Bohaty *et al.* 1998; Scherer *et al.* 1998), and therefore even a wholly early Pleistocene age for the formation cannot be ruled out. Lower Pleistocene (2.2 - 1.8 Ma) sediments from Prydz Bay contain diatoms that suggest warmer reduced sea-ice conditions occurred (Mahood and Barron 1996). Until more accurate resolution is forthcoming, a broad age assignment of late Pliocene (<3.1 Ma) to early Pleistocene (>1 Ma) for the whole Bardin Bluffs Formation is considered here to be appropriate.

At Adamson Spur the strata are considered to be equivalent to Member 1 (of the Bardin Bluffs sequence), and consist of ~15 m of thin-bedded laminated sandstones and siltstones (Figures 43 and 45), which are draped over the unconformity surface. These strata may be similar in origin to the tidal cyclopsams and cyclopels of Macriewicz *et al.* (1984) and Powell and Molnia (1989); however, definite tidal couplets could not be distinguished.



Unlike at Bardin Bluffs, a weathering profile on the unconformity surface is not apparent. An accurate stratigraphy of the sequence at Adamson Spur was difficult to reconstruct because there is considerable glaciotectionic deformation. This has caused sediment overfolding and thrusting, in response to forces from the south and southeast. Higher in the section are little-deformed diamicts, similar to those near the base of Member 2 at Bardin Bluffs. These are interbedded with a few brown sandstones and graded conglomerates. Similar brown sandstones occur interbedded with Member 2 diamicts at Quike Gully (Figure 45).

### 8A.3 Discussion

Four aspects of the stratigraphy of the Bardin Bluffs Formation warrant discussion.

1) Away from Pagodroma Gorge, the base of the Bardin Bluffs Formation is well exposed (i) overlooking the southern shore of Bainmedart Cove and (ii), overlooking the southeastern and southern shores of Radok Lake. However, at both these locations Member 1 is absent and the diamicts of Member 2 rest directly upon an unweathered and glacially striated erosion surface on the Amery Group (Hambrey and McKelvey in press). Similarly, above the northeastern shores of Radok Lake, although the exposures are poor, Member 2 diamicts of the Bardin Bluffs Formation directly overlie the glacially cut unconformity surface on the Amery Group.

Member 1 appears to be restricted to the lower parts of the unconformity surface (<50 m above sea-level), where it infills small valleys that constitute the oldest part of that surface. In some places the unconformity surface beneath Member 1 retains a chemically weathered profile and is devoid of striations. There are yet no data to suggest that this surface is of glacial origin. It is assumed that chemical weathering occurred during subaerial exposure of the Amery Group. Similar weathering surfaces are not developing on extant Amery Group exposures, which suggests that weathering occurred in a warmer climate than that of today.

Two separate unconformity surfaces should be recognised. A younger glacially striated erosion surface cut on the Amery Group and an older, very restricted, weathered surface preserved beneath Member 1 at Bardin Bluffs and near Bardin Knoll. Because the known aerial distribution of Member 1 and the older erosional surface is small it was not possible to confidently define two separate unconformity surfaces.

Member 1 and Member 2 may represent two distinct depositional episodes, separated by a major disconformity. Alternatively, the two members could record a transition from (relatively) distal glacial marine fjordal deposition to that of more ice-proximal waterlain and lodgment till sedimentation, in the course of a single glacial advance. However, strong evidence of lodgment till fabrics within the Member 2 is so far lacking (Hambrey and McKelvey in press). In either case, the disconformity separating the two members at Bardin Bluffs is also the unconformity surface beneath Member 2, in those areas where the latter rests directly upon the Amery Group.

2) Member 1 of the Bardin Bluffs Formation occurs at four of the six localities where sections were measured (Figures 44 and 45). Of these four localities, Member 1 is thickest (at ~12.5 m) in the type section at Bardin Bluffs. The variation in thickness seen, and the apparent absence of the member elsewhere in the Amery Oasis, is considered here to be due to the relief on both the unconformity and disconformity surfaces, bounding the base and top of Member 1 respectively. The Member 1 sequences in each of the sections also differ somewhat lithologically, and may reflect facies variations. For this reason more detailed, intra-member, correlations between the individual sequences were not attempted. Nevertheless, in all instances Member 1 is composed predominantly of silty sandstones and sandy siltstones, that contain sparse to abundant macrofossil debris, and lack the brown surface-weathering that is characteristic of Member 2. In contrast, the silty sandstones exposed in Quike Gully, and in the upper part of the Adamson Spur exposure, were brown in colour, contained no macrofossils, and are interbedded with diamicts. Therefore, these were assigned to Member 2 of the Bardin Bluffs Formation (Figure 5).

3) The relative stratigraphic positions within Member 1 of the shallow water (<50 m), benthic diatom flora in sample 20-12 (Bardin and Belevich 1985), and the deeper water, more open-marine foraminifera and radiolarian fossils in sample 90-7 (Webb, pers. comm. 1999) merits comment. It is possible that these reflect a relative sea-level transgression and overlapping marine deposition. The benthic flora occurs a few metres above the aerially weathered unconformity surface at Bardin Bluffs. In turn, this is overlain by the deep water foraminifera and radiolarian fossils.

4) Several palaeogeographic considerations arise from this study. For instance, there is little information concerning the origin and palaeogeographic setting of the erosion surface preserved beneath Member 1 at Bardin Bluffs. As stated previously, the preserved

weathering profile and apparent lack of striations does not suggest any glacial influence. In contrast, away from Pagodroma Gorge the smoothed and striated erosion surface cut on the Amery Group, beneath Member 2, suggests this was once part of a fjord floor that was cut as the Lambert Glacier grounding line advanced northwards during East Antarctic Ice Sheet expansion. The blanketing glacial marine strata of Member 2 were subsequently deposited as the glacier receded, in the late Pliocene or early Pleistocene. During the deposition of Member 2 the grounding line may have continued to fluctuate. The contacts between individual diamicts exposed at Bardin Bluffs could well be interpreted as disconformities. However, there is as yet little evidence of proven lodgment tills in Member 2 (Hambrey and McKelvey in press).

## **8A.4 Summary**

In the Amery Oasis of the northern Prince Charles Mountains, the glacial marine Bardin Bluffs Formation of the Pagodroma Group was deposited between the Upper Pliocene (<3.1 Ma) and early Pleistocene (>1 Ma). The formation provides evidence of (i) a reduced East Antarctic Ice Sheet compared to that of the present day and (ii) a subsequent Plio-Pleistocene ice sheet expansion.

The older, basal Member 1 is approximately 12.5 m thick, divided into three lithological units. It consists predominantly of sandy siltstones and silty sandstones, containing relatively minor IRD, showing only minor evidence of ice rafting, and containing molluscs, foraminifera, a radiolarian and diatoms. In summary, the member is indicative of marine sedimentation in a slightly ice-influenced setting.

Member 1 deposition occurred ~250 km inland from the present edge of the Amery Ice Shelf, and so indicates a considerably smaller East Antarctic Ice Sheet than that of today. Member 1 is restricted to the area about the northeastern end of Pagodroma Gorge where it infills a chemically weathered valley-form erosion surface cut on the Permo-Triassic Amery Group. Weathering occurred during aerial exposure of the Amery Oasis in a warmer climate than that of today.

The younger Member 2 exceeds 40 m in thickness and is made up of coarse ice proximal glacial marine diamicts, from wet-based or polythermal glacial marine sedimentation in a fjordal setting. It overlies disconformably Member 1 at Pagodroma Gorge. Elsewhere, Member 2 rests directly upon a younger smoothed and striated erosion surface, cut on the

Amery Group, which once was part of a fjord floor. This erosional surface and facies contrast between the two members indicate a later East Antarctic Ice Sheet expansion and Lambert Glacier grounding line advance. The facies contrasts between the two members, coupled with the disconformity separating them, records a major advance in the Lambert Glacier grounding line and therefore the size of the East Antarctic Ice Sheet at that time.

## **8B. Diatom Biostratigraphy of the Pagodroma Group**

### **8B.1 Introduction**

#### **8B.1.1 Aims**

The present study reports on new diatom data that provide age control for the Pagodroma Group. These data also enable the identification of times when the East Antarctic Ice Sheet (EAIS) was reduced in extent and volume and when marine conditions extended up the Lambert Graben.

#### **8B.1.2 Previous Work**

Marine molluscs, foraminifera, radiolarians and diatoms have been previously recovered from the Pagodroma Group (Bardin and Belevich 1985; Bardin and Chepalyga 1989; Harwood in McKelvey and Stephenson 1990; Harper and Harwood 1992; Laiba and Pushina 1995, 1997; Whitehead *et al.* 1996; McKelvey *et al.* in press; Webb, pers. comm. 1999). Of all these fossil groups, diatoms have the greatest potential for dating Southern Ocean sediments deposited during the last 35 million years. Marine and non-marine diatoms occur in diamict and siltstone from the Bardin Bluffs Formation (Bardin and Belevich 1985; Harwood, in McKelvey and Stephenson 1990; Harper and Harwood 1992; Whitehead *et al.* 1996) and in siltstone from the Fisher Bench Formation (Laiba and Pushina 1995, 1997). The biostratigraphic interpretation of the diatoms in the Pagodroma Group is reported in this study.

### **8B.2 Methods**

Twenty-nine sediment samples were collected from the Prince Charles Mountains during Australian National Antarctic Research Expeditions (ANARE) in 1987/88, 89/90 and 94/95. Sample locations were mapped (Figure 46), their stratigraphic position illustrated (Figures 47), and lithology recorded (Appendix 5).

Samples were prepared for siliceous microfossil analysis in a laboratory facility at the University of Nebraska dedicated to the extraction of rare microfossils from glacial deposits. Samples which yielded diatoms upon initial examination of a strewn slide were prepared in a different laboratory, in order to avoid cross contamination. As most of the samples contained too much terrigenous material for standard microfossil preparation, it was necessary to concentrate the microfossils using a series of procedures involving

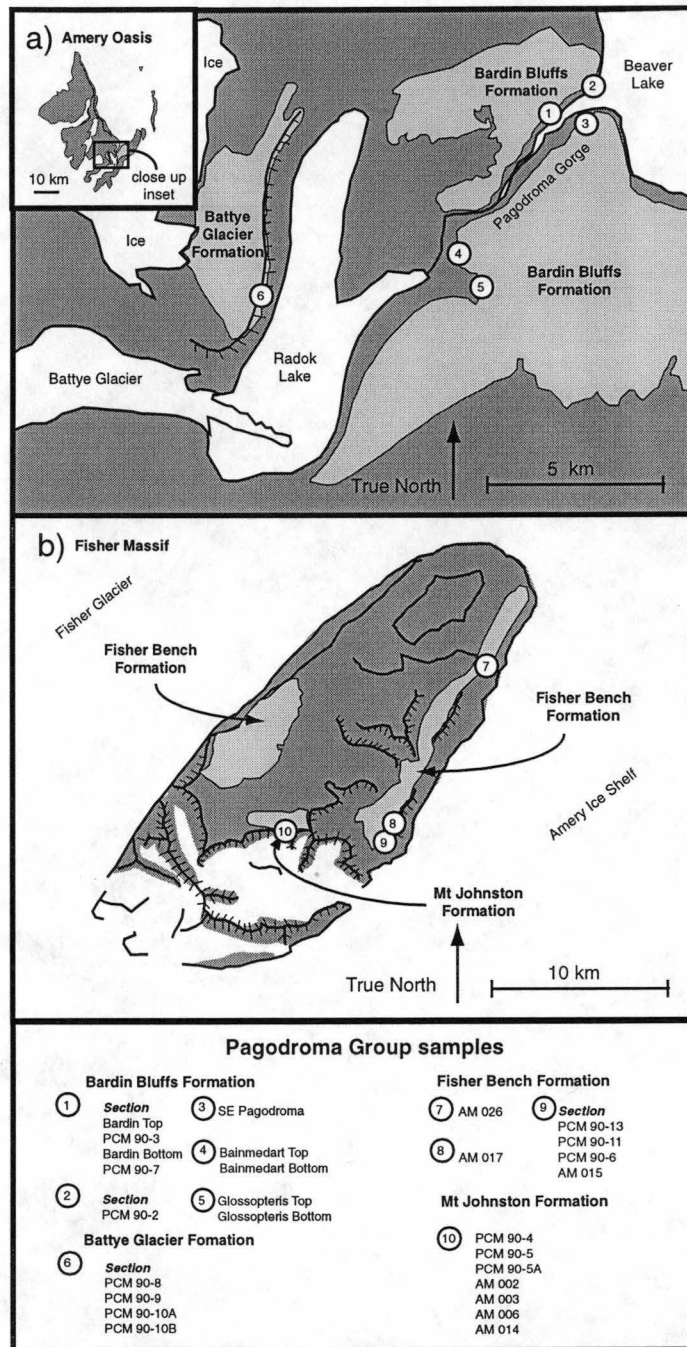


**Figure 46.** Location of Pagodroma Group samples studied for microfossils.

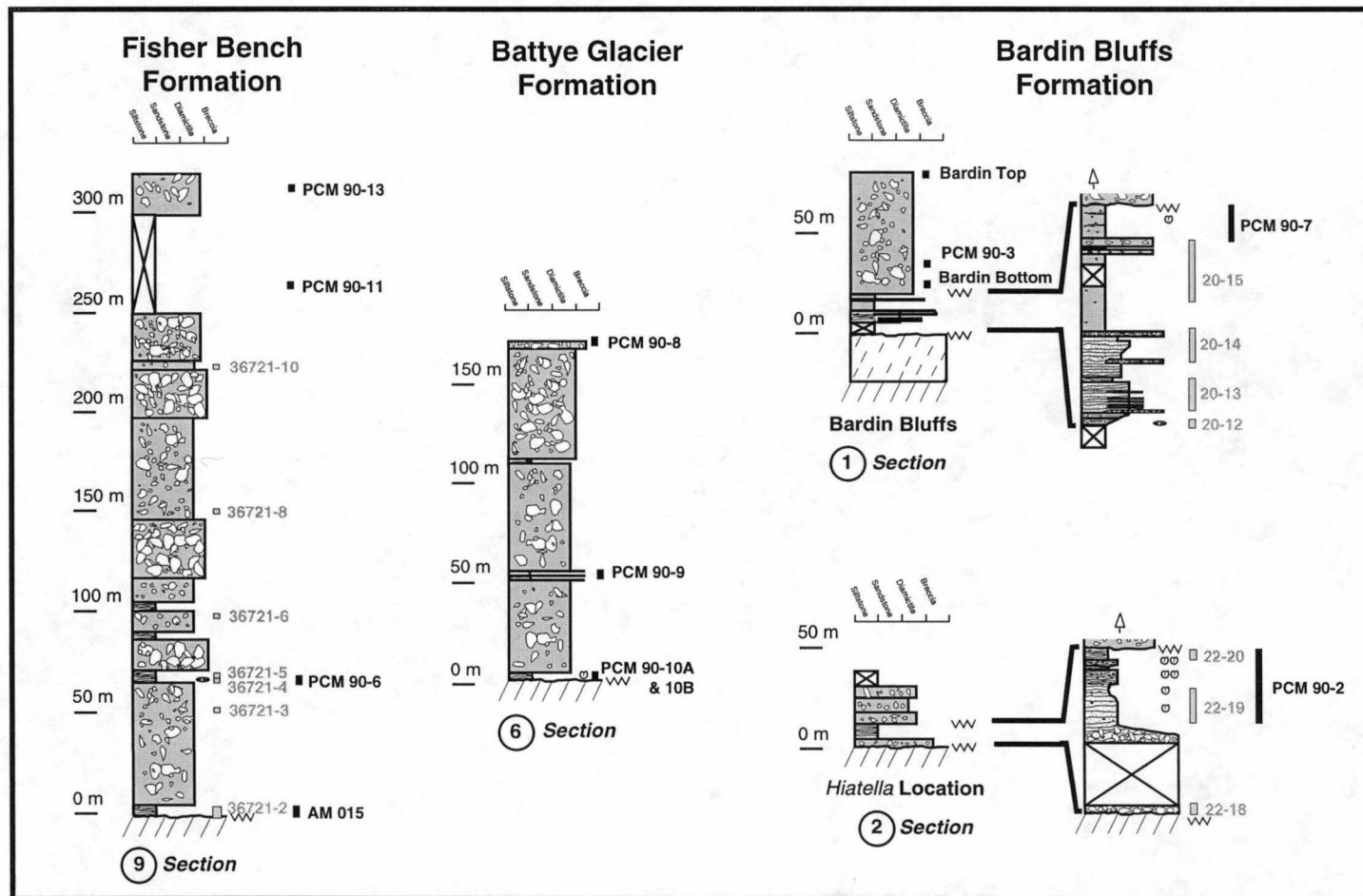


**Figure 47.** Stratigraphic position of some Pagodroma Groups samples (Fisher Bench Formation stratigraphy from Laiba and Pushina 1997, Battye Glacier Formation from Hambrey and McKelvey in press)

elutriation, sieving, gravity-settling and heavy-liquid density separation (using sodium polytungstate), as described in Harwood and Rose (1998). Microfossil concentrates were made into permanent slides and mounted with Norland Optical Adhesive 61 (refractive index = 1.56). Siliceous microfossils (predominately diatoms) were identified and recorded (Appendix 5). The concentration technique and the often fragmentary nature of the fossils prevented collection of quantitative data of microfossil abundance. However, a qualitative judgment was made on the abundance of fossils in each sample: that is, recorded as either barren (no specimens observed), very low (at least one specimen per slide), low (a few specimens per slide), moderate-low (numerous specimens per slide), moderate (many specimens per slide), moderate-high (a specimen every few fields of view), or very high (specimens on every field of view) (Appendix 5).

Diatom biostratigraphy was carried out on the Pagodroma Group (Table 8) using established datums reported in Harwood (1989), Harwood and Maruyama (1992) and Winter and Harwood (1997), revised from the Berggren *et al.* (1985a, b) geomagnetic time scales to the Berggren *et al.* (1995) time scale. Revised ages for these datums in Shackleton *et al.* (1995), Bohaty *et al.* (1998), Gersonde and Bárcena (1998) and Harwood *et al.* (in press) were also applied. Unrevised dates, for sediments compared to those in the Pagodroma Group, in this study are written in italics.

## **8B.3 Results and Discussion**

### **8B.3.1 Diatom Taphonomy**

Complete diatoms (intact frustules) and diatom fragments (broken valves) were recovered in 21 of the 29 samples examined. Diatom abundance varied from absent to very high (Appendix 5), and were generally greater in siltstone than diamict samples. The assemblages consist largely of planktic marine species. Minor mixing of diatom assemblages of different ages was noted in some samples (e.g. PCM 90-7), whilst others appeared unmixed (e.g. AM 015). All the diatoms occurred in a sand or silt matrix (in the diamict or siltstone samples); however, some diatoms contained diatomaceous sediment 'trapped' within their valves, suggesting that they have been reworked from more diatomaceous sediment (e.g. in PCM 90-2).

The state of diatom preservation differed between many samples; some diatoms occurred as fragments, some as single but intact valves, and others as whole frustules with both valves joined.



**Table 8.** Pagodroma Group biostratigraphy. Unrevised and revised datums (as discussed in the text) provided for key species, and deposit age based on these diatoms.

Pagodroma Group Diatom Biostratigraphy								
Formation	Samples	Lithology	Key diatoms	Diatom Biostratigraphy				Deposit age
				Unrevised ages (Ma)		Revised ages (Ma)		Revised (Ma)
				FAD	LAD	FAD	LAD	Unrevised (Ma)
Mt Johnnton	AM 006	diamict	<i>Pyxilla reticulata</i>	-	<u>32.3</u>	-	<u>30.2</u>	<u>&lt;-36.6</u>
			<i>Stephanopyxis splendidus</i> (T. hydra)	<u>(~36.6)</u>	<u>(~30)</u>	<u>(~36.6)</u>	<u>(~30)</u>	<u>&lt;-36.6</u>
Fisher Bench	AM O15	siltstone	<i>Actinocyclus ingens</i> var. <i>nodus</i>	14.5	<u>12.3</u>	14.6	<u>12.5</u>	<u>14.2(12.6)-12.5</u>
			<i>Actinocyclus ingens</i>	16.4	0.62	16.2	0.67	<u>14.2(12.5)-12.3</u>
			<i>Denticulopsis simonsenii</i>	<u>14.2</u>	<u>5.6-5.7</u>	<u>14.2</u>	<u>6.2-6.3</u>	
			<i>Proboscia barboi</i>	12.5		12.6	1.8	
	36721-4 (Laiba and Pushina 1997)	siltstone	<i>Actinocyclus ingens</i>	16.4	0.62	16.2	0.8	<u>14.2-6.5</u>
			<i>Denticulopsis hustedii</i>	<u>14.2</u>	<u>5.6-5.7</u>	<u>14.2</u>	<u>6.2-6.3</u>	<u>14.2 - 5.6</u>
Battye Glacier	PCM 90-8	diamicts	<i>Thalassiothrix</i> sp	mid-late	0.0	-	0.0	< mid-late Oligocene
	PCM 90-10B			Oligocene				
Bardin Bluffs	PCM 90-7	siltstone	<i>Actinocyclus actinochilus</i>	<u>3.0</u>	0.0	<u>3.1</u>	0.0	<u>3.1-1.8</u>
			<i>Fragilaropsis praeinterfrigidana</i>	4.5	3.5	4.9	3.7	<u>3.0-1.7</u>
			<i>Actinocyclus karstenii</i>	11.7	<u>1.7-2.8</u>	12.2	<u>1.8-2.9</u>	
			<i>Nitzschia reinholdii</i>	5.8	-	6.4	0.62	
	20-12 (Bardin and Belevich 1985)	siltstone	<i>Actinocyclus actinochilus</i>	<u>3.0</u>	0.0	<u>3.1</u>	0.0	<u>&lt;3.1</u>
			<i>Thalassiosira oestrupii</i>	5.1	0.0	5.6	0.0	<u>&lt;3.0</u>
	PCM 90-2	siltstone	<i>Actinocyclus ingens</i>	16.4	<u>0.62</u>	16.2	<u>0.67</u>	<u>6.4-0.67</u>
			<i>Thalassiosira oliverana</i>	<u>5.8</u>	0	<u>6.4</u>	0	<u>5.8-0.62</u>
	Bardin oldest	diamicts	<i>Fragilaropsis kerguelensis</i>	<u>3.1</u>	0.0	<u>3.2</u>	0.0	<u>&lt;3.2</u>
	Bardin top		<i>Fragilaropsis curta</i>	3.5	0.0	3.7	0.0	<u>&lt;3.1</u>
	Glossopteris old		<i>Fragilaropsis interfrigidana</i>	3.6	2.6	3.8	2.8	
	Glossopteris young		<i>Thalassiosira inura</i>	4.5 (4.8)	1.8	4.6 (4.9)	1.9	
	Pagodroma SE-side		<i>Fragilaropsis praeinterfrigidana</i>	4.5	3.5	4.9	3.7	
	Bainmedart 1		<i>Rouxia heteropolara</i>	4.3	2.5	5.1	2.6	
	Bainmedart 2		<i>Denticulopsis dimorpha</i>	11.9 (12.2)	8	12.2 (12.4)	(~10.8)	
			<i>Denticulopsis hustedii</i>	14.2	5.6-5.7	14.2	6.5-6.7	
			<i>Denticulopsis praedimorpha</i>	12.6	11.1	12.8	(~11.7)	

Diatom preservation reflects the degree of silica dissolution and mechanical breakage (Shemesh *et al.* 1989; Leventer 1998). Dissolution favors the preservation of heavily silicified diatoms (Shemesh *et al.* 1989; Pichon *et al.* 1992; Leventer 1998). On the Antarctic continental shelf dissolution may be less important in controlling the surface sediment diatom assemblage than in deeper water areas of the Southern Ocean (Leventer and Dunbar 1996). Fragmentation of diatoms tends to reflect mechanical transport and bioturbation (Truesdale and Kellogg 1979; McMinn 1995). Grazing in the water column causes little diatom breakage; for example, nearly all diatom deposition in McMurdo Sound consists of unbroken diatoms that have settled within fecal pellets (Dunbar *et al.* 1991; DeMaster *et al.* 1992). The mechanical breakage of diatoms in the Ross Sea has been attributed partially to water current transport (Truesdale and Kellogg 1979). It is possible that severe mechanical breakage could occur also during glacial reworking.

Preservational and taxonomic differences between the Pagodroma Group diatoms suggest that they have originated from a variety of sources, and that various modes of transport, deposition, and *in situ* production may have contributed to these assemblages. Identifying the sources and transport mechanism of diatoms in the Pagodroma Group is crucial to correct biostratigraphical and palaeoenvironmental interpretation of these deposits.

It is unlikely that marine diatoms recovered from the Pagodroma Group are aeolian in origin. There are no known modern exposures that could represent an aeolian source for all the species and multiple ages represented by diatoms recovered from the Pagodroma Group. Furthermore, airborne diatoms found in recent (<20 000 years) Antarctic ice cores are predominately small freshwater and benthic taxa (Burckle *et al.* 1988b; Kellogg and Kellogg 1996; Harwood and Webb 1998), which is in strong contrast with the predominantly marine planktic assemblages in the Pagodroma Group (Appendix 5). Similar observations, based on the abundance of freshwater versus marine diatoms, have been used to comment on the origin of the diatom in the Sirius Group (Burckle *et al.* 1988b; Harwood *et al.* 1999). The Pagodroma Group diatoms are also unlikely to have originated from meteorite impact ejecta. For example, the Eltanin meteorite impact in the Southern Ocean ~2.15 Ma is thought to have reworked Cenozoic sediment over Antarctica spanning the last 50 My in age (Gersonde *et al.* 1997). Whilst there is biostratigraphic mixing in diatom assemblages from the Bardin Bluffs Formation, this does not span the last ~50 Ma, furthermore, some samples from other older formations (e.g. AM 015 in the Fisher Bench Formation) contain no sign of mixed ages, whilst some samples contain no diatoms at all. As exposures of the Pagodroma Group are actively eroding, the persistence

of debris from marine meteorite ejecta on the outcrop surface for the last 2.15 My is extremely unlikely. The most likely source of the marine diatoms in the Pagodroma Group is from *in situ* marine deposition and from glacial reworking of previous marine deposits, as illustrated in Figure 48.

### **8B.3.2 Pagodroma Group Biostratigraphic and Palaeoenvironmental Interpretation**

#### **Mt Johnston Formation**

Diamicts from the Mt Johnston Formation (Figures 46) contain rare diatoms and diatom fragments (Appendix 5). All of the recovered specimens are planktic marine species. The presence of *Stephanopyxis splendidus* (Greville) Harwood and *Pyxilla reticulata* Grove *et* Sturt indicates marine deposition during the late Eocene to early Oligocene (Harwood 1989; Wilson *et al.* 1998). The age may be constrained further by the lack of biostratigraphic mixing with the local, and stratigraphically younger, Middle to Upper Miocene Fisher Bench Formation (discussed below). Stratigraphic relationships suggest deposition of the Mt Johnston Formation sometime during the late Eocene to middle Miocene. It is likely that planktic marine diatoms in the Mt Johnston Formation were reworked by glacial ice from marine sediments deposited inland of Fisher Massif in the late Eocene to early Oligocene.

#### **Fisher Bench Formation**

Siltstone and diamict facies of the Fisher Bench Formation (Figure 46 and 47) contain marine diatoms and diatom fragments (Appendix 5). These fossils are abundant in two siltstone beds near the base of the section (sample AM 015) and ~70 m above the base of the section (sample 36721-4, reported by Laiba and Pushina 1997). The siltstones contain planktic and benthic marine diatoms, which overlap biostratigraphically in the Miocene. Diatoms in the lower siltstone bed (AM 015) were deposited in the middle Miocene, between 14.2 and 12.5 Ma. This is indicated by the presence of *Actinocyclus ingens* var. *nodus* Baldauf, (FAD 14.2 Ma; LAD 12.5 Ma) and *Denticulopsis simonsenii* Yanagisawa *et* Akiba (referred to as *Denticulopsis hustedtii* (Simonsen *et* Kanaya) Simonsen in previous literature) (FAD 14.2 Ma). The older age range could be also interpreted from the presence of *Proboscia barboi* (Brün) Jordan and Priddle (FAD 12.6 Ma); however, this datum is less reliable than the FAD of *D. hustedtii* (Harwood, pers. comm. 1997) applied here. The siltstone bed ~70 m up the section (36721-4) was deposited between 14.2 and 6.5 Ma (middle to late Miocene), as indicated by the presence of *D. simonsenii* (FAD 14.2 Ma and LAD 6.5 Ma) (Laiba and Pushina 1997).

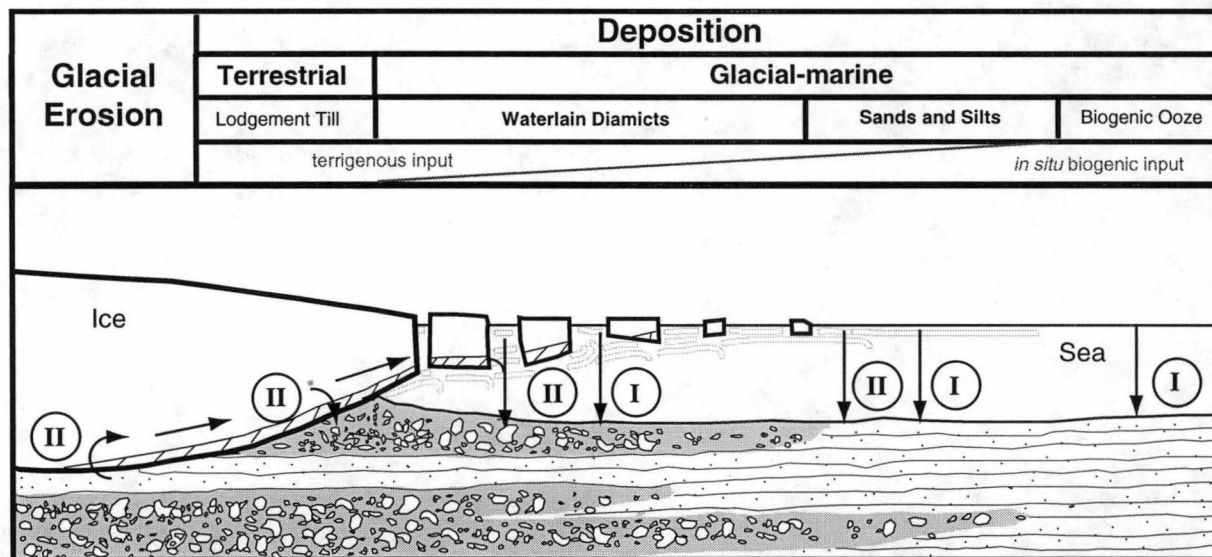


**Figure 48.** Likely source, transport and depositional pathways for marine planktic diatoms in the Pagodroma Group. (I) *In situ* marine deposition and (II) glacial, glacial-marine, reworking of older subglacial marine deposits.

Biostratigraphic interpretations are generally made from planktic taxa with a widespread distribution; however, in the Fisher Bench Formation siltstones benthic species support a Neogene age. *Rhabdonema japonica* Tempere *et* Brun, Gen. *et* sp. indet. C Harwood (1986a) and *Isthmia* sp. occur in AM 015; *Hyalodiscus obsoletus* Sheshukova, *Rhabdonema* sp. and *Rhaphoneis* spp. occur in 36721-4. These taxa are no longer found in the modern Antarctic environment (Whitehead, unpublished obs.), but were present in Neogene shallow marine sediments in the Ross Sea (Harwood 1986a, 1986b; Harwood *et al.* 1989; Winter 1995; Barrett *et al.* 1998) and the Vestfold Hills (Harwood 1986a).

Along strike from sample 36721-4, sample PCM 90-6 contained a few complete diatoms and diatom fragments (Appendix 5), but these specimens add no further constraint on the age. Diatoms in sample AM 015 indicate that deposition of the Fisher Bench Formation began in the middle Miocene. The diatoms are abundant, they are restricted in occurrence to the siltstone bed, there is no evidence of mixing from different ages or environments, thus indicating this is a natural *in situ* accumulation of diatoms in an open-marine environment, rather than a reworked assemblage.

Diamicts in the Fisher Bench Formation are either barren of diatoms (e.g. PCM 90-13) or contain a moderate amount of diatoms and diatom fragments (e.g. PCM 90-11). Sample PCM 90-11 contains an assemblage that differs bi-modally in preservation, taxonomy and ecology. The more abundant, well preserved diatoms are *Gomphonema angustatum* var. sp. A, *G. angustatum* var. sp. B, *Diploneis* sp. A and *Amphora* sp. A, which frequently occurs as complete frustules with their valves joined, all are benthic taxa (Round *et al.* 1990). *Gomphonema angustatum* is a fresh water species (Cramer 1979; Beaver 1981), as could be the variants *G. angustatum* var. sp. A, *G. angustatum* var. sp. B. *Diploneis* and *Amphora* are found in modern marine and lake environments (Whitehead and McMinn 1997; Roberts and McMinn 1999); however, the preservational association of *Diploneis* sp. A and *Amphora* sp. A with *G. angustatum* var. sp. A and B may suggest that these species are also derived from a freshwater deposit. Similar preservation is seen in some non-marine diatoms from the Sirius Group (Mount Feather, Transantarctic Mountains), which were interpreted as *in situ* or as having formed nearby (Harwood and Rose 1998). It is possible that the well-preserved diatoms in PCM 90-11 originated syndepositionally from lake discharges into the Lambert Graben during deposition of the Fisher Bench Formation. The less abundant, fragmented, diatoms in the assemblage are planktic marine species, and have a poor age constraint with the youngest datum constrained by the presence of *P. barboi* (with uncertain FAD at 12.6 Ma, mentioned above). There is no

evidence of biostratigraphic mixing in PCM 90-11. The marine diatoms in this sample were probably glacially reworked from marine sediments that may have existed further inland, up glacier.

#### Battye Glacier Formation

Diatom fragments are rare in diamict and siltstone facies of the Battye Glacier Formation (samples PCM 90-8 and PCM 90-10B) (Figures 46 and 47; Appendix 5). The fragments are of extant planktic marine *Thalassiothrix* sp., which provide no biostratigraphic age control. These diatom fragments were probably glacially reworked from marine sediments that may have existed further inland.

#### Bardin Bluffs Formation

The Bardin Bluffs Formation (Figures 46 and 47) has two lithological members (Chapter 8A). The basal Member 1 consists largely of siltstone and sand. It is disconformably overlain by Member 2, which consists largely of diamict (Chapter 8A). Diatoms were recovered from siltstone and diamict samples throughout the formation (Appendix 5).

##### *Member 1*

Two fossiliferous siltstone beds occur in Member 1 of the Bardin Bluffs Formation at the type section (Chapter 8A). Abundant diatoms were recovered from the stratigraphically lower siltstone (sample 20-12, Figure 3) (Bardin and Belevich 1985). *Actinocyclus actinochilus* (Ehrenberg) Simonsen is noted in Bardin and Belevich (1985) Plate 1, photo 4, as *Charcotia actinochilus*. It is an extant species with a FAD in the late Pliocene, 3.1 Ma (Bohaty *et al.* 1998), indicating that Member 1 is less than 3.1 My old. The diatom assemblage from sample 20-12 also contains many Antarctic benthic marine diatoms, and a few planktic diatoms, suggesting that deposition occurred in a shallow, euphotic environment of water depth less than 75 m (Bardin and Belevich 1985).

A stratigraphically higher, and younger, Member 1 siltstone bed at Bardin Bluffs (sample PCM 90-7, Figure 47) contains a moderately high abundance of diatoms and diatom fragments. The assemblage contains *A. actinochilus*, which, again indicates deposition <3.1 Ma ago. The presence of foraminifera and a radiolarian suggests that deposition occurred between 5 - 1 Ma (Webb, pers. comm. 1999). Together, these datums support a late Pliocene (3.1 Ma) to early Pleistocene (1 Ma) age for Member 1 (proposed in Chapter 8A). The diatom assemblage from sample PCM 90-7 is also biostratigraphically mixed, with the co-occurrence of *A. actinochilus* and *Fragilariopsis praeinterfrigidaria*

(McCollum) Gersonde *et* Barcena (LAD 3.7 Ma). The assemblage is almost exclusively planktic, with the exception of one benthic diatom, *Cocconeis pinnata* Gregory. The low abundance of benthic diatoms suggests that deposition occurred in water depth exceeding euphotic depths (>75 m).

Differences between the diatom assemblages in sample 20-12 and PCM 90-7 indicate that environmental changes occurred during deposition of Member 1 at the type section. The lower siltstone bed (sample 20-12) contains the extant species *A. actinochilus*, *Thalassiosira antarctica* Comber and *Thalassiosira oestrupii* (Ostenfeld) Proschkina-Lavrenko, which are absent from sample PCM 90-7. In turn, the older taxa *N. reinholdii* and *F. praeinterfrigidaria* present in PCM 90-7 were not noted from sample 20-12. The ecology of the two assemblages also differs; sample 20-12 contains many shallow marine benthic diatoms (Bardin and Belevich 1985), yet sample PCM 90-7 consists almost exclusively of planktic taxa. The foraminiferal assemblage in PCM 90-7 is also from a deep water environment (Webb, pers. comm. 1999). The change from a predominately benthic diatom assemblage (sample 20-12) to a planktic diatom assemblage (sample PCM 90-7) up Member 1 suggests that a relative rise in sea-level occurred. This is supported by transgressive sea-level evidence in Chapter 8A.

A moderate abundance of diatoms were recovered in the siltstone of Member 1 from the *Hiatella* Location, sample PCM 90-2 (Figure 47, Appendix 5). The assemblage consisted largely of extant planktic diatoms, with the exception of extinct taxa *Actinocyclus ingens* Ratray (LAD 0.67 Ma) and *Rouxia isopolica* Schrader. The presence of *Thalassiosira oliverana* (O'Meara) Sournia (FAD 6.4 Ma) indicates deposition occurred after 6.4 Ma. However, the absence of *A. actinochilus* prevents a direct correlation to the siltstone beds at Bardin Bluffs. Some diatoms from sample PCM 90-2 occur in diatomaceous sediment aggregates, suggesting that part of the assemblage was reworked from a diatomaceous sediment source.

The absolute abundance of diatoms in siltstone samples 20-12 (as indicated by Figure 1, Plate 1 in Bardin and Belevich, 1985), PCM 90-7 and PCM 90-2 is low. Geochemical analysis on samples from these intervals indicate that the biogenic silica content (largely from diatoms) is <3% (Whitehead, unpublished data). This is much less than in modern Antarctic continental shelf sediments, which contain 10 - 90% biogenic silica (Stockwell *et al.* 1991; McMinn *et al.* 1998). Terrigenous input may have been higher during deposition of the Pagodroma Group, compared to the modern environment. This could have

increased water turbidity (Elverhøi 1984), decreased light levels (Maffione 1998), reduced diatom productivity, and diluted the biogenic input. Infaunal mollusc fossils collected from sample PCM 90-7, are species that were able to dig upwards through the accumulating sediment and could have survived in areas with a high sediment input (Hart, pers. comm. 1998). The glacial style during deposition of the Pagodroma Group is, is more wet-based and, thought to have been warmer than today (Hambrey and McKelvey in press), which resulted in higher erosion rates at the glacier bed, faster glacier flow and higher sedimentary input into the nearby marine environment. The glacially transported sediment probably contained reworked diatoms and diatomaceous sediment (Figure 48), which resulted in the biostratigraphic mixing, of different aged diatoms, observed in the Bardin Bluffs Formation.

### *Member 2*

Many of the diamicts in Member 2 of the Bardin Bluffs Formation contain diatoms. The diatoms are predominantly planktic marine taxa that lived in the Southern Ocean during the Miocene, Pliocene (Harwood in McKelvey and Stephenson 1990) and Pliocene - Quaternary (Appendix 5, Table 8). The presence of *Fragilariopsis kerguelensis* (O'Meara) Hasle (FAD of 3.2 Ma) indicates that the diamicts were deposited after 3.2 Ma. However, the diamict assemblages are also biostratigraphically mixed (Table 8) and contain occasional fragments and diatomaceous sediment aggregates consisting of planktic freshwater diatoms (Harper and Harwood 1992) of the genera *Cyclotella*, *Stephanodiscus* and *Aulacoseira* and a specimen of *Tabellaria fenestrata* (Lyngb.) Kutzing. The first two genera are indicative of a late Miocene to recent age (Bradbury and Krebs 1995). Diatoms in the Bardin Bluffs Formation diamicts probably originated from a variety of subglacial sources such as lake and marine deposits.

The Bardin Bluffs Formation diamicts of Member 2 are thought to have been deposited in a marine environment heavily influenced by icebergs (Hambrey and McKelvey in press). The diatom evidence indicates that there were times during the Pliocene to Quaternary when diatoms were deposited under open marine conditions that existed between deposition of the diamicts. Miocene, Pliocene and Pliocene-Quaternary planktic diatoms were probably glacially reworked from inland marine deposits and incorporated into the diamicts of Member 2. Reworked Miocene marine diatoms in the diamicts include *Denticulopsis dimorpha* (Schrader) Simonsen and *Denticulopsis praedimorpha* Barron ex Akiba, which lived between 12.2 Ma (12.4 Ma) and ~10.8 Ma. Neither species was recovered from the Fisher Bench Formation, providing indirect evidence for other



intervals of EAIS reduction and marine deposition. Similar EAIS reductions may have occurred during the Pliocene (4.9 - 3.7 Ma) when *F. praeinterfrigidaria*, which now occurs as reworked fossils throughout some parts of the formation, was deposited. Pliocene-Quaternary diatoms in the diamicts may have also been reworked from Member 1 siltstones, or correlative strata. There are, however, some taxonomic differences between the Member 1 siltstone and the diamict assemblages, which could reflect ecological and temporal differences between the reworked and preserved parts of Member 1. Alternately, these diatoms could have come from completely unrelated marine deposits from elsewhere in the Lambert Graben.

The freshwater planktic lake diatoms *Aulacoseira* sp., *Stephanodiscus* sp., *Cyclotella* sp. and *T. fenestrata* in the Bardin Bluffs Formation diamicts may have come from a fresh water lake deposits. The size of these aggregates could help identify if they are aeolian or glacially reworked (Harwood and Webb 1998). Aeolian diatomaceous material found in Antarctic ice cores is <25 µm in diameter (Harwood and Webb 1998). There is currently, however, a lack of data to identify which source is most likely for the freshwater diatoms in the Pagodroma Group. Planktic freshwater diatoms are not present in Antarctic lakes today (Harper and Harwood 1992).

### **8B.3.3 Palaeoenvironmental Significance of the Pagodroma Group and Correlation with other Records**

Planktic marine diatoms in the Mt Johnston Formation were probably reworked from Upper Eocene / Lower Oligocene deposits south of 72°S latitude by glaciers during the Oligocene to middle Miocene. The closest known *in situ* Lower Oligocene marine sediments occur in Prydz Bay, ODP Site 739 (Baldauf and Barron 1991; Barron and Mahood, 1993). Two marine intervals in Site 739 contain diatoms similar to those in the Mt Johnston Formation, with the co-occurrence of *P. reticulata*, *S. splendidus* and *Stephanopyxis grunowii* Grove *et al.* These may have been deposited in Prydz Bay at a similar time to the marine sediment reworked within the formation; however, a direct correlation would be tenuous. Both of these deposits indicate that major EAIS fluctuations occurred in the late Eocene to early Oligocene. The Lower Oligocene marine sediments in Prydz Bay are bound by disconformities, which formed during EAIS expansion when the Lambert Glacier grounded at the continental shelf break (Hambrey *et al.* 1991). Upper Eocene to Lower Oligocene marine diatoms in the Mt Johnston Formation suggest that there was at least one intervening episode of glacial retreat, during which the grounding line may have moved ~600 km southward, enabling marine deposition inland of Fisher

Massif. Dramatic changes in the glacial conditions of the Lambert Graben may also explain the high amount of ice-rafted-debris in lower Oligocene sediment on the Kerguelen Plateau (36.0 - 35.8 Ma) (Breza and Wise 1992). These may have been deposited during a major interval of iceberg release, either associated with wet-based glacial conditions or glacial reduction. A similar assemblage to the Mt Johnston Formation diatoms also occurs in lower Oligocene marine sediments from the CIROS-1 drillcore in McMurdo Sound (Harwood 1989). The CIROS -1 strata (366 to 500 m below surface) consist of interbedded diamicts and marine sediment, which also suggest that glacial conditions fluctuated in the late Eocene to early Oligocene (Barrett 1989; Wilson *et al.* 1998).

Grounded ice was thought to have filled much of the Lambert Graben through the early Oligocene until the late Miocene (10 Ma) (Hambrey *et al.* 1991). It has been traditionally viewed that Antarctic ice volume has fluctuated little since the Middle Miocene (e.g. Flower and Kennett 1994). *In situ* marine diatoms in the Fisher Bench Formation and reworked diatoms in the Bardin Bluffs Formation indicate that glacial conditions and ice volume continued to vary significantly after the Middle Miocene. At times, the Lambert Glacier grounding line retreated more than 600 km inland from the continental shelf break, southward beyond 72° S.

*In situ* marine diatoms in the Fisher Bench Formation indicate that significant EAIS reduction occurred between 14.2 - 12.5 Ma (14.2 - 12.3 Ma) (in sample AM 015) and 14.2 - 6.5 Ma (14.2 - ~5.65 Ma) (in sample 36721-4). These EAIS reduction are notably younger than the Middle Miocene oxygen isotope shift (Shackleton and Kennett 1975), which was used to infer permanent establishment of the present EAIS during this time (Sugden 1992; Denton *et al.* 1993; Kennett and Hodell 1995). There is much supporting evidence for EAIS fluctuations from the Middle Miocene to Pliocene. Climate fluctuations 16-12.5 Ma led to the deposition of alternating cold and warm water facies on the Maud Rise and Kerguelen Plateau (Rack 1993). Cool water nannoplankton were absent from Kerguelen Plateau 15.2 - 14.07 Ma and 12.84 - 8.92 Ma (Beaufort and Aubry 1992). Middle to late Miocene reductions in the volume of the EAIS may have enabled marine deposition in the Antarctic subglacial Wilkes, Pensacola (Harwood 1983; Harwood 1986a; Webb *et al.* 1984; Faure and Harwood 1990) and Ross-Bentley embayments, now beneath ice sheets or ice shelves (Scherer 1989, 1991; Harwood *et al.* 1989). Late Miocene warm intervals have also been recognised from open water diatom assemblages in the Western Ross Sea in the DVDP-11 drillcore (Winter and Harwood 1997), and nearby in the Wright Valley, where warm late Miocene (somewhere between 10.5-7.5 Ma)

glacial marine sediments of the Jason Diamicton were deposited (Prentice *et al.* 1993). Recently, Prentice *et al.* (1999) reported significant negative excursion of oxygen isotopes in carbonate from the DVDP drillcores, which reflect extensive discharge of glacial meltwater into the western Ross Sea.

Reworked Pliocene diatoms in the Bardin Bluffs Formation suggest marine deposition occurred in the Lambert Graben during warmer climatic conditions 4.9 - 3.7 Ma (4.5 - 3.5 Ma). This may correlate with deposition of the Sørødal Formation (4.1 - 4.5 Ma (3.8 - 4.1 Ma), Harwood *et al.* in press), which was deposited on the nearby Vestfold Hills during warm climatic conditions (Harwood 1986a; Pickard *et al.* 1986, 1988; Quilty 1991, 1992, 1993; Fordyce and Quilty 1994). Mid-Pliocene warming is thought to have peaked between ~4.8 and 4.4 Ma, with the southerly occurrence of low- and mid- latitude radiolarian and diatom species in the Southern Ocean, when marine temperatures were 5° to 10°C warmer than today (Abelmann *et al.* 1990). The Antarctic Polar Front Zone (APFZ) was also considered further south ~4.4 to 4.2 Ma, as indicated from high biogenic accumulation, low biogenic silica concentrations, and the presence of warm-water diatoms and silicoflagellates in ODP Site 704 (Froelich *et al.* 1991). Climatic conditions probably fluctuated between 4.5 - 3.5 Ma, as indicated by the occurrence of warmer water silicoflagellates on the Kerguelen Plateau (ODP Sites 751 and 748), which suggest warming up to 4°C, occurred in the intervals ~4.5 Ma, ~4.3 Ma and ~3.6 Ma (Bohaty and Harwood 1998). These suggest that the APFZ was either ~900 km further south or the temperature gradient across the associated ocean fronts became shallower (Bohaty and Harwood 1998).

Pliocene temperatures were apparently high enough to support the growth of *Nothofagus* in the Transantarctic Mountains, as suggested from two independent lines of evidence: the *in situ* *Nothofagus* leaf fossils in the Sirius Group (Hill *et al.* 1996) and a peak at 3.0 Ma of *Nothofagidites* pollen in DSDP Site 274 (Fleming and Barron 1994, 1996). It is likely that reduction in volume of the EAIS and marine deposition in the Lambert Graben (at 71°S) occurred during one or more of these warm events.

The type section of the Bardin Bluffs Formation was deposited between 3.1 and 1 Ma. *In situ* marine diatoms in samples 20-12 and PCM 90-7 indicate that marine conditions occurred ~250 km inland of the current edge of the Amery Ice Shelf. In support of this, Lower Pleistocene (2.2 - 1.8 Ma) sediments in nearby Prydz Bay contain diatoms that suggest warmer marine water than at present and reduced sea-ice (Mahood and Barron

1996). Silicoflagellates data from the Kerguelen Plateau indicate that a significant warming occurred 3.1 - 2.64 Ma, with a 3° to 4.5 C° rise in sea-surface temperature at 62° S (GC 34) (Chapter 6). This could have only occurred if the APFZ was either ~1200 km further south or the temperature gradient across the associated ocean fronts became significantly shallower (Chapter 6). Diatoms recovered from the Sirius Group suggest that the EAIS extent and volume were reduced, by as much as third of today's size, as recently as <3.1 Ma (Harwood 1983; Webb *et al.* 1984, 1996). It is possible that marine conditions in the Wilkes and Pensacola Basins, as suggested by Sirius Group data, were contemporaneous with marine incursions into the Lambert Graben as indicated here from diatom evidence from the Pagodroma Group. It is unknown how the Lambert Glacier-Amery Ice Shelf system responded to subsequent warming of the Antarctic region identified during the early Pleistocene (Bohaty *et al.* 1998) and the late Pleistocene (Scherer 1991).

Global eustatic sea-level data suggest that EAIS volume fluctuated during the Neogene (Haq *et al.* 1987; Dowsett and Cronin 1990; Wardlaw and Quinn 1991; Miller *et al.* 1996). The magnitude of some of these eustatic highstands can only be accounted for by a reduction in EAIS volume (Bohaty and Harwood 1998). The direct evidence that these rises in sea-level result from ice volume changes in Antarctica is reported herein by *in situ* glacial marine sediments of the middle Miocene Fisher Massif Formation and the Pliocene Bardin Bluffs Formation, which were deposited deep within the Lambert Graben embayment during significant retreat of the Antarctic Ice Sheet.

## 8B.4 Summary

*In situ* and glacially reworked marine diatoms in the Pagodroma Group, on the Amery Oasis, suggest marine deposition occurred >250 km inland from the modern Amery Ice Shelf edge repeatedly during the Pliocene - Pleistocene (<3.1 Ma), Pliocene (4.9 - 3.7 Ma) and middle Miocene (12.2 - 11.7 Ma). Similar data, on Fisher Massif, suggests that marine deposition also occurred >300 km inland in the Miocene (14.2 - 12.5 Ma and 14.2 - 6.2 Ma) and the late Eocene to early Oligocene. At these times of marine deposition there was significantly less ice on East Antarctica than today. Diatoms provide age control for three formations of the Pagodroma Group and for the marine conditions suggested. At high elevations on Fisher Massif, diamicts of the Mt Johnston Formation were probably deposited after the late Eocene but before the late Miocene. At a lower elevation on Fisher Massif, deposition of the Fisher Bench Formation began during the

middle Miocene (14.2 - 12.5 Ma). At a lower elevation and further down-glacier in the Amery Oasis, the Bardin Bluffs Formation was deposited after 3.1 Ma. To a lesser degree some of the diatoms in the Pagodroma Group come from non-marine sources. A proximal lake assemblage was recovered from the Fisher Bench Formation. Freshwater planktic diatoms in the Bardin Bluffs Formation may be aeolian or from glacially reworked lake sediments, which were deposited in a deglaciated landscape where large lakes developed under a climate significantly warmer than at present. Diatoms in the Pagodroma Group provide new evidence in support of dynamic Antarctic glacial conditions and warmer climatic intervals through the Neogene.

## **8C. Palaeoenvironmental Conditions during Miocene Marine Deposition of the Fisher Bench Formation, Fisher Massif.**

### **8C.1 Introduction**

#### **8C.1.1 Aims**

Diatoms are used here to interpret the palaeoenvironment during Miocene marine, siltstone, deposition in the Fisher Bench Formation, 300 km inland from the modern coastline (Figures 41a and b). These findings address three study aims: 1) what were Antarctic glacial conditions like in the Miocene, 2) what was the climate like during past East Antarctic Ice Sheet (EAIS) retreat, 3) how does the geological evidence of palaeoclimate and EAIS volume compare to the expected EAIS response to global warming determined from numerical ice sheet models.

#### **8C.1.2 Previous Work**

There is currently much conjecture about Antarctic glacial conditions during the Miocene. Miocene sediments deposited in Antarctica during intervals of warmer global climate provide an opportunity to comment on Antarctic climatic conditions during glacial retreat. It is generally accepted that Antarctic glaciation developed prior to the Miocene due to the continent's thermal isolation ~24 Ma (Mercer 1983; Barker *et al.* 1988; Kennett and Barker 1990; Robert and Maillott 1990). Although the exact time of ice sheet development is unclear, there is a general consensus that glacial conditions were unstable, and the glacial style wet-based / polythermal until the middle Miocene (Barker *et al.* 1988; Flower and Kennett 1994). Interpretations of Antarctica's glacial history diverge at the middle Miocene. Conditions either remained unstable and wet-based / polythermal through the Neogene (Webb and Harwood 1991, 1993; Harwood *et al.* 1991; 1992; Moriwaki *et al.* 1992a; Wilson 1995), or the ice sheet expanded, became stable and dry-based, and remained so through to today (Sugden 1992; Denton *et al.* 1993; Huybrechts 1993; Kennett and Hodell 1993; Marchant *et al.* 1993a, 1993b; Flower and Kennett 1994; Cowen 1995; Marchant *et al.* 1996; Sugden *et al.* 1995a, 1995b). Antarctica's glacial history and ice sheet response to past climatic warming needs to be resolved if geological evidence is to help predict Antarctica's response to future global warming.

#### **8C.1.3 Geological Setting**

On Fisher Massif, part of the Pagodroma Group is represented by the Fisher Bench Formation (Hambrey and McKelvey in press) (Figure 41). On the eastern side of the

massif the formation is exposed in a cliff section (Figures 46 and 47). In profile view from the south, its lower contact with the basement inclines steeply, but vertically down-section this gently curves and flattens out beneath the formation. The basement contact was once the wall and floor of the Lambert Graben fjord and has been partially infilled with sediment of the Fisher Bench Formation. Glacial recutting has since removed much of the sediment and reshaped the basement (Hambrey and McKelvey in press). A 320 m thick section of the Fisher Bench Formation has been preserved here, near the former fjord wall. Glacial down cutting, together with tectonic (Laiba and Pushina 1997) and isostatic uplift may have raised the base of the Fisher Bench Formation, 360 m above sea-level, and exposed it in a cliff section (Figure 47).

Laiba and Pushina (1997) and Hambrey and McKelvey, (in press) have logged the lithology of the Fisher Bench Formation from adjacent spurs on the cliff exposure. The formation has been interpreted as ice-proximal glacial marine sediment, including sub- and supra-glacially derived sediments released as iceberg rain-out (Hambrey and McKelvey in press). Much of this consists of waterlain diamicts (Hambrey and McKelvey in press); however, minor siltstone beds also occur (Laiba and Pushina 1997; Hambrey and McKelvey in press). A siltstone bed 66 m up the section (sample 36721-4), contains middle-Upper Miocene marine diatoms (Laiba and Pushina 1997; Chapter 8B). The later assemblage is rich in benthic diatoms, suggesting deposition occurred in a marine environment less than 50 m deep or transported down-slope from shallow sediments deposited near the former fjord wall (Laiba and Pushina 1997). Planktic diatoms dominate the AM 015 assemblage and provide more information about the oceanographic conditions during glacial retreat studied here.

## **8C.2 Methods**

During the Australian National Antarctic Research Expeditions (ANARE) 1994/95 field season, a section of siltstone from the base of the Fisher Bench Formation was sampled (sample AM 015) (Figure 47). This sample was prepared for siliceous microfossil analysis in a clean laboratory facility at the University of Nebraska-Lincoln. Permanent slide mounts were made from the original sample by suspending the sediment in deionized water, and then dried on a cover slip. This was mounted in Norland Optical Adhesive 61 mounting medium (refractive index =1.56) and studied with an Olympus light microscope. The sample was too terrigenous for detailed fossil analysis, so it was concentrated by filtered water flotation, settling and heavy liquid separation (with sodium polytungstate)

(Harwood and Rose 1998). Permanent slide mounts were made with Norland Optical Adhesive 61 mounting medium, and the fossils observed had a very high abundance (specimens on every field of view) (Chapter 8B). As a result, this sample warranted more detailed investigation. Quantitative relative abundance data was collected, by counting ~400 diatom valves. The slides were also scanned for rarer microfossils. Some diatom species were often broken and occurred as valve ends fragments. The diatom data were adjusted for this preferential preservation and converted into relative percentage abundance (Table 9).

### 8C.3 Results

Diatom data from AM 015 have been tabulated (Table 9). Much of the assemblage is dominated by extinct *Actinocyclus ingens* Rattray (~69%), and to a lesser degree by the extant taxon, *Coscinodiscus radiatus* Ehrenberg (~10%) and extinct *Denticulopsis simonsenii* Yanagisawa and Akiba (~7%). Another 21 diatom species in the assemblage occur at a relative abundance of <4%. Biogenic silica is a minor matrix component in AM 015, and qualitatively appears to be <10% of the sediment.

### 8C.4 Discussion

#### 8C.4.1 Diatom assemblage

The total abundance of diatoms in AM 015 appears low, <10% biogenic silica, due to the high terrigenous content of the sediment. The diatoms are moderately well preserved, but do not appear as well preserved as in modern Antarctic marine sediments. The fossils occur as fragments or single specimens with the valves rarely joined. Some valves contain silt, which was similar in grain size to that in the supporting matrix. All the taxa have been documented previously in other Southern Ocean assemblages (Fenner *et al.* 1976; Schrader 1976; Harwood 1986a, 1986b, 1989; Baldauf and Barron 1990; Harwood and Maruyama 1992). Approximately 87% of the total relative abundance of the diatom specimens are extinct. Some of these species have been used to date the formation (Chapter 8B). Extant planktic species comprise the other ~13% and have been used to interpret sea-ice conditions and sea-surface temperature (SST). Benthic diatoms constitute <1% of the total, and enable comment to be made on water depth.



**Table 9.** Microfossil relative abundance data from siltstone sample AM 015.

Species list Fisher Massif (AM 015)	Raw Data	Preservation Quality	Adjusted Counts	Percentage
<b>DIATOMS</b>				
<i>Actinocyclus ingens</i>	301	Full valves	301.0	68.67
<i>Actinocyclus</i> aff. <i>ingens</i>	3	Full valves	3.0	0.68
<i>Actinocyclus ingens</i> var. <i>nodus</i>	R	Full valves	0.2	0.05
<i>Actinocyclus octonarius</i> var. <i>asteriscus</i>	R	1/3 valves	0.2	0.05
<i>Chaetoceros</i> sp. cyst (smooth)	2	x2 (whole diatoms)	4.0	0.91
<i>Coscinodiscus oculus-indis</i>	18	1/3 valves	6.0	1.37
<i>Coscinodiscus radiatus</i>	130	1/3 valves	43.0	9.81
<i>Coscinodiscus</i> sp. A	52	1/3 valves	17.0	3.88
<i>Denticulopsis ovata</i>	13	Full valves	13.0	2.97
<i>Denticulopsis simonsenii</i>	30	Full valves	30.0	6.84
<i>Eucampia antarctica</i> var. <i>recta</i>	4	Full valves	4.0	0.91
<i>Isthmia</i> sp	1	1/3 valves	0.3	0.07
<i>Proboscia barboi</i>	2	Full valves	2.0	0.46
<i>Rhabdonema japonica</i>	1	Full valves	1.0	0.23
<i>Rhaphoneis</i> sp. A	R	Full valves	1.0	0.23
Gen. et sp. indet. A (Harwood 1986a)	R	Full valves	0.2	0.05
<i>Rhizosolenia hebetata</i> (group)	3	1/2 (Valve ends)	1.5	0.34
<i>Stellarima microtrnas</i>	7	Full valves	7.0	1.60
<i>Stellarima stellaris</i>	1	1/3 valves	0.3	0.07
<i>Stephanopyxis grunowii</i>	R	Full valves	0.2	0.05
<i>Stephanopyxis turris</i>	1	Full valves	1.0	0.23
<i>Thalassionema nitzschioides</i>	2	1/3 valves	0.7	0.16
<i>Thalassionema/Thalassiothrix</i> (frag.)	2	1/3 valves	0.7	0.16
<i>Trinacria excavata</i>	1	Full valves	1.0	0.23
<b>OTHER</b>				
<i>Chaetoceros</i> sp. spines	20			
<b>SILICOFLAGELLATES</b>				
<i>Distephanus speculum</i>	R			
<b>EBRIDIANs</b>				
<i>Pseudommodochium lingii</i>	13			
<b>SPONGE SPICULES</b>				
	12			

**Notes:**

R= rare occurrence

Full valves = intact valve

1/3 Valve = Fragment, ~1/3 of af the valve

1/2 Valve = Only valve ends seen

x2 (Complete Diatom) = Cyst representing whole diatom

#### 8C.4.2 Diatom Palaeoecology

Siltstone in the Fisher Bench Formation was deposited when marine conditions occurred ~300 km inland from the current Amery Ice Shelf edge. This would have occurred during glacial reduction when climatic conditions were warmer than today. Diatoms in the siltstones enable comment on the climatic conditions during glacial retreat. At least nine diatom and one silicoflagellate species in AM 015 are extant species. The current temperature ranges of some of these are known (Figure 49).

Winter valves of *Eucampia antarctica* var. *recta* (Mangin) Fryxell *et* Prasad were identified in AM 015. Winter valves are an alternative to resting spores (Fryxell 1994), and are thought to be produced by *E. antarctica* var. *recta*, due to low light conditions (Fryxell and Prasad 1990) and, in part, to a change in temperature (Fryxell 1994). These conditions are generally associated with the formation of winter sea-ice. Only heavily silicified winter frustules were identified in AM 015, as these were probably preferentially preserved over the less silicified summer form. Today the distribution of this species appears to be restricted to cold Antarctic waters and in association with the seasonal moving sea-ice cover south of the Antarctic Convergence, where sea-surface temperatures are  $<5^{\circ}\text{C}$  (Fryxell 1991; Fryxell and Prasad 1990; Kaczmarek *et al.* 1993).

Resting spores of *Stellarima microtrias* (Ehrenberg) Hasle and Sims are present in AM 015. The vegetative stage, which was not present in AM 015, occurs in sea-ice, ice edge and adjacent open water conditions (Garrison *et al.* 1987; Ligowski 1987; Hasle *et al.* 1988; Garrison and Buck 1989; Garrison *et al.* 1993; Garrison and Close 1993; Kang and Fryxell 1993; Moisan and Fryxell 1993). In the modern environment *S. microtrias* occurs in SSTs of  $-2^{\circ}$  to  $1^{\circ}\text{C}$  (Zielinski and Gersonde 1997). The resting spores form during the winter, when light conditions are unfavorable (Fryxell 1994). Winter vegetative forms can also occur (Fryxell 1994), but these were not seen in AM 015. The close association of these species with sea-ice habitats, suggests reduced sea-ice associated conditions during deposition of AM 015.

Open water diatoms *Thalassionema nitzschioides* Grunow group, *Stellarima stellaris* (Roper) Hasle and Sims and *Coscinodiscus radiatus* Ehrenberg also occur in AM 015. *Thalassionema* spp. are generally found in modern surface waters with SST  $>0^{\circ}\text{C}$  (Zielinski and Gersonde 1997). Apart from trace occurrences in sea-ice covered regions they are not associated with sea-ice cover (Armand 1997). *Stellarima stellaris* is typically a temperate and warmer water species (Hasle *et al.* 1988) not found in areas covered by sea-

ice (Armand 1997), but has been found in the northern part of the Antarctic Zone where surface waters are  $>3.5^{\circ}\text{C}$  (Armand 1997). *Coscinodiscus radiatus* is generally a warmer water species that occurs north of the Antarctic Polar Front where the summer SST is  $>5^{\circ}\text{C}$  (Cassie 1963). However, *C. radiatus* has been found south of here, around South Georgia (Hirano 1965), where the summer SST is approximately  $3^{\circ}\text{C}$  (Gordon and Molinelli 1982).

Sedimentary diatom assemblages may provide a composite records of the annual diatom successional cycle. Depending on the deposition rate and depth of sediment mixing, a single sample could contain a mixed record of this succession, spanning a season to several years of deposition. However, only a small percentage of the living assemblages is preserved, due to mechanical breakage and dissolution (Shemesh *et al.* 1989) causing a preservational bias towards heavily silicified diatoms (Leventer 1998). Lightly silicified diatoms and other phytoplankton groups can sometimes dominate the phytoplankton assemblage (McMinn and Hodgson 1993; Arrigo *et al.* 1998a, 1998b), but are rarely evident in the fossil record. Given that the sediment in AM 015 is very terrigenous, suggesting a high deposition rate, it is unlikely that the sample spans a long time interval. This assemblage may reflect a mixture of diatoms deposited through seasonal climate changes over a short time span. The temperature ranges of some diatoms in AM 015 do not overlap (Figure 49). The occurrence of sea-ice associated *E. antarctica* var. *recta* and *S. microtrias* provides compelling evidence for the presence of sea-ice. Sea-ice forms when the SST reaches  $-1.8^{\circ}\text{C}$  (Ackley 1996), which may represent the winter SST in AM 015 (Figure 50). Open water taxa, such as *Thalassionema* spp., *C. radiatus* and *S. stellaris*, do not live in cold sea-ice associated waters (Cassie 1963; Hasle *et al.* 1988; Armand 1997; Zielinski and Gersonde 1997). These were deposited in AM 015 during summer as the sea-surface temperature increased  $>0^{\circ}\text{C}$ ,  $>3^{\circ}\text{C}$  and  $>3.5^{\circ}\text{C}$ , respectively (Figure 50). *Stellarima microtrias* does not occur in waters  $>1^{\circ}\text{C}$ , and probably formed resting spores to evade the higher summer sea-surface temperatures. The maintenance of vegetative *E. antarctica* var. *recta*, which cannot form resting spores during unfavorable conditions, indicates that summer SST remained  $<5^{\circ}\text{C}$  (Figures 49 and 50). It is unlikely that this species could retreat to colder East Antarctic regions if temperatures were higher, although a retreat further south into the Lambert Graben may have been possible.

The ratio of benthic to planktic diatoms in AM 015 and 36721-4 provides further palaeoenvironmental information. The AM 015 diatom assemblage is predominantly planktic, although rare ( $<1\%$  of the assemblage) benthic diatoms occur, i.e. *Rhabdonema*

*japonica*, Gen. et sp. indet. C (in Harwood 1986a) and fragments of *Isthmia* sp. These suggest that deposition may have occurred close to euphotic water depths, ~50 m, or close to a shallow water area. The later could also imply localised slumping or resuspension from nearby shallow water areas up the ancestral fjord wall. Approximately 70 m up the section, abundant benthic diatoms in 36721-4, indicate deposition within euphotic water depths <50 m (Laiba and Pushina 1997). The increase in benthic diatoms from AM 015 to 36721-4 possibly indicates a relative shallowing in water depth with time.

#### **8C.4.3 Diatom Taphonomy**

The diatoms in the Fisher Bench Formation siltstones were probably deposited *in situ* in a distal glacial marine environment. However, the siltstones are not similar to modern Antarctic marine sediments. Biogenic silica generally comprises 10 - 75% of the sediment on the modern Antarctic continental shelves (DeMaster 1981; Gersonde and Wefer 1987; Stockwell *et al.* 1991; Domack 1993; Harris *et al.* 1998) and up to 90% of the sediment in anoxic fjord basins in the Vestfold Hills (McMinn *et al.* 1998). In AM 015 the biogenic silica content appears <10%, which is generally much less than in the modern marine environment. Higher silt deposition probably diluted the biogenic input increases water turbidity (Elverhøi 1984) and decreases light levels (Maffione 1998), in turn reducing the diatom productivity. It is possible that modern analogues to the siltstone deposition in the Fisher Bench Formation may be found in the fjords of East Greenland, where the adjacent glaciers are polythermal, and provide considerable sediment to the marine environment (Hambrey and McKelvey in press).

#### **8C.4.4 Stability of the Amery Ice Shelf and the East Antarctic Ice Sheet**

The climate conditions during which Miocene marine sediments at Fisher Massif were deposited provide a unique opportunity to test the computer models that have been developed to determine the interaction between temperature and ice volume (e.g. Huybrechts 1990, 1992, 1993; Prentice *et al.* 1992; Warner and Budd 1998). The Fisher Bench Formation is thought to have been deposited in the absence of the Amery Ice Shelf, and perhaps even other Antarctic ice shelves. This contrasts dramatically to today, where ice shelves border ~50% of the continent. It is unclear what caused many of these to form, or how stable they currently are (Fahnestock 1996), but temperature is known to greatly affect their stability (Doake and Vaughan 1991). The modern, mean annual sea-surface temperature (SST) at the front of Antarctic ice shelves is -1.9°C (Barkov 1985). Summer SST at the front of the Amery Ice Shelf ranges between -0.6° to -1.1°C (Kerry *et al.* 1987a, 1987b).

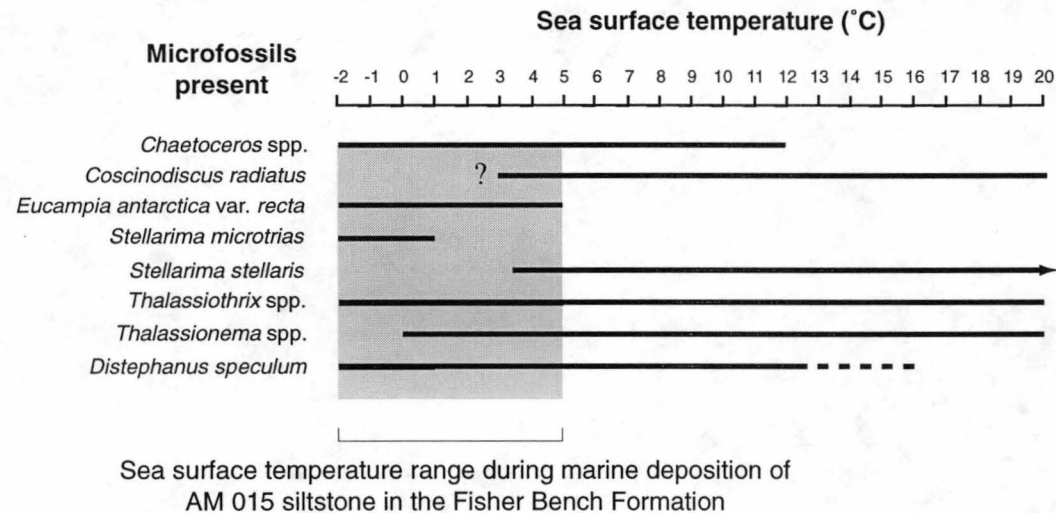


**Figure 49.** Temperature range of extant microfossils present in the Fisher Bench Formation sample AM 015. based on DeFelice and Wise (1981), Fryxell (1991), Armand (1997), Zielinski and Gersonde (1997).

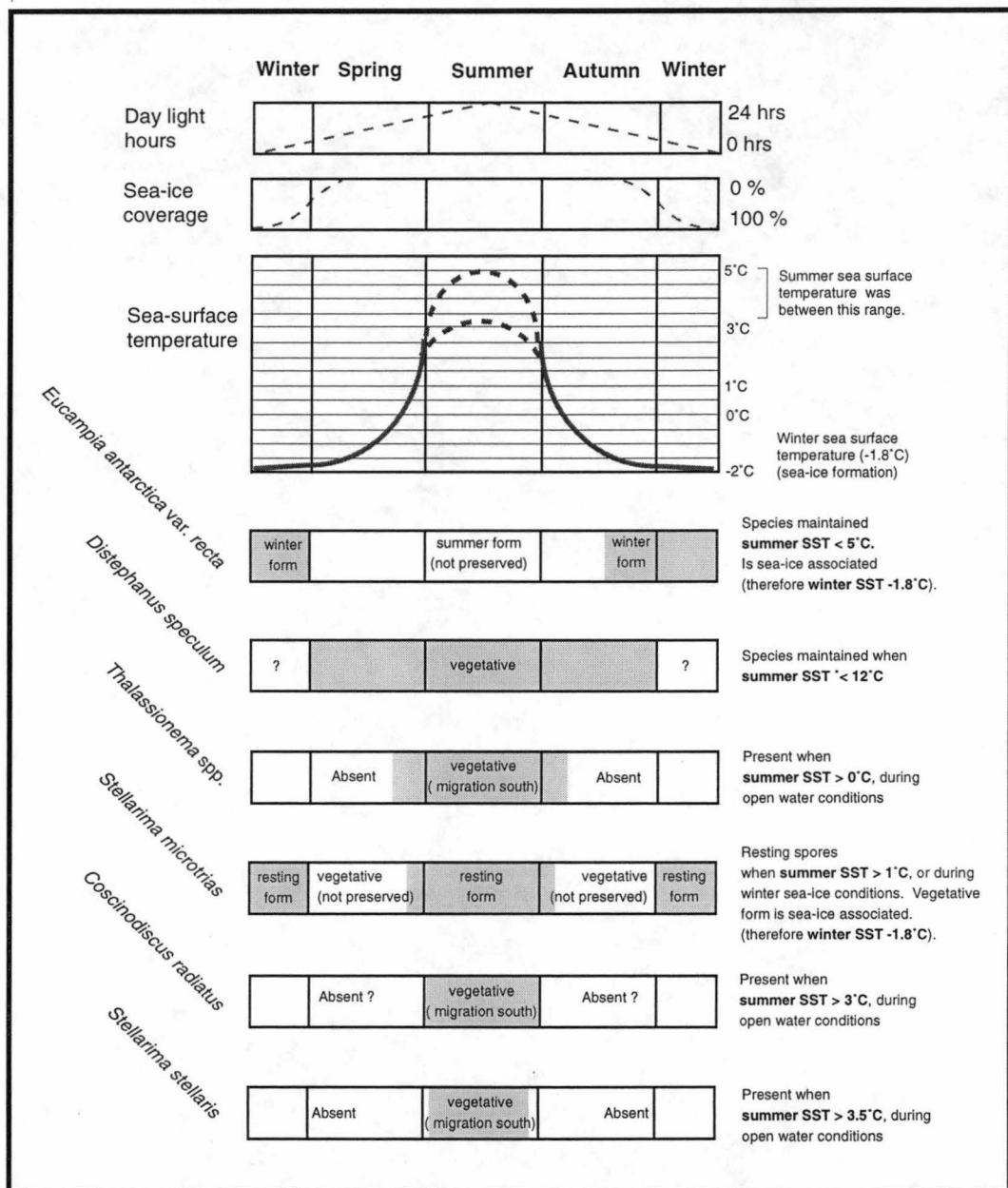


**Figure 50.** Possible seasonal succession in the AM 015 diatoms.

On the western side of the Antarctic Peninsula, summer SST is  $<1^{\circ}\text{C}$  (Gordon and Molinelli 1982), and ice shelves do not occur where mean coastal air temperatures are  $>-4^{\circ}\text{C}$  (Reynolds 1981; Fahnestock 1996).

Loss of the Amery Ice Shelf from the current shelf edge to Fisher Massif, a distance of  $\sim 300$  km, may have occurred when mean coastal air temperatures were  $>-4^{\circ}\text{C}$ . Diatoms in AM 015 support this hypothesis. Based on the species present, it is estimated that summer SST was between  $3.5^{\circ}$  and  $5^{\circ}\text{C}$  at the time of deposition, although winter sea-ice still formed. If the minimum, mean annual air temperature at Fisher Massif was  $-4^{\circ}\text{C}$ , this would represent a temperature approximately  $15^{\circ}\text{C}$  higher than today (calculated from Rubin and Weyant 1965). Modeling studies suggest that such a warming could cause partial deglaciation not only of the Lambert Graben, but the rest of Antarctica (Figure 51).

Glacial reduction in the Lambert Graben is supported by geological and palaeontological evidence in the Fisher Bench Formation. It has been suggested that pre-Pliocene climatic conditions in Antarctica were at least  $15^{\circ}$  to  $20^{\circ}\text{C}$  higher than today (Harwood *et al.* 1991). These temperatures may be similar to those that occurred at Fisher Massif during the middle Miocene. It has been also suggested that reduction in the EAIS occurred when summer SST was  $2^{\circ}$  to  $6^{\circ}\text{C}$  (Harwood 1986b), with the loss of sea-ice assisting Antarctic deglaciation (Harwood *et al.* 1994).

## 8C.5 Summary

Distal glacial marine siltstones were deposited on Fisher Massif 14.2 - 12.5 Ma (sample AM 015) and 14.2 - 6.5 Ma (sample 36721-4) respectively. The sedimentological facies suggest that the Fisher Bench Formation was deposited in a warmer wet-based / polythermal glacial marine environment, in the absence of the Amery Ice Shelf (Hambrey and McKelvey in press). Diatoms in the older siltstone bed (AM 015) indicate summer sea-surface temperatures were  $>3.5^{\circ}\text{C}$  (to explain the occurrence of *S. stellaris*), but  $<5^{\circ}\text{C}$  (for the maintenance of *E. antarctica* var. *recta*). The warmer conditions allowed marine deposition  $\sim 300$  km inland from the modern Amery Ice Shelf edge. Modeling studies suggest that a warming of  $15^{\circ}\text{C}$  would cause partial deglaciation of the Lambert Graben, and the rest of Antarctica (Figure 51). Summer SST from AM 015 are consistent with temperatures that occur in warmer areas where ice-shelves are absent. However, reduced

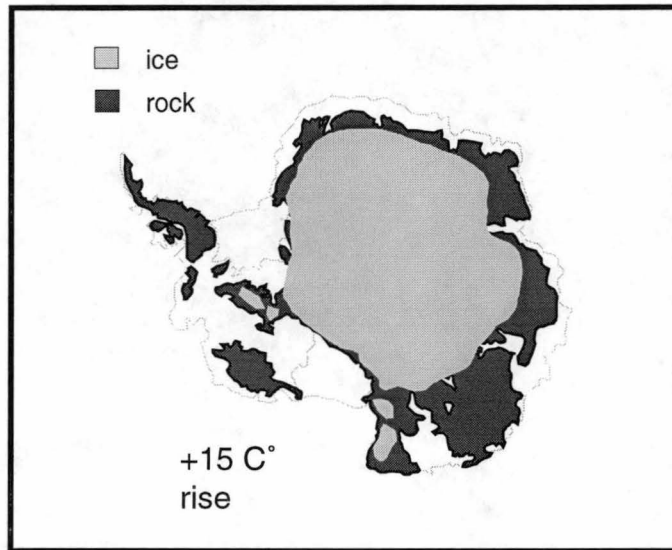


**Figure 51.** Ice sheet changes due to climatic warming 15°C higher than today (modified from Huybrechts 1993).



sea-ice conditions still occurred during winter, and possibly in spring and autumn, explaining the presence of *S. microtrias* and winter valves of *E. antarctica* var. *recta*.

The Fisher Bench Formation siltstones were deposited in a distal glacial marine environment (Hambrey and McKelvey in press). The terrigenous input from glacial melt out was high during the deposition of AM 015, where diatoms make up <10% of the sediment. The high terrigenous input probably diluted the biogenic input and increased water turbidity, which may have lowered the light levels, and decreased the diatom productivity.

The assemblage in AM 015 consists largely of planktic diatoms, which indicated the water depth exceeded euphotic depths. However, the euphotic depth may have been shallow due to the high water turbidity. In contrast, the assemblage in 36721-4 is rich in benthic diatoms (Laiba and Pushina 1997). The difference between the samples may represent a relative shallowing in water depth; although it is not possible to discern bathymetric changes through the intervening interval. The Fisher Bench Formation on Fisher Massif was deposited close to the former fjord wall, and the shallow assemblage in 36721-4 may reflect close proximity to this old shoreline.

## **9. Cenozoic glacial history of the Menzies Range, Southern Prince Charles Mountains, Antarctica.**

### **9.1 Introduction**

Glacial retreat in the past is evident in marine and glacial marine sediments of the Pagodroma Group in the Northern Prince Charles Mountains (nPCM), East Antarctica (see Chapter 8). Pagodroma Group deposit on the Amery Oasis and Fisher Massif, indicate that glacial retreat occurred 250 km and 300 km inland, from the modern Amery Ice Shelf edge, in the past. Further inland, 750 km from the coast, are unstudied Cenozoic strata on the Southern Prince Charles Mountains (sPCM); which could contain evidence of even larger past glacial retreat. Field work was carried out during the Australian National Antarctic Research Expeditions (ANARE) 1997/98 season to study the Cenozoic strata in the Southern Prince Charles Mountains (sPCM).

#### **9.1.1 Aims**

The aim of the field programme was to:

1. Locate and describe Cenozoic strata distributed along the central Menzies Range.
2. Interpret the glacial regimes represented by these strata.
3. Identify if these Cenozoic sediments were fjordal deposits of the Pagodroma Group.

Landform evolution of the region was integrated with the sedimentological study.

#### **9.1.2 Geological Setting**

The sPCM extend inland up to 750 km from the coast of Prydz Bay, on either side of the Lambert Graben (Figure 52). They consist of widely scattered nunataks that are comprised largely of Pre-Cambrian metasediments and gneisses (Tingey 1982, 1991), covered in places by little-known Cenozoic glaciogene sediments (Trail 1964). Within the sPCM, the Menzies Range trends east-west (Figure 52) and is ~65 km long. The range is bounded on its northern side by the east - flowing Fisher Glacier. Fisher Glacier is ~2100 m thick, and its surface descends from 2100 m to 1600 m in elevation (Morgan and Budd 1975). The southern side of the range is bounded by the northeast-flowing Geysen Glacier, of which most of the surface is above 2000 m in elevation. Both glaciers merge and flow into the head of the Lambert Glacier, ~110 km further to the east. Two unnamed glaciers also carry ice from the Geysen to the Fisher Glacier, and separate

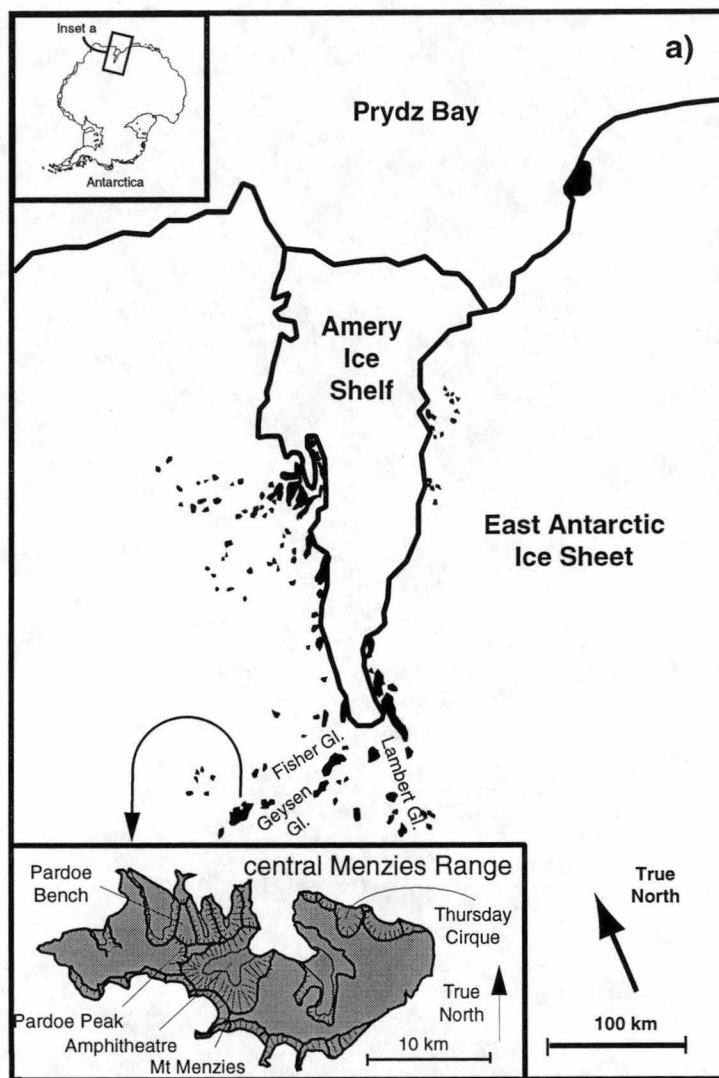


**Figure 52.** The central Menzies Range, Southern Prince Charles Mountains, East Antarctica.

Mt Bayliss (~2025 m) from Mt Mather (~2340 m), at the eastern and western ends of the Menzies Range respectively.

At the centre of the Menzies Range lie the two highest peaks: Mt Menzies (~3355 m) and Pardoe Peak (~2920 m), which are also the highest peaks in the PCMs. On either side of the central Menzies Range, large cirque valleys open out onto both the Geysen and the Fisher Glaciers. Those that open on the southern side are filled with ice from the Geysen Glacier. In contrast, those opening onto the Fisher Glacier are essentially devoid of ice, except where lateral Fisher Glacier ice flows down into their mouths. The largest two of these cirque valleys, immediately northwest of Mt Menzies, have sheer walls between 1000 m and 1500 m in height, and are informally referred to herein as the “Amphitheatre”.

The location and elevation of the Menzies Range generates a frigid climate. Air temperatures are  $<-18^{\circ}\text{C}$  in summer and  $<-35^{\circ}\text{C}$  in winter (extrapolated from Allison 1999). During the course of the field season, only minor liquid water was observed in small ice-covered ponds. The modern glacial conditions are dry-based and cause negligible erosion and sediment deposition.

### **9.1.3 Previous Work**

Few details of the Menzies Range geology are known. The greatest part of the range consists of Archaean metasediments, including metaquartzite and metapelites, intruded by Proterozoic tholeiitic (now lower amphibolite facies) sills and dykes (Tingey 1982, 1991). Complex deformation includes recumbent folding. Mt Bayliss consists, in the main, of older Archaean augen gneiss, cataclastic granite and amphibolite (Tingey 1982, 1991).

Cenozoic glacigene strata, the subject of this study, blanket much of the Archaean basement (Trail 1963). Glacial deposits ~50 m thick cover the eastern end of the central Menzies Range (Trail 1964); these deposits have benched surfaces that were cut by later glacial valleys (Trail 1964). Air photo interpretation of the central Menzies Range has revealed moraine ridges, glacial trim-lines, ice cored moraines, and the development of diverse patterned ground on these older Cenozoic surfaces (Derbyshire and Peterson 1978), indicating an intricate glacial history.

### **9.1.4 Glacial Sedimentology**

Temperature largely determines the way in which glaciers move, how they erode the landscape, and the types of sedimentary deposits that they form (Drewry 1986; Hambrey

1994; McLane 1995). Warmer, wet-based glaciers move largely by sliding along on their base (Menziés 1995). In contrast, dry-based glaciers move very little along their base, and instead move largely through internal ice deformation (Menziés 1995; Bennett and Glasser 1996). As a result, the greater amount of basal sliding beneath wet-based glaciers causes a greater amount of erosion, and subsequent deposition than that from dry-based glaciers (Hambrey 1994; Bennett and Glasser 1996) (Chapter 3.1.1, Figure 13). Using these sedimentological principals, the climatic regime and stratigraphy of landform development and deposition on the central Menziés Range is studied.

## 9.2 Stratigraphy

It is proposed here that the pre-Quaternary Cenozoic strata of the Menziés Range be termed the Menziés deposits, until further work can incorporate these into a Menziés Group. The Menziés deposits are overlain disconformably by boulder and cobble grade gravels, deposited in later dry-based glacial conditions during the Quaternary. The latter deposits are not part of this study.

On the central Menziés Range, four Cenozoic deposits have been recognised. These are, in order of decreasing age:

- (1) Pardoe Formation, >240 m thick.
- (2) Trail diamict, >100 m thick.
- (3) Amphitheatre diamict, >10 m thick.
- (4) Quaternary boulder and cobble grade gravels (<10m thick).

More detailed field work will almost certainly lead to subdivision of the Trail diamict, with the recognition of at least one further separate deposit (see Discussion). Most of the central Menziés Range strata are non-lithified. For this reason exposure is generally poor, as the sequences are mantled by loose scree, and horizontal surfaces are modified by patterned ground development. The provenance of much of the central Menziés Range strata appears to be the local Precambrian basement. However, further work is required on the basement geology and clast lithologies, within the Menziés Group, to identify the glacial provenance.

### Pardoe Formation

The Pardoe Formation is at least 240 m thick at location 1 (Figures 53 and 54b).

However, the best exposures so far known are at location 8 (73°24'S; 61°54'E), which is

designated here as the type section (Figure 55). The formation contains three contrasting sediment facies. Variable diamicts are the predominate facies,, with subordinate amounts of sandstone, and laminated siltstone. The facies allow recognition within the formation of four members, all were identified in the sections examined at locations 2, 3 and 8 (Figure 53b).

Member 1, a matrix supported diamict (~60% clasts), ranges in thickness from 15 m in the type section, to 1.5 m at location 2, and only ~ 0.1 m at location 3. The average clast size varies between 2 cm and 20 cm. Member 2 shows considerable variation, consisting of silts, fine sands, slightly lithified sandstone, and a minor thin clast-rich muddy diamict (in the sense of Moncrieff 1989).

Member 2 ranges in thickness from 35 m in the type section (Figure 55), to ~0.5 m at location 6. The sandstone tends to be massive, whereas the silt and fine sand vary from massive to laminated. At location 6, Member 2 rests upon basement directly. In two adjacent sections at Pardoe Bench (i.e. location 2), the basal two members overlie the rugged unconformity surface at altitudes of 2100 m and 2300 m, respectively (Figure 54). In both instances Member 3 overlies Member 2. The lack of intervening exposure made it impossible to determine whether Members 1 and 2 are continuous between the two sections. It is possible that in the higher outcrop the facies interpreted as Members 1 and 2 are younger, as yet unrecognised members, separated from the lower exposures by a disconformity (See Discussion).

Members 3 and 4 are similar, indistinctly stratified diamicts. However, these are considered to be different members, as Member 3 averages ~50% clasts, whereas Member 4 averages ~70%. In both instances the clasts are usually of cobble grade, although a few scattered blocks in Member 4 exceed 2 m in diameter. Members 2 and 4 form the bulk of the sequences at locations 2, 3 and 8 (Figure 54). At location 8, Member 3 is ~110 m thick, and an incomplete Member 4 exceeds 45 m in thickness. At location 2, Member 3 is 150 m thick and an incomplete Member 4 exceeds ~70 m. At location 1, only Member 4 is evident, and here it probably exceeds 200 m in thickness. The base of the sequence is not exposed. At locations 2 and 8, the basal part of Member 3 contains abundant soft-sediment clasts of laminated silt and fine sand, almost certainly derived from the underlying Member 2. At the base of Member 3, in the type section (Figure 55), a 15 m thick diamict interval contains in places up to 80% of such intraformational clasts.

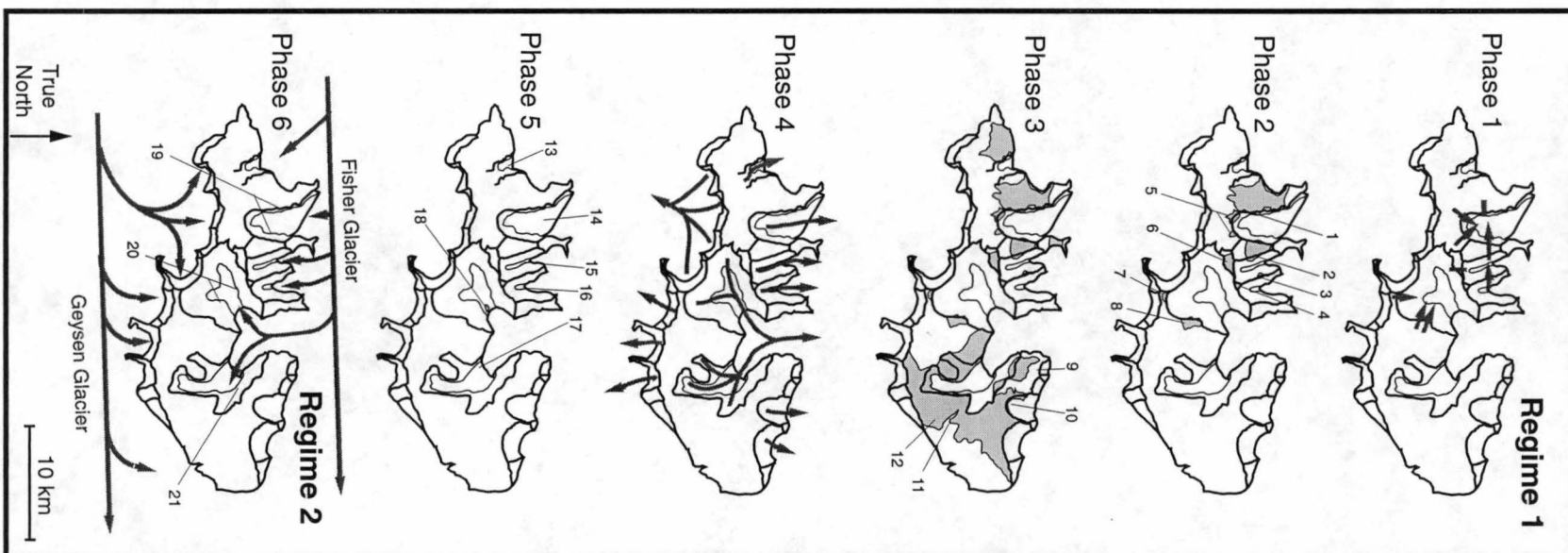


**Figure 53.** Cenozoic Stratigraphic history of the central Menzies Range. Deposits are in grey, arrows indicating ice flow direction, and locations described in the text are numbered

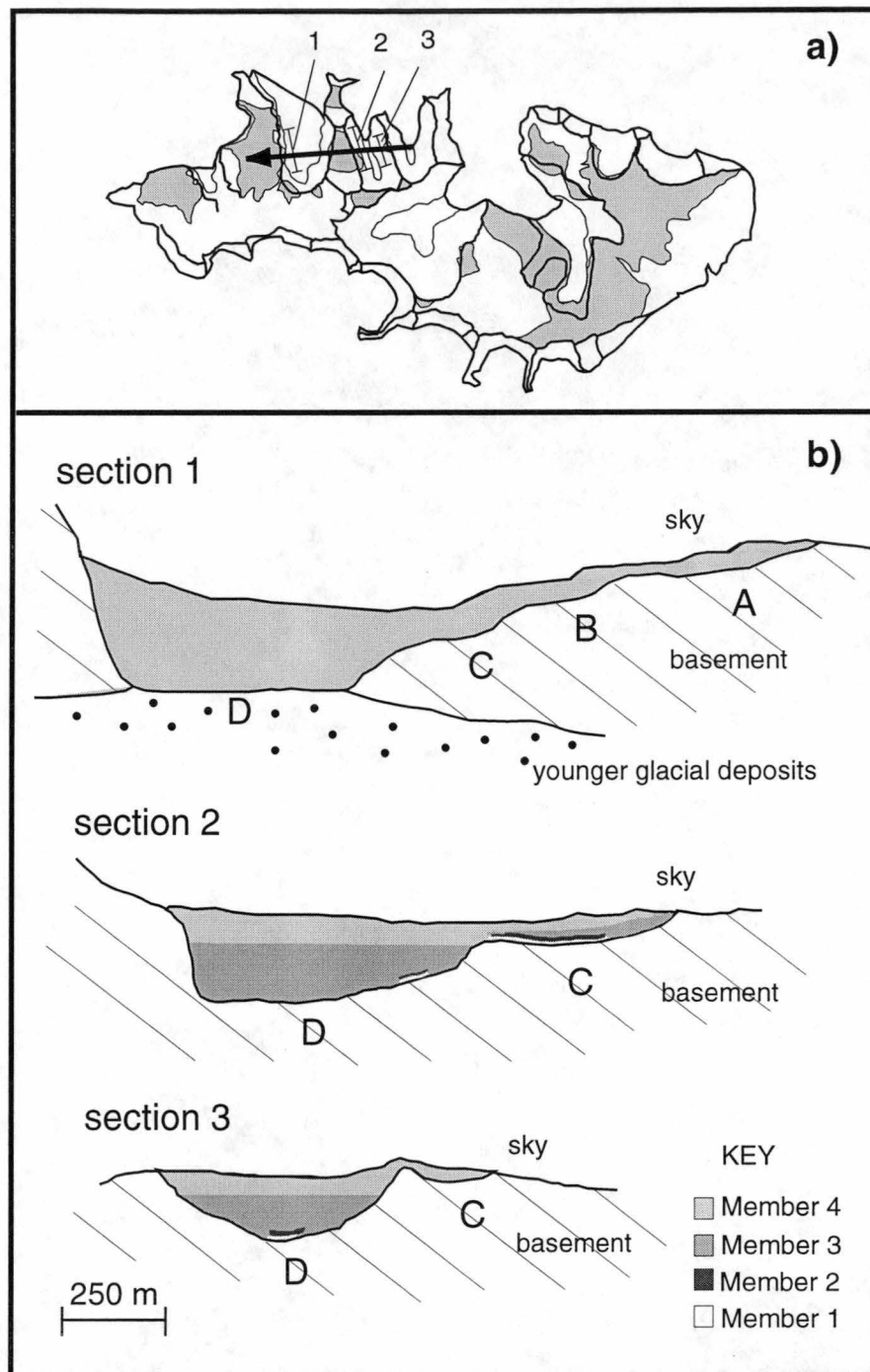


**Figure 54.** Menzies Group deposits on the central Menzies Range (a), with the location of three sections (1, 2, and 3) through the Pardoe Formation (b). These are possibly sections from a single valley, called here the Pardoe Palaeovalley. Four steps were identified (A, B, C and D) on the unconformity surface on the northern wall of the palaeovalley (b). The position of four member within the Pardoe Formation is illustrated (b).



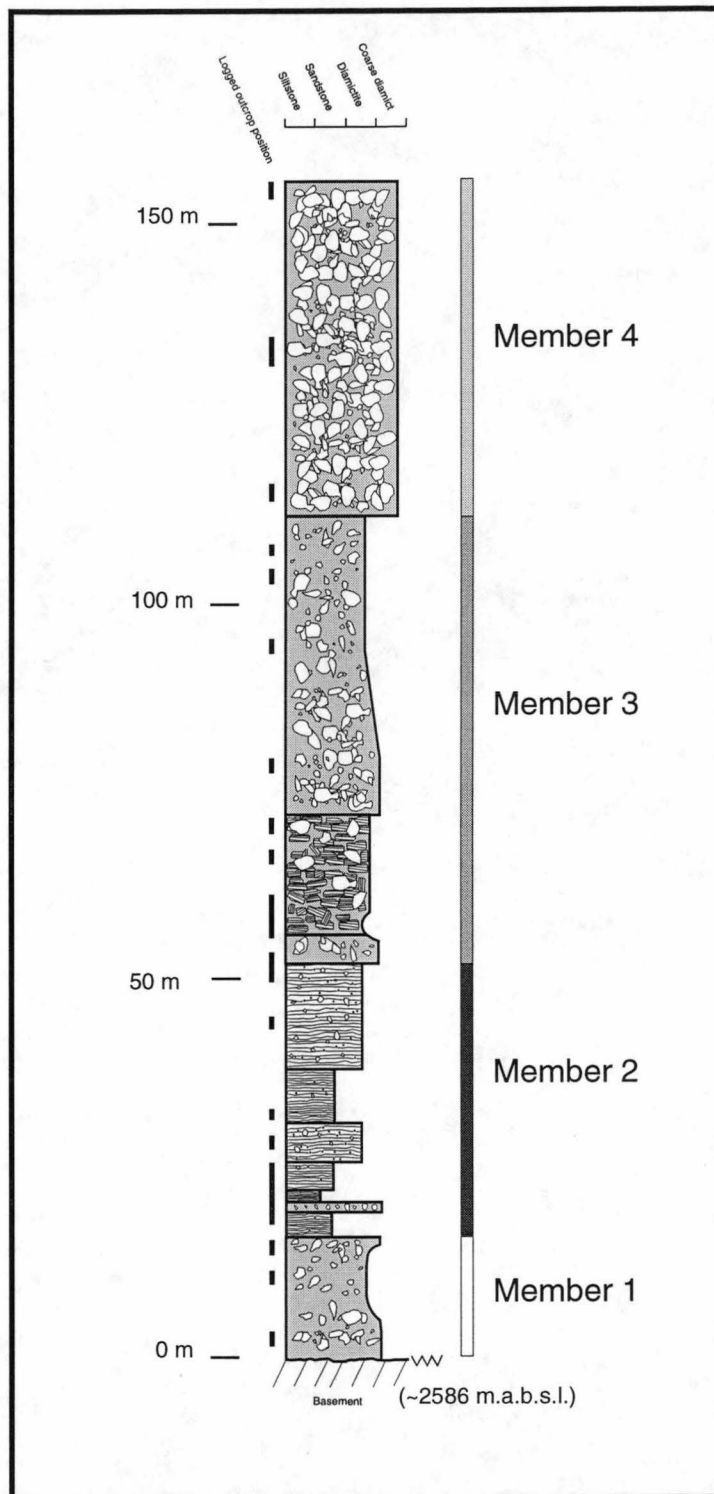


**Figure 55.** The Pardoe Formation type section (lat. 73° 27' S.; long. 61° 54' E.) at location 8 in Figure 53

### The Sub-Pardoe Formation Erosion Surface

The Pardoe Formation inliers overlie a rugged erosion surface cut into the Precambrian basement rocks. On the Menzies Range the altitudes of the exposed fragments of this unconformity surface (i.e. locations 1, 2, 3, 5, 6, 7 and 8) range from <1700 m to ~2800 m. Overall, the exposed remnants' altitude appear to increase south and east, in the direction of the summit of Mt Menzies. In all cases the unconformity surface appears fresh and non-weathered. The precise palaeogeographic relationships between the individual surface remnants were not always evident; however, some reconstruction of the erosion surface is possible. At locations 1, 2 and 3, steep exposures (on the sides of the cirque valley ridges) reveal cross-sections of a single east to west trending palaeovalley. For convenience of description, this exhumed feature is referred to as the "Pardoe Palaeovalley". The axis of the palaeovalley descends westwards over a distance of 6 km, from a height of 2150 m at location 3 to less than 1700 m at location 1 where it is obscured by younger, dry-based glacial deposits (possibly from the Last Glacial Maximum). At location 2, striations cut on the unconformity surface are compatible with the east-west trend of the palaeovalley axis.

At location 2 the Pardoe Palaeovalley is exposed in a cliff cross section, ~1.5 km across. The Pardoe Formation infills the palaeovalley, and is at least 200 m thick. The basement surface of the palaeovalley in this cross-section is notably asymmetrical. The southern wall is steep, whereas the northern wall is more gently inclined, and stepped in places (Figures 54a and 54b). The shallow cross section of another palaeovalley is apparent at Location 6. This section is ~0.75 km across and is infilled with <75 m of the Pardoe Formation. The palaeovalley floor, here at ~2500 m elevation, appears to descend gently north-west, towards the Pardoe Palaeovalley. These two features may have been contiguous originally.

The palaeogeographic setting of the unconformity fragments preserved at locations 4, 5 and 8 is unclear. All are exposed remnants of palaeovalleys that drained to the north or north-west. The configuration of the basement rocks and the Pardoe Formation at location 8 is that of a buttress unconformity.

### Trail diamict

The Trail diamict generally ranges from cobble-grade, poorly sorted conglomerate to clast-rich, sandy diamicts. The sediments mantle the eastern and western flanks of the central Menzies Range, as an incomplete blanket, at altitudes of 1600 m to 2200 m. The Trail

diamict rests on Precambrian basement and was nowhere observed to directly overlie the Pardoe Formation. However, the coarse sediment grade of the Trail diamict and abundance of clasts is similar to Member 4 of the Pardoe Formation (Figure 53b). Therefore, Member 4 of the Pardoe Formation and the Trail diamict may be stratigraphically the same unit. Further work is required to resolve this relationship.

The Trail diamict probably exceeds 100 m in thickness. It is difficult to make an accurate estimate as the base of the Trail diamict is only exposed at the thinned (by erosion) edges of the sediment blanket, along the north-eastern margin of the central part of the range. Exposure is poor as the diamict surface has been modified greatly by patterned ground development, and all scarps are mantled by scree. Moraine ridges also modify the surface, and partial erosion has resulted in scattered trim-lines (Derbyshire and Peterson 1978). The surface morphology of the Trail diamict, including the moraine ridges, indicates more than one depositional episode. There is further evidence for this near the eastern margin of the central part of the range (Figure 53, location 11), where the floor of an erosional depression exposes a deeply chemically weathered diamict surface, which clearly represents an interval of ice retreat and sub-aerial weathering. This surface underlies non-weathered Trail diamict.

The basement surface underlying the Trail diamict is exposed intermittently along the north-eastern margin of the central Menzies Range, at altitudes of 2000 m to 2080 m. In marked contrast to the basement surface underlying the Pardoe Formation, that beneath the Trail diamict at one location exhibits considerable chemical weathering (Figure 53, location 9). There are few data available from which to determine the configuration of the sub-Trail diamict erosion surface. In this region, the surface falls gently southwards to less than ~1680 m, before rising again towards the crest of the Menzies Range. This suggests an elongate shallow depression, oriented northwest-southeast, and descending gently towards the Fisher Glacier. However, in the back wall of Thursday Cirque (informal name) a northeast-southwest palaeovalley form within the erosion surface is apparent (Figure 53, location 10). This smaller feature, ~80 m deep, appears to trend at a high angle to the northwest-oriented, shallow regional depression defined by the sub-Trail diamict erosion surface.

#### Amphitheatre diamict

In the floor of the Amphitheatre are scattered exposures of matrix-rich pebble grade diamicts with sub-rounded clasts (Figure 53, location 18). A noticeable feature of the

diamict is an abundance of plutonic *cf.* metamorphic clasts. The matrix varied from fine sand, silty sand and was at times indistinctly laminated. The matrices have a distinctive greyish-green (10 GY 5/2) colour. In appearance, the Amphitheatre diamicts are more matrix-rich than those of the Pardoe Formation and Trail diamict. Thin lenses of pebble conglomerate and sand were rare. These outcrops are the only known of the Amphitheatre diamict. It is not possible to estimate the diamicts thickness, as only ~10 m is stratigraphically evident in exposures. The Amphitheatre diamicts probably occupy the floors of the cirque valleys to the west and east of the Amphitheatre (Figure 53, locations 13, 14, 15, 16 and 17), concealed beneath the coarse Quaternary gravels deposited from dry-based ice.

#### The Sub-Amphitheatre diamict Erosion surface

The erosion surface upon which the Amphitheatre diamict rests is part of a rugged landscape that includes the Amphitheatre (Figure 53, location 18), and other ice-free cirque valleys further to the west and east (Figure 53, locations 13, 14, 15, 16, and 17). Similar major excavations developed on the southern side of the range, but these are now concealed largely beneath the Geysen Glacier. This landscape, with an elevation up to 1500 m, is much more rugged than that underlying the Trail diamict. West and east of the Amphitheatre, the sub-Amphitheatre diamict erosion surface is deeply incised into the Trail diamict and Pardoe Formation (e.g. Figure 54).

#### Quaternary Cobble-Boulder Gravels

A thin veneer (<4 m) of cobble and boulder gravels (in the sense of Hambrey (1994) and Moncrieff (1989)) devoid of matrix, overlies the floors and lower walls of the ice-free cirque valleys, including the Amphitheatre, defining a spectacular trim-line (Figure 53, location 19 and 20) (see Tingey 1991, Figure 23). Within the Amphitheatre the altitude of the trim line decreases gradually southwards, from ~1880 m near the valley mouth, to ~1720 m, 3 km up-valley.

### **9.3 Discussion**

The Cenozoic history of the Menzies Range records two different climatic regimes. The Cenozoic Pardoe Formation, Trail and Amphitheatre diamicts and Quaternary cobble-boulder gravels on the Menzies Range record at least four intervals of glaciogene sedimentation. The Pardoe Formation and Amphitheatre diamict followed periods of terrestrial glacial erosion. These erosive events produced the sub-Pardoe and sub-

Ampitheatre surfaces. These rugged erosion surfaces and the sediments overlying them suggest conditions of wet-based alpine glaciation. Erosive wet-based alpine glaciers today occur in temperate climatic conditions. The youngest depositional event recognisable on the Menzies Range is the deposition of the Quaternary gravels. These are interpreted to have been laid down from polar dry-based ice, similar to that of the present glacial regime. The Cenozoic history of the central Menzies range can be divided into at least six phases of glacial erosion and deposition, during two different climatic regimes, which merits discussion:

### **9.3.1 Regime 1 Warm Wet-based Glaciation**

#### **Phase 1. The sub-Pardoe Formation erosion surface**

It is not possible to reconstruct the complete topography of the sub-Pardoe Formation erosion surface, but the form of the Pardoe Palaeovalley is apparent (See Stratigraphy). The floor of the Pardoe Palaeovalley descends westwards and glacial ice would have clearly flowed west. This contrasts completely with the present eastward flow of the Fisher Glacier. The palaeovalley surface remnant preserved at location 6 may be part of a former tributary that fed down into Pardoe Palaeovalley.

It is not clear why the marked cross-section asymmetry of the Pardoe Palaeovalley is present, as portrayed by the steep southern wall and contrasting gently-sloped, stepped northern wall (Figure 54b). Two hypotheses may explain the formation of this erosion surface: 1) it is possible that the stepped northern wall records periods of renewed down glacial cutting, in response to uplift, or 2) separate intervals of glaciation and glacial erosion. The steeper southern palaeovalley wall joins the steep face of Pardoe Peak, which could have acted also as a snow fence, concentrating snow accumulation along this edge of the palaeovalley, causing more erosion here and preventing the formation of steps. Fault movement co-incident with the southern wall is also a possible factor in the development of the asymmetry, but there is no firm field evidence to support this.

At present, there is no firm field evidence to indicate which of these two hypotheses is more likely. Nevertheless, glacial down cutting, due to uplift or separate glaciation, would have influenced sediment deposition, reworking and preservation within the palaeovalley. At location 2 (Figure 54b, Section 2), on Step C, sediments from the basal Members 1 and 2 of the Pardoe Formation are present. The strata on Step C may be the oldest strata preserved in the Pardoe Palaeovalley at this locality. Subsequent down-cutting could have been followed by the deposition of a similar glacial sedimentation

sequence on the lower Step D (Figure 54b). In this situation, a disconformity would separate the sequence overlying Step D from the higher older sequence resting on Step C. Alternatively, much of the palaeovalley could have been infilled with Members 1 and 2, covering both Steps C and D. Latter glacial down-cutting would then have removed almost all of this strata, from the palaeovalley, above Step D.

#### Phase 2. Deposition of the Pardoe Formation

All four members of the Pardoe Formation, including the glacial lacustrine facies indicate wet-based (temperate) glacial sedimentation. Within the diamicts, the relative abundance of fine matrix (30 - 50%) and the sub-rounded or sub-angular clast shapes, point to erosion and abrasion by basal-sliding ice. The presence of soft-sediment intraformational clasts within the oldest horizons of some diamicts further illustrates basal (i.e. wet-based) glacial erosion. The presence of Member 4 only, infilling Pardoe Palaeovalley at location 1, suggests either erosion (of at least Member 3) prior to the deposition of Member 4. Alternatively, the presence of the relatively clast-rich member may be a consequence of a down-valley facies change, due to the reworking of the more clast-rich Member 3.

The sandstone, silty sand and sandy silt of Member 2 clearly record aqueous deposition. The absence of obvious cross-stratification and only moderate sorting suggests a low-energy, aqueous regime, with a considerable component of suspension current sedimentation. The presence of ice rafted debris (i.e. as in the thin clast-rich muddy diamicts at location 8 suggests ice rafting (Figure 55) . The rugged morphology of the discontinuous sub-Pardoe Formation erosion surface, and the apparent absence of marine fossils (e.g. molluscs), suggest that this was an alpine depositional setting. It is assumed therefore that Member 2 reflects either terrestrial, quiet fluvial sedimentation or, more likely, glaciolacustrine sedimentation. In these circumstances, much of Member 2 may have been eroded prior to deposition of the overlying diamicts. There are no data available to indicate the altitude of Pardoe Palaeovalley at that time.

#### Phase 3. Deposition of the Trail diamict

Weathering preceded deposition of the Trail diamict. The added fact that considerable chemical weathering has been observed only on the sub-Trail diamict surface (Figure 53, location 9) lends strong support to this view.

The source of the Trail diamict is not apparent. It may have been deposited from a more southern ice source, flowing north across the lower ends of the range. Not until the

basement petrography of the Prince Charles Mountains is better documented, will it be possible to determine accurately the provenance of various widespread glacial formations distributed throughout the region.

#### Phase 4. The sub-Amphitheatre diamict erosion surface

The relict sub-Amphitheatre erosion surface dominates the current topography of the Central Menzies Range, having produced large alpine glacial valleys now largely devoid of ice.

#### Phase 5. Deposition of the Amphitheatre diamict

There are few data recovered yet concerning the deposition of the Amphitheatre diamict. These attest, yet again, to deposition from temperate wet-based ice. The provenance of these diamicts is uncertain, although the diversity of their clasts suggests south-flowing ice (entering the Amphitheatre cirque), from the generally east-flowing Fisher Glacier. Should ongoing provenance studies substantiate this, then a major reversal in the Menzies Range ice drainage system will be established and constitute a significant event in the glacial history. This would resemble a change in the drainage direction from that in Phase 4 to that similar to Phase 6, which resembles today's ice flow direction (Figure 53).

### **9.3.2 Regime 2: Cold Dry-based Glaciation**

#### Phase 6. Quaternary dry-based cobble-boulder gravels

The thin blanket of boulder and cobble gravels, mantling the lower slopes of the Menzies Range, record the change from temperate, wet-based glaciation to cold, polar dry-based glaciation. The spectacular trim-lines along the north side of the central range (e.g. Figure 53, locations 19, 20 and 21), record a major episode of south-flowing ice and are possibly related to the LGM. However, it is likely that more than one pulse of Quaternary dry-based ice is recorded about the slopes of the Menzies Range. Derbyshire and Peterson (1978, Figure 2) delineated several discontinuous moraine ridges, some apparently older, and others younger than the trim-line referred to above.

### **9.3.3 Palaeoclimate Considerations**

Temperate wet-based glaciation on Menzies Range occurred during markedly warmer Cenozoic climate than exists presently. The large amount of glacial excavation represented by the erosion surfaces beneath the Pardoe and Amphitheatre Formations indicates higher snow precipitation than at present, for no appreciable (i.e. erosionally competent) alpine glaciers exist on the Menzies Range today.

The elevation of the ice sheet surrounding the Menzies Range prior to the Quaternary is difficult to assess. Should the Trail Formation have been deposited by ice-sheet derived ice (from the Geysen and Fisher Glaciers), then a past higher ice sheet level is indicated. However, subsequent tectonic uplift here could have been a factor. The current presence of Geysen Glacier ice largely overwhelming the cirque valleys on the southern side of the range suggest strongly that lower ice sheet levels existed in the past.

During cold glacial intervals there is reduced snow precipitation in Antarctica, due to reduced evaporation in the surrounding marine environment (Jouzel *et al.* 1989). This leads to the retreat of alpine glaciers on Antarctic nunataks, but only a relatively minor decline in the thickness of the interior ice sheets (Jouzel *et al.* 1989). In contrast, during extreme warming it is possible that the Lambert Graben and Fisher Glacier Valley were deglaciated, or experienced lowered ice sheet levels (e.g. Figure 56). Warmer climatic conditions would be expected to increase marine evaporation and snow precipitation on Antarctica (Domack *et al.* 1991; Zwally 1994), creating a smaller, but higher, ice-sheet relative to its current size (Prentice *et al.* 1992). The altered coastal configuration of the ice sheet margin, due to ice sheet retreat, may have enabled increased snow accumulation on the Menzies Range (if closer to the coast), whilst the surrounding ice sheet elevation was lower (e.g. Figure 56). This scenario may explain the formation of wet-based alpine glaciers on the central Menzies Range, during Phases 1 and 4. In support of this hypothesis, the Phase 4 glacial valleys extend below the height of the current ice sheet. It is possible that tectonic lowering of the mountain could offer an alternative explanation for this observation; however, a warmer climate had to have existed during the formation of these alpine glacial valleys.

#### **9.3.4 The Age of the Menzies Range Landforms and Deposits**

Comparison of the Menzies Range landforms and deposits with other Antarctic records may help to constrain their age. The earliest Cenozoic glaciers in Antarctica were probably alpine glaciers on the Gamburtsev Mountains and other mountainous regions in the Antarctic interior (Drewry 1975; Huybrechts 1993), such as the Prince Charles Mountains (Hambrey and Barrett 1993). The glaciers eventually joined and developed into the first East Antarctic Ice Sheet (EAIS) (Drewry 1975; Hambrey and Barrett 1993), which flowed into Prydz Bay via the Lambert Graben (Barker *et al.* 1998).



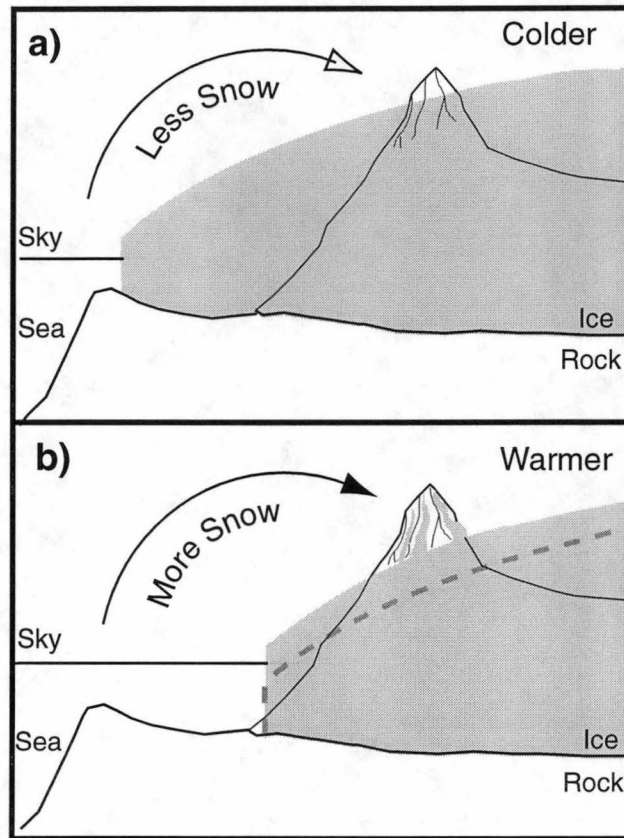


**Figure 56.** Model of current condition on the central Menzies Range (a), with advanced ice sheet and low snow accumulation inland. Therefore, the Menzies Range is largely ice free and surrounding ice sheet elevation is high. During warmer climatic conditions the ice sheet may retreat (b), although there is more snow accumulation. The increase in snow accumulation increases the relative thickness of the ice sheet, however, glacial retreat may place the Menzies Range closer to the ice sheet margin where the ice thickness was less. This would enable increased snow accumulation and alpine glaciation on the Menzies Range, whilst the surrounding ice sheet elevation was lower.

The oldest evidence for Antarctic glaciation comes from late Eocene to early Oligocene glacial sediments in Prydz Bay, ODP Site 739 and 742 (Hambrey *et al.* 1994). Due to the southern position of the Menzies Range in the Lambert Graben system, it is likely that the region was first glaciated during or after the late Eocene to early Oligocene.

Landforms and deposits, similar to those on the Menzies Range, have been found in the Transantarctic Mountains and Dronning Maud Land. These include regional, terrestrial wet-based glacial deposits (like Member 4), well preserved large-scale wet-based erosion of alpine glacial valleys (like those from Phase 4), and a relatively recent change to colder dry-based glacial conditions (as with the change from Regime 1 to Regime 2). Large-scale, terrestrial, wet-based glacial deposits, similar to Member 4, were deposited in the Transantarctic Mountains as the Sirius Group in the late Pliocene- Pleistocene (<3.1 Ma) (Webb *et al.* 1987; Webb and Harwood 1993) and possibly the Miocene (Webb *et al.* 1996); however, the group may consist of deposits of significantly different ages (McKelvey *et al.* 1991). Similar deposits in the Sør-Rondane Mountains were deposited in the Miocene to Early Pliocene (Moriwaki *et al.* 1992b). Large-scale alpine glacial erosion, like Phase 4 on the Menzies Range, occurred here during the mid to late Pliocene (Moriwaki *et al.* 1992b). Wet-based glacial cirques have been exposed recently by the lowering of the modern dry-based ice sheet in the Yamato Mountains (~300 km east of the Sør-Rondanes) (Yoshida 1983). Pre-Quaternary, wet-based, glacially eroded valleys have been identified on Borg Massif (Brunk 1989) and beneath the EAIS, near Vestfjella and Heimefrontjella Nunataks (Holmlund and Näslund 1994) in Dronning Maud Land. Wet-based, alpine glacial cirques and valleys preserved in the Transantarctic Mountains may have formed during different times. For example, Wright Valley in the Dry Valley region may have formed >9 My ago (Prentice *et al.* 1993). In Victoria Land (northern Transantarctic Mountains) alpine glaciation followed deposition of the Sirius Group (Van der Wateren and Verbers 1991; Verbers and Damm 1994; Passchier *et al.* 1999), with deep valley cutting occurring in the early Pleistocene (Van der Wateren and Verbers 1991).

A significant climate event at 2.6 Ma identified globally, correlates to the onset of bipolar glaciation, and has been suggested to have caused a dramatic change in Antarctic erosion and sedimentation, from warm, wet-based / polythermal glaciation, to colder, dry-based glaciation (Webb and Harwood 1991, 1993; Harwood *et al.* 1991; 1992; Moriwaki *et al.*, 1992a; Wilson 1995). Cold, dry-based glacial deposition in the Sør-Rondane Mountains began in the early Pleistocene (Moriwaki *et al.* 1992b), or near the Plio-Pleistocene Boundary (Matsuoka 1995). The first regime of erosion and deposition on the Menzies

Range is wet-based, and would be assumed therefore to predate the onset of bipolar glaciation and the development of cold, dry-based Antarctic glaciation. Nevertheless, warmer Antarctic Pleistocene episodes have been identified (Scherer 1991; Barrett *et al.* 1998; Bohaty *et al.* 1998; Scherer *et al.* 1998) and an early Pleistocene age for some of these Phases can not be ignored. In contrast, the second regime of erosion and deposition on the Menzies Range is dry-based, and is therefore probably Quaternary in age. The broad comparisons of the landforms and deposits on the Menzies Range with those elsewhere in Antarctica are, at best, tentative. Nevertheless, they provide some indication of the approximate age of the landscapes and deposits observed.

Cenozoic glacial marine deposits of the Pagodroma Group can be found nearer the coast in the Northern Prince Charles Mountains, on the Amery Oasis and Fisher Massif (Hambrey and McKelvey 2000). They were deposited in a fjordal environment, within the Lambert Graben largely during warmer climatic conditions of the Neogene (Hambrey and McKelvey 2000). The terrestrial Menzies Range strata deposited during warmer conditions may be contemporaneous with all or part of the Pagodroma Group. However, no temporal relationships are yet established.

## 9.4 Summary

The Cenozoic geology of the Menzies Range contains evidence for two very different climatic regimes. Glacial landforms and deposits formed on the central Menzies Range sometime after the onset of Antarctic glaciation <40 Ma. The first climatic regime was warmer, whilst the latter was cold and more similar to today. Numerous Antarctic records suggest this climatic transition occurred ~2.6 Ma.

The central Menzies Range stands ~1500 m above the surrounding ice and is deeply incised by relict (ice-free), alpine glacial valleys. Cenozoic deposits have been cut by the alpine glacial valleys, exposing deposits up to 240 m thick. The deposits consist largely of clast-supported diamicts with minor sandstones, sands and silts. It is proposed here that the pre-Quaternary Cenozoic strata on the Menzies Range be called the Menzies deposits, until further work can incorporate these into a “Menzies Group”. Four Cenozoic deposits have been recognised. These are:

- (1) Pardoe Formation – oldest
- (2) Trail diamict

- (3) Amphitheatre diamict
- (4) Quaternary boulder and cobble grade gravels - youngest

At least six different phases of glacial erosion and deposition were identified on the central Menzies Range. During Phase 1, alpine glacial valleys formed, which trend at high angles to the current drainage system. They were infilled by the Pardoe Formation during Phase 2. During Phase 3, further erosion occurred along with the deposition of the Trail diamict, which blankets the lower elevated areas on the eastern and western side of the central Menzies Range. Both of these deposits were cut by later, Phase 4, alpine glacial erosion, which produced the alpine glacial valleys of the sub-Amphitheatre diamict erosion surface, that dominates the geomorphology of the central Menzies Range today. The head of the glacial valleys are now ice-free on the northern side of the range. During Phase 5, glacial deposits of the Amphitheatre diamicts were deposited on the floor of at least one of the Phase 4 glacial valleys.

The Menzies deposits, and associated landforms, formed during temperate wet-based glacial conditions. During the warmer conditions, the ice sheet may have been relatively lower compared to today, although snow accumulation on the central Menzies Range was higher than today. These conditions created the alpine glacial landscape. The warmest conditions occurred during deposition of the Pardoe Formation, with terrestrial proglacial lacustrine, or quiet proglacial fluvial deposits developing. Later, Phase 6 Quaternary cobble-boulder gravels that were deposited over the Menzies deposits, and associated landforms, during dry-based glacial conditions like today. Phase 6 includes the most recent depositional events on the Menzies Range. These deposits formed under, cold, dry-based glacial conditions, like today, causing minor erosion and deposition.

The terrestrial setting of the Menzies deposits contrasts with the marine depositional setting of the Pagodroma Group. It is possible that both formed contemporaneously; however, precise temporal relationships are yet to be established. The Menzies deposits, like the Pagodroma Group, records warmer climatic condition in Antarctica during the Cenozoic.

## 10. Past Biogeographical Barriers to Terrestrial Migration in Antarctica.

### 10.1 Introduction

#### 10.1.1 Aims

This chapter discusses 1) the current lack of evidence for Neogene terrestrial higher plant fossils in the Lambert Graben catchment region and 2) the results of the search for such fossils on the Menzies Range. A hypothesis is formulated in this chapter to explain the question of Antarctic Neogene terrestrial biogeography and its relationship to Antarctica's glacial history.

#### 10.1.2 Previous Work

There has been continuing debate about Antarctic Neogene ice sheet history and climate, in particular about the late Pliocene. Much of the debate has concentrated on the Transantarctic Mountains, but it is now considering other East Antarctic locations where new data are emerging. The discovery of *Nothofagus beardmorensis* Hill, Harwood *et al.* Webb (southern beech) in the Sirius Group, of the Transantarctic Mountains at 80° S, provides evidence for a much warmer climate at some time in the past (Webb and Harwood 1993). These fossils may be Plio-Pleistocene (<3.8 Ma) in age, based upon glacially recycled and biostratigraphically datable diatoms in till deposits on which the *Nothofagus* grew (Hill and Truswell 1993; Webb and Harwood 1993; Hill *et al.* 1996). *Nothofagidites* pollen has also been found in reliably dated Pliocene (~3.0 Ma) marine sediments in the Ross Sea (Fleming and Barron 1994, 1996). This vegetation may have survived in Antarctica until <3.1 Ma (Webb *et al.* 1987; Webb and Harwood 1993), long after the generally accepted date for the development of cold polar climatic conditions like today, ~14 Ma (Flower and Kennett 1994).

East Antarctic Ice Sheet (EAIS) reductions occurred at intervals through out the Neogene (evident in Chapter 8). Diatoms in siltstones from the Fisher Bench Formation (AM 015) suggest that the mean annual air temperature, during one of these ice sheet reductions was at least 15 C° warmer than today (Chapter 8C). This is consistent with Antarctic mean temperature estimates of 15° to 20°C (Harwood *et al.* 1991), or 13° to 15°C (Hill *et al.* 1996), required for *Nothofagus* growth on the Transantarctic Mountains. During these conditions, large areas of East Antarctica were probably deglaciated, and could have been capable of supporting terrestrial higher plants. When mean air temperatures were >15 C°,

glacial reduction may have created a land bridge from the Transantarctic Mountains to other regions of East Antarctica. This chapter discusses the current lack of evidence for vegetation in the East Antarctic Lambert Graben catchment region. These observations create biogeographical questions that will be addressed here.

## **10.2 Methods**

Ancient lake sediments of the Pardoe Formation were found on the central Menzies Range during the 1997/98 Australian National Antarctic Research Expeditions (ANARE) (Chapter 9). They were deposited with wet-based glacial till and occupy palaeovalleys, sectioned by later wet-based glacial erosion (Chapter 9). These deposits are poorly exposed, mantled by scree; however, they were mapped, logged and sampled where possible.

Samples from one palaeovalley, containing the Pardoe Formation type section (Figure 57), were prepared commercially for palynological analysis by Lada Pty. Ltd. Andrew McMinn examined these slide preparations on a Zeiss Axioskop with 63x oil objective lens.

## **10.3 Results and Discussion**

### **10.3.1 Palynology on the Pardoe Formation Lake Sediments**

No plant macrofossils were found on Menzies Range, nor were there any pollen from the Pardoe Formation type section. Pollen dispersed by wind or water, and deposited in the Pardoe Bench Formation lakes could have been used to indicate the presence of vegetation within the region when these deposits formed. Lakes are an ideal place for the preservation of pollen records. The lack of pollen in ancient lake sediments on the Menzies Range may suggest that no higher plants occurred in this region during lake deposition.

### **10.3.2 Biogeographical Barriers**

The earliest Cenozoic glaciers in Antarctica are thought to have been alpine glaciers on the Gamburtsev Mountains and other mountainous regions in the Antarctic interior (Drewry 1975; Huybrechts 1993), such as the Prince Charles Mountains (Hambrey and Barrett 1993).

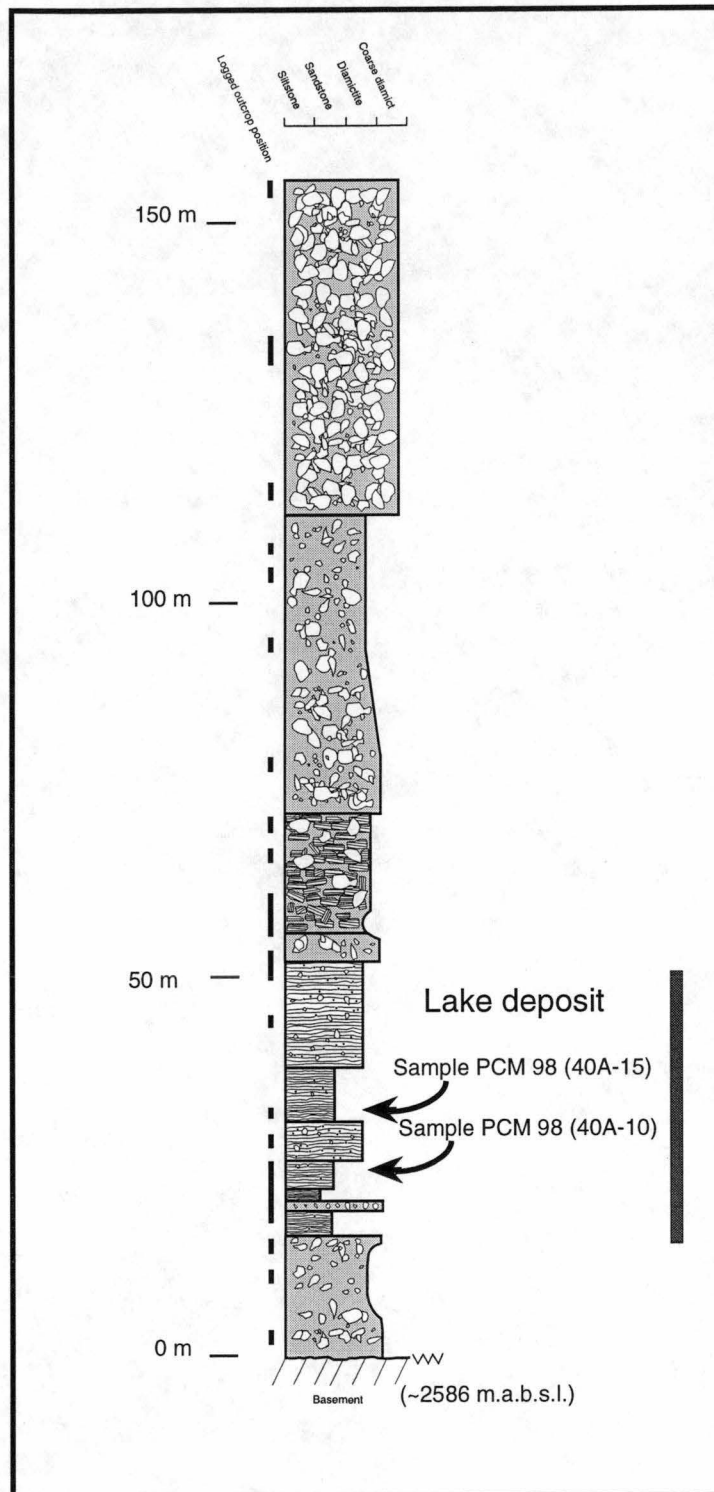


**Figure 57.** The Pardoe Formation type section (lat. 73° 27' S.; long. 61° 54' E.) at location 8 in Figure 53, palynological samples.

The glaciers eventually joined and developed into the first East Antarctic Ice Sheet (EAIS) (Drewry 1975; Hambrey and Barrett 1993), which flowed into Prydz Bay via the Lambert Graben (Barker *et al.* 1998). The oldest evidence for East Antarctic glaciation comes from late Eocene to early Oligocene glacial sediments in Prydz Bay ODP Sites 739 and 742 (Hambrey *et al.* 1991, 1994).

Prior to the formation of the EAIS, vascular plants vegetated the East Antarctic coastal margin in the middle – late Eocene (Truswell 1983; Quilty *et al.* 1999). As the EAIS expanded, it eliminated the vegetation; however, the timing of this event is uncertain. *Nothofagus* may have persisted in the Transantarctic Mountains and Antarctic Peninsula until intense cooling in the Plio-Pleistocene, <3.1 Ma (Webb *et al.* 1987; Webb and Harwood 1993). *Nothofagus* is unable to disperse vegetatively across seaways, nor is the seed easily transported by wind (Humphries 1981; Burckle and Pokras 1991; Hill *et al.* 1996).

If a similar flora, once present in the rest of East Antarctica, had been lost due to earlier Eocene – Oligocene, or later, EAIS expansion, geographical and environmental barriers may have prevented recolonisation from the Transantarctic Mountains. The rest of East Antarctica may have been geographically separated from the Transantarctic Mountains during deglaciation by the Wilkes-Pensacola-Aurora seaway (Figure 58F, Webb *et al.* 1984, Denton 1985). However, other reconstructions of Antarctica's subglacial topography indicate that there could have been a partial landbridge (Figure 58E, Drewry 1983), or even a major land connection between the Transantarctic Mountains and the rest of East Antarctic (Figure 58D, Bentley 1991; Denton 1995). Given most recent interpretation of Antarctica's sub-glacial topography and its response to deglaciation, it was likely that there was a land connection throughout East Antarctica (Denton 1995). Nevertheless, geographical and environmental barriers could have existed during partial glaciation. A reduced ice sheet on the Gamburtsev Mountains, for example, probably created a barrier between the Transantarctic Mountains and the rest of East Antarctica. During warmer intervals, elevated regions in the Transantarctic Mountains and Gamburtsev Mountains would have been high enough, and cold enough, due to isostatic rebound, to allow accumulation of sufficient snow to support an ice sheet locked between them (Prentice *et al.* 1992). A reconstruction of this ice sheet, when mean annual surface-air temperatures over the continent were 15 C°, 19 C° and 20 C° higher than today, is illustrated (Figure 58) (Huybrechts 1993).



Unique biogeographical provinces could have formed due to geographic separation by the ice sheet, seaways and marine embayments. Marine inundation, due to isostatic depression and the formation of outlet glaciers would have strengthened these barriers. If unfavorable conditions, such as deserts, existed across land connections they also would have formed environmental barriers to migration. The East Antarctic regions between the Lambert Graben, Wilkes and Aurora Basins are thought to have been connected to the Transantarctic Mountains when the mean annual surface-air temperature over the continent was  $>15\text{ }^{\circ}\text{C}$  warmer than today (Huybrechts 1993) (Figures 58A, B and C). Dronning Maud Land, Enderby Land and the Western Prince Charles Mountains it is thought, remained separate from the rest of Antarctica until temperatures were  $>19\text{ }^{\circ}\text{C}$  warmer than today (Huybrechts 1993) (Figures 58A and B).

The loss of East Antarctic terrestrial higher plants due to earlier Eocene–Oligocene, or later, EAIS expansion could explain the lack of these fossils in Neogene, East Antarctic, marine and glacial marine deposits. No terrestrial plant fossils have been found in the Lambert Graben catchments Northern Prince Charles Mountains, (Miocene and Pliocene Pagodroma Group), and Prydz Bay (Miocene and Pliocene ODP 119 and 120 Sites), nor along the East Antarctic coastal margins of the Larsemann Hills (Pliocene) and Vestfold Hills (Pliocene Sørødal Formation) (Quilty 1996). The palynology results from the Menzies Range are consistent with these observations. Biogeographical barriers could have prevented the recolonisation of higher plants back into East Antarctica from refuges in the Transantarctic Mountains. Nevertheless, the lack of terrestrial plant fossils from Neogene East Antarctic sediments requires further investigation, especially if mean annual surface-air temperatures over the continent were ever  $>15\text{ }^{\circ}\text{C}$  warmer than today. Such conditions could have caused deglaciation and created a major land connection between vegetated areas in the Transantarctic Mountains and the rest of East Antarctica. During an interval in the early Pliocene, mean sea-surface temperature was  $3.0^{\circ}\text{C}$ , which would have caused an elevation in mean annual surface-air temperature over the continent of  $17\text{ }^{\circ}\text{C}$  (Prentice *et al.* 1992). Associated changes in the Antarctic ice sheet were relatively modest, compared to those during even warmer temperatures that may have occurred during warmer intervals in the late Pliocene (Quilty 1996). Data from  $62^{\circ}\text{S}$  on the Kerguelen Plateau indicate that the summer sea-surface temperature in the late Pliocene  $<3.2\text{ Ma}$  was  $3.5^{\circ}$  to  $4.5\text{ }^{\circ}\text{C}$  warmer than today (Chapter 6). During late Pliocene warming the Antarctic ice volume may have been reduced by a third of its present size (Harwood 1983; Harwood 1986a; McKelvey *et al.* 1991; Webb *et al.* 1984, 1986, Webb and Harwood 1991).

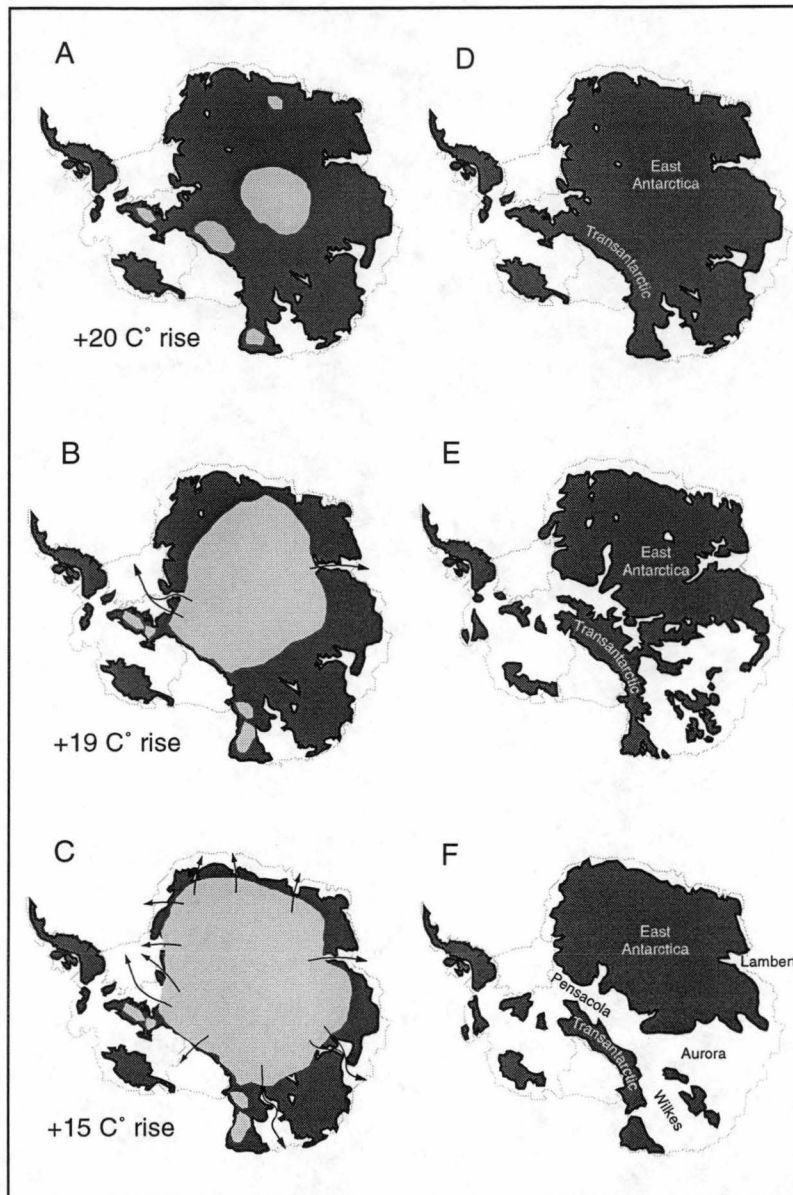


**Figure 58.** (A, B and C) Predicted ice sheet extent at higher mean annual air temperatures, determined from computer models (Huybrechts 1993), modified to illustrate geographical barriers due to glacial outflow (indicated by arrows). Different reconstructions of a deglaciated Antarctic, (F) illustrate no terrestrial connection between the Transantarctic Mountains and the rest of East Antarctica (isostatically corrected and sea-level elevated due to deglaciation, from Webb *et al.* 1984, Denton 1985), (E) a partial land connection (without isostatic correction nor sea-level elevation, from Drewry 1983), (D) or a major land connection (isostatically corrected and sea-level elevated due to deglaciation, from Bentley 1991, Denton 1995).

This could have created a continuous land connection from the Transantarctic Mountains to the Lambert Graben, enabling higher plant migration into East Antarctica, but evidence for this has not been found.

## 10.4 Summary

The lack of pollen in samples from post Eocene, lake sediments on the Menzies Range, supports other evidence for the absence of higher plants from post-Eocene deposits around the Lambert Graben catchment and adjacent coastal margin regions. These regions may have been denuded of higher plants by Eocene–Oligocene, or later, EAIS expansion; whilst this vegetation persisted in the Transantarctic Mountains until the Plio-Pleistocene (<3.1 Ma). Biogeographical barriers probably prevented its migration and recolonisation back into the rest of East Antarctica. The Transantarctic Mountains may have been geographically separated from other parts of East Antarctica during deglaciation by the Wilkes-Pensacola-Aurora seaway (Webb *et al.* 1984, Denton 1985), but if a land connection existed, as currently thought (Denton 1995), geographical separation still could have occurred during partial glaciation. A reduced ice sheet between the Gamburtsev and Transantarctic Mountains, for example, could create a barrier between the rest of East Antarctica and the Transantarctic Mountains, when mean annual surface air temperatures over the continent were <15 °C higher than today. Geographic barriers to plant migration could be caused by the ice sheet, seaways and partially flooded marine embayments. Further marine inundation, due to isostatic depression and the formation of outlet glaciers would have strengthened these barriers. If unfavorable conditions existed across land connections, such as deserts, they would form environmental barriers to plant migration. During periods of warmer temperatures, i.e. >15 °C warmer than today, these barriers would be breached; however, Dronning Maud Land, Enderby Land, and the western Prince Charles Mountains (including the Menzies Range), would remain isolated from the rest of Antarctica at temperatures <19 °C higher than today. Nevertheless, higher temperatures may have enabled a complete Antarctic land connection. Further investigation is required into the lack of Neogene higher plant fossils within the Lambert Graben catchment and along the adjacent coastal margin, especially if mean annual surface-air temperature over the continent were ever raised >15 °C during the late Pliocene.

## 11. Thesis Conclusion

Southern Ocean and Antarctic sediments from the Kerguelen Plateau, Vestfold Hills and Prince Charles Mountains have yielded evidence indicating that climatic conditions and ice sheet volume have fluctuated during the Cenozoic, in particular, after the Middle Miocene. At intervals through the Neogene the Southern Ocean and Antarctic climate was significantly warmer and the East Antarctic Ice Sheet (EAIS) smaller than today. This contrasts with traditional views from isotope (e.g. Flower and Kennett 1994) and geomorphological studies (e.g. Sugden *et al.* 1995a, 1995b; Sugden 1996), which suggest that the EAIS expanded, became stable and dry-based in the Middle Miocene and has remained so to the present day. In contrast, the results from this thesis indicate that warmer and reduced ice sheet conditions occurred in the Neogene. This is consistent with Neogene palaeoenvironmental interpretations from microfossils and terrestrial higher plant fossils found in the Sirius Group of the Transantarctic Mountains (e.g. Webb *et al.* 1983, 1984; Faure and Harwood 1990; Harwood 1991; Webb and Harwood 1987; Webb *et al.* 1987; Hill and Truswell 1993; Webb and Harwood 1993; Hill *et al.* 1996). Marine fossils have been used in this thesis to date intervals of ice sheet retreat and Southern Ocean warming. These fossils also enable reconstruction of the climatic conditions during glacial retreat. These findings correspond with some of the predicted climatic conditions during ice sheet retreat, identified by computer models (e.g. Huybrechts 1993; Warner and Budd 1998). The major findings from the three study regions are as follows:

### 11.1 Southern Kerguelen Plateau

Gravity cores from the Southern Kerguelen Plateau contain two Quaternary intervals, three Pliocene intervals, and at least three disconformities. The disconformities formed during intense glacial intervals during which the velocity of the Antarctic Circumpolar Current increased. Increased current velocity winnowed away the finer biogenic sediment, to create ice rafted debris lags that protected the underlying sediment. Sediment deposition occurred during the warmer climatic intervals. In these deposits, three assemblages were identified amongst the extant diatoms: assemblage I, an interglacial Antarctic open water assemblage; assemblage II, a glacial pack-ice associated assemblage, and assemblage III, a Pliocene interglacial Antarctic open water assemblage. Changes in the dominance of these assemblages imply that sea-ice conditions have changed with time over the Kerguelen Plateau. Assemblage II is uncommon today and may reflect differences in the sea-ice habitat during colder intervals in the past. There is a strong negative correlation between

the total abundance of diatoms in assemblage I versus assemblage II during the Quaternary. The ratios between assemblages I and II were plotted down core, and compared to modern surface sediment ratios, to reconstruct Quaternary sea-ice, salinity and water temperatures. Silicoflagellate ratios were used to reconstruct Pliocene summer sea-surface temperatures. Fluctuating climatic conditions were identified in the Quaternary and Pliocene. Two intervals with surface water temperatures higher than today were identified in the Pliocene, during which conditions were 3° to 4.5 C° warmer 3.1 - 2.64 Ma, and 4.5 C° warmer 3.2 - 3.1 Ma as far south as 62° S. This could have only occurred if the Antarctic Polar Front Zone was either ~1200 km further south or the temperature gradient across the associated ocean fronts became significantly shallower. The Pliocene intervals contain a high amount of ice rafted debris that may reflect a heavy iceberg influence due to warmer glacial conditions in Antarctica, which could have increased sediment discharge and iceberg calving.

## 11.2 Vestfold Hills

Quantitative diatom data from modern surface sediments in Prydz Bay and the Kerguelen Plateau with diatom assemblages from the Sørødal Formation, Vestfold Hills, to indicate that the climate was warmer than present during the early Pliocene (4.5 - 4.1 Ma). The presence of extant, sea-ice associated diatoms are significantly less abundant throughout the Sørødal Formation than in the modern Antarctic coastal zone. Extant diatoms in the Sørødal Formation, including *Stellarima stellaris*, *Thalassiosira oliverana*, *Fragilariopsis sublinearis*, *Pseudo-nitzschia turgiduloides* and *Eucampia antarctica* var. *recta*, are consistent with annual sea-surface temperatures (SST) of between -1.8° and 5.0°C. The presence of *Stellarima stellaris* indicates that the summer SSTs were >3°C during some intervals. The absence of calcareous coccoliths and the silicoflagellate *Dictyocha* suggests that the upper limit for summer SST was <5°C. These data indicate that early Pliocene summer SST were between 1.6° and 3 C° warmer than today. Abundant *Chaetoceros* cysts infer that stratified, open-water conditions were present during summer / spring. Ice sheet models show that warming of the magnitude evident in the Sørødal Formation ( 3 C°) would have resulted initially in increased snow accumulation and ice sheet growth. However, ice sheet growth was probably short-lived, as the long-term response to this warming in the early Pliocene resulted in a significant decrease in ice volume and deposition of the Sørødal Formation. Other factors, such as increased basal-ice sliding and higher discharge (icebergs and melt-water), probably led to significantly elevated ablation rates from the Pliocene ice sheet, resulting in ice sheet retreat.

### 11.3 Prince Charles Mountains

i) The Pagodroma Group of the northern Prince Charles Mountains consists largely of diamict, and to a lesser degree, siltstone and sand that were deposited in the Lambert Graben during reduced East Antarctic Ice Sheet volume. *In situ* and glacially reworked marine diatoms in the Pagodroma Group from the Amery Oasis and Fisher Massif suggest marine conditions occurred >250 km inland from the modern Amery Ice Shelf edge during the Plio-Pleistocene (3.1 - 1 Ma), Pliocene (4.9 - 3.7 Ma) and middle Miocene (12.2 - 11.7 Ma), and >300 km inland in the Miocene (14.2 - 12.5 Ma and 14.2 - 6.2 Ma) and Oligocene (~36.6 - 30.2 Ma). These diatoms provide age control for three formations in the Pagodroma Group. At high elevations on Fisher Massif, diamict of the Mt Johnston Formation was probably deposited between 36.6 - 12.5 Ma. At lower elevations on Fisher Massif, the basal 70 m of the Fisher Bench Formation was deposited during the Middle to late Miocene (14.2 - 6.2 Ma). On the Amery Oasis the Bardin Bluffs Formation was deposited less than 3.1 My ago. Diatom evidence from the Pagodroma Group indicates a history of significant ice volume changes in the EAIS throughout much of the late Cenozoic.

ii) The Bardin Bluffs Formation in the Amery Oasis was deposited between the late Pliocene (<3.1 Ma) and earliest Pleistocene (>1 Ma). The formation provides evidence of a reduced East Antarctic Ice Sheet compared to that of the present day and a subsequent Plio-Pleistocene ice sheet expansion. The formation consists of two members. The older, basal Member 1 is approximately 12.5 m thick and consists of relatively ice-distal silty sand and sparsely fossiliferous fjordal strata. Member 1 reflects largely ice free marine sedimentation ~250 km inland from the current Amery Ice Shelf edge. The member is restricted to the northeastern end of Pagodroma Gorge where it infills a chemically weathered valley-form erosion surface cut on the Permo-Triassic Amery Group. Weathering occurred during aerial exposure of the Amery Oasis in a warmer climate than today. The younger Member 2 exceeds 60 m in thickness and is made up of coarse ice proximal glacial marine diamicts. It disconformably overlies Member 1 at Pagodroma Gorge. Elsewhere, Member 2 rests directly upon a younger smoothed and striated erosion surface cut on the Amery Group, which was part of a fjord floor. The erosional disconformity and facies contrast between the two members indicate a later East Antarctic Ice Sheet expansion and Lambert Glacier grounding line advance.

iii) The Fisher Bench Formation on Fisher Massif contains a marine siltstone bed at its base that was deposited in the middle Miocene (14.2 - 12.5 Ma). The presence of the diatoms *Stellarima stellaris* and *Eucampia antarctica* var. *recta* suggests the summer SST was between 3.5° and 5°C. An associated relative mean annual air temperature rise >15°C, during ice shelf absence, caused deglaciation of the Lambert Graben. Marine deposition in the Lambert Graben during these temperatures is consistent with the predicted response of the EAIS from glacial models (e.g. Huybrechts 1993). The diatoms also suggest that reduced sea-ice conditions occurred during winter, and possibly in spring and autumn. The assemblage consists predominantly of planktic diatoms, indicating deposition in water exceeding euphotic depths. Diatoms are low in abundance, making up <10% of the sediment, due to the high terrigenous input from glacial melt out in the warmer glacial environment.

iv) The Cenozoic geology of the Menzies Range, in the Southern Prince Charles Mountains, formed during at least six phases of erosion and deposition during two very different climatic regimes. The range stands ~1500 m above the surrounding ice and is deeply incised by relict (ice free), alpine glacial valleys. Cliff sections in the sides of the valleys expose Cenozoic deposits up to 240 m thick. The glacial landforms and deposits formed sometime after the onset of Antarctic glaciation <40 Ma. The first climatic regime was warmer, whilst the latter was cold like today. Comparison with other Antarctic records suggests this climatic transition occurred ~2.6 Ma (e.g. Moriwaki *et al.* 1992a). The older Cenozoic deposits consist largely of clast-supported diamict with minor sandstone, sand and silt. These strata have been called the Menzies deposits, and consist of one distinct formation and two diamict deposits. These are, in order of decreasing age: the Pardoe Formation, Trail diamict and Amphitheatre diamict. The Menzies deposits and its associated landforms formed during, temperate, wet-based glacial conditions. At least five phases of glacial erosion and deposition were identified. The Menzies deposits and their landforms are overlain in places by latter Quaternary cobble-boulder gravels, of phase six. The Quaternary deposits formed under, cold, dry-based glacial conditions like today, which caused minor erosion and deposition.

v) Previous researchers have found controversial terrestrial higher plant fossils in the Transantarctic Mountains, which indicate a warmer Antarctic climate than today through much of the late Neogene (Webb and Harwood 1987; Webb *et al.* 1987; Hill and Truswell 1993; Webb and Harwood 1993; Hill *et al.* 1996). The lack of a similar flora in the Vestfold Hills and Prince Charles Mountains may reflect earlier denudation of this

vegetation during ice sheet development. Vascular plants vegetated the East Antarctic coastal margin near Prydz Bay in the middle – late Eocene (Truswell 1983).

Biogeographical barriers may have prevented recolonisation from the Transantarctic Mountains to other East Antarctic regions during later episodes of deglaciation, such as those identified in the Lambert Graben catchment during this study.



## 11.4 Summary

Results from this study suggest that the EAIS was a dynamic feature during the Neogene. After the middle Miocene the EAIS remained wet-based / polythermal and continued to be unstable, fluctuating in size at least until the late Pliocene <3.0 Ma. Southern Ocean conditions also continued to vary after the middle Miocene, with changes in the velocity of the Antarctic Circumpolar Current and in the position and / or temperature gradients across associated ocean fronts. Warming in the Pliocene on the Southern Kerguelen Plateau during the late Pliocene <3.2 Ma, could have only occurred if the Antarctic Polar front was 1200 km further south or a significant shallowing in the temperature gradient occurred across the associated ocean fronts.

The palaeoclimatic conditions during glacial retreat identified here show a general consensus with the conditions currently predicted from computer ice sheet models. In summary, marine deposition ~300 km inland of the current Amery Ice Shelf edge, at Fisher Massif, occurred during ice shelf absence. During ice shelf absence the mean annual temperature would have been  $>-4^{\circ}\text{C}$ , which is  $15^{\circ}\text{C}$  higher than today. Marine microfossils here indicate summer SST consistent with this view. East Antarctic Ice Sheet retreat detected at this palaeotemperature is consistent with the ice sheet response from computer models (e.g. Huybrechts 1993). At lower temperature increases ( $<5^{\circ}\text{C}$ ) some glacial models predict ice sheet expansion due to increased accumulation versus ablation (Huybrechts 1993). However, microfossils from the Vestfold Hills suggest that the ice sheet retreated when temperatures were approximately  $2.0^{\circ}$  to  $3.5^{\circ}\text{C}$  higher than today. This is inconsistent with Huybrechts (1993), but may support more recent models, which calculate ice sheet retreat due to an associated, albeit minor, rise in sea-surface temperature. An increase in sea-surface temperature would increase ice shelf and ice margin melting, decreasing ice sheet stability and increasing the rate of ice outflow (Warner and Budd 1998).

## 12. References

- Abbott, W.H., 1973, Investigation of diatoms in Southern Ocean deep sea cores. *Antarctic Journal of the United States*, 8(5), 286-287.
- Abbott, W.H., 1974, Temporal and spatial distribution of Pleistocene diatoms from the southeastern Indian Ocean. *Nova Hedwigia*, 25, 291-347.
- Abelmann, A., Gersonde, R., and Spiess, V., 1990, Pliocene-Pleistocene Paleooceanography in the Weddell Sea- Siliceous microfossil evidence. (In, Bleil, U. and Thiede, J. (Editors), *Geological History of the Polar Oceans: Arctic Versus Antarctic*. Kluwer Academic Publishers, Netherlands, pp. 729-759).
- Ackley, S.F., 1996, Sea ice. *Encyclopedia of Applied Physics*, 17, 81-103.
- Adamson, D.A. and Pickard, J., 1983, Late Quaternary ice movement across the Vestfold Hills, East Antarctica. (In, Oliver, R.L., James, P.R. and Jago, J.B. (Editors), *Antarctic Earth Science*. Cambridge University Press, Cambridge, pp. 465-469).
- Adamson, D.A. and Pickard, J., 1986a, Cainozoic history of the Vestfold Hills. (In, Pickard, J. (Editor), *Antarctic Oasis. Terrestrial Environments and History of the Vestfold Hills*. Academic Press, Sydney, pp. 63-97).
- Adamson, D.A. and Pickard, J., 1986b, Physiology and geomorphology of the Vestfold Hills. (In, Pickard, J. (Editor), *Antarctic Oasis. Terrestrial Environments and History of the Vestfold Hills*. Academic Press, Sydney, pp.99-139).
- Adamson, D. and Darragh, A., 1991, Field evidence on Cainozoic history and landforms in the Northern Prince Charles Mountains, East Antarctica. (In, Gillieson, D.J. and Fitzsimons, S.J. (Editors), *Quaternary Research in Australian Antarctica: Future Directions*. Department of Geography and Oceanography, Canberra, Special Publication 3, pp. 5-14).
- Adamson, D.A., Mabin, M.C.G., and Luly, J.G., 1997, Holocene isostasy and late Cenozoic development of landforms including Beaver and Radok Lake basins in the Amery Oasis, Prince Charles Mountains, Antarctica. *Antarctic Science*, 9(3), 299-306.
- Akiba, F., 1982, *Late Quaternary diatom biostratigraphy of the Bellingshausen Sea, Antarctic Ocean*. Report of the Technology Research Center, J.N.O.C., 16, 31-74.
- Akiba, F., 1985, Lower Miocene to Quaternary diatom biostratigraphy of Leg 57, off northeastern Japan, Deep Sea Drilling Project. *Initial Reports of the Deep Sea Drilling Project*, 56-57(2), 641-685.
- Alley, R.B., 1989, Deforming-bed origin for southern Laurentide till sheets? *Journal of Glaciology*, 37, 67-76.

- Alley, R.B., 1991, Water-pressure coupling of sliding and bed deformation: II. Velocity depth profiles. *Journal of Glaciology*, 35, 108-118.
- Alley, R.B. and Whillans, I.M., 1991, Changes in the West Antarctic ice sheet. *Science*, 254, 959-963.
- Allison, I., 1999, Surface climate of the interior of the Lambert Graben basin, Antarctica, from automatic weather station data. *Annals of Glaciology*, 27, 515-520.
- Anderson, J.B., Kurtz, D.B., and Weaver, F.M., 1979, Sedimentation on the Antarctic continental slope. *Society of Economic Paleontology and Mineralogy, Special Publication*, 27, 265-283.
- Anderson, J.B., Kurtz, D.D., Domack, E.W., and Balshaw, K.M., 1980, Glacial and glacial marine sediments of the Antarctic continental shelf. *Journal of Geology*, 88, 399-414.
- Anderson, J.B. and Molnia, B. (Editors), 1989, *Glacial Marine Sedimentation. Short Course in Geology*. American Geophysical Union, Washington, pp. 57.
- Anderson, J.B., Kennedy, D.S., Smith, M.J., and Domack, E.W., 1991, Sedimentary facies association with Antarctica's floating ice masses. (In, Anderson, J.B. and Ashley, G.M. (Editors), *Glacial Marine Sedimentation; Paleoclimatic Significance*. The Geological Society of America, Special Paper 261, 25 p.).
- Anderson, J.B. and Bartek, L.R., 1992, Cenozoic glacial history of the Ross Sea revealed by intermediate resolution seismic reflection data combined with drill site information. *Antarctic Research Series*, 56, 231-263.
- Anderson, J.B., 1993, Antarctic glacial-marine sedimentation. (In, Bryan, J.R. (Editor), *Workshop on Antarctic glacial marine and biogenic sedimentation notes for a shortcourse, I*. Tallahassee, Florida, pp. 1-88).
- Anderson, J.B., 1994, Marine Geological Record of the Ross Sea Glacial History. *Landscape Evolution in the Ross Sea Area*, 65-68.
- Armand, L.A., 1997, *The Use of Diatom Transfer Functions in Estimating Sea-surface Temperature and Sea-ice in Cores From the Southeast Indian Ocean*. Ph.D. Thesis, Australian National University, Canberra, 391 p.
- Arrigo, K.A., Robinson, D.H., Worthen, D.L., Schieber, B., and Lizotte, M.P., 1998a, Bio-optical properties of the southwestern Ross Sea. *Journal of Geophysical Research*, 103(C10), 21,683-21,695.
- Arrigo, K.A., Weiss, A.M., and Smith, W.O., Jr., 1998b, Physical forcing of phytoplankton dynamics in the southwestern Ross Sea. *Journal of Geophysical Research*, 103(C1), 1007-1021.

- Ashworth, A.C., 1999, The fossils of the Meyer Desert Formation, Sirius Group, Transantarctic Mountains. (In, Skinner, D.N.B. (Editor), *Programme and Abstracts, VIII International Symposium on Antarctic Earth Sciences*, Wellington, p. 28).
- Ashworth, A.C., Harwood, D.M., Webb, P.N., and Mabin, M.C.G., 1997, A weevil from the heart of Antarctica. *Quaternary Proceedings*, 5, 15-22.
- Baldauf, J. G. and Barron, J. A., 1980, *Actinocyclus ingens* var. *nodus*; a new, stratigraphically useful diatom of the Circum-North Pacific. *Micropaleontology*, 26(1), 103-110.
- Baldauf, J.G. and Barron, J.A., 1990, Evolution of biosiliceous sedimentation patterns - Eocene through Quaternary: paleoceanographic response to polar cooling. (In, Bleil, U. and Thiede, J. (Editors), *Geological History of the Polar Oceans: Arctic Versus Antarctic, NATO ASI Series*, Kluwer Academic Publishers, Dordrecht, pp. 575-609).
- Baldauf, J.G. and Barron, J.A., 1991, Diatom biostratigraphy: Kerguelen Plateau and Prydz Bay regions of the Southern Ocean. *Proceedings of the Ocean Drilling Program, Scientific Results*, 119, 547-598.
- Baldauf, J.G., 1993, Middle Eocene through early Miocene diatom floral turnover. (In, Prothero, D. and Berggren, W.A. (Editors), *Eocene-Oligocene climatic and biotic evolution*. Princeton University Press, Princeton, pp. 310-326).
- Bardin, V.I. and Suyetova, I.A., 1967, Basic morphometric characteristics for Antarctica and budget of the Antarctic ice cover. *Japanese Antarctic Research Expeditions, Scientific Reports, Special Issue*, 1, 92-100
- Bardin, V.I., 1975, Glacial geomorphology of Lambert Glacier and of its mountainous frame. *Antarktika*, 14, 110-127.
- Bardin, V.I., 1980, Moraines of the Antarctic continent. *26<sup>th</sup> International Geological Congress, Abstracts*, 26(2), 14-21.
- Bardin, V.I., 1982, Composition of East Antarctic Moraines and Some Problems of Cenozoic History. (In, Craddock, C. (Editor), *Antarctic Geoscience*. University of Wisconsin Press, Madison, pp. 1069-1076).
- Bardin, V.I. and Kolosova, G.N., 1983, Early glaciation deposits in the Prince Charles Mountains, *Antarktika*, 22, 68-76.
- Bardin, V.I. and Kolosova, G.N., 1988, Ancient glacial deposits at Radok Lake, *Antarktika; doklady komissi*, 27, 66-75.
- Bardin, V.I. and Belevich, A.M., 1985, On the study of early glacial deposits in the Prince Charles Mountains. *Antarktika*, 24, 76-81.

- Bardin, V.I. and Chepalyga, A.L., 1989, Molluscs in early glacial deposits on the shore of Beaver Lake. (East Antarctica, Prince Charles Mountains). *Antarktika*, 28, 35-38.
- Barker, P.F., 1977, Underway geophysical observations, Leg 36 Deep Sea Drilling Project. *Initial Reports of the Deep Sea Drilling Project*, 36, 945-970.
- Barker, P.F., Kennett, J.P., and Scientific Party, 1988, Weddell Sea palaeoceanography: preliminary results of ODP Leg 113. *Palaeogeography, Palaeoclimatology, Palaeoecology*, 67, 75-102.
- Barker, P., Fontes, J.C., Gasse, F. and Druart, J.C., 1994, Experimental dissolution of diatom silica in concentrated salt solutions and implications for palaeoenvironmental reconstruction. *Limnology and Oceanography*, 39(1), 99-110.
- Barker, P.F., Barrett, P.J., Cooper, A.K., Davey, F.J., Domack, E.W., Escutia, C., Kristoffersen, Y., and O'Brien, P.E., 1998, Ice Sheet history from Antarctic Continental Margin sediments: the ANTOSTRAT approach. *Terra Antarctica*, 5(4), 737-769.
- Barkov, N.I., 1985, *Ice shelves of Antarctica*. A. A. Balkema, Rotterdam, 262 p.
- Barrett, P. J., 1982, Proposal for Cenozoic investigations in the western Ross Sea (CIROS). *New Zealand Antarctic record*, 4(2), 32-39.
- Barrett, P.J., 1989, Antarctic Cenozoic history from the CIROS-1 drillhole, McMurdo Sound. *DSIR Bulletin*, 245, 254.
- Barrett, P.J., 1996, Antarctic paleoenvironments through Cenozoic times - a review. *Terra Antarctica*, 3, 103-119.
- Barrett, P.J., Adams, C.J., McIntosh, W.C., Swisher, C.C., and Wilson, G.S., 1992, Geochronological evidence supporting Antarctic deglaciation three million years ago. *Nature*, 359, 816-818.
- Barrett, P.J., 1992, Debate: Antarctic ice sheets and global warming. *Antarctic Science*, 12(10), 330-334.
- Barrett, P.J., Bleakley, N.L., Dickinson, W.W., Hannah, M.J., and Harper, M.A., 1997, Distribution of Siliceous Microfossils on Mount Feather, Antarctica, and the Age of the Sirius Group. (In, Ricci C.A. (Editor), *The Antarctic Region; Geological Evolution and Processes; Proceedings of the VII International Symposium on Antarctic Earth Sciences*. Siena (Italy), pp. 763-770).
- Barrett, P.J., Fielding, C., Wise, S.W., 1998, Initial Report on CRP-1, Cape Roberts Project, Antarctica. *Terra Antarctica*, 5(1), 187.

- Barron, J.A., 1980, Lower Miocene to Quaternary diatom biostratigraphy of Leg 57, off northeastern Japan. *Initial Reports of the Deep Sea Drilling Project*, 56-57(2) 641-685.
- Barron, J.A., 1981, Marine diatom biostratigraphy of the Montesano Formation near Aberdeen, Washington. *Geological Society of America*, Special Report 184, pp. 113-126.
- Barron, J.A., 1985, Miocene to Holocene planktic diatoms. (In, Bolli H.M, Saunders, J.B. and Perch-Nielsen, K. (Editors), *Plankton Stratigraphy*. Cambridge University Press, Cambridge, pp. 763-809).
- Barron, J.A., Larsen, B., and Ship board scientific party, 1989a, Introduction, *Proceedings of the Ocean Drilling Program, Initial Reports*, 119, 5-14.
- Barron, J.A., Larsen, B., Baldauf, J.G., Albert, C., Berkowitz, S.P., Caulet, J.-P., Chambers, S.R., Cooper, A.K., Cranston, R., Dorn, W.U., Ehrmann, W.U., Fox, R., Fryxell, G., Hambrey, M.J., Huber, B.T., Jenkins, C.J., Kang, S.-H., Keating, B.H.H., Mehl, K.W., Il, N., Ollier, G., Pittenger, A., Sakai, H., Schroder, C.J., Solheim, A., Stockwell, D., Thierstein, H.R., Tocher, B.A., Turner, B., and Wei, W., 1989b, Ocean Drilling Program; early glaciation of Antarctica, *Nature*, 333, 303-304.
- Barron, J.A., 1992, Neogene diatom datum levels in the equatorial and North Pacific, (In, Ishizki, K, and Saito, T., (Editors), *The Centenary of Japanese Micropaleontology*, Tokyo University Press, Tokyo, p. 413-425).
- Barron, J.A., 1993, Diatoms. (In Lipps, J.H. (Editor), *Fossil Prokaryotes and Protists*. Blackwell Scientific Publications, Boston, pp. 155-168).
- Barron, J.A. and Mahood, A.D., 1993, Exceptionally well-preserved early Oligocene diatoms from glacial sediments of Prydz Bay, East Antarctica. *Micropaleontology*, 39(1), 29-45.
- Barron, J.A. and Baldauf, J.G., 1995, Cenozoic marine diatom biostratigraphy and application to paleoclimatology and paleoceanography. (In, Babcock, L.E. and Ausich, W.I. (Editors), *Siliceous microfossils. Short Courses in Paleontology*, 8. University of Tennessee Publication, pp. 107-118).
- Barron, J.A., 1996, Diatom constraints on the position of the Antarctic Polar Front in the middle part of the Pliocene. *Marine Micropalaeontology*, 27, 195-213.
- Bartek, L.R, Anderson, J.B., Emmet, P.A, and Wu, S., 1991, Effect of Cenozoic ice sheet fluctuations in Antarctica on the stratigraphic signature of the Neogene. *Journal of Geophysical Research*, 96, 6753-6778.

- Bartek, L.R., Henrys S.A., Anderson, J.B., and Barrett, P.J., 1996, Seismic stratigraphy of McMurdo Sound, Antarctica: implications for glacially influenced early Cenozoic eustatic change? *Marine Geology*, 130, 79-98.
- Basile, I., Grousset, F.E., Revel, M., Petit, J.R., Biscaye, P.E. and Barkov, N.I., 1997, Patagonian origin of glacial dust deposited in East Antarctica (Vostok and Dome C) during glacial stages 2, 4 and 6. *Earth and Planetary Science Letters*, 146, 573-589.
- Bearman, G., 1989, *Seawater: its composition, properties and behaviour*, Pergamon Press, Oxford, 165 p.
- Beaufort, L. and Aubry, M.-P., 1992, Paleooceanographic implications of a 17 M.y. long record of High latitude Miocene calcareous nannoplankton fluctuations. *Proceedings of the Ocean Drilling Program, Scientific Results*, 120, 539-549.
- Beaver, J., 1981, *Apparent Ecological Characteristics of Some Common Freshwater Diatoms*. Ontario Ministry of the Environment, 517 p.
- Benn, D.I. and Evans, D.J.A., 1998, *Glaciers and Glaciation*. Edward Arnold, London, 734 p.
- Bennett, M.R. and Glasser, N.F., 1996, *Glacial Geology Ice Sheets and Landforms*. John Wiley and Sons Ltd., West Sussex, 364 p.
- Benson, R.H., 1975, The origin of the psychrosphere as recorded in changes of deep sea ostracode assemblages. *Lethaia*, 8, 69-83.
- Bentley, C.R., 1991, Configuration and structure of the subglacial crust. (In, Tingey, R.J. (Editor.), *The Geology of Antarctica*. Oxford Monographs on Geology and Geophysics, 17, pp. 335-364).
- Bentley, C.R., 1997, Rapid Sea-Level Rise Soon from West Antarctic Ice Sheet Collapse. *Science*, 275, 1077- 1078.
- Berggren, W.A., Kent, D.V., Flynn, J.J., and Van Couvering, J.A., 1985a, Cenozoic geochronology. *GSA Bulletin*, 96, 1407-1418.
- Berggren, W.A., Kent, D.V., and Van Couvering, J.A., 1985b, The Neogene: Part 2, Neogene geochronology and chronostratigraphy. (In, Snelling, N.J. (Editor), *The Chronology of the Geological Record*, Geological Society of London Memoirs, 10, pp. 211-260.
- Berggren, W.A., Kent, D.V., Swisher, C.C., and Aubry, M.P., 1995, A revised Cenozoic geochronology and chronostratigraphy. (In Berggren, W.A., Kent, D.V., Aubry, M.P. and Hardenbol, J.A., (Editors.), *Geochronology, Time Scales and Global Stratigraphic Correlation*, Special Publication, Society for Sedimentary Geology, 54, pp. 129-212).

- Bianchi, F., Boldrin, A., Cioce, F., Dieckmann, G., Kuosa, H., Larsson, A.-M., Nöthig, E.-M., Sehlstedt, P.-I., Socal, G., and Syversten, E.E., 1992, Phytoplankton distribution in relation to sea ice, hydrography and nutrients in the northwestern Weddell Sea in early spring 1988 during EPOS. *Polar Biology*, 12, 225-235.
- Bindschadler, R. and Bentley, C.E., 1997, West Antarctic Ice Sheet collapse? *Science*, 276, 662-663.
- Bindschadler, R., 1998, Future of the West Antarctic Ice Sheet. *Science*, 282, 428-429.
- Birkenmajer, K. 1987, Oligocene-Miocene glaciomarine sequences of King George (South Shetland Islands), Antarctica. *Palaeontologia Polonica*, 49, 9-36.
- Bodén, P., 1992, Quantitative biostratigraphy of Neogene diatoms from the Norwegian Sea, North Atlantic and North Pacific. *ACTA Universitatis Stockholmiensis, Stockholm Contributions in Geology*, 42(3), 121-215.
- Bohaty, S.M. and Harwood, D.M., 1998, Southern Ocean Pliocene paleotemperature variation from high resolution silicoflagellate biostratigraphy. *Marine Micropaleontology*, 33, 241-272.
- Bohaty, S.M., Scherer, R.P. and Harwood, D.M. 1998. Quaternary diatom biostratigraphy and palaeoenvironments of the CRP-1 drillcore, Ross Sea, Antarctica. *Terra Antarctica*, 5(3), 431-453.
- Boulton, G.S., 1987, A theory of drumlin formation by subglacial sediments deformation, (In, Menzies, J. and Rose, J. (Editors), *Drumlin Symposium*. A.A. Balkema, Rotterdam, pp. 25-80).
- Braarud, T., 1979, The temperature change of the non-motile stage of *Coccolithus pelagicus* in the North Atlantic region. *British Phycology Journal*, 14, 349-352.
- Bradbury, J. and Krebs, W. N., 1995, Fossil continental diatoms: paleolimnology, evolution and biochronology. (In, Babcock, L.E. and Ausich, W.I. (Editors), *Siliceous microfossils. Short Courses in Paleontology*, 8. University of Tennessee Publication, pp. 119-138).
- Brady, H.T. and Martin, H., 1979, Ross Sea region in the Middle Miocene: a glimpse of a past. *Science*, 203, 437-438.
- Breza, J.R., 1992, High-resolution study of Neogene ice-rafted debris, Site 751, Southern Kerguelen Plateau, *Proceedings of the Ocean Drilling Program, Scientific Results*, 120 (1), 207-221.
- Breza, J.R., and Wise, S.W., 1992, Lower Oligocene ice-rafted debris on the Kerguelen Plateau: evidence for East Antarctic continental glaciation. *Proceedings of the Ocean Drilling Program, Scientific Results*, 120 (1), 161-178.



- Brown, R.W., Fabel, D., Gleadow, A.J.W., Gallagher, K., and Summerfield, M.A., 1995, Reconstructing the long-term topographic history of the Prince Charles Mountains, East Antarctica. (In, Ricci C.A. (Editor), *The Antarctic Region; Geological Evolution and Processes; Proceedings of the VII International Symposium on Antarctic Earth Sciences*. Siena (Italy), p. 64).
- Brunk, K., 1989, Large-scale geomorphologic-glaciological mapping of the arid high-polar Borgmassivet, New Schwabenland, Antarctica. *Berichte zur Polarforschung*, 66, 85-102.
- Bryan, J.R., 1993, *Workshop on Antarctic glacial marine and biogenic sedimentation notes for a shortcourse*. Sedimentology Research Laboratory Contribution No. 57., Tallahassee, 104 p.
- Budd, W, Jenssen, D. and Radock, U., 1970, The extent of basal melting in Antarctica. *Polarforschung*, 6, 293-306.
- Budd, W.F., Jensen, D. and Radok, U., 1971, Derived physical characteristics of the Antarctic Ice Sheet. *Australian National Antarctic Expeditions Interim Reports, Series A(IV) Glaciology*. Publication No. 120, 178 p.
- Burckle, L.H. and Abrams, N., 1986, Biotic response to two late Neogene intervals of global climatic change: evidence from the deep-sea record. *Suid-Afrikaanse Tydskrif vir Wetenskap*, 82, 69.
- Burckle, L.H. and Cirilli, J., 1987, Origin of diatom ooze belt in the Southern Ocean: Implications for the late Quaternary paleoceanography. *Micropalaeontology*, 33(1), 82-86.
- Burckle, L.H., Jacobs, S.S. and McLaughlin, R., 1987, Late Spring diatom distribution between New Zealand and Ross Sea: Correlation with hydrography and bottom sediments. *Micropaleontology*, 33, 74-81.
- Burckle, L.H., Gayley, R.I., Ram, M. and Petit, J.-R., 1988a, Biogenic particles in Antarctic ice cores and the source of Antarctic dust. *Antarctic Journal of the United States*, 23(5), 71-72.
- Burckle, L.H., Gayley, R.I., Ram, M., and Petit, J.-R., 1988b, Biogenic particles in Antarctic ice cores and the source of Antarctic dust. *Antarctic Journal of the United States*, 23(5), 71-72.
- Burckle, L.H. and Pokras, E.M., 1991, Implications of a Pliocene stand of *Nothofagus* (southern Beech) within 500 kilometres of the South Pole/ *Antarctic Science*, 3 (4), 389-403.

- Burckle, L.H., Mortlock, R., and Rudolph, S., 1996, No evidence for extreme, long term warming in early Pliocene sediments of the Southern Ocean. *Marine Micropaleontology*, 27, 215-226.
- Burckle, L.H. and Potter, N. Jr., 1996, Pliocene-Pleistocene diatoms in Paleozoic and Mesozoic sedimentary and igneous rocks from Antarctica: A Sirius problem solved. *Geology*, 24, 235-238.
- Burckle, L.H., Kellogg, D.E., Kellogg, T.B., and Fastook, J.L., 1997, A mechanism for emplacement and concentration of diatoms in glacial deposits. *Boreas*, 26(1), 55-60.
- Burckle, L.H. and Delaney, J.S., 1999, Terrestrial microfossils in Antarctic ordinary chondrites. *Meteoritic and Planetary Science*, 34, 475-478.
- Burgess, J.S., Spate, A.P., and Shevlin, J., 1994, Onset of deglaciation in the Larsemann Hills, eastern Antarctica. *Antarctic Science*, 6(4), 491-495.
- Calvert, S.E., 1974, Deposition and diagenesis of silica in marine sediments. (In, Hsu, K.J., and Jenkyns, H.C. (Editors), *Pelagic Sediments on Land and Under the Sea*. International Association of Sedimentologists, Blackwell Scientific Publications, Oxford, pp. 273-299).
- Carlquist, S., 1987, Pliocene *Nothofagus* wood from the Transantarctic Mountains. *Aliso*, 11(4), 571-583.
- Carmack, E.C., 1990, Large-scale physical oceanography of Polar Oceans. (In, Smith, W.O., Jr., (Editor), *Polar Oceanography, Part A Physical Science*. Academic Press, Inc., San Diego, pp. 171-222).
- Cassie, V., 1963, Distribution of surface phytoplankton between New Zealand and Antarctica, December 1957. *Trans-Antarctic Expedition 1955-1958, Scientific Reports*, 7, 11.
- Cavalieri, D.J. and Parkinson, C.L., 1981, Large-scale variations in observed Antarctic sea ice extent and associated atmospheric circulation. *Monthly Weather Reviews*, 109, 2323-2336.
- Cavalieri, D.J. and Martin, S., 1985, A passive microwave study of polynyas along the Antarctic Wilkes Land coast. *Antarctic Research Series*, 43, 227-252.
- Ciesielski, P.F., Weaver, F.M., 1973, Southern ocean Pliocene paleotemperatures based on silicoflagellates from deep sea cores, *Antarctic journal of the United States*, 8(5), 295-297.
- Ciesielski, P.F., 1974, Silicoflagellate paleotemperature curve for the Southern Ocean. *Antarctic Journal of the United States*, 9, 269-270.

- Ciesielski, P.F. and Weaver, F.M., 1974, Early Pliocene Temperature changes in the Antarctic Seas. *Geology*, 2(10), 511-515.
- Ciesielski, P.F. and Wise, S., 1977, Geological history of the Maurice Ewing Bank of the Falkland Plateau (Southwest Atlantic Sector of the Southern Ocean) based on piston and drill cores. *Marine Geology*, 25, 175-207.
- Ciesielski, P.F., Ledbetter, M.T., and Ellwood, B., 1982, The development of Antarctic glaciation and the Neogene paleoenvironment of the Maurice Ewing Bank. *Marine Geology*, 46, 1-51.
- Ciesielski, P.F., 1983, The Neogene and Quaternary diatom biostratigraphy of subantarctic sediments, Deep Sea Drilling Project Leg 71. *Initial Reports of the Deep Sea Drilling Project*, 90(2), 635-665.
- Ciesielski, P.F., 1986, Middle Miocene to Quaternary diatom biostratigraphy of Deep Sea Drilling Project Site 594, Chatham Rise, south west Pacific. *Initial Reports of the Deep Sea Drilling Project*, 90, 863-885.
- Ciesielski, P.F. and Grinstead, G.P., 1986, Pliocene variation in the position of the Antarctic convergence in the Southwest Atlantic. *Paleoceanography*, 1(2), 197-232.
- Clapperton, C.M. and Sugden, D.E., 1990, Late Cenozoic glacial history of the Ross Embayment, Antarctica. *Quaternary Science Reviews*, 9, 253-272.
- Clarke, A., 1996a, Benthic marine habitats in Antarctica. *Antarctic Research Series*, 70, 123-133.
- Clarke, A., 1996b, The distribution of Antarctic marine benthic communities. *Antarctic Research Series*, 70, 219-230.
- CLIMAP Project Members, 1981, *Seasonal Reconstructions of the Earth's Surface at the Last Glacial Maximum*, Geological Society of America: Map and Chart Series MC-36.
- Colbeck, S.C., 1980, *Dynamics of Snow and Ice Masses*. Academic Press, New York, 468 p.
- Colbert, E.H., 1991, Mesozoic and Cainozoic tetrapod fossils from Antarctica. (In, Tingey, R.J. (Editor), *The Geology of Antarctica*. Clarendon Press, Oxford, pp. 568-587).
- Colhoun, E.A., 1991, Geological evidence for changes in the East Antarctica ice sheet (60 degrees -120 degree E.) during the last glaciation. *Polar Record*, 27(163), 345-355.
- Colhoun, E.A., 1997, Review of geomorphological research in Bunger Hills and expansion of the East Antarctic Ice Sheet during the Last Glacial Maximum. (In, Ricci C.A. (Editor), *The Antarctic Region; Geological Evolution and Processes*;

- Proceedings of the VII International Symposium on Antarctic Earth Sciences*. Siena (Italy), pp. 801-807).
- Comiso, J.C. and Gordon, A.L., 1996, The Cosmonaught Polynya in the Southern Ocean: structure and variability. *Journal of Geophysical Research*, 101(C8), 18297-18313.
- Comiso, J.C. and Zwally, H.J., 1984, Concentration gradients and growth/decay characteristics of the seasonal sea ice cover. *Journal of Geophysical Research*, 89(C5), 8081-8103.
- Contant, H. and Duthie, H.C., 1978, The phytoplankton of Lac St-Jean, Quebec. *Bibliotheca Phycologica*, 40, 43 p.
- Cooke, D.W. and Hays, J. D., 1982, Estimates of Antarctic Ocean seasonal sea-ice cover during glacial intervals. *Antarctic Geoscience*, 131, 1017-1025.
- Cooper, A.K., Barrett, P.J., Hinz, K., Traube, V., Leitchenkov, G., and Stagg, H.M.J., 1991, Cenozoic prograding sequences of the Antarctic continental margin: a record of glacio-eustatic and tectonic events. *Marine Geology*, 102, 175-213.
- Cowan, E.A. and Powell, R.D., 1991, Ice-proximal sediment accumulation rates in a temperate glacial fjord, southeastern Alaska. (In, Anderson, J.B. and Ashley, G.M. (Editors), *Glacial Marine Sedimentation; Paleoclimatic Significance*. Geological Society of America. Special Paper, 261, pp. 61-73).
- Cowen, R., 1995, Ice's age? More than 8 million years. *Science News*, 148, 87.
- Cramer, J., 1979, The algae of Southern Victoria Land, Antarctica. *Bibliotheca Phycologica*, 46, 163 p.
- Crawford, R.M., 1979, Taxonomy and frustular structure of the marine centric diatom *Paralia sulcata*. *Journal of Phycology*, 15, 200-210.
- Crosta, X., Pichon, J.-J. and Labracherie, M., 1997, Distribution of *Chaetoceros* resting spores in modern peri-Antarctic sediments. *Marine Micropaleontology*, 29, 283-299.
- Crosta, X., Pichon, J.-J. and Burckle, L.H., 1998, Application of modern analog technique to marine Antarctic diatoms: Reconstruction of maximum sea-ice extent at the Last Glacial Maximum. *Paleoceanography*, 13(3), 284-297.
- Crowley, T.J., 1996, Pliocene climates: the nature of the problem. *Marine Micropaleontology*, 27, 3-12.
- Cunningham, W.L., 1997, *The Use of Modern and Fossil Diatom Assemblages as Climate Proxies in the Central and Western Ross Sea, Antarctica*. Masters Thesis, University of Colorado, 233 p.

- Cunningham, W.L., Leventer, A., Andrews, J.T., Jennings, A.E. and Licht, K.J., 1999, Late Pleistocene-Holocene marine conditions in the Ross Sea, Antarctica: evidence from the diatom record. *The Holocene*, 9(2), 129-139.
- Daniels, J. 1996, *Systematics of Pliocene dolphins (Odontoceti: Delphinidae) from Marine Plain, Antarctica*. MSC Thesis, University of Otago, 400 p.
- Davis-A.M.J. and McNider R.T., 1997, The development of Antarctic katabatic winds and implications for the coastal ocean. *Journal of the Atmospheric Sciences*, 54, 1248-1261.
- Dayton, P. K., 1969, Anchor-ice formation in McMurdo Sound, Antarctica, and its biological effects. *Science*, 163, 273-274.
- Dayton, P.K., Robilliard, G.A. and DeVries, A.L., 1969, Anchor ice formation in McMurdo Sound, Antarctica, and its biological significance. *Science*, 163, 273-275.
- Dayton, P. K., Bobilliard, G. A. and Paine, R. T., 1970, Benthic faunal zonation as a result of anchor ice at McMurdo Sound, Antarctica. (In, Holdgate, M. W. (Editor), *Antarctic Ecology, Volume 1, The Scientific Committee on Antarctic Research*. Academic Press, New York, pp. 244-258).
- Dayton, P.K. and Martin, S., 1971, observations on ice stalactites in McMurdo Sound, Antarctica. *Journal of Geophysical Research*, 76, 1579.
- DeFelice, D.R. and Wise, S.W., 1981, Surface lithofacies, biofacies, and diatom diversity patterns as models for delineation of climatic change in the Southeast Atlantic Ocean. *Marine Micropaleontology*, 6, 29-70.
- Delmas, R.J. and Legrand, M., 1989, Long-term changes in the concentrations of major chemical compounds (soluble and insoluble) along deep ice cores. (In, Oeschger, H. and Langway, C. C. Jr. (Editors), *Environmental Record in Glaciers and Ice Sheets*. John Wiley and Sons, New York, pp.319-341).
- Delmas, R.J., and Petit, J.R., 1994, Present Antarctic aerosol composition: A memory of ice age atmospheric dust? *Geophysical Research Letters*, 21(10), 879-882.
- DeMaster, D.J., 1981, The supply and accumulation of silica in the marine environment. *Geochimie et Cosmochimie Acta*, 45, 1715-1732.
- DeMaster, D.J., Dunbar, R.B., Gordon, L.I., Leventer, A.R., Morrison, J.M., Nelson, D.M., Nittrouer, C.A. and Smith, W.O. Jr., 1992, Cycling and accumulation of biogenic silica and organic matter in high-latitude environments: the Ross Sea. *Oceanography*, 5(3), 146-153.
- Denton, G.H. and Hughes, T.J., 1981, *The Last Great Ice Sheets*. John Wiley and Sons, New York, 484 p.

- Denton, G.H., 1985, Did the Antarctic Ice Sheet influence Late Cainozoic climate and evolution in the southern hemisphere? *South African Journal of Science*, 81, 224-229.
- Denton, G.H., Prentice, M.L., and Burckle, L.H., 1991, Cainozoic history of the Antarctic ice sheet, (In, Tingey, R.J., (Editors), *The Geology of Antarctica*. Clarendon Press, Oxford, pp. 365-433).
- Denton, G.H., Sugden, D.M., Marchant, D.R., Hall, B.L., and Wilch, T.I., 1993, East Antarctic Ice Sheet sensitivity to Pliocene climatic change from a Dry Valleys perspective. *Geografiska Annaler*, 75A, 155-204.
- Denton, G.H., 1995, The problem of Pliocene paleoclimate and ice sheet evolution in Antarctica. (In, Vrba, E.S, Denton, G.H, Partridge, T.C. and Burckle, L.H. (Editors), *Paleoclimate and Evolution, with Emphasis on Human Origins*. Yale university Press, New Haven, pp. 213-229).
- Derbyshire, E. and Peterson, J. A., 1978, A photo-geomorphic map of the Mt Menzies nunatak, Prince Charles Mountains, Australian Antarctic Territory. *Zeitschrift für Gletscherkunde und Glazialgeologie*, 14 (1), 17-26.
- De Santis, L., Brancolini, G., Buseti, M., and Marchetti, A., 1997, Seismic sequence and Late Cenozoic glacial history in the Ross Sea. (In, Ricci C.A. (Editor), *The Antarctic Region; Geological Evolution and Processes; Proceedings of the VII International Symposium on Antarctic Earth Sciences*. Siena (Italy), pp. 781-790).
- Dieckmann, G.S. Lange, M.A. Ackley, S.F., and Jennings, J.C., 1991, The nutrient status in sea ice of the Weddell Sea during winter: effects of sea ice texture and algae. *Polar Biology*, 11, 449-456.
- Dingle, R.V., McArthur, J.M., and Vroon, P., 1997, Oligocene and Pliocene interglacial events in the Antarctic Peninsula dated using strontium isotope stratigraphy. *Journal of the Geological Society of London*, 154, 257-264.
- Dmitriyenko, O.B., 1989, Some general features of the distribution of calcareous nannoplankton in the upper Quaternary sediments of the oceans. *Oceanology*, 29(2), 190-195.
- Doake, C.S.M. and Vaughan, D.G., 1991, Rapid disintegration of the Wordie Ice Shelf in response to atmospheric warming. *Nature*, 350, 328.
- Domack, E.W. and Molnia, B.F., 1983, Facies of late Pleistocene glacial-marine sediments on Whidbey Island, Washington; an isostatic glacial-marine sequence, *Glacial-marine Sedimentation*. Plenum Press, New York, pp. 535-570.

- Domack, E.W., 1988, Biogenic facies in the Antarctic glacimarine environment: basis for a polar glaciomarine summary. *Palaeogeography, Palaeoclimatology, Palaeoecology*, 63, 357-372.
- Domack, E.W. and Domack, C.R., 1991, *Cenozoic Glaciation; the Marine Record Established by Ocean Drilling*. JOI/USSAC, Washington, DC, 49 p.
- Domack, E.W., Jull, A.J.T., and Nakao, S., 1991, Advance of East Antarctic outlet glaciers during the Hypsithermal: Implications for the volume state of the Antarctic ice sheet under global warming. *Geology*, 19, 1059-1062.
- Domack, E.W., 1993, Stratigraphy and paleoclimatic analysis of deep water Antarctic glacial marine sediments. (In, Bryan J.R. (Editor), *Workshop on Antarctic Glacial Marine and Biogenic Sedimentation. Notes for a Short Course, Part 1, Glacial Marine Sedimentation*. Sedimentary Research Laboratory, Tallahassee, 57, pp.89-104).
- Domack, E.W. and Harris, P.T., 1998, A new depositional model for ice shelves, based upon sediment cores from the Ross Sea and Mac. Robertson shelf, Antarctica. *Journal of Glaciology*, 27, 281-284.
- Domack, E., O'Brien, P., Harris, P., Taylor, F., Quilty, P.G., De Santis, L., and Raker, B., 1998, Late Quaternary sediment facies in Prydz Bay, East Antarctica and their relationship to glacial advance onto the continental shelf. *Antarctic Science*, 10(3), 234-244.
- Dowsett, H.J. and Cronin, T.M., 1990, High eustatic sea level during the middle Pliocene: evidence from the southeastern U.S. Atlantic Coastal Plain. *Geology*, 18, 435-438.
- Dreimanis, A., 1988, Till: their genetic terminology and classification. (In, Goldthwait, R.P. and Matsch, C.L. (Editors), *Genetic Classification of Glacigenic Deposits*. A.A. Balkema, Rotterdam, pp. 17-83).
- Drewry, D., 1975, Initiation and growth of the East Antarctic ice sheet. *Journal of the Geological Society of London*, 131(3), 255-273.
- Drewry, D.J., 1981, Record of Late Cenozoic glacial events in East Antarctica (60°-171°E). (In, Hambrey, M.J. and Harland, W.B. (Editors), *Earth's Pre-Pleistocene Glacial Record*. Cambridge University Press, Cambridge, pp. 212-216.
- Drewry, D.J., Jordan, S.R. and Jankowski, E., 1982, Measured properties of the Antarctic Ice Sheet: surface configuration, ice thickness, volume and bedrock characteristics, *Annals of Glaciology*, 3, p. 83-91.
- Drewry, D., 1983, *Antarctica: Glaciological and Geophysical Folio*. Cambridge University Press, Cambridge.

- Drewry, D., 1986, *Glacial Geologic Processes*. Edward Arnold, London, 276 p.
- Drum, R.W., 1969, Light and electron microscope observations on the tube-dwelling diatom *Amphipleura rutilans* (Trentopohl) Cleveland. *Journal of Phycology*, 5, 21-26.
- Dunbar, R.B., Leventer, A.R. and Stockton, W.L., 1989, Biogenic sedimentation in McMurdo Sound, Antarctica. *Marine Geology*, 85, 155-179.
- Dunbar, R.B., Mucciarone, D.A. and Leventer, A., 1991, Sediment-trap experiments in the central and western Ross Sea, January and February 1990. *Antarctic Journal of the United States*, 26(5), 115-117.
- Edwards, M., 1986, Glacial Environments. (In, Reading, H.G., (Editor), *Sedimentary Environments and Facies*. Blackwell Scientific Publishers, London, pp. 445-470).
- Ehrmann, W.E., Grobe, H., and Fütterer, 1992, Late Miocene to Holocene glacial history of the East Antarctica revealed by sediments from Sites 745 and 746. *Proceedings of the Ocean Drilling Program, Scientific Results*, 119, 239-289.
- El-Sayed, S.Z., 1971, Observations of a phytoplankton bloom in the Weddell Sea. *Antarctic Research Series*, 17, 301-312.
- Elverhøi, A., 1984, Glacigenic and associated marine sediments in the Weddell Sea, fjords of Spitsbergen and the Barents Sea: a review. *Marine Geology*, 57, 53-88.
- Fahnestock, M., 1996, An ice shelf breakup. *Science*, 271, 775-776.
- Faure, G. and Harwood, D.M., 1990, Marine microfossils in till clasts of the Elephant Moraine on the east Antarctic ice sheet. *Antarctic Journal of the United States*, 25(5), 23-25.
- Fenner J., Schrader H.J. and Weinigk H., 1976, Diatom phytoplankton studies in the southern Pacific Ocean, composition and correlation to the Antarctic convergence and it's paleoecological significance. *Initial Reports of the Deep Sea Drilling Project*, 35, 757-814.
- Fenner, J., 1984, Eocene-Oligocene planktic diatom stratigraphy in the low latitudes and the high southern latitudes. *Micropaleontology*, 30, 319-342.
- Fenner, J.M., 1991, Late Pliocene-Quaternary quantitative diatom stratigraphy in the Atlantic sector of the Southern Ocean. *Proceedings of the Ocean Drilling Program, Scientific Results*, 114, 97-121.
- Field, J., Clark, K. and Warrick, R., 1982, A practical strategy for analysing multispecies distribution patterns. *Marine Ecology Progress Series*, 8, 37-52.
- Fielding, C.R. and Webb, J.A., 1995, Sedimentology of the Permian Radok Conglomerate in the Beaver Lake area of Mac.Robertson Land, East Antarctica. *Geological Magazine*, 132(1), 51-63.



- Fitzsimons, S., 1990, Ice-marginal depositional processes in a polar maritime environment, Vestfold Hills, Antarctica. *Journal of Glaciology*, 36(124), 279-286.
- Fleming, R.F. and Barron, J.A., 1994, Evidence of Pliocene *Nothofagus* in Antarctica from DSDP/ODP Cores. *Pliocene High-Latitude Climate Records*. USGS Workshop Abstracts, Herndon, Virginia, July 25-27, U.S. Geological Survey, p. 13.
- Fleming, R.F. and Barron, J.A., 1996, Evidence of Pliocene *Nothofagus* in Antarctica from Pliocene marine sedimentary deposits (DSDP Site 274). *Marine Micropaleontology*, 27, 227-236.
- Flower, B.P. and Kennett, J.P., 1994, The middle Miocene climatic transition: East Antarctic ice sheet development, deep ocean circulation and global carbon cycling. *Palaeogeography, Palaeoclimatology, Palaeoecology*, 108(3/4), 537-555.
- Fordyce, R.E. and Quilty, P.G., 1994, Pliocene whales and dolphins (Cetacea) from the Vestfold Hills, Antarctica (abstract). *Records of the South Australian Museum*, 27(2), 219.
- Foster, T.D., Foldvik, A., and Middleton, J.H., 1987, Mixing and bottom water formation in the shelf break region of the southern Weddell Sea. *Deep Sea Research*, 34, 1771-1794.
- Foster, T.D., 1995, Abyssal water mass formation off the eastern Wilkes Land coast of Antarctica/ *Deep Sea Research*, 42(4), 501-522.
- Frakes, L.A. and Crowell, J.C., 1975, Characteristics of modern glacial marine sediments: application to Gondwana glacials. (In, Campbell, K.S.W., (Editor), *Gondwana Geology*. Australian National University Press, Canberra, pp. 373-376).
- Franklin, D., 1997, *The Sedimentology of Holocene Prydz Bay: Sedimentary Patterns and Processes*. Ph.D. Thesis, University of Tasmania, 259 p.
- Froelich, P.N., Malone, P.N., Hodell, D.A., Ciesielski, P.F., Warnke, D.A., Westall, F., Hailwood, E.A., Nobes, D.C., Fenner, J., Mienert, J., Mwenifumbo, C.J., and Müller, D.W., 1991, Biogenic opal and carbonate accumulation rates in the Sub-Antarctic South Atlantic: the Late Neogene of Meteor Rise Site, 704. *Proceedings of the Ocean Drilling Program, Scientific Results*, 114, 515-550.
- Fryxell, G.A. and Hasle, G.R., 1979, The genus *Thalassiosira* (Algae): species with internal extensions of the strutted processes. *Phycologia*, 18(4), 378-393.
- Fryxell, G.A., Kang, S. and Reap, M., 1987, AMERIEZ 1986: phytoplankton at the Weddell Sea ice edge. *Antarctic Journal of the United States*, 22, 173-175.

- Fryxell, G.A. and Kendrick, G.A., 1988, Austral spring microalgae across the Weddell Sea ice edge: spatial relationships found along a northward transect during AMERIEZ 83. *Deep Sea Research*, 35(1A), 1-20.
- Fryxell, G.A., 1989, Marine phytoplankton at the Weddell Sea ice edge: seasonal changes at the specific level. *Polar Biology*, 10, 1-18.
- Fryxell, G.A. and Prasad, A.K.S.K., 1990, *Eucampia antarctica* var. *recta* (Mangin) stat. nov. (Biddulphiaceae, Bacillariophyceae): life stages at the Weddell Sea ice edge. *Phycologia*, 29(1), 27-38.
- Fryxell, G.A., 1991, Comparison of winter and summer growth stages of the diatom *Eucampia antarctica* from the Kerguelen Plateau and south of the Antarctic Convergence Zone. *Proceedings of the Ocean Drilling Program, Scientific Results*, 19, 675-685.
- Fryxell, G.A., 1994, Planktonic marine diatom winter stages: Antarctic alternatives to resting spores. *Memoirs of the California Academy of Science*, 17, 437-448.
- Garrison, , D.L., Buck, K.R., and Silver, M.W., 1982, Ice algal communities in the Weddell Sea. *Antarctic Journal of the United States*, 17, 157-159.
- Garrison, , D.L., Buck, K.R. and Silver, M.W., 1983, Studies of ice-algal communities in the Weddell Sea. *Antarctic Journal of the United States*, 18, 179-181.
- Garrison, D.L. and Buck, K.R., 1985, Sea-ice algal communities in the Weddell Sea: species composition in ice and plankton assemblages. (In, Gray, J.S. and Christiansen, M.E. (Editors), *Marine Biology of Polar Regions and Effects of Stress on Marine Organisms*, John Wiley and Sons, New York, pp. 103-122).
- Garrison, D.L., Buck, K.R., and Fryxell, G.A., 1987, Algal assemblages in Antarctic pack ice and ice-edge plankton. *Journal of Phycology*, 23, 564-572.
- Garrison, D.L. and Buck, K.R., 1989, The biota of Antarctic pack ice in the Weddell Sea and Antarctic Peninsula regions. *Polar Biology*, 10, 211-219.
- Garrison, D.L., 1991, Antarctic sea ice biota. *American Zoologist*, 31, 17-33.
- Garrison, D.L., Buck, K.R., and Gowing, M.M., 1993, Winter plankton assemblages in the ice edge zone of the Weddell and Scotia Seas: composition, biomass and spatial distributions *Deep Sea Research*, 40(2), 311-338.
- Garrison, D.L. and Close, A.R., 1993, Winter ecology of the sea ice biota in Weddell Sea pack ice. *Marine Ecology Progress Series*, 96, 17-31.
- Gaudichet, A. , Petit, J.R., Lefevre, R., and Lorius, C., 1986, An investigation by analytical transmission electron microscopy of individual insoluble microparticles from Antarctic (Dome C) ice core samples. *Tellus*, 38(B), 250-261.

- Gaudichet, A., De Angelis, M., Lefevre, R., Petit, J.R., Korotkevitch, Y.S., and Petrov, V.N., 1988, Mineralogy of insoluble particles in the Vostok Antarctic ice core over the last climatic cycle (150 kyr). *Geophysical Research Letters*, 15(13), 1471-1474.
- Gersonde, R. and Wefer, G., 1987, Sedimentation of biogenic siliceous particles in Antarctic waters from the Atlantic sector. *Marine Micropaleontology*, 11, 311-322.
- Gersonde, R., 1990, Taxonomy and morphostructure of Neogene diatoms from the Southern Ocean, ODP Leg 113. *Proceedings of the Ocean Drilling Program, Scientific Results*, 113, 791-802.
- Gersonde, R., Abelmann, A., Burckle, L.H., Hamilton, N., Lazarus, D., McCartney, K., O'Brien, P., Spieß, V., and Wise, S.W., Jr., 1990, Biostratigraphic synthesis of Neogene siliceous microfossils from the Antarctic Ocean, ODP Leg 113 (Weddell Sea). *Proceedings of the Ocean Drilling Program, Scientific Results* 113, 915-936.
- Gersonde, R. and Burckle, L.H., 1990, Neogene diatom biostratigraphy of ODP Leg 113, Weddell Sea (Antarctic Ocean). *Proceedings of the Ocean Drilling Program, Scientific Results*, 113, 761-789.
- Gersonde, R., 1991, Taxonomy and morphostructure of Late Neogene diatoms from Maud Rise (Antarctic Ocean). *Polarforschung*, 59(3), 141-171.
- Gersonde, R., Kyte, F.T., Bleil, U., Diekmann, B., Flores, J.A., Gohl, K., Grahl, G., Hagen, R., Kuhn, G., Sierro, F.J., Völker, D., Abelmann, A., Bostwick, J.A., 1997, Geological record and reconstruction of the late Pliocene impact of the Eltanin asteroid in the Southern Ocean. *Nature*, 27, 357-363.
- Gersonde, R. and Bárcena, M.A., 1998, Revision of the upper Pliocene-Pleistocene diatom biostratigraphy for the northern belt of the Southern Ocean. *Micropaleontology*, 44(1), 84-98.
- Gibson, J.A., 1998, Carbon flow through inshore marine environments of the Vestfold Hills, East Antarctica, *ANARE Reports*, 139, 221 p.
- Giovietto, M.B. and Bentley, C.R., 1985, Surface balance in ice drainage systems of Antarctica. *Antarctic Journal of the U.S.*, 20(4), 6-13.
- Gloersen, P., Campell, W.J., Cavalieri, D.J., Comiso, J.C., Parkinson, C.L. and Zwally, H.J., 1992, *Arctic and Antarctic Sea Ice, 19878-1987: Satellite Passive-Microwave Observations and Analysis*. NASA Special Publication (511), Washington D.C., 290 p.
- Gombos, A.M., 1976, Paleogene and Neogene diatoms from the Falkland Plateau and Malvinas Outer Basin: Leg 36 Deep Sea Drilling Project. *Initial Reports of Deep Sea Drilling Project*, 36, 575-687.

- Gombos, A.M., 1977, Paleogene and Neogene diatoms from the Falkland Plateau and Malvinas outer basin, Leg 36, Deep Sea Drilling Project, *Initial Reports of Deep Sea Drilling Project*, 36, 575-687.
- Gombos, A.M. and Ciesielski, P.F., 1983, Late Eocene to early Miocene diatoms from the southwestern Atlantic. *Initial Reports of Deep Sea Drilling Project*, 90(2), 583-634.
- Goodell, H.G., 1973, Marine sediments of the Southern Ocean. *Antarctic Map Folio Series*, 17, 1-9.
- Gordon, A.L., 1971, Oceanography of Antarctic waters. *Antarctic Research Series*, 15, 169-203.
- Gordon, A.L. and Tchernia, P., 1972, Waters of the continental margin off Adélie Coast, Antarctica. (In, Hayes, D.E. (Editor), *Antarctic Oceanography II: The Australian-New Zealand Sector*, American Geophysical Union, Washington D.C., pp. 59-69.
- Gordon, A.L. and Molinelli, E.J., 1982, Thermohaline and chemical distributions and the atlas data set. (In, Gordon, A.L., Molinelli, E.J., and Baker, T.N. (Editors), *Southern Ocean Atlas*. A.A. Balkema, Rotterdam, 34 p).
- Gordon, A.L., 1988, Spatial and temporal variability within the Southern Ocean. (In, Sahrhage, D. (Editor), *Antarctic Ocean and resources variability: Scientific Seminar on Antarctic Ocean Variability and its Influence on Marine Living Resources, Particularly Krill*, Springer-Verlag, Berlin, pp. 41-56).
- Gordon, A.L. and Comiso, J.C. (1988) Polynyas in the Southern Ocean. *Scientific American*, 258, 70-77.
- Gow, A.J., Epstein, S., and Sheehy, W., 1979, On the origin of stratified debris in ice cores from the bottom of the Antarctic ice sheet. *Journal of Glaciology*, 23(89), 185-192.
- Gow, A.J. and Tucker III, W.B., 1990, Sea Ice in the Polar Regions. (In, Smith, W.O., Jr., (Editor), *Polar Oceanography, Part A Physical Science*. Academic Press Inc., San Diego, pp. 47-122).
- Grobe, H., and Mackenson, A., 1992, Late Quaternary climatic cycles as recorded in sediments from the antarctic continental margin *Antarctic Research Series*, 56, 349-376.
- Grousset, F.E., Biscaye, P.E., Revel, M., Petit, J-R, Pye, K., Joussaume, S., and Jouzel, J., 1992, Antarctic (Dome C) ice-core dust at 18 k.y. B.P. Isotopic constraints on origins. *Earth and Planetary Science Letters*, 111, 175-182.

- Hambrey, M.J., Erhmann, W.U., and Larsen, B., 1991, The Cenozoic glacial record from the Prydz Bay continental shelf, East Antarctica. *Proceedings of the Ocean Drilling Program, Scientific Results*, 119, 77-132.
- Hambrey, M.J., Barrett, P.J., Ehrmann, W.U., and Larsen, B., 1992, Cenozoic sedimentary processes on the Antarctic continental margin and the record from deep drilling. *Zeitschrift für Geomorphologie*, 86, 77-103.
- Hambrey, M.J. and Barrett, P.J., 1993, Cenozoic sedimentary and climatic record, Ross Sea region, Antarctica. *Antarctic Research Series*, 60, 91-124.
- Hambrey, M.J., 1994, *Glacial Environments*. University of British Columbia Press, Vancouver, 296 p.
- Hambrey, M.J., Ehrman, W.U., and Larsen, B., 1994, The Cenozoic Sedimentary Record of the Prydz Bay Continental Shelf, East Antarctica. *Terra Antarctica*, 1(2), 399-402.
- Hambrey, M.J. and McKelvey, B.C., 1995, Neogene Glacigenic Facies and Environments in the Northern Prince Charles Mountains, East Antarctica. (In, Ricci C.A. (Editor), *The Antarctic Region; Geological Evolution and Processes; Proceedings of the VII International Symposium on Antarctic Earth Sciences*. Siena (Italy), p. 179.
- Hambrey, M.J. and McKelvey, B.C., in press, Neogene fjordal sedimentation on the western margin of the Lambert Graben, East Antarctica. *Sedimentology*.
- Haq, B.U., Hardenbol, J., Vail, P.R., 1987, Chronology of fluctuating sea levels since the Triassic. *Science*, 235, 1156-1167.
- Hargraves, P.E. and French, F., 1983, Diatom resting spores: significance and strategies. (In, Fryxell, G.A. (Editor), *Survival strategies of the algae*, Cambridge University Press, Cambridge, pp. 49-68).
- Harper, M.A. and Harwood, D.M., 1992, Ancient fresh water diatoms in Antarctica. *Abstract, New Zealand Limnological Society Newsletter*, 18, 26.
- Harris, G.P., 1986, *Phytoplankton Ecology Structure, Function and Fluctuation*. Chapman and Hall, London.
- Harris, P.T., O'Brien, P.E., Quilty, P.G., Taylor, F., Domack, E., De Santis, L., and Raker, B., 1997, *Post Cruise Report, Antarctic CRC Marine Geoscience: Vincennes Bay, Prydz Bay and Mac. Robertson Shelf: AGSO Cruise 186, ANARE Voyage 5, 1996/97 (BRAD)*. AGSO Record 1997/51, 75p.
- Harris, P.T., Taylor, F., Pushina, Z., Leitchenkov, G., O'Brien, P.E., Smirnov, V., and Masotov, V.N., 1998, Lithofacies distribution in relation to the geomorphic provinces of Prydz Bay, East Antarctica. *Antarctic Science*, 10(3), 227-235.

- Hart, C.P. and McKelvey, B.C., 1991, Tertiary marine molluscs from the Pagodroma Tillite, Prince Charles Mountains, East Antarctica. *6<sup>th</sup> International Symposium on Antarctic Earth Sciences*. Cambridge University Press, Cambridge, vol. 6, p. 219
- Hart, C.P., 1994, Amino acid analysis of Antarctic Pliocene macrofossils; chronology, correlation, taxonomy. *Geological Society of America, Abstracts*, 26(7), 143.
- Harwood, D.M., 1983, Diatoms from the Sirius Formation, Transantarctic Mountains. *Antarctic Journal of the United States*, 18(5), 98-100.
- Harwood, D.M., 1985, Late Neogene climatic fluctuations in the southern high latitudes of a warm Pliocene and deglaciated Antarctic continent. *South African Journal of Science*, 81, 239-241.
- Harwood, D.M., 1986a, *Diatom Biostratigraphy and Paleoecology With a Cenozoic History of Antarctic Ice Sheets*. Ph.D. Dissertation, Ohio State University, 592 p.
- Harwood, D.M. 1986b, Diatoms. (In, Barrett, P.J. (Editor), *Antarctic Cenozoic History from the MSSTS-1 Drillhole, McMurdo Sound*. New Zealand Department of Scientific and Industrial Research Bulletin, 237, pp. 69-109).
- Harwood, D.M., 1989, Siliceous microfossils. (In, Barrett, P.J. (Editor), *Antarctic Cenozoic History from the MSSTS-1 Drillhole, McMurdo Sound*. New Zealand Department of Scientific and Industrial Research Bulletin, 245, pp. 67-97).
- Harwood, D.M., Scherer, R.P., and Webb, P.N., 1989, Multiple Miocene marine productivity events in West Antarctica as recorded in Upper Miocene sediments beneath the Ross Ice Shelf (Site J-9). *Marine Micropaleontology*, 15, 91-115.
- Harwood, D.M., 1991, Cenozoic diatom biogeography in the southern high latitudes: inferred biogeographic barriers and progressive endemism. (In, Thomson, M.R.A. *et al.* (Editors), *Geological Evolution of Antarctica*. Cambridge University Press, Cambridge, pp. 667-672).
- Harwood, D.M., Webb, P.N., Barrett, P.J., and McKelvey, B.C., 1991, The changing style of Cenozoic Antarctic glaciations. *6<sup>th</sup> International Symposium on Antarctic Earth Sciences*. Tokyo (Japan), p. 220.
- Harwood, D.M. and Maruyama, T., 1992, Middle Eocene to Pleistocene diatom biostratigraphy of Southern Ocean Sediments from the Kerguelen Plateau. *Proceedings of the Ocean Drilling Program, Scientific Results*, 120, 683-733.
- Harwood, D.M., Webb, P.N., and Barrett, P.J., 1992, The search for consistency between several indices of Antarctic Cenozoic glaciation. *Cenozoic Glaciations and Deglaciations, Abstracts*. Burlington House, London, pp. 61-63.

- Harwood, D.M., Srivastav, A., and Winter, D.M., 1994, Sea-ice absence and 3°C seas – is this all it takes? *Pliocene High-Latitude Climate Records*. Abstracts from USGS Workshop, U.S. Geological Survey, p. 15.
- Harwood, D.M. and Rose, S.A., 1998, Report on diatom analysis of Mount Feather COMRAC Cores. (In, Wilson, G. and Barron, J. (Editors), *Mount Feather Sirius Group Core Workshop and Collaborative Sample Analysis*. Byrd Polar Research Center Report, Ohio State University, vol. 14, pp. 79- 89).
- Harwood, D.M. and Webb, P.N., 1998, Glacial Transport of Diatoms in the Antarctic Sirius Group: Pliocene Refrigerator. *GSA Today*, 8(4), 1-8.
- Harwood, D.M., Spaulding, S.A., and McMinn, A., 1999. Fossil marine diatom distribution in modern surface sediments, lakes and fiords: aeolian transport pitfalls, potential and remaining questions. *8<sup>th</sup> International Symposium on Antarctic Earth Sciences*, Wellington (New Zealand), p. 138.
- Harwood D.M. and Bohaty, S.M., in press, Marine Diatom Assemblages from Eocene and Younger Erratics, McMurdo Sound, Antarctica. (In, Stilwell, J.D. and Feldmann, R.M. (Editors), *Paleobiology and Paleoenvironments of Eocene fossiliferous Erratics, McMurdo Sound, East Antarctica*. American Geophysical Union, Antarctic Research
- Harwood, D.M., McMinn, A., and Quilty, P., in press, Diatom biostratigraphy of the Pliocene Sørødal Formation, Vestfold Hills, East Antarctica. *Antarctic Science*.
- Hasegawa, H., Iwata, S. and Matsuoka, N., 1992, Observation of clayey till and underlying glacier ice in the central Sør Rondane Mountains, East Antarctica. (In, Yoshida *et al.* (Editors), *Recent Progress in Antarctic Earth Science*. Terra Scientific Publishing Co., Tokyo, pp. 679-681).
- Hasle, G.R. and Heimdal, B.R., 1968, Morphology and distribution of the marine centric diatom *Thalassiosira antarctica* Comber. *Journal of the Royal Microscopy Society*, 88, 357-369.
- Hasle, G.R. and Syvertsen, E.E., 1985, An Arctic ice-diatom assemblage. *2<sup>n</sup> International Phycological Congress Book of Abstracts*, Copenhagen, p. 62.
- Hasle, G.R. and Semina, H.J., 1987, The marine planktonic diatoms *Thalassiothrix longissima* and *Thalassiothrix antarctica* with comments on *Thalassionema* spp. and *Synedra reinboldii*. *Diatom Research*, 2(2), 175-192
- Hasle G.R, Sims P.A. and Syvertsen E.E., 1988, Two Recent *Stellarima* Species: *S. microtrias* and *S. stellaris* (Bacillariophyceae). *Botanica Marina*, 31, 195-206.
- Hays, J. D., 1967, Quaternary sediments of the Antarctic Ocean. *Progress in Oceanography*, 4, 117-131.

- Hays, J.D., Lozano, J.A., Shackleton, N. and Irving, G., 1976, Reconstruction of the Atlantic and western Indian Ocean sectors of the 18,000 B.P. Antarctic Ocean. *Geological Society of America Memoir*, 145, 337-372.
- Heath, G, 1974, Dissolved silica and deep-sea sediments. *Studies in Paleooceanography, Special Publication No. 20. Society of Economic Paleontologists and Mineralogists*, pp. 77-93).
- Heidelberg, D.B., Manchester, I.D., Paris, F.J., Tempe, M.M., and Bern, B.M., 1991, *Ice Composition and Glacier Dynamics. Springer Series in Physical Environment*, 8. Springer Verlag, Berlin, 207 p.
- Hill, R.S. and Truswell, E.M., 1993, *Nothofagus* fossils in the Sirius Group, Transantarctic Mountains: leaves and pollen and their climatic implications. *Antarctic Research Series*, 60, 67-73.
- Hill, R.S., Harwood, D.M., and Webb, P.N., 1996, *Nothofagus beardmorensis* (Nothofagaceae), a new species based on leaves from the Pliocene Sirius Group, Transantarctic Mountains, Antarctica, *Review of Palaeobotany and Palynology*, 94, 11-24.
- Hirano, M, 1965, Freshwater algae in the Antarctic region. (In, van Mighem, J., van Oye, P. and Schell, J. (Editors), *Biogeography and Ecology in Antarctica. Monographiae Biologicae*, 15, 127-193).
- Hodell, D.A. and Ciesielski, P.F., 1990, Southern Ocean response to the intensification of northern hemisphere glaciation at 2.4 Ma. (In, Bleil, U. and Theide, J. (Editors), *Geological History of the Polar Oceans: Arctic Versus Antarctic*. Kluwer Academic Publishers, Netherlands, pp. 707-728).
- Hodell, D.A. and Warnke, D.A, 1991, Climatic evolution of the Southern Ocean during the Pliocene epoch from 4.8 to 2.6 million years ago. *Quaternary Science Reviews*, 10, 205-214.
- Hodell, D.A. and Venz, K., 1992, Towards a high-resolution stable isotopic record of the southern ocean during the Plio-Pleistocene (4.8 to 0.8 Ma). *Antarctic Research Series*, 56, 265-310.
- Holmlund, P. and Näslund, J., 1994, The glacially sculptured landscape in Dronning Maud Land, Antarctica, formed by wet-based mountain glaciation and not by the present ice sheet. *Boreas*, 23, 139-148.
- Honjo, S., Manganini, S., and Poppe, L., 1982, Sedimentation of lithogenic particles in the deep ocean. *Marine Geology*, 50, 199-220.



- Honjo, S., 1990, Particle fluxes and modern sedimentation in the polar oceans. (In, W.O. Smith (Editor), *Polar Oceanography. Part B: Chemistry, Biology, and Geology*. Academic Press, San Diego, pp.687-739).
- Hooke, R.LeB., 1998, *Principles of Glacier Mechanics*. Prentice Hall, New Jersey, 248 p.
- Hopkins, J.T., 1966, Diatom locomotion: An explanation. *Protoplasma*, 62, 1-33.
- Hoshiai, T., 1977, Seasonal change of ice communities in the sea ice near Syowa Station, Antarctica. (In, Dunbar, M.J. (Editor), *Polar Oceans*. Arctic Institute of North America, Calgary, pp. 307-317).
- Hosie, G.W., 1994, Multivariate analyses of the macrozooplankton communities and euphausiid larval ecology in the Prydz Bay region, Antarctica. *ANARE Reports*, 137, 209 p.
- Horner, R. 1985, *Sea Ice Biota*, CRC Press, Boca Ranton, pp. 83-103.
- Horner, R.A., Syvertsen, E.E., Thomas, D.P. and Lange, C., 1988, Proposed terminology and reporting units for sea-ice algal assemblages. *Polar Biology*, 8, 249-253.
- Horner, R., 1990, Ice-associated ecosystems. (In, Medlin, L.K. and Priddle, J. (Editors), *Polar Marine Diatoms*. British Antarctic Survey, Cambridge, pp. 9-34).
- Howard, W.R. and Prell, W.L., 1994, Late Quaternary CaCO<sub>3</sub> production and preservation in the Southern Ocean: Implications for oceanic and atmospheric carbon cycling. *Paleoceanography*, 9(3), 453-482.
- Hsiao, S.I.C., 1980), Quantitative composition, distribution, community structure and standing stock of sea ice microalgae in the Canadian Arctic. *Arctic*, 33, 768-793.
- Humlum, O., 1982, Rock glacier types on Disko, central west Greenland. *Norsk Geografisk Tidsskrift*, 82, 59-66.
- Humphreys, K.A., and Fitzsimons, S.J., 1996, Landforms and sediments associations of dry-based glaciers in arid polar environments. *Zeitschrift fur Geomorphologie. Supplementband*, 105, 21-33.
- Humphries, C.J., 1981, Biogeographical methods and the southern beeches. (In, Forey, P.L. (Editor), *The Evolving Biosphere*. Cambridge University Press, Cambridge, pp. 283-297).
- Hurd, D., 1972, Factors affecting solution rate of biogenic opal in seawater. *Earth and Planetary Science Letters*, 15, 411-417.
- Huybrechts, P., 1990, 3-D model for the Antarctic ice sheet: a sensitivity study on the glacial-interglacial contrast *Climate dynamics*, 5(2), 79-92.

- Huybrechts, P. and Oerlemans, J., 1990, Response of the Antarctic ice sheet to future greenhouse warming. *Climate Dynamics*, 5, 93-102.
- Huybrechts, P., 1992, Antarctic ice sheet and environmental change: a three dimensional modeling study. *Berichte zur Polarforschung*, 99, 223-241.
- Huybrechts, P., 1993, Glaciological modeling of the Late Cenozoic East Antarctic ice sheet: stability or dynamism? *Geografiska Annaler*, 75A, 221-238.
- Imbrie, J. and Kipp, N. G., 1971, A new micropalaeontological method for quantitative palaeoclimatology: application to a late Pleistocene Caribbean core. (In, Turekian, K. (Editor), *Late Cenozoic Glacial Ages*. Yale University Press, New Haven, pp. 71-181).
- IPCC (Intergovernmental Panel on Climate Change), 1990, *Climate Change. The IPCC Scientific Assessment*. Cambridge University Press, Cambridge, 364 p.
- Jacka, T.H., 1983, Computer data base for Antarctic sea ice extent. *ANARE Research Notes*, 13, 54 p.
- Jacobs, S.S., Amos, A.F., and Bruchhausen, P.M., 1970, Ross Sea oceanography and Antarctic Bottom Water formation, *Deep Sea Research*, 17, 935-962.
- Jacobs, S.S., Fairbanks, R.G., and Horibe, Y., 1985, Origin and evolution of water masses near the Antarctic continental margin; evidence from H (sub 2) (super 18) O/H (sub 2) (super 16) O ratios in seawater. *Antarctic Research Series*, 43, 59-85.
- Jacques, G. and Fukushi, M., 1994, Phytoplankton of the Indian Antarctic Ocean. (In, El-Sayed, S.Z. (Editor), *Southern Ocean Ecology: the BIOMASS Perspective*. Cambridge University Press, Cambridge, pp. 63-78).
- Jefferies, M.O. and Weeks, W.F., 1992, Structural characteristics and development of sea-ice in the western Ross Sea, *Antarctic Science*, 5(1), 63-75.
- Jefferies, M.O. and Adolphs, U., 1997, Early winter snow and ice thickness distribution, ice structure and development of western Ross Sea pack ice between the ice edge and the Ross ice shelf. *Antarctic Science*, 9(2), 188-200.
- Jendrzewski, J.P. and Zarillo, G.A., 1972, Late Pleistocene paleotemperature oscillations defined by silicoflagellate changes in a subantarctic deep-sea core, *Deep Sea Research*, 19, 327-329.
- Johansen, J.R. and Fryxell, G.A., 1985, The genus *Thalassiosira* (Bacillariophyceae): studies on species occurring south of the Antarctic Convergence Zone. *Phycologia*, 24(2), 155-179.
- Jorgensen, E.G., 1955, Solubility of silica in diatoms. *Physiology Plantarum*, 8, 846-851.

- Jousé, A., Kozlova, O. and Muhina, V., 1971, Distribution of diatoms in the surface layer of sediment from the Pacific Ocean. (In, Funnell, B.M. and Riedel, W.R. (Editors), *The Micropalaeontology of Oceans*. Cambridge University Press, Cambridge, pp. 263-269).
- Jouzel, R., Raisbeck, G., Benoist, J.P., Yiou, F., Lorius, C., Raynard, D., Petit, J.R., Barkov, N.I., Korotkevich, Y.S., and Kotlyakov, V.M., 1989, A comparison of deep Antarctic ice core and their implication for climate change between 65,000 and 15,000 years ago. *Quaternary Research*, 31, 135-150.
- Kaczmarska, I., Barbrick, N.E., Ehrman, J.M., and Cant, G.P., 1993, *Eucampia* index as an indicator of the Late Pleistocene oscillations of the winter sea-ice extent at the Leg 119 Site 745B at the Kerguelen Plateau. *Hydrobiologia*, 269/270, 103-112.
- Kamatani, A. and Riley, J., 1979, Rate of dissolution of diatom silica walls in seawater. *Marine Biology*, 55, 29-53.
- Kang, S.-H. and Fryxell, G.A., 1993, Phytoplankton in the Weddell Sea, Antarctica: composition, abundance and distribution in water-column assemblages of the marginal ice-edge zone during austral autumn. *Marine Biology*, 116, 335-348.
- Kellogg, D.E. and Kellogg, T.B., 1984, Diatoms from the McMurdo Ice Shelf, Antarctica. *Antarctic Journal of the United States*, 19(5), 76-77.
- Kellogg, D.E. and Kellogg, T.B., 1986, Diatom biostratigraphy of sediment cores beneath the Ross Ice Shelf. *Micropaleontology*, 3, 301-345.
- Kellogg, D.E. and Kellogg, T.B., 1987, Diatoms of the McMurdo Ice Shelf, Antarctica: implications for sediment and biotic reworking. *Palaeogeography, Palaeoclimatology, Palaeoecology*, 60, 77-96.
- Kellogg, T.B. and Kellogg, D.E., 1988, Antarctic cryogenic sediments: biotics and inorganic facies of ice shelf and marine-based ice sheet environments. *Palaeogeography, Palaeoclimatology, Palaeoecology*, 67, 51-74.
- Kellogg, D.E. and Kellogg, T.B., 1996, Diatoms in South Pole ice: implications for aeolian contamination of Sirius Group deposits. *Geology*, 24, 115-118.
- Kennett, J.P., 1977, Cenozoic Evolution of Antarctic Glaciation, the Circum-Antarctic Ocean, and Their Impact on Global Paleooceanography. *Journal of Geophysical Research*, 82(27), 3843-3860.
- Kennett, J.P., 1978a, Cenozoic Planktonic Biogeographic Evolution in the Southern Ocean. (In, *Proceedings of the International Symposium on Marine Biogeography and Evolution in the Southern Hemisphere (Volume 1)*, New Zealand DSIR Information Series, 137, pp. 187-201).

- Kennett, J.P. 1978b, The Development of Planktonic Biogeography in the Southern Ocean during the Cenozoic. *Marine Micropaleontology*, 3, 301-345.
- Kennett, J.P. 1978c, Cainozoic evolution of circumantarctic palaeoceanography, (In, Van Zinderen Bakker, E.M., Rotterdam, Sr., Balkema, A.A. (Editors.), *Antarctic Glacial History and World Palaeoenvironments*. A. A. Balkema, Rotterdam, pp. 41-53).
- Kennett, J. P., 1980, Cenozoic climate history. (In, Dornsiepen U.F. and Haak, V. (Editors), *International Alfred-Wegener-Symposium*. Berliner Geowissenschaftliche Abhandlungen, Reihe A: Geologie und Palaeontologie, 19, pp.107-109).
- Kennett, J.P. and Barker, P.F., 1990, Latest Cretaceous to Cenozoic climate and oceanographic developments in the Weddell Sea, Antarctica: An ocean-drilling perspective. *Proceedings of the Ocean Drilling Program, Scientific Results*, 113, 937-962.
- Kennett, J.P. and Stott, L.D., 1990, Proteus and Proto-oceanus: ancestral Paleogene oceans as revealed from Antarctic stable isotopic results; ODP Leg 113. *Proceedings of the Ocean Drilling Program, Scientific Results*, 113, 865-878.
- Kennett, J.P. and Hodell, D.A., 1993, Evidence for relative climatic stability of Antarctica during the Early Pliocene: a marine perspective. *Geografiska Annaler*, 75A, 205-220.
- Kennett, J.P., 1995, A review of polar climatic evolution during the Neogene, based on the marine sediment record. (In, Vrba, E.S., Denton, G.H, Partridge, T.C., and Burckle, L.H. (Editors), *Paleoclimate and Evolution, with Emphasis on Human Origins*. Yale University Press, New Haven, pp. 49-64).
- Kennett, J.P. and Hodell, D.A., 1995, Stability or instability of Antarctic ice sheets during warm climates of the Pliocene? *GSA Today*, 5(1), 10-13.
- Kerr, R.A., 1981, Staggered Antarctic ice sheet formation supported. *Science*, 213, 427-428.
- Kerry, K.R., Woehler, E.J., Wright, S., and Dong, Z., 1987a, Oceanographic data: Prydz Bay region-MV Nella Dan, January-March 1981. *ANARE Research Notes*, 49, 114 p.
- Kerry, K.R., Woehler, E.J., and Robb, M.S., 1987b, Oceanographic data: Prydz Bay region-SIBEX II, MV Nella Dan, January 1985. *ANARE Research Notes*, 53, 122 p.
- Key, J.R., 1990, Ice. (In, Glasby, G.P. (Editor), *Antarctic Sector of the Pacific*. Elsevier Oceanography Series, 51, pp. 95-123).

- Knox, G.A., 1990, Primary production and consumption in McMurdo Sound, Antarctica. (In, Kerry, K.R. and Hempel, G. (Editors), *Antarctic Ecosystems: Ecological Change and Conservation*. Springer-Verlag, Berlin, pp. 115-128).
- Knox, G.A., 1994, *Studies in Polar Research, The Biology of the Southern Ocean*. Cambridge University Press, Cambridge, 444 p.
- Koizumi, I., 1973, The Late Cenozoic diatoms of sites 183-193, Leg 19 Deep Sea Drilling Project. *Initial Reports of the Deep Sea Drilling Project*, 19, 805-855.
- Koizumi, I. and Tanimura, Y., 1982, Neogene diatom biostratigraphy of the middle latitude western north Pacific, Deep Sea Drilling Project Leg 86. *Initial Reports of the Deep Sea Drilling Project*, 86, 269-300.
- Kozlova, O.G., 1966, *Diatoms in the Indian and Pacific Sectors of the Antarctic*. Israel Program for Scientific Translations, Jerusalem, 168p. (Translated from Russian).
- Kozlova, O.G. and Mukhina, V.V., 1967, Diatoms and silicoflagellates in suspension and floor sediments of the Pacific Ocean. *International Geology Review*, 9(10), 1322-1342.
- Krantz, D.E., 1991, A chronology of Pliocene sea-level fluctuations: the U.S. Middle Atlantic coastal plain record. *Quaternary Science Reviews*, 10, 163-174.
- Krebs, K.A., 1997, Mawson Escarpment alpine-type glaciers and the Lambert Glacier Grounding Zone. *Proceedings of the Antarctic Co-operative Research Centre - Antarctica and Global Change Conference*, July 13-17, 1997, Hobart, Australia.
- Krebs, K.A., 1998, *The Morphology and Dynamics of the Lower Lambert Glacier and Amery Ice Shelf System*. M.Sc. Thesis, University of Tasmania.
- Krebs, W.N., 1977, *Ecology and preservation of neritic marine diatoms, Arthur Harbour, Antarctica*. Ph.D. Dissertation, University of California, 216 p.
- Krebs, W.N., 1983, Ecology of neritic marine diatoms, Arthur Harbour, Antarctica. *Micropaleontology*, 29(3), 267-297.
- Krebs, W.N., Lipps, J.H., and Burckle, L.H., 1987, Ice diatom floras, Arthur Harbor, Antarctica. *Polar Biology*, 7, 163-171.
- Kuijpers, A., 1989, Southern Ocean circulation and global climate in the Middle Pleistocene (early Brunhes). *Palaeogeography, Palaeoclimatology, Palaeoecology*, 76(1/2), 80-83.
- Kurinin, R.G. and Aleshkova, N.D., 1987, Bedrock relief of Enderby Land, Mac.Robertson Land and Princess Elizabeth Land, East Antarctica. *Antarctic Committee Reports*, 26, 62-65.

- Laiba, A. and Pushina, Z. 1995, Glacial-Marine Deposits on the Fisher Massif, Prince Charles Mountains (East Antarctica), *VII International Symposium on Antarctic Earth Sciences*, Sienna (Italy), p. 234.
- Laiba, A. and Pushina, Z., 1997, Glacial-Marine Deposits in the Fisher Massif, Prince Charles Mountains (East Antarctica). (In, Ricci C.A. (Editor), *The Antarctic region; geological evolution and processes; proceedings of the VII international symposium on Antarctic Earth sciences*. Siena (Italy), pp. 977-984).
- Laws, R.M., 1984, *Antarctic Ecology*. Academic Press, London.
- Lawson, D.E., 1995, Sedimentary and hydrologic processes within modern terrestrial valley glaciers. (In, Menzies, J., (Editor), *Modern Glacial Environments Processes, Dynamics and Sediments*. Butterworth Heinemann Ltd., Oxford, pp. 337- 363).
- Ledbetter, M.T. and Ciesielski, P.F., 1986, Post Miocene disconformities and paleoceanography in the Atlantic sector of the Southern Ocean. *Marine Geology*, 52, 185-214.
- Lee, R.E., 1989, *Phycology*. Cambridge University Press, Cambridge, pp. 467-508.
- Leitchenkov, G., Stagg, H., Gandjukhin, V., Cooper, A.K., Tanahashi, M. and O'Brien, P., 1994, Cenozoic Seismic Stratigraphy of Prydz Bay (Antarctica). *Terra Antarctica*, 1(2), 395-397.
- LeMasurier, W.E., Harwood, D.M. and Rex, D.C., 1994, Geology of Mount Murphy Volcano: An 8-m.y. history of interaction between a rift volcano and the West Antarctic ice sheet. *GSA Bulletin*, 106, 265-280.
- Leventer, A. and Dunbar, R. B., 1987, Diatom flux in McMurdo Sound, Antarctica. *Marine Micropaleontology*, 12, 49-64.
- Leventer, A. and Dunbar, R. B., 1988, Recent diatom record of McMurdo Sound, Antarctica: Implications for history of sea-ice extent. *Paleoceanography*, 3, 259-274.
- Leventer, A., 1991, Sediment trap diatom assemblages from the northern Antarctic Peninsula region. *Deep Sea Research*, 38(8), 1127-1143.
- Leventer A., 1992, Modern distribution of diatoms in sediments from the George V Coast, Antarctica. *Marine Micropaleontology*, 19, 315-332.
- Leventer, A. and Harwood, D.M., 1993, *The Geological Use of Polar Marine Diatoms. Workshop on Antarctic Glacial Marine Biogenic Sedimentation. Notes for a Short Course. Part 2. Biogenic Sedimentation*, pp. 134-253.
- Leventer, A., Domack, E.W., Ishman, S.E., Brachfeld, S., McClennen, C.E. and Manley, P., 1996, Productivity cycles of 200-300 year in the Antarctic Peninsula

- region: Understanding linkages among the sun, atmosphere, oceans, sea ice, and biota. *GSA Bulletin*, 108, 626-1644.
- Leventer, A. and Dunbar, R. B., 1996, Factors influencing the distribution of diatoms and other algae in the Ross Sea. *Journal of Geophysical Research*, 101(C8), 18489-18500.
- Leventer, A., 1998, The fate of Antarctic "sea-ice diatoms" and their use as paleoenvironmental indicators. *Antarctic Research Series*, 73, 121-137.
- Lewin, J.C., 1957, Silicon metabolism in diatoms. IV. Growth and frustule formation in *Navicula pelliculosa*. *Canadian Journal of Microbiology*, 46, 361-367.
- Lewin, J.C., 1961, The dissolution of silica from diatom walls. *Geochimica Cosmochimica Acta*, 21, 182-198.
- Ligowski, R., 1987, Sea ice microalgae community of the floating ice in the Admiralty Bay (South Shetland Islands). *Polish Polar Research*, 8(4), 367-380.
- Ligowski, R., Lipski, M., and Zielinski, K., 1988, Algae of drifting sea ice north of Elephant Island (BIOMASS III, October 1986). *Polish Polar Research*, 9(2-3), 217-229.
- Lisitzin, A., 1971, Distribution of siliceous microfossils in suspension and in bottom sediments. (In, Funnell B. and Riedel, W. (Editors), *The Micropalaeontology of Oceans*, Cambridge University Press, Cambridge, pp. 173-195).
- Mabin, M.C.G., 1990, The glacial history of the Lambert Glacier - Prince Charles Mountains area and comparisons with the record from the Transantarctic Mountains. (In, Gillieson, D. and Fitzsimons, S. (Editors), *Quaternary Research in Australian Antarctica: Future Directions*. Australian Defense Force Academy, Canberra, Special Publication, 3, pp. 15-23).
- Mackenson, A., Barrera, E., and Hubberten, H.W., 1992, Neogene circulation in the southern Indian Ocean: evidence from benthic foraminifers, carbonate data, and stable isotope analysis (Site 751). *Proceedings of the Ocean Drilling Program, Scientific Results*, 120, 867- 878.
- Mackenson, A. and Ehrmann, W.U., 1992, Middle Eocene through Early Oligocene climate history and paleoceanography in the Southern Ocean: Stable oxygen and carbon isotopes from ODP sites on Maud Rise and Kerguelen Plateau. *Marine Geology*, 108, 1-27.
- Mackiewicz, N.E., Powell, R.D., Carlson, P. R., and Molnia, B.F., 1984, Interlaminated ice-proximal glacimarine sediments in Muir Inlet, Alaska. *Marine Geology*, 57, 113-147.

- Maffione, R.A., 1998, Theoretical developments on the optical properties of highly turbid waters and sea ice. *Limnology and Oceanography*, 43(1), 29-33.
- Mahood, A.D. and Barron, J.A., 1996, Late Pliocene diatoms in a diatomite from Prydz Bay, East Antarctica. *Micropaleontology*, 42(3), 285-302.
- Mandra, Y.T., 1969, Silicoflagellates: a new tool for the study of Tertiary climates. *Antarctic Journal of the United States*, 4, 172-174.
- Mandra, Y.T. and Mandra, H., 1970, Antarctic Tertiary marine climate based on silicoflagellates. *Antarctic Journal of the United States*, 5, 178-180.
- Marchant, D.R., Denton, G.H., and Swisher, C.C., 1993a, Miocene-Pliocene-Pleistocene glacial history of Arena Valley, Quatermain Mountains, Antarctica. *Geographiska Annaler Stockholm*, 75A, 269-302.
- Marchant, D.R., Swisher, C.C., Lux, D.R., West, D.P.Jr., and Denton, G.H., 1993b, Pliocene Palaeoclimate and East Antarctic ice-sheet history from surficial ash deposits. *Science*, 260, 667-670.
- Marchant, D.R., Denton, G.H., Swisher, C.C. and Potter, N.Jr., 1996, Late Cenozoic Antarctic paleoclimate reconstruction from volcanic ashes in the Dry Valleys region of southern Victoria Land. *GSA Bulletin*, 108, 181-194.
- Martin, J.H., Gordon, R.M. and Fitzwater, S.E., 1991, Iron limitation? *Limnology and Oceanography*, 36(8), 1793-1802.
- Martinez-Macchiavello, J.C., Tatur, A., Servant-Vildary, S.S., and Del Valle, R., 1996, Holocene environmental change in a marine-estuarine-lacustrine sediment sequence, King George Island, South Shetland Islands. *Antarctic Science*, 18(4), 313-322.
- Matsuoka, N., 1995, Rock weathering processes and landform development in the Sør Rondane Mountains, Antarctica. *Geomorphology*, 12, 323-339.
- Matthews, R.K. and Poore, R.Z., 1980, Tertiary  $^{18}\text{O}$  record and glacio-eustatic sea-level fluctuations. *Geology*, 8, 501-504.
- Maykut, G.A., 1985, An introduction to ice in the polar oceans. Report APL-UW 8510. Department of Atmospheric Sciences / Geophysics Program, University of Washington, Seattle, U.S.A. (In, Medlin, L.K. and Priddle, J. (Editors), *Polar Marine Diatoms*, British Antarctic Survey, Cambridge, pp. 3-8).
- Maynard, N.G., 1968, Significance of air-borne algae. *Zeitschrift für Allg. Mikrobiologie*, 8(3), 225-226.
- McCartney, K., 1977, Subantarctic Mode Water. (In, Angel, M., (Editor), *A Voyage to Discovery*. Pergamon Press, Oxford, pp. 103-119).
- McCollum, D.W., 1975, Diatom stratigraphy of the Southern Ocean. *Initial Reports Deep Sea Drilling Project*, 28, 515-571.



- McConville, M.J. and Wetherbee, R., 1983, The bottom-ice microalgal community from the annual ice in the inshore waters of East Antarctica. *Journal of Phycology*, 19, 431-439.
- McElroy, M.B. and Mintzer, I.M., 1993, Changes in climates of the past; lessons for the future. (In, Mintzer, I.M. (Editor), *Confronting Climate Change; Risk, Implications and Responses*, Cambridge University Press, Cambridge, pp. 65-83).
- McKelvey, B.C. and Stephenson, N.C.N., 1990, A geological reconnaissance of the Radok Lake area, Amery Oasis, Prince Charles Mountains. *Antarctic Science*, 2(1), 53-66.
- McKelvey, B.C., Webb, P.N., Harwood, D.M., and Mabin, M.C.G., 1991, The Dominion Range Sirius Group: a record of the Late Pliocene-Early Pleistocene Beardmore Glacier. (In, Thomson, M.R.A., Crame, J.A., and Thomson, J.W., (Editors), *Geological Evolution of Antarctica*. Cambridge University Press, Cambridge, pp. 675-682).
- McKelvey, B.C., 1994, The Pagodroma Tillite and the Sirius Group - a comparison. (In, van der Wateren, F.M., Verbers, A.L.L.M. and Tessensohn, F., (Editors), *LIRA Workshop on Landscape Evolution: A Multidisciplinary Approach to the Relationship Between Cenozoic Climate Change and Tectonics in the Ross Sea Area, Antarctica*. Ministerie van Economische Zaken, pp. 112-116).
- McKelvey, B.C., Hambrey, M.J., Mabin, M.C.G., Harwood, D.M. and Webb, P.N., 1995, The Neogene Pagodroma Group in the northern Prince Charles Mountains, East Antarctica. (In, Ricci C.A. (Editor), *The Antarctic Region; Geological Evolution and Processes; Proceedings of the VII International Symposium on Antarctic Earth Sciences*. Siena (Italy), p. 262).
- McKelvey, B.C., Hambrey, M.J., Harwood, D.M., Mabin, M.C.G., Webb, P.N. and Whitehead, J.M., 1997, The Pagodroma Group - The Neogene record in the Northern Prince Charles Mountains of a dynamic Lambert Glacier on the East Antarctic Ice Sheet. *Antarctica and Global Change, Symposium*, Hobart, Tasmania, paper 310.
- McKelvey, B., Hambrey, M., Harwood, D., Mabin, M., Webb, P., and Whitehead, J., (in press), The Pagodroma Group - The Neogene Record in the Northern Prince Charles Mountains of a Dynamic Lambert Glacier and East Antarctic Ice Sheet, *Antarctic Science*
- McLane, M., 1995, *Sedimentology*. Oxford University Press, New York, 423 p.
- McLeod, I.R., 1958, *Report on geological and glaciological work by the 1958 Australian National Antarctic Research Expedition*. Commonwealth of Australia, Department

- of National Development, Bureau of mineral resources geology and geophysics, record 1958/131.
- McLoughlin, S. and Drinnan, A.N., 1997, Revised stratigraphy of the Permian Bainmedart Coal Measures, northern Prince Charles Mountains, East Antarctica. *Geological magazine*, 134(3), 335-353.
- McMinn, A. and Hodgson, D., 1993, Summer phytoplankton succession in Ellis Fjord, eastern Antarctica. *Journal of Phytoplankton Research*, 15(8), 925-938.
- McMinn, A., 1994, Preliminary investigation of a method for determining past winter temperatures at Ellis Fjord, eastern Antarctica, from fast-ice diatom assemblages. *Memoirs of the National Institute of Polar Research, Special Issue*, 50, 34-40.
- McMinn, A., 1995, Comparison of diatom preservation between oxic and anoxic basins in Ellis Fjord, Antarctica. *Diatom Research*, 10(1), 145-151.
- McMinn, A. and Harwood, D.M., 1995, Biostratigraphy and paleoecology of early Pliocene diatom assemblages from the Larsemann Hills, eastern Antarctica. *Antarctic Science*, 7, 115-116.
- McMinn, A., 1996, Preliminary investigation of the contribution of fast-ice algae to the spring phytoplankton bloom in Ellis Fjord, eastern Antarctica. *Polar Biology*, 16, 301-307.
- McMinn, A., Bloxham, J.J., Whitehead, J., 1998, Modern surface sediments and non-deposition in Ellis Fjord, eastern Antarctica. *Australian Journal of Earth Sciences*, 45, 645-652.
- Medlin, L.K. and Priddle, J., 1990, *Polar Marine Diatoms*, British Antarctic Survey, 241 p.
- Meier, M.F., 1984, Contribution of Small Glaciers to Global Sea Level. *Science*, 226, 1418-1421.
- Menzies, J., 1995, *Modern Glacial Environments, Dynamics and Sediments*. Butterworth-Heinemann Ltd., Oxford, 590 p.
- Mercer, J.H., 1983, Cenozoic glaciations in the southern hemisphere. *Annual Review of Earth and Planetary Science*, 11, 99-132.
- Middleton, J.H. and Humphries, S.E., 1989, Thermohaline structure and mixing in the region of Prydz Bay, Antarctica. *Deep-sea Research*, (36)8, 1255-1266.
- Mikhail, V. and Saltzman, B., 1994, Heinrich-type glacial surges in a low-order dynamic climate model. *Climate Dynamics*, 10, 39-47.
- Miller, K.G., Mountain, G.S., the Leg 150 Shipboard Party, and Members of the New Jersey Coastal Plain Drilling Project, 1996, Drilling and dating New Jersey

- Oligocene - Miocene sequences: ice volume, global sea level, and Exxon Records. *Science*, 271, 1092-1095.
- Morgan, V.I., Budd, W.F., 1975, Radio-echo sounding of the Lambert Glacier basin. *Journal of glaciology*, 15(73), 103-111.
- Moisan, T.A. and Fryxell, G.A., 1993, The distribution of Antarctic diatoms in the Weddell Sea during austral winter. *Botanica Marina*, 36, 489-497.
- Moncrieff, A. C. M., 1989, Classification of poorly-sorted sedimentary rocks, *Sedimentary Geology*, 65(1-2), 191-194.
- Moriwaki, K., Yoshida, Y., and Harwood, D.M., 1992a, Cenozoic Glacial History of Antarctica - a correlative synthesis. (In, Yoshida, Y. *et al.* (Editors), *Recent Progress in Antarctic Earth Science*. Terra Scientific Publication Company, Tokyo, pp. 773-780).
- Moriwaki, K., Hirakawa, K., Hayashi, M., and Iwata, S., 1992b, Late Cenozoic Glacial History in the Sør-Rondane Mountains, East Antarctica. (In, Yoshida, Y. *et al.* (Editors), *Recent Progress in Antarctic Earth Science*. Terra Scientific Publication Commune, Tokyo, pp. 661-667).
- Morrison, R. and Kukla, G., 1998,. The Pliocene-Pleistocene (Tertiary-Quaternary) boundary should be placed at about 2.6 Ma, not at 1.8 Ma. *GSA Today*, 1(8), 9.
- Morrow, R., Church, J., Coleman, R., Chelton, D. and White, N., 1992, Eddy momentum flux and it's contribution to the Southern Ocean momentum balance. *Nature*, 357, 482-484.
- Muir, H., 1996, Giant lake lurks beneath Antarctica's ice. *New Scientist*, 150, 16.
- Nelson, D.M. and Goering, J.J., 1977, Near-surface silica dissolution in the upwelling region off Northwest Africa. *Deep Sea Research*, 24, 65-73.
- Nelson, D.M. and Treguer, P., 1992, Role of silicon as a limiting nutrients to Antarctic diatoms: evidence from kinetic studies in the Ross Sea ice-edge zone. *Marine Ecology Progress Series*, 80, 255-264.
- Nicol, S. and Allison, I., 1997, The frozen skin of the Southern Ocean. *American Scientist*, 85, 426-439.
- Niiler, P.P., Amos, A., and Hu, J.-H., 1991, Water masses and 200 m relative geostrophic circulation in the western Bransfield Strait region. *Deep Sea Research*, 38, 943-959.
- O'Brien, P.E., Franklin, D., and O'Loughlin, M.O., 1993, *Post Cruise Report - Prydz Bay and Mac.Robertson Shelf, Antarctica, January-March, 1993*. AGSO Record 1993/78, 39 p.

- O'Brien, P.E., and Harris, P.T., 1995, Prydz Trough Mouth Fan – a major Record of Antarctic Glacial History. (In, Ricci C.A. (Editor), *The Antarctic Region; Geological Evolution and Processes; Proceedings of the VII International Symposium on Antarctic Earth Sciences*. Siena (Italy), p. 283).
- O'Brien, P.E., Harris, P.T., Quilty, P.G., Taylor, F., and Wells, P., 1995, *Antarctic CRC Marine Geoscience, Prydz Bay, Mac. Robertson Shelf and Kerguelen Plateau, Post cruise Report*. AGSO Record 1995/29, 119 p.
- OECD/EIA (Organisation for Economic Co-operation and Development / International Energy Agency), 1994, *Climate Change and Policy Initiatives*, 1, OECD Countries, Paris, 217 p.
- Orsi, A.H., Whitworth, T., and Nowlin, W.D., 1995, On the meridional extent and fronts of the Antarctic Circumpolar Current. *Deep Sea Research*, 42(5), 641-673.
- Osborn, N.I., Ciesielski, P.F., and Ledbetter, M.T., 1983, Disconformities and paleoceanography in the southeast Indian Ocean during the past 5.4 million years. *GSA Bulletin*, 94, 1345-1358.
- Palmisano, A.C. and Sullivan, C.W., 1982, Physiology of sea ice diatoms. I. Response of three polar diatoms to a simulated summer-winter transition. *Journal of Phycology*, 18, 489-498.
- Park, Y., Gamberoni, L., and Charriaud, E., 1993, Frontal Structure, water masses, and circulation in the Crozet Basin. *Journal of Geophysical Research*, 98(C7), 12361-12385.
- Parkinson, C.L. and Cavalieri, D.J., 1982, Interannual sea-ice variations and sea-ice/atmosphere interactions in the Southern Ocean, 1973-1975. *Annals of Glaciology*, 3, 249-254.
- Passchier, S., Verbers, A.L.L.M., van der Wateren, F.M., and Vermeulen, F.J.M., 1999, Provenance, geochemistry and grain-sizes of glaciogene sediments, including the Sirius Group, and Late Cenozoic glacial history of the southern Prince Albert Mountains, Victoria Land, Antarctica. *Annals of Glaciology*, 27, 290-296.
- Patterson, S.L. and Whitworth, T., 1990, Physical Oceanography. (In, Glasby, G.P., (Editor), *Antarctic Sector of the Pacific*. Elsevier Oceanography Series, 51, Amsterdam, pp. 55-94).
- Phillips, H.A., Allison, I., Craven, M., Krebs, K., and Morgan, P., 1996, Ice velocity, mass flux and the grounding line location in the Lambert glacier - Amery Ice Shelf system, Antarctica. *Congress Proceedings of the 12<sup>th</sup> Australian Institute of Physics Congress*, Hobart.

- Pichon, J.J., Labracherie, M., Labeyrie, L.D., and Duprat, J., 1987, Transfer function between diatom assemblages and surface hydrology in the Southern Ocean. *Palaeogeography, Palaeoclimatology, Palaeoecology*, 61, 79-95.
- Pichon, J.J., Bareille, G., Labracherie, M., Labeyrie, L.D., Baudrimont, A., and Turon, J.L., 1992, Quantification of the biogenic silica dissolution in Southern Ocean sediments. *Quaternary Research*, 37, 361-378.
- Pickard, J., 1986, *Antarctic Oasis: Terrestrial Environments and History of the Vestfold Hills*. Academic Press, Sydney, 367 p.
- Pickard, J., Adamson, D.A., Harwood, D.M., Miller, G.H., Quilty, P.G., and Dell, R.K., 1986, Early Pliocene marine sediments in the Vestfold Hills, East Antarctica: implications for coastline, ice sheet and climate. *South African Journal of Science*, 82, 520-521.
- Pickard, J., Adamson, D.A., Harwood, D.M., Miller, G.H., Quilty, P.G., and Dell, R.K., 1988, Early Pliocene marine sediments, coastline, and climate of east Antarctica. *Geology*, 16(2), 158-161.
- Pickard, G.L. and Emery, W.J., 1990, *Descriptive physical oceanography. An Introduction*. Pergamon Press, Oxford, 320 p.
- Pickett-Heaps, J.D., Hill, D.R.A., and Wetherbee, R., 1986, Cellular movement in the centric diatom, *Odontella sinensis*. *Journal of Phycology*, 22, 334-339.
- Pimentel, R. A., 1993, *BIO TAT II A multivariate Statistical Toolbox*. Sigma Software, United States.
- Potter, M.J., 1995, *An Evaluation of Polynyas in East Antarctica*. Honours Thesis, Institute of Antarctic and Southern Ocean Studies, University of Tasmania, 168 p.
- Powell, R.D. and Molnia, B.F., 1989, Glacimarine sedimentary processes, facies and morphology of the south-southeast Alaska shelf and fjords. *Marine Geology*, 85(2/4), 359-390.
- Powell, R.D., 1990, Glacimarine processes at grounding-line fans and their growth to ice-contact deltas. (In, Dowdeswell, J.A. and Scourse, J.D., (Editors), *Glacimarine Environments: Processes and Sediments*. Geological Society of London, Special Publication, 53, pp. 53-73).
- Prentice, M.L. and Matthews, R.K., 1991, Tertiary ice sheet dynamics: the snow gun hypothesis. *Journal of Geophysical Research*, 96, 6811-6827.
- Prentice, M.L., Fastook, J.L., and Oglesby, R.J., 1992, Early Pliocene Antarctic interglaciations: Climate and ice-sheet modeling results. *Antarctic Journal of the United States*, 92, 35-37.

- Prentice, M.L., Bockheim, J.G., Wilson, S.C., Burckle, L.H., Hodell, D.A., Schlüchter, C., and Kellogg, D.E., 1993, Late Neogene Antarctic Glacial history: evidence from Central Wright Valley. *Antarctic Research Series*, 60, 207-250.
- Prentice, M., Ishman, S., Clemens, S. McIntosh, B., and Clarke, K., 1999, Late Neogene stable isotope records from fjords within the McMurdo Dry Valleys, Antarctica, *VIII International Symposium on Antarctic Earth Sciences*, Wellington (New Zealand) Abstracts, p. 249.
- Priddle, J. and Fryxell, G., 1985, *Handbook of the Common Plankton of the Southern Ocean: Centrales Except the Genus Thalassiosira*. British Antarctic Survey, Cambridge, 365 p.
- Priddle, J., 1990, The Antarctic Planktonic ecosystem. (In, Medlin, L.M. and Priddle, J. (Editors), *Polar Marine Diatoms*. British Antarctic Survey, Cambridge, pp. 25-46).
- Pye, K., 1987, *Aeolian Dust and Dust Deposits*. Academic Press, London, 334 p.
- Quilty, P.G., 1988, Foraminifera from Neogene sediments, Vestfold Hills, Antarctica. *Hydrobiologia*, 165, 213-220.
- Quilty, P.G., 1991, The geology of Marine Plain, Vestfold Hills, East Antarctica. (In, Thompson, M.R.A., Crame, J.A. and Thomson, J.W., (Editors), *The Geological Evolution of Antarctica*. Cambridge University Press, Cambridge, pp. 683-686).
- Quilty, P.G., 1992, Late Neogene sediments of coastal East Antarctica-an overview. (In, Yoshida, Y., Kaminuma, K. and Shiraishi, K. (Editors), *Recent Progress in Antarctic Earth Science*. Terra Scientific Publishing Company, Tokyo, pp. 699-705).
- Quilty, P.G., 1993, Coastal East Antarctic Neogene sections and their contribution to the ice sheet evolution debate. *Antarctic Research Series*, 60, 251-264.
- Quilty, P.G., 1994, Preliminary results of 1993/1994 fieldwork, Marine Plain, Vestfold Hills, East Antarctica. *Terra Antarctica*, 1(2), 409-410.
- Quilty, P.G., 1996, The Pliocene environment of Antarctica. *Papers and Proceedings of the Royal Society of Tasmania*, 130(2), 1-8.
- Quilty, P.G., Truswell, E.M., O'Brien, P.E., and Taylor, F., 1999, Palaeocene-Eocene biostratigraphy and palaeoenvironment of East Antarctica; new data from Mac.Robertson Shelf and western Prydz Bay. *AGSO Journal of Australian Geology and Geophysics*, 17, 133-143.
- Quilty, P.G., Lirio, J.M. and Jillett, D., in press, Lithostratigraphy and postdepositional disruption of marine Pliocene sediments, Marine Plain, Vestfold Hills, Antarctica. *Antarctic Science*

- Rabus, B.T. and Echelmeyer, K.A., 1997, The flow of a polythermal glacier: McCall Glacier, Alaska, U.S.A.. *Journal of Glaciology*, 43(145), 522-536.
- Rack, F.R., 1993, A geologic perspective on the Miocene evolution of the Antarctic Circumpolar Current system. *Tectonophysics*, 222, 397-415.
- Rack, F.R., and Palmer-Julson, A., 1992, Sediment microfabric and physical properties record of late Neogene Polar Front migration, Site 751. *Proceedings of the Ocean Drilling Program, Scientific Results*, 120 (2), 179-205.
- Ram, M., Gayley, R.I., and Petit, J.R., 1988, Insoluble particles in Antarctic ice: background aerosol size distribution and diatom concentration. *Journal of Geophysical Research*, 93(D7), 8378-8382.
- Ramsay, D.C., Colwell, M.F., Davies, H.L., Hill, P.J., Pigram, C.J., and Stagg, H.M.J., 1986, New Findings from the Kerguelen Plateau. *Geology*, 14, 589-593.
- Rattray, J., 1890, A revision of the genus *Actinocyclus* Ehrenberg. *Quekett Microscopy Club Journal Series*, 2(4), 137-212.
- Raven, P.H., Evert, R.F., and Eichhorn, S. E., 1986, *Biology of Plants*. Worth Publishing Inc., New York, 519 p.
- Raymo, M.E., Grant, B., Horowitz, M. and Rau, G.H., 1996, Mid-Pliocene warmth: stronger greenhouse and stronger conveyor, *Marine Micropaleontology*, 27, 313-326.
- Reading, H., 1986, *Sedimentary Environments and Facies*. Blackwell Scientific Publishers, Oxford, 615 p.
- Reynolds, J.M., 1981, The distribution of mean annual air temperatures in the Antarctic Peninsula. *British Antarctic Survey Bulletin*, 54, 123-133.
- Richardson, M. D. and Hedgpeth, J. W., 1977, Antarctic soft-bottom, macrobenthic community adaptations to a cold, stable, highly productive, glacially affected environment. (In, Llano, G. A. (Editor), *Proceedings of the Third SCAR Symposium on Antarctic Biology, Adaptations Within Antarctic Ecosystems*, Smithsonian Institution, Washington, D.C., pp. 181-196).
- Riedel, G.F. and Nelson, D.M., 1985, Silicon uptake by algae with no known Si requirement. II. Strong pH dependence of uptake kinetic parameters in *Phaeodactylum tricornutum* (Bacillariophyceae). *Journal of Phycology*, 21, 196-171.
- Rintoul, S.R. and Church, J.A., 1993, A late winter section between Tasmania and Antarctica : circulation, transport and water mass formation. *Forth International Conference on Southern Hemisphere Meteorology and Oceanography March 29-*

- April 2, Hobart, Australia Preprint Volume. American Meteorological Society, pp. 21-22.
- Rintoul, S.R., Donguy, J.-R., and Roemmich, D.H., 1997, Seasonal evolution of upper ocean thermal structure between Tasmania and Antarctica. *Deep Sea Research*, 44, 1185-1202.
- Ritz, C., 1989, Interpretation of the temperature profile measured at Vostok, East Antarctica. *Annals of Glaciology*, 12, 138-144.
- Rivikin, R.B. and Putt, M., 1987, Photosynthesis and cell division by Antarctic microalgae: Comparison of benthic, planktonic and ice algae. *Journal of Phycology*, 23, 223-229.
- Robert, C. and Maillot, H., 1990, Paleoenvironments in the Weddell Sea area and Antarctic climates, as deduced from clay mineral association and geochemical data, ODP Leg 113. *Proceedings of the Ocean Drilling Program, Scientific Results*, 113, 51-70.
- Roberts D. and McMinn, A., 1996, Relationship between surface sediment diatom assemblages and water chemistry gradients in saline lakes of the Vestfold Hills, Antarctica. *Antarctic Science*, 8(4), 331-341.
- Roberts D. and McMinn, A., 1997, Palaeosalinity reconstruction from saline lake diatom assemblages in the Vestfold Hills, Antarctica. (In Lyons, W.B., Howard-Williams, C. and Hawes, I. (Editors), *Ecosystems Processes in Antarctic Ice-free Landscapes*. A.A. Balkema, Rotterdam, pp. 207-219).
- Roberts D. and McMinn, A., 1998, A weighted-averaging regression and calibration model for inferring lakewater salinity from fossil diatom assemblages in saline lakes of the Vestfold Hills: a new tool for interpreting Holocene lake histories in Antarctica. *Journal of Paleolimnology*, 19, 99-113.
- Roberts D. and McMinn, A., 1999, Diatoms of the saline lakes of the Vestfold Hills, Antarctica. *Bibliotheca Diatomologica*, 44, 83 p.
- Robin, G., de Q., 1986, Changing the sea level. (In, Bolin, B., Döös, B.R., Jäger, J., and Warrick, R.A., (Editors), *SCOPE 29 The Greenhouse Effect, Climate Change, and Ecosystems*. John Wiley and Sons, Chichester, pp. 323-359).
- Round, F.E., 1981, *The Ecology of Algae*. Cambridge University Press, Cambridge, pp. 122-125.
- Round, F.E., Crawford, R.M., and Mann, D.G., (1990), *The Diatoms, Biology and Morphology of the Genera*. Cambridge University Press, Cambridge, 747 p.
- Rubin, M.J. and Weyant, W.S., 1965, Antarctic meteorology. (In, Hatherton, T. (Editor), *Antarctica*. Methuen, London, pp. 375-401).



- Saari, M.R., Yuen, D.A., and Schubert, G., 1987, Climatic warming and basal melting of large ice sheets, Possible implications for East Antarctica. *Geophysical Research Letters*, 14(1), 33-36.
- Salisbury, F.B. and Ross, C.W., 1985, *Plant Physiology*. Wadsworth Publishers Inc., New York, 100 p.
- Sarnthein, M., Winn, K., Jung, S.J.A., Duplessy, J.-C., Labeyrie, L., Erlenkeusser, H., and Ganssen, G., 1994, Changes in east Atlantic deepwater circulation over the last 30, 000 years : Eight time slice reconstructions. *Paleoceanography*, 9(2), 209-267.
- SCCCS (Steering Committee on the Climate Change Study), 1995, *Climate Change Science: Current Understanding and Uncertainties*. Australian Academy of Technology, Science and Engineering, Parkville, Victoria, 100 p.
- Scharek, R., Smetacek, V., Fahrback, E., Gordon, L.I., Rohardt, G., and Moore, S., 1994, The transition from winter to early spring in the eastern Weddell Sea, Antarctica: Plankton biomass and composition in relation to hydrology and nutrients. *Deep Sea Research*, 41(8), 1231-1250.
- Scherer, R.P., Harwood, D.M., Ishman, S., and Webb, P., 1988, Micropaleontological analyses of sediments from Crary Ice Rise. *Antarctic Journal of the United States*, 23(5), 34-36.
- Scherer, R.P., 1989, Paleoenvironmental studies of the West Antarctic interior: microfossil study of sediments below Upstream B. *Antarctic Journal of the United States*, 22(5), 35-37.
- Scherer, R.P., 1991, Quaternary and Tertiary microfossils from beneath Ice Stream B: Evidence for a dynamic west Antarctic Ice Sheet history. *Palaeogeography, Palaeoclimatology, Palaeoecology*, 90, 395-412.
- Scherer, R.P., Aldahan, A., Tulaczyk, S., Possnert, G., Engelhardt, H., and Lamb, B., 1998, Pleistocene collapse of the West Antarctic Ice Sheet., *Science*, 281, 82-85.
- Schmaljohann, R. and Röttger, R., 1978, The ultrastructure and taxonomic identity of the symbiotic algae of *Heterostegina depressa* (Foraminifera: Nummulitidae). *Journal of The Marine Association of the United Kingdom*, 58, 227-237.
- Schrader, H.J., 1973a, Cenozoic planktonic diatom biostratigraphy of the Southern Pacific Ocean. *Initial Reports of the Deep Sea Drilling Project*, 18, 673-797.
- Schrader, H., 1973b, Cenozoic diatoms from the Northeast Pacific, Leg 18. *Initial Reports of the Deep Sea Drilling Project*, 36, 673-797.
- Schrader, H.J., 1976, Cenozoic planktonic diatom biostratigraphy of the Southern Pacific Ocean. *Initial Reports of the Deep Sea Drilling Project*, 35, 605-672.

- Schwerdtfeger, W., 1984, *Developments in Atmospheric Sciences, Vol.15*. Elsevier, New York, 261 p.
- Scott, P.A., 1992, *Physical Parameters Influencing Diatom Abundance and Species Composition in Antarctic Sea-ice*. Honours Thesis, University of Melbourne, 140 p.
- Scott, P., McMinn, A., and Hosie, G., 1994, Physical parameters influencing diatom community structure in eastern Antarctic sea ice. *Polar Biology*, 14, 507-517.
- Shackleton, N.J. and Kennett, J.P., 1975, Paleotemperature history of the Cenozoic and the initiation of Antarctic glaciation: oxygen and carbon isotope analyses in DSDP sites 277, 279 and 281. *Initial Reports of the Deep Sea Drilling Project*, 29, 742-755.
- Shackleton, N. J. and Opdyke, N. D. 1977 Oxygen isotope and palaeomagnetic evidence for early Northern Hemisphere glaciation. *Nature*, 270, 216-219.
- Shackleton, N.J., 1995, New data on the Evolution of Pliocene Climatic Variability. (In, Vrba, E.S., Denton, G.H., Partridge, T.C., and Burckle, L.H. (Editors), *Paleoclimate and Evolution, with Emphasis on Human Origins*. Yale university Press, New Haven, pp. 242-248).
- Shackleton, N.J., Hall, M.A., and Pate, D., 1995, Pliocene stable isotope stratigraphy of Site 846. *Proceedings of the Ocean Drilling Program, Scientific Results*, 138, 337-353.
- Shaw, G.E., 1979, Considerations on the origin and properties of the Antarctic aerosol. *Reviews of Geophysics and Space Physics*, 17(8), 1983-1998.
- Shaw, J., 1983, Drumlin formation related to inverted meltwater erosion marks. *Journal of Glaciology*, 29, 461-479.
- Shaw, J. and Kvill, D., 1984, A glaciofluvial origin for drumlins of the Lingstone Lake area, Saskatchewan. *Canadian Journal of Earth Sciences*, 12, 1426-1440.
- Shaw, J., 1985, Subglacial and ice marginal environments, (In Ashley, G.M., Shaw, J. and Smith, N.D. (Editors), *Glacial Sedimentary Environments, Society of Economic Palaeontologists and Mineralogists, Short Course 16*. Tulsa, Oklahoma, pp. 7-84).
- Shemesh, A., Burckle, L.H., and Froelich, P.N., 1989, Dissolution and Preservation of Antarctic Diatoms and the Effects on Sediment Thanatocoenoses. *Quaternary Research*, 31, 288-308.
- Shi, G.R., 1993, Multivariate data analysis in palaeoecology and palaeobiogeography - a review, *Palaeogeography, Palaeoclimatology, Palaeoecology*, 105(3-4), 199-234.

- Shi, G., 1995, Spatial aspects of palaeobiogeographical data and multivariate analysis. *Memoirs of the Association of Australian Palaeontologists*, 18, 179-188.
- Siegert, M.J. and Ridley, J.K., 1998, Analysis of the ice-sheet surface and subsurface topography above the Vostok Station subglacial lake, central East Antarctica. *Journal of Geophysical Research*, 103(B5), 10 195-10 207.
- Siesser, W.G., 1993, Calcareous nannoplankton. (In, Lipps, J.H. (Editor), *Fossil Prokaryotes and Protists*. Blackwell Scientific Publications, Boston, pp. 169-201).
- Smetacek, V., 1985, Role of sinking in diatom life-history cycles, ecological, evolutionary and geological significance. *Marine Biology*, 84, 239-251.
- Smith, N.R., Zhaoqian, D., Knowles, K., and Wright, S., 1984, Water masses and circulation in the region of Prydz Bay, Antarctica. *Deep Sea Research*, 31(9), 1121-1147.
- Smith, N. and Tréguer, P., 1994, Physical and Chemical Oceanography in the Vicinity of Prydz Bay, Antarctica. (In, El-Sayed, S.Z. (Editor), *Southern Ocean Ecology: The BIOMASS Perspective*. Cambridge University Press, Cambridge, pp. 25-45).
- Smith, W.O. and Nelson, D.M., 1986, The importance of ice edge phytoplankton production in the Southern Ocean. *BioScience*, 36, 251-257.
- Smith, W.O., Jr., Nelson, D.M., DiTullio, G.R., and Leventer, A.R., 1996, Temporal and spatial patterns in the Ross Sea: phytoplankton biomass, elemental composition, productivity and growth rates *Journal of Geophysical Research*, 101(C8), 18455-18465.
- Squire, V.A., 1990, Sea ice: its formation, distribution and properties. (In, Medlin, L.K. and Priddle, J. (Editors), *Polar Marine Diatoms*, British Antarctic Survey, pp. 3-8).
- Stockwell, D. A., 1991, Distribution of *Chaetoceros* resting spores in the Quaternary sediments from Leg 119. *Proceedings of the Ocean Drilling Program, Scientific Results*, 119, 599-610.
- Stockwell, D.A, Kang, S. and Fryxell, G.A., 1991, Comparison of diatom biocoenoses with Holocene sediment assemblages in Prydz Bay, Antarctica. *Proceedings of the Ocean Drilling Program, Scientific Results*, 119, 667-673.
- Strelnikova, N.I., 1990, Evolution of diatoms during the Cretaceous and Paleogene periods. (In, Simola, H., (Editor), *Proceedings of the Tenth International Diatom Symposium*. Koeltz Scientific Books, Koenigstein, pp. 195-204).
- Strelnikova, N.I., 1991, Evolution of marine diatoms: Cretaceous and Paleogene. *Algologia*, 1, 65-72.

- Stroeven, A.P., Prentice, M.J., and Borns, H.W., 1992, Mt Fleming Upper Valley Drift: evidence for Neogene glacial history of Antarctica. *Antarctic Journal Review*, 27(5), 51-54.
- Stroeven, A.P., Prentice, M.L., and Kleman, J., 1996, On marine microfossil transport and pathways in Antarctica during the late Neogene: Evidence from the Sirius Group at Mount Fleming. *Geology*, 24, 727-730.
- Stroeven, A.P., Burckle, L.H., Kleman, J., and Prentice, M.L., 1998, Atmospheric transport of diatoms in the Antarctic Sirius Group: Pliocene deep freeze. *GSA Today*, 8(4), 1-6.
- Sugden, D.E. and John, B.S., 1976, *Glaciers and Landscapes - a Geomorphological Approach*. John Wiley and Sons, New York, 376 p.
- Sugden, D.E., 1992, Antarctic ice sheets at risk? *Nature*, 359, 775-776.
- Sugden, D.E., Marchant, D.R., Potter, N.Jr., Souchez, R.A., Denton, G.H., Swisher, C.C., and Tison, J-L, 1995a, Preservation of Miocene glacier ice in East Antarctica. *Nature*, 376, 412-414.
- Sugden, D.E., Denton, G.H., and Marchant, D.R., 1995b, Landscape evolution of the Dry Valleys, Transantarctic Mountains: tectonic implications. *Journal of Geophysical Research*, 100(B7), 9949-9967.
- Sugden, D.E., 1996, East Antarctic Ice Sheet: unstable ice or unstable ideas? *Institute of British Geographers. Transactions*, 21(3), 443-454.
- Sullivan, C.W., Arrigo, K.R., McClain, C.R., Comiso, J.C., and Firestone, J., 1993, Distributions of phytoplankton blooms in the Southern Ocean. *Science*, 262, 1832-1837.
- Sverdrup, H.U; Johnson, M.W. and Fleming, R.H., 1942, The oceans, their physics, chemistry, and general biology, Prentice-Hall, New York, p. 1087.
- Tanimura, Y., Fukuchi, M., Watanabe, K., and Moriwaki, K., 1990, Diatoms in the water column and sea-ice in Lützow-Holm Bay, Antarctica, and their preservation in the underlying sediments. *Bulletin of the National Science Museum, Tokyo, Series C*, 18(1), 15-39.
- Taylor, F., McMinn, A., and Franklin, D., 1997, Distribution of diatoms in surface sediments of Prydz Bay, Antarctica. *Marine Micropaleontology*, 32, 209-229.
- Taylor, F., 1999, *Sedimentary Diatom Assemblages of Prydz Bay and Mac.Robertson Shelf, East Antarctica, and Their Use as Palaeoecological Indicators*. Ph.D. Thesis, University of Tasmania, 284 p.
- Tchernia, P., 1980, *Descriptive Regional Oceanography; An Elementary Description of*

- the Four Main Divisions of the World Ocean, of Their Limits, Forms, Topography, Wind Systems, Climatology, Surface Circulation, and Hydrological Characteristics and Structure. Pergamon Marine Series (3).* Pergamon Press, Oxford, 253 p.
- Thomas, R.H., 1979, The dynamics of marine ice sheets. *Journal of Glaciology*, 24, 167-177.
- Thomas, W.H., Hollibaugh, J.T., and Seibert, D.L.R., 1980, Effects of heavy metals on the morphology of some marine phytoplankton. *Phycologia*, 19, 202-209.
- Tingey, R.J., 1982, Geologic evolution of the Prince Charles Mountains--an Antarctic Archean cratonic block, (In, Craddock, C. (Editor), *Symposium on Antarctic Geology and Geophysics*, University of Wisconsin Press, International Union of Geological Sciences Publication, B(4), pp.455-464).
- Tingey, R.J. (Editor), 1991, *Geology of Antarctica*. Oxford, Clarendon Press, 1991, p.1-73.
- Tomczak, M. and Godfrey, J.S., 1994, *Regional Oceanography: An Introduction*. Pergamon Press, Oxford, 422 p.
- Tootill, E., 1984, *The Penguin Dictionary of Botany*. Penguin Books, London, 83p.
- Trail, D.S., 1963, Low-grade metamorphic rocks from the Prince Charles Mountains, East Antarctica. *Nature* 197, 548-550.
- Trail, D.S., 1964, The glacial geology of the Prince Charles Mountains. (In, Adie, R.J. (Editor), *Antarctic Geology*. North Holland, Amsterdam, pp. 143-151).
- Tréguer, P. and Jacques, G., 1992, Dynamics of nutrients and phytoplankton, and fluxes of carbon, nitrogen and silicon in the Antarctic Ocean. *Polar Biology*, 12, 149-162.
- Tréguer, P., 1994, Southern ocean: biogeochemical cycles and climate changes. (In, Hempel, G. (Editor), *Antarctic Science: Global Concerns*. Springer Verlag, Berlin, pp.110-128).
- Truesdale, R.S. and Kellogg, T.B., 1979, Ross Sea diatoms: modern assemblage distributions and their relationship to ecologic, oceanographic, and sedimentary conditions. *Marine Micropaleontology*, 4, 13-31.
- Truswell, E.M., 1983, Geological implications of recycled palynomorphs in continental shelf sediments around Antarctica, (In, Oliver, R.L., James, P.R. and Jago, J.B. (Editors), *Antarctic earth science; fourth international symposium*. Cambridge University Press, 1983, p.394-399).
- Tucholke, B.E., Hollister, C.D., Weaver, F.M., and Vennum, W.R., 1976, Continental rise and abyssal plain sedimentation in the Southeast Pacific Basin, Leg 35 Deep Sea Drilling Project. *Initial Reports of the Deep Sea Drilling Project*, 35, 359-400).

- Tulaczyk, S., Kamb, B., Scherer, R.P., and Engelhardt, H.F., 1998, Sedimentary processes at the base of a West Antarctic ice stream: constraints from textural and compositional properties of subglacial debris. *Journal of sedimentary research*, 68(3), 487-496.
- Van Bennekon, A.J., Berger, G.W., Van der Gaast, S.J., and De Vries, R.T.P., 1988, Primary productivity and the silica cycle in the Southern Ocean (Atlantic sector). *Palaeogeography, Palaeoclimatology, Palaeoecology*, 67, 19-30.
- Van der Wateren, F.M. and Hindmarsh, R., 1995, Stabilists strike again. *Nature*, 376, 389-376.
- Van der Wateren, F.M. and Verbers, A.L.L.M., 1991, Glacial geology and mountain uplift in Northern Victoria Land. *Abstracts, Sixth International Symposium on Antarctic Earth Sciences*. National Institute of Polar Research, Tokyo, p. 637.
- Verbers, A.L.L.M. and Damm, V., 1994, Morphology and late Cenozoic (<5Ma) glacial history of the area between David and Mawson Glaciers, Victoria Land, Antarctica. *Annals of Glaciology*, 20, 55-60.
- Walton, D.W.H., 1987, *Antarctic Science*. Cambridge University Press, Cambridge, 78 p.
- Wardlaw, B.R. and Quinn, T.M., 1991, The record of Pliocene sea-level change at Enewetak atoll. *Quaternary Science Reviews*, 10, 247-258.
- Warner, R.C. and Budd, W.F., 1998, Modeling the long-term response of the Antarctic ice-sheet to global warming. *Journal of Glaciology*, 27, 161-168.
- Warren, C.R. and Ashley, G.M., 1994, Origins of the ice contact stratified ridges (eskers) of Ireland. *Journal of Sedimentary Research*, A64, 433-449.
- Wasell, A. and Håkansson, H. 1992, Diatom stratigraphy in a lake on Horseshoe Island, Antarctica: A marine-brackish-fresh water transition with comments on the systematics and ecology of the most common diatoms. *Diatom Research*, 7(1), 157-194.
- Warrick, R. and Oerlemans, J., 1990, Sea Level Rise. (In, Houghton, J.T., Jenkins, G.J. and Ephraums, J.J. (Editors), *Climate Change, The IPCC Scientific Assessment*. Cambridge University Press, Cambridge, pp. 263-281).
- Watkins, A.B. and Simmonds, I., 1998, Relationships between Antarctic sea-ice concentration, wind stress and temperature temporal variability, and their changes with distance from the coast. *Annals of Glaciology*, 27, 409-412.
- WCRP (World Climate Research Program), 1990, *Global Climate Change*. Scientific Review, 35 p.

- Weaver, F.M. and Gombos, A.M., 1981, Southern high-latitude diatom biostratigraphy. (In, Warne, T.E., Douglas, R.G. and Winterer, E.L. (Editors), *The Deep Sea Drilling Project: A decade of progress*. Special Publication of the Society of Economic Paleontology and Minerals, 32, pp. 445-470).
- Webb, P.N., Harwood, D.M., McKelvey, B.C., Mercer, J.H., and Stott, L.D., 1983, Late Neogene and older Cenozoic microfossils in high elevation deposits of the Transantarctic Mountains: Evidence for marine sedimentation and ice volume variation on the east Antarctic craton. *Antarctic Journal of the United States*, 18(5), 96-97.
- Webb, P.N., Harwood, D.M., McKelvey, B.C., Mercer, J.H., and Stott, L.D., 1984, Cenozoic marine sedimentation and ice-volume variation on the East Antarctic craton. *Geology*, 12, 287-291.
- Webb, P.N. and Harwood, D.M., 1987, Terrestrial flora of the Sirius Formation: its significance for Late Cenozoic glacial history. *Antarctic Journal of the United States*, 22(4), 7-11.
- Webb, P.N., McKelvey, B.C., Harwood, D.M., Mabin, M.C.G., and Mercer, J.H., 1987, Sirius Formation of the Beardmore Glacier region. *Antarctic Journal of the United States*, 22(1/2), 8-13.
- Webb, P.N. and Harwood, D.M., 1991, Late Cenozoic glacial history of the Ross Sea embayment. *Quaternary Science Reviews*, 10, 215-223.
- Webb, P.N. and Harwood, D.M., 1993, Pliocene fossil *Nothofagus* (Southern Beech) from Antarctica: phyogeography, dispersal strategies, and survival in high latitude glacial - deglacial environments. (In, Alden, J., et al. (Editor), *Forest Development in Cold Regions*. Plenum Press, New York, pp. 135-165).
- Webb, P.N., Harwood, D.M., Mabin, M.G.C., and McKelvey, B.C., 1996, A marine and terrestrial Sirius Group succession, middle Beardmore Glacier-Queen Alexandra Range, Transantarctic Mountains, Antarctica. *Marine Micropaleontology*, 27, 273-297.
- Webb, T. and Bryson, R., 1972, Late- and postglacial climate change in the Northern Midwest, USA: quantitative estimates derived from fossil pollen spectra by multivariate statistical analysis. *Quaternary Research*, 2, 70-115.
- Weeks, W.F. and Ackley, S.F., 1982, The growth, structure, and properties of sea-ice. *CCREL Monograph 82-1*; United States Army Cold Regions Research and Engineering Laboratory, Hanover, 130 p.

- Weeks, W.F., Ackley, S.F., and Govoni, J., 1989, Sea ice ridging in the Ross Sea, Antarctica, as compared with sites in the Arctic. *Journal of Geophysical Research*, 94(C10), 4984-4988.
- Wei, W. and Thierstein, H.R., 1991, Upper Cretaceous and Cenozoic calcareous nannofossils Kerguelen Plateau (southern Indian Ocean) and Prydz Bay (East Antarctica). *Proceedings of the Ocean Drilling Program, Scientific Results*, 120,
- Weier, T.E., Stocking, G.R., Barbour, M.G., and Rost, T.L. 1982, *Botany: An Introduction to Plant Biology*. John Wiley and Sons, New York, 221 p.
- Westall, F. and Fenner, J., 1991, Pliocene-Holocene Polar Front Zone in the South Atlantic: Changes in its position and sediment-accumulation rate from holes 699A, 701C, and 704B. *Proceedings of the Ocean Drilling Program, Scientific Results*, 114, 609-646.
- Whitaker, T.M. and Richardson, M.G., 1980, Morphology and chemical composition of a natural population of an ice-associated Antarctic diatom *Navicula glaciei*. *Journal of Phycology*, 16, 25-257.
- Whitehead, J.M., Harwood, D.M., McKelvey, B.C., and McMinn, A., 1996, Preliminary diatom data from the Pagodroma Group, northern Prince Charles Mountains, Antarctica, (In, Wilson, C. (Editors), *Prince Charles Mountain Workshop*. University of Melbourne, Melbourne, p. 18).
- Whitehead, J.M. and McMinn, A., 1997, Paleodepth determination from Antarctic benthic diatom assemblages. *Marine Micropaleontology*, 29, 301-318.
- Whitworth, T., 1988, The Antarctic Circumpolar Current. *Oceanus*, 31, 53-58.
- Whitworth, T., Orsi, A.H., Kim, S.-J., and Nowlin, W.D. Jr., 1998, Water masses and mixing near the Antarctic slope front. *Antarctic Research Series*, 75, 1-27.
- Williams, M, Dunkerley, D., DeDeckker, P., Kershaw, P., and Chappell, J., 1998, *Quaternary Environments*. Edward Arnold, London, 329 p.
- Wilson, G.S., 1995, The Neogene East Antarctic ice sheet: A dynamic or stable feature? *Quaternary Science Reviews*, 14, 101-123.
- Wilson, G.S., Harwood, D.M., Askin, R.A. and Levy, R.H., 1998, Late Neogene Sirius Group strata in Reedy Valley, Antarctica: a multiple-resolution record of climate, ice-sheet and sea-level events. *Journal of Glaciology*, 44(148), 437-447.
- Winter, D.M., 1995, *Upper Neogene diatom biostratigraphy from coastal drillcores in Southern Victoria Land, Antarctica.*, M.S. Thesis, University of Nebraska-Lincoln, 146 p.
- Winter, D.M. and Harwood, D.M., 1997, Intergrated diatom biostratigraphy of Late Neogene drillholes in Southern Victoria Land and correlation to Southern Ocean



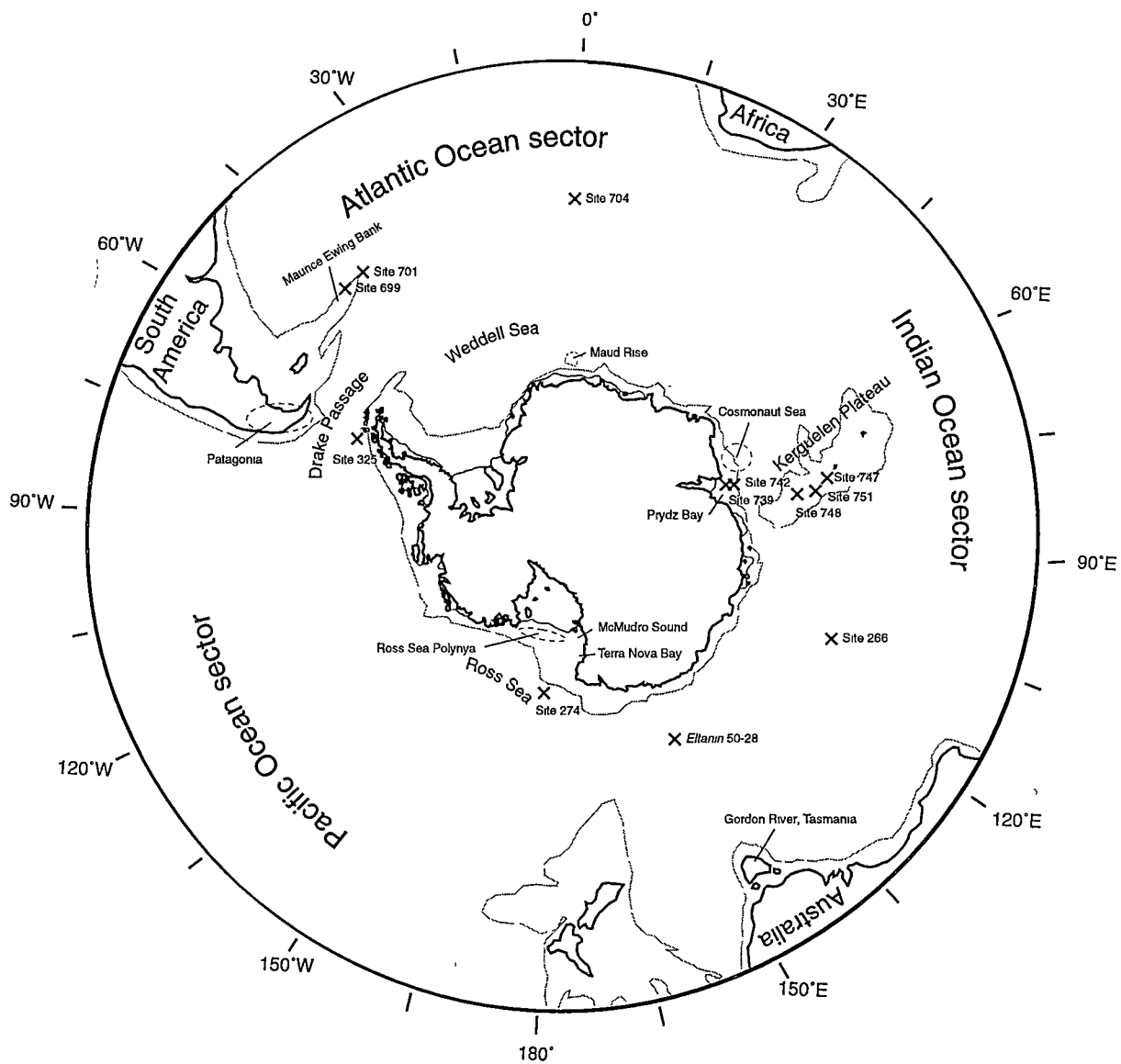
- records. (In, Ricci C.A. (Editor), *The Antarctic Region; Geological Evolution and Processes; Proceedings of the VII International Symposium on Antarctic Earth Sciences*. Siena (Italy), pp. 985-992).
- Wise, S.W., Breza, J.R., Harwood, D.M., Wuchang, W., and Zachos, J.C., 1992, Paleogene glacial history of Antarctica in light of Leg 120 drilling results. *Proceedings of the Ocean Drilling Program, Scientific Results*, 120, 1001-1030.
- Won Hyung, K., Mi-Ock, K. and Byong-Kwon, P., 1991, Diatoms in the Holocene Sediments of the Maxwell Bay, King George Island, Antarctica. *Korean Journal of Polar Research*, 2(1), 159-177.
- Wong, A., 1994, *Structure and Dynamics of Prydz Bay, Antarctica, as inferred from a Summer Hydrographic Data Set*. MPOSc Thesis, Institute of Antarctic and Southern Ocean Studies, University of Tasmania, 104 p.
- Wong, A.P.S., Bindoff, N.L. and Forbes, A. 1998, Ocean-ice shelf interactions and possible bottom water formation in Prydz Bay, Antarctica. *Antarctic Research Series*, 75, 173-187.
- Worby, A.P., Bindoff, N.L., Lytle, V.I., Allison, I., and Massom, R.A., 1996, Winter ocean/sea ice interactions in the East Antarctic Pack ice. *EOS Transactions*, 77(43), 456-457.
- Worby, A.P., Massom, R.A., Allison, I., Lytle, V.I. and Heil, P., 1998, East Antarctic sea ice: a review of its structure, properties and drift. *Antarctic Research Series*, 74, 41-67.
- Wornardt, W.W., 1967, Miocene and Pliocene marine diatoms from California. *Occasional papers of the California Academy of Sciences*, 63, 108.
- Yanagisawa, Y. and Akiba, F., 1990, Taxonomy and phylogeny of the three marine diatom genera *Crucidenticula*, *Denticulopsis* and *Neodenticula*. *Bulletin of the Geological Survey of Japan*, 41(5), 197-301.
- Yoshida, Y., 1983, Physiography of the Prince Olav and Prince Harald Coasts, East Antarctica. *Tokyo National Institute of Polar Research Memoirs*, 13(C), 83 p.
- Young, N.W., Turner, D., Hyland, G., and Williams, R.N., 1998, Near-coastal ice berg distribution in East Antarctica 50-145° E. *Annals of Glaciology*, 27, 68-75.
- Zachos, J. C., Stott, L. D., and Lohmann, K C., 1994, Evolution of early Cenozoic marine temperatures. *Paleoceanography*, 9(2), 353-387.
- Zachos, J.C., Flower, B.P., and Paul, H., 1997, Orbitally paced climate oscillations across the Oligocene/Miocene boundary. *Nature*, 388, 567-570.
- Zar, J.H., 1984, *Biostatistical Analysis*. Prentice-Hall Inc., New Jersey, 718 p.

- Zhang, Q., 1983, Periglacial landforms in the Vestfold Hills, East Antarctica: preliminary observations and measurements, (In, Oliver, R.L., James, P.R. and Jago, J.B. (Editors), *Antarctic earth science; fourth international symposium*. Cambridge University Press, 1983, p.478-481).
- Zhang, Q., 1989, Evolution of the Antarctic ice sheet since late Pleistocene. *International Symposium on Antarctic Research. Proceedings*. China Ocean Press, Tianjin, 67-73.
- Zhang, Q. and Peterson, J.A, 1984, A geomorphology and late Quaternary geology of the Vestfold Hills, Antarctica. *ANARE Reports*, 133, 84 p.
- Zhang, Q., Xie, Y., and Li, Y., 1983, A preliminary study of the evolution of the post late Pleistocene Vestfold Hills environment, East Antarctica. (In, Oliver, R.L., James, P.R. and Jago, J.B., (Editors), *Antarctic Earth Science*. Cambridge University Press, Cambridge, pp. 473-477).
- Zielinski, U. and Gersonde, R., 1997, Diatom distribution in Southern Ocean surface sediments (Atlantic sector): Implications for paleoenvironmental reconstructions. *Palaeogeography, Palaeoclimatology, Palaeoecology*, 129, 213-250.
- Zwally, H.J., Comiso, J.C., Parkinson, C.L., Campbell, W.J., Carsey, F.D., and Gloersen, P., 1983, *Antarctic Sea Ice, 1973-1976 satellite passive-microwave observations*. NASA Scientific and Technical Information Branch, NASA SP- 459, Washington, 206 p.
- Zwally, H.J., Comiso, J.C., and Gordon, A.L., 1985, Antarctic offshore leads and polynyas and oceanographic effects. *Antarctic Research Series*, 43, 203-226.
- Zwally, H.J., 1994, Detection of Change in Antarctica. (In, Hempel, G., (Editor), *Antarctic Science and Global Concerns*. Springer-Verlag, Berlin, pp. 126-143).

---

**Appendix 1:**  
**Southern Ocean Locations in the Thesis Text**

---



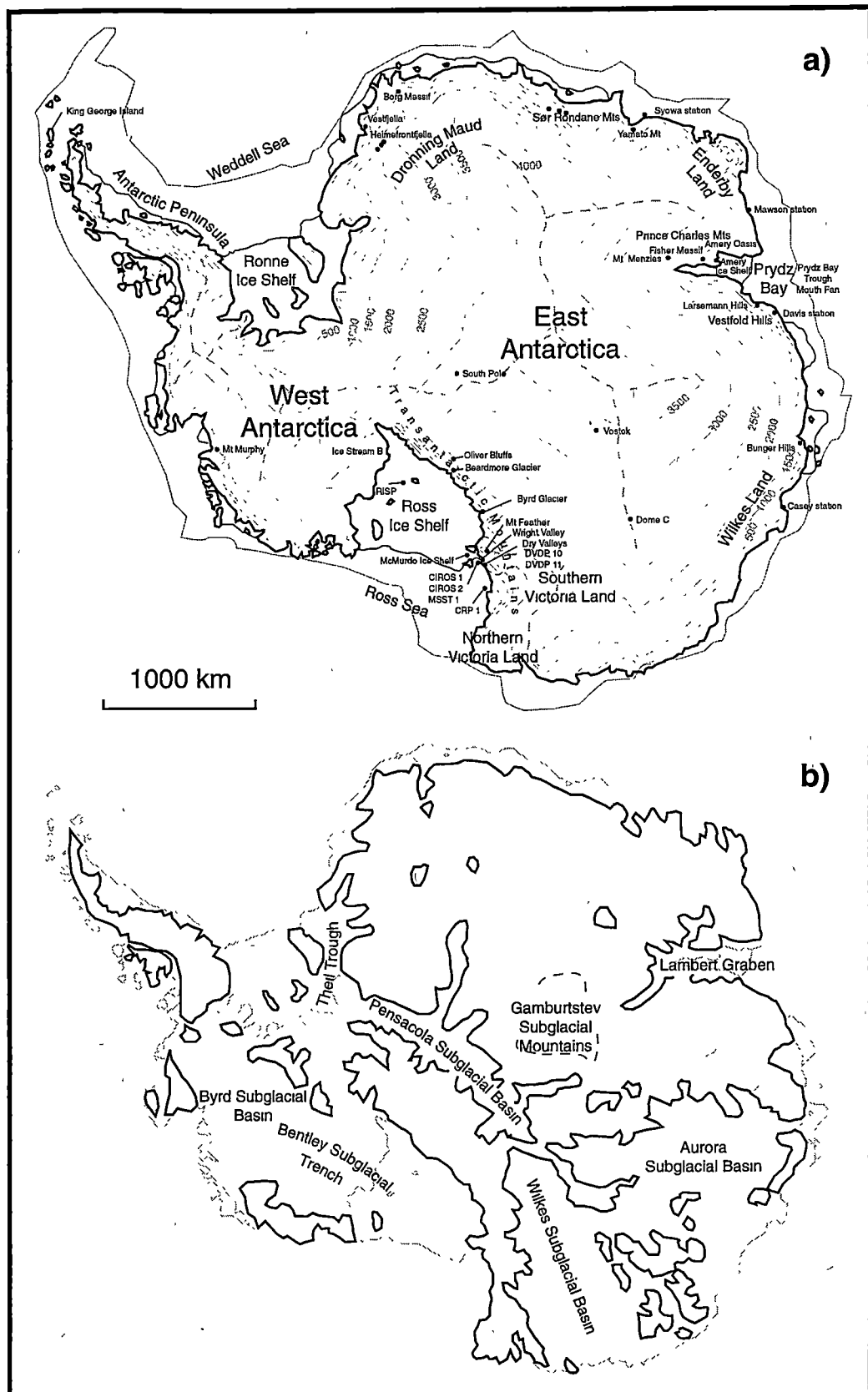
**Appendix 1.** Southern Ocean locations mentioned in the text.

---

## **Appendix 2:**

### **Antarctic Locations in the Thesis Text**

---



**Appendix 2.** Antarctic locations mention in the text, illustrated on modern surface and continental shelf (a) and subglacial topographic maps (b).

---

**Appendix 3:**  
**Southern Kerguelen Plateau Diatom Data**

---

### Appendix 3. Quantitative relative abundance (%) of diatoms in Kerguelen Plateau cores.

GC 48 (lat 58°31'0"S, long 81°73'0"E)																					
CORE DEPTH (cm)		0	10	20	30	40	50	60	70	80	90	100	110	120	130	140	150	160	170	180	190
DIATOMS																					
<i>Actinocyclus actinochilus</i>		1.24	0.00	0.30	0.65	0.37	1.13	0.99	0.85	0.00	0.53	0.00	0.00	0.00	0.45	0.19	0.49	0.57	0.39	0.00	0.46
<i>Actinocyclus dimorphus</i>		0.00	0.00	0.00	0.00	0.00	0.00	0.00	0.00	0.00	0.00	0.00	0.00	0.00	0.00	0.00	0.00	0.00	0.00	0.00	0.00
<i>Actinocyclus fasciculatus</i>		0.00	0.00	0.00	0.00	0.00	0.00	0.00	0.00	0.00	0.00	0.00	0.00	0.00	0.00	0.00	0.00	0.00	0.00	0.00	0.00
<i>Actinocyclus ingens</i>		0.00	0.00	0.00	0.00	0.00	1.30	9.70	6.84	34.44	41.11	27.30	12.24	11.56	13.62	8.92	22.00	37.64	20.70	34.39	14.09
<i>Actinocyclus karstenii</i>		0.00	0.00	0.00	0.00	0.00	0.00	0.00	0.00	0.00	0.00	0.00	0.00	0.00	0.00	0.00	0.00	0.00	0.00	0.00	0.00
<i>Asteromphalus hookeri</i>		0.00	0.00	0.00	0.00	0.00	0.00	0.00	0.00	0.00	0.00	0.00	0.00	0.00	0.00	0.00	0.00	0.38	0.19	0.00	0.00
<i>Asteromphalus hepaticus / parvulus</i>		0.16	0.00	0.15	0.00	0.00	0.00	0.40	0.00	0.00	0.00	0.00	0.00	0.00	0.45	0.00	0.16	1.14	0.00	0.00	0.00
<i>Asteromphalus hyalinus</i>		0.16	0.52	0.30	0.16	0.00	0.00	0.00	0.00	0.00	0.00	0.00	0.00	0.00	0.00	0.19	0.00	0.00	0.00	0.00	0.00
<i>Azpetia tabulans</i>		0.16	0.17	0.30	0.16	0.00	0.00	0.00	0.00	0.00	0.53	0.00	0.00	0.00	0.00	0.00	0.00	0.00	0.00	0.00	0.00
<i>Chaetoceros bulbosum</i>		0.16	0.34	0.30	0.00	0.19	0.00	0.00	0.21	0.22	0.80	0.77	0.23	0.00	0.45	0.00	0.33	0.00	0.19	0.00	0.00
<i>Chaetoceros cysts</i>		0.00	0.17	1.07	0.82	1.12	1.94	2.77	1.28	1.56	0.27	1.02	0.68	0.71	0.89	0.56	0.16	0.00	0.19	0.00	1.07
<i>Corethron crophilum</i>		0.00	0.00	0.00	0.00	0.00	0.00	0.00	0.00	0.00	0.00	0.00	0.00	0.00	0.00	0.00	0.00	0.00	0.00	0.00	0.00
<i>Coscinodiscus spp</i>		0.16	0.00	0.00	0.16	0.00	0.16	0.00	0.00	0.00	0.00	0.51	0.00	0.47	0.45	0.74	0.33	0.38	0.39	0.33	0.31
<i>Dactylosolen antarcticus</i>		3.89	5.51	4.26	7.53	1.49	3.08	3.37	1.50	2.89	2.39	7.14	17.69	8.25	4.02	5.76	2.63	1.71	2.71	1.67	2.76
<i>Denticulopsis spp</i>		0.00	0.00	0.00	0.00	0.00	0.00	0.00	0.00	0.00	0.00	0.00	0.00	0.00	0.00	0.00	0.00	0.00	0.00	0.00	0.00
<i>Eucampia antarctica</i>		0.93	0.52	0.15	2.13	0.56	2.11	2.57	0.43	1.78	0.00	0.26	1.13	1.18	0.22	0.93	0.33	0.76	0.39	0.33	0.31
<i>Fragilaropsis aurica</i>		0.00	0.00	0.00	0.00	0.00	0.00	0.00	0.00	0.00	0.00	0.00	0.00	0.00	0.00	0.00	0.00	0.00	0.00	0.00	0.00
<i>Fragilaropsis barronii</i>		0.00	0.00	0.00	0.00	0.00	0.00	0.00	0.00	0.00	0.00	0.00	0.00	0.00	0.00	0.00	0.00	0.00	0.00	0.00	0.00
<i>Fragilaropsis barronii</i> var A + B		0.00	0.00	0.00	0.00	0.00	0.00	0.79	4.49	8.67	8.22	18.62	20.41	13.44	20.31	8.36	25.29	21.67	27.27	16.36	11.18
<i>Fragilaropsis curta</i>		4.04	6.88	2.28	2.45	3.72	5.02	4.55	8.12	4.22	9.02	9.18	12.93	5.90	10.49	17.29	9.85	3.23	7.16	6.51	33.08
<i>Fragilaropsis cylindrus</i>		0.00	0.17	0.00	0.16	0.00	0.65	0.40	0.21	0.00	0.53	0.51	0.23	0.24	0.45	0.93	0.00	0.00	0.58	0.00	1.68
<i>Fragilaropsis interfrigidana</i>		0.00	0.00	0.00	0.00	0.00	0.00	0.00	0.00	0.00	0.27	0.00	0.00	0.24	0.22	0.56	0.00	0.00	0.39	0.17	0.00
<i>Fragilaropsis kerguelensis</i>		61.43	64.72	71.54	65.47	70.76	56.89	36.44	37.82	14.22	5.57	3.32	6.35	19.58	13.84	0.37	2.79	2.09	5.80	13.36	0.92
<i>Fragilaropsis obliquecostata</i>		0.00	0.00	0.00	0.00	0.19	0.00	0.20	0.00	0.00	0.00	0.00	0.00	0.00	0.00	0.19	0.00	0.00	0.58	0.00	0.15
<i>Fragilaropsis praecurta</i> (?)		0.00	0.00	0.00	0.00	0.00	0.00	0.00	0.00	0.00	0.00	0.00	0.00	0.00	0.00	0.00	0.33	0.00	0.97	0.17	0.61
<i>Fragilaropsis praeterfrigidana</i>		0.00	0.00	0.00	0.00	0.00	0.00	0.00	0.00	0.00	0.00	0.00	0.00	0.00	0.00	0.00	0.00	0.00	0.00	0.00	0.00
<i>Fragilaropsis ritscheri</i>		0.78	1.03	1.37	1.31	0.56	2.27	9.11	11.54	6.89	1.86	4.59	1.81	1.65	1.12	1.12	3.45	0.38	0.77	3.17	0.31
<i>Fragilaropsis rhombica</i>		1.24	0.52	1.22	2.13	1.12	2.11	0.99	1.07	0.22	1.06	0.77	0.45	0.24	0.22	1.12	3.61	0.38	0.77	0.33	0.77
<i>Fragilaropsis separanda</i>		11.04	9.12	4.87	6.22	8.75	6.16	9.31	9.83	7.33	6.63	6.12	0.91	5.42	2.68	2.23	3.61	0.76	0.58	0.83	0.77
<i>Fragilaropsis separanda</i> var A		0.00	0.00	0.00	0.00	0.00	0.00	0.00	0.00	0.00	0.00	0.00	0.00	0.00	0.00	0.00	0.00	0.00	0.00	0.00	0.00
<i>Fragilaropsis sublinearis</i>		0.00	0.00	0.00	0.33	0.00	0.00	0.59	0.21	0.44	0.27	0.26	0.45	0.00	0.22	1.12	0.66	0.19	0.00	0.33	0.77
<i>Fragilaropsis weaveri</i>		0.00	0.00	0.00	0.00	0.00	0.00	0.00	0.00	0.00	0.00	0.00	0.00	0.00	0.00	0.00	0.00	0.00	0.00	0.00	0.00
<i>Hemidiscus karstenii</i>		0.00	0.00	0.00	0.00	0.00	0.00	0.00	0.00	0.00	0.00	0.00	0.00	0.00	0.00	0.00	0.00	0.00	0.19	0.00	0.00
<i>Navicula directa</i>		0.00	0.00	0.15	0.16	1.12	0.49	0.20	0.85	0.00	0.00	0.00	0.45	0.00	0.00	0.00	0.00	0.00	0.00	0.00	0.00
<i>Navicula glaciei</i>		0.00	0.00	0.00	0.00	0.00	0.00	0.00	0.00	0.00	0.00	0.00	0.00	0.00	0.00	0.00	0.00	0.00	0.00	0.00	0.00
<i>Nitzschia fossilis</i>		0.00	0.00	0.00	0.00	0.00	0.00	0.00	0.00	0.00	0.00	0.00	0.00	0.00	0.00	0.19	0.00	0.00	0.00	0.00	0.00
<i>Nitzschia perrillii</i>		0.00	0.00	0.00	0.00	0.00	0.00	0.20	0.21	0.00	0.00	0.26	0.91	0.47	0.67	0.37	0.33	0.19	0.77	0.00	0.92
<i>Nitzschia reinholdii</i>		0.00	0.00	0.00	0.00	0.00	0.00	0.00	0.00	0.00	0.00	0.00	0.00	0.00	0.00	0.00	0.00	0.00	0.00	0.00	0.00
<i>Proboscia alata</i>		0.00	0.00	0.00	0.00	0.00	0.00	0.00	0.00	0.00	0.00	0.00	0.00	0.00	0.00	0.00	0.00	0.00	0.00	0.00	0.00
<i>Proboscia barbol</i>		0.00	0.00	0.00	0.00	0.00	0.00	0.00	0.00	0.00	0.00	0.00	0.00	0.00	0.00	0.00	0.00	0.00	0.00	0.00	0.15
<i>Rhizosolenia hebetata</i> (group)		0.31	0.00	0.00	0.16	0.00	0.00	0.00	0.21	0.00	1.86	2.30	0.91	0.71	0.00	0.19	0.00	0.00	0.19	0.17	0.00
<i>Rhizosolenia styliformis</i> (group)		0.16	0.69	0.46	0.82	0.93	0.65	1.98	1.92	3.78	5.31	3.83	2.27	1.65	1.56	1.12	3.28	2.85	3.87	0.50	1.23
<i>Rhizosolenia</i> sp A		0.00	0.00	0.00	0.00	0.00	0.00	0.00	0.00	0.44	0.80	2.55	2.49	2.83	2.46	1.67	1.15	0.57	0.77	0.17	0.15
<i>Rhizosolenia</i> spp		0.00	0.00	0.00	0.00	0.00	0.00	0.20	0.00	0.00	0.00	0.00	0.00	0.00	0.00	0.19	0.16	0.38	0.00	0.00	0.00
<i>Rouxia antarctica</i>		0.00	0.00	0.00	0.00	0.00	0.00	0.00	0.00	0.00	0.00	0.00	0.91	0.71	0.67	0.37	0.00	0.00	0.00	0.00	0.00
<i>Rouxia heteropolara</i>		0.00	0.00	0.00	0.00	0.00	0.00	0.00	0.00	0.00	0.00	0.00	0.00	0.00	0.00	0.00	0.00	0.00	0.00	0.00	0.00
<i>Rouxia isoplocia</i>		0.00	0.00	0.00	0.00	0.37	0.97	3.17	4.49	2.89	1.06	1.02	4.54	3.77	5.80	29.18	4.11	1.33	3.09	1.84	5.05
<i>Rouxia leventerae</i>		0.00	0.00	0.00	0.00	0.00	0.00	0.00	0.00	0.00	0.00	0.00	0.00	0.00	0.00	0.00	0.00	0.00	0.00	0.00	0.00
<i>Rouxia naviculoides</i>		0.00	0.00	0.00	0.00	0.00	0.00	0.00	0.00	0.00	0.00	0.00	0.00	0.00	0.00	0.00	0.38	1.16	0.50	0.00	0.00
<i>Stellarima microtrias</i>		0.78	0.00	0.15	0.33	0.00	0.49	0.20	0.00	0.00	0.53	0.51	0.23	0.24	1.12	0.00	0.49	0.76	0.00	0.33	0.00
<i>Stephanopyxis</i> spp		0.00	0.00	0.00	0.00	0.00	0.00	0.00	0.00	0.00	0.00	0.00	0.00	0.00	0.00	0.00	0.00	0.00	0.00	0.00	0.00
<i>Thalassionema nitzschoides</i> (group)		0.00	0.00	0.00	0.00	0.00	0.00	0.00	0.00	0.00	0.00	0.00	0.00	0.00	0.00	0.00	0.00	0.00	0.00	0.00	0.00
<i>Thalassionema nitzschoides</i> var parva		0.00	0.00	0.00	0.00	0.00	0.00	0.00	0.00	0.00	0.00	0.00	0.00	0.00	0.00	0.00	0.00	0.00	0.00	0.00	0.00
<i>Thalassiosira antarctica</i>		0.00	0.00	0.00	0.00	0.00	0.00	0.00	0.00	0.00	0.00	0.00	0.00	0.00	0.00	1.67	0.00	0.00	0.00	0.00	0.00
<i>Thalassiosira complicata</i>																					



# Appendix 3. continued

GC 48		200	210	220	230	240	250	260	270	280	290	300	310	320	330	340	350	360	370	380	390
CORE DEPTH (cm)																					
DIATOMS																					
<i>Actinocyclus actinocylus</i>		0.00	0.00	0.00	0.16	0.00	0.36	0.17	0.42	0.18	0.00	0.17	0.00	0.00	0.00	0.00	0.17	0.00	0.00	0.33	0.00
<i>Actinocyclus dimorphus</i>		0.00	0.00	0.00	0.00	0.00	0.00	0.00	0.00	0.00	0.00	0.00	0.00	0.00	0.00	0.00	0.00	0.00	0.00	0.00	2.72
<i>Actinocyclus fasciculatus</i>		0.00	0.00	0.00	0.00	0.00	0.00	0.00	0.00	0.00	0.00	0.00	0.00	0.00	0.00	0.00	0.00	0.00	0.19	0.00	6.52
<i>Actinocyclus ingens</i>	25.93	32.23	20.65	20.62	14.88	39.89	37.76	30.57	16.64	13.79	14.93	14.78	4.41	13.07	12.48	19.16	18.66	25.23	21.85	1.09	
<i>Actinocyclus karstenii</i>	0.00	0.00	0.00	0.00	0.00	0.00	0.00	0.00	0.00	0.00	0.00	0.00	0.00	0.00	0.00	0.00	0.00	0.00	0.00	0.00	0.00
<i>Asteromphalus hookeri</i>	0.15	0.00	0.00	0.00	0.00	0.18	0.17	0.00	0.00	0.19	0.00	0.34	0.00	0.00	0.00	0.00	0.00	0.00	0.37	0.00	0.00
<i>Asteromphalus hepaticus / parvulus</i>	0.00	0.00	0.15	0.31	0.00	0.18	0.00	0.00	0.00	0.00	0.00	0.00	0.00	0.00	0.00	0.54	0.17	0.00	0.19	0.33	0.00
<i>Asteromphalus hyalinus</i>	0.00	0.00	0.00	0.00	0.00	0.00	0.00	0.00	0.00	0.19	0.17	0.17	0.00	0.35	0.00	0.17	0.18	0.19	0.17	0.00	0.00
<i>Azpeitia tabularis</i>	0.00	0.00	0.00	0.00	0.00	0.00	0.00	0.00	0.00	0.00	0.00	0.00	0.00	0.00	0.00	0.00	0.00	0.00	0.00	0.00	0.00
<i>Chaetoceros bulbosum</i>	0.00	0.00	0.00	0.16	0.00	0.18	0.00	0.21	0.00	0.19	0.00	0.00	0.30	0.00	0.00	0.00	0.18	0.00	0.33	0.00	0.00
<i>Chaetoceros cysts</i>	0.00	0.00	0.00	0.00	0.46	0.00	0.00	0.21	0.36	0.00	0.00	0.00	0.00	0.00	0.00	0.00	0.00	0.00	0.00	0.18	0.00
<i>Corethron crophilum</i>	0.00	0.00	0.00	0.00	0.00	0.00	0.00	0.00	0.00	0.00	0.00	0.00	0.00	0.00	0.00	0.00	0.00	0.00	0.00	0.00	0.00
<i>Coscinodiscus spp</i>	0.31	0.31	0.15	0.00	0.00	0.00	0.00	0.21	0.54	1.55	0.52	0.52	0.00	0.35	0.18	0.35	0.00	0.56	0.00	0.00	0.00
<i>Dactylosolen antarcticus</i>	5.25	4.87	8.32	10.23	0.46	2.86	2.80	2.34	2.53	0.00	7.29	8.42	2.58	2.30	2.35	1.05	1.76	0.58	1.66	5.43	
<i>Denticulopsis spp</i>	0.00	0.00	0.00	0.00	0.00	0.00	0.00	0.00	0.00	0.00	0.00	0.00	0.00	0.00	0.00	0.00	0.00	0.00	0.00	0.00	0.00
<i>Eucampia antarctica</i>	0.31	0.47	0.00	0.00	0.92	0.89	0.35	0.21	0.36	0.19	0.00	0.34	0.00	0.35	0.36	0.17	0.53	1.11	0.83	0.54	
<i>Fragilaropsis aurica</i>	0.00	0.00	0.00	0.00	0.00	0.00	0.00	0.00	0.00	0.00	0.00	0.00	0.00	0.00	0.00	0.00	0.00	0.00	0.00	0.00	0.00
<i>Fragilaropsis baronii</i>	0.00	0.00	0.00	0.00	0.00	0.00	0.00	0.00	0.00	0.00	0.00	0.00	0.00	0.00	0.00	0.00	0.00	0.00	0.00	0.54	
<i>Fragilaropsis baronii var A + B</i>	18.67	15.25	35.36	17.36	3.07	11.45	10.14	5.73	9.22	18.25	13.54	14.26	10.33	10.07	12.30	14.98	13.03	7.05	10.93	2.90	
<i>Fragilaropsis curta</i>	10.96	9.12	8.62	19.84	0.46	1.25	6.64	3.18	5.61	6.21	12.33	9.97	46.81	13.60	14.47	8.01	12.50	4.45	7.12	16.67	
<i>Fragilaropsis cylindrus</i>	0.62	0.31	0.15	0.00	0.00	0.00	0.00	0.00	0.00	0.19	0.00	0.00	0.00	0.00	0.00	0.00	0.00	0.00	0.00	0.00	0.00
<i>Fragilaropsis interfrigidaria</i>	0.77	0.16	0.15	0.00	0.00	0.18	0.35	0.00	0.00	0.00	0.00	0.00	0.00	0.00	0.00	0.00	0.00	0.00	0.00	0.00	0.00
<i>Fragilaropsis kerguelensis</i>	6.33	1.73	10.10	6.82	50.31	14.67	3.15	11.25	20.25	1.94	1.56	1.20	0.61	0.88	3.98	5.57	5.28	5.01	6.62	1.63	
<i>Fragilaropsis obliquecostata</i>	0.00	0.16	0.00	0.16	0.00	0.18	0.00	0.00	0.00	0.19	0.00	0.00	0.00	0.00	0.00	0.00	0.00	0.00	0.33	0.00	0.00
<i>Fragilaropsis praecurta (?)</i>	0.31	0.47	0.15	0.16	0.00	0.18	0.35	0.64	1.81	5.83	3.65	4.12	1.06	5.65	2.53	1.74	1.94	1.48	1.32	3.62	
<i>Fragilaropsis praeterfrigidaria</i>	0.00	0.00	0.00	0.00	0.00	0.00	0.00	0.00	0.00	0.00	0.00	0.00	0.00	0.00	0.00	0.00	0.18	0.00	0.17	0.54	
<i>Fragilaropsis ritscheri</i>	1.54	0.31	0.89	0.16	0.46	0.00	0.70	0.42	0.00	0.39	0.17	0.52	0.00	0.35	0.18	0.52	0.53	0.19	0.00	0.72	
<i>Fragilaropsis rhombica</i>	0.62	0.00	0.00	0.00	0.31	0.36	0.35	0.64	0.18	0.00	0.69	0.00	0.00	0.00	0.36	0.00	0.00	0.00	0.66	0.36	
<i>Fragilaropsis separanda</i>	0.77	0.00	0.00	0.16	2.91	0.18	0.17	0.21	0.18	0.00	0.00	0.00	0.00	0.00	0.00	0.00	0.00	0.00	0.00	0.00	0.00
<i>Fragilaropsis separanda var A</i>	0.00	0.00	0.00	0.00	0.00	0.00	0.00	0.00	0.00	0.00	0.00	0.00	0.00	0.00	0.00	0.00	0.00	0.00	0.00	0.00	0.00
<i>Fragilaropsis sublinearis</i>	0.15	0.79	0.00	0.31	0.46	0.36	0.00	0.00	0.36	0.19	0.35	0.86	0.30	0.18	0.36	0.00	0.35	0.00	0.00	0.54	
<i>Fragilaropsis weaveri</i>	0.00	0.00	0.00	0.00	0.00	0.00	0.00	0.00	0.00	0.00	0.00	0.00	0.00	0.00	0.00	0.00	0.00	0.00	0.00	0.00	0.00
<i>Hemidiscus karstenii</i>	0.00	0.00	0.00	0.00	0.00	0.00	0.00	0.00	0.00	0.00	0.00	0.00	0.00	0.00	0.00	0.00	0.00	0.00	0.00	0.00	0.00
<i>Navicula directa</i>	0.15	0.31	0.00	0.00	0.00	0.00	0.00	0.00	0.00	0.00	0.00	0.00	0.00	0.00	0.00	0.00	0.00	0.00	0.00	0.00	0.00
<i>Navicula glaciei</i>	0.00	0.31	0.00	0.16	0.00	0.00	0.00	0.00	0.00	0.00	0.00	0.00	0.00	0.00	0.00	0.00	0.00	0.00	0.00	0.00	0.00
<i>Nitzschia fossilis</i>	0.15	0.00	0.00	0.00	0.00	0.00	0.00	0.00	0.00	0.00	0.00	0.35	0.00	0.15	0.18	0.00	0.00	0.00	0.00	0.18	0.00
<i>Nitzschia perrigalli</i>	1.23	2.04	0.45	1.55	0.00	0.36	0.87	0.00	0.00	0.97	0.35	0.69	1.52	0.53	0.18	1.57	0.53	0.19	0.00	0.72	
<i>Nitzschia reinholdii</i>	0.00	0.00	0.00	0.00	0.00	0.00	0.00	0.00	0.00	0.00	0.00	0.00	0.00	0.00	0.00	0.00	0.00	0.00	0.00	0.00	0.00
<i>Proboscia alata</i>	0.00	0.00	0.00	0.00	0.00	0.00	0.00	0.00	0.00	0.00	0.00	0.00	0.00	0.00	0.00	0.00	0.00	0.00	0.00	0.00	0.00
<i>Proboscia barboi</i>	0.00	0.00	0.00	0.00	0.00	0.00	0.00	0.00	0.21	0.00	0.00	0.00	0.00	0.00	0.00	0.00	0.00	0.00	0.00	0.00	0.00
<i>Rhizosolenia hebetata (group)</i>	0.00	0.00	0.00	0.00	0.00	0.00	0.00	0.00	0.00	0.00	0.17	0.00	0.15	0.00	0.18	0.00	0.00	0.00	0.00	0.00	0.00
<i>Rhizosolenia styliformis (group)</i>	0.62	0.79	1.19	0.16	0.61	1.07	1.92	0.85	0.18	0.97	0.87	1.03	0.46	0.88	0.90	0.87	0.88	1.48	1.82	2.90	
<i>Rhizosolenia sp. A</i>	0.31	0.31	0.89	0.31	0.00	0.00	0.00	0.00	0.18	0.19	0.17	0.69	2.74	0.53	0.18	0.17	0.00	0.19	0.17	1.27	
<i>Rhizosolenia spp</i>	0.15	0.00	0.00	0.00	0.00	0.00	0.17	0.00	0.00	0.00	0.00	0.00	0.00	0.00	0.00	0.00	0.00	0.00	0.00	0.00	0.00
<i>Rouxia antarctica</i>	0.00	0.00	0.00	0.00	0.00	0.72	4.90	2.97	10.31	15.92	12.67	13.23	8.97	16.43	16.27	7.84	8.27	7.42	5.63	13.59	
<i>Rouxia heteropolara</i>	0.00	0.00	0.00	0.00	0.00	0.00	0.00	0.00	0.00	0.00	0.00	0.00	0.00	0.00	0.00	0.00	0.00	0.00	0.00	0.00	0.00
<i>Rouxia isopolara</i>	4.48	11.01	1.19	2.17	0.46	1.25	1.40	0.21	0.36	0.39	0.69	0.69	1.67	1.94	1.63	0.52	0.18	0.00	0.37	0.50	1.27
<i>Rouxia leventerae</i>	0.00	0.00	0.00	0.00	0.00	0.00	0.00	0.00	0.00	0.00	0.00	0.00	0.00	0.00	0.00	0.00	0.00	0.00	0.00	0.00	0.00
<i>Rouxia naviculoides</i>	0.31	0.00	0.30	0.00	0.61	3.76	11.54	18.90	9.22	10.49	8.68	8.76	5.17	5.65	6.51	5.57	5.81	4.27	5.63	8.15	
<i>Stellaria microtrias</i>	0.00	0.00	0.00	0.00	0.00	0.00	0.00	0.21	0.00	0.39	0.35	0.52	0.00	0.35	0.18	0.00	0.53	0.37	0.33	0.00	0.00
<i>Stephanopyxis spp</i>	0.00	0.00	0.00	0.00	0.00	0.00	0.00	0.00	0.00	0.00	0.00	0.00	0.00	0.00	0.00	0.00	0.00	0.00	0.00	0.00	0.00
<i>Thalassionema nitzschoides (group)</i>	0.00	0.00	0.00	0.00	2.91	0.36	0.00	0.64	0.00	0.00	0.00	0.00	0.00	0.00	0.00	0.00	0.00	0.00	0.00	0.00	0.00
<i>Thalassionema nitzschoides var parva</i>	0.00	0.00	0.00	0.00	0.00	0.00	0.00	0.00	0.00	0.00	0.00	0.00	0.00	0.00	0.00	0.00	0.00	0.00	0.00	0.00	0.00
<i>Thalassiosira antarctica</i>	0.00	0.00	0.00	0.00	0.00	0.00	0.00	0.00	0.00	0.00	0.17	0.00	0.00	0.00	0.00	0.00	0.00	0.00	0.00	0.00	0.00
<i>Thalassiosira complicata</i>	0.00	0.00	0.00	0.00	0.00	0.00	0.00	0.00	0.00	0.00	0.00	0.00	0.00	0.00	0.00	0.00	0.00	0.00	0.00	0.00	0.00
<i>Thalassiosira elliptica</i>	0.31	0.47	0.30	0.00	0.18	0.17	0.00	0.18	0.00	0.00	0.00	0.00	0.00	0.18	0.00	0.00	0.00	0.19	0.17	0.00	0.00
<i>Thalassiosira fasciculata</i>	0.93	0.63	0.74	0.00	0.00	0.72	0.35	0.42	0.54	0.97	1.39	1.03	0.46								

# Appendix 3. continued

GC 48								
CORE DEPTH (cm)	400	410	420	430	440	450	460	470
DIATOMS								
<i>Actinocyclus actinocylus</i>	0.00	0.00	0.00	0.00	0.00	0.00	0.00	0.00
<i>Actinocyclus dimorphus</i>	0.00	0.00	0.00	0.00	0.00	0.00	0.00	0.00
<i>Actinocyclus fasciculatus</i>	1.59	0.99	0.85	0.17	0.00	0.00	0.00	0.00
<i>Actinocyclus ingens</i>	3.34	1.82	2.39	0.51	0.34	0.00	0.38	0.00
<i>Actinocyclus karstenii</i>	1.91	2.48	2.56	2.91	0.00	0.00	0.00	0.00
<i>Asteromphalus hooker</i>	0.00	0.00	0.00	0.00	0.00	0.00	0.00	0.00
<i>Asteromphalus hepaticus / parvulus</i>	0.00	0.00	0.34	0.00	0.00	0.18	0.00	0.00
<i>Asteromphalus hyalinus</i>	0.32	0.33	0.00	0.00	0.00	0.00	0.00	0.00
<i>Azpeitia tabularis</i>	0.00	0.00	0.00	0.00	0.00	0.36	0.00	0.00
<i>Chaetoceros bulbosum</i>	0.00	0.00	0.00	0.00	0.00	0.18	0.00	0.21
<i>Chaetoceros cysts</i>	0.64	1.49	0.68	0.68	2.85	6.42	4.73	4.18
<i>Corethron criophilum</i>	0.00	0.00	0.17	0.17	1.34	0.71	1.51	2.51
<i>Coscinodiscus spp</i>	0.16	0.00	0.17	0.00	0.00	0.00	0.00	0.00
<i>Dactylosolen antarcticus</i>	6.52	8.91	9.22	9.25	16.42	15.33	8.88	15.24
<i>Denticulopsis spp</i>	0.16	0.00	0.00	0.00	0.00	0.00	0.00	0.00
<i>Eucampia antarctica</i>	1.11	0.99	0.85	0.68	0.34	0.36	0.38	0.42
<i>Fragilaropsis aunca</i>	0.00	0.00	0.00	0.00	0.00	0.00	0.00	0.00
<i>Fragilaropsis barronii</i>	0.32	1.98	1.54	8.05	20.10	18.54	27.98	27.77
<i>Fragilaropsis barronii</i> var A + B	4.29	6.60	4.78	4.45	2.35	2.50	0.95	0.42
<i>Fragilaropsis curta</i>	13.35	15.18	16.04	6.68	7.04	6.42	9.26	5.85
<i>Fragilaropsis cylindrus</i>	0.00	0.00	0.00	0.00	0.00	0.00	0.00	0.00
<i>Fragilaropsis interfrigidana</i>	0.00	0.99	0.51	0.86	3.02	1.60	0.85	1.04
<i>Fragilaropsis kerguelensis</i>	0.79	0.66	0.00	0.00	0.00	0.00	0.00	0.00
<i>Fragilaropsis obliquecostata</i>	0.00	0.17	0.00	0.00	0.00	0.18	0.00	0.00
<i>Fragilaropsis praecurta</i> (?)	2.86	1.49	2.90	0.51	0.00	0.00	0.00	0.00
<i>Fragilaropsis praeinterfrigidana</i>	0.32	0.66	1.19	5.14	6.87	3.92	10.21	7.31
<i>Fragilaropsis ritscheri</i>	0.48	0.17	0.85	1.54	0.17	0.00	0.00	0.00
<i>Fragilaropsis rhombica</i>	0.00	0.00	0.00	0.00	0.00	0.00	0.00	0.00
<i>Fragilaropsis separanda</i>	0.00	0.00	0.00	0.00	0.00	0.00	0.00	0.00
<i>Fragilaropsis separanda</i> var A	0.00	0.00	0.00	0.00	0.00	0.00	0.00	0.00
<i>Fragilaropsis sublineans</i>	0.79	0.33	0.51	0.51	0.50	0.18	0.00	0.00
<i>Hemidiscus karstenii</i>	0.00	0.00	1.02	0.00	0.00	0.00	0.00	0.00
<i>Navicula directa</i>	0.00	0.00	0.00	0.17	0.00	0.00	0.00	0.00
<i>Navicula glaci</i>	0.00	0.00	0.00	0.00	0.00	0.00	0.00	0.00
<i>Nitzschia fossilis</i>	0.48	0.83	0.51	0.17	0.00	0.18	0.19	0.00
<i>Nitzschia parrigallii</i>	0.16	0.00	0.34	0.51	0.00	0.18	0.00	0.00
<i>Nitzschia reinholdii</i>	0.00	0.00	0.00	0.00	0.00	0.00	0.00	0.00
<i>Fragilaropsis weaveri</i>	0.00	0.00	r	r	0.00	0.36	0.38	0.21
<i>Proboscia alata</i>	0.00	0.00	0.00	0.00	0.00	0.00	0.00	0.00
<i>Proboscia barboi</i>	0.16	0.00	0.00	0.34	0.17	0.00	0.19	0.21
<i>Rhizosolenia hebetata</i> (group)	0.00	0.00	0.17	0.00	0.00	0.00	0.00	0.00
<i>Rhizosolenia styliformis</i> (group)	4.77	3.14	2.22	2.23	0.67	0.36	0.38	2.09
<i>Rhizosolenia</i> sp A	0.95	1.82	2.39	0.51	2.01	1.25	1.32	1.04
<i>Rhizosolenia</i> spp	0.00	0.33	0.51	0.17	0.00	0.18	0.00	0.00
<i>Rouxia antarctica</i>	9.06	9.57	8.53	5.82	5.86	6.24	6.81	5.01
<i>Rouxia heteropolara</i>	0.00	0.00	0.00	0.00	0.00	0.00	0.00	0.00
<i>Rouxia isopolica</i>	1.59	2.31	4.10	2.57	2.01	3.39	1.32	2.30
<i>Rouxia leventerae</i>	2.38	6.11	4.27	3.94	1.51	2.14	0.57	1.25
<i>Rouxia naviculoides</i>	7.79	3.30	1.71	4.28	6.87	4.81	5.10	5.22
<i>Stellarima microtrias</i>	0.48	0.17	0.34	0.17	0.00	0.00	0.00	0.00
<i>Stephanopyxis spp</i>	0.00	0.00	0.00	0.00	0.00	0.00	0.00	0.00
<i>Thalassionema nitzschoides</i> (group)	0.00	0.00	0.00	0.00	0.00	0.00	0.00	0.00
<i>Thalassionema nitzschoides</i> var parva	0.00	0.00	0.00	0.00	0.00	0.00	0.00	0.00
<i>Thalassiosira antarctica</i>	0.00	0.17	0.17	0.00	0.00	0.00	0.00	0.00
<i>Thalassiosira complicata</i>	0.00	0.00	0.00	0.00	0.00	0.00	0.00	0.00
<i>Thalassiosira elliptipora</i>	0.00	0.00	0.00	0.00	0.00	0.00	0.00	0.00
<i>Thalassiosira fasciculata</i>	0.16	0.00	0.00	0.00	0.00	0.00	0.00	0.00
<i>Thalassiosira frenguelli</i>	0.00	0.00	0.00	0.17	0.00	0.00	0.00	0.00
<i>Thalassiosira gracilis</i> var <i>expecta</i>	0.00	0.17	0.00	0.00	0.00	0.00	0.00	0.00
<i>Thalassiosira gracilis</i> var <i>gracilis</i>	0.00	0.00	0.00	0.00	0.00	0.00	0.00	0.00
<i>Thalassiosira gravida</i>	0.00	0.00	0.00	0.00	0.00	0.00	0.00	0.00
<i>Thalassiosira inura</i>	0.00	0.00	0.34	1.03	0.84	1.60	2.84	2.09
<i>Thalassiosira inura-insigna</i> (transition)	0.79	4.29	2.05	2.74	1.34	0.36	0.38	0.00
<i>Thalassiosira insigna</i>	6.04	3.30	2.73	10.96	4.69	4.81	2.08	0.21
<i>Thalassiosira kolbei</i>	0.16	0.00	0.34	0.00	0.00	0.18	0.00	0.00
<i>Thalassiosira lentiginosa</i>	7.63	4.62	4.78	1.20	1.01	2.50	0.76	0.21
<i>Thalassiosira maculata</i>	1.75	1.98	1.54	1.54	0.84	1.07	1.13	1.46
<i>Thalassiosira oestrupii</i>	7.79	4.46	3.41	3.77	5.36	7.49	8.70	10.23
<i>Thalassiosira oliverana</i>	1.75	1.82	1.37	0.86	1.01	0.36	0.57	0.21
<i>Thalassiosira oliverana</i> (coarse)	0.95	0.99	0.17	1.03	0.50	0.89	0.38	0.63
<i>Thalassiosira stnata</i>	0.00	0.00	0.00	0.00	0.00	0.00	0.00	0.00
<i>Thalassiosira torokina</i>	0.16	0.00	0.00	0.00	0.00	0.00	0.00	0.00
<i>Thalassiosira vulnifica</i>	1.59	1.16	5.63	5.82	0.34	0.18	0.00	0.00
<i>Thalassiosira webbi</i>	0.00	0.00	0.00	0.00	0.00	0.00	0.00	0.00
<i>Thalassiothrix spp</i>	0.00	0.00	0.51	0.34	0.50	0.18	0.00	0.00
<i>Trichotoxon reinboldii</i>	1.11	1.16	1.54	2.05	0.50	1.60	1.13	0.21
OTHER	1.27	0.99	2.39	1.54	0.17	0.89	0.00	0.42
SILICOFLAGELLATES	2.07	2.15	1.37	2.91	2.51	1.96	0.57	2.09

# Appendix 3. continued

GC 51 (lat.57°07' 2"S, long 78°27' 2"E)

CORE DEPTH (cm)

DIATOMS

	0	10	20	30	40	50	60	70	80	90	100	110	119	120	130	140	149	150	160	170
<i>Actinocyclus actinocilius</i>	0.00	0.16	0.23	0.50	0.49	1.07	0.52	1.44	0.39	0.00	0.23	0.15	0.18	0.59	0.00	0.00	0.18	0.00	0.00	0.15
<i>Actinocyclus dimorphus</i>	0.00	0.00	0.00	0.00	0.00	0.00	0.00	0.00	0.00	0.00	0.00	0.00	0.00	0.00	0.00	0.00	0.00	0.00	0.00	0.00
<i>Actinocyclus fasciculatus</i>	0.00	0.00	0.00	0.00	0.00	0.27	0.00	0.00	0.00	0.00	0.00	0.00	0.00	0.00	0.00	0.00	0.00	0.00	0.00	0.00
<i>Actinocyclus ingens</i>	0.00	0.00	0.00	0.00	0.32	1.33	21.52	6.88	3.47	24.04	24.32	2.77	56.56	3.37	43.64	15.23	24.64	10.98	13.34	30.00
<i>Actinocyclus karstenii</i>	0.00	0.00	0.00	0.00	0.00	0.00	0.00	0.00	0.00	0.00	0.00	0.00	0.00	0.00	0.00	0.00	0.00	0.00	0.00	0.00
<i>Asteromphalus hookeri</i>	0.00	0.00	0.45	0.13	0.16	0.00	0.00	0.00	0.00	0.64	0.23	0.00	0.00	0.15	0.00	0.00	0.00	0.00	0.00	0.00
<i>Asteromphalus hepaticus / parvulus</i>	0.00	0.16	0.45	0.00	0.00	0.27	0.00	0.00	0.00	0.00	0.00	0.15	0.18	0.29	0.29	0.00	0.00	0.00	0.00	0.00
<i>Asteromphalus hyalinus</i>	0.33	0.00	0.23	0.13	0.97	0.00	0.00	0.22	0.00	0.00	0.00	0.00	0.00	0.00	0.00	0.00	0.00	0.00	0.00	0.00
<i>Azpeitia tabularis</i>	0.00	0.00	0.68	0.38	1.30	0.27	0.26	0.22	0.00	0.00	0.00	0.15	0.00	0.00	0.00	0.00	0.00	0.00	0.00	0.00
<i>Chaetoceros bulbosum</i>	0.00	0.16	0.23	0.00	0.32	0.00	0.00	0.00	0.00	0.00	0.00	0.00	0.00	0.00	0.00	0.00	0.00	0.00	0.16	0.15
<i>Chaetoceros cysts</i>	0.00	0.00	0.11	0.38	0.32	3.20	1.05	0.78	0.77	1.06	0.23	0.62	0.00	0.29	0.00	0.00	0.00	0.00	0.00	0.00
<i>Corethron criophilum</i>	0.17	0.00	0.00	0.00	0.00	0.00	0.00	0.00	0.00	0.23	0.00	0.00	0.00	0.00	0.00	0.00	0.00	0.00	0.00	0.00
<i>Coscinodiscus spp</i>	0.00	0.00	0.23	0.00	0.00	0.27	0.00	0.00	0.00	0.00	2.93	0.00	1.85	0.00	0.00	0.00	0.55	0.00	0.00	0.29
<i>Dactylosolen antarcticus</i>	7.14	10.46	3.05	2.77	2.27	7.47	3.41	1.55	4.83	1.49	1.35	3.54	0.37	3.81	0.00	4.67	2.19	1.67	0.94	1.32
<i>Denticulopsis spp</i>	0.00	0.00	0.00	0.00	0.00	0.00	0.00	0.11	0.00	0.00	0.00	0.00	0.00	0.00	0.29	0.00	0.00	0.00	0.00	0.00
<i>Eucampia antarctica</i>	0.17	0.16	0.34	0.00	1.13	2.13	0.79	4.33	0.39	2.77	0.90	1.08	1.48	0.73	2.31	0.98	0.00	0.24	0.00	0.15
<i>Fragilaria aurica</i>	0.00	0.00	0.00	0.00	0.00	0.00	0.00	0.00	0.00	0.00	0.00	0.00	0.00	0.00	0.00	0.00	0.00	0.00	0.00	0.00
<i>Fragilaria barronii</i>	0.00	0.00	0.00	0.00	0.00	0.00	0.00	0.00	0.00	0.00	0.00	0.00	0.00	0.59	1.16	3.44	0.36	0.72	0.00	0.15
<i>Fragilaria barronii var A + B</i>	0.00	0.00	0.00	0.00	0.00	0.27	19.69	4.44	2.12	7.02	7.66	0.15	5.18	4.69	2.02	11.06	6.93	9.31	8.01	8.97
<i>Fragilaria curta</i>	2.33	5.23	2.03	2.64	0.81	5.33	10.24	3.33	8.69	3.83	7.66	6.16	0.74	10.10	3.18	8.35	9.12	19.81	6.75	5.15
<i>Fragilaria cylindrus</i>	0.17	0.16	0.11	0.25	0.16	4.80	0.79	2.11	1.35	2.34	0.45	1.23	0.00	1.90	1.45	0.49	1.46	7.16	0.31	1.18
<i>Fragilaria interfrigidiana</i>	0.00	0.00	0.00	0.00	0.00	0.00	0.26	0.00	0.00	0.00	0.00	0.00	0.00	0.00	0.00	0.00	0.00	0.24	0.00	0.15
<i>Fragilaria kerguelensis</i>	66.61	54.08	43.23	50.69	48.14	50.67	13.91	52.83	44.98	25.32	7.88	58.55	4.25	51.83	16.18	6.39	7.85	10.26	17.11	3.38
<i>Fragilaria obliquecostata</i>	0.00	0.00	0.11	0.63	0.81	0.27	0.79	0.44	0.19	0.21	0.45	0.31	0.00	0.88	0.29	0.00	0.55	0.48	0.16	0.29
<i>Fragilaria praecurta (?)</i>	0.00	0.00	0.00	0.00	0.00	0.00	0.00	0.00	0.00	0.00	0.00	0.00	0.00	0.00	0.00	0.00	0.00	0.00	0.00	0.00
<i>Fragilaria praeinterfrigidiana</i>	0.00	0.00	0.00	0.00	0.00	0.00	0.00	0.00	0.00	0.00	0.00	0.00	0.00	0.00	0.00	0.00	0.00	0.00	0.00	0.00
<i>Fragilaria ritscheri</i>	0.17	0.33	0.23	0.63	0.97	0.53	0.52	1.11	0.19	2.98	11.94	2.00	2.77	3.51	13.01	16.46	8.58	9.55	14.29	9.85
<i>Fragilaria rhombica</i>	0.50	3.10	3.72	5.41	2.59	5.07	3.15	2.33	5.98	0.43	0.45	2.47	0.00	5.12	0.29	0.25	3.28	5.25	3.14	1.03
<i>Fragilaria separanda</i>	11.30	16.18	15.24	15.97	6.16	5.07	2.62	3.22	13.13	4.04	0.23	5.55	0.00	3.81	0.87	0.25	2.01	2.86	1.73	0.29
<i>Fragilaria separanda var A</i>	0.00	0.00	0.00	0.00	0.00	0.53	0.00	0.00	0.19	0.21	0.68	0.00	0.00	0.00	0.58	0.49	0.00	0.24	0.16	0.15
<i>Fragilaria sublinearis</i>	0.00	0.00	0.00	0.00	0.00	0.00	0.00	0.00	0.19	0.21	0.23	0.62	0.00	0.29	0.00	0.55	0.24	0.00	0.00	0.00
<i>Fragilaria weaveri</i>	0.00	0.00	0.00	0.00	0.00	0.00	0.00	0.00	0.00	0.00	0.00	0.00	0.00	0.00	0.00	0.00	0.00	0.00	0.00	0.00
<i>Hemidiscus karstenii</i>	0.00	0.00	0.00	0.00	0.00	0.00	0.00	0.00	0.00	0.00	0.00	0.00	0.00	0.00	0.00	0.00	0.00	0.00	0.00	0.00
<i>Navicula directa</i>	0.00	0.00	0.00	0.00	0.16	0.53	0.00	0.00	0.00	0.21	0.00	0.31	0.00	0.00	0.00	0.00	0.00	0.00	0.00	0.00
<i>Navicula glaciei</i>	0.00	0.00	0.00	0.00	0.00	0.00	0.00	0.00	0.00	0.00	0.00	0.00	0.00	0.00	0.00	0.00	0.00	0.00	0.00	0.00
<i>Nitzschia fossilis</i>	0.00	0.00	0.00	0.00	0.00	0.00	0.00	0.00	0.00	0.00	0.00	0.00	0.00	0.00	0.00	0.00	0.00	0.00	0.00	0.00
<i>Nitzschia perrillii</i>	0.00	0.00	0.00	0.00	0.00	0.00	0.00	0.00	0.00	0.00	0.00	0.15	0.00	0.00	0.00	4.42	1.64	0.48	0.00	0.74
<i>Nitzschia reinholdii</i>	0.00	0.00	0.11	0.13	0.32	0.00	0.00	0.00	0.00	0.00	0.00	0.00	0.00	0.00	0.00	0.00	0.00	0.00	0.00	0.00
<i>Proboscidea alata</i>	0.00	0.00	0.00	0.00	0.00	0.00	0.00	0.00	0.00	0.00	0.00	0.00	0.00	0.00	0.00	0.00	0.00	0.00	0.00	0.00
<i>Proboscidea barboi</i>	0.00	0.00	0.00	0.00	0.00	0.00	0.00	0.00	0.00	0.00	0.00	0.00	0.00	0.00	0.00	0.00	0.00	0.00	0.00	0.00
<i>Rhizosolenia hebetata (group)</i>	0.00	0.33	0.00	0.00	0.00	0.00	0.00	0.00	0.00	0.00	0.00	0.00	0.00	0.00	0.00	0.00	0.00	0.00	0.00	0.00
<i>Rhizosolenia styliformis (group)</i>	0.17	0.49	0.11	0.00	0.00	0.00	0.00	0.22	0.00	0.00	0.00	0.00	0.00	0.00	0.00	0.00	0.00	0.00	0.00	1.47
<i>Rhizosolenia sp A</i>	0.00	0.00	0.00	0.00	0.00	0.00	0.00	0.00	0.00	0.00	0.00	0.00	0.00	0.00	0.00	0.00	0.00	0.00	0.00	0.00
<i>Rhizosolenia spp</i>	0.00	0.00	0.00	0.00	0.00	0.00	0.00	0.22	0.00	0.21	0.00	0.46	0.18	0.29	0.87	0.74	0.36	0.24	0.31	0.00
<i>Rouxia antarctica</i>	0.00	0.00	0.00	0.00	0.00	0.00	0.52	0.00	0.00	0.00	0.15	0.00	0.00	0.00	0.00	0.00	0.00	0.00	0.16	0.00
<i>Rouxia heteropolara</i>	0.00	0.00	0.11	0.00	0.00	0.00	0.00	0.00	0.00	0.00	0.00	0.00	0.00	0.00	0.00	0.00	0.00	0.00	0.00	0.00
<i>Rouxia isoplica</i>	0.00	0.00	0.00	0.00	0.00	0.53	1.05	0.00	1.16	0.85	1.80	0.31	0.37	0.00	0.00	3.19	1.09	1.67	0.94	0.00
<i>Rouxia leventerae</i>	0.00	0.00	0.00	0.00	0.00	0.00	0.00	0.00	0.00	0.00	0.00	0.00	0.00	0.00	0.00	0.00	0.00	0.00	0.00	0.00
<i>Rouxia naviculoides</i>	0.00	0.00	0.00	0.00	0.00	0.27	0.00	0.00	0.00	0.00	0.00	0.00	0.00	0.00	0.00	0.00	0.55	0.00	0.16	0.15
<i>Stellarima microtrias</i>	0.00	0.00	0.00	0.00	0.00	0.00	0.00	0.00	0.00	0.68	0.31	0.18	0.00	0.29	0.00	0.18	0.00	0.00	0.00	0.00
<i>Stephanopyxis spp</i>	0.00	0.00	0.00	0.00	0.00	0.00	0.00	0.00	0.00	0.00	0.00	0.00	0.00	0.00	0.00	0.00	0.00	0.00	0.00	0.00
<i>Thalassionema nitzschoides (group)</i>	0.00	0.00	0.00	0.00	0.00	0.00	0.00	0.00	0.00	0.00	0.00	0.00	0.00	0.00	0.00	0.00	0.00	0.00	0.00	0.00
<i>Thalassionema nitzschoides var parva</i>	0.00	0.00	0.00	0.00	0.00	0.00	0.00	0.00	0.00	0.00	0.00	0.00	0.00	0.00	0.00	0.00	0.00	0.00	0.00	0.00
<i>Thalassiosira antarctica</i>	0.00	0.00	0.00	0.00	0.00	0.00	0.00	0.00	0.00	0.00	0.00	0.00	0.00	0.00	0.00	0.25	0.00	0.00	0.00	0.00
<i>Thalassiosira complicata</i>	0.00	0.00	0.00	0.00	0.00	0.00	0.00	0.00	0.00	0.00	0.00	0.00	0.00	0.00	0.00	0.00	0.00	0.00	0.00	0.00
<i>Thalassiosira elliptica</i>	0.00	0.00	0.00	0.00	0.00	0.00	0.26	0.11	0.00	0.43	0.23	0.00	0.18	0.15	0.87	0.74	0.00	0.00	0.16	0.29
<i>Thalassiosira fasciculata</i>	0.00	0.00	0.00	0.00	0.00	0.00	0.22	0.19	0.43	0.23	0.00	0.18	0.15	0.29	0.25	0.36	0.24	0.16	0.15	0.00
<i>Thalassiosira frenguelli</i>	0.17	0.00	0.00	0.00	0.00	0.00	0.00	0.00	0.00	0.00	0.00	0.00	0.15	0.00	0.00	0.00	0.00	0.00	0.00	0.00
<i>Thalassiosira gracilis var expecta</i>	0.50	0.98	0.23	2.89	1.13	1.33	1.31	0.33	2.12	0.43	0.23	0.62	0.00	0.29	0.29	1.23	1.46	0.72	0.94	0.29
<i>Thalassiosira gracilis var gracilis</i>	0.66	0.33	9.26	6.04	6.0															

# Appendix 3. continued

GC 51	180	190	200	210	220	230	240	249	250	260	270	280	290	299	300	310	320	330	340	349
CORE DEPTH (cm)																				
<b>DIATOMS</b>																				
<i>Actinocyclus actinocylus</i>	0.34	0.00	0.00	0.00	0.00	0.00	0.00	0.00	0.00	0.00	0.00	0.18	0.00	0.00	0.13	0.00	0.00	0.00	0.18	0.00
<i>Actinocyclus dimorphus</i>	0.00	0.00	0.00	0.00	0.00	0.00	0.00	0.00	0.00	0.00	0.00	0.00	0.00	0.00	0.00	0.00	0.00	0.00	0.00	0.00
<i>Actinocyclus fasciculatus</i>	0.00	0.00	0.00	0.00	0.00	0.00	0.00	0.00	0.00	0.00	0.00	0.00	0.00	0.00	0.17	0.00	0.00	0.00	0.00	0.71
<i>Actinocyclus ingens</i>	37.90	11.96	27.99	39.45	25.41	9.23	7.95	22.27	44.42	18.80	9.98	10.31	6.84	7.82	9.80	14.96	8.57	9.10	4.60	5.70
<i>Actinocyclus karstenii</i>	0.00	0.00	0.00	0.00	0.00	0.00	0.00	0.00	0.00	0.00	0.00	0.00	0.00	0.00	0.00	0.00	0.00	0.00	0.00	0.24
<i>Asteromphalus hookeri</i>	0.00	0.00	0.17	0.00	0.00	0.28	0.00	0.00	0.19	0.32	0.00	0.37	0.00	0.00	0.00	0.59	0.00	0.15	0.00	0.00
<i>Asteromphalus hepaticus / parvulus</i>	0.00	0.00	0.00	0.00	0.00	0.00	0.00	0.00	0.00	0.00	0.00	0.00	0.00	0.00	0.00	0.00	0.00	0.31	0.00	0.24
<i>Asteromphalus hyalinus</i>	0.00	0.00	0.00	0.00	0.00	0.00	0.29	0.00	0.00	0.17	0.55	0.00	0.00	0.00	0.15	0.22	0.31	0.00	0.00	0.24
<i>Azpeitia tabularis</i>	0.00	0.00	0.00	0.00	0.00	0.00	0.00	0.00	0.00	0.00	0.00	0.00	0.00	0.00	0.00	0.00	0.00	0.00	0.00	0.00
<i>Chaetoceros bulbosum</i>	0.17	0.00	0.00	0.00	0.00	0.00	0.00	0.00	0.00	0.32	0.00	0.00	0.15	0.00	0.25	0.00	0.22	0.15	0.18	0.00
<i>Chaetoceros cysts</i>	0.00	0.19	0.00	0.00	0.00	0.00	0.00	0.00	0.00	0.00	0.00	0.00	0.00	0.00	0.00	0.00	0.00	0.00	0.00	0.00
<i>Corethron criophilum</i>	0.00	0.00	0.00	0.00	0.00	0.00	0.00	0.00	0.19	0.00	0.00	0.00	0.00	0.00	0.13	0.29	0.00	0.00	0.18	0.24
<i>Coscinodiscus spp</i>	0.00	0.19	0.00	0.00	0.00	0.14	0.00	0.15	0.37	0.16	0.00	0.18	0.44	0.67	0.00	2.20	0.33	0.15	0.18	0.71
<i>Dactylosolen antarcticus</i>	1.35	3.74	2.02	2.44	1.23	0.28	0.96	0.87	1.67	6.00	3.55	4.60	7.42	2.16	3.27	1.03	2.45	0.46	0.71	2.38
<i>Denticulopsis spp</i>	0.00	0.00	0.00	0.00	0.00	0.00	0.00	0.00	0.00	0.00	0.00	0.00	0.00	0.00	0.00	0.00	0.00	0.00	0.18	0.00
<i>Eucampia antarctica</i>	0.68	0.00	0.51	0.43	0.00	0.42	0.00	0.00	0.56	0.00	0.17	0.00	0.00	0.00	0.13	0.15	0.22	0.62	0.00	0.00
<i>Fragilariopsis aurica</i>	0.00	0.00	0.00	0.00	0.00	0.28	0.24	0.00	0.00	0.00	1.02	0.18	0.00	0.00	0.00	0.00	0.00	0.00	0.00	0.00
<i>Fragilariopsis barroni</i>	0.00	0.00	0.00	0.00	0.00	0.14	0.00	0.00	0.00	0.16	0.00	0.00	0.00	0.00	0.00	0.00	0.00	0.93	0.01	0.00
<i>Fragilariopsis barroni var A + B</i>	4.91	10.28	8.94	10.90	3.69	0.28	4.10	10.77	6.13	10.27	9.31	13.63	5.82	16.31	10.68	7.33	10.80	6.64	9.03	5.94
<i>Fragilariopsis curta</i>	8.12	25.23	10.46	12.77	2.05	0.58	4.10	7.42	4.65	9.79	14.04	13.44	29.40	21.80	23.37	17.45	23.05	12.19	23.89	17.34
<i>Fragilariopsis cylindrus</i>	0.85	1.50	2.53	0.72	0.20	0.00	0.00	1.16	0.56	0.00	0.68	0.00	0.73	0.00	0.25	0.00	0.11	0.15	0.00	0.00
<i>Fragilariopsis interfrigidaria</i>	0.17	0.00	0.51	0.14	0.61	0.00	0.24	0.15	0.19	0.32	0.68	0.18	0.00	0.33	0.00	0.15	0.33	0.62	0.00	0.95
<i>Fragilariopsis kerguelensis</i>	3.21	6.92	6.41	3.87	40.98	54.83	44.82	13.97	4.83	3.16	14.72	3.31	2.33	1.33	2.26	1.76	5.90	5.40	9.73	3.80
<i>Fragilariopsis obliquecostata</i>	0.51	0.93	0.17	0.14	0.00	0.00	0.24	0.15	0.19	0.95	0.51	0.18	0.44	0.00	0.38	0.15	0.11	0.15	0.00	0.48
<i>Fragilariopsis praecurta (?)</i>	0.00	0.00	0.00	0.00	0.00	0.00	0.24	0.87	0.74	1.90	2.37	4.97	4.80	3.83	2.26	4.55	5.46	0.46	4.25	4.51
<i>Fragilariopsis praeterfrigidaria</i>	0.00	0.00	0.00	0.00	0.00	0.00	0.00	0.00	0.00	0.00	0.00	0.00	0.00	0.00	0.00	0.00	0.00	0.00	0.00	0.00
<i>Fragilariopsis ritscheri</i>	5.08	9.72	11.30	4.30	5.94	2.38	5.78	7.86	2.23	5.06	8.63	8.84	5.09	4.83	3.39	3.67	5.01	7.56	8.85	4.28
<i>Fragilariopsis rhombica</i>	0.34	2.06	0.34	0.00	0.00	0.00	0.72	1.02	0.56	0.32	1.18	0.00	0.15	0.00	0.25	0.00	0.33	0.31	0.71	0.00
<i>Fragilariopsis separanda</i>	0.17	0.75	0.34	0.00	1.23	9.37	2.17	2.04	0.74	0.00	2.37	0.37	0.15	0.00	0.00	0.00	0.33	0.00	0.00	0.00
<i>Fragilariopsis separanda var A</i>	0.00	0.75	0.00	0.00	0.00	0.00	0.00	0.00	0.00	0.00	0.00	0.37	0.58	1.50	0.63	0.44	0.89	0.15	0.00	2.38
<i>Fragilariopsis sublinearis</i>	0.00	0.00	0.00	0.00	0.00	0.00	0.00	0.00	0.00	0.00	0.00	0.00	0.00	0.00	0.00	0.00	0.00	0.00	0.00	0.00
<i>Fragilariopsis weaveri</i>	0.00	0.00	0.00	0.00	0.00	0.00	0.00	0.00	0.00	0.00	0.00	0.00	0.00	0.00	0.00	0.00	0.00	0.00	0.00	0.00
<i>Hemidiscus karstenii</i>	0.00	0.00	0.00	0.00	0.00	0.00	0.00	0.00	0.00	0.00	0.00	0.00	0.00	0.00	0.00	0.00	0.00	0.00	0.00	0.00
<i>Navicula directa</i>	0.00	0.00	0.00	0.00	0.00	0.00	0.00	0.00	0.00	0.00	0.00	0.00	0.00	0.00	0.00	0.00	0.00	0.00	0.00	0.00
<i>Navicula glaciei</i>	0.00	0.00	0.00	0.00	0.00	0.00	0.00	0.00	0.00	0.00	0.00	0.00	0.00	0.00	0.00	0.00	0.22	0.00	0.00	0.00
<i>Nitzschia fossilis</i>	0.00	0.00	0.00	0.00	0.00	0.00	0.00	0.00	0.00	0.00	0.00	0.00	0.00	0.00	0.00	0.00	0.00	0.00	0.00	0.00
<i>Nitzschia perigalli</i>	1.18	1.68	1.18	1.72	0.00	0.00	0.96	0.73	0.74	1.26	0.88	1.10	0.29	0.50	0.75	1.03	0.45	0.46	0.18	0.00
<i>Nitzschia reinholdii</i>	0.00	0.00	0.00	0.00	0.00	0.00	0.00	0.00	0.00	0.00	0.00	0.00	0.00	0.00	0.50	0.00	0.00	0.00	0.00	0.00
<i>Proboscia alata</i>	0.00	0.00	0.00	0.00	0.00	0.00	0.00	0.00	0.00	0.00	0.00	0.00	0.00	0.00	0.00	0.00	0.00	0.00	0.00	0.00
<i>Proboscia barboi</i>	0.00	0.00	0.00	0.00	0.00	0.00	0.00	0.00	0.00	0.00	0.00	0.00	0.00	0.00	0.00	0.00	0.00	0.00	0.00	0.00
<i>Rhizosolenia hebetata (group)</i>	0.00	0.00	0.00	0.00	0.00	0.00	0.00	0.00	0.00	0.00	0.00	0.00	0.15	0.00	0.00	0.00	0.00	0.00	0.00	0.00
<i>Rhizosolenia styliformis (group)</i>	0.34	0.00	0.34	0.43	0.20	0.14	0.00	0.44	0.37	0.32	0.00	0.00	0.44	0.17	0.13	0.29	0.00	0.15	0.18	0.00
<i>Rhizosolenia sp A</i>	0.00	0.00	0.00	0.00	0.00	0.00	0.00	0.00	0.00	0.00	0.00	0.18	0.00	0.00	0.00	0.15	0.11	0.00	0.00	0.00
<i>Rhizosolenia spp</i>	0.00	0.19	0.00	0.00	0.00	0.00	0.00	0.00	0.00	0.00	0.00	0.37	0.00	0.00	0.13	0.29	0.00	0.00	0.00	0.24
<i>Rouxia antarctica</i>	0.00	0.00	0.00	0.00	0.00	0.00	1.69	1.89	1.67	3.00	2.37	3.68	4.22	2.16	3.14	1.32	1.67	2.47	3.54	5.23
<i>Rouxia heteropolara</i>	0.00	0.00	0.00	0.14	0.00	0.00	0.00	0.00	0.00	0.00	0.00	0.00	0.00	0.00	0.00	0.00	0.00	0.00	0.00	0.00
<i>Rouxia isopolara</i>	6.26	2.99	1.01	0.72	0.00	0.28	0.24	0.58	0.37	1.42	2.88	1.10	0.29	0.17	0.50	0.15	0.45	0.00	0.18	0.24
<i>Rouxia leventerae</i>	0.00	0.00	0.00	0.00	0.00	0.00	0.00	0.00	0.00	0.00	0.00	0.00	0.00	0.00	0.00	0.00	0.11	0.00	0.00	1.90
<i>Rouxia naviculoides</i>	0.00	0.37	0.00	1.00	0.61	1.26	8.19	5.39	7.81	19.12	11.17	8.10	10.63	13.14	10.90	7.62	10.91	17.13	11.50	12.35
<i>Stellarima microtrias</i>	0.17	0.00	0.17	0.00	0.00	0.00	0.00	0.00	0.19	0.00	0.00	0.00	0.00	0.00	0.00	0.44	0.00	0.15	0.00	0.00
<i>Stephanopyx spp</i>	0.00	0.00	0.00	0.00	0.00	0.00	0.00	0.00	0.00	0.00	0.00	0.00	0.00	0.00	0.00	0.00	0.00	0.00	0.00	0.00
<i>Thalassionema nitzschoides (group)</i>	0.00	0.00	0.00	0.00	0.82	1.54	0.96	0.15	0.00	0.00	0.00	0.00	0.00	0.00	0.00	0.00	0.00	0.00	0.00	0.00
<i>Thalassionema nitzschoides var parva</i>	0.00	0.00	0.00	0.00	0.00	0.00	0.00	0.00	0.00	0.00	0.00	0.00	0.00	0.00	0.00	0.00	0.00	0.00	0.00	0.00
<i>Thalassiosira antarctica</i>	0.17	0.00	0.00	0.00	0.00	0.14	0.00	0.00	0.00	0.00	0.00	0.18	0.00	0.00	0.00	0.00	0.00	0.00	0.00	0.24
<i>Thalassiosira complicata</i>	0.00	0.00	0.00	0.00	0.00	0.00	0.00	0.00	0.00	0.00	0.00	0.00	0.00	0.00	0.00	0.00	0.00	0.00	0.00	0.00
<i>Thalassiosira elliptipora</i>	0.34	0.19	0.34	0.14	0.00	0.24	0.44	0.19	0.00	0.00	0.18	0.15	0.00	0.00	0.00	0.15	0.00	r	0.00	r
<i>Thalassiosira fasciculata</i>	0.34	0.37	0.84	0.29	0.00	0.00	0.29	0.19	0.47	0.17	0.55	0.87	0.50	0.75	1.03	0.67	0.15	0.35	0.24	
<i>Thalassiosira frenguelli</i>	0.00	0.00	0.00	0.00	0.00	0.00	0.00	0.00	0.00	0.00	0.00	0.00	0.00	0.00	0.00	0.00	0.00	0.00	0.00	0.00
<i>Thalassiosira gracilis var expecta</i>	0.68	2.43	0.51	0.72	0.00	0.00	0.24	0.87	0.74	2.05	0.34	0.00	1.02	1.33	1.76	0.29	1.00	0.46	1.06	0

# Appendix 3. continued

GC 51															
CORE DEPTH (cm)	350	360	370	380	390	400	401	410	420	430	440	450	460	470	
DIATOMS															
<i>Actinocyclus actinocilius</i>	0.00	0.00	0.00	0.00	0.00	0.00	0.00	0.00	0.00	0.00	0.00	0.00	0.00	0.00	
<i>Actinocyclus dimorphus</i>	0.00	0.00	0.00	0.00	0.00	0.29	0.00	0.00	0.00	0.00	0.00	0.00	0.00	0.00	
<i>Actinocyclus fasciculatus</i>	0.18	0.63	0.67	0.00	0.00	0.00	0.00	0.00	0.00	0.00	0.20	0.00	0.00	0.00	
<i>Actinocyclus ingens</i>	2.50	1.46	3.35	2.46	0.54	0.58	0.26	0.00	0.38	0.00	0.00	0.19	1.10	2.31	
<i>Actinocyclus karstenii</i>	0.36	1.04	3.13	3.28	0.54	0.29	0.00	0.00	0.38	0.21	0.78	0.58	0.55	0.21	
<i>Asteromphalus hookeri</i>	0.00	0.00	0.00	0.00	0.00	0.00	0.00	0.00	0.00	0.00	0.00	0.00	0.00	0.00	
<i>Asteromphalus hepaticus / parvulus</i>	0.18	0.00	0.00	0.27	0.00	0.00	0.00	0.00	0.00	0.00	0.00	0.00	0.00	0.00	
<i>Asteromphalus hyalinus</i>	0.00	0.00	0.00	0.00	0.00	0.00	0.00	0.00	0.00	0.00	0.00	0.00	0.00	0.00	
<i>Azpeitia tabularis</i>	0.00	0.00	0.00	0.00	0.00	0.00	0.00	0.00	0.19	0.00	0.00	0.00	0.00	0.00	
<i>Chaetoceros bulbosum</i>	0.18	0.00	0.00	0.00	0.18	0.58	0.26	0.21	0.19	0.21	0.20	0.19	0.00	0.00	
<i>Chaetoceros cysts</i>	0.71	0.00	0.00	0.00	0.00	0.00	0.00	0.00	0.00	0.00	0.00	0.00	0.00	0.00	
<i>Corethron cnophillum</i>	2.50	0.84	0.67	0.27	2.14	1.17	2.55	2.36	1.53	4.34	2.94	1.17	0.37	0.42	
<i>Coscinodiscus spp</i>	0.00	0.21	0.00	0.00	0.00	0.29	0.00	0.00	0.19	0.00	0.00	0.00	0.00	0.00	
<i>Dactylosolen antarcticus</i>	15.89	7.93	5.58	7.92	9.29	16.08	8.16	11.35	10.71	8.68	16.05	15.92	12.50	10.71	
<i>Denticulopsis spp</i>	0.00	0.00	0.00	0.27	0.36	0.00	0.00	0.21	0.00	0.00	0.00	0.00	0.37	0.00	
<i>Eucampia antarctica</i>	0.71	0.21	0.67	1.64	1.07	0.29	0.26	0.21	0.19	0.21	0.20	0.19	0.92	2.10	
<i>Fragilaropsis aunca</i>	0.00	0.00	4.69	1.37	0.71	0.58	0.51	0.21	0.00	0.00	0.00	0.00	0.00	0.00	
<i>Fragilaropsis barroni</i>	0.00	0.21	0.22	4.64	3.93	8.19	10.20	16.49	14.72	35.95	24.66	25.05	24.45	31.09	
<i>Fragilaropsis barroni</i> var A + B	6.25	9.81	11.16	3.28	2.50	0.00	0.26	0.86	0.96	0.00	0.00	0.00	0.00	0.00	
<i>Fragilaropsis curta</i>	9.64	22.96	15.18	8.47	4.82	7.89	6.12	6.21	4.02	3.93	6.26	4.27	1.65	0.63	
<i>Fragilaropsis cylindrus</i>	0.00	0.00	0.00	0.00	0.00	0.00	0.00	0.00	0.00	0.00	0.00	0.00	0.00	0.00	
<i>Fragilaropsis interfrigidaria</i>	1.79	1.46	0.22	0.82	1.79	0.58	0.77	1.50	2.29	1.65	0.98	1.36	0.55	1.47	
<i>Fragilaropsis kerguelensis</i>	1.43	1.88	0.22	0.27	0.00	0.29	0.00	0.00	0.00	0.00	0.20	0.00	0.00	0.21	
<i>Fragilaropsis obliquecostata</i>	0.36	0.42	0.45	0.00	0.00	0.00	0.00	0.00	0.00	0.00	0.20	0.00	0.00	0.00	
<i>Fragilaropsis praecurta</i> (?)	1.61	0.21	0.00	0.00	0.00	0.00	0.00	0.00	0.00	0.00	0.00	0.00	0.00	0.00	
<i>Fragilaropsis praeinterfrigidiana</i>	0.18	0.00	0.89	4.10	9.82	7.31	10.46	7.49	8.03	10.54	10.76	11.65	7.90	3.36	
<i>Fragilaropsis ntschen</i>	2.68	4.38	3.79	5.74	10.71	10.53	13.52	10.28	12.24	4.96	5.68	6.21	4.41	4.83	
<i>Fragilaropsis rhombica</i>	0.00	0.63	0.22	0.00	1.43	4.97	5.10	7.92	5.74	3.93	3.91	1.75	1.29	0.63	
<i>Fragilaropsis separanda</i>	0.18	0.00	0.00	0.00	0.00	0.00	0.00	0.00	0.00	0.00	0.00	0.00	0.00	0.00	
<i>Fragilaropsis separanda</i> var A	1.61	1.25	0.00	0.55	0.00	0.00	0.00	0.00	0.00	0.00	0.00	0.00	0.00	0.00	
<i>Fragilaropsis sublineans</i>	0.00	0.00	0.00	0.00	0.00	0.00	0.00	0.00	0.00	0.00	0.00	0.00	0.00	0.00	
<i>Hemidiscus karstenii</i>	0.00	0.00	0.00	0.00	0.36	0.00	0.00	0.00	0.00	0.00	0.00	0.00	0.00	0.00	
<i>Navicula directa</i>	0.00	0.00	0.00	0.00	0.00	0.00	0.00	0.00	0.00	0.00	0.00	0.00	0.00	0.00	
<i>Navicula glaciei</i>	0.00	0.00	0.00	0.00	0.00	0.00	0.00	0.00	0.00	0.00	0.00	0.00	0.00	0.00	
<i>Nitzschia fossilis</i>	0.00	0.00	r	0.00	0.00	0.00	0.77	0.21	0.57	0.41	0.39	0.58	0.37	0.00	
<i>Nitzschia perngalli</i>	0.00	0.21	0.00	0.00	0.00	0.00	0.00	0.00	0.00	0.00	0.00	0.00	0.00	0.00	
<i>Nitzschia reinholdii</i>	0.00	0.00	0.00	0.00	0.00	0.00	0.00	0.00	0.00	0.00	0.00	0.00	0.00	0.00	
<i>Fragilaropsis weaveri</i>	0.00	0.00	0.22	1.37	0.18	0.29	1.28	0.00	r	r	0.59	0.00	8.46	1.47	
<i>Proboscia alata</i>	0.00	0.00	0.00	0.55	0.54	0.58	0.26	0.00	0.00	0.00	0.00	0.00	0.00	0.00	
<i>Proboscia barboi</i>	0.00	0.00	0.00	0.82	0.00	2.34	0.51	1.07	0.19	0.41	0.59	0.39	0.37	0.21	
<i>Rhizosolenia hebetata</i> (group)	0.00	0.00	0.00	0.00	0.00	0.29	0.00	0.00	0.00	0.00	0.00	0.00	0.00	0.00	
<i>Rhizosolenia styliformis</i> (group)	0.00	1.25	0.22	0.00	0.00	0.00	0.00	0.00	0.00	0.00	0.00	0.00	0.00	0.00	
<i>Rhizosolenia</i> sp A	0.36	0.00	0.22	0.00	0.00	0.00	0.00	0.21	0.00	0.00	0.00	0.00	0.00	0.00	
<i>Rhizosolenia</i> spp	0.00	0.21	0.45	1.09	0.18	0.29	0.26	0.43	0.00	0.00	0.20	0.00	0.00	0.21	
<i>Rouxia antarctica</i>	6.79	2.51	0.89	0.55	2.32	2.05	3.06	1.93	1.15	0.83	1.17	0.97	1.47	2.73	
<i>Rouxia heteropolara</i>	2.50	3.76	3.13	0.55	0.36	0.58	0.51	0.43	0.19	0.41	0.39	0.39	0.37	0.21	
<i>Rouxia isopolica</i>	2.50	0.84	0.67	0.82	1.79	0.88	1.02	0.43	0.96	0.62	0.39	0.39	1.65	3.57	
<i>Rouxia leventerae</i>	0.00	0.00	1.56	0.00	0.00	0.00	0.00	0.00	0.00	0.00	0.20	0.00	0.00	0.00	
<i>Rouxia naviculoides</i>	11.43	8.98	2.46	2.46	7.14	5.56	8.42	7.71	7.84	5.79	4.31	6.99	7.54	13.87	
<i>Stellarima microtrias</i>	0.36	0.21	0.22	0.00	0.00	0.29	0.26	0.00	0.00	0.00	0.00	0.00	0.37	0.63	
<i>Stephanopyxis spp</i>	0.00	0.00	0.00	0.00	0.00	0.00	0.00	0.00	0.00	0.00	0.00	0.00	0.00	0.00	
<i>Thalassionema nitzschloides</i> (group)	0.00	0.00	0.00	0.00	0.00	0.00	0.00	0.00	0.00	0.00	0.20	0.19	0.00	0.21	
<i>Thalassionema nitzschloides</i> var parva	0.00	0.00	0.00	0.00	0.00	0.00	0.00	0.00	0.00	0.00	0.00	0.00	0.00	0.00	
<i>Thalassiosira antarctica</i>	0.00	0.00	0.00	0.00	0.00	0.00	0.00	0.00	0.00	0.00	0.00	0.00	0.00	0.00	
<i>Thalassiosira complicata</i>	0.00	0.00	0.00	r	0.00	0.29	0.00	0.00	0.19	0.00	0.00	0.00	0.18	r	
<i>Thalassiosira elliptipora</i>	r	0.00	0.00	0.00	0.00	0.00	0.00	0.00	0.00	0.00	0.00	0.00	0.00	0.00	
<i>Thalassiosira fasciculata</i>	0.18	0.00	0.67	0.27	0.00	0.00	0.00	0.00	r	0.00	0.00	0.00	0.00	0.00	
<i>Thalassiosira frenguelli</i>	0.00	0.00	0.00	0.00	0.00	0.00	0.00	0.00	0.00	0.00	0.00	0.00	0.00	0.00	
<i>Thalassiosira gracilis</i> var <i>expecta</i>	1.43	1.04	0.45	0.00	0.00	0.29	0.00	0.21	0.19	0.21	0.20	0.00	0.00	0.00	
<i>Thalassiosira gracilis</i> var <i>gracilis</i>	0.89	0.00	0.00	0.00	0.00	0.00	0.00	0.00	0.00	0.00	0.00	0.00	0.00	0.00	
<i>Thalassiosira gravida</i>	0.54	0.00	0.00	0.00	0.18	0.00	0.00	0.00	0.00	0.00	0.00	0.00	0.00	0.00	
<i>Thalassiosira inura</i>	0.54	1.46	1.56	5.74	8.04	6.14	5.36	2.78	4.21	1.45	1.96	2.14	4.96	3.57	
<i>Thalassiosira inura-insigna</i> (transition)	0.00	0.00	0.00	0.00	0.00	0.00	0.00	0.00	0.00	0.00	0.00	0.00	0.00	0.00	
<i>Thalassiosira insigna</i>	1.25	0.42	2.90	11.20	6.43	1.17	3.83	0.43	0.38	0.00	r	0.19	0.18	0.21	
<i>Thalassiosira kolbei</i>	0.00	0.21	0.89	0.27	0.18	0.29	0.26	0.00	0.00	0.21	0.20	0.00	0.74	2.31	
<i>Thalassiosira lentiginosa</i>	2.32	5.43	8.71	8.74	3.93	0.58	1.53	0.21	0.19	0.41	1.57	2.72	4.60	1.05	
<i>Thalassiosira maculata</i>	0.71	1.04	3.57	2.46	2.14	0.88	3.57	0.86	1.15	1.86	1.76	1.17	1.84	0.63	
<i>Thalassiosira oestrupii</i>	15.18	12.73	8.04	4.37	6.61	7.31	5.87	14.35	13.58	8.47	8.61	7.77	2.39	3.15	
<i>Thalassiosira oliverana</i>	0.00	0.42	4.46	1.91	0.71	2.92	1.79	0.21	0.38	0.21	0.59	1.17	0.92	0.84	
<i>Thalassiosira oliverana</i> (coarse)	0.00	0.00	0.00	0.00	0.00	0.00	0.00	0.00	0.00	0.00	0.00	0.00	0.00	0.00	
<i>Thalassiosira strata</i>	0.00	0.00	0.00	0.00	0.00	0.00	0.00	0.00	0.00	0.00	0.00	0.00	0.00	r	
<i>Thalassiosira torokina</i>	0.18	0.21	0.45	0.00	0.18	0.29	0.00	0.00	0.19	0.00	0.00	0.00	0.00	0.21	
<i>Thalassiosira vulnifica</i>	0.36	0.21	4.69	6.28	0.54	0.00	0.26	0.00	0.38	0.21	0.00	0.00	0.00	0.00	
<i>Thalassiosira webbi</i>	0.00	0.00	0.00	0.00	0.00	0.00	0.00	0.00	0.00	0.21	0.00	0.00	0.00	0.00	
<i>Thalassiothrix spp</i>	0.00	0.21	0.00	0.00	0.00	0.00	0.00	0.00	0.00	0.00	0.19	0.00	0.00	0.00	

# Appendix 3. continued

GC 34 (lat 62°20'4"S, long 81°14'9"E)																				
CORE DEPTH (cm)	0	10	20	30	40	50	60	70	80	90	100	110	120	130	140	150	160	170	180	190
DIATOMS																				
<i>Actinocyclus actinocylus</i>	0.94	1.08	1.22	2.68	1.98	1.19	0.70	1.92	2.43	1.49	0.82	0.52	0.21	0.65	0.50	0.21	0.00	0.22	0.00	0.00
<i>Actinocyclus dimorphus</i>	0.00	0.00	0.00	0.00	0.00	0.00	0.00	0.00	0.00	0.00	0.00	0.00	0.00	0.00	0.00	0.00	0.00	0.00	0.00	0.00
<i>Actinocyclus fasciculatus</i>	0.00	0.00	0.00	0.00	0.00	0.00	0.00	0.00	0.00	0.00	0.00	0.00	0.00	0.00	0.00	0.00	0.00	0.00	0.00	0.00
<i>Actinocyclus ingens</i>	0.19	0.00	0.17	0.00	0.59	15.20	16.01	22.53	20.13	15.10	22.28	23.96	17.13	24.56	37.97	41.75	37.34	40.43	30.84	13.57
<i>Actinocyclus karstoni</i>	0.00	0.00	0.00	0.00	0.00	0.00	0.00	0.00	0.00	0.00	0.00	0.00	0.00	0.00	0.00	0.00	0.00	0.00	0.00	0.00
<i>Asteromphalus hookeri</i>	0.57	0.15	0.00	0.14	0.00	0.48	1.39	0.00	0.22	0.74	0.27	0.52	0.00	0.00	0.00	0.00	0.21	0.22	0.00	0.00
<i>Asteromphalus hepaticus / parvulus</i>	0.38	1.08	0.35	0.00	0.00	1.19	1.39	0.00	0.00	0.00	0.82	0.26	0.00	0.66	0.25	0.84	0.42	0.22	0.00	0.00
<i>Asteromphalus hyalinus</i>	0.38	0.93	0.00	0.28	0.00	0.00	0.00	0.00	0.00	0.00	0.00	0.00	0.00	0.00	0.00	0.00	0.00	0.00	0.00	0.00
<i>Azpeitia tabularis</i>	0.00	0.00	0.00	0.00	0.00	0.00	0.00	0.00	0.00	0.00	0.00	0.26	0.43	0.00	0.00	0.00	0.00	0.22	0.00	0.00
<i>Chaetoceros bulbosum</i>	0.57	0.15	0.17	0.00	0.00	0.24	0.00	0.00	0.00	0.00	0.54	0.26	0.21	0.22	1.49	0.84	0.63	0.00	0.23	0.00
<i>Chaetoceros cysts</i>	0.84	0.00	0.35	0.00	0.66	0.00	0.00	0.00	0.00	0.50	0.27	0.00	0.00	0.22	0.00	0.00	0.00	0.00	0.00	0.00
<i>Corethron criophilum</i>	0.00	0.00	0.00	0.00	0.00	0.00	0.00	0.00	0.00	0.00	0.00	0.00	0.00	0.00	0.00	0.00	0.00	0.00	0.00	0.00
<i>Coscinodiscus spp</i>	0.57	0.31	0.35	0.00	0.00	0.24	0.23	0.00	0.22	0.00	0.00	1.30	0.00	0.00	0.50	0.21	0.00	0.22	0.00	0.00
<i>Dactylosolen antarcticus</i>	3.21	3.56	1.40	2.12	1.54	1.66	4.41	4.40	1.11	0.74	1.63	1.04	1.50	0.88	0.50	2.30	2.95	1.72	3.74	3.81
<i>Denticulopsis spp</i>	0.00	0.00	0.00	0.00	0.00	0.00	0.00	0.00	0.00	0.00	0.00	0.00	0.00	0.00	0.00	0.00	0.00	0.00	0.00	0.00
<i>Eucampia antarctica</i>	0.57	0.15	1.05	2.40	0.88	0.24	1.39	4.40	2.21	1.24	1.09	0.78	0.64	0.66	0.99	1.46	1.48	0.22	1.87	0.48
<i>Fragilaropsis aurica</i>	0.00	0.00	0.00	0.00	0.00	0.00	0.00	0.00	0.00	0.00	0.26	0.00	0.22	0.00	0.00	0.00	0.00	0.00	0.00	0.00
<i>Fragilarlopsis barronii</i>	0.00	0.00	0.00	0.00	0.00	0.00	0.00	0.27	0.00	0.00	0.00	0.00	0.00	0.00	0.00	0.00	0.00	0.00	0.00	0.00
<i>Fragilarlopsis barronii var A + B</i>	0.00	0.00	0.00	0.00	0.00	2.14	11.83	0.82	3.76	1.49	3.26	4.69	10.28	3.32	10.42	8.56	8.23	7.74	10.51	33.33
<i>Fragilaropsis curta</i>	6.79	3.25	0.70	3.53	3.30	4.04	2.09	0.82	0.66	0.74	2.45	1.82	6.64	3.76	1.99	2.51	6.96	9.68	5.14	8.33
<i>Fragilaropsis cylindrus</i>	2.08	0.15	0.00	0.00	0.00	0.00	0.00	0.55	0.00	0.25	0.00	0.52	0.21	0.00	0.00	0.00	0.00	0.21	0.00	0.00
<i>Fragilaropsis Interfrigidiana</i>	0.00	0.00	0.00	0.00	0.00	0.00	0.00	0.00	0.00	0.00	0.00	0.00	0.00	0.00	0.00	0.00	0.00	0.00	0.00	0.00
<i>Fragilarlopsis kerguelensis</i>	52.45	62.23	74.83	53.39	57.27	16.63	12.06	28.02	34.96	32.67	27.72	19.79	17.13	16.15	12.66	4.59	5.27	4.52	18.93	17.38
<i>Fragilaropsis obliquecostata</i>	0.38	0.46	0.35	0.14	0.00	0.48	0.00	0.00	0.00	0.00	0.00	0.00	0.00	0.00	0.00	0.00	0.00	0.00	0.00	0.00
<i>Fragilaropsis praecurta (?)</i>	0.00	0.00	0.00	0.00	0.00	0.00	0.00	0.00	0.00	0.00	0.00	0.00	0.00	0.00	0.00	0.00	0.00	0.00	0.00	0.00
<i>Fragilarlopsis praeterfrigidiana</i>	0.00	0.00	0.00	0.00	0.00	0.00	0.00	0.00	0.00	0.00	0.00	0.00	0.00	0.00	0.00	0.00	0.00	0.00	0.00	0.00
<i>Fragilaropsis ritscheri</i>	0.75	0.62	0.70	1.27	1.98	23.52	24.36	8.52	11.73	6.93	4.35	6.25	13.70	10.18	8.44	8.35	7.81	8.17	9.81	1.67
<i>Fragilarlopsis rhombica</i>	3.40	2.17	1.22	2.26	0.66	0.48	0.00	0.00	0.00	0.00	0.00	0.00	0.00	0.00	0.00	0.00	0.00	0.00	0.00	0.00
<i>Fragilaropsis separanda</i>	8.68	4.02	6.29	18.22	9.03	10.93	6.50	4.67	8.41	11.39	2.99	3.65	7.71	6.19	6.45	3.34	3.59	4.52	0.70	7.86
<i>Fragilaropsis separanda var A</i>	0.00	0.00	0.00	0.00	0.00	0.00	0.00	0.00	0.00	0.00	0.00	0.00	0.00	0.00	0.00	0.00	0.00	0.00	0.00	0.00
<i>Fragilaropsis sublinearis</i>	0.00	0.00	0.00	0.00	0.22	0.48	0.46	0.27	0.00	0.25	0.00	0.78	0.86	0.88	0.25	0.84	0.21	0.00	0.47	1.19
<i>Fragilaropsis weaveri</i>	0.00	0.00	0.00	0.00	0.00	0.00	0.00	0.00	0.00	0.00	0.00	0.00	0.00	0.00	0.00	0.00	0.00	0.00	0.00	0.00
<i>Hemidiscus karstenii</i>	0.00	0.00	0.00	0.00	0.00	0.00	0.00	0.00	0.00	0.00	0.00	0.00	0.00	0.00	0.00	0.00	0.00	0.00	0.00	0.00
<i>Navicula directa</i>	0.00	0.15	0.00	0.00	0.00	0.48	0.23	0.00	0.00	0.00	0.00	0.00	0.00	0.00	0.00	0.00	0.00	0.00	0.00	0.00
<i>Navicula glaciei</i>	0.00	0.00	0.00	0.00	0.00	0.00	0.00	0.00	0.00	0.00	0.00	0.00	0.00	0.00	0.00	0.00	0.00	0.00	0.00	0.00
<i>Nitzschia fossilis</i>	0.00	0.00	0.00	0.00	0.00	0.00	0.00	0.00	0.00	0.00	0.00	0.00	0.00	0.00	0.00	0.00	0.00	0.00	0.00	0.00
<i>Nitzschia pergalii</i>	0.00	0.00	0.00	0.00	0.00	0.00	0.00	0.00	0.00	0.00	0.00	0.26	0.43	0.00	0.00	0.00	0.00	0.00	0.00	0.00
<i>Nitzschia reinholdii</i>	0.00	0.00	0.00	0.00	0.00	0.00	0.00	0.00	0.00	0.00	0.00	0.00	0.00	0.00	0.00	0.00	0.00	0.00	0.00	0.00
<i>Proboscia alata</i>	0.00	0.00	0.00	0.00	0.00	0.00	0.00	0.00	0.00	0.00	0.00	0.26	0.21	0.00	0.00	0.00	0.00	0.00	0.00	0.00
<i>Proboscia barboi</i>	0.00	0.00	0.00	0.00	0.00	0.00	0.00	0.00	0.00	0.00	0.00	0.00	0.00	0.00	0.00	0.00	0.00	0.00	0.00	0.00
<i>Rhizosolenia hebetata (group)</i>	0.00	0.15	0.00	0.00	0.00	0.00	0.00	0.00	0.00	0.00	0.00	0.00	0.00	0.00	0.00	0.21	0.00	0.22	0.00	0.00
<i>Rhizosolenia styliformis (group)</i>	0.75	0.46	0.70	0.85	1.32	2.38	0.46	1.65	0.44	0.74	1.90	3.13	3.00	3.32	0.25	1.46	1.90	0.65	0.47	0.24
<i>Rhizosolenia sp A</i>	0.00	0.00	0.00	0.00	0.00	0.00	0.00	0.00	0.00	0.00	0.00	0.00	0.00	0.22	0.50	0.00	0.00	0.00	0.00	0.24
<i>Rhizosolenia spp</i>	0.00	0.00	0.17	0.28	0.00	0.00	0.46	0.27	0.00	0.74	0.27	0.26	0.00	0.22	0.00	0.00	0.00	0.00	0.00	0.48
<i>Rouxia antarctica</i>	0.00	0.00	0.00	0.00	0.00	0.00	0.00	0.00	0.00	0.00	0.00	0.26	0.21	0.00	0.00	0.00	0.00	0.22	0.00	0.48
<i>Rouxia heteropolara</i>	0.00	0.00	0.00	0.00	0.00	0.00	0.00	0.00	0.00	0.00	0.00	0.00	0.00	0.00	0.00	0.00	0.00	0.00	0.00	0.00
<i>Rouxia isopolica</i>	0.00	0.00	0.00	0.00	1.10	3.56	5.80	3.85	3.54	7.43	8.42	4.17	1.93	2.65	0.25	1.46	2.32	2.80	2.10	2.38
<i>Rouxia leventerae</i>	0.00	0.00	0.00	0.00	0.00	0.00	0.00	0.00	0.00	0.00	0.00	0.00	0.00	0.00	0.00	0.00	0.00	0.00	0.00	0.00
<i>Rouxia naviculoides</i>	0.00	0.00	0.00	0.00	0.00	0.00	0.00	0.00	0.00	0.00	0.00	0.00	0.00	0.00	0.00	0.00	0.00	0.00	0.00	0.00
<i>Stellarima microtrias</i>	0.00	0.00	0.00	0.00	0.00	0.48	0.23	0.27	0.22	0.25	0.27	0.52	0.00	0.22	0.25	0.42	0.21	0.22	0.47	0.24
<i>Stephanopyxis spp</i>	0.00	0.00	0.00	0.00	0.00	0.00	0.00	0.00	0.0											

**Appendix 3. continued**

GC 34																					
CORE DEPTH (cm)	200	210	220	230	240	250	260	270	280	290	300	310	320	330	340	350	360	370	380	390	
DIATOMS																					
<i>Actinocyclus actinocylitus</i>	0.23	1.08	0.19	0.44	0.43	0.22	0.39	0.23	0.00	0.17	0.00	0.21	0.00	0.20	0.20	0.00	0.00	0.72	0.47	0.61	
<i>Actinocyclus dimorphus</i>	0.00	0.00	0.00	0.00	0.00	0.00	0.00	0.00	0.00	0.00	0.00	0.00	0.00	0.00	0.00	0.00	0.00	0.00	0.00	0.00	
<i>Actinocyclus fasciculatus</i>	0.00	0.00	0.00	0.00	0.00	0.00	0.00	0.00	0.00	0.00	0.00	0.00	0.00	0.00	0.00	0.00	0.00	0.00	r	0.00	
<i>Actinocyclus ingens</i>	20.50	26.29	14.62	20.00	25.22	33.04	21.26	27.70	35.28	39.32	44.80	36.91	12.52	21.19	12.24	15.64	14.39	9.55	15.19	7.94	
<i>Actinocyclus karstenii</i>	0.00	0.00	0.00	0.00	0.00	0.00	0.00	0.00	0.00	0.00	0.00	0.00	0.00	0.00	0.00	0.00	0.00	0.00	r	0.00	
<i>Asteromphalus hookeri</i>	0.00	0.00	0.19	0.00	0.00	0.00	0.00	0.00	0.18	0.17	0.00	0.00	0.38	0.00	0.00	0.00	0.00	0.00	0.23	0.00	
<i>Asteromphalus hepaticus / parvulus</i>	0.46	0.00	0.00	0.00	0.22	0.00	0.20	0.23	0.00	0.34	0.60	0.43	1.90	0.59	0.41	0.56	1.20	0.00	1.17	0.61	
<i>Asteromphalus hyalinus</i>	0.00	0.00	0.19	0.00	0.00	0.00	0.00	0.00	0.00	0.00	0.00	0.00	0.00	0.00	0.00	0.84	0.48	0.72	0.23	1.63	
<i>Azpeitia tabularis</i>	0.00	0.00	0.00	0.00	0.00	0.00	0.00	0.00	0.00	0.00	0.00	0.00	0.00	0.00	0.00	0.00	0.24	0.00	0.00	0.00	
<i>Chaetoceros bulbosum</i>	0.00	0.00	0.00	0.00	0.00	0.00	0.39	0.00	0.00	0.17	0.00	0.00	0.19	0.00	0.20	0.28	0.00	0.00	0.00	0.41	
<i>Chaetoceros cysts</i>	0.00	0.00	0.00	0.00	0.22	0.22	0.00	0.00	0.00	0.00	0.20	0.21	0.00	0.20	0.20	0.00	0.00	0.00	0.23	0.20	
<i>Corethron crophillum</i>	0.00	0.00	0.00	0.00	0.00	0.00	0.00	0.00	0.00	0.00	0.00	0.00	0.00	0.00	0.00	0.00	0.00	0.00	0.00	0.00	
<i>Coscinodiscus spp</i>	0.00	0.27	0.19	0.22	0.00	1.56	0.20	0.47	0.55	0.17	0.40	0.21	0.00	1.19	2.86	0.28	0.72	1.91	1.87	2.24	
<i>Dactylosolen antarcticus</i>	0.68	2.17	0.77	0.44	0.86	1.12	3.94	1.88	1.28	0.51	4.20	1.07	2.09	0.99	2.45	2.51	3.60	10.74	3.50	1.63	
<i>Denticulopsis spp</i>	0.00	0.00	0.00	0.00	0.00	0.00	0.00	0.00	0.00	0.00	0.00	0.00	0.00	0.00	0.00	0.00	0.00	0.00	0.00	0.00	
<i>Eucampia antarctica</i>	1.59	0.54	0.00	1.33	0.43	1.56	0.20	1.17	0.37	1.19	0.20	0.00	0.00	0.59	0.61	0.28	2.40	0.95	1.17	0.20	
<i>Fragilaropsis aurca</i>	0.00	0.00	0.00	0.00	0.00	0.00	0.00	0.00	0.00	0.00	0.00	0.00	0.00	0.00	0.00	0.00	0.00	0.00	0.00	0.00	
<i>Fragilaropsis barronii</i>	0.00	0.00	0.00	0.00	0.00	0.00	0.00	0.00	0.00	0.00	0.120	0.21	0.00	0.40	0.61	0.28	0.00	0.24	0.23	0.20	
<i>Fragilaropsis barronii var A + B</i>	17.08	11.65	17.88	18.89	29.31	7.37	12.20	6.57	12.61	12.20	15.40	9.01	10.06	8.91	12.65	11.73	7.67	7.16	3.50	9.78	
<i>Fragilaropsis curta</i>	6.15	8.94	33.46	14.44	15.09	4.24	15.16	9.39	14.99	4.24	7.00	4.29	3.80	7.13	9.39	4.75	6.24	2.15	r	9.98	
<i>Fragilaropsis cylindrus</i>	0.00	0.00	0.96	0.00	0.00	0.22	0.79	0.23	0.18	0.00	0.00	0.00	0.00	0.00	0.00	0.28	0.24	0.00	0.00	0.61	
<i>Fragilaropsis interfrigidiana</i>	0.00	0.00	0.00	0.00	0.00	0.00	0.00	0.00	0.00	0.00	0.00	0.00	0.00	0.00	0.00	0.00	0.00	0.00	0.00	0.00	
<i>Fragilaropsis kerguelensis</i>	24.15	4.88	3.46	1.33	3.66	3.57	6.50	1.64	2.38	5.93	7.60	14.81	26.62	5.94	2.65	1.96	0.48	1.43	1.40	3.87	
<i>Fragilaropsis obliquecostata</i>	0.00	0.00	0.00	0.00	0.00	0.00	0.00	0.00	0.00	0.00	0.00	0.00	0.00	0.00	0.00	0.00	0.00	0.00	0.00	0.00	
<i>Fragilaropsis praecurta (?)</i>	0.00	0.00	0.00	0.00	0.00	0.00	0.00	0.47	0.00	0.00	0.00	0.00	0.38	0.79	2.24	1.68	3.12	2.39	5.37	1.63	
<i>Fragilaropsis praeinterfrigidiana</i>	0.00	0.00	0.00	0.00	0.00	0.00	0.00	0.00	0.00	0.00	0.00	0.00	0.00	0.00	0.00	0.00	0.00	0.00	0.00	0.00	
<i>Fragilaropsis nitscheri</i>	1.59	0.54	1.54	1.11	0.00	1.12	3.15	1.88	1.65	1.02	0.20	0.64	0.00	0.00	0.00	0.00	0.00	0.00	0.23	0.61	
<i>Fragilaropsis rhombica</i>	0.00	0.00	0.00	0.00	0.00	0.00	0.00	0.00	0.00	0.00	0.00	0.00	0.00	0.00	0.00	0.00	0.00	0.00	0.00	0.00	
<i>Fragilaropsis separanda</i>	5.92	1.08	3.85	0.89	1.08	1.34	2.17	0.00	0.37	0.00	0.40	0.00	2.47	1.19	0.41	0.00	0.00	0.00	0.47	0.20	
<i>Fragilaropsis separanda var A</i>	0.00	0.00	0.00	0.00	0.00	0.00	0.00	0.00	0.00	0.00	0.00	0.00	0.00	0.00	0.00	0.00	0.00	0.00	0.00	0.00	
<i>Fragilaropsis sublineans</i>	0.23	0.54	0.38	0.67	0.43	1.56	1.57	0.94	1.83	1.19	0.80	1.50	0.19	0.59	0.41	0.28	1.44	2.15	1.17	0.20	
<i>Fragilaropsis weaveri</i>	0.00	0.00	0.00	0.00	0.00	0.00	0.00	0.00	0.00	0.00	0.00	0.00	0.00	0.00	0.00	0.00	0.00	0.00	0.00	0.00	
<i>Hemidiscus karstenii</i>	0.00	0.00	0.00	0.00	0.00	0.00	0.00	0.00	0.00	0.00	0.00	0.00	0.00	0.00	0.00	0.00	0.00	0.00	0.00	0.00	
<i>Navicula directa</i>	0.00	0.00	0.00	0.00	0.00	0.00	0.00	0.00	0.00	0.00	0.00	0.00	0.00	0.00	0.00	0.00	0.00	0.00	0.00	0.00	
<i>Navicula glaciei</i>	0.00	0.00	0.00	0.00	0.00	0.00	0.00	0.00	0.00	0.00	0.00	0.00	0.00	0.00	0.00	0.00	0.00	0.00	0.00	0.00	
<i>Nitzschia fossilis</i>	0.00	0.00	0.00	0.00	0.22	0.00	0.00	0.00	0.00	0.00	0.00	0.00	0.00	0.00	0.00	0.28	0.00	0.00	0.00	0.00	
<i>Nitzschia perrigallii</i>	0.00	0.54	0.19	0.00	0.22	0.00	0.58	0.23	0.00	0.00	0.60	0.21	0.00	0.00	0.00	0.00	0.24	0.00	0.00	1.22	
<i>Nitzschia reinholdii</i>	0.00	0.00	0.00	0.00	0.00	0.00	0.00	0.00	0.00	0.00	0.00	0.00	0.00	0.00	0.00	0.00	0.00	0.00	0.00	0.00	
<i>Proboscia alata</i>	0.00	0.00	0.00	0.00	0.00	0.00	0.00	0.00	0.00	0.00	0.00	0.00	0.00	0.00	0.00	0.00	0.00	0.00	0.00	0.00	
<i>Proboscia barbori</i>	0.00	0.00	0.00	0.00	0.00	0.00	0.00	0.00	0.00	0.00	0.00	0.00	0.00	0.00	0.00	0.00	0.00	0.00	0.00	0.00	
<i>Rhizosolenia hebetata (group)</i>	0.00	0.00	0.00	0.00	0.00	0.00	0.00	0.00	0.00	0.00	0.00	0.00	0.00	0.00	0.00	0.00	0.00	0.00	0.23	0.41	
<i>Rhizosolenia styliformis (group)</i>	1.37	1.90	1.35	2.67	1.08	2.46	1.18	0.23	1.28	1.02	1.20	1.50	0.38	0.40	0.61	0.28	0.96	0.72	0.47	1.02	
<i>Rhizosolenia sp A</i>	0.00	0.27	0.00	0.00	0.00	0.00	0.00	0.23	0.18	0.00	0.00	0.00	0.19	0.00	0.00	0.28	0.24	0.24	0.00	1.83	
<i>Rhizosolenia spp</i>	0.23	0.00	0.00	0.22	0.22	0.22	0.20	0.00	0.00	0.00	0.00	0.00	0.00	0.00	0.00	0.00	0.00	0.00	0.00	0.00	
<i>Rouxia antarctica</i>	0.46	0.54	0.38	0.00	0.22	0.00	0.00	0.94	0.00	0.34	0.00	0.00	0.38	4.16	4.90	3.07	8.39	9.31	12.62	9.16	
<i>Rouxia heteropolara</i>	0.00	0.00	0.00	0.00	0.00	0.00	0.00	0.00	0.00	0.00	0.00	0.00	0.00	0.00	0.00	0.00	0.00	0.00	0.00	0.00	
<i>Rouxia isopolica</i>	1.59	3.79	2.31	2.67	1.51	2.46	0.59	19.72	5.48	3.73	1.80	2.15	0.19	0.59	0.61	0.56	1.92	2.63	1.64	0.81	
<i>Rouxia leventerae</i>	0.00	0.00	0.00	0.00	0.00	0.00	0.00	0.00	0.00	0.00	0.00	0.00	0.00	0.00	0.00	0.00	0.00	0.00	0.00	0.00	
<i>Rouxia naviculoides</i>	0.00	0.00	0.00	0.00	0.00	0.00	0.20	0.00	0.00	0.17	0.20	4.51	11.76	20.00	18.98	17.32	12.47	8.35	6.78	9.16	
<i>Stellarima microtrias</i>	0.00	0.54	0.00	0.00	0.00	0.45	0.00	0.00	0.34	0.20	0.00	0.00	0.20	0.61	1.12	0.72	0.48	1.17	0.41		
<i>Stephanopyxus spp</i>	0.00	0.00	0.00	0.00	0.00	0.00	0.00	0.00	0.00	0.00	0.00	0.00	0.00	0.00	0.00	0.00	0.00	0.00	0.00	0.00	
<i>Thalassionema nitzschloides (group)</i>	0.00	0.00	0.00	0.00	0.00	0.00	0.00	0.00	0.00	0.00	0.00	0.21	5.31	0.00	0.00	0.00	0.00	0.00	0.00	0.00	
<i>Thalassionema nitzschloides var parva</i>	0.00	0.00	0.00	0.00	0.00	0.00	0.00	0.00	0.00	0.00	0.00	0.00	r	0.00	0.00	0.00	0.00	0.00	0.00	0.00	
<i>Thalassiosira antarctica</i>	0.00	0.00	0.00	0.00	0.00	0.00	0.00	0.00	0.00	0.00	0.00	0.00	0.19	0.00	1.43	0.00	0.00	0.00	0.00	0.00	
<i>Thalassiosira complicata</i>	0.00	0.00	0.00	0.00	0.00	0.00	0.00	0.00	0.00	0.00	0.00	0.00	0.00	0.00	0.00	0.00	0.00	0.00	0.00	0.00	
<i>Thalassiosira elliptipora</i>	0.00	1.08	0.19	1.11	0.22	1.56	0.20	0.70	0.55	0.68	0.20	0.43	0.38	0.00	0.00	0.28	0.24	0.00	0.23	0.00	
<i>Thalassiosira fasciculata</i>	0.23	0.27	0.00	0.67	1.08	0.45	0.00	0.23	1.10	1.02	0.20	0.64	0.19	0.00	0.82	0.00	1.92	0.72	0.00	0.41	
<i>Thalassiosira frenguelli</i>	0.00	0.00	0.00	0.00	0.00	0.00	0.20	0.00	0.00	0.00	0.00	0.00	0.00	0.20	0.00	0.00	0.48	0.00	0.23	0.00	
<i>Thalassiosira gracilis var expecta</i>	0.00	0.00	0.58	0.00	0.22	0.45	0.00	0.00	0.00	0.17	0.00	0.00	0.00	0.00	0.00	0.00	0.24	0.00	0.00	0.00	
<i>Thalassiosira gracilis var gracilis</i>	0.23	0.00	1.73	0.89	1.29	1.12	0.20	0.00	0.00	0.00	0.20	0.21	0.00	0.00	0.00	0.00	0.00	0.00	0.00	0.00	
<i>Thalassiosira gravida</i>	0.00	0.00	0.00	0.00	0.22	0.00	0.39	0.00	0.00	0.00	0.00	0.00	0.00	0.40	0.41	0.28					

# Appendix 3. continued

GC 34		399	410	420	430	440	450	460	470	480	490	500	510	520	530	540	550	560	570
CORE DEPTH (cm)																			
DIATOMS																			
<i>Actinocyclus actinocylus</i>		0.23	0.97	1.01	0.51	0.23	0.00	1.29	0.29	0.16	0.00	0.37	0.00	0.00	0.00	0.00	0.00	0.31	0.00
<i>Actinocyclus dimorphus</i>		0.00	0.00	0.00	0.00	0.00	0.00	0.00	0.00	0.00	0.00	0.00	0.00	0.00	0.00	0.00	0.00	0.00	0.00
<i>Actinocyclus fasciculatus</i>		r	r	0.50	1.80	1.87	1.15	3.00	0.58	0.00	0.18	0.00	0.00	0.00	0.00	0.00	0.00	0.00	0.00
<i>Actinocyclus ingens</i>		18.78	16.46	16.33	10.03	5.84	2.08	0.86	0.58	0.47	0.18	0.18	0.00	0.00	0.00	0.23	0.58	0.00	0.00
<i>Actinocyclus karstenii</i>		r	0.24	0.50	1.29	1.17	3.00	1.50	1.45	1.40	1.27	0.37	0.00	0.00	0.00	0.00	0.00	0.00	0.00
<i>Asteromphalus hookeri</i>		0.00	0.00	0.00	0.00	0.00	0.00	0.00	0.00	0.00	0.00	0.00	0.00	0.00	0.00	0.00	0.00	0.00	0.00
<i>Asteromphalus hepaticus / parvulus</i>		0.00	0.00	0.00	0.51	0.00	0.00	0.00	0.00	0.00	0.00	0.00	0.00	0.00	0.00	0.00	0.00	0.00	0.00
<i>Asteromphalus hyalinus</i>		0.68	1.45	1.01	1.29	1.17	1.15	0.84	0.58	0.16	0.00	0.18	0.00	0.00	0.00	0.00	0.00	0.00	0.00
<i>Azpetia tabularis</i>		0.00	0.00	0.00	0.00	0.00	0.00	0.00	0.00	0.00	0.00	0.00	0.00	0.00	0.00	0.00	0.00	0.00	0.00
<i>Chaetoceros bulbosum</i>		0.00	0.00	0.00	0.00	0.00	0.00	0.21	0.00	0.00	0.00	0.00	0.00	0.00	0.00	0.00	0.00	0.00	0.00
<i>Chaetoceros cysts</i>		0.23	0.00	0.00	0.00	0.47	2.08	0.64	1.45	0.00	0.54	0.37	1.03	0.00	0.47	0.45	0.00	0.62	1.62
<i>Corethron crophilum</i>		0.00	0.00	0.00	0.00	0.00	0.23	0.00	0.00	0.00	0.00	0.00	0.00	0.00	0.00	0.00	0.00	0.00	0.00
<i>Coscinodiscus spp</i>		0.00	0.48	1.26	0.77	0.93	0.69	0.43	0.29	0.16	0.00	0.37	0.00	0.00	0.00	0.91	0.58	0.00	0.00
<i>Dactylosolen antarcticus</i>		2.71	2.66	4.52	2.57	4.44	4.62	5.36	3.49	3.74	5.06	9.61	15.72	18.13	23.08	22.50	15.74	11.21	11.35
<i>Denticulopsis spp</i>		0.00	0.00	0.00	0.00	0.00	0.00	0.00	0.00	0.16	0.18	0.00	0.00	0.00	0.47	0.23	0.29	0.93	0.54
<i>Eucampia antarctica</i>		0.45	0.48	0.25	1.03	2.34	2.31	3.43	2.62	2.80	0.72	0.74	0.52	0.27	0.00	0.00	0.00	0.00	0.00
<i>Fragilaropsis aunca</i>		0.00	0.00	0.00	0.00	r?	0.00	0.00	0.00	0.00	0.00	0.00	0.00	r	0.00	r	0.58	5.30	14.05
<i>Fragilaropsis barronii</i>		0.90	0.24	0.25	0.51	r	0.69	r	1.16	3.74	2.71	7.95	15.21	13.60	17.41	15.23	6.41	2.49	0.54
<i>Fragilaropsis barronii var A + B</i>		6.33	3.39	2.01	2.06	2.34	0.92	1.29	0.29	0.31	0.54	0.00	1.03	0.00	0.00	0.00	0.00	0.00	0.00
<i>Fragilaropsis curta</i>		9.28	5.33	2.76	6.94	5.14	8.08	6.65	6.98	4.98	2.89	3.33	1.80	2.13	1.65	5.00	5.25	1.87	2.70
<i>Fragilaropsis cylindrus</i>		0.00	0.00	0.00	0.00	0.00	0.00	0.00	0.00	0.00	0.00	0.00	0.00	0.00	0.00	0.00	0.00	0.00	0.00
<i>Fragilaropsis interfrigidaria</i>		0.00	r	0.00	0.00	r	r	r	r	r	0.54	0.00	0.00	1.60	0.24	1.59	2.33	3.12	3.24
<i>Fragilaropsis kerguelensis</i>		3.17	6.30	3.02	1.80	0.70	0.92	0.00	0.00	0.31	0.00	0.00	0.00	0.00	0.00	0.00	0.00	0.00	0.00
<i>Fragilaropsis obliquecostata</i>		0.00	0.24	0.00	0.00	0.00	0.00	0.00	0.00	0.00	0.00	0.00	0.00	0.00	0.00	0.00	0.00	0.62	0.00
<i>Fragilaropsis praecurta (?)</i>		4.75	6.05	4.02	4.11	4.21	3.23	2.36	2.03	1.09	1.99	1.66	2.58	1.07	0.94	0.00	0.58	0.31	0.00
<i>Fragilaropsis praeterfrigidaria</i>		0.00	0.00	0.00	0.00	r	r	0.64	0.29	1.87	2.35	2.59	3.61	4.27	2.59	1.59	1.17	r	r
<i>Fragilaropsis nitscheri</i>		0.00	0.00	0.00	0.00	0.00	0.00	0.00	0.00	0.00	2.89	1.85	1.03	0.27	0.47	0.00	0.00	0.00	0.00
<i>Fragilaropsis rhombica</i>		0.00	0.00	0.00	0.00	0.00	0.00	0.00	0.00	0.00	0.00	0.00	0.00	0.00	0.00	0.00	0.00	0.00	0.00
<i>Fragilaropsis separanda</i>		0.45	0.00	0.00	0.00	0.23	0.00	0.00	0.00	0.00	0.00	0.00	0.00	0.00	0.00	0.00	0.00	0.00	0.00
<i>Fragilaropsis separanda var A</i>		0.00	0.00	0.00	0.00	0.00	0.00	0.00	0.00	0.00	0.00	0.00	0.00	0.00	0.00	0.00	0.00	0.00	0.00
<i>Fragilaropsis sublineans</i>		0.00	1.21	1.01	1.03	0.47	0.92	0.64	0.58	0.00	0.18	0.37	0.00	0.00	0.00	0.00	0.00	0.00	0.54
<i>Hemidiscus karstenii</i>		0.00	0.00	0.00	0.00	0.00	0.00	0.00	0.00	0.00	0.00	0.00	0.00	0.00	0.00	0.00	0.00	0.00	0.00
<i>Navicula directa</i>		0.00	0.00	0.00	0.00	0.00	0.00	0.00	0.00	0.00	0.00	0.00	0.00	0.00	0.00	0.00	0.00	0.00	0.00
<i>Navicula glaciei</i>		0.00	0.00	0.00	0.00	0.00	0.00	0.00	0.00	0.00	0.00	0.00	0.00	0.00	0.00	0.00	0.00	0.00	0.00
<i>Nitzschia fossilis</i>		0.00	0.00	0.00	0.00	0.00	0.00	0.00	0.00	0.00	0.00	0.00	0.00	0.00	0.00	0.00	0.00	0.31	0.00
<i>Nitzschia perrigallii</i>		0.00	0.00	0.00	0.00	0.00	0.00	0.00	0.00	0.00	0.00	0.00	0.00	0.00	0.00	0.00	0.00	0.00	0.00
<i>Nitzschia reinholdii</i>		0.00	0.00	0.00	0.00	0.00	0.00	0.00	0.00	0.00	0.00	0.00	0.00	0.00	r	0.00	r	0.00	0.00
<i>Fragilaropsis weaveri</i>		0.00	r	0.00	0.00	r	0.00	r	0.00	r	0.00	0.00	0.00	0.00	0.00	0.00	r	0.00	0.00
<i>Proboscia alata</i>		0.00	0.00	0.00	0.00	0.00	0.00	0.00	0.00	0.00	0.00	0.00	0.00	0.00	0.00	0.00	0.00	0.31	0.00
<i>Proboscia barboi</i>		0.00	0.00	0.00	0.00	0.00	0.00	0.00	0.00	0.00	0.00	0.00	0.00	0.00	0.00	0.00	0.00	0.00	0.00
<i>Rhizosolenia hebelata (group)</i>		0.00	0.00	0.00	0.00	0.00	0.23	0.00	0.00	0.00	0.00	0.00	0.00	0.00	0.00	0.00	0.00	0.93	0.00
<i>Rhizosolenia styliformis (group)</i>		2.26	2.66	2.01	2.31	4.21	1.62	2.15	0.29	0.31	0.18	0.74	1.55	0.80	1.41	1.36	2.33	0.62	1.08
<i>Rhizosolenia sp A</i>		1.13	0.24	0.00	0.51	0.93	0.69	0.43	0.00	0.00	0.00	0.00	0.00	0.00	0.00	0.00	0.00	0.00	0.00
<i>Rhizosolenia spp</i>		0.00	0.00	0.00	0.00	0.00	0.00	0.00	0.00	0.00	0.00	0.00	0.00	0.00	0.00	0.00	0.00	0.00	0.00
<i>Rouxia antarctica</i>		13.57	8.47	8.29	8.23	5.37	9.70	4.94	1.45	0.93	1.27	1.66	1.55	6.93	5.18	4.09	5.83	4.98	7.03
<i>Rouxia heteropolara</i>		0.00	0.00	0.00	0.00	0.00	0.00	0.00	0.00	0.78	0.36	0.00	0.77	0.80	0.47	0.91	0.58	0.93	0.54
<i>Rouxia isopolica</i>		0.90	0.00	0.50	0.77	0.23	0.92	1.07	0.87	0.62	0.54	0.55	1.80	2.13	1.41	2.95	4.08	6.54	12.97
<i>Rouxia leventerae</i>		0.00	0.00	0.75	0.26	0.70	2.54	4.29	2.91	1.56	0.36	0.92	0.00	0.00	0.00	r	0.00	0.00	r
<i>Rouxia naviculoides</i>		6.56	4.36	12.06	8.74	4.91	8.08	4.08	4.36	2.34	3.07	5.91	15.46	18.40	15.53	15.00	14.29	14.95	17.30
<i>Stellarima microtrus</i>		0.00	0.73	0.50	0.51	0.70	0.46	0.43	0.29	0.31	0.36	0.37	0.26	0.27	0.00	0.00	0.29	0.00	0.00
<i>Stephanopyxis spp</i>		0.00	0.00	0.00	0.00	0.00	0.00	0.00	0.00	0.00	0.00	0.00	0.00	0.00	0.00	0.68	0.00	0.00	0.00
<i>Thalassionema nitzschioides (group)</i>		0.00	0.00	0.00	0.00	0.00	0.00	0.00	0.00	0.00	0.00	0.00	0.00	0.00	0.24	0.00	0.58	1.25	7.03
<i>Thalassionema nitzschioides var parva</i>		0.00	0.00	0.00	0.00	0.00	0.00	0.00	0.00	0.00	0.00	0.00	0.00	0.00	0.00	r	0.00	0.00	0.00
<i>Thalassiosira antarctica</i>		0.00	0.00	0.00	0.00	0.00	0.00	0.00	0.00	0.00	0.00	0.00	0.00	0.00	0.00	0.00	0.00	0.00	0.00
<i>Thalassiosira complicata</i>		0.00	0.00	0.00	0.00	r	0.00	r	0.00	0.47	0.18	0.18	0.52	1.60	1.88	1.14	1.17	0.31	0.00
<i>Thalassiosira elliptora</i>		r	0.00	0.00	0.00	0.00	0.00	r?	0.00	0.00	0.00	0.00	0.00	0.00	0.00	0.00	0.00	0.00	0.00
<i>Thalassiosira fasciculata</i>		0.90	0.48	0.50	1.29	0.00	0.23	0.00	0.00	0.00	0.00	0.00	0.00	r	0.00	0.00	0.00	0.00	0.00
<i>Thalassiosira frenguelli</i>		0.00	0.00	0.00	0.00	0.00	0.00	0.00	0.00	0.00	0.00	0.00	0.00	0.00	0.00	0.00	0.00	0.00	0.00
<i>Thalassiosira gracilis var expecta</i>		0.00	0.00	0.00	0.00	0.00	0.00	0.00	0.00	0.16	0.00	0.00	0.00	0.00	0.00	0.00	0.00	0.00	0.00
<i>Thalassiosira gracilis var gracilis</i>		0.00	0.00	0.00	0.00	0.00	0.00	0.00	0.00	0.00	0.00	0.00	0.00	0.00	0.00	0.00	0.00	0.00	0.00
<i>Thalassiosira gravida</i>		0.00	0.24	0.00	0.00	0.00	0.00	0.21	0.00	0.00	0.00	0.00	0.00	0.00	0.00	0.00	0.00	0.00	0.00
<i>Thalassiosira inura</i>		0.00	r	0.00	0.51	0.93	1.62	1.07	1.16	0.31	2.35	1.29	1.55	2.67	4.24	4.32	6.71	4.36	5.95
<i>Thalassiosira inura-insigna (transition)</i>		0.00	r	2.26	2.31	0.47	0.00	0.00	0.40	6.54	11.39	11.09	6.44	1.60	0.24	0.91	0.87	1.87	0.00
<i>Thalassiosira insigna</i>		r	0.97	1.51	1.03	3.27	7.85	14.16	21.22	29.13	33.45	23.29	5.67	2.40	0.94	0.23	0.87	0.00	1.08
<i>Thalass</i>																			



# Appendix 3. continued

GC 50 (lat 57°45 1'E, long 77°32 1'E)																				
CORE DEPTH (cm)	0	10	20	30	40	50	60	70	80	90	100	110	120	130	140	150	160	170	180	190
DIATOMS																				
<i>Actinocyclus actinocylus</i>	0 15	0 47	0 15	0 26	0 21	9 96	1 22	1 09	0 39	0 45	0 20	0 00	0 00	0 00	0 00	0 00	0 19	0 33	0 00	0 00
<i>Actinocyclus dimorphus</i>	0 00	0 00	0 00	0 00	0 00	0 00	0 00	0 00	0 00	0 00	0 00	0 00	0 00	0 00	0 00	0 00	0 00	0 00	0 00	0 00
<i>Actinocyclus fasciculatus</i>	0 00	0 00	0 00	0 00	0 00	0 00	0 00	0 00	0 00	0 00	0 00	0 00	0 00	0 00	0 00	0 00	0 00	0 00	0 00	0 00
<i>Actinocyclus ingens</i>	0 00	0 00	0 00	0 00	0 42	1 85	0 61	1 37	0 97	2 25	31 00	20 25	36 24	41 40	23 63	6 68	29 57	20 42	21 77	12 73
<i>Actinocyclus karstenii</i>	0 00	0 00	0 00	0 00	0 00	0 00	0 00	0 00	0 00	0 00	0 00	0 00	0 00	0 00	0 00	0 00	0 00	0 00	0 00	0 15
<i>Asteromphalus hookeri</i>	0 45	0 16	0 00	0 00	0 00	0 00	0 00	0 14	0 00	0 15	0 20	0 21	0 19	0 23	0 53	0 00	0 19	0 00	0 34	0 00
<i>Asteromphalus hepaticus / parvulus</i>	0 45	0 16	0 15	0 00	0 00	0 28	0 20	0 96	0 19	0 30	0 80	0 42	0 00	0 00	0 00	0 00	0 00	0 33	0 00	0 00
<i>Asteromphalus hyalinus</i>	0 15	0 31	0 15	0 00	0 00	0 00	0 20	0 14	0 19	0 00	0 00	0 00	0 00	0 00	0 00	0 00	0 00	0 33	0 00	0 00
<i>Azpeitia tabularis</i>	0 00	0 47	0 15	0 13	0 21	0 00	0 00	0 14	0 00	0 00	0 00	0 00	0 00	0 00	0 00	0 00	0 00	0 00	0 00	0 00
<i>Chaetoceros bulbosum</i>	0 30	0 16	0 00	0 00	0 00	0 14	0 00	0 00	0 00	0 15	0 20	0 00	0 00	0 00	0 00	0 00	0 19	0 00	0 00	0 00
<i>Chaetoceros cysts</i>	0 30	0 00	0 00	3 12	2 97	0 14	2 65	1 09	1 36	0 75	0 20	2 30	0 00	0 00	0 00	0 00	0 19	0 33	0 17	0 76
<i>Corethron coryphium</i>	0 00	0 00	0 00	0 00	0 00	0 00	0 00	0 14	0 00	0 00	0 00	0 00	0 00	0 00	0 00	0 00	0 00	0 00	0 00	0 00
<i>Coscinodiscus spp</i>	0 00	0 00	0 15	0 00	0 00	1 42	0 00	0 68	0 19	0 75	0 80	0 00	0 57	0 00	0 35	0 18	1 51	0 82	0 00	0 15
<i>Dactylosolen antarcticus</i>	6 14	2 18	1 93	11 31	3 81	1 71	3 27	3 01	10 68	3 44	1 40	3 13	4 74	0 00	2 12	5 45	2 26	4 41	4 59	5 45
<i>Denticulopsis spp</i>	0 00	0 00	0 00	0 00	0 00	0 00	0 00	0 00	0 19	0 00	0 00	0 00	0 00	0 14	0 00	0 00	0 00	0 00	0 00	0 00
<i>Eucampia antarctica</i>	0 75	0 93	0 89	0 39	0 64	3 56	2 24	3 15	1 75	2 69	0 40	0 00	0 19	0 47	0 18	0 18	0 94	0 49	0 00	0 00
<i>Fragilariopsis aunca</i>	0 00	0 00	0 00	0 00	0 00	0 00	0 00	0 00	0 00	0 00	0 00	0 00	0 00	0 00	0 00	0 00	0 00	0 00	0 00	0 00
<i>Fragilariopsis barronii</i>	0 00	0 00	0 00	0 00	0 00	0 00	0 00	0 00	0 00	0 00	0 00	0 00	0 00	0 00	0 00	0 00	0 00	0 00	0 00	0 00
<i>Fragilariopsis barronii var A + B</i>	0 00	0 00	0 30	0 00	0 00	0 00	0 20	0 14	0 39	0 30	24 20	16 28	11 39	0 00	18 17	23 73	13 37	9 80	14 46	29 85
<i>Fragilariopsis curta</i>	0 75	0 78	0 30	11 57	13 56	5 97	12 24	7 39	13 98	4 34	9 60	15 87	7 02	8 37	3 70	20 21	6 97	11 60	13 78	12 12
<i>Fragilariopsis cylindrus</i>	0 00	0 16	0 00	0 52	2 97	0 43	5 51	0 27	2 14	0 45	0 00	1 46	0 19	0 00	0 00	0 70	0 19	0 00	0 17	0 00
<i>Fragilariopsis interfrigidana</i>	0 00	0 00	0 00	0 13	0 00	0 00	0 00	0 00	0 00	0 00	0 00	0 00	0 00	0 23	0 00	0 00	0 38	0 65	0 17	0 15
<i>Fragilariopsis kerguelensis</i>	64 22	63 92	79 64	49 41	52 54	52 63	53 67	57 05	48 16	60 63	3 40	9 19	5 88	3 49	13 93	11 42	3 39	2 78	10 37	13 18
<i>Fragilariopsis obliquecostata</i>	0 00	0 00	0 00	0 26	1 48	0 57	0 61	0 27	0 39	0 45	0 00	0 00	0 00	0 00	0 00	0 00	0 19	0 00	0 17	0 30
<i>Fragilariopsis praecurta (?)</i>	0 00	0 00	0 00	0 00	0 00	0 28	0 00	0 00	0 00	0 00	0 60	0 00	0 00	0 00	0 35	0 18	0 00	0 00	0 00	0 00
<i>Fragilariopsis praeterfrigidana</i>	0 00	0 00	0 00	0 00	0 00	0 00	0 00	0 00	0 00	0 00	0 00	0 00	0 00	0 00	0 00	0 00	0 00	0 00	0 00	0 00
<i>Fragilariopsis ritscheri</i>	0 90	0 78	0 45	0 65	0 85	1 56	0 61	1 50	2 14	1 80	0 00	0 84	0 19	0 00	0 18	0 18	0 56	3 59	2 89	0 45
<i>Fragilariopsis rhombica</i>	2 25	1 40	0 89	6 63	10 17	3 27	6 12	4 51	2 91	3 74	0 00	6 68	0 00	0 00	0 35	0 70	0 00	0 65	1 19	1 36
<i>Fragilariopsis separanda</i>	4 79	4 51	4 31	7 41	4 24	2 13	1 43	3 28	2 72	2 84	0 00	2 51	1 33	0 47	1 06	1 93	0 19	0 33	0 34	0 61
<i>Fragilariopsis separanda var A</i>	0 00	0 00	0 00	0 00	0 00	0 00	0 00	0 00	0 00	0 00	0 00	0 00	0 00	0 00	0 00	0 00	0 00	0 00	0 00	0 00
<i>Fragilariopsis sublinearis</i>	0 00	0 00	0 00	0 00	0 00	0 00	0 20	0 41	0 39	0 15	0 20	0 00	0 00	0 00	0 35	0 53	1 13	0 98	1 19	0 45
<i>Fragilariopsis weaven</i>	0 00	0 00	0 00	0 00	0 00	0 00	0 00	0 00	0 00	0 00	0 00	0 00	0 00	0 00	0 00	0 00	0 00	0 00	0 00	0 00
<i>Hemidiscus karstenii</i>	0 00	0 00	0 00	0 00	0 00	0 00	0 00	0 00	0 00	0 00	0 00	0 00	0 00	0 00	0 00	0 00	0 00	0 00	0 00	0 00
<i>Navicula directa</i>	0 15	0 16	0 15	0 26	0 42	0 14	0 00	0 00	0 00	0 15	0 00	0 00	0 00	0 00	0 00	0 00	0 00	0 00	0 00	0 00
<i>Navicula glaciei</i>	0 00	0 00	0 00	0 00	0 00	0 00	0 00	0 00	0 00	0 00	0 00	0 00	0 00	0 00	0 00	0 00	0 00	0 00	0 00	0 00
<i>Nitzschia fossilis</i>	0 00	0 00	0 00	0 00	0 00	0 00	0 00	0 00	0 00	0 00	0 00	0 00	0 00	0 00	0 00	0 00	0 00	0 00	0 00	0 00
<i>Nitzschia perigalli</i>	0 00	0 00	0 00	0 00	0 00	0 00	0 00	0 00	0 00	0 00	0 00	0 00	0 57	0 70	0 18	0 53	0 56	1 14	1 02	0 15
<i>Nitzschia reinholdii</i>	0 00	0 00	0 00	0 00	0 00	0 00	0 00	0 00	0 00	0 00	0 00	0 00	0 00	0 00	0 00	0 00	0 00	0 00	0 00	0 00
<i>Proboscia alata</i>	0 00	0 00	0 00	0 00	0 00	0 00	0 00	0 00	0 00	0 00	0 00	0 00	0 00	0 00	0 00	0 00	0 00	0 00	0 00	0 00
<i>Proboscia barboi</i>	0 00	0 00	0 00	0 00	0 00	0 00	0 00	0 00	0 00	0 00	0 00	0 00	0 00	0 00	0 00	0 00	0 00	0 00	0 00	0 00
<i>Rhizosolenia hebetata (group)</i>	0 00	0 00	0 00	0 00	0 21	0 14	0 00	0 00	0 19	0 30	0 00	0 00	0 00	0 00	0 00	0 00	0 00	0 16	0 00	0 00
<i>Rhizosolenia styliformis (group)</i>	0 60	0 31	0 15	0 52	0 64	0 14	1 22	0 82	1 55	0 60	1 00	1 46	1 14	1 63	0 53	1 41	0 56	0 49	1 19	0 45
<i>Rhizosolenia sp A</i>	0 00	0 00	0 00	0 00	0 00	0 00	0 00	0 00	0 00	0 15	0 20	1 25	0 19	0 70	0 00	3 16	0 38	1 14	0 17	0 61
<i>Rhizosolenia spp</i>	0 00	0 00	0 00	0 00	0 00	0 00	0 00	0 00	0 00	0 00	0 00	0 00	0 00	0 23	0 00	0 00	0 00	0 16	0 17	0 00
<i>Rouxia antarctica</i>	0 00	0 00	0 00	0 00	0 00	0 00	0 00	0 00	0 00	0 15	0 20	0 00	0 00	0 47	0 00	0 18	0 00	0 00	0 68	0 00
<i>Rouxia heteropolara</i>	0 00	0 00	0 00	0 00	0 00	0 00	0 00	0 00	0 00	0 00	0 00	0 00	0 00	0 00	0 00	0 00	0 00	0 00	0 00	0 00
<i>Rouxia isopolica</i>	0 00	0 00	0 00	0 00	0 64	0 57	1 22	0 82	0 39	0 75	3 00	0 84	1 52	3 02	0 71	6 15	2 45	14 87	4 08	2 73
<i>Rouxia leventerae</i>	0 00	0 00	0 00	0 00	0 00	0 00	0 00	0 00	0 00	0 00	0 00	0 00	0 00	0 00	0 00	0 00	0 00	0 00	0 00	0 00
<i>Rouxia naviculoides</i>	0 00	0 00	0 00	0 13	0 00	0 00	0 00	0 00	0 39	0 00	0 20	0 00	0 19	0 00	0 00	0 00	0 00	0 51	0 00	0 00
<i>Stellarima microstas</i>	0 00	0 00	0 00	0 00	0 00	0 14	0 00	0 00	0 00	0 45	0 00	0 00	0 00	0 00	0 00	0 00	1 13	0 00	0 00	0 00
<i>Stephanopyxis spp</i>	0 00	0 00	0 00	0 00	0 00	0 00	0 00	0 00	0 00	0 00	0 00	0 00	0 00	0						

# Appendix 3. continued

GC 50	200	210	220	230	240	250	260	270	280	290	300	310	320	330	340	350	360	370	380	390
CORE DEPTH (cm)																				
<b>DIATOMS</b>																				
<i>Actinocyclus actinocylus</i>	0.16	0.00	0.00	0.00	0.00	0.00	0.17	0.15	0.15	0.15	0.13	0.00	0.16	0.00	0.19	0.00	0.19	0.00	0.00	0.00
<i>Actinocyclus dimorphus</i>	0.00	0.00	0.00	0.00	0.00	0.00	0.00	0.00	0.00	0.00	0.00	0.00	0.00	0.00	0.00	0.00	0.00	0.00	0.00	0.00
<i>Actinocyclus fasciculatus</i>	0.00	0.00	0.00	0.00	0.00	0.00	0.00	0.00	0.00	0.00	0.00	0.00	0.00	0.00	0.00	0.00	0.00	0.00	r	0.00
<i>Actinocyclus ingens</i>	16.89	28.62	27.60	22.46	12.58	28.48	36.64	23.47	17.46	15.93	15.01	6.21	7.63	5.83	6.02	14.08	8.33	5.97	8.26	6.64
<i>Actinocyclus karstenii</i>	0.00	0.00	0.00	0.00	0.00	0.00	0.00	0.00	0.00	0.00	0.00	0.00	0.00	0.00	0.00	0.00	0.00	0.00	r	r
<i>Asteromphalus hookeri</i>	0.33	0.17	0.17	0.31	0.32	0.46	0.67	0.15	0.15	0.15	0.13	0.00	0.00	0.00	0.00	0.00	0.16	0.19	0.19	0.15
<i>Asteromphalus hepaticus / parvulus</i>	0.33	0.34	0.17	0.31	0.96	0.15	0.17	0.00	0.44	0.15	0.27	0.00	0.48	0.34	0.00	0.32	0.00	0.00	0.00	0.17
<i>Asteromphalus hyalinus</i>	0.00	0.17	0.00	0.00	0.32	0.15	0.00	0.00	0.15	0.15	0.00	0.16	0.16	0.34	0.38	0.16	0.19	0.37	0.44	0.00
<i>Azperia tabularis</i>	0.00	0.00	0.00	0.00	0.00	0.15	0.00	0.00	0.00	0.00	0.00	0.00	0.00	0.00	0.00	0.00	0.00	0.00	0.00	0.00
<i>Chaetoceros bulbosum</i>	0.00	0.34	0.00	0.00	0.16	0.00	0.00	0.00	0.00	0.00	0.13	0.33	0.16	0.17	0.75	0.16	0.39	0.37	0.00	0.00
<i>Chaetoceros cysts</i>	0.82	0.00	0.34	0.16	0.48	0.15	0.34	0.61	0.30	0.00	0.00	0.00	0.00	0.17	0.38	0.00	0.97	0.19	0.00	0.00
<i>Corethron criophilum</i>	0.00	0.00	0.00	0.00	0.00	0.61	0.00	0.00	0.00	0.00	0.00	0.00	0.00	0.00	0.00	0.00	0.00	0.19	0.15	0.00
<i>Coscinodiscus spp</i>	0.16	0.17	0.00	0.16	0.32	0.00	0.17	0.15	0.44	0.74	0.40	0.65	0.16	0.51	0.19	1.11	0.19	0.00	0.15	0.17
<i>Dactylosolen antarcticus</i>	3.61	4.21	4.94	2.81	2.71	4.75	9.41	2.91	4.59	5.16	7.64	6.86	6.68	5.49	2.44	0.63	1.74	0.56	2.21	4.15
<i>Denticulopsis spp</i>	0.00	0.00	0.00	0.00	0.00	0.00	0.00	0.00	0.00	0.00	0.00	0.00	0.00	0.00	0.00	0.16	0.19	2.61	0.15	0.17
<i>Eucampia antarctica</i>	0.00	0.00	0.17	0.16	0.48	0.15	0.17	0.46	0.15	0.29	0.40	0.00	0.16	0.17	0.19	0.32	0.19	0.56	0.15	0.17
<i>Fragilaropsis aunca</i>	0.00	0.00	0.00	0.00	0.00	0.00	0.00	0.00	0.00	0.00	0.00	0.00	0.00	0.00	0.00	0.00	0.00	0.00	0.00	0.00
<i>Fragilaropsis barronii</i>	0.00	0.00	0.00	0.00	0.00	0.00	0.00	0.00	0.00	0.00	0.00	0.00	0.00	0.00	0.00	0.00	0.19	0.00	0.15	0.00
<i>Fragilaropsis barronii var A + B</i>	20.98	17.85	10.05	7.96	4.30	10.72	5.71	17.33	13.31	15.19	11.80	13.24	22.42	10.46	13.16	16.30	11.24	15.86	15.19	11.63
<i>Fragilaropsis curta</i>	18.20	3.87	4.09	1.87	3.34	9.80	8.91	7.06	8.58	10.32	13.54	34.64	14.94	21.61	21.62	6.96	27.52	28.36	24.04	20.60
<i>Fragilaropsis cylindrus</i>	0.00	0.00	0.17	0.00	0.00	0.00	0.17	0.00	0.15	0.00	0.00	0.00	0.00	0.00	0.00	0.00	0.19	0.00	0.15	0.50
<i>Fragilaropsis interfrigidiana</i>	0.16	0.00	0.00	0.00	0.32	0.00	0.00	0.00	0.00	0.00	0.00	0.00	0.16	0.00	0.00	0.00	0.19	0.00	0.00	0.17
<i>Fragilaropsis karguelensis</i>	10.16	21.55	26.41	38.07	47.77	3.06	0.50	6.29	7.40	8.26	2.82	2.94	2.70	3.95	3.38	6.80	6.20	10.45	9.00	8.14
<i>Fragilaropsis obliquecostata</i>	0.16	0.00	0.00	0.16	0.00	0.31	0.00	0.00	0.00	0.00	0.00	0.00	0.00	0.00	0.00	0.00	0.00	0.00	0.00	0.00
<i>Fragilaropsis praecurta (?)</i>	0.00	0.00	0.00	0.00	0.00	0.00	0.00	0.00	1.04	1.18	2.95	0.98	1.75	3.43	1.32	1.27	1.94	1.12	1.77	3.49
<i>Fragilaropsis praeinterfrigidiana</i>	0.00	0.00	0.00	0.00	0.00	0.00	0.00	0.00	0.00	0.00	0.00	0.00	0.00	0.00	0.00	0.00	0.00	0.00	0.15	0.17
<i>Fragilaropsis nitscheri</i>	0.66	0.34	0.17	0.31	1.91	3.37	1.51	0.46	3.11	0.59	0.27	0.16	0.00	0.17	0.19	0.47	0.19	0.19	0.15	0.17
<i>Fragilaropsis rhombica</i>	0.66	0.00	0.00	0.16	0.00	0.15	0.00	0.46	1.18	0.15	0.00	0.16	0.00	0.00	0.19	0.16	0.19	0.19	0.88	0.66
<i>Fragilaropsis separanda</i>	0.16	0.00	0.51	0.78	0.16	0.00	0.17	0.00	0.44	0.00	0.00	0.00	0.00	0.17	0.00	0.16	0.19	0.00	0.00	0.33
<i>Fragilaropsis separanda var A</i>	0.00	0.00	0.00	0.00	0.00	0.00	0.00	0.00	0.00	0.00	0.00	0.00	0.00	0.00	0.00	0.00	0.00	0.00	0.00	0.00
<i>Fragilaropsis sublinearis</i>	0.98	0.17	0.17	0.00	0.00	0.31	0.84	0.15	0.15	0.29	0.40	0.33	0.16	0.17	0.19	0.00	0.19	0.19	0.15	0.50
<i>Fragilaropsis weaveri</i>	0.00	0.00	0.00	0.00	0.00	0.00	0.00	0.00	0.00	0.00	0.00	0.00	0.00	0.00	0.00	0.00	0.00	0.00	0.00	0.50
<i>Hemidiscus karstenii</i>	0.00	0.00	0.00	0.00	0.00	0.00	0.00	0.00	0.00	0.00	0.00	0.00	0.00	0.00	0.00	0.16	0.00	0.00	0.00	0.00
<i>Navicula directa</i>	0.00	0.00	0.00	0.00	0.00	0.00	0.00	0.00	0.00	0.00	0.00	0.00	0.00	0.00	0.00	0.00	0.00	0.00	0.15	0.00
<i>Navicula glaciei</i>	0.00	0.00	0.00	0.00	0.00	0.00	0.00	0.00	0.00	0.00	0.00	0.00	0.00	0.00	0.00	0.00	0.00	0.00	0.00	0.00
<i>Nitzschia fossilis</i>	0.00	0.00	0.00	0.00	0.00	0.00	0.17	0.00	0.00	0.00	0.40	0.00	0.32	0.00	0.00	0.16	0.00	0.00	0.00	0.17
<i>Nitzschia perigallii</i>	1.15	0.17	0.17	0.00	0.00	0.00	0.00	0.15	1.33	0.29	0.00	0.49	1.11	0.00	0.38	0.16	0.58	0.37	0.00	0.17
<i>Nitzschia reinholdii</i>	0.00	0.00	0.00	0.00	0.00	0.00	0.00	0.00	0.00	0.00	0.00	0.00	0.00	0.00	0.00	0.00	0.00	0.00	0.00	0.00
<i>Proboscia alata</i>	0.00	0.00	0.00	0.00	0.00	0.00	0.00	0.00	0.00	0.00	0.13	0.00	0.00	0.00	0.00	0.00	0.00	0.00	0.00	0.17
<i>Proboscia barboi</i>	0.00	0.00	0.00	0.00	0.00	0.00	0.00	0.00	0.00	0.00	0.00	0.00	0.00	0.00	0.00	0.00	0.00	0.00	0.00	0.00
<i>Rhizosolenia hebetata (group)</i>	0.00	0.00	0.00	0.00	0.00	0.15	0.17	0.15	0.00	0.00	0.13	0.00	0.16	0.34	0.19	0.00	0.00	0.19	0.15	0.00
<i>Rhizosolenia styliformis (group)</i>	0.82	0.00	0.68	1.25	0.32	0.46	1.51	0.61	0.59	0.74	0.54	0.16	0.16	0.69	0.19	0.47	0.78	0.93	0.74	0.66
<i>Rhizosolenia sp A</i>	1.48	0.67	0.51	0.16	0.00	0.31	0.84	0.15	0.59	0.29	0.67	1.63	1.27	2.74	3.01	0.79	1.16	0.56	0.44	1.33
<i>Rhizosolenia spp</i>	0.00	0.00	0.00	0.31	0.00	0.00	0.00	0.00	0.00	0.00	0.00	0.00	0.00	0.00	0.00	0.00	0.00	0.00	0.00	0.17
<i>Rouxia antarctica</i>	0.00	0.17	0.17	0.16	0.80	8.27	9.41	4.45	8.28	9.44	8.58	6.37	10.97	12.18	13.91	5.22	9.30	5.04	7.23	8.31
<i>Rouxia heteropolara</i>	0.00	0.00	0.00	0.00	0.00	0.00	0.00	0.00	0.00	0.00	0.00	0.00	0.00	0.00	0.00	0.00	0.00	0.00	0.00	0.00
<i>Rouxia isoplica</i>	3.77	0.67	0.17	0.00	0.00	2.45	1.01	1.07	3.11	0.74	0.40	0.65	0.95	2.06	2.63	0.47	1.16	0.56	1.18	0.66
<i>Rouxia leventerae</i>	0.00	0.00	0.00	0.00	0.00	0.00	0.00	0.00	0.00	0.00	0.00	0.00	0.00	0.00	0.19	0.00	0.19	0.19	0.00	0.00
<i>Rouxia naviculoides</i>	0.00	0.84	1.02	0.62	0.96	5.21	6.89	9.97	6.36	6.19	4.69	4.74	4.13	6.00	5.26	4.91	6.59	6.16	5.46	4.15
<i>Stellarima microtrias</i>	0.00	0.00	0.00	0.00	0.16	0.00	0.00	0.15	0.00	0.00	0.13	0.00	0.00	0.17	0.00	0.16	0.19	0.00	0.15	0.00
<i>Stephanopyxis spp</i>	0.00	0.00	0.00	0.00	0.00	0.00	0.00	0.00	0.00	0.00	0.00	0.00	0.00	0.00	0.00	0.00	0.00	0.00	0.15	0.00
<i>Thalassionema nitzschoides (group)</i>	0.00	0.17	0.00	0.16	0.16	0.00	0.00	0.00	0.30	0.15	0.00	0.00	0.00	0.00	0.00	0.00	0.19	0.00	0.29	0.17
<i>Thalassionema nitzschoides var parva</i>	0.00	0.00	0.00	0.00	0.00	0.00	0.00	0.00	0.00	0.00	0.00	0.00	0.00	0.00	0.00	0.00	0.00	0.00	0.00	0.00
<i>Thalassiosira antarctica</i>	0.00	0.00	0.00	0.00	0.00	0.15	0.17	0.00	0.00	0.00	0.13	0.00	0.00	0.00	0.00	0.00	0.00	0.00	0.00	0.17
<i>Thalassiosira complicata</i>	0.00	0.00	0.00	0.00	0.00	0.00	0.00	0.00	0.00	0.00	0.00	0.00	0.00	0.00	0.00	0.00	0.00	0.00	0.00	0.00
<i>Thalassiosira elliptica</i>	0.49	0.17	0.17	0.16	0.16	0.31	0.17	0.00	0.15	0.00	0.27	0.16	0.16	0.17	0.19	0.00	0.19	0.19	r	0.00
<i>Thalassiosira fasciculata</i>	0.49	0.34	0.68	0.16	0.16	0.15	0.50	1.07	0.30	0.29	0.40	0.16	0.32	0.51	0.19	0.32	0.58	0.37	0.15	0.17
<i>Thalassiosira frenguelli</i>	0.00	0.17	0.00	0.00	0.00	0.00	0.00	0.15	0.00	0.00	0.00	0.00	0.00	0.00	0.00	0.00	0.00	0.00	0.00	0.00
<i>Thalassiosira gracilis var expecta</i>	0.82	0.17	0.00	0.00	0.00	0.00	0.00	0.46	0.59	0.15	0.13	1.63	0.48	0.00	0.56	0.95	0.39	0.00	0.00	0.00

## Appendix 3. continued

GC 50						
CORE DEPTH (cm)	400	410	420	430	440	C.C
<b>DIATOMS</b>						
<i>Actinocyclus actinocilius</i>	0 00	0 00	0 16	0 00	0 00	0 00
<i>Actinocyclus dimorphus</i>	0 00	0 00	0 00	0 00	0 00	0 00
<i>Actinocyclus fasciculatus</i>	0 17	1 32	0 80	0 16	0 17	0 16
<i>Actinocyclus ingens</i>	7 76	4 53	1 28	2 38	0 86	0 32
<i>Actinocyclus karstenii</i>	0 17	1 46	2 88	0 94	0 00	0 00
<i>Asteromphalus hookeri</i>	0 17	0 15	0 16	0 00	0 17	0 00
<i>Asteromphalus hepaticus / parvulus</i>	0 17	0 15	0 00	0 16	0 00	0 16
<i>Asteromphalus hyalinus</i>	0 00	0 00	0 00	0 00	0 00	0 00
<i>Azpeitia tabularis</i>	0 00	0 00	0 00	0 00	0 00	0 00
<i>Chaetoceros bulbosum</i>	0 00	0 15	0 32	0 16	0 34	0 32
<i>Chaetoceros</i> cysts	0 17	0 88	1 44	1 26	3 44	1 46
<i>Corethron croophilum</i>	0 00	0 58	0 48	1 10	1 55	1 46
<i>Coscinodiscus</i> spp	0 00	0 15	0 16	0 16	0 34	0 65
<i>Dactylosolan antarcticus</i>	2 59	1 90	6 24	6 14	12 56	11 83
<i>Denticulopsis</i> spp	0 17	0 00	0 16	0 16	0 17	0 00
<i>Eucampia antarctica</i>	0 17	0 15	0 80	1 57	0 17	0 16
<i>Fragilaropsis aurica</i>	0 00	0 00	0 48	0 31	0 17	0 00
<i>Fragilaropsis barroni</i>	0 00	0 58	2 56	8 03	20 83	22 69
<i>Fragilaropsis barroni</i> var A + B	7 24	7 60	7 52	7 09	3 44	2 43
<i>Fragilaropsis curta</i>	26 55	20 61	12 96	7 40	4 13	3 57
<i>Fragilaropsis cylindrus</i>	0 69	0 00	0 00	0 00	0 00	0 00
<i>Fragilaropsis interfrigidaria</i>	0 00	0 44	0 64	0 47	0 34	0 65
<i>Fragilaropsis kerguelensis</i>	2 24	4 53	1 28	0 31	0 34	0 32
<i>Fragilaropsis obliquecostata</i>	0 00	0 00	0 00	0 00	0 00	0 00
<i>Fragilaropsis praecurta</i> (?)	2 59	2 19	2 08	0 79	0 00	0 49
<i>Fragilaropsis praeterfrigidaria</i>	0 17	0 58	1 92	2 99	5 34	4 05
<i>Fragilaropsis ritscheri</i>	0 86	0 15	0 48	0 47	0 00	0 00
<i>Fragilaropsis rhombica</i>	0 34	0 15	0 48	0 31	0 17	0 49
<i>Fragilaropsis separanda</i>	0 00	0 15	0 16	0 00	0 00	0 00
<i>Fragilaropsis separanda</i> var A	0 00	0 00	0 00	0 00	0 00	0 00
<i>Fragilaropsis sublineans</i>	0 17	0 44	0 64	0 16	0 17	0 65
<i>Hemidiscus karstenii</i>	0 00	0 15	0 00	0 16	0 00	0 00
<i>Navicula directa</i>	0 00	0 00	0 00	0 00	0 00	0 00
<i>Navicula glaciel</i>	0 17	0 15	0 16	0 00	0 00	0 00
<i>Nitzschia fossilis</i>	0 00	0 58	0 16	0 16	0 00	0 00
<i>Nitzschia perrigallii</i>	0 17	0 00	0 00	0 00	0 00	0 00
<i>Nitzschia reinholdii</i>	0 00	0 00	0 00	0 00	0 00	0 00
<i>Fragilaropsis weaveri</i>	0 00	0 00	0 32	0 31	1 03	0 16
<i>Proboscia alata</i>	0 00	0 00	0 16	0 31	0 17	0 16
<i>Proboscia barboi</i>	0 00	0 00	0 00	0 00	0 52	0 00
<i>Rhizosolenia hebetata</i> (group)	0 00	0 29	0 16	0 00	0 00	0 00
<i>Rhizosolenia styliformis</i> (group)	0 86	1 32	1 92	0 79	0 86	0 81
<i>Rhizosolenia</i> sp A	1 38	3 36	2 56	1 10	3 27	0 81
<i>Rhizosolenia</i> spp	0 00	0 00	0 00	0 31	0 17	0 16
<i>Rouxia antarctica</i>	7 76	7 89	7 36	4 25	2 75	3 73
<i>Rouxia heteropolara</i>	0 00	0 00	0 00	0 00	0 00	0 00
<i>Rouxia isopolica</i>	1 03	1 32	1 76	1 57	1 38	3 40
<i>Rouxia leventerae</i>	0 17	2 78	2 08	1 42	1 03	0 65
<i>Rouxia naviculoides</i>	8 28	6 73	3 84	1 89	2 58	4 54
<i>Stellatma microtrias</i>	0 17	0 29	0 00	0 47	0 17	0 16
<i>Stephanopyxis</i> spp	0 17	0 15	0 16	0 00	0 00	0 00
<i>Thalassionema nitzschioides</i> (group)	0 52	0 00	0 00	0 00	0 00	0 00
<i>Thalassionema nitzschioides</i> var parva	0 00	0 00	0 00	0 00	0 00	0 00
<i>Thalassiosira antarctica</i>	0 00	0 00	0 00	0 00	0 17	0 00
<i>Thalassiosira complicata</i>	0 00	0 00	0 00	0 00	0 00	0 00
<i>Thalassiosira elliptipora</i>	0 00	0 00	0 00	0 00	0 00	0 00
<i>Thalassiosira fasciculata</i>	0 52	0 73	0 16	0 16	0 00	0 16
<i>Thalassiosira frenguelli</i>	0 00	0 00	0 00	0 00	0 00	0 00
<i>Thalassiosira gracilis</i> var expecta	0 34	0 58	0 48	0 00	0 00	0 49
<i>Thalassiosira gracilis</i> var gracilis	0 00	0 15	0 16	0 00	0 00	0 00
<i>Thalassiosira gravida</i>	0 52	0 15	0 00	0 00	0 00	0 00
<i>Thalassiosira inura</i>	0 17	0 15	0 48	1 73	1 55	4 70
<i>Thalassiosira inura-insigna</i> (transition)	0 86	2 49	3 04	1 73	1 89	1 30
<i>Thalassiosira insigna</i>	0 69	1 32	2 56	9 76	6 37	2 59
<i>Thalassiosira kolbei</i>	0 17	0 73	0 64	0 63	0 17	0 49
<i>Thalassiosira lentiginosa</i>	8 28	5 12	10 08	8 98	3 79	4 70
<i>Thalassiosira maculata</i>	0 86	0 88	1 28	0 94	1 89	2 43
<i>Thalassiosira oestrupii</i>	5 34	4 39	3 52	3 94	5 68	4 38
<i>Thalassiosira oliverana</i>	2 41	3 22	3 52	5 20	2 93	3 40
<i>Thalassiosira oliverana</i> (coarse)	2 59	1 90	0 80	0 63	0 17	0 16
<i>Thalassiosira strata</i>	0 00	0 00	0 16	0 00	0 00	0 00
<i>Thalassiosira torokuna</i>	0 17	0 15	0 16	0 00	0 17	0 16
<i>Thalassiosira vulnifica</i>	0 34	0 29	2 08	3 62	0 52	0 49
<i>Thalassiosira webbi</i>	0 17	0 00	0 00	0 00	0 34	0 32
<i>Thalassiothrix</i> spp	0 00	1 02	0 48	0 94	0 62	0 65
<i>Tnchotoxon reinboldii</i>	0 86	0 88	1 12	1 42	0 86	2 43
OTHER	0 86	0 73	0 64	2 05	1 03	0 81
<b>SILICOFLAGELLATES</b>	1 21	1 17	1 60	2 36	2 58	2 59

# Appendix 3. continued

GC 49 (lat 57°36'2"S, long 78°18'1"E)																				
CORE DEPTH (cm)	0	10	20	31	41	51	61	71	81	101	114	124	134	144	154	164	174	184	194	204
DIATOMS																				
<i>Actinocyclus actinocylus</i>	0.36	0.12	0.13	0.28	1.32	0.47	0.63	0.58	1.11	0.00	0.72	0.00	0.00	0.00	0.00	0.00	0.00	0.23	0.00	0.00
<i>Actinocyclus dimorphus</i>	0.00	0.00	0.00	0.00	0.00	0.00	0.00	0.00	0.00	0.00	0.00	0.00	0.00	0.00	0.00	0.00	0.00	0.00	0.00	0.00
<i>Actinocyclus fasciculatus</i>	0.00	0.00	0.00	0.00	0.00	0.00	0.00	0.00	0.00	0.00	0.00	0.00	0.00	0.00	0.00	0.00	0.00	0.00	0.00	0.00
<i>Actinocyclus ingens</i>	0.00	0.00	0.00	0.00	0.49	0.00	0.47	3.17	4.07	1.61	7.40	8.73	3.95	34.33	25.49	19.23	38.83	19.49	36.05	23.33
<i>Actinocyclus karstenii</i>	0.00	0.00	0.00	0.00	0.00	0.00	0.00	0.00	0.00	0.00	0.00	0.00	0.00	0.00	0.00	0.00	0.00	0.00	0.00	0.00
<i>Asteromphalus hookeri</i>	0.00	0.00	0.13	0.14	0.00	0.00	0.47	0.00	0.00	0.00	0.24	0.00	0.00	0.00	0.00	0.00	0.00	0.00	0.00	0.00
<i>Asteromphalus hepaticus / parvulus</i>	0.00	0.12	0.13	0.00	0.16	0.00	0.47	0.14	0.00	0.00	0.24	0.00	0.00	0.00	0.00	0.00	0.00	0.00	0.00	0.00
<i>Asteromphalus hyalinus</i>	0.84	0.12	0.51	0.28	0.33	0.00	0.00	0.43	0.00	0.29	0.00	0.22	0.00	0.19	0.25	0.00	0.00	0.00	0.23	0.20
<i>Azpettia tabulans</i>	0.60	0.93	0.51	0.14	0.00	0.00	0.78	0.14	0.00	0.00	0.00	0.00	0.00	0.00	0.00	0.00	0.00	0.00	0.00	0.00
<i>Chaetoceros bulbosum</i>	0.24	0.00	0.00	0.00	0.16	0.00	0.00	0.00	0.37	0.00	0.00	0.00	0.00	0.00	0.00	0.35	0.00	0.00	0.23	0.00
<i>Chaetoceros cystis</i>	0.24	0.00	0.00	1.26	1.97	1.11	0.78	0.86	0.56	0.29	0.00	0.00	0.33	0.00	0.00	0.00	0.00	0.00	0.47	0.00
<i>Corethron criophilum</i>	0.00	0.00	0.00	0.00	0.00	0.00	0.00	0.00	0.00	0.00	0.00	0.00	0.00	0.00	0.00	0.00	0.00	0.00	0.00	0.00
<i>Coscinodiscus</i> spp	0.00	0.00	0.00	0.00	0.00	0.00	0.00	0.00	0.00	0.00	0.00	0.00	0.00	0.00	0.00	0.00	0.00	0.00	0.00	0.00
<i>Dactylosolen antarcticus</i>	7.76	6.53	3.57	6.00	5.92	4.90	4.07	3.60	4.26	2.49	3.82	13.10	6.91	2.44	5.39	8.04	4.27	5.10	8.37	2.03
<i>Denticulopsis</i> spp	0.00	0.00	0.00	0.00	0.00	0.00	0.00	0.00	0.00	0.00	0.00	0.00	0.00	0.00	0.00	0.00	0.00	0.00	0.00	0.00
<i>Eucampia antarctica</i>	0.95	0.58	0.26	0.14	0.99	0.16	0.00	0.43	0.19	0.00	0.48	0.66	0.00	0.38	0.74	0.70	0.78	0.23	0.23	0.20
<i>Fragilaropsis aurica</i>	0.00	0.00	0.00	0.00	0.00	0.00	0.00	0.00	0.00	0.00	0.00	0.00	0.33	0.00	0.00	0.00	0.00	0.00	0.00	0.00
<i>Fragilaropsis barronii</i>	0.00	0.00	0.00	0.00	0.00	0.00	0.00	0.00	0.00	0.00	0.00	0.22	0.00	0.19	0.25	0.35	0.00	0.00	0.00	0.41
<i>Fragilaropsis barronii</i> var A + B	0.00	0.00	0.00	0.00	0.16	0.47	0.00	1.44	1.85	1.91	6.44	17.69	37.50	20.64	14.46	16.08	17.86	27.38	23.02	4.67
<i>Fragilaropsis curta</i>	4.53	1.75	1.53	1.81	7.89	4.42	8.29	9.37	16.85	0.59	5.73	18.12	7.57	5.44	8.09	19.93	4.47	12.76	7.44	1.42
<i>Fragilaropsis cylindrus</i>	0.00	0.00	0.00	0.14	0.49	0.16	0.63	1.87	3.89	0.00	0.72	0.22	1.32	0.38	0.49	0.70	0.19	0.00	0.00	0.00
<i>Fragilaropsis interfrigidaria</i>	0.00	0.00	0.00	0.00	0.00	0.00	0.00	0.00	0.00	0.00	0.00	0.00	0.00	0.00	0.00	0.00	0.19	0.00	0.00	0.00
<i>Fragilaropsis kerguelensis</i>	60.50	65.93	74.49	66.67	61.51	65.40	57.28	52.45	41.11	69.35	36.52	0.66	2.63	5.82	5.88	3.50	4.47	11.83	0.93	46.04
<i>Fragilaropsis obliquecostata</i>	0.00	0.00	0.00	0.00	0.33	0.32	0.31	0.29	0.00	0.00	0.00	0.00	0.00	0.00	0.00	0.00	0.00	0.00	0.00	0.00
<i>Fragilaropsis praecurta</i> (?)	0.00	0.00	0.00	0.00	0.00	0.00	0.00	0.00	0.00	0.00	0.00	0.00	0.00	0.00	0.74	0.00	0.00	0.00	0.00	0.00
<i>Fragilaropsis praeterfrigidiana</i>	0.00	0.00	0.00	0.00	0.00	0.00	0.00	0.00	0.00	0.00	0.00	0.00	0.00	0.00	0.00	0.00	0.00	0.00	0.00	0.00
<i>Fragilaropsis nitscheni</i>	0.36	0.35	0.64	1.95	3.29	3.32	3.13	3.31	2.04	9.97	9.55	12.45	7.57	5.63	1.96	2.80	0.39	3.02	0.23	0.81
<i>Fragilaropsis rhombica</i>	1.19	0.58	0.26	0.42	0.66	0.16	0.47	0.43	0.00	0.00	0.00	0.00	0.00	0.00	0.00	0.00	0.00	0.00	0.00	0.00
<i>Fragilaropsis separanda</i>	9.79	11.44	9.06	13.81	8.72	12.48	14.71	11.38	17.41	2.64	11.93	1.97	11.84	6.38	2.70	1.75	0.19	0.23	0.00	1.83
<i>Fragilaropsis separanda</i> var A	0.00	0.00	0.00	0.00	0.00	0.00	0.00	0.00	0.00	0.00	0.00	0.00	0.00	0.00	0.00	0.00	0.00	0.00	0.00	0.00
<i>Fragilaropsis sublineans</i>	0.00	0.00	0.00	0.00	0.00	0.32	0.47	0.29	0.19	0.00	0.00	1.97	0.33	0.38	0.25	1.05	0.58	0.70	0.70	0.00
<i>Fragilaropsis weaveri</i>	0.00	0.00	0.00	0.00	0.00	0.00	0.00	0.00	0.00	0.00	0.00	0.00	0.00	0.00	0.00	0.00	0.00	0.00	0.00	0.00
<i>Hemidiscus karstenii</i>	0.00	0.00	0.00	0.00	0.00	0.00	0.00	0.00	0.00	0.00	0.00	0.00	0.00	0.00	0.00	0.00	0.00	0.00	0.00	0.00
<i>Navicula directa</i>	0.00	0.00	0.00	0.00	0.00	0.00	0.16	0.14	0.00	0.00	0.00	0.00	0.00	0.00	0.00	0.00	0.00	0.00	0.00	0.00
<i>Navicula glaciei</i>	0.00	0.00	0.00	0.00	0.00	0.00	0.00	0.00	0.00	0.00	0.00	0.00	0.00	0.00	0.00	0.00	0.00	0.00	0.00	0.00
<i>Nitzschia fossilis</i>	0.00	0.00	0.00	0.00	0.00	0.00	0.00	0.00	0.00	0.00	0.00	0.00	0.00	0.00	0.00	0.35	0.00	0.00	0.00	0.00
<i>Nitzschia pennigalli</i>	0.00	0.00	0.00	0.00	0.00	0.00	0.00	0.00	0.00	0.00	0.24	0.22	0.66	0.19	1.47	0.35	0.00	0.23	0.23	0.00
<i>Nitzschia reinholdii</i>	0.00	0.00	0.00	0.00	0.00	0.00	0.00	0.00	0.00	0.00	0.00	0.00	0.00	0.00	0.00	0.00	0.00	0.00	0.00	0.00
<i>Proboscidea alata</i>	0.00	0.12	0.00	0.00	0.00	0.16	0.00	0.00	0.19	0.00	0.00	0.00	0.00	0.00	0.25	0.35	0.00	0.00	0.00	0.00
<i>Proboscidea barboi</i>	0.00	0.00	0.00	0.00	0.00	0.00	0.00	0.00	0.00	0.00	0.00	0.00	0.00	0.00	0.00	0.00	0.00	0.00	0.00	0.00
<i>Rhizosolenia hebetata</i> (group)	0.24	0.00	0.00	0.00	0.00	0.00	0.00	0.00	0.19	0.15	0.00	0.22	0.33	0.19	0.00	0.00	0.00	0.00	0.00	0.00
<i>Rhizosolenia styliformis</i> (group)	0.00	0.00	0.13	0.00	0.00	0.32	0.16	0.86	0.19	0.59	0.95	0.44	1.32	1.13	2.94	0.70	0.39	1.39	0.47	0.00
<i>Rhizosolenia</i> sp A	0.00	0.00	0.00	0.00	0.00	0.00	0.00	0.14	0.56	0.00	0.24	1.31	1.32	0.00	0.98	1.40	0.97	0.46	0.23	0.00
<i>Rhizosolenia</i> spp	0.00	0.00	0.00	0.00	0.00	0.00	0.00	0.00	0.00	0.00	0.00	0.00	0.00	0.00	0.00	0.00	0.00	0.00	0.00	0.00
<i>Rouxia antarctica</i>	0.00	0.00	0.00	0.00	0.16	0.00	0.00	0.14	0.00	0.00	0.00	0.00	0.00	0.00	0.00	0.00	0.00	0.00	0.00	0.00
<i>Rouxia heteropolara</i>	0.00	0.00	0.00	0.00	0.00	0.00	0.00	0.00	0.00	0.00	0.00	0.00	0.00	0.00	0.00	0.00	0.00	0.00	0.00	0.00
<i>Rouxia isopolica</i>	0.00	0.00	0.00	0.00	1.32	0.47	2.19	1.87	0.37	0.15	2.15	6.33	6.91	1.31	4.90	3.15	3.88	4.18	3.02	0.41
<i>Rouxia leventerae</i>	0.00	0.00	0.00	0.00	0.00	0.00	0.00	0.00	0.00	0.00	0.00	0.00	0.00	0.00	0.00	0.00	0.00	0.00	0.00	0.00
<i>Rouxia naviculoides</i>	0.00	0.00	0.00	0.00	0.00	0.00	0.00	0.14	0.00	0.00	0.00	0.00	0.00	0.00	0.00	0.35	0.19	0.23	0.23	0.81
<i>Stellarima microstas</i>	0.12	0.00	0.00	0.00	0.00	0.00	0.00	0.00	0.19	0.00	0.00	0.00	0.00	0.00	0.00	0.00	0.19	0.00	0.00	0.00
<i>Stephanopyxis</i> spp	0.00	0.00	0.00	0.00	0.00	0.00	0.00													

# Appendix 3. continued

GC 49																				
CORE DEPTH (cm)	214	224	234	244	254	264	274	284	291	300	310	320	330	340	350	360	370	380	C. C.	
DIATOMS																				
<i>Actinocyclus actinochilus</i>	0 00	0 00	0 00	0 00	0 00	0 00	0 00	0 00	0 22	0 00	0 00	0 00	0 00	0 00	0 00	0 00	0 00	0 00	0 00	
<i>Actinocyclus dimorphus</i>	0 00	0 00	0 00	0 00	0 00	0 00	0 00	0 00	0 00	0 00	0 00	0 00	0 00	0 00	0 00	0 00	0 00	0 00	0 00	
<i>Actinocyclus fasciculatus</i>	0 00	0 00	0 00	0 00	0 00	0 00	0 00	0 00	0 00	0 00	0 00	0 00	0 00	0 00	0 00	0 00	0 00	0 00	0 00	
<i>Actinocyclus ingens</i>	21 97	4 76	34 25	31.12	14 57	12 54	12 96	3 56	16 41	13 81	17 95	15 67	15 17	15 67	18 10	12 55	11 53	8 89	26 48	
<i>Actinocyclus karstenii</i>	0 00	0 00	0 00	0 00	0 00	0 00	0 00	0 00	0 00	0 21	0 18	0 00	0 00	0 00	0 00	0 20	0 00	0 00	0 00	
<i>Asteromphalus hookeri</i>	0 00	0 18	0 20	0 20	0 00	0 57	0 00	0 21	0 22	0 41	0 00	0 39	0 33	0 00	0 35	0 00	0 00	0 20	0 00	
<i>Asteromphalus hepalicus / parvulus</i>	0 00	0 35	0 20	0 20	0 00	0 28	0 00	0 00	0 44	0 82	0 18	0 00	0 16	0 00	0 00	0 40	0 00	0 59	0 00	
<i>Asteromphalus hyalinus</i>	0 00	0 00	0 00	0 00	0 00	0 00	0 00	0 00	0 00	0 21	0 36	1 16	0 16	0 00	0 35	0 00	0 40	0 20	0 00	
<i>Azpeitia tabularis</i>	0 00	0 00	0 00	0 00	0 00	0 00	0 00	0 00	0 00	0 00	0 00	0 00	0 00	0 00	0 00	0 00	0 00	0 00	0 00	
<i>Chaetoceros bulbosum</i>	0 00	0 00	0 20	0 00	0 00	0 00	0 00	0 84	0 00	0 21	0 18	0 39	0 16	0 00	0 18	0 20	0 00	0 20	0 28	
<i>Chaetoceros cysts</i>	0 00	0 18	0 00	0 00	0 00	0 00	0 00	0 00	0 00	0 00	0 00	0 00	0 00	0 00	0 00	0 00	0 00	0 00	0 00	
<i>Corethron criophilum</i>	0 00	0 00	0 00	0 00	0 00	0 00	0 00	0 00	0 00	0 00	0 00	0 00	0 00	0 00	0 00	0 00	0 00	0 00	0 00	
<i>Coscinodiscus spp</i>	0 00	0 00	0 59	0 20	0 45	0 00	1 32	1 46	2 22	2 27	0 72	1 55	2 61	2 07	0 88	0 80	0 60	3 36	5 92	
<i>Dactylosolen antarcticus</i>	1 35	0 71	1 97	5 42	18 16	7 98	5 03	8 16	5 54	6 19	5 75	3 87	1 63	2 07	2 46	4 78	1 59	4 55	1 13	
<i>Denticulopsis spp</i>	0 00	0 00	0 00	0 00	0 00	0 00	0 00	0 00	0 00	0 00	0 00	0 00	0 00	0 00	0 00	0 00	0 00	0 00	0 00	
<i>Eucampia antarctica</i>	0 22	0 35	0 20	0 80	0 00	0 00	0 00	0 00	0 44	0 41	0 00	0 39	0 33	0 00	0 00	0 00	0 20	0 20	0 00	
<i>Fragilaropsis aunca</i>	0 00	0 00	0 00	0 00	0 00	0 00	0 00	0 00	0 00	0 00	0 00	0 00	0 00	0 00	0 18	0 00	0 00	0 00	0 00	
<i>Fragilaropsis barronii</i>	0 45	0 18	0 00	0 20	0 00	0 00	0 00	0 00	0 00	0 00	0 00	0 00	0 00	0 00	0 35	0 20	0 00	0 20	0 00	
<i>Fragilaropsis barronii</i> var A + B	2 69	2 82	7 87	17 87	16 59	19 94	15 87	9 62	12 64	11 75	15 62	15 86	6 69	9 45	11 95	14 54	15 71	15 61	5 35	
<i>Fragilaropsis curta</i>	3 14	0 00	1 97	10 84	21 52	7 41	25 66	21 76	5 54	11 13	13 11	14 70	15 50	14 98	13 36	14 74	20 68	12 06	5 63	
<i>Fragilaropsis cylindrus</i>	0 00	0 00	0 00	0 00	0 22	0 00	0 00	0 00	0 00	0 00	0 00	0 19	0 49	0 23	0 00	0 00	0 00	0 00	0 00	
<i>Fragilaropsis interfrigidiana</i>	0 00	0 00	0 00	0 00	0 00	0 00	0 00	0 00	0 00	0 00	0 00	0 00	0 00	0 00	0 00	0 00	0 00	0 00	0 00	
<i>Fragilaropsis kerguelensis</i>	50 90	73 37	19 69	2 21	4 48	10 26	3 97	1 26	0 44	0 82	0 72	1 16	0 65	0 69	1 41	2 39	3 38	1 19	5 63	
<i>Fragilaropsis obliquecostata</i>	0 00	0 00	0 00	0 00	0 00	0 00	0 00	0 00	0 00	0 00	0 00	0 00	0 00	0 00	0 00	0 00	0 00	0 00	0 00	
<i>Fragilaropsis praecurta</i> (?)	0 00	0 00	0 00	0 00	0 00	1 71	0 00	6 07	5 32	4 33	2 69	4 45	3 92	3 23	2 28	3 39	1 19	3 36	0 56	
<i>Fragilaropsis praeinterfrigidiana</i>	0 00	0 00	0 00	0 00	0 00	0 00	0 00	0 00	0 00	0 00	0 00	0 00	0 00	0 00	0 00	0 00	0 00	0 00	0 00	
<i>Fragilaropsis ritscheri</i>	0 45	0 71	0 00	0 20	0 00	0 85	0 26	0 42	0 00	0 21	0 00	0 19	0 00	0 00	0 00	0 20	0 40	0 00	0 28	
<i>Fragilaropsis rhombica</i>	0 00	0 00	0 00	0 00	0 00	0 00	0 00	0 00	0 00	0 00	0 00	0 00	0 00	0 00	0 00	0 00	0 00	0 00	0 00	
<i>Fragilaropsis separanda</i>	5 38	2 65	2 76	0 00	2 24	0 00	1 06	0 00	0 00	0 00	0 00	0 00	0 00	0 00	0 00	0 00	0 00	0 00	0 00	
<i>Fragilaropsis separanda</i> var A	0 00	0 00	0 00	0 00	0 00	0 00	0 00	0 00	0 00	0 00	0 00	0 00	0 00	0 00	0 00	0 00	0 00	0 00	0 00	
<i>Fragilaropsis sublineans</i>	0 00	0 00	0 00	0 80	0 22	0 00	0 00	0 84	1 55	0 00	0 00	0 39	0 16	0 46	0 00	0 20	0 60	0 40	0 00	
<i>Fragilaropsis weaveri</i>	0 00	0 00	0 00	0 00	0 00	0 00	0 00	0 00	0 00	0 00	0 00	0 00	0 00	0 00	0 00	0 00	0 00	0 00	0 00	
<i>Hemidiscus karstenii</i>	0 00	0 00	0 00	0 00	0 00	0 00	0 00	0 00	0 00	0 00	0 00	0 00	0 00	0 00	0 00	0 00	0 00	0 00	0 00	
<i>Navicula directa</i>	0 00	0 00	0 00	0 00	0 00	0 00	0 00	0 00	0 00	0 00	0 00	0 00	0 00	0 00	0 00	0 00	0 00	0 00	0 00	
<i>Navicula glaciei</i>	0 00	0 00	0 00	0 00	0 00	0 00	0 00	0 00	0 00	0 00	0 00	0 00	0 00	0 00	0 00	0 00	0 00	0 00	0 00	
<i>Nitzschia fossilis</i>	0 00	0 00	0 00	0 00	0 00	0 00	0 00	0 00	0 00	0 21	0 00	0 19	0 00	0 23	0 00	0 00	0 00	0 00	0 00	
<i>Nitzschia perigalli</i>	0 00	0 00	0 00	0 00	0 00	0 00	0 00	1 67	0 67	0 62	1 08	1 16	0 98	0 92	0 88	1 59	0 99	1 38	0 28	
<i>Nitzschia reinholdii</i>	0 00	0 00	0 00	0 00	0 00	0 00	0 00	0 00	0 00	0 00	0 00	0 00	0 00	0 00	0 00	0 00	0 00	0 00	0 00	
<i>Proboscia alata</i>	0 00	0 00	0 00	0 00	0 00	0 00	0 00	0 00	0 00	0 00	0 00	0 00	0 00	0 00	0 00	0 00	0 00	0 00	0 00	
<i>Proboscia barboi</i>	0 00	0 00	0 00	0 00	0 00	0 00	0 00	0 00	0 00	0 00	0 00	0 00	0 00	0 00	0 00	0 00	0 00	0 00	0 00	
<i>Rhizosolenia hebetata</i> (group)	0 00	0 00	0 00	0 00	0 00	0 00	0 00	0 00	0 00	0 00	0 00	0 00	0 00	0 23	0 00	0 00	0 00	0 00	0 00	
<i>Rhizosolenia styliformis</i> (group)	0 00	0 18	0 20	1 20	0 67	0 85	0 26	0 21	1 33	0 41	0 18	0 39	0 16	0 23	0 53	0 20	0 60	0 00	0 28	
<i>Rhizosolenia</i> sp A	0 00	0 00	0 00	0 00	0 00	0 57	0 26	0 00	0 44	0 21	0 00	0 00	0 33	0 46	0 00	0 80	0 40	0 20	0 85	
<i>Rhizosolenia</i> spp	0 00	0 18	0 00	0 00	0 00	0 00	0 00	0 00	0 00	0 00	0 36	0 19	0 00	0 00	0 00	0 00	0 40	0 40	0 28	
<i>Rouxia antarctica</i>	0 00	0 00	2 76	3 82	3 81	6 55	8 47	23 64	14 63	11 13	12 93	6 38	10 28	11 06	8 96	7 97	8 15	11 26	2 54	
<i>Rouxia heteropolara</i>	0 00	0 00	0 00	0 00	0 00	0 00	0 00	0 00	0 00	0 00	0 00	0 00	0 00	0 00	0 00	0 00	0 00	0 00	0 00	
<i>Rouxia isopolica</i>	0 00	0 00	0 00	0 20	0 67	0 57	0 79	0 42	1 33	1 03	0 72	0 19	0 98	1 15	1 23	0 20	0 60	0 79	0 00	
<i>Rouxia leventerae</i>	0 00	0 00	0 00	0 00	0 00	0 00	0 00	0 00	0 22	0 00	0 00	0 00	0 00	0 00	0 00	0 00	0 00	0 00	0 00	
<i>Rouxia naviculoides</i>	0 67	0 18	3 94	10 04	7 40	6 55	10 58	9 41	6 43	5 98	5 39	5 61	7 50	5 76	5 62	8 17	8 95	9 88	1 41	
<i>Stellarima microtnas</i>	0 00	0 00	0 00	0 00	0 00	0 00	0 00	0 00	0 22	0 00	0 00	0 00	0 00	0 00	0 00	0 00	0 20	0 00	0 28	
<i>Stephanopyxis</i> spp	0 00	0 00	0 00	0 00	0 00	0 00	0 00	0 00	0 00	0 00	0 00	0 00	0 00	0 00	0 00	0 00	0 00	0 00	0 00	
<i>Thalassionema nitzschoides</i> (group)	0 45	0 18	0 59	0 00	0 00	0 28	0 00	0 00	0 00	0 00	0 00	0 00	0 33	0 00	0 00	0 00	0 00	0 20	0 00	
<i>Thalassionema nitzschoides</i> var parva	0 00	0 00	0 00	0 00	0 00	0 00	0 00	0 00	0 00	0 00	0 00	0 00	0 00	0 00	0 00	0 00	0 00	0 00	0 00	
<i>Thalassiosira antarctica</i>	0 00	0 18	0																	

---

## **Appendix 4**

### **Sørsdal Formation Diatom Data**

---

**Appendix 4.** Quantitative relative abundance (%) of diatoms in the Sørødal Formation. (r and \* designate species occurrences in Harwood *et al.* in press)

SAMPLES	2(0-10)	2A(10-20)	2A(20-30)	2A(30-40)	2A(40-50)	2A(80-90)	2A(90-100)	2A(120-130)	2A(130-140)	2A(140-150)
CORE DEPTH (cm)	10	175	185	195	205	245	255	285	295	305
DIATOMS										
<i>Actinocyclus ingens</i>	0 00	0 00	0 00	0 00	0 00	0 00	0 00	0 00	0 00	r
<i>Actinocyclus karstenii</i>	r	r	0 21	0 00	0 00	0 00	0 59	0 00	0 00	r
<i>Actinocyclus octonarius</i> var <i>astenscuss</i>	0 00	r	0 00	0 00	0 00	0 00	0 00	0 00	0 00	r
<i>Actinocyclus</i> sp A	0 48	0 00	0 00	0 00	0 00	0 00	0 00	0 00	0 00	0 00
<i>Achnanthes brevipes</i>	r	0 23	1 03	0 91	2 02	1 53	1 97	2 61	3 63	r
<i>Amphora</i> sp A	2 15	1 15	2 26	0 73	2 02	2 62	0 00	1 74	1 45	0 89
<i>Amphora</i> sp B	0 00	0 00	0 21	0 00	0 00	0 00	0 59	0 00	0 00	0 22
<i>Amphora</i> spp	0 24	0 00	0 21	0 73	0 00	0 44	0 79	0 44	0 48	1 12
<i>Anaulus ellipticus</i>	r	0 00	0 00	0 00	0 00	0 00	0 00	0 00	0 00	r
<i>Anaulus scalaris</i>	0 00	0 00	0 00	0 00	0 00	0 00	0 00	0 00	0 00	0 00
<i>Chaetoceros dichæta</i> (vege)	2 86	9 40	6 38	5 29	6 73	5 24	3 35	8 93	3 63	8 93
<i>Chaetoceros</i> (extant cysts)	56 56	54 13	40 95	54 20	47 09	38 86	31 30	40 96	34 14	50 45
<i>Chaetoceros lorenzianus</i> (cyst)	0 00	r	0 82	0 18	0 67	0 66	2 95	1 74	0 00	0 67
<i>Cocconeis costata</i>	0 95	r	1 03	0 73	0 45	0 22	1 57	1 31	1 94	0 22
<i>Cocconeis fasciolata</i>	2 63	2 06	4 73	3 47	4 04	1 75	7 28	4 58	4 36	2 46
<i>Cocconeis gautieri</i>	0 00	r	0 00	0 00	0 00	0 00	0 00	0 00	0 00	0 00
<i>Cocconeis pinnata</i>	1 19	r	0 41	0 00	0 67	0 66	1 57	1 74	0 73	r
<i>Cocconeis schuettii</i>	0 72	r	0 00	0 18	0 00	0 00	0 39	0 44	0 00	r
<i>Cocconeis</i> sp A	0 48	0 00	0 62	0 00	0 00	0 66	0 39	0 87	0 73	0 22
<i>Cocconeis</i> sp B	0 48	0 23	0 62	0 00	0 67	0 22	1 38	0 65	0 48	0 45
<i>Coscinodiscus</i> spp	0 72	r	1 03	0 36	0 00	0 00	1 38	0 44	0 97	r
<i>Coretheron crotaphilum</i>	0 00	0 00	0 00	0 00	0 00	0 00	0 00	0 00	0 00	0 00
<i>Dactylosira antarctica</i>	0 00	0 00	0 00	0 00	0 22	0 00	0 00	0 22	0 00	r
<i>Diploneis frickel</i>	0 24	0 00	0 00	0 00	0 00	0 00	0 00	0 00	0 00	r
<i>Diploneis splendida</i>	1 67	0 23	0 21	0 00	0 22	0 00	0 79	0 00	0 00	0 22
<i>Diploneis subovalis</i>	1 91	r	0 00	0 00	0 00	0 00	0 59	0 00	0 00	r
<i>Diploneis</i> sp A	0 00	0 00	0 00	0 00	0 00	0 00	0 00	0 00	0 00	0 00
<i>Drepanotheca bivittata</i>	0 00	0 00	0 00	0 00	0 00	0 00	0 00	0 00	0 00	0 00
<i>Eucampia antarctica</i> var <i>recta</i>	0 00	r	0 00	0 00	0 00	1 31	0 39	0 00	0 97	r
<i>Eunota</i> sp A	0 00	r	0 00	0 00	0 00	0 00	0 00	0 00	0 00	r
<i>Fragilaria construens</i> var <i>venter</i>	0 24	2 52	0 82	0 73	2 02	2 40	1 38	0 00	0 48	3 57
<i>Fragilaria</i> sp A	13 37	18 58	18 52	22 81	24 89	24 02	17 72	14 16	26 63	22 10
<i>Fragilariopsis barronii</i>	0 00	0 46	2 67	0 36	0 00	0 87	0 00	0 22	0 24	0 67
<i>Fragilariopsis curta</i>	0 00	r	0 00	0 00	0 00	0 00	0 20	0 00	0 00	r
<i>Fragilariopsis</i> sp cf <i>obliquecostata</i>	0 00	0 00	0 00	0 00	0 00	0 00	0 20	0 00	0 00	0 00
<i>Fragilariopsis praecurta</i>	0 00	0 23	0 00	0 00	0 00	0 00	0 39	0 00	0 00	0 00
<i>Fragilariopsis praeinterfrigidaria</i>	0 00	r	0 00	0 00	0 00	0 00	0 20	0 00	0 00	r
<i>Fragilariopsis ritscheri</i>	0 00	0 00	0 00	0 00	0 00	0 00	0 20	0 00	0 00	0 00
<i>Fragilariopsis separanda</i>	0 00	0 00	0 62	0 36	0 00	0 22	0 00	0 22	0 00	0 00
<i>Fragilariopsis sublinearis</i>	0 24	0 46	1 03	0 00	0 00	0 44	0 00	0 00	0 73	r
<i>Gomphonemopsis</i> sp A	0 72	0 23	0 21	0 00	0 00	0 00	0 79	0 00	0 24	0 00
<i>Grammatophora</i> spp	r	r	0 00	0 00	0 00	0 00	0 00	0 00	0 00	r
Gen et sp indet A + B	0 72	0 00	0 41	0 55	0 67	0 44	0 00	0 87	0 24	0 45
<i>Hyalodiscus</i> spp	0 00	0 00	0 00	0 00	0 00	0 00	0 00	0 00	0 48	0 00
<i>Isthmia</i> sp	0 48	r	0 00	0 00	0 22	0 22	0 00	0 22	0 48	r
<i>Navicula</i> sp cf <i>cancellata</i>	0 72	0 92	1 03	0 55	0 22	0 44	0 59	1 09	0 97	0 89
<i>Navicula directa</i>	0 00	0 00	0 00	0 00	0 00	0 00	0 20	0 00	0 00	0 00
<i>Navicula perminuta</i>	0 00	0 46	0 82	0 18	0 00	0 00	0 59	0 44	0 73	0 45
<i>Navicula</i> spp	0 24	0 00	0 21	0 00	0 00	0 00	0 20	0 00	0 00	0 00
<i>Nitzschia</i> spp	0 00	0 46	0 82	0 00	0 22	0 44	0 00	0 22	0 24	0 00
<i>Odontella punctata</i>	0 00	r	0 00	0 00	0 00	0 00	0 00	0 00	0 00	r
<i>Odontella weissflogii</i>	0 00	0 00	0 00	0 00	0 00	0 00	0 00	0 00	0 00	r
<i>Paralia</i> spp	3 34	0 23	0 41	0 18	0 22	1 75	0 20	1 31	1 94	r
<i>Pinnularia quadratarea</i>	0 48	0 00	0 00	0 18	0 22	0 00	0 00	1 09	0 48	r
<i>Pinnularia</i> spp	0 24	0 00	0 00	0 00	0 00	0 44	0 00	0 00	0 00	0 00
<i>Podosira</i> sp	r	0 69	1 85	0 00	0 67	0 44	0 00	0 00	0 00	r
<i>Porosira pseudodenticulata</i>	0 00	0 00	0 00	0 00	0 00	0 00	0 00	0 44	0 00	0 00
<i>Pseudogomphonema kamtschaticum</i>	0 00	0 00	0 00	0 00	0 00	0 00	0 00	0 00	0 00	0 00

#### Appendix 4. continued

[illegible]



## Appendix 4. continued

SAMPLES	2A(150-160)	2A(170-180)	2A(180-190)	2A(190-200)	2A(210-220)	2A(240-250)	2A(260-265)	2A(265-270)	2A(270-280)	2A(280-290)
CORE DEPTH (cm)	315	335	345	355	375	405	420	425	435	445
<b>DIATOMS</b>										
<i>Actinocyclus ingens</i>	0 00	0 00	0 00	0 00	0 00	0 00	0 00	0 00	0 00	0 00
<i>Actinocyclus karstenii</i>	0 00	0 22	r	0 20	0 00	0 22	0 20	0 00	0 00	0 20
<i>Actinocyclus octonarius</i> var <i>asteriscus</i>	0 00	0 00	r	0 00	0 00	0 00	r	0 00	r	0 00
<i>Actinocyclus</i> sp A	0 00	0 00	0 00	0 00	0 00	0 00	0 00	0 00	0 00	0 00
<i>Achnanthes brevipes</i>	1 71	1 35	0 43	1 23	0 82	2 17	0 81	0 60	0 99	0 61
<i>Amphora</i> sp A	1 28	5 38	1 95	1 43	2 04	2 39	1 61	2 80	3 96	3 69
<i>Amphora</i> sp B	0 00	0 00	0 00	0 00	0 41	0 43	0 20	0 00	0 17	0 20
<i>Amphora</i> spp	0 21	0 22	0 00	0 20	0 41	0 22	0 20	0 60	0 00	0 20
<i>Anaulus ellipticus</i>	0 00	0 00	0 00	0 00	0 00	0 00	0 00	0 00	0 00	0 00
<i>Anaulus scalars</i>	0 00	0 00	0 00	0 00	0 00	0 00	0 00	0 00	0 00	0 20
<i>Chaetoceros dictyeta</i> (vege)	9 64	6 73	4 77	3 07	4 50	2 39	3 63	6 20	7 10	2 05
<i>Chaetoceros</i> (extant cysts)	52 46	38 12	22 34	30 74	38 24	43 17	33 67	46 80	40 92	35 66
<i>Chaetoceros lorenzianus</i> (cyst)	0 00	0 00	0 22	1 64	0 82	0 00	r	0 00	r	0 20
<i>Cocconeis costata</i>	0 21	0 45	0 65	1 02	0 41	1 52	1 01	1 40	0 66	1 64
<i>Cocconeis fasciolata</i>	2 57	3 36	1 74	4 10	4 50	6 51	5 44	9 40	5 78	5 12
<i>Cocconeis gautieri</i>	0 00	0 00	0 00	0 00	0 00	0 00	0 00	0 00	0 00	0 00
<i>Cocconeis pinnata</i>	0 86	0 45	0 43	1 23	0 00	1 30	0 60	1 00	0 33	0 82
<i>Cocconeis schuettii</i>	0 00	0 00	0 00	0 00	0 00	0 22	0 00	0 60	0 17	0 20
<i>Cocconeis</i> sp A	0 00	0 22	r	0 20	0 61	0 22	0 60	0 60	0 50	0 82
<i>Cocconeis</i> sp B	0 43	0 00	0 22	0 00	0 41	0 43	0 60	2 20	0 99	1 02
<i>Coscinodiscus</i> spp	0 00	0 00	0 22	0 41	0 20	0 00	r	0 60	r	0 41
<i>Coretheron criophilum</i>	0 00	0 00	0 00	0 00	0 00	0 00	0 00	0 00	0 00	0 00
<i>Dactylosolen antarcticus</i>	0 00	0 00	r	0 00	0 00	0 00	0 00	0 00	0 00	0 00
<i>Diploneis frickei</i>	0 00	0 00	0 00	0 00	0 00	0 00	0 00	0 00	0 00	0 20
<i>Diploneis splendida</i>	0 43	0 22	0 43	0 20	0 00	0 22	r	0 60	0 00	0 20
<i>Diploneis subovalis</i>	0 00	0 00	r	0 00	0 20	0 00	r	0 00	0 17	0 00
<i>Diploneis</i> sp A	0 00	0 22	0 00	0 00	0 20	0 00	0 20	0 00	0 17	0 00
<i>Drepanotheca bivittata</i>	0 00	0 00	0 00	0 00	0 00	0 00	0 00	0 00	0 00	0 00
<i>Eucampia antarctica</i> var <i>recta</i>	0 00	0 22	0 22	0 82	0 20	0 22	0 00	0 00	0 00	0 00
<i>Eunotia</i> sp A	0 00	0 00	r	0 00	0 00	0 00	0 00	0 00	0 17	0 00
<i>Fragilaria construens</i> var <i>venter</i>	0 86	0 45	4 12	1 23	1 02	1 74	5 85	0 00	1 82	5 33
<i>Fragilaria</i> sp A	18 20	27 35	50 76	35 04	19 63	20 17	33 06	0 00	18 32	18 85
<i>Fragilaropsis barronii</i>	0 00	0 22	0 22	0 20	1 02	0 00	0 40	0 20	0 33	1 02
<i>Fragilaropsis curta</i>	0 00	0 00	r	0 00	0 00	0 00	0 20	0 00	0 33	0 20
<i>Fragilaropsis</i> sp cf <i>obliquecostata</i>	0 00	0 00	0 00	0 00	0 00	0 00	0 00	0 00	0 00	0 00
<i>Fragilaropsis praecurta</i>	0 00	0 00	0 00	0 00	0 00	0 00	0 00	0 20	0 17	0 20
<i>Fragilaropsis praelinterfrigidana</i>	0 00	0 00	0 00	0 00	0 00	0 22	0 00	0 00	r	r
<i>Fragilaropsis ritscheri</i>	0 00	0 00	0 00	0 00	0 00	0 00	0 00	0 00	0 00	0 00
<i>Fragilaropsis separanda</i>	0 00	0 00	0 43	0 00	0 00	0 22	0 00	0 60	0 00	0 00
<i>Fragilaropsis sublinearis</i>	0 00	0 22	0 22	0 41	0 20	0 43	0 00	0 00	0 17	0 61
<i>Gomphonemopsis</i> sp A	0 64	0 00	0 00	0 41	0 00	0 22	0 60	0 00	0 17	0 00
<i>Grammatophora</i> spp	0 00	0 00	r	0 00	0 00	0 00	0 00	0 00	0 00	0 00
<i>Gen et sp indet A + B</i>	1 28	0 22	0 65	0 41	1 02	0 00	0 40	0 80	0 33	0 20
<i>Hyalodiscus</i> spp	0 00	0 00	0 43	0 00	0 20	0 00	0 20	0 00	0 00	0 20
<i>Isthmia</i> sp	0 43	0 22	0 43	0 00	0 20	0 22	0 20	0 20	r	0 20
<i>Navicula</i> sp cf <i>cancellata</i>	0 86	1 35	0 87	1 23	0 82	0 87	0 00	1 40	1 49	0 82
<i>Navicula directa</i>	0 00	0 00	0 00	0 20	0 00	0 00	0 00	0 40	0 17	1 02
<i>Navicula perminuta</i>	0 43	0 67	0 22	0 20	1 43	0 00	0 81	2 00	2 15	1 23
<i>Navicula</i> spp	0 00	0 00	0 22	0 20	0 20	0 22	0 81	0 60	0 66	0 41
<i>Nitzschia</i> spp	0 21	0 00	0 00	0 00	0 20	0 00	0 40	1 40	0 00	0 00
<i>Odontella punctata</i>	0 00	0 00	r	0 00	0 00	0 00	0 00	0 00	r	0 20
<i>Odontella weissflogii</i>	0 00	0 00	0 00	0 00	0 00	0 00	0 00	0 00	0 00	0 00
<i>Paralia</i> spp	0 64	0 00	0 87	1 23	0 20	2 60	1 41	1 40	0 83	0 41
<i>Pinnularia quadratarea</i>	0 00	0 45	0 00	0 20	0 41	0 00	0 00	0 40	0 17	0 20
<i>Pinnularia</i> spp	0 00	0 00	0 00	0 00	0 00	0 00	0 00	0 00	0 00	0 00
<i>Podosira</i> sp	0 00	0 45	0 87	2 05	1 43	1 08	r	1 20	0 17	0 41
<i>Porosira pseudodenticulata</i>	0 00	0 00	0 00	0 00	0 00	0 00	0 00	0 00	0 00	0 00
<i>Pseudogomphonema kamtschaticum</i>	0 00	0 00	0 00	0 00	0 00	0 22	0 00	0 00	0 00	0 00

## (

1

### Appendix 4. continued

SAMPLES	2B(0-10)	2B(20-30)	2B(40-50)	2B(50-60)	2B(60-70)	2B(75)	2B(70-80)	2B(85-90)	2B(80-90)	2B(90-95)
CORE DEPTH (cm)	460	480	500	510	520	525	530	540	540	545
DIATOMS										
<i>Actinocyclus ingens</i>	0 00	0 00	0 00	0 00	0 00	0 00	0 00	0 00	0 00	0 00
<i>Actinocyclus karstenii</i>	r	0 22	0 00	r	0 21	0 00	0 77	0 20	0 00	0 19
<i>Actinocyclus octonarius</i> var <i>astenscus</i>	r	0 22	0 00	r	0 00	0 00	0 00	0 00	0 00	0 00
<i>Actinocyclus</i> sp A	0 00	0 00	0 00	0 00	0 00	0 00	0 00	0 00	0 00	0 00
<i>Achnanthes brevipes</i>	0 67	0 65	0 21	0 98	0 42	0 22	0 58	0 80	0 23	0 58
<i>Amphora</i> sp A	1 55	2 80	1 87	1 95	1 48	0 66	2 31	1 80	1 85	3 48
<i>Amphora</i> sp B	0 00	0 43	0 00	0 00	0 21	0 00	0 19	0 20	0 00	0 00
<i>Amphora</i> spp	0 44	0 43	0 42	0 00	0 42	0 00	0 19	0 80	0 23	0 00
<i>Anaulus ellipticus</i>	0 00	0 00	0 00	0 00	0 00	0 00	0 00	0 00	0 00	0 00
<i>Anaulus scalaris</i>	0 00	0 00	0 00	0 00	0 00	0 00	0 00	0 00	0 00	0 00
<i>Chaetoceros dichaela</i> (vege)	0 44	3 88	3 74	5 47	8 03	8 30	7 31	3 79	3 23	7 16
<i>Chaetoceros</i> (extant) cysts	65 30	57 11	72 14	60 74	47 36	67 69	47 31	66 27	65 36	57 83
<i>Chaetoceros lorenzianus</i> (cyst)	0 00	0 00	0 00	0 00	0 00	0 00	0 00	0 00	0 00	0 00
<i>Cocconeis costata</i>	0 67	1 08	0 83	0 98	2 11	1 53	1 73	1 00	0 92	1 55
<i>Cocconeis fasciolata</i>	5 76	8 41	4 78	8 20	13 95	4 80	14 62	7 39	9 24	7 74
<i>Cocconeis gauteri</i>	0 00	0 00	0 00	0 00	0 00	0 00	0 00	0 00	0 00	0 00
<i>Cocconeis pinnata</i>	r	1 29	0 21	1 37	1 90	0 44	4 62	0 40	0 46	1 16
<i>Cocconeis schuettii</i>	0 67	0 65	0 21	0 00	0 21	0 22	0 00	0 00	0 23	0 58
<i>Cocconeis</i> sp A	r	0 43	0 21	0 59	0 85	0 44	0 77	0 40	0 23	1 16
<i>Cocconeis</i> sp B	1 77	0 86	1 04	0 20	0 42	0 44	0 19	0 40	0 46	0 58
<i>Coscinodiscus</i> spp	r	0 00	0 21	0 20	0 42	0 00	0 58	0 00	0 00	0 00
<i>Coretheron crenophitum</i>	0 00	0 00	0 00	0 00	0 00	0 00	0 00	0 00	0 00	0 00
<i>Dactylosira antarctica</i>	r	0 00	0 00	0 00	0 00	0 00	0 19	0 00	0 00	0 19
<i>Diploneis frickei</i>	0 00	0 00	0 00	0 00	0 00	0 00	0 00	0 00	0 00	0 00
<i>Diploneis splendida</i>	r	0 22	0 21	r	0 21	0 22	0 58	0 00	0 00	0 00
<i>Diploneis subovalis</i>	0 00	0 00	0 00	0 20	0 00	0 00	0 00	0 00	0 00	0 00
<i>Diploneis</i> sp A	0 00	0 00	0 00	0 00	0 00	0 00	0 00	0 00	0 00	0 00
<i>Drepanotheca breviflata</i>	0 00	0 00	0 00	0 00	0 00	0 00	0 00	0 00	0 00	r
<i>Eucampia antarctica</i> var <i>recta</i>	0 00	0 00	0 00	0 00	0 00	0 00	0 00	0 00	0 23	0 58
<i>Eunotia</i> sp A	0 44	0 00	0 00	r	0 21	0 00	0 00	0 00	0 00	0 00
<i>Fragilaria construens</i> var <i>venter</i>	0 44	0 00	0 00	0 98	0 21	0 44	0 38	0 00	0 46	0 00
<i>Fragilaria</i> sp A	5 32	10 34	4 99	6 05	4 65	6 11	2 69	3 39	5 31	2 13
<i>Fragilariopsis barronii</i>	0 67	0 22	0 42	0 39	0 63	0 22	1 15	0 00	1 15	0 39
<i>Fragilariopsis curta</i>	?	0 22	0 00	0 00	0 21	0 00	0 00	1 40	0 00	0 00
<i>Fragilariopsis</i> sp cf. <i>obliquecostata</i>	0 00	0 00	0 00	0 00	0 00	0 00	0 00	0 00	0 00	0 00
<i>Fragilaropsis praecurta</i>	0 00	0 00	0 00	0 00	1 27	0 00	0 00	0 00	0 00	0 19
<i>Fragilariopsis praeinterfrigidana</i>	r	0 00	0 00	r	0 00	0 00	0 00	0 00	0 23	0 00
<i>Fragilaropsis ritscheri</i>	0 00	0 00	0 00	0 00	0 00	0 00	0 00	0 00	0 00	0 00
<i>Fragilaropsis separanda</i>	0 67	0 22	1 04	0 78	0 00	0 44	0 19	0 60	0 00	0 97
<i>Fragilaropsis sublinearis</i>	0 00	0 00	0 42	0 20	0 42	0 22	0 77	0 40	0 00	0 58
<i>Gomphonemopsis</i> sp A	0 00	0 86	0 21	0 78	0 00	0 00	0 60	0 60	0 00	0 00
<i>Grammatophora</i> spp	0 00	0 00	0 00	0 20	0 00	0 00	0 00	0 00	0 00	0 00
Gen et sp indet A + B	1 11	0 22	0 62	0 98	0 63	0 44	0 38	1 40	0 00	0 00
<i>Hyalodiscus</i> spp	0 00	0 00	0 00	0 00	0 85	0 00	0 00	0 00	0 23	0 00
<i>Isthmia</i> sp	0 22	0 22	0 21	r	0 00	0 22	0 00	0 40	0 00	0 19
<i>Navicula</i> sp cf. <i>cancellata</i>	2 66	2 16	0 42	0 59	0 42	0 66	0 58	0 80	0 92	1 16
<i>Navicula directa</i>	0 00	0 22	0 00	0 00	0 42	0 00	0 00	0 00	0 23	0 39
<i>Navicula perminuta</i>	3 77	0 86	0 83	0 59	0 21	0 87	0 00	1 20	0 92	0 97
<i>Navicula</i> spp	0 22	0 22	0 21	0 59	0 63	0 22	0 00	0 40	0 46	0 39
<i>Nitzschia</i> spp	0 00	0 00	0 00	0 39	0 00	0 00	0 38	0 00	0 00	0 00
<i>Odontella punctata</i>	0 00	0 00	0 00	0 39	0 00	0 00	0 00	0 00	0 00	0 00
<i>Odontella weissflogii</i>	0 00	0 00	0 00	0 00	0 00	0 00	0 00	0 00	0 00	0 00
<i>Paralia</i> spp	0 67	0 86	0 83	1 17	2 11	0 66	1 92	1 00	0 23	1 93
<i>Pinnularia quadratarea</i>	0 00	0 22	0 00	0 20	0 00	0 22	0 77	0 00	0 00	0 19
<i>Pinnularia</i> spp	0 00	0 00	0 00	0 00	0 00	0 00	0 00	0 00	0 23	0 19
<i>Podosira</i> sp	r	0 65	0 21	0 39	0 42	0 00	0 77	0 00	0 00	0 58
<i>Porosira pseudodenticulata</i>	0 00	0 00	0 00	0 00	0 00	0 00	0 00	0 00	0 00	0 00
<i>Pseudogomphonema kamtschaticum</i>	0 00	0 00	0 00	0 00	0 00	0 00	0 00	0 00	0 00	0 00

SAMPLES	2B(0-10)	2B(20-30)	2B(40-50)	2B(50-60)	2B(60-70)	2B(75)	2B(70-80)	2B(85-90)	2B(80-90)	2B(90-95)
CORE DEPTH (cm)	460	480	500	510	520	525	530	540	540	545
DIATOMS										
<i>Rhizosolenia hebetata</i> (group)	0 00	0 00	0 00	0 00	0 00	0 00	0 00	0 00	0 00	0 39
<i>Rhizosolenia styliformis</i> (group)	0 00	0 00	0 00	0 00	0 21	0 22	0 58	0 00	0 00	0 00
<i>Rhizosolenia</i> sp A	0 00	0 00	0 00	0 39	0 63	0 00	0 19	0 00	0 00	0 00
<i>Rouxia antarctica</i>	r	0 00	0 00	r	0 42	0 22	0 00	0 00	0 23	0 00
<i>Rouxia isopolica</i>	0 22	0 00	0 00	0 00	0 00	0 00	0 19	0 00	0 00	0 00
<i>Rouxia leventerae</i>	0 00	0 22	0 00	0 00	0 00	0 22	0 00	0 00	0 00	0 19
<i>Rouxia naviculoides</i>	0 00	0 00	0 00	0 00	0 00	0 00	0 00	0 00	0 00	0 19
<i>Rouxia</i> fragments	0 44	0 65	0 21	0 39	0 85	0 00	0 19	0 40	0 00	0 58
<i>Stellarima microtrias</i>	0 00	0 43	0 62	r	0 21	0 44	0 38	0 60	0 46	0 97
<i>Stellarima stellans</i>	0 00	0 00	0 00	0 00	0 00	0 00	0 00	0 00	0 00	0 00
<i>Stephanopyxis grunowii</i>	0 00	0 00	0 21	0 00	0 00	0 00	0 38	0 40	0 00	0 00
<i>Stephanopyxis turnis</i>	r	0 00	0 42	r	0 42	0 66	0 58	0 20	0 69	0 39
<i>Sticodiscus hardmanianus</i>	0 00	0 00	0 00	0 00	0 00	0 00	0 00	0 00	0 00	0 00
<i>Synedra</i> spp	4 21	0 86	0 62	2 15	2 33	0 87	0 77	1 40	1 39	1 16
<i>Thalassionema nitzschoides</i> (group)	0 22	0 65	0 21	1 37	1 27	1 09	1 35	1 20	0 92	0 77
<i>Thalassiosira antarctica</i> (?)	0 00	0 00	0 00	0 00	0 00	0 00	0 00	0 00	0 00	0 00
<i>Thalassiosira complicata</i>	0 00	0 00	0 00	0 00	0 00	0 00	0 00	0 00	0 00	0 00
<i>Thalassiosira fasciculata</i>	0 00	0 00	0 00	0 00	0 00	0 00	0 00	0 00	0 00	0 00
<i>Thalassiosira inura</i>	0 00	0 22	0 21	0 00	0 42	0 00	0 00	0 00	0 00	0 00
<i>Thalassiosira inura- insigna</i> (transitional)	0 00	0 00	0 00	0 00	0 00	0 00	0 00	0 00	0 00	0 00
<i>Thalassiosira gracilis</i> var <i>expecta</i>	0 00	0 00	0 21	0 00	0 00	0 00	0 19	0 00	2 08	0 00
<i>Thalassiosira gracilis</i> var <i>gracilis</i>	0 00	0 00	0 00	0 00	0 00	0 00	0 58	0 00	0 23	0 39
<i>Thalassiosira maculata</i>	0 00	0 00	0 00	0 00	0 00	0 00	0 00	0 00	0 00	0 00
<i>Thalassiosira oestrupii</i>	0 22	0 00	0 21	r	1 06	0 44	1 15	0 00	0 46	0 58
<i>Thalassiosira oliverana</i>	0 00	0 00	0 00	0 00	0 00	0 22	0 19	0 20	0 00	0 00
<i>Thalassiosira striata</i>	0 00	0 00	0 00	0 00	0 00	0 00	0 19	0 00	0 00	0 00
<i>Thalassiosira torokana</i>	0 22	0 22	0 00	r	0 00	0 00	0 00	0 00	0 00	0 39
<i>Thalassiosira oliverana</i> (coarse)	0 00	0 00	0 00	0 00	0 00	0 00	0 00	0 00	0 00	0 00
<i>Thalassiothrix</i> spp	0 00	0 00	0 42	0 20	0 00	0 00	0 00	0 20	0 00	0 58
<i>Trachyneis aspera</i>	0 00	0 22	0 21	0 00	0 42	0 00	1 15	0 40	0 46	0 00
<i>Trichotoxon</i> sp	0 00	0 22	0 00	0 00	0 00	0 00	0 00	0 00	0 00	0 39
<i>Trigonium arcticum</i>	0 00	0 22	0 00	0 00	0 00	0 00	0 00	0 00	0 00	0 00
Other spp	0 00	0 00	0 00	0 00	0 21	0 00	0 00	0 00	0 00	0 00
<i>Pseudo-nitzschia turgiduloides</i> *										
<i>Proboscia barboi</i> *										

## Appendix 4. continued

SAMPLES	2B(100-110)	2B(110-120)	2B(140-150)	2B(170-180)	2B(210-220)	2B(235-237)
CORE DEPTH (cm)	560	570	600	630	670	687
<b>DIATOMS</b>						
<i>Actinocyclus ingens</i>	0.00	0.00	0.00	0.00	0.00	0.00
<i>Actinocyclus karstenii</i>	0.00	r	0.23	r	r	0.00
<i>Actinocyclus octonarius</i> var <i>astenscus</i>	0.00	0.00	0.00	r	0.00	0.00
<i>Actinocyclus</i> sp. A	0.00	0.00	0.00	0.22	0.00	0.00
<i>Achnanthes brevipes</i>	1.45	0.82	0.23	0.86	0.78	0.44
<i>Amphora</i> sp. A	1.86	1.91	2.49	4.30	1.17	1.31
<i>Amphora</i> sp. B	0.00	0.00	0.00	0.00	0.00	0.00
<i>Amphora</i> spp.	0.21	1.09	0.45	0.43	0.00	0.00
<i>Anaulus ellipticus</i>	0.00	0.00	0.00	0.00	0.00	0.00
<i>Anaulus scalaris</i>	0.00	0.00	0.00	0.00	0.00	0.00
<i>Chaetoceros dichæta</i> (vege)	3.93	10.11	5.67	3.44	9.73	3.92
<i>Chaetoceros</i> (extant cysts)	72.31	53.01	53.74	49.03	57.98	60.78
<i>Chaetoceros lorenzianus</i> (cyst)	0.00	0.00	0.00	0.00	0.00	0.00
<i>Cocconeis costata</i>	1.24	1.09	1.36	1.72	1.56	2.61
<i>Cocconeis fasciolata</i>	4.55	7.38	5.90	8.60	9.53	14.16
<i>Cocconeis gautieri</i>	0.00	0.00	0.00	0.00	0.00	0.00
<i>Cocconeis pinnata</i>	0.83	0.82	0.00	0.65	0.58	1.74
<i>Cocconeis schuettii</i>	0.21	0.00	0.23	0.65	0.00	0.44
<i>Cocconeis</i> sp. A	0.83	0.55	0.00	2.15	1.17	0.87
<i>Cocconeis</i> sp. B	0.41	0.00	1.13	2.58	0.00	1.31
<i>Coscinodiscus</i> spp.	0.21	r	0.23	r	0.58	0.44
<i>Coretheron criophilum</i>	0.00	0.00	0.00	0.22	0.00	0.00
<i>Dactylosolen antarcticus</i>	0.00	0.00	0.00	0.86	r	0.00
<i>Diploneis frickei</i>	0.00	0.00	0.00	0.00	0.00	0.00
<i>Diploneis splendida</i>	0.00	0.55	0.45	r	r	0.00
<i>Diploneis subovalis</i>	0.41	0.00	0.00	0.00	0.19	0.00
<i>Diploneis</i> sp. A	0.00	0.00	0.00	0.00	0.00	0.00
<i>Drepanotheca bivitata</i>	0.00	0.00	0.00	0.00	0.00	0.00
<i>Eucampia antarctica</i> var <i>recta</i>	0.00	r	0.23	0.00	r	0.22
<i>Eunotia</i> sp. A	0.00	0.55	0.00	r	0.00	0.22
<i>Fragilaria construens</i> var <i>venter</i>	0.00	0.55	0.23	0.00	0.19	0.00
<i>Fragilaria</i> sp. A	3.10	12.02	10.43	1.08	4.28	1.53
<i>Fragilaropsis baronii</i>	0.21	0.55	0.45	0.43	0.00	0.22
<i>Fragilaropsis curta</i>	0.00	0.00	0.23	0.00	0.00	0.00
<i>Fragilaropsis</i> sp. cf. <i>obliquecostata</i>	0.00	0.00	0.00	0.00	0.00	0.00
<i>Fragilaropsis praecurta</i>	0.00	0.00	0.00	0.00	0.00	0.00
<i>Fragilaropsis praeinterfrigidaria</i>	0.00	0.00	0.00	0.00	r	0.00
<i>Fragilaropsis nitscheni</i>	0.00	0.00	0.00	0.00	0.00	0.00
<i>Fragilaropsis separanda</i>	0.41	0.27	0.68	0.00	0.39	0.65
<i>Fragilaropsis sublineans</i>	0.00	0.00	0.45	0.00	0.00	0.00
<i>Gomphonemopsis</i> sp. A	0.00	0.82	0.00	2.58	0.19	0.00
<i>Grammatophora</i> spp.	0.00	r	0.00	0.00	0.00	0.00
<i>Gen. et sp. indet. A + B</i>	0.21	0.27	1.13	0.65	1.36	0.44
<i>Hyalodiscus</i> spp.	0.00	0.00	r	0.00	0.00	0.00
<i>Isthmia</i> sp.	0.00	0.82	0.45	0.43	0.19	0.00
<i>Navicula</i> sp. cf. <i>cancellata</i>	0.83	0.55	1.81	1.94	0.39	1.09
<i>Navicula directa</i>	0.00	0.00	0.00	0.00	0.39	0.00
<i>Navicula perminuta</i>	0.21	0.00	0.68	8.17	0.19	0.87
<i>Navicula</i> spp.	0.00	1.09	0.00	0.00	0.39	0.00
<i>Nitzschia</i> spp.	0.62	0.00	0.91	0.00	0.19	0.44
<i>Odontella punctata</i>	0.00	0.00	0.00	0.00	0.00	0.00
<i>Odontella weissflogii</i>	0.00	0.00	0.00	0.00	0.00	0.00
<i>Paralia</i> spp.	0.62	r	0.68	0.65	0.19	0.87
<i>Pinnularia quadratarea</i>	0.41	0.00	0.23	0.00	0.00	0.00
<i>Pinnularia</i> spp.	0.00	0.00	0.00	0.43	0.00	0.00
<i>Podosira</i> sp.	0.21	0.55	0.00	r	0.58	0.65
<i>Porosira pseudodenticulata</i>	0.00	0.00	0.00	0.00	0.00	0.00
<i>Pseudogomphonema kamtschaticum</i>	0.00	0.00	0.00	0.22	0.00	0.00

## Appendix 4. continued

SAMPLES	2B(100-110)	2B(110-120)	2B(140-150)	2B(170-180)	2B(210-220)	2B(235-237)
CORE DEPTH (cm)	560	570	600	630	670	687
<b>DIATOMS</b>						
<i>Rhizosolenia hebetata</i> (group)	0 00	0 00	0 00	0 00	0 19	0 00
<i>Rhizosolenia styliformis</i> (group)	0 21	r	0 23	0 00	1 36	0 00
<i>Rhizosolenia</i> sp A	0 00	0 00	0 00	0 00	0 00	0 00
<i>Rouxia antarctica</i>	0 00	0 27	0 00	0 22	r	0 00
<i>Rouxia isopolica</i>	0 41	0 00	0 00	0 00	0 00	0 22
<i>Rouxia leventerae</i>	0 00	0 00	0 00	0 22	0 00	0 00
<i>Rouxia naviculoides</i>	0 00	0 00	0 00	r	0 00	0 44
<i>Rouxia</i> fragments	0 00	0 82	1 59	0 00	0 39	0 00
<i>Stellarima microtrias</i>	0 21	0 27	0 23	0 65	0 39	0 44
<i>Stellarima stellans</i>	0 00	0 00	0 00	r	r	0 00
<i>Stephanopyxis grunowii</i>	0 00	r	0 45	0 22	0 00	0 00
<i>Stephanopyxis turris</i>	0 00	0 00	0 00	r	r	0 22
<i>Sticodiscus hardmanianus</i>	0 00	0 00	0 00	0 00	0 00	0 00
<i>Synedra</i> spp	1 03	0 27	1 59	2 15	1 75	1 74
<i>Thalassionema nitzschioides</i> (group)	0 83	1 91	1 13	1 72	1 36	0 65
<i>Thalassiosira antarctica</i> (?)	0 00	0 27	0 00	0 00	0 00	0 00
<i>Thalassiosira complicata</i>	0 00	0 00	0 00	0 00	0 00	0 00
<i>Thalassiosira fasciculata</i>	0 00	0 00	0 00	0 00	0 00	0 00
<i>Thalassiosira inura</i>	0 00	0 00	0 00	0 00	0 19	0 00
<i>Thalassiosira inura- insigna</i> (transitional)	0 00	0 00	0 00	0 00	0 00	0 00
<i>Thalassiosira gracilis</i> var <i>expecta</i>	0 00	0 27	0 00	0 00	0 00	0 00
<i>Thalassiosira gracilis</i> var <i>gracilis</i>	0 21	0 00	0 00	0 22	0 00	0 00
<i>Thalassiosira maculata</i>	0 00	0 00	0 00	0 00	0 00	0 00
<i>Thalassiosira oestrupii</i>	0 21	0 55	1 81	0 22	1 36	0 22
<i>Thalassiosira oliverana</i>	0 00	0 00	0 00	0 22	0 00	0 00
<i>Thalassiosira striata</i>	0 00	0 00	0 23	0 00	0 00	0 00
<i>Thalassiosira torokina</i>	0 41	r	0 00	r	0 19	0 22
<i>Thalassiosira oliverana</i> (coarse)	0 00	0 00	0 23	0 00	0 00	0 00
<i>Thalassiothrix</i> spp	0 00	0 00	0 23	0 86	0 00	0 00
<i>Trachyneis aspera</i>	0 62	0 00	0 91	1 08	0 39	0 65
<i>Trichotoxon</i> sp	0 41	0 00	0 23	0 00	0 00	0 00
<i>Trigonum arcticum</i>	0 00	0 00	0 00	0 00	r	0 00
Other spp	0 21	0 00	0 45	0 00	0 19	0 00
<i>Pseudo-nitzschia turgiduloides</i> *						
<i>Proboscia barboi</i> *						

---

**Appendix 5**  
**Pagodroma Group Diatom Data**

---

**Appendix 5.** Microfossils identified in the Pagodroma Group, including quantitative abundance information and sample lithology.

FORMATIONS	Bardins Bluffs									Battye		Fisher Bench					Mt Johnston				
SAMPLE Location	1	1	5	5	3	4	4	2	1	6	6	9	9	9	8	7	10	10	10	10	10
SAMPLE Name	Bardin	Bardin	Gloss	Gloss	Pago	Bain	Bain	PCM	PCM	PCM	PCM	PCM	PCM	AM	AM	AM	PCM	PCM	AM	AM	AM
SAMPLE Position/Number	top	bottom	top	bottom	SE	top	bottom	90-2	90-7	90-8	90-10a	90-6	90-11	15	17	26	90-4	90-5	OO3	OO6	14
LITHOLOGY	diamict	diamict	diamict	diamict	diamict	diamict	diamict	siltst.	siltst.	diamict	diamict	siltst.	diamict	siltst.	siltst.	diamict	diamict	diamict	diamict	diamict	diamict
DIATOM ABUNDANCE	m-l	m	m	m-l	m-l	m-l	m-l	m	m-h	v l	v l	l	m	v h	m	v l	l	l	v l	l	l
DIATOMS																					
Planktic marine																					
<i>Actinocyclus actinocylus</i>									X												
<i>Actinocyclus ingens</i>	X	X	X	X	X		X	X						X	X						
<i>Actinocyclus ingens</i> var <i>nodus</i>														X							
<i>Actinocyclus aff ingens</i>														X							
<i>Actinocyclus karstenii</i>	X								X												
<i>Actinocyclus octonarius</i> var <i>astenscus</i>													X								
<i>Actinocyclus senarius</i>									X												
<i>Actinocyclus</i> sp A									X												
<i>Actinocyclus</i> spp (fragments)								X	X												
<i>Astromphalus</i> spp (fragments)									X												
<i>Azpeitia tabularis</i>	X		X?																		
<i>Chaetoceros</i> spp (cyst)	X				X			X	X?				X	X							
<i>Chaetoceros</i> spp (spines)	X				X			X	X				X	X							
<i>Coscinodiscus oculis-iridis</i>														X	X						
<i>Coscinodiscus oculoides</i>															X						
<i>Coscinodiscus radiatus</i>															X						
<i>Coscinodiscus marginatus</i>			X	X	X		X		X												
<i>Coscinodiscus</i> sp A	X													X							
<i>Coscinodiscus</i> spp (whole and frags )									X				X	X					X		
<i>Dactylosolen antarcticus</i>	X		X	X	X	X	X	X	X				X								
<i>Denticulopsis dimorpha</i>	X		X	X		X															
<i>Denticulopsis hustedii</i>			X																		
<i>Denticulopsis ovata</i>	X		X	X	X	X								X							
<i>Denticulopsis praedimorpha</i>	X																				
<i>Denticulopsis simonseni</i>	X		X											X							
<i>Denticulopsis</i> spp (whole and frags )	X		X				X		X				X								
<i>Eucampia antarctica</i> var <i>recta</i>	X		X	X	X				X				X	X							
<i>Fragilaria curta</i>					X																
<i>Fragilaria interfrigidana</i>		X																			
<i>Fragilaria kerguelensis</i>		X	X	X	X		X														
<i>Fragilaria obliquecostata</i>																					
<i>Fragilaria praeinterfrigidana</i>			X		X				X					X							
<i>Fragilaria</i> spp	X	X	X	X	X	X	X		X												
<i>Nitzschia reinholdii</i>					?				X												
<i>Fragilaria</i> spp weaven / <i>N reinholdii</i>				X					X												
<i>Paralia sulcata</i>					X																
<i>Proboscia barboi</i>														X	X						
<i>Prorocentrum reticulata</i>					X				X?											X	
<i>Rhizosolenia hebetata</i> (group)				X	X				X					X	X						
<i>Rhizosolenia styliformis</i> (group)				X	X				X					X							
<i>Rouxia heteropolara</i>		X																			
<i>Rouxia isopolara</i>								X	X												
<i>Rouxia</i> spp (fragments)				X	X	X		X	X												
<i>Stellarima microtrias</i>														X?		X					
<i>Stellarima stellaris</i>															X						
<i>Stephanopyxis grunowii</i>															X					X	X
<i>Stephanopyxis splendidus</i>																			X		
<i>Stephanopyxis turris</i>					X										X						
<i>Stephanopyxis</i> sp															X				X		
<i>Thalassiothrix</i> sp (fragments)	X		X	X	X		X	X		X	X	X					X				
<i>Thalassiothrix/Thalassionema</i> (frag )	X	X	X	X	X	X	X	X	X					X	X			X			
<i>Thalassionema nitzschioides</i>									X	X				X	X						
<i>Thalassionema nitzschioides</i> var <i>parva</i>									X	X											
<i>Thalassiosira insigna</i>				X																	
<i>Thalassiosira inura</i>							X														
<i>Thalassiosira nativa</i>	X							X	X												
<i>Thalassiosira oliverana</i>			X	X					X												
<i>Thalassiosira</i> sp (concentric areolae)								X													



## Appendix 5. continued

[illegible]

---

## **Appendix 6:**

### **Microfossil Taxonomy**

---

## Class Bacillariophyceae (Diatoms)

### Genus *Achnanthes* Bory 1822

*Achnanthes brevipes* Agardh 1824

Occurrence: Sørødal Formation

Synonymy: *Achnanthes charcotii*, Harwood *et al.* submitted, fig 10.i-j.

Reference:

Roberts and McMinn 1999, p. 67, pl. 1, fig 3,4.

### Genus *Actinocyclus* Ehrenberg 1838

*Actinocyclus actinochilus* (Ehrenberg) Simonsen 1982

This study: Plate 1, Figure 1; Plate 14, Figure 4.

Occurrence: Southern Kerguelen Plateau, Sørødal Formation

Basionymy: *Coscinodiscus actinochilus* Ehrenberg 1844

Reference:

Harwood and Maruyama 1992, p. 726, pl. 12, fig. 11;

Winter 1995, p. 119, pl. 1, fig. 1.

*Actinocyclus dimorphus* (Castracane) Harwood and Maruyama 1992

Occurrence: Southern Kerguelen Plateau

Reference:

Harwood and Maruyama 1992, p. 727, pl. 13, fig. 3-5.

*Actinocyclus fasciculatus* Harwood and Maruyama 1992

This study: Plate 1, Figures 2-4.

Occurrence: Southern Kerguelen Plateau

Basionymy: *Actinocyclus fasciculatus* Harwood and Maruyama 1992, p. 727, pl. 13, fig. 14, 15.

Reference:

Harwood and Maruyama 1992, p. 727, pl. 13, fig. 14, 15;

Winter 1995, p. 119, pl. 1, fig. 4.

*Actinocyclus ingens* Rattray 1890

This study: Plate 1, Figure 5; Plate 8, Figure 9; Plate 17, Figure 1.

Occurrence: Southern Kerguelen Plateau, Sørødal Formation, Pagodroma Group

Reference:

Rattray 1890, p. 149, pl. 11;

Schrader 1973, p. 666, pl. 13, fig. 8;

Gombos 1976, p. 607, pl. 2, fig. 1, 2;

Barron 1981, p. p. 118, pl. 1, fig. 9; p. 122, pl. 2, fig. 6;

Akiba 1982, p. 51, pl. 5, fig. 7-14;

Akiba 1985, p. 467, pl. 16, fig. 6,9;

Harwood and Maruyama 1992, p. 722, pl. 8, fig. 10; p. 725, pl. 11, fig. 4, 6; p. 726, pl. 12, fig. 8;

Winter 1995, p. 119, pl. 1, fig. 10.

*Actinocyclus aff. ingens* Rattray 1891

This study: Plate 17, Figure 6.

Occurrence: Pagodroma Group

Reference:

Schrader 1973, p. 663, pl. 11, fig. 6,7.

Notes: This diatom is thought to be more common in the Miocene (Schrader 1973).

***Actinocyclus ingens* var. *nodus*** Baldauf in Baldauf *et* Barron 1980

This study: Plate 14, Figures 5, 6; Plate 17, Figures 2, 3.

Occurrence: Pagodroma Group

Synonymy: *Actinocyclus ingens* var. 1, Barron 1980, p. 683, pl. 5, fig. 8, 12.

Reference:

Baldauf and Barron 1980, p. 109, pl. 1, fig. 1-9;

Barron 1985, p. 794, fig. 9, fig. 4;

Ciesielski 1986, p. 880, pl. 1, fig. 8-9;

Gersonde 1990, p. 797, pl. 1, fig. 6.

***Actinocyclus karstenii*** Van Heurck 1909

This study: Plate 8, Figure 4.

Occurrence: Southern Kerguelen Plateau, Sørsdal Formation, Pagodroma Group

Synonymy:

*Actinocyclus polysculptrus* Mann 1937

*Cestodiscus* sp. 1, Schrader 1973, p. 664, pl. 12, fig. 6.

Reference:

Harwood 1986a, p. 324, pl. 24, fig. 7;

Winter 1995, p. 119, pl. 1, fig. 5-9;

Harwood and Maruyama 1992, p. 727, pl. 13, fig. 1, 2, 6-6, 10, 11, 13.

***Actinocyclus octonarius* var. *asteriscus*** Barron *sensu* Harwood 1986

This study: Plate 8, Figure 8; Plate 16, Figure 6.

Occurrence: Sørsdal Formation, Pagodroma Group

Synonymy: *Actinocyclus ehrenbergii* var. *asteriscus* Barron 1975

Reference:

Harwood 1986b, p. 326, pl. 25, fig. 1-9, 11, 12;

Harwood 1986a, p. 326, pl. 25, fig. 7-12;

Winter 1995, p. 119, pl. 2, fig. 2.

***Actinocyclus* sp. A.**

Occurrence: Sørsdal Formation

### Genus *Actinoptycus* Ehrenberg 1843

***Actinoptycus senarius*** Ehrenberg 1838

This study: Plate 15, Figure 11.

Occurrence: Pagodroma Group

Reference:

Synonymy: *Actinoptycus undulatus* (Bailey) Ralfs

Wornardt 1967, p. 45, fig. 67;

McCollum 1975, p. 541, pl. 1, fig. 3-6;

Gombos 1976, p. 655, pl. 26, fig. 1-3;

Harwood 1986b, p. 99, pl. 4, fig. 14.

***Actinoptycus* sp. A**

This study: Plate 15, Figure 12.

Occurrence: Pagodroma Group

Genus *Anaulus* Ehrenberg 1844

*Anaulus ellipticus* Hendey 1937

Occurrence: Sørødal Formation

Reference:

Harwood *et al.* in press, Fig. 11. b.

*Anaulus scalaris* Ehrenberg 1854

This study: Plate 12, Figure 8.

Occurrence: Sørødal Formation

Reference:

Harwood *et al.* in press, fig 11. a.

Genus *Amphora* (Ehrenberg) Kützting 1844

***Amphora* sp. A.**

This study: Plate 11, Figures 14-16.

Occurrence: Sørødal Formation

Synonymy: *Amphora* sp. A. Roberts *et* McMinn 1999

Reference:

Roberts and McMinn 1999, p. 67, pl. 1, fig 6, 7.

***Amphora* sp. B**

This study: Plate 11, Figure 17.

Occurrence: Sørødal Formation

Synonymy: *Amphora* sp. E Roberts *et* McMinn 1999

Reference:

Roberts and McMinn 1999, p. 67, pl. 1, fig 12, 13.

***Amphora* sp. C**

This study: Plate 15, Figure 5.

Occurrence: Pagodroma Group

***Amphora* spp. (fragments)**

Occurrence: Sørødal Formation, Pagodroma Group

Genus *Astromphalus* Ehrenberg 1844

*Astromphalus hookeri* Ehrenberg 1844

Occurrence: Southern Kerguelen Plateau

Reference:

Priddle and Fryxell 1985, p. 119, fig A, B, D, F.

*Astromphalus hepaticus* (Brébisson) Ralphs, in Pritchard 1861 / *Astromphalus. parvulus* Karsten 1905

This study: Plate 1, Figures 6, 9.

Occurrence: Southern Kerguelen Plateau

Reference:

Priddle and Fryxell 1985, p. 117, fig A-F.

Note: *A. hepaticus* and *A. parvulus* were not differentiated from each other in this study.

***Astromphalus hyalinus* Karsten 1905**

This study: Plate 1, Figures 7, 8.

Occurrence: Southern Kerguelen Plateau

Reference:

Abbott 1974, p. 329, pl. 2, fig. b;

Priddle and Fryxell 1985, p. 121, fig A-E.

***Astromphalus* spp.**

Occurrence: Southern Kerguelen Plateau, Pagodroma Group

Note: Only *Astromphalus* spp. fragments were identified in the Pagodroma Group.

**Genus *Aulacoseira* Thwaites 1848**

***Aulacoseira* sp. A**

This study: Plate 16, Figure 11.

Occurrence: Pagodroma Group

**Genus *Azpeitia* Pergallo in Tempère et Pergallo 1912**

***Azpeitia tabularis* (Grunow) Fryxell et Sims 1986**

This study: Plate 2, Figure 3.

Occurrence: Southern Kerguelen Plateau, Pagodroma Group

Synonymy:

*Coscinodiscus tabularis*, Schrader 1973, p. 663, pl. 11, fig. 5

Reference:

Schrader 1973, p. 785, pl. 20, fig. 3,4;

Akiba 1982, p. 55, pl. 2, fig. 6a, 9;

Winter 1995, p.139, pl. 11, fig. 5.

**Genus *Caloneis* Cleve 1894**

***Caloneis* sp.**

Occurrence: Pagodroma Group

**Genus *Chaetoceros* Ehrenberg 1844**

***Chaetoceros bulbosum* (Ehrenberg) Heiden 1928**

This study: Plate 7, Figures 15, 16.

Occurrence: Southern Kerguelen Plateau

Reference:

Priddle and Fryxell 1985, p. 25 fig C.

Note: when recorded in the data this represented vegetative cells

***Chaetoceros dictyota* Ehrenberg 1844**

This study: Plate 13, Figures 8, 9.

Occurrence: Southern Kerguelen Plateau, Sørødal Formation

Reference:

Abbott 1974, p. 345, pl. 10, fig. f.

Note: when recorded in the data this represented vegetative cells

***Chaetoceros lorenzianus* (*Diocladia pylea* Hanna and Grant)**

This study: Plate 13, Figure 6.

Occurrence: Southern Kerguelen Plateau, Sørødal Formation

Reference:

Harwood and Maruyama 1992, p. 732, pl. 18, fig. 11;

Harwood *et al.* in press, fig 8.q.

Note: Restings spores identified

***Chaetoceros* spp.**

Occurrence: Sørødal Formation, Pagodroma Group

Note: resting spores undifferentiated

Reference:

Armand 1997, pl. 3, fig 9-27.

Note: vegetative spines undifferentiated.

This study: Plate 18, Figure 8.

**Genus *Cocconeis* Ehrenberg 1838**

***Cocconeis costata* Gregory 1855**

This study: Plate 11, Figure 2.

Occurrence: Sørødal Formation

Synonymy: *Cocconeis fasciolata*, Harwood *et al.* in press, fig. 10.c-d.

Reference:

Roberts and McMinn 1999, p. 69, pl. 2, fig 5.

***Cocconeis fasciolata* (Ehrenberg) Brown 1920**

This study: Plate 11, Figures 1, 3.

Occurrence: Sørødal Formation

Synonymy: *Cocconeis costata* Harwood 1986b, p. 103, pl. 6, fig. 10.

Synonymy: *Cocconeis pinnata*, Harwood *et al.* in press, fig. 10.g.

Reference:

Roberts and McMinn 1999, p. 69, pl. 2, fig 4.

***Cocconeis gauteri* Van Heurck 1909**

This study: Plate 11, Figure 7.

Occurrence: Sørødal Formation

Reference:

Harwood *et al.* in press, fig. 10. e.

***Cocconeis pinnata* Gregory *ex* Greville 1859**

This study: Plate 11, Figure 4.

Occurrence: Sørødal Formation, Pagodroma Group

Synonymy: *Cocconeis costata*, Harwood 1986b, p. 103, pl. 6, fig. 10;

Harwood *et al.* in press, fig. 10. h.

Reference:

Roberts and McMinn 1999, p. 69, pl. 2, fig 6.

***Cocconeis schuettii* Van Heurck 1909**

This study: Plate 11, Figure 8.

Occurrence: Sørødal Formation

Reference:

Harwood 1986a, p. 315, pl. 20, fig. 1, 2, 6;

Harwood *et al.* in press, fig 10.a, b, f.

Note: Quantitative data grouped here may also contain the species *Navicula spectabilis* var. *oamaruensis*

Grove, Mann (This study: Plate 11, figure 6).

***Cocconeis* sp A.**

This study: Plate 11, Figure 5.

Occurrence: Sørødal Formation

Reference:

Harwood *et al.* in press, fig 10.u-v.

***Cocconeis* sp B.**

This study: Plate 13, Figures 16, 17.

Occurrence: Sørødal Formation

Reference:

Synonymy: *Cocconeis* sp A., Roberts and McMinn 1999, p. 69, pl. 2, fig 7-10.

**Genus *Corethron* Castracane 1886**

***Corethron criophilum* group Castracane 1886**

This study: Plate 7, Figure 14.

Occurrence: Southern Kerguelen Plateau, Sørødal Formation

Reference:

Harwood and Maruyama 1992, p. 733, pl. 19, fig 13-14.

**Genus *Coscinodiscus* Ehrenberg 1838**

***Coscinodiscus oculus-iridis* Ehrenberg 1839**

This study: Plate 10, Figures 1, 3; Plate 17, Figure 5.

Occurrence: Sørødal Formation, Pagodroma Group

Reference:

Harwood 1986b, p. 101, pl. 5, fig. 9;

Harwood 1989, p. 87, pl. 1, fig. 1.

***Coscinodiscus oculoides* Karsten 1905**

Occurrence: Sørødal Formation, Pagodroma Group

Reference:

Harwood 1986a, p. 324, pl. 24, fig. 3-5.

***Coscinodiscus radiatus* Ehrenberg 1939**

This study: Plate 17, Figure 7.

Occurrence: Pagodroma Group

Reference:

Harwood 1986a, p. 324, pl. 24, fig. 11;

Harwood 1989, p. 87, pl. 1, fig. 5;

Winter 1995, p. 123, pl. 3, fig. 6.

***Coscinodiscus marginatus* Ehrenberg; Hustedt 1930**

This study: Plate 16, Figure 1.

Occurrence: Pagodroma Group

Reference:

Koizumi, 1973, p. 845, pl. 3, fig. 12-13;

Schrader 1973, p. 664, pl. 12, fig. 2;

McCollum 1975, p. 571, pl. 16, fig. 2, 3;

Barron 1981, p. 118, pl. 1, fig. 2;

Akiba 1985, p. 468, pl. 17, fig. 5;

Harwood 1986b, p. 99, pl. 4, fig. 19.



***Coscinodiscus* sp. A**

This study: Plate 17, Figure 8

Occurrence: Pagodroma Group

Note: large fragments found in the Pagodroma Group

***Coscinodiscus* spp.**

Occurrence: Southern Kerguelen Plateau, Sørødal Formation, Pagodroma Group

Note: All *Coscinodiscus* spp. in the Kerguelen cores were grouped together.

**Genus *Cyclotella* Kützing 1834**

***Cyclotella* sp.**

Occurrence: Pagodroma Group

**Genus *Dactyliosolen* Castracane 1886**

***Dactyliosolen antarcticus* Castracane 1886**

This study: Plate 7, Figure 12; Plate 13, Figures 4, 5.

Occurrence: Southern Kerguelen Plateau, Sørødal Formation, Pagodroma Group

Reference:

Harwood 1986b, p. 101, pl. 5, fig. 17; p. 132, pl. 18, fig. 12.

**Genus *Denticulopsis* (Simonsen) Akiba et Yanagisawa 1990**

***Denticulopsis dimorpha* (Schrader) Simonsen 1979**

This study: Plate 7, Figures 6, 7; Plate 15, Figures 6, 7.

Occurrence: Pagodroma Group

Reference:

Schrader 1973, p. 649, pl. 4, fig. 27,29-32;

Barron 1980, p. 675, pl. 1, fig. 21;

Ciesielski 1986, p. 881, pl. 2, fig. 5-8;

Gersonde and Burckle 1990, p. 788, pl. 4, fig. 10-12;

Baldauf and Barron 1991, p. 598, pl. 7, fig. 4;

Harwood and Maruyama 1992, p. 720, pl. 6, fig. 5-7; p. 721, pl. 7, fig. 10; p. 723, pl. 9, fig. 5-9, 15-18, 22, 23; p. 724, pl. 10, fig. 14.

***Denticulopsis hustedtii* (Simonsen and Kanaya) Simonsen 1979**

This study: Plate 15, Figure 8.

Occurrence: Pagodroma Group

Basionymy: *Denticula hustedtii* Simonsen and Kanaya 1961

Reference:

Schrader 1973, p. 649, pl. 4, fig. 2, 4?, 8, 9?;

Akiba 1985, p. 479, pl. 28, fig. 9, 16-18;

Barron 1985, p. 802, fig. 13, fig. 22, 23;

Kellogg and Kellogg 1986, p. 83, pl. 2, fig. 4;

Baldauf and Barron 1991, p. 598, pl. 7, fig. 1;

Harwood and Maruyama 1992, p. 721, pl. 7, fig. 14; p. 722, pl. 8, fig. 1-3, 16; p. 723, pl. 9, fig. 19,20.

***Denticulopsis ovata* (Schrader) Yanagisawa et Akiba 1990**

Occurrence: Pagodroma Group

Basionymy: *Denticula hustedtii* var. *ovata* Schrader, 1976, p. 632, pl. 4, figs. 5, 6, 12, 14, 15.

Synonymy: *Denticulopsis meridionalis* Maruyama in Harwood et Maruyama 1992

Reference:

Yanagisawa and Akiba, 1990 p. 257-258, pl. 6, figs. 6-14, 24-32;  
Harwood and Maruyama 1992, p. 720, pl. 6, fig. 1-4; p. 721, pl. 7, fig. 1-4, 6-9, 11-13; p. 723, pl. 9,  
fig. 1-4,10-14; p. 724, pl. 10, fig. 7.

***Denticulopsis praedimorpha* Barron ex Akiba 1982**

Occurrence: Pagodroma Group

References used:

Akiba 1982, p. 73, pl. 11, fig. 9-27;  
Akiba 1985, p. 477, pl. 26, fig. 8; p. 478, pl. 27, fig. 14-2;  
Barron 1985, p. 802, fig. 13, fig. 24, 25;  
Baldauf and Barron 1991, p. 598, pl. 7, fig. 9;  
Bodén 1992, p. 209, pl. 3, fig. 4, 5;  
Harwood and Maruyama 1992, p. 720, pl. 6, fig. 8-10, 12, 14-17; p. 723, pl. 9, fig. 1-4,10-14;  
p. 724, pl. 10, fig. 7.

***Denticulopsis simonsenii* Yanagisawa et Akiba 1990**

This study: Plate 7, Figure 8; Plate 14, Figure 3; Plate 17, Figure 10.

Occurrence: Pagodroma Group

Synonymy: *Denticula hustedtii* Simonsen et Kanaya 1961

Synonymy: *Denticulopsis hustedtii* (Simonsen et Kanaya) Simonsen emend. Yanagisawa et Akiba 1990

Reference:

Schrader 1973, p. 649, pl. 4, fig. 9;  
Barron 1985, p. 802, fig. 13, fig. 17;  
Ciesielski 1986, p. 881, pl. 2, fig. 1, 2;  
Gersonde and Burckle 1990, p. 789, pl. 5, fig. 10-13;  
Harwood and Maruyama 1992, p. 724, pl. 10, fig. 4.

Note: This species in the Southern Ocean persisted into the Lower Pliocene, just beyond the FAD of *D. hustedtii* (Yanagisawa and Akiba 1990)

***Denticulopsis* spp.**

Occurrence: Southern Kerguelen Plateau, Pagodroma Group

Note: *Denticulopsis* spp. were not differentiated in the Kerguelen cores. Some *Denticulopsis* spp. fragments in the Pagodroma Group could not be identified to species level.

**Genus *Diploneis* Ehrenberg 1844**

***Diploneis frickei* (Van Heurck) Heiden and Kolbe 1958**

This study: Plate 11, Figure 12.

Occurrence: Sørøsdal Formation

Reference:

Harwood et al. in press, fig 10. m.;  
Harwood 1986a, p. 315, pl. 20, fig. 13.

***Diploneis splendida* Gregory 1856**

This study: Plate 11, Figure 13.

Occurrence: Sørøsdal Formation

Reference:

Harwood 1986a, p. 315, pl. 20, fig. 11, 12;  
Roberts and McMinn 1999, p. 71, pl. 3, fig 1.

***Diploneis subovalis* Cleve 1894**

This study: Plate 11, Figure 9.

Occurrence: Sørøsdal Formation

Reference:

Harwood 1986a, p. 315, pl. 20, fig. 14;  
Harwood *et al.* in press, fig 10. 1.

***Diploneis* sp. A**

This study: Plate 11, Figures 10, 11.

Occurrence: Sørødal Formation

Synonymy: *Diploneis* sp B., Roberts *et* McMinn 1999

Reference:

Roberts and McMinn 1999, p. 71, pl. 3, fig 2.

***Diploneis* sp. B**

This study: Plate 15, Figure 1.

Occurrence: Pagodroma Group

***Diploneis* spp. / *Navicula* spp. (fragments)**

Occurrence: Pagodroma Group

**Genus *Drepanotheca* Schrader 1969**

***Drepanotheca bivittata* (Grunow and Pantocsek) Schrader 1969**

This study: Plate 12, Figure 1.

Occurrence: Sørødal Formation

Reference:

Harwood 1986b, p. 97, pl. 3, fig. 10.

**Genus *Endictya* Ehrenberg 1845**

***Endictya* sp. A**

Occurrence: Pagodroma Group

**Genus *Eucampia* Ehrenberg 1839**

***Eucampia antarctica* var. *recta* (Mangin) Fryxell *et* Prasad 1990**

This study: Plate 6, Figure 3; Plate 12, Figures 6, 7; This study: Plate 16, Figure 9; Plate 17, Figure 9.

Occurrence: Southern Kerguelen Plateau, Sørødal Formation, Pagodroma Group

Bastonymy: *Eucampia antarctica* (Castracane) Mangin f. *recta* Mangin 1915

Synonymy:

*Hemiaulus antarcticus* Ehrenberg 1844

*Eucampia balaustium* f. *hiberna* Castracane 1886

Reference:

Gombos 1976, p. 605, pl. 1, fig. 1-6;

Akiba 1982, p. 53, pl. 6, fig. 1-9;

Syvertsen and Hasle, 1983, p. 206, pl. 10.

**Genus *Eunotia* Ehrenberg 1837**

***Eunotia* sp. A**

This study: Plate 12, Figure 4.

Occurrence: Sørødal Formation

Reference:

Synonymy: *Eunotia* sp., Harwood 1986a, p. 318, pl. 21, fig. 3;

Synonymy: *Eunotia* sp., Harwood *et al.* in press, fig 11. c.

## Genus *Fragilaria* Lyngbye 1819

***Fragilaria construens* var. *venter*** (Ehrenberg) Grunow, in Van Heurck 1881

Occurrence: Sørødal Formation

Reference:

Roberts and McMinn 1999, p. 71, pl. 3, fig 4-5.

***Fragilaria* sp. A**

This study: Plate 13, Figure 7.

Occurrence: Sørødal Formation

Reference:

Roberts and McMinn 1999, p. 71, pl. 3, fig 6-7.

## Genus *Fragilariopsis* Hustedt 1913

***Fragilariopsis aurica*** (Gersonde) Gersonde *et* Bárcena 1998

This study: Plate 4, Figure 6.

Occurrence: Southern Kerguelen Plateau

Basionymy: *Nitzschia aurica* Gersonde 1991

Reference:

Gersonde 1991, p. 153, pl. 1, fig. 18-25;

Harwood and Maruyama 1992, p. 731, pl. 17., fig 21-23.

***Fragilariopsis barronii*** (Gersonde) Gersonde *et* Bárcena 1998

This study: Plate 5, Figures 12, 13.

Occurrence: Southern Kerguelen Plateau, Sørødal Formation

Basionymy: *Nitzschia barronii* Gersonde 1991

Reference:

Gersonde 1991, p. 161, pl. 5, fig. 7-17;

Harwood and Maruyama 1992, p. 731, pl. 17., fig 27-28.

***Fragilariopsis barronii* var. A**

This study: Plate 5, Figures 6, 7.

Occurrence: Southern Kerguelen Plateau

***Fragilariopsis barronii* var. B**

This study: Plate 5, Figures 7, 8.

Occurrence: Southern Kerguelen Plateau

***Fragilariopsis curta*** (Van Heurck) Hasle 1958

This study: Plate 4, Figure 10; Plate 13, Figure 2; Plate 16, Figure 5.

Occurrence: Southern Kerguelen Plateau, Sørødal Formation, Pagodroma Group

Basionymy: *Fragilaria curta* Van Heurck 1909

Synonymy: *Nitzschia curta* (Van Heurck) Hasle 1972

Reference:

Schrader 1973, p. 671, pl. 15, fig. 21;

Akiba 1982, p. 71, pl. 10, fig. 1, 2;

Kellogg and Kellogg 1986, p. 83, pl. 2, fig 18-23, 25-31;

Harwood and Maruyama 1992, p. 731, pl. 17, fig. 1-4.

***Fragilariopsis cylindrus*** (Grunow) Krieger 1954

This study: Plate 4, Figure 11.

Occurrence: Southern Kerguelen Plateau

Basionymy: *Fragilaria cylindrus* Grunow in Cleve 1883

Synonymy: *Nitzschia cylindrus* (Grunow) Hasle 1972

Reference:

Medlin and Priddle 1999, p. 193, pl. 24.6, fig 6-11.

***Fragilariopsis interfrigidaria*** (McCollum) Gersonde *et* Bárcena 1998

This study: Plate 4, Figures 3-5; Plate 16, Figure 4.

Occurrence: Southern Kerguelen Plateau, Pagodroma Group

Basionymy: *Nitzschia interfrigidaria* McCollum 1975

Reference:

McCollum 1975, p. 557, pl. 9, fig. 7-9;

Gombos 1976, p. 617, pl. 7, fig. 1;

Ciesielski 1983, p. 659, pl. 1, fig. 11-18; p. 660, pl. 2, fig. 3, 5-8, 13-16;

Barron 1985, p. 804, fig. 14, fig. 3,4;

Kellogg and Kellogg 1986, p. 83, pl. 2, fig. 13-15;

Gersonde and Burckle 1990, p. 785, pl. 1, fig. 1-3;

Baldauf and Barron 1991, p. 598, pl. 7, fig. 12.

Note: sometimes this species has been mistaken for *Nitzschia praeinterfrigidaria* in previous literature.

***Fragilariopsis kerguelensis*** (O'Meara) Hasle 1952

This study: Plate 5, Figures 1-5; Plate 14, Figures 7, 8.

Occurrence: Southern Kerguelen Plateau, Pagodroma Group

Basionymy: *Terebraria kerguelensis* O'Meara 1877

Synonymy: *Nitzschia kerguelensis* (O'Meara) Hasle 1972

Reference:

Fenner *et al.* 1976, p. 789, pl. 2, fig. 20-25;

Barron 1985, p. 804, fig. 14, fig. 1, 2;

Medlin and Priddle 1990, p. 185, pl. 24.2, fig. 11-18; p. 187, pl. 24.3, fig. 9.

***Fragilariopsis lacrima*** (Gersonde) Gersonde *et* Bárcena 1998

This study: Plate 7, Figure 13.

Occurrence: Southern Kerguelen Plateau

Basionymy: *Nitzschia lacrima* Gersonde 1991

Reference:

Gersonde 1991, p. 153, pl. 1, fig. 1-6.

Note: Occur rarely in the Kerguelen cores and have been included in the category OTHER.

***Fragilariopsis obliquecostata*** (Van Heurck) Heiden in Heiden *et* Kolbe 1928

This study: Plate 4, Figure 12; Plate 6, Figures, 4, 5.

Occurrence: Southern Kerguelen Plateau, Sørøsdal Formation

Basionymy: *Fragilaria obliquecostata* Van Heurck 1909

Synonymy: *Nitzschia obliquecostata* (Van Heurck) Hasle 1972

Reference:

Akiba 1982, p. 69, pl. 9, fig. 11;

Winter 1995, p. 129, pl. 6, fig. 5,6

***Fragilariopsis praecurta*** (Gersonde) Gersonde *et* Bárcena 1998

This study: Plate 13, Figure 3.

Occurrence: Southern Kerguelen Plateau, Sørøsdal Formation

Basionymy: *Nitzschia praecurta* Gersonde 1991

Reference:

Gersonde 1991, p. 153, pl. 1, fig. 7-17;

Harwood and Maruyama 1992, p. 731, pl. 17, fig 25, 26.

Note: In the Kerguelen cores *F. praecurta* may have been misidentified from *F. separanda* var. A

***Fragilariopsis praeinterfrigidaria*** (McCollum) Gersonde *et* Bárcena 1998

This study: Plate 4, Figures 1, 2; Plate 13, Figure 1; Plate 15, Figure 9.

Occurrence: Southern Kerguelen Plateau, Sørødal Formation, Pagodroma Group

Basionymy: *Nitzschia praeinterfrigidaria* McCollum 1975

Reference:

Barron 1985, p. 804, fig. 14, fig. 5,6;

McCollum 1975, p. 559, pl. 10, fig. 1;

Gombos, 1976, p. 617, pl. 7, fig. 2;

Ciesielski 1983, p. 659, pl. 1, fig. 1, 2;

Gersonde and Burckle 1990, p. 785, pl. 1, fig. 4-10;

Winter 1995, p. 129, pl. 6, fig. 11.

***Fragilariopsis ritscheri*** Hustedt 1958

This study: Plate 5, Figures, 16-18.

Occurrence: Southern Kerguelen Plateau, Sørødal Formation

Synonymy: *Nitzschia ritscheri* (Hustedt) Hasle 1972

Reference:

Abbott 1974, p. 339, pl. 7, fig. I-K;

Bohaty *et al.* 1999, p.448, pl. 1, fig. 8.

***Fragilariopsis rhombica*** (O'Meara) Hustedt 1952

This study: Plate 4, Figures, 7, 8.

Occurrence: Southern Kerguelen Plateau

Synonymy:

*Diatoma rhombica* O'Meara

*Nitzschia rhombica* in Abbott 1974

*Nitzschia angulata* Hasle

Reference:

Abbott 1974, p. 339, pl. 7, fig. D-E;

***Fragilariopsis separanda*** Hustedt 1958

This study: Plate 4, Figure 9.

Occurrence: Southern Kerguelen Plateau, Sørødal Formation

Synonymy: *Nitzschia separanda* (Hustedt) Hasle 1972

Reference:

Medlin and Priddle 1990, p. 189, pl. 24.2, fig. 7-10.

***Fragilariopsis separanda* var. A**

This study: Plate 5, Figures 14, 15.

Occurrence: Southern Kerguelen Plateau

***Fragilariopsis sublinearis*** (Van Heurck) Heiden 1928

This study: Plate 5, Figure 20.

Occurrence: Southern Kerguelen Plateau, Sørødal Formation

Basionymy: *Fragilaria sublinearis* Van Heurck 1901

Synonymy: *Nitzschia sublineata* Hasle 1972

Reference:

Medlin and Priddle 1990, p. 191, pl. 14.5, fig. 1-10.

***Fragilariopsis weaveri*** (Ciesielski) Gersonde *et* Bárcena 1998

This study: Plate 5, Figures 10, 11.

Basionymy: *Nitzschia weaveri* Ciesielski 1983

Occurrence: Southern Kerguelen Plateau

Reference:

Ciesielski 1983, p. 655, pl. 1, fig. 1-10.

Genus *Gomphonema* Agardh 1824

***Gomphonema angustatum* var. A**

This study: Plate 15, Figure 3.

Occurrence: Pagodroma Group

Synonymy: *Navicula* sp. Winter 1995, p. 131, pl. 7, fig. 2-4.

***Gomphonema angustatum* var. B**

This study: Plate 15, Figure 4.

Occurrence: Pagodroma Group

Genus *Gomphonemopsis* Medlin 1986

***Gomphonemopsis* sp. A**

This study: Plate 13, Figure 12.

Occurrence: Sørødal Formation

Reference:

Roberts and McMinn 1999, p. 71, pl. 3, fig. 11.

Genus *Grammatophora* Ehrenberg 1840

***Grammatophora* spp. Ehrenberg 1840**

Occurrence: Sørødal Formation

Note. *Grammatophora* spp. recorded in the Sørødal Formation are a grouping of the species:

*G. arcuata* Ehrenberg

Reference:

Harwood *et al.* in press, fig 11. i.

*G. charcoti* Peragallo

This study: Plate 10, Figure 8.

Reference:

Harwood *et al.* in press, fig 11. e.

*G. marina* (Lyngbye) Kutzing 1844

This study: Plate 10, Figure 9.

Reference:

Harwood *et al.* in press, fig 4. d,j.

Genus *Hemidiscus* Wallich 1860

***Hemidiscus karstenii* Jousé 1962**

This study: Plate 7, Figure 11.

Occurrence: Southern Kerguelen Plateau

Reference:

Barron 1985, p. 804, fig. 14.20.

Genus *Hyalodiscus* Ehrenberg 1845

***Hyalodiscus* spp. Ehrenberg 1845**

Occurrence: Sørødal Formation

Note. *Hyalodiscus* spp. recorded in the Sørødal Formation are a grouping of the species:

*H. radiatus* (O'Meara) Grunow, in Cleve *et* Grunow 1880

This study: Plate 9, Figure 3.

Reference:

Harwood *et al.* in press, fig 9. g.  
*H. valens* Schmidt 1888  
This study: Plate 9, Figures 1, 4, 5.  
Reference:

Wornardt 1967, p. 19, fig 3.  
*H. zonulatus* Peragallo  
This study: Plate 9, Figure 2.  
Reference:  
Harwood *et al.* in press, fig 9. l.

### Genus *Isthmia* Agardh 1832

#### ***Isthmia* sp.**

This study: Plate 10, Figure 2; Plate 17, Figure 4.  
Occurrence: Sørøsdal Formation, Pagodroma Group  
Reference:  
Harwood 1986b, p. 107, pl. 8, fig. 17;  
Harwood 1986a, p. 320, pl. 22, fig. 1; p. 322 pl. 23, fig. 4, 5;  
Winter 1995, p. 125, pl. 4, fig. 7 8.

### Genus *Navicula* Bory 1822

#### ***Navicula* sp. cf *cancellata* Donkin 1873**

This study: Plate 13, Figure 10.  
Occurrence: Sørøsdal Formation  
Reference:  
Roberts and McMinn 1999, p. 73, pl. 4, fig. 5.

#### ***Navicula directa* (Smith) Ralfs in Pritchard 1861**

Occurrence: Southern Kerguelen Plateau, Sørøsdal Formation  
Reference:  
Krebs 1983, p. 291, pl. 3, fig. 7.  
Roberts and McMinn 1999, p. 73, pl. 4, fig. 13.

#### ***Navicula perminuta* Grunow, in Van Heurck 1880**

Occurrence: Sørøsdal Formation  
Reference:  
Roberts and McMinn 1999, p. 73, pl. 4, fig. 15.

#### ***Navicula spectabilis* var. *oamaruensis* Grove, Mann 1937**

Occurrence: Sørøsdal Formation  
Reference:  
Harwood *et al.* in press, fig 11. 0.

#### ***Navicula* spp.**

Occurrence: Sørøsdal Formation, Pagodroma Group

### Genus *Nitzschia* Hassall 1845

#### ***Nitzschia fossilis* (Frenguelli) Kanaya 1970**

Occurrence: Southern Kerguelen Plateau  
Reference:  
Gersonde and Burckle 1990, p. 785, pl 1, fig. 19-20.



***Nitzschia grossepunctata* Schrader 1976**

Occurrence: Pagodroma Group

Reference:

Schrader 1973, p. 647, pl. 3, fig. 1-4;

Gersonde and Burckle 1990, p. 786, pl. 2, fig. 3-6.

***Nitzschia peragallii* Hasle 1965**

This study: Plate 5, Figure 21.

Occurrence: Southern Kerguelen Plateau

Reference:

Medlin and Priddle 1990, p. 189, pl. 24.2, fig. 11-12.

***Nitzschia reinholdii* Kanaya ex Barron and Bauldauf 1986**

This study: Plate 5, Figure 19; Plate 15, Figure 13.

Occurrence: Southern Kerguelen Plateau, Pagodroma Group

Reference:

Schrader 1973b, p. 753, pl. 4, fig. 12-16; p. 755, pl. 5, fig. 1-9;

McCollum 1975, p. 571, pl. 16, fig. 4, 5;

Barron 1980, p. 677, pl. 2, fig. 11; p. 679, pl. 3, fig. 1;

Koizumi and Tanimura 1982, p. 300, pl. 6, fig. 3, 4;

Akiba 1985, p. 472, pl. 22, fig. 4, 5;

Barron 1985, p. 802, fig. 13, fig. 4;

Gersonde and Burckle 1990, p. 786 pl. 2, fig. 1.

***Nitzschia* spp.**

Occurrence: Sørøsdal Formation, Pagodroma Group

Note: Occur as fragments in some samples from the Pagodroma Group

**Genus *Odontella* Agardh 1832**

***Odontella punctata* (Greville 1864)**

Occurrence: Sørøsdal Formation

Reference:

Harwood *et al.* in press fig. 9.a.

***Odontella weissflogii* (Janisch) Grunow**

Occurrence: Sørøsdal Formation

Reference:

Hoban *et al.* 1980, p. 597, fig. 24.

**Genus *Paralia* Heiberg 1863**

***Paralia sulcata* (Ehrenberg) Cleve 1873**

Occurrence: Pagodroma Group

Reference:

Crawford 1979, p. 202, fig. 6, 7, 8, 9;

Akiba 1985, p. 480, pl. 29, fig. 4, 5;

Harwood and Maruyama 1992, p. 715, pl. 1, fig. 9

***Paralia* spp.**

This study: Plate 10, Figure 7.

Occurrence: Sørøsdal Formation

Notes: *Paralia* spp. in the Sørøsdal Formation is a collective grouping of the species:

*P. omma* (Cleve)

Synonymy: *Melosira omma* Cleve 1885

Reference:

Harwood 1986a, pl. 18, fig 22.

*P. pantocseki* Van Heurck 1909

This study: Plate 9, Figure 7.

Reference:

Harwood *et al.* in press fig. 9. j-k..

*P. sol* (Ehrenberg)

This study: Plate 9, Figure 6.

Reference:

Harwood *et al.* in press fig. 9. f.

*P. sol* var. *marginalis* (Peragallo) Harwood 1989

This study: Plate 9, Figure 8.

Reference:

Winter 1995, p. 131, pl. 7, fig 9.

### Genus *Pinnularia* Ehrenberg 1841

*Pinnularia quadratarea* (Schmidt) Cleve 1895

This study: Plate 13, Figures 12, 13.

Occurrence: Sørødal Formation

Reference:

Harwood 1986a, p. 318, pl. 21, fig. 5;

Harwood *et al.* in press, fig 11.f.

### *Pinnularia* sp.-A

This study: Plate 15, Figure 2.

Occurrence: Pagodroma Group

### Genus *Pleurosigma* Smith 1852

*Pleurosigma* sp A.

This study: Plate 10, Figure 5.

Occurrence: Sørødal Formation

Reference:

Roberts and McMinn 1999, p. 79, pl. 7, fig. 1.

### Genus *Proboscia* Sudström 1986

*Proboscia alata* (Hustedt) Jousé 1962

Occurrence: Southern Kerguelen Plateau

Reference:

Armand 1997, pl. 10, fig. 2, 3.

*Proboscia barboi* (Brün) Jordan and Priddle 1991

This study: Plate 6, Figure 9; Plate 18, Figure 9.

Occurrence: Southern Kerguelen Plateau, Sørødal Formation, Pagodroma Group

Basionymy: *Rhizosolenia barboi* (Brün) Tempere and Peragallo

Synonymy:

*Simonseniella barboi* (Brün) Fenner

Reference:

Schrader, 1973, p. 659, pl. 9, fig. 11-13;

Schrader, 1976, p. 635, pl. 9, fig. 11-13;

McCollum, 1975, p. 561, pl. 11, fig. 13;

Koizumi and Tanimura, 1982, p. 300, pl. 6, fig. 16;  
Barron, 1980, p. 677, pl. 2, fig. 17;  
Barron, 1981, p. 118, pl. 1, fig. 12;  
Akiba, 1985, p. 469, pl. 18, fig. 2;  
Barron, 1985, p. 800, fig. 12, fig. 5;  
Ciesielski, 1986, p. 882, pl. 3, fig. 22;  
Bodén, 1992, p. 205, pl. 1, fig. 2-4;  
Harwood and Maruyama, 1992, p. 725, pl. 11, fig. 13.

#### Genus *Podosira* Ehrenberg 1840

##### ***Podosira* sp.**

Occurrence: Sørødal Formation

#### Genus *Porosira* Jørgensen 1905

##### ***Porosira pseudeodenticulata* (Hustedt) Jousé 1962**

This study: Plate 2, Figures 4, 5.

Occurrence: Sørødal Formation

Reference:

Krebs 1983, p. 293, pl. 4, fig. 13.

#### Genus *Pseudogomphonema* Medlin 1986

##### ***Pseudogomphonema kamtschaticum* Grunow 1986**

Occurrence: Sørødal Formation

Reference:

Medlin and Priddle 1990, p. 158, pl. 20.1, fig. 1.

#### Genus *Pseudo-nitzschia* H. Pergallo in H. Pergallo et M. Pergallo 1900

##### ***Pseudo-nitzschia turgiduloides* (Hasle) Hasle 1995**

Occurrence: Sørødal Formation

Synonymy: *Nitzschia turgiduloides* Hasle

Reference:

Medlin and Priddle 1990, p. 173, pl. 22.3, fig. 9-14.

#### Genus *Pyxilla* Greville 1865

##### ***Pyxilla reticulata* Grove et Sturt 1887**

This study: Plate 14, Figure 2.

Occurrence: Pagodroma Group

Reference:

Harwood 1989, p. 91, pl. 3, fig. 7-10

Notes: fragments

#### Genus *Rhabdonema* Kützing 1844

##### ***Rhabdonema japonica* group Tempere et Brun in Brun et Tempere 1889**

This study: Plate 18, Figure 3.

Occurrence: Pagodroma Group

Reference:

Harwood, 1986a, p. 105, pl. 7, fig. 31.

Genus *Rhaphoneis* Ehrenberg 1845

***Rhaphoneis* sp. A**

This study: Plate 18, Figure 7.

Occurrence: Pagodroma Group

Genus *Rhizosolenia* Brightwell 1858

***Rhizosolenia hebetata* group Bailey 1856**

This study: Plate 7, Figure 5; Plate 16, Figure 8.

Occurrence: Southern Kerguelen Plateau, Sørødal Formation, Pagodroma Group

Reference:

Koizumi, 1973, p. 849, pl. 5, fig. 35;

Winter, 1995, p. 133, pl. 8, fig. 1, 2.

***Rhizosolenia styliiformis* group Brightwell 1858**

This study: Plate 7, Figures 3, 4.

Occurrence: Southern Kerguelen Plateau, Sørødal Formation, Pagodroma Group

Reference:

Schrader 1973, p. 659, pl. 9, fig. 4;

Schrader 1973b, p. 765, pl. 10, fig. 18-21;

Fenner *et al.* 1976, p. 811, pl. 13, fig. 3-5, 9;

Akiba 1982, p. 65, pl. 7, fig. 3, 4;

Harwood and Maruyama 1992, p. 732, pl. 18, fig. 20;

Winter 1995, p. 133, pl. 8, fig. 3.

***Rhizosolenia* sp. A**

This study: Plate 7, Figures 9, 10.

Occurrence: Southern Kerguelen Plateau, Sørødal Formation

***Rhizosolenia* spp.**

Occurrence: Southern Kerguelen Plateau

Note: Rare *Rhizosolenia* spp. in the Kerguelen cores have been grouped together, these include

*R. costata* var. A

This study: Plate 7, Figure 1.

Reference:

Harwood and Maruyama 1992, p. 732, pl. 18, fig. 3, 4.

*R. sp. B*

This study: Plate 13, Figure 11.

*R. sp. C*

This study: Plate 7, Figure 2.

Reference:

Harwood and Maruyama 1992, p. 732, pl. 18, fig. 5, 6.

Genus *Rouxia* Brun *et* Heribaud 1893

***Rouxia antarctica* (Heiden) Hanna 1930**

This study: Plate 4, Figure 16; Plate 13, Figure 19.

Occurrence: Southern Kerguelen Plateau, Sørødal Formation

Synonymy: *Rouxia peragalli* var. *antarctica* Heiden

Reference:

Schrader 1976, p. 651, pl. 5, fig. 3-8;

Harwood and Maruyama 1992, p. 731, pl. 17, fig. 15;

Winter 1995, p. 133, pl. 8, fig. 6;

Bohaty et al. 1999, p. 448, pl. 1, fig 7.

***Rouxia heteropolara* Gombos 1974**

This study: Plate 4, Figure 13; Plate 15, Figure 14.

Occurrence: Southern Kerguelen Plateau, Pagodroma Group

Reference:

Gombos 1976, p. 617, pl. 7, fig. 14, 15;

Harwood 1986b, p. 731, pl. 17, fig. 15;

Gersonde and Burckle 1990, p. 789, pl. 5, fig. 2.

***Rouxia isopolica* Schrader 1976**

This study: Plate 4, Figure 14; Plate 13, Figure 20.

Occurrence: Southern Kerguelen Plateau, Sørødal Formation, Pagodroma Group

Synonymy: *Rouxia peragalli* Brun et Hérubaud

Reference:

Schrader 1976, p. 651, pl. 5, fig. 14-15;

Harwood 1986b, p. 731, pl. 17, fig. 13;

Winter 1995, p. 133, pl. 8, fig. 8.

***Rouxia leventerae* Bohaty et al. 1998**

This study: Plate 4, Figure 15.

Occurrence: Southern Kerguelen Plateau

Reference:

Bohaty et al. 1998, p. 448, pl 1, fig 1-6.

***Rouxia naviculoides* Schrader 1976**

This study: Plate 4, Figure 17; Plate 13, Figure 18.

Occurrence: Southern Kerguelen Plateau, Sørødal Formation

Reference:

Schrader 1976, p. 651, pl. 5, fig. 13, 18.

**Genus *Stephanopyxis* Ehrenberg 1845**

***Stephanopyxis grunowii* Grove et Sturt 1888**

Occurrence: Sørødal Formation, Pagodroma Group

Reference:

McCollum, 1975, p. 563, pl. 12, fig. 9,10;

Gombos, 1976, p. 659, pl. 28, fig. 3-5; p. 665, pl. 31, fig. 1,2, 7; p. 667, pl. 32, fig. 1-3;

Harwood, 1986a, p. 99, pl. 4, fig. 6,7;

Harwood, 1986b, p. 324, pl. 24, fig. 1;

Harwood, 1989, p. 89, pl. 2, fig. 1, 2-4.

Note: Found in early Oligocene sediments from OPD Hole 739A (Baldauf and Barron 1991)

***Stephanopyxis turris* (Greville and Arnott) Ralfs, in Pritchard 1861**

This study: Plate 15, Figure 10.

This study: Plate 8, Figures 5, 6.

Occurrence: Sørødal Formation, Pagodroma Group

Reference:

Koizumi, 1973, p. 851, pl. 6, fig. 13-16;

Schrader, 1973b, p. 775, pl. 15, fig. 1-7;

McCollum, 1975, p. 563, pl. 12, fig. 4;

Gombos, 1976, p. 607, pl. 2, fig. 5;

Akiba, 1982, p. 53, pl. 1, fig. 9;

Harwood, 1986a, p. 99, pl. 4, fig. 4;

Harwood, 1986b, p. 324, pl. 24, fig. 2;  
Harwood, 1989, p. 89, pl. 2, fig. 21-23;  
Winter, 1995, p. 133, pl. 8, fig. 9,10.

***Stephanopyxis splendidus* (Greville) Harwood 1989**

This study: Plate 14, Figure 1.

Occurrence: Pagodroma Group

Synonymy: *Thalassiosira hydra*

Reference:

Gombos and Cieselski 1983, p. 615, pl. 7, fig. 1-6;

Harwood 1989, p. 89, pl. 2, fig. 1, 2-4.

Note: Early Oligocene in age (Gombos and Cieselski 1983)

***Stephanopyxis* spp.**

This study: Plate 6, Figures 1, 2.

Occurrence: Sørødal Formation, Pagodroma Group

Note: *Stephanopyxis* spp. in the Kerguelen cores were not differentiated. Some *Stephanopyxis* spp. fragments were also identified in the Pagodroma Group and could not be identified to the species level.

**Genus *Stephanodiscus* Ehrenberg 1845**

***Stephanodiscus* spp.**

This study: Plate 16, Figure 3.

Occurrence: Pagodroma Group

Note: Undifferentiated fragments.

**Genus *Stellarima* Hasle et Sims 1986**

***Stellarima microtrias* (Ehrenberg) Hasle et Sims 1986**

This study: Plate 2, Figure 1; Plate 18, Figure 2.

Occurrence: Sørødal Formation, Pagodroma Group

Basionymy: *Symbolophora* (?) *microtrias* Ehrenberg 1844

Synonymy: *Coscinodiscus stellaris* var. *symbolophorus* Grunow 1884

Reference:

Harwood 1989, p. 87, pl. 1, fig. 4;

Winter 1995, p. 135, pl. 9, fig. 1.

***Stellarima stellaris* (Roper) Hasle et Sims 1986**

This study: Plate 8, Figure 7; Plate 18, Figure 1.

Occurrence: Sørødal Formation, Pagodroma Group

Basionymy: *Coscinodiscus* (?) *stellaris* Roper 1858

Synonymy: *Coscinodiscus stellaris* Roper

Reference:

Harwood 1986a, p. 324, pl. 24, fig. 10, 13;

Harwood 1989, p. 87, pl. 1, fig. 3;

Winter 1995, p. 135, pl. 9, fig. 2-4.

**Genus *Stictodiscus* Greville 1861**

***Stictodiscus hardmanius* Greville 1865**

Occurrence: Pagodroma Group

Reference:

Winter 1995, p. 135, pl. 9, fig. 5;

McCollum 1975, p. 565, pl. 13, fig. 1-4;

Harwood 1986b, p. 93, pl. 1, fig. 8, 9;  
Harwood 1989, p. 87, pl. 1, fig. 6.

Genus *Synedra* Ehrenberg 1832

*Synedra* sp. A

Occurrence: Sørødal Formation

Genus *Tabellaria* Ehrenberg ex Kutzing 1844

*Tabellaria* sp. cf. *fenestrata* (Lyngb.) Kutzing 1844

Occurrence: Pagodroma Group

Reference:

Contant and Duthie 1978, p. 43 pl. XV figs. 4-7.

Genus *Thalassionema* Grunow in Van Heurck 1881

*Thalassionema nitzschioides* group Grunow, in Van Heurck

This study: Plate 4, Figures, 19-21; Plate 15, Figure 17.

Occurrence: Southern Kerguelen Plateau, Sørødal Formation, Pagodroma Group

*Thalassionema nitzschioides* var. *parva* Heiden 1928

This study: Plate 4, Figure 18; Plate 15, Figure 16.

Occurrence: Southern Kerguelen Plateau, Pagodroma Group

Reference:

Koizumi and Tanimura 1982, p. 300, pl. 6, fig. 11;

Winter 1995, p. 145, pl. 14, fig. 1.

*Thalassionema* spp. / *Thalassiothrix* spp.

Occurrence: Pagodroma Group

Note: *Thalassionema* spp. / *Thalassiothrix* spp. fragments are common in some Pagodroma Group samples. The occasional lack of characteristic end pieces prevented the separation of these genera.

Genus *Thalassiosira* Cleve 1873

*Thalassiosira antarctica* Comber 1896

This study: Plate 8, Figure 12.

Occurrence: Sørødal Formation

Reference:

Johansen and Fryxell 1985, p. 163, fig. 37-39;

Roberts and McMinn 1999, p. 83, pl. 9, fig. 3-4.

Note: Unsure if this is *T. antarctica* in the Sørødal Formation, as this planktic diatom has not been recorded on other Antarctic and Southern Ocean Neogene sediments.

*Thalassiosira complicata* Gersonde 1991

This study: Plate 3, Figure 12; Plate 8, Figure 13.

Occurrence: Southern Kerguelen Plateau, Sørødal Formation

Basionymy: *Thalassiosira complicata* Gersonde 1991

Reference:

Gersonde 1991, p. 163, pl. 6, fig. 1-6;

Harwood and Maruyama 1992, p. 728, pl. 14, fig. 18-21;

Winter 1995, p. 137, pl. 10, fig. 1, 2.

***Thalassiosira elliptipora* (Donahue) Fenner 1991**

This study: Plate 2, Figure 9.

Occurrence: Southern Kerguelen Plateau

Reference:

Harwood and Maruyama 1992, p. 730, pl. 16, fig. 12;

Winter 1995, p. 143, pl. 13, fig 12.

***Thalassiosira fasciculata* Harwood and Maruyama 1992**

This study: Plate 2, Figure 8.

Occurrence: Southern Kerguelen Plateau

Synonym: *Coscinodiscus bullatus* Janisch sensu Hustedt 1958

Reference:

Harwood and Maruyama 1992, p. 729, pl. 15, fig. 4-6;

Winter 1995, p. 143, pl. 13, fig 2-4.

***Thalassiosira frenguelli* Kozlova 1967**

Occurrence: Southern Kerguelen Plateau

Reference:

Johansen and Fryxell 1985, p. 169, fig 64;

Medlin and Priddle 1990, p. 101, pl. 11.8, fig. 2.

***Thalassiosira gracilis* var. *gracilis* (Karsten) Hustedt 1958**

This study: Plate 3, Figure 4.

Occurrence: Southern Kerguelen Plateau, Sørødal Formation

Reference:

Johansen and Fryxell 1985, p. 167, fig 58, 59.

***Thalassiosira gracilis* var. *expecta* (Van Landingham) Fryxell et Hasle 1979**

This study: Plate 3, Figures 5, 6; Plate 8, Figures 10, 11.

Occurrence: Southern Kerguelen Plateau, Sørødal Formation

Synonymy: *Thalassiosira delicatula* sensu (Hustedt)

Reference:

Johansen and Fryxell 1985, p. 167, fig 60-63.

***Thalassiosira gravida* Cleve 1896**

Occurrence: Southern Kerguelen Plateau

Reference:

Johansen and Fryxell 1985, p. 164, fig 43.

***Thalassiosira insigna* (Jousé) Harwood and Maruyama 1991**

This study: Plate 3, Figure 8.

Occurrence: Southern Kerguelen Plateau, Pagodroma Group

Basionymy: *Cosmiodiscus insignis* Jousé 1959

Reference:

Koizumi 1973, p. 864, pl. 4, fig. 7-11;

Gombos 1976, p. 611, pl. 4, fig. 4, 5;

Akiba 1985, p. 468, pl. 17, fig. 1;

Harwood and Maruyama 1992, p. 728, pl. 14, fig. 3-5;

Winter 1995, p. 137, pl. 10, fig. 3,4.

***Thalassiosira inura* Gersonde 1991**

This study: Plate 3, Figure 7; Plate 8, Figure 2; Plate 16, Figure 2.

Occurrence: Southern Kerguelen Plateau, Sørødal Formation, Pagodroma Group

Basionymy: *Thalassiosira inura* Gersonde 1991



Reference:

- Gersonde 1991, p. 163, pl. 6, fig. 7-14;  
Baldauf and Barron 1991, p. 597, pl. 6, fig. 9;  
Harwood and Maruyama 1992, p. 719, pl. 5, fig. 14; p. 728, pl. 14, fig. 12-14, 16;  
Winter 1995, p. 137, pl. 10, fig. 5.

***Thalassiosira inura / insigna*** (transitional forms)

Occurrence: Southern Kerguelen Plateau, Sørødal Formation

Reference:

- Harwood and Maruyama 1992, p. 728, pl. 14, fig. 7-10.

***Thalassiosira kolbei*** (Jousé) Gersonde 1990

This study: Plate 3, Figure 1.

Occurrence: Southern Kerguelen Plateau

Basionymy: *Coscinodiscus kolbei* (Jousé)

Reference:

- McCollum 1975, p. 527, pl. 4, fig. 7-9;  
Winter 1995, p. 139, pl. 11, fig. 1-3.

***Thalassiosira lentiginosa*** (Janisch) Fryxell 1977

This study: Plate 2, Figure 2.

Occurrence: Southern Kerguelen Plateau

Synonymy: *Coscinodiscus lentiginosus* Janisch in Schmidt 1978

Reference:

- Abbott 1974, p. 331, pl. 3, fig. D-F;  
Johansen and Fryxell 1985, p. 166, fig. 49; 50;  
Winter 1995, p. 143, pl. 13, fig. 5, 6.

***Thalassiosira maculata*** Fryxell et Johansen 1985

This study: Plate 3, Figure 10.

Occurrence: Southern Kerguelen Plateau, Sørødal Formation

Synonymy: *Coscinodiscus bullatus* (Janisch) Hustedt 1958

Reference:

- Johansen and Fryxell 1985, p. 172, fig. 72-74.

***Thalassiosira nativa*** Sheshukova-Poretzkaya 1959

Occurrence: Pagodroma Group

Reference:

- Schrader 1973, p. 665, pl. 12, fig. 8-11;  
Barron 1985, p. 798, fig. 11, fig. 4;  
Baldauf and Barron 1991, p. 597, pl. 6, fig. 5.

***Thalassiosira oestrupii*** (Ostenfeld) Hasle 1972

This study: Plate 2, Figure 6.

Occurrence: Southern Kerguelen Plateau, Sørødal Formation

Reference:

- Abbott 1974, p. 337, pl. 6, fig. E;  
Winter 1995, p. 137, pl. 10, fig. 8,9.

***Thalassiosira oliverana*** (O'Meara) Makarova et Nikolaev 1983

This study: Plate 3, Figure 11; Plate 8, Figure 3.

Occurrence: Southern Kerguelen Plateau, Sørødal Formation, Pagodroma Group

Synonymy: *Schimperella antarctica* Karsten in Abbott 1973

References used:

Abbott 1974, p. 329, pl. 2, fig. D-F;

Winter 1995, p. 137, pl. 10, fig 10.

Note: at times a coarse variety was identified and recorded in samples from the Southern Kerguelen Plateau and Sørødal Formation

This study: Plate 3, Figures 2 and 3; Plate 10, Figure 6

Reference:

Harwood and Maruyama 1992, p. pl. 14, fig. 6, 11).

Note: *Thalassiosira oliverana* var. *sparsa* was indentified but recorded as *Thalassiosira oliverana*

This study: Plate 15, Figure 18.

Reference:

Harwood *et al.* 1989b, pl 2, fig 7.

***Thalassiosira striata*** Harwood and Maruyama 1992

Occurrence: Southern Kerguelen Plateau, Sørødal Formation

Reference:

Harwood and Maruyama 1992, p. 720, pl. 15, fig. 7-9.

***Thalassiosira torokina*** Brady 1977

This study: Plate 3, Figure 9; Plate 8, Figure 1.

Occurrence: Southern Kerguelen Plateau, Sørødal Formation

Reference:

Winter 1995, p. 139, pl. 11, fig 7.

***Thalassiosira vulnifica*** (Gombos) Fenner 1991

This study: Plate 2, Figure 7.

Basionym: *Coscinodiscus vulnificus* Gombos 1977

Reference:

Harwood and Maruyama 1992, p. 729, pl. 15, fig 1;

Winter 1995, p. 141, pl. 12, fig 4-6.

***Thalassiosira webbi*** Harwood and Maruyama 1992

Occurrence: Southern Kerguelen Plateau

Reference:

Harwood and Maruyama 1992, p. 729, pl. 5, fig 2-3;

Winter 1995, p. 139, pl. 11, fig 4-6.

Genus ***Thalassiothrix*** Cleve *et* Grunow 1880

***Thalassiothrix antarctica*** Cleve *et* Grunow 1880

This study: Plate 6, Figure 7.

Occurrence: Pagodroma Group

Reference:

Schrader 1973, p. 643, pl. 1, fig. 5, 17;

Hasle and Semina 1987, p. 183, fig. 32-43;

Harwood and Maruyama 1992, p. 725, pl. 11, fig. 12.

***Thalassiothrix spp.***

Occurrence: Southern Kerguelen Plateau, Sørødal Formation, Pagodroma Group

Genus '***Tigeria***' Harwood *et al.* 1999

***'Tigeria' spp.*** group Harwood *et al.* 1999

This study: Plate 12, Figures 12-14.

Occurrence: Sørødal Formation

Note. Rare occurrence in the Sørødal Formation and have been recorded as OTHER.

Reference:

Harwood, pers. comm. 1999.

Genus *Trachyneis* Cleve 1894

*Trachyneis aspera* (Ehrenberg) Cleve 1884

This study: Plate 11, Figure 18.

Occurrence: Sørødal Formation

Reference:

Krebs 1983, p. 297, pl. 6, fig. 2;

Roberts and McMinn 1999, p. 79, pl. 7, fig. 9.

Genus *Trichotoxon* Reid et Round 1987

*Trichotoxon reinboldii* (Van Heurck) Reid et Round 1987

This study: Plate 6, Figure 6; Plate 12, Figure 11.

Occurrence: Southern Kerguelen Plateau, Sørødal Formation

Synonymy: *Syndera reinboldii* (Van Heurck)

Reference:

Medlin and Priddle 1990, p. 135, pl. 17.1, fig. 7-9.

Genus *Trigonium* Cleve 1868

*Trigonium arcticum* (Brightwell) Cleve 1868

This study: Plate 10, Figure 4.

Occurrence: Sørødal Formation, Pagodroma Group

Reference:

Winter 1995, p. 145, pl. 14, fig. 5,6;

Harwood 1986a, p. 320, pl. 22, fig. 3.

Genus *Trinacria* Heiberg 1863

*Trinacria excavata* Heiberg 1863

This study: Plate 18, Figure 6.

Occurrence: Pagodroma Group

Reference:

Schrader 1973, p. 669, pl. 14, fig. 15;

McCollum 1975, p. 569, pl. 15, fig. 1, 2;

Harwood 1986b, p. 95, pl. 2, fig. 13;

Harwood 1989, p. 91, pl. 3, fig. 1.

**Gen. et sp. indet. A**

This study: Plate 12, Figures 2, 3; Plate 18, Figure 5.

Occurrence: Pagodroma Group

Synonym: Gen et sp. C, Harwood *et al.* in press, fig. 10.s-t.

**Gen. et sp. indet. B**

This study: Plate 12, Figure 9.

Occurrence: Sørødal Formation

Class **Dinophyceae**  
(Dinoflagellates)

Genus ***Actiniscus*** Ehrenberg 1854

***Actiniscus pentasteris*** (Ehrenberg) Ehrenberg 1854  
Occurrence: Pagodroma Group

Class **Dictyochophyceae**  
(Silicoflagellates)

Genus ***Dictyocha*** Ehrenberg 1839

***Dictyocha aspera*** (Lemmermann) Burkry *et* Foster 1973  
This study: Plate 6, Figure 12.  
Occurrence: Southern Kerguelen Plateau  
Reference:  
Bohaty and Harwood 1998, p. 247, pl. 1, fig. 5.

Genus ***Distephanus*** Stoechr 1880

***Distephanus pseudofibula*** (Schulz) Burkry 1976  
This study: Plate 15, Figure 15.  
Occurrence: Pagodroma Group  
Reference:  
Bohaty and Harwood 1998, p. 247, pl. 1, fig. 7.

***Distephanus speculum*** (Ehrenberg) Haeckel 1887  
This study: Plate 6, Figure 10; This study: Plate 16, Figure 10; Plate 18, Figure 10.  
Occurrence: Southern Kerguelen Plateau, Pagodroma Group  
Reference:  
Bohaty and Harwood 1998, p. 247, pl. 1, fig. 1, 4.

***Distephanus crux*** (Ehrenberg) Locker 1974  
This study: Plate 6, Figure 11.  
Occurrence: Southern Kerguelen Plateau  
Reference:  
Bohaty and Harwood 1998, p. 247, pl. 1, fig. 6.

Class **Ebriophyceae**  
(Ebridians)

Genus ***Pseudammodochium***

***Pseudammodochium lingii*** Bohaty and Harwood 2000  
This study: Plate 18, Figure 4.  
Occurrence: Pagodroma Group  
Reference:  
Bohaty, pers. comm. 1999.

## **Plate 1.**

- |   |                           |
|---|---------------------------|
| <b>1</b> <i>Actinocyclus actinochilus</i> , | (Kerguelen GC 34, 130 cm) |
| <b>2</b> <i>Actinocyclus fasciculatus</i> , | (Kerguelen GC 34, 390 cm) |
| <b>3</b> <i>Actinocyclus fasciculatus</i> , | (Kerguelen GC 50, 410 cm) |
| <b>4</b> <i>Actinocyclus fasciculatus</i> , | (Kerguelen GC 34, 390 cm) |
| <b>5</b> <i>Actinocyclus ingens</i> ,       | (Kerguelen GC 34, 250 cm) |
| <b>6</b> <i>Astromphalus hepaticus</i> ,    | (Kerguelen GC 34, 320 cm) |
| <b>7</b> <i>Astromphalus hyalinus</i> ,     | (Kerguelen GC 34, 10 cm)  |
| <b>8</b> <i>Astromphalus hyalinus</i> ,     | (Kerguelen GC 34, 10 cm)  |
| <b>9</b> <i>Astromphalus hepaticus</i> ,    | (Kerguelen GC 34, 320 cm) |
-

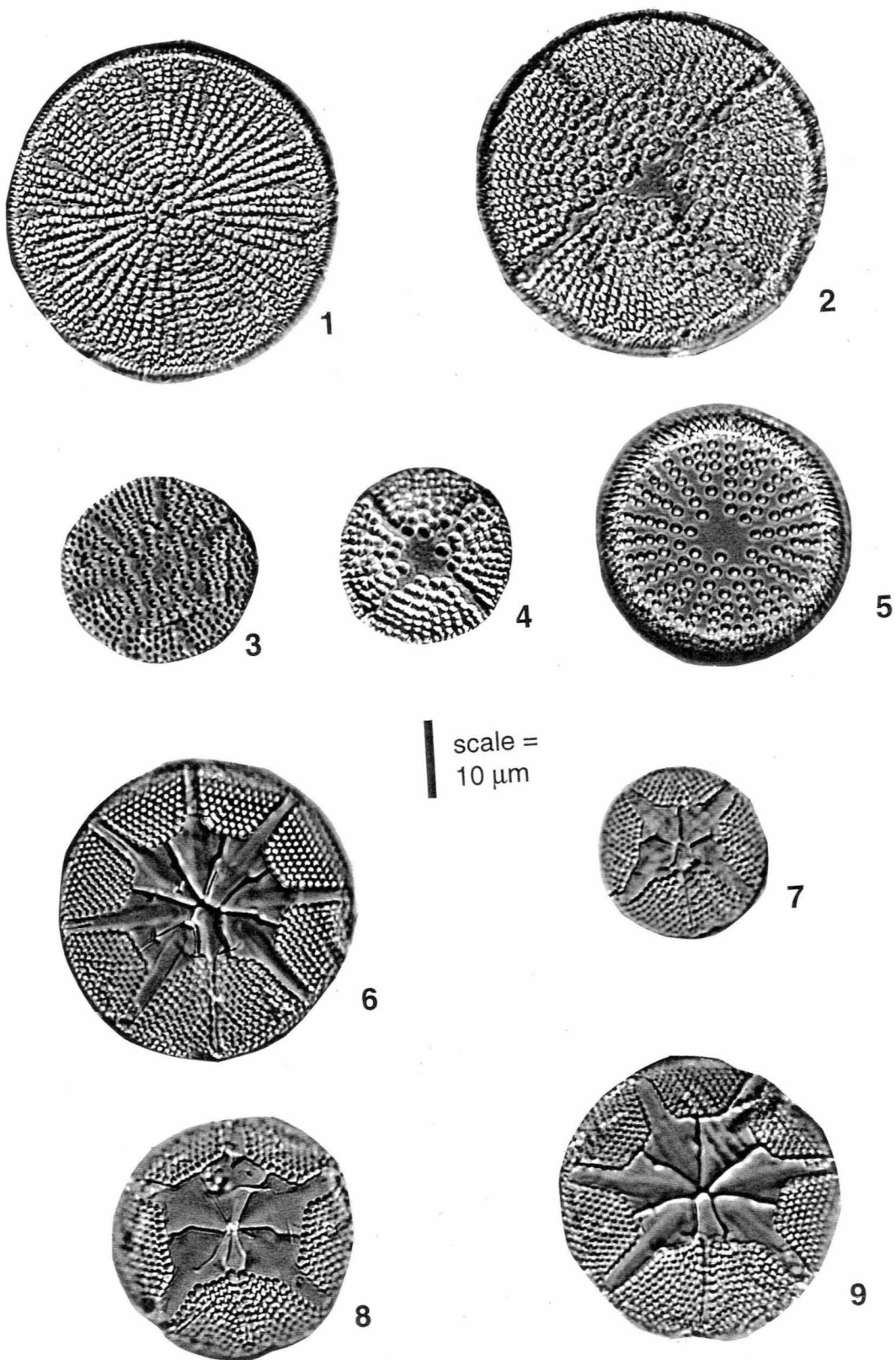
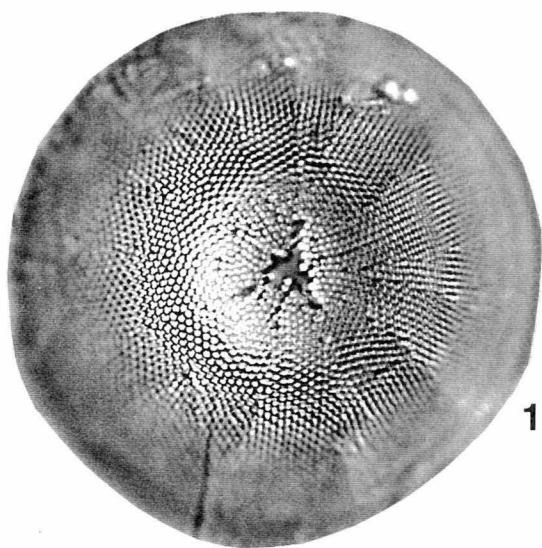
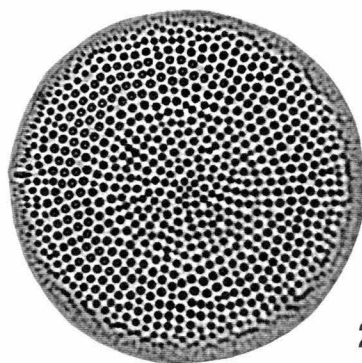


## Plate 2.

- |   |                           |
|---|---------------------------|
| <b>1</b> <i>Stellarima microtrias</i> ,                   | (Kerguelen GC 34, 130 cm) |
| <b>2</b> <i>Thalassiosira lentiginosa</i> ,               | (Kerguelen GC 34, 30 cm)  |
| <b>3</b> <i>Azpeitia tabularis</i> ,                      | (Kerguelen GC 49, 71 cm)  |
| <b>4</b> <i>Porosira pseudodenticulata</i> ,              | (Kerguelen GC 34, 520 cm) |
| <b>5</b> <i>Porosira pseudodenticulata</i> ,              | (Kerguelen GC 34, 520 cm) |
| <b>6</b> <i>Thalassiosira oestrupii</i> ,                 | (Kerguelen GC 48, 420 cm) |
| <b>7</b> <i>Thalassiosira vulnifica</i> ,                 | (Kerguelen GC 48, 420 cm) |
| <b>8</b> <i>Thalassiosira fasciculata</i> ,               | (Kerguelen GC 51, 300 cm) |
| <b>9</b> <i>Thalassiosira elliptipora</i> ,<br>(fragment) | (Kerguelen GC 48, 170 cm) |

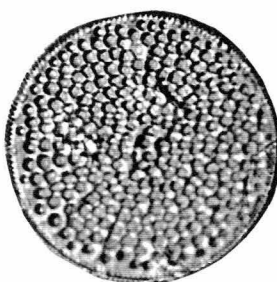


1

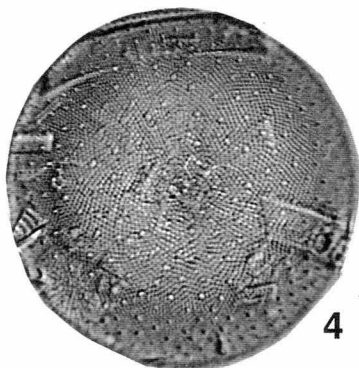


2

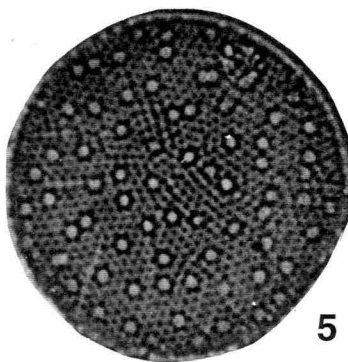
scale =  
10  $\mu$ m



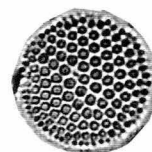
3



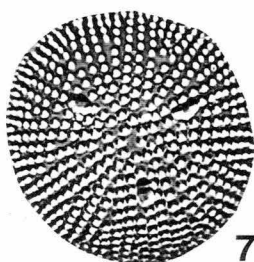
4



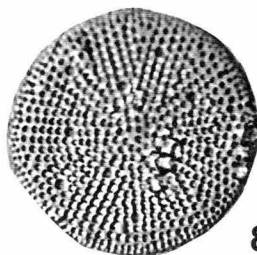
5



6



7



8



9



### Plate 3.

- |  |                           |
|--|---------------------------|
| 1 <i>Thalassiosira kolbei</i> ,                        | (Kerguelen GC 34, 480 cm) |
| 2 <i>Thalassiosira oliverana</i> (coarse),             | (Kerguelen GC 34, 390 cm) |
| 3 <i>Thalassiosira oliverana</i> (coarse),             | (Kerguelen GC 48, 120cm)  |
| 4 <i>Thalassiosira gracilis</i> var. <i>gracilis</i> , | (Kerguelen GC 34, 130 cm) |
| 5 <i>Thalassiosira gracilis</i> var. <i>expecta</i> ,  | (Kerguelen GC 49, 380 cm) |
| 6 <i>Thalassiosira gracilis</i> var. <i>expecta</i> ,  | (Kerguelen GC 49, 380 cm) |
| 7 <i>Thalassiosira inura</i> ,                         | (Kerguelen GC 34, 390 cm) |
| 8 <i>Thalassiosira insigna</i> ,                       | (Kerguelen GC 34, 480 cm) |
| 9 <i>Thalassiosira torokina</i> ,                      | (Kerguelen GC 48, 250 cm) |
| 10 <i>Thalassiosira maculata</i> ,<br>(girdle band)    | (Kerguelen GC 34, 130 cm) |
| 11 <i>Thalassiosira oliverana</i> ,                    | (Kerguelen GC 49, 320 cm) |
| 12 <i>Thalassiosira complicata</i> ,                   | (Kerguelen GC 34, 540 cm) |

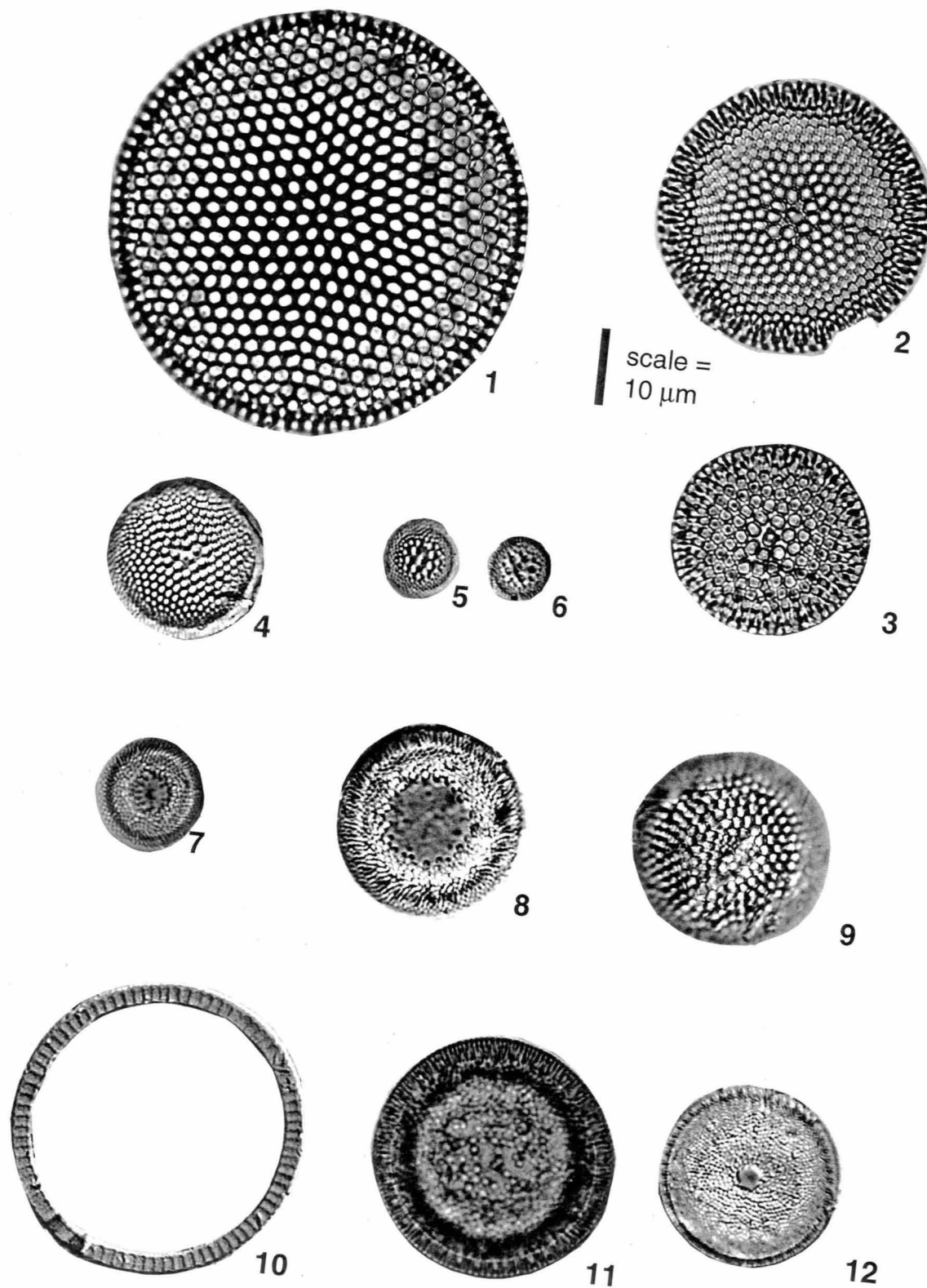


#### **Plate 4.**

- |   |                           |
|---|---------------------------|
| <b>1</b> <i>Fragilariopsis praeinterfrigidaria</i> ,            | (Kerguelen GC 48, 440 cm) |
| <b>2</b> <i>Fragilariopsis praeinterfrigidaria</i> ,            | (Kerguelen GC 48, 440 cm) |
| <b>3</b> <i>Fragilariopsis interfrigidaria</i> ,                | (Kerguelen GC 50, 390 cm) |
| <b>4</b> <i>Fragilariopsis interfrigidaria</i> ,                | (Kerguelen GC 50, 390 cm) |
| <b>5</b> <i>Fragilariopsis interfrigidaria</i> ,                | (Kerguelen GC 50, 390 cm) |
| <b>6</b> <i>Fragilariopsis aurica</i> ,                         | (Kerguelen GC 34, 550 cm) |
| <b>7</b> <i>Fragilariopsis rhombica</i> ,                       | (Kerguelen GC 49, 71 cm)  |
| <b>8</b> <i>Fragilariopsis rhombica</i> ,                       | (Kerguelen GC 49, 71 cm)  |
| <b>9</b> <i>Fragilariopsis separanda</i> ,                      | (Kerguelen GC 50, 50 cm)  |
| <b>10</b> <i>Fragilariopsis curta</i> ,                         | (Kerguelen GC 50, 50 cm)  |
| <b>11</b> <i>Fragilariopsis cylindrus</i> ,                     | (Kerguelen GC 34, 380 cm) |
| <b>12</b> <i>Fragilariopsis obliquecostata</i> ,                | (Kerguelen GC 51, 370 cm) |
| <b>13</b> <i>Rouxia heteropolara</i> ,                          | (Kerguelen GC 34, 370 cm) |
| <b>14</b> <i>Rouxia isopolica</i> ,                             | (Kerguelen GC 51, 470 cm) |
| <b>15</b> <i>Rouxia leventerae</i> ,                            | (Kerguelen GC 51, 470 cm) |
| <b>16</b> <i>Rouxia antarctica</i> ,                            | (Kerguelen GC 51, 470 cm) |
| <b>17</b> <i>Rouxia naviculoides</i> ,                          | (Kerguelen GC 34, 410 cm) |
| <b>18</b> <i>Thalassionema nitzchioides</i> var. <i>parva</i> , | (Kerguelen GC 34, 530 cm) |
| <b>19</b> <i>Thalassionema nitzschoides</i> (group)             | (Kerguelen GC 34, 530 cm) |
| <b>20</b> <i>Thalassionema nitzschoides</i> (group)             | (Kerguelen GC 34, 530 cm) |
| <b>21</b> <i>Thalassionema nitzschoides</i> (group)             | (Kerguelen GC 34, 530 cm) |

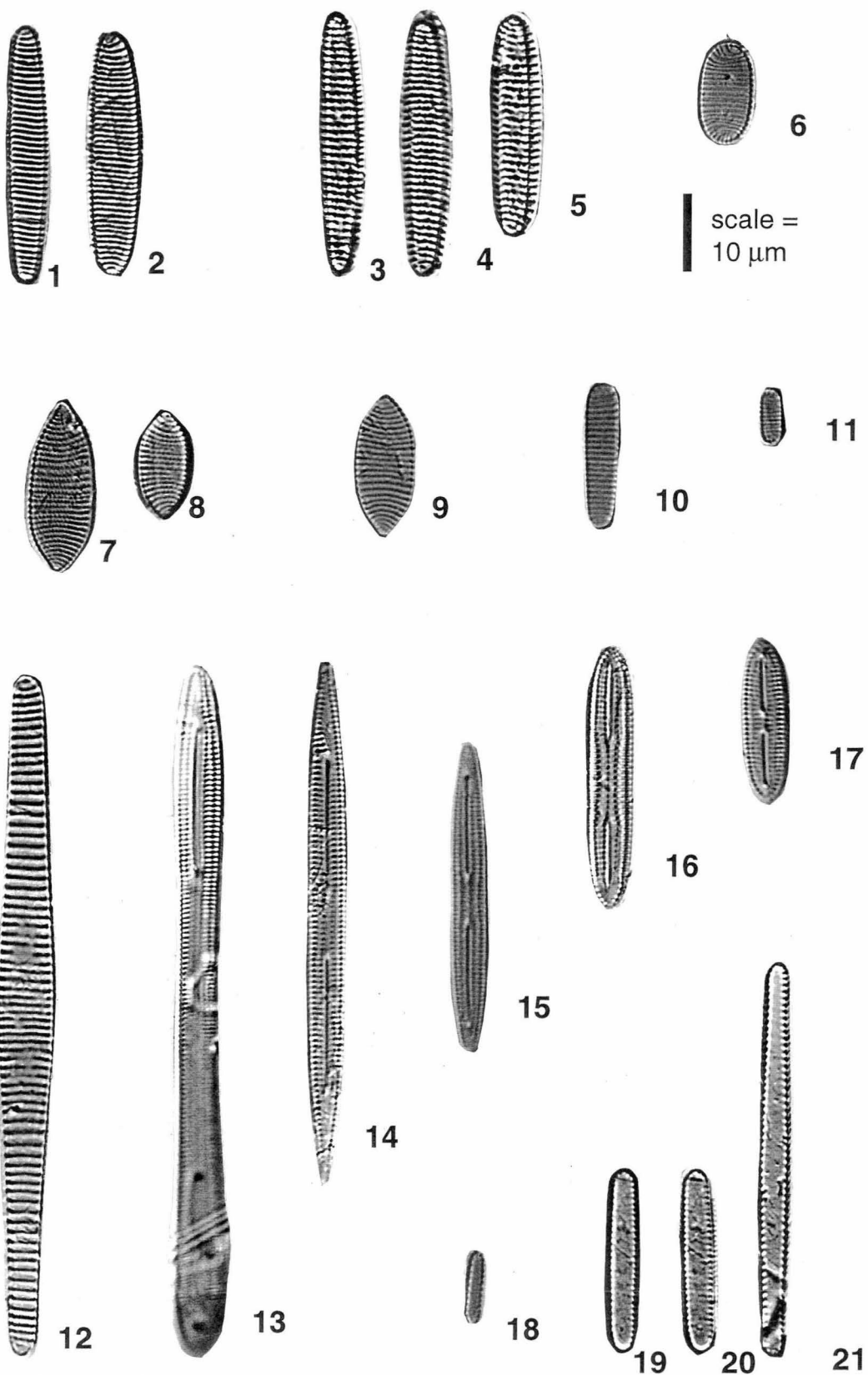


## Plate 5.

- |  |                           |
|--|---------------------------|
| 1 <i>Fragilariopsis kerguelensis</i> ,     | (Kerguelen GC 48, 50 cm)  |
| 2 <i>Fragilariopsis kerguelensis</i> ,     | (Kerguelen GC 48, 50 cm)  |
| 3 <i>Fragilariopsis kerguelensis</i> ,     | (Kerguelen GC 48, 50 cm)  |
| 4 <i>Fragilariopsis kerguelensis</i> ,     | (Kerguelen GC 48, 50 cm)  |
| 5 <i>Fragilariopsis kerguelensis</i> ,     | (Kerguelen GC 48, 50 cm)  |
| 6 <i>Fragilariopsis barronii</i> var. A,   | (Kerguelen GC 49, 291 cm) |
| 7 <i>Fragilariopsis barronii</i> var. A,   | (Kerguelen GC 49, 291 cm) |
| 8 <i>Fragilariopsis barronii</i> var. B,   | (Kerguelen GC 49, 291 cm) |
| 9 <i>Fragilariopsis barronii</i> var. B,   | (Kerguelen GC 49, 291 cm) |
| 10 <i>Fragilariopsis weaveri</i> ,         | (Kerguelen GC 48, 440 cm) |
| 11 <i>Fragilariopsis weaveri</i> ,         | (Kerguelen GC 48, 440 cm) |
| 12 <i>Fragilariopsis barronii</i> ,        | (Kerguelen GC 50, 470 cm) |
| 13 <i>Fragilariopsis barronii</i> ,        | (Kerguelen GC 50, 470 cm) |
| 14 <i>Fragilariopsis separanda</i> var. A, | (Kerguelen GC 51, 320 cm) |
| 15 <i>Fragilariopsis separanda</i> var. A, | (Kerguelen GC 51, 320 cm) |
| 16 <i>Fragilariopsis ritscheri</i> ,       | (Kerguelen GC 34, 60 cm)  |
| 17 <i>Fragilariopsis ritscheri</i> ,       | (Kerguelen GC 34, 60 cm)  |
| 18 <i>Fragilariopsis ritscheri</i> ,       | (Kerguelen GC 34, 60 cm)  |
| 19 <i>Nitzschia reinholdii</i> ,           | (Kerguelen GC 34, 550 cm) |
| 20 <i>Fragilariopsis sublinearis</i> ,     | (Kerguelen GC 48, 440 cm) |
| 21 <i>Nitzschia peragallii</i> ,           | (Kerguelen GC 49, 61 cm)  |

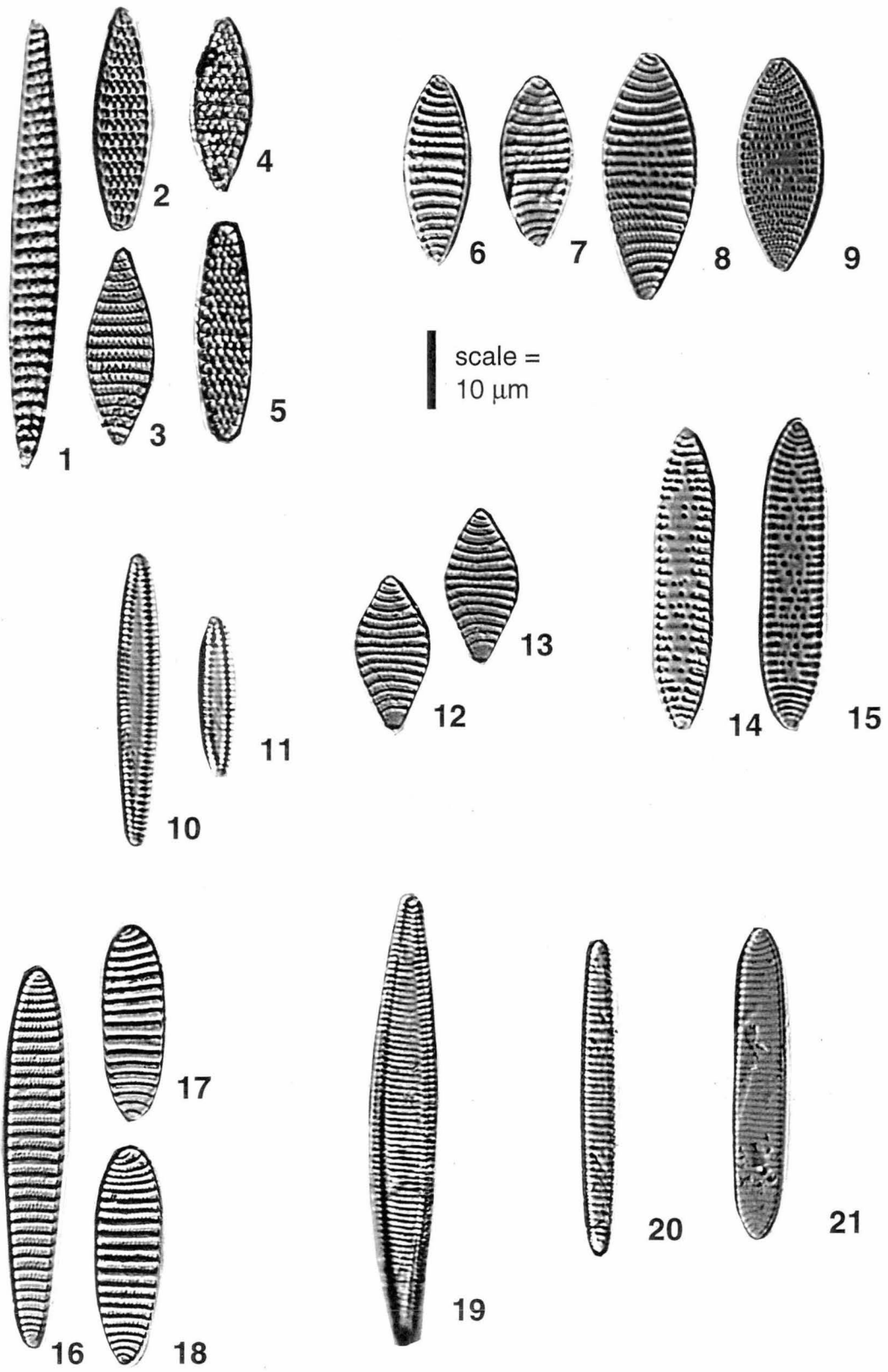
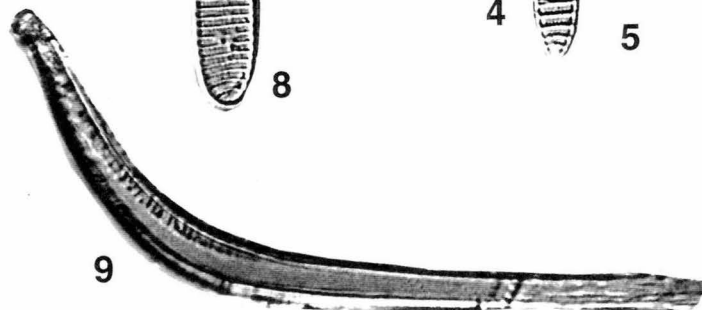
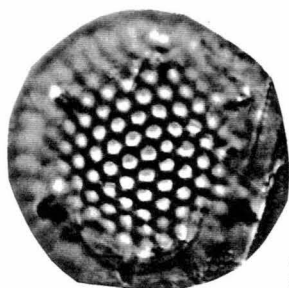
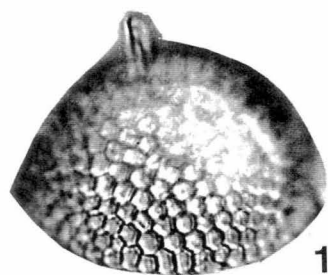


## Plate 6.

- |  |                           |
|--|---------------------------|
| 1 <i>Stephanopyxis</i> sp.,                            | (Kerguelen GC 34, 10 cm)  |
| 2 <i>Stephanopyxis</i> sp.,                            | (Kerguelen GC 34, 10 cm)  |
| 3 <i>Eucampia antarctica</i> var. <i>recta</i> ,       | (Kerguelen GC 48, 60 cm)  |
| 4 <i>Fragilariopsis obliquecostata</i> ,               | (Kerguelen GC 50, 40 cm)  |
| 5 <i>Fragilariopsis obliquecostata</i> ,               | (Kerguelen GC 50, 40 cm)  |
| 6 <i>Trichotoxon reinboldii</i> ,<br>(fragment)        | (Kerguelen GC 51, 370 cm) |
| 7 <i>Thalassiothrix antarctica</i> ,<br>(fragment)     | (Kerguelen GC 49, 51 cm)  |
| 8 <i>Fragilariopsis praecurta</i> ,                    | (Kerguelen GC 48, 470 cm) |
| 9 <i>Proboscia barboi</i> ,                            | (Kerguelen GC 34, 170 cm) |
| 10 <i>Distephanus speculum</i> ,<br>(silicoflagellate) | (Kerguelen GC 50, 170 cm) |
| 11 <i>Distephanus crux</i> ,<br>(silicoflagellate)     | (Kerguelen GC 34, 570 cm) |
| 12 <i>Dictyocha aspera</i> ,<br>(silicoflagellate)     | (Kerguelen GC 50, 170 cm) |



scale =  
10  $\mu$ m

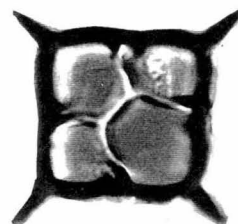
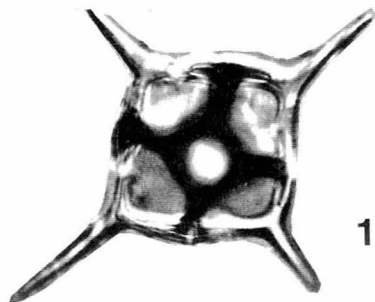
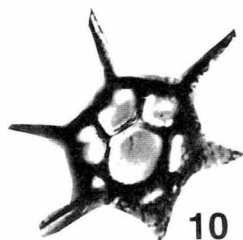




## Plate 7.

- |   |                           |
|---|---------------------------|
| <b>1</b> <i>Rhizosolenia costata</i> var. A,<br>(fragment)    | (Kerguelen GC 51, 370 cm) |
| <b>2</b> <i>Rhizosolenia</i> sp. C,<br>(fragment)             | (Kerguelen GC 51, 370 cm) |
| <b>3</b> <i>Rhizosolenia styliformis</i> ,                    | (Kerguelen GC 34, 390 cm) |
| <b>4</b> <i>Rhizosolenia styliformis</i> ,                    | (Kerguelen GC 34, 390 cm) |
| <b>5</b> <i>Rhizosolenia hebetata</i> ,                       | (Kerguelen GC 34, 540 cm) |
| <b>6</b> <i>Denticulopsis dimorpha</i> ,                      | (Kerguelen GC 34, 530 cm) |
| <b>7</b> <i>Denticulopsis dimorpha</i> ,                      | (Kerguelen GC 34, 530 cm) |
| <b>8</b> <i>Denticulopsis simonsenii</i> ,                    | (Kerguelen GC 34, 530 cm) |
| <b>9</b> <i>Rhizosolenia</i> sp. A,                           | (Kerguelen GC 48, 140 cm) |
| <b>10</b> <i>Rhizosolenia</i> sp. A,<br>(fragment)            | (Kerguelen GC 48, 140 cm) |
| <b>11</b> <i>Hemidiscus karstenii</i> ,                       | (Kerguelen GC 34, 30 cm)  |
| <b>12</b> <i>Dactyliosolen antarcticus</i> ,<br>(girdle band) | (Kerguelen GC 48, 440 cm) |
| <b>13</b> <i>Fragilariopsis lacrima</i> ,                     | (Kerguelen GC 50, 440 cm) |
| <b>14</b> <i>Corethron criophilum</i> ,                       | (Kerguelen GC 34, 560 cm) |
| <b>15</b> <i>Chaetoceros bulbosum</i> ,<br>(vegetative)       | (Kerguelen GC 51, 420 cm) |
| <b>16</b> <i>Chaetoceros bulbosum</i> ,<br>(vegetative)       | (Kerguelen GC 51, 420 cm) |

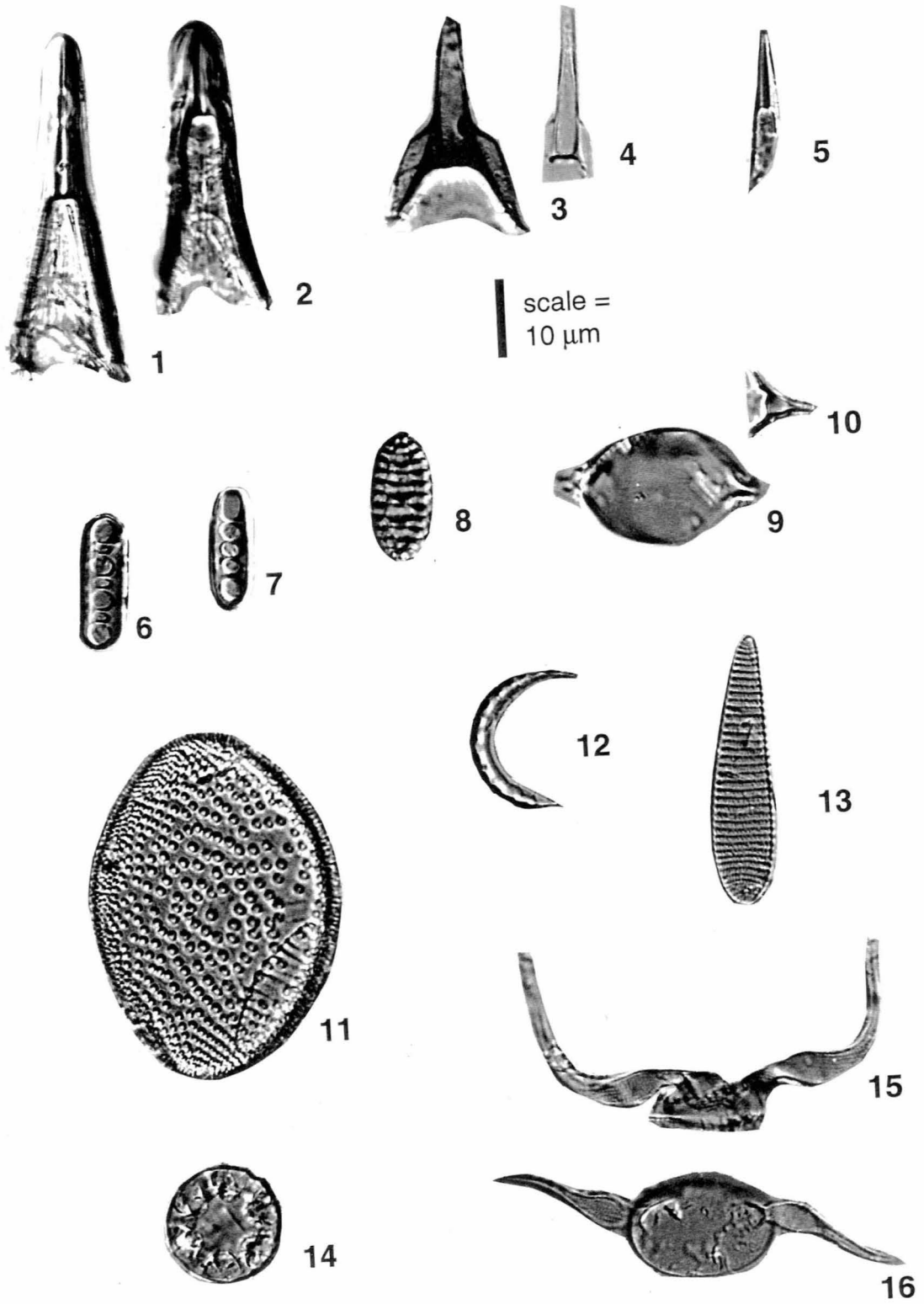
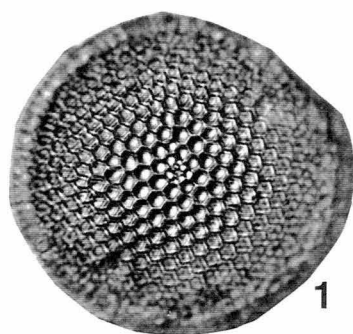


## Plate 8.

- |  |   |
|--|---|
| <b>1</b> <i>Thalassiosira torokina</i> ,                                       | (Sørsdal Formation 2A, 210-220 cm)          |
| <b>2</b> <i>Thalassiosira inura</i> ,  | (Sørsdal Formation 2A, 150-160 cm)          |
| <b>3</b> <i>Thalassiosira oliverana</i> ,                                      | (Sørsdal Formation 2A, 150-160 cm)          |
| <b>4</b> <i>Actinocyclus karstenii</i> ,                                       | (Sørsdal Formation 2A, 150-160 cm)          |
| <b>5</b> <i>Stephanopyxis turris</i> ,   | (Sørsdal Formation 2A, 210-220 cm)          |
| <b>6</b> <i>Stephanopyxis turris</i> ,   | (Sørsdal Formation 2A, 210-220 cm)          |
| <b>7</b> <i>Stellarima stellaris</i> ,<br>(fragment)                           | (Sørsdal Formation, photo by David Harwood) |
| <b>8</b> <i>Actinocyclus octonarius</i> var. <i>asteriscus</i> ,<br>(fragment) | (Sørsdal Formation 2A, 190-200 cm)          |
| <b>9</b> <i>Actinocyclus ingens</i> ,  | (Sørsdal Formation 2A, 150-160 cm)          |
| <b>10</b> <i>Thalassiosira gracilis</i> var. <i>expecta</i> ,                  | (Sørsdal Formation 2A, 210-220 cm)          |
| <b>11</b> <i>Thalassiosira gracilis</i> var. <i>expecta</i> ,                  | (Sørsdal Formation 2A, 210-220 cm)          |
| <b>12</b> <i>Thalassiosira antarctica</i> (?),                                 | (Sørsdal Formation 2A, 210-220 cm)          |
| <b>13</b> <i>Thalassiosira complicata</i> ,                                    | (Sørsdal Formation 2A, 150-160 cm)          |



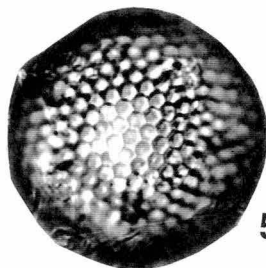
1



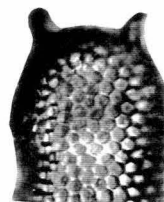
2



3

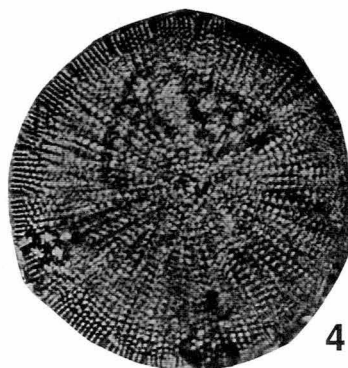


5

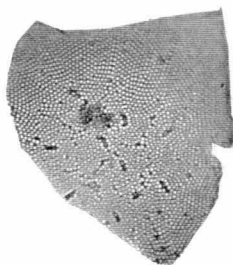


6

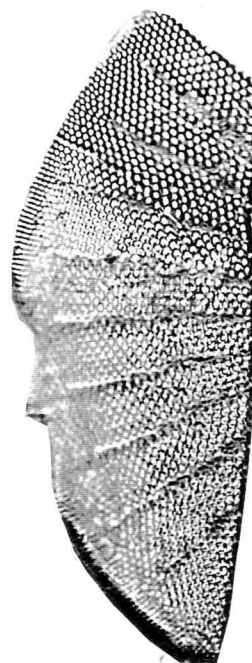
scale =  
10  $\mu$ m



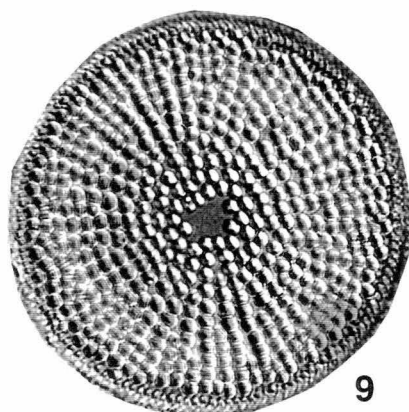
4



7



8



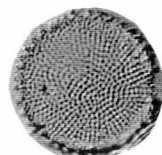
9



10



11



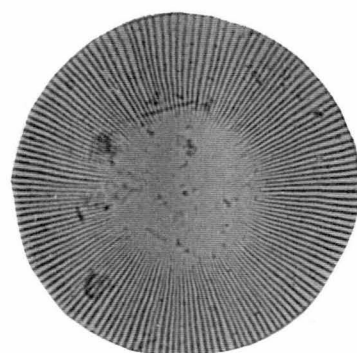
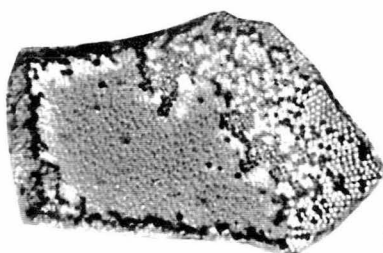
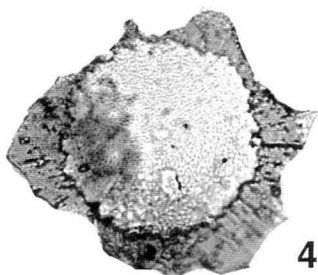
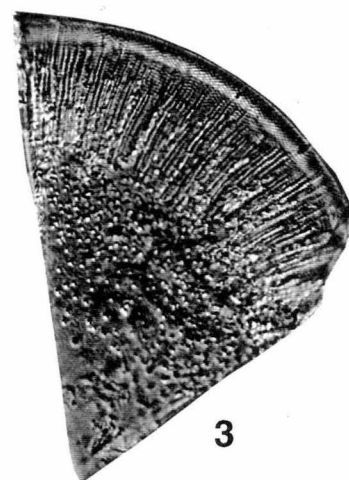
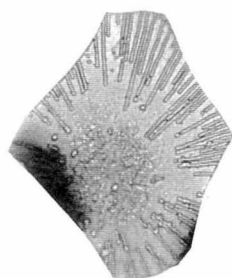
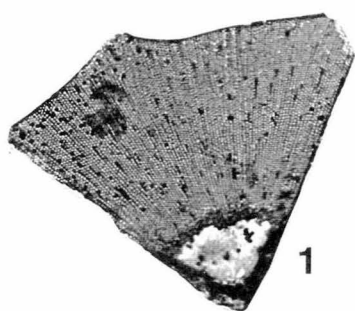
12



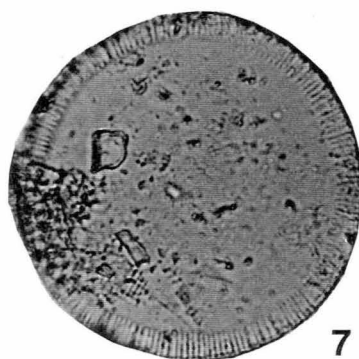
13

## Plate 9.

- |   |   |
|---|---|
| <b>1</b> <i>Hyalodiscus valens</i> ,<br>(fragment)    | (Sørsdal Formation, photo by David Harwood) |
| <b>2</b> <i>Hyalodiscus zonulatus</i> ,<br>(fragment) | (Sørsdal Formation, photo by David Harwood) |
| <b>3</b> <i>Hyalodiscus radiatus</i> ,<br>(fragment)  | (Sørsdal Formation 2A, 210-220 cm)          |
| <b>4</b> <i>Hyalodiscus valens</i> ,<br>(fragment)    | (Sørsdal Formation 2A, 190-200 cm)          |
| <b>5</b> <i>Hyalodiscus valens</i> ,<br>(fragment)    | (Sørsdal Formation 2A, 190-200 cm)          |
| <b>6</b> <i>Paralia sol</i> ,                         | (Sørsdal Formation, photo by David Harwood) |
| <b>7</b> <i>Paralia pantocseki</i> ,                  | (Sørsdal Formation, photo by David Harwood) |
| <b>8</b> <i>Paralia sol</i> var. <i>maginalis</i>     | (Sørsdal Formation 2A, 190-200 cm)          |



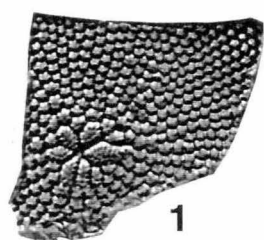
scale =  
10  $\mu$ m



10  $\mu$ m

## Plate 10.

- |   |   |
|---|---|
| <b>1</b> <i>Coscinodiscus oculus-iridus</i> ,<br>(fragment) | (Sørsdal Formation 2A, 150-160 cm)          |
| <b>2</b> <i>Isthmia</i> sp.,<br>(fragment)                  | (Sørsdal Formation 2A, 150-160 cm)          |
| <b>3</b> <i>Coscinodiscus oculus-iridus</i> ,<br>(fragment) | (Sørsdal Formation 2A, 150-160 cm)          |
| <b>4</b> <i>Trigonium arcticum</i> ,                        | (Sørsdal Formation, photo by David Harwood) |
| <b>5</b> <i>Pleurosigma</i> sp. A.,<br>(fragment)           | (Sørsdal Formation 2A, 90-100 cm)           |
| <b>6</b> <i>Thalassiosira oliverana</i> (coarse),           | (Sørsdal Formation 2A, 150-160 cm)          |
| <b>7</b> <i>Paralia</i> sp.,                                | (Sørsdal Formation 2A, 150-160 cm)          |
| <b>8</b> <i>Grammatophora charcoti</i> ,                    | (Sørsdal Formation, photo by David Harwood) |
| <b>9</b> <i>Grammatophora marina</i> ,                      | (Sørsdal Formation 2A, 210-220 cm)          |



scale =  
10  $\mu$ m

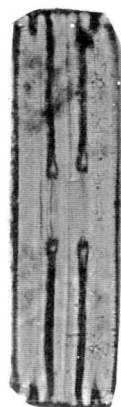
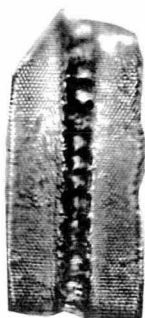
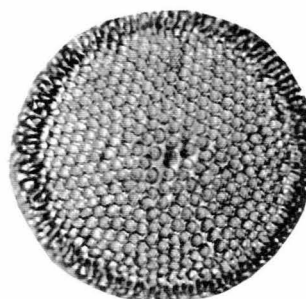
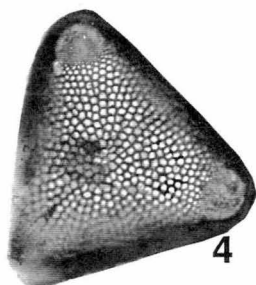
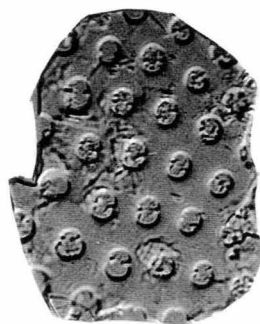




## Plate 11.

- |   |   |
|---|---|
| 1 <i>Cocconeis fasciolata</i> ,                                       | (Sørsdal Formation 2A, 190-200 cm)          |
| 2 <i>Cocconeis costata</i> ,  | (Sørsdal Formation 2A, 150-160 cm)          |
| 3 <i>Cocconeis fasciolata</i> ,                                       | (Sørsdal Formation 2A, 90-100 cm)           |
| 4 <i>Cocconeis pinnata</i> ,<br>(fragment)                            | (Sørsdal Formation 2A, 140-150 cm)          |
| 5 <i>Cocconeis</i> sp. A,   | (Sørsdal Formation 2B, 90-95 cm)            |
| 6 <i>Navicula spectabilis</i> var. <i>oamaruensis</i> ,<br>(fragment) | (Sørsdal Formation, photo by David Harwood) |
| 7 <i>Cocconeis gauteri</i> ,  | (Sørsdal Formation, photo by David Harwood) |
| 8 <i>Cocconeis schuettii</i> ,  | (Sørsdal Formation 2A, 150-160 cm)          |
| 9 <i>Diploneis subovalis</i> ,  | (Sørsdal Formation 2, 0-10 cm)              |
| 10 <i>Diploneis</i> sp. A,  | (Sørsdal Formation 2A, 210-220 cm)          |
| 11 <i>Diploneis</i> sp. A,  | (Sørsdal Formation 2A, 210-220 cm)          |
| 12 <i>Diploneis frickei</i> ,   | (Sørsdal Formation 2A, 140-150 cm)          |
| 13 <i>Diploneis splendida</i> ,                                       | (Sørsdal Formation 2B, 90-95 cm)            |
| 14 <i>Amphora</i> sp. A.,   | (Sørsdal Formation 2A, 150-160 cm)          |
| 15 <i>Amphora</i> sp. A.,   | (Sørsdal Formation 2A, 150-160 cm)          |
| 16 <i>Amphora</i> sp. A.,   | (Sørsdal Formation 2A, 210-220 cm)          |
| 17 <i>Amphora</i> sp. B,  | (Sørsdal Formation 2A, 190-200 cm)          |
| 18 <i>Trachyneis aspera</i> ,<br>(fragment)                           | (Sørsdal Formation 2A, 140-150 cm)          |

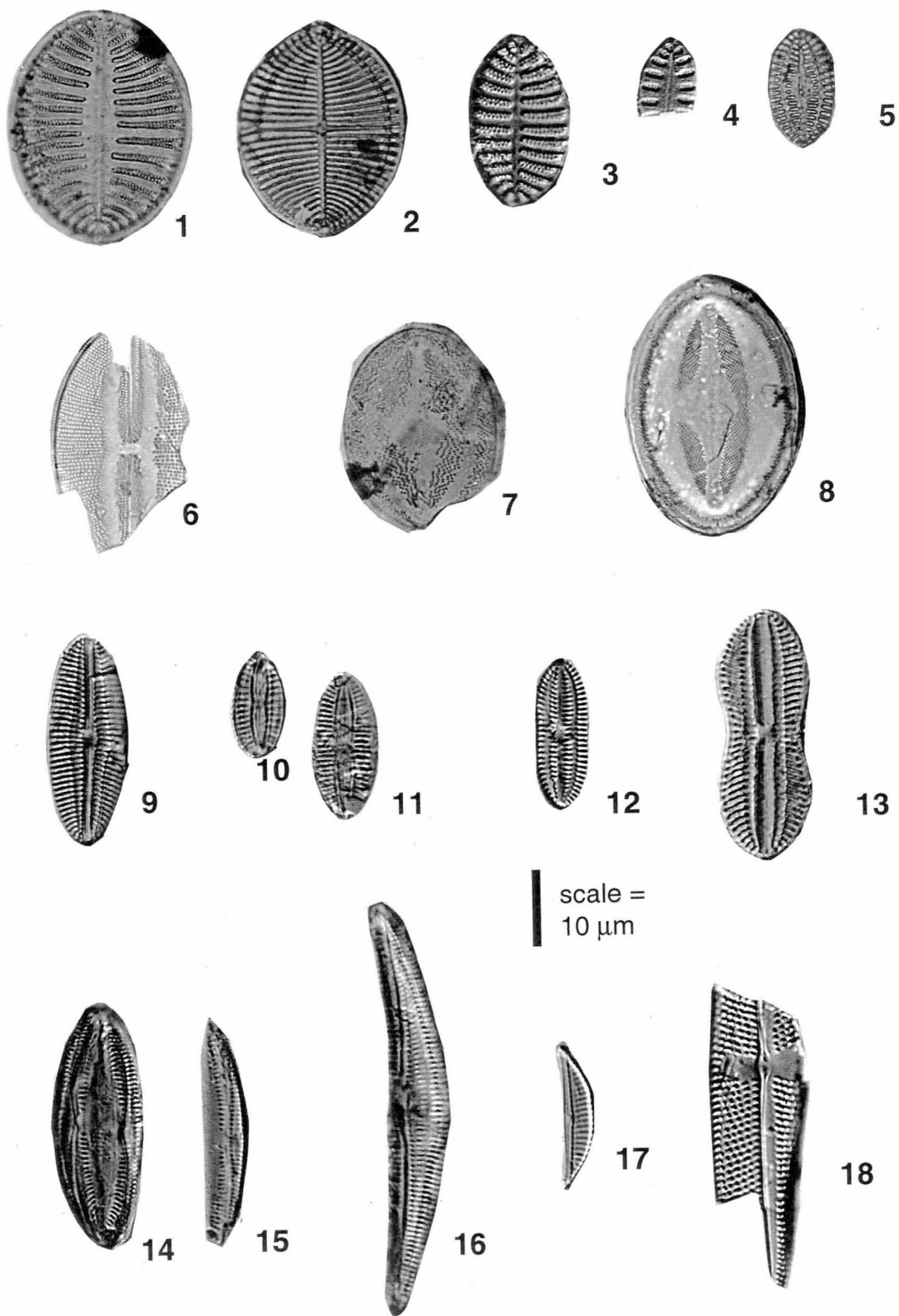


## Plate 12.

- |   |   |
|---|---|
| <b>1</b> <i>Drepanotheca bivittata</i> ,                | (Sørsdal Formation 2B, 90-95 cm)            |
| <b>2</b> Gen. <i>et</i> sp. indet. A,                   | (Sørsdal Formation 2A, 190-200 cm)          |
| <b>3</b> Gen. <i>et</i> sp. indet. A,                   | (Sørsdal Formation 2A, 190-200 cm)          |
| <b>4</b> <i>Eunotia</i> sp. A,<br>(fragment)            | (Sørsdal Formation 2A, 190-200 cm)          |
| <b>5</b> <i>Odontella punctata</i> ,                    | (Sørsdal Formation, photo by David Harwood) |
| <b>6</b> <i>Eucampia antarctica</i> var. <i>recta</i> , | (Sørsdal Formation 2B, 90-95 cm)            |
| <b>7</b> <i>Eucampia antarctica</i> var. <i>recta</i> , | (Sørsdal Formation 2B, 90-95 cm)            |
| <b>8</b> <i>Anaulus scalaris</i> ,                      | (Sørsdal Formation 2A, 280-290 cm)          |
| <b>9</b> Gen. <i>et</i> sp. indet. B,                   | (Sørsdal Formation 2A, 150-160 cm)          |
| <b>10</b> <i>Synedra</i> sp. A,                         | (Sørsdal Formation 2A, 210-220 cm)          |
| <b>11</b> <i>Trichotoxon reinboldii</i> ,<br>(fragment) | (Sørsdal Formation 2B, 90-95 cm)            |
| <b>12</b> ' <i>Tigeria</i> ' spp.,<br>(fragment)        | (Sørsdal Formation 2B, 90-95 cm)            |
| <b>13</b> ' <i>Tigeria</i> ' spp.,                      | (Sørsdal Formation 2B, 90-95 cm)            |
| <b>14</b> ' <i>Tigeria</i> ' spp.,<br>(fragment)        | (Sørsdal Formation 2B, 90-95 cm)            |



1



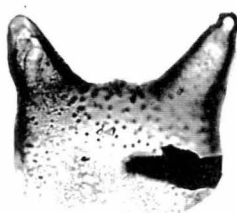
2



3



4



5



6



7



8



9

scale =  
10  $\mu$ m



10



11



12



13



14

## Plate 13.

- |   |                                    |
|---|------------------------------------|
| 1 <i>Fragilariopsis praeinterfrigidaria</i> ,         | (Sørsdal Formation 2B, 80-90 cm)   |
| 2 <i>Fragilariopsis curta</i> ,                       | (Sørsdal Formation 2B, 85-90 cm)   |
| 3 <i>Fragilariopsis praecurta</i> ,                   | (Sørsdal Formation 2B, 60-70 cm)   |
| 4 <i>Dactyliosolen antarcticus</i> ,<br>(girdle band) | (Sørsdal Formation 2B, 170-180 cm) |
| 5 <i>Dactyliosolen antarcticus</i> ,<br>(girdle band) | (Sørsdal Formation 2B, 170-180 cm) |
| 6 <i>Chaetoceros lorenzianus</i> ,                    | (Sørsdal Formation 2A, 140-150 cm) |
| 7 <i>Fragilaria</i> sp. A,                            | (Sørsdal Formation 2A, 140-150 cm) |
| 8 <i>Chaetoceros dictyota</i> ,<br>(vegetative)       | (Sørsdal Formation 2B, 90-95 cm)   |
| 9 <i>Chaetoceros dictyota</i> ,<br>(vegetative)       | (Sørsdal Formation 2B, 90-95 cm)   |
| 10 <i>Navicula</i> sp. cf. <i>cantellata</i> ,        | (Sørsdal Formation 2A, 150-160 cm) |
| 11 <i>Rhizosolenia</i> sp. B,<br>(fragment)           | (Sørsdal Formation 2A, 140-150 cm) |
| 12 <i>Gomphonemopsis</i> sp. A,                       | (Sørsdal Formation 2B, 90-95 cm)   |
| 13 <i>Pinnularia quadratarea</i> ,                    | (Sørsdal Formation 2A, 210-220 cm) |
| 14 <i>Pinnularia quadratarea</i> ,<br>(fragment)      | (Sørsdal Formation 2A, 210-220 cm) |
| 15 <i>Achnanthes brevipes</i> ,                       | (Sørsdal Formation 2A, 150-160 cm) |
| 16 <i>Cocconeis</i> sp. B,                            | (Sørsdal Formation 2A, 210-220 cm) |
| 17 <i>Cocconeis</i> sp. B,                            | (Sørsdal Formation 2A, 210-220 cm) |
| 18 <i>Rouxia naviculoides</i> ,                       | (Sørsdal Formation 2A, 210-220 cm) |
| 19 <i>Rouxia antarctica</i> ,<br>(fragment)           | (Sørsdal Formation 2B, 90-95 cm)   |
| 20 <i>Rouxia isopolica</i> ,<br>(fragment)            | (Sørsdal Formation 2B, 100-110 cm) |



1



2



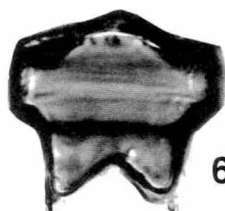
3



4



5



6



7



8



9



10



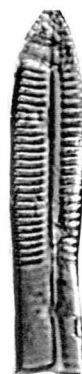
11



12



13



14

scale =  
10  $\mu$ m



15



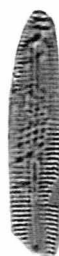
16



17



18



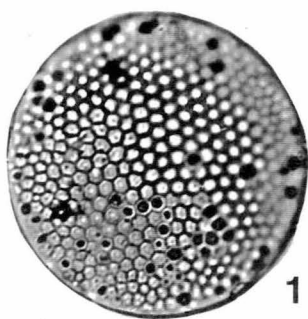
19



20

## Plate 14.

- |   |  |
|---|--|
| <b>1</b> <i>Stephanopyxis splendidus</i> ,  | (Mt Johnston Formation AM 003)                 |
| <b>2</b> <i>Pyxilla reticulata</i> ,<br>(fragment)  | (Mt Johnston Formation AM 003)                 |
| <b>3</b> <i>Denticulopsis simonsenii</i> ,  | (Fisher Bench Formation AM 015)                |
| <b>4</b> <i>Actinocyclus actinochilus</i> ,   | (Bardin Bluffs Formation PCM 90-7)             |
| <b>5</b> <i>Actinocyclus ingens</i> var. <i>nodus</i> ,   | (Fisher Bench Formation AM 015)                |
| <b>6</b> <i>Actinocyclus ingens</i> var. <i>nodus</i> ,   | (Fisher Bench Formation AM 015)                |
| <b>7</b> <i>Fragilariopsis kerguelensis</i> ,   | (Bardin Bluffs Formation, Glossopteris bottom) |
| <b>8</b> <i>Fragilariopsis kerguelensis</i> ,<br>(fragment within a diatomaceous sediment aggregate). | (Bardin Bluffs Formation, Bardin bottom)       |



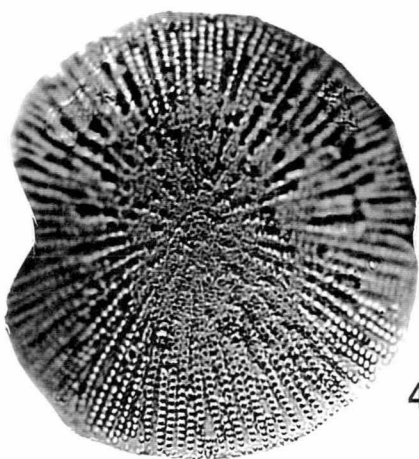
1



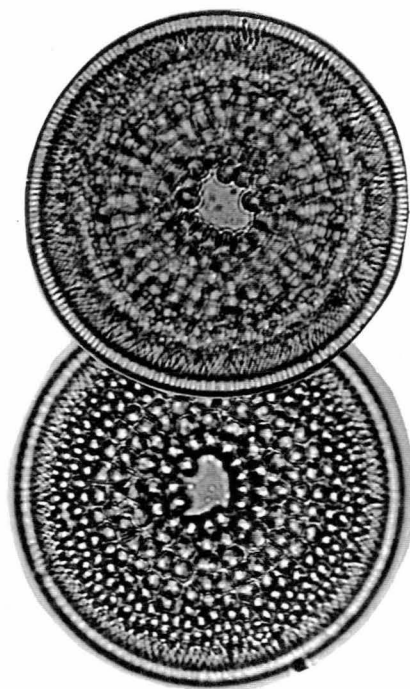
2



3



4



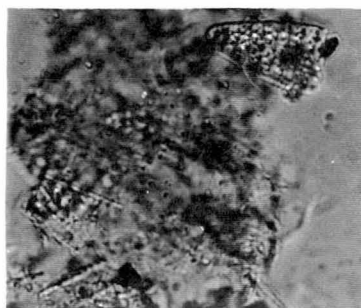
6

5

scale =  
10  $\mu$ m



7



8



## Plate 15.

- |  |   |
|--|---|
| 1 <i>Diploneis</i> sp. B,  | (Fisher Bench Formation PCM 90-11)          |
| 2 <i>Pinnularia</i> sp. A.,  | (Fisher Bench Formation PCM 90-11)          |
| 3 <i>Gomphonema angustatum</i> var. A,   | (Fisher Bench Formation PCM 90-11)          |
| 4 <i>Gomphonema angustatum</i> var. B,   | (Fisher Bench Formation PCM 90-11)          |
| 5 <i>Amphora</i> sp. C,  | (Fisher Bench Formation PCM 90-11)          |
| 6 <i>Denticulopsis dimorpha</i> ,  | (Bardin Bluffs Formation, Bardin top)       |
| 7 <i>Denticulopsis dimorpha</i> ,  | (Bardin Bluffs Formation, Bardin top)       |
| 8 <i>Denticulopsis hustedtii</i> ,   | (Bardin Bluffs Formation, Glossopteris top) |
| 9 <i>Fragilariopsis praeinterfrigidaria</i> ,  | (Bardin Bluffs Formation PCM 90-7)          |
| 10 <i>Stephanopyxis turris</i> ,<br>(fragment)   | (Mt Johnston Formation AM 006)              |
| 11 <i>Actinoptycus senarius</i> ,  | (Bardin Bluffs Formation PCM 90-7)          |
| 12 <i>Actinoptycus</i> sp. A,  | (Bardin Bluffs Formation PCM 90-7)          |
| 13 <i>Nitzschia reinholdii</i> ,<br>(fragment)   | (Bardin Bluffs Formation PCM 90-7)          |
| 14 <i>Rouxia heteropolara</i> ,  | (Bardin Bluffs Formation, Bardin bottom)    |
| 15 <i>Distephanus pseudofibula</i> .<br>(silicoflagellate containing diatomaceous sediment). | (Bardin Bluffs Formation, Glossopteris top) |
| 16 <i>Thalassionema nitzschioides</i> var. <i>parva</i> ,                                    | (Bardin Bluffs Formation PCM 90-7)          |
| 17 <i>Thalassionema nitzschioides</i> ,  | (Bardin Bluffs Formation PCM 90-7)          |
| 18 <i>Thalassiosira oliverana</i> var. <i>sparsa</i> .                                       | (Bardin Bluffs Formation PCM 90-2)          |



1



2



3



4



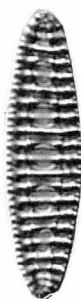
5



6



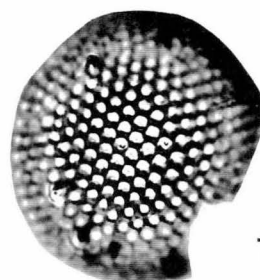
7



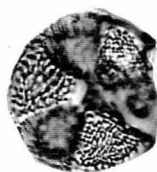
8



9



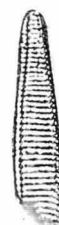
10



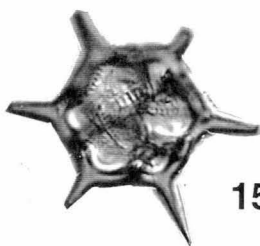
11



12



13



15

scale =  
10  $\mu$ m



14



16



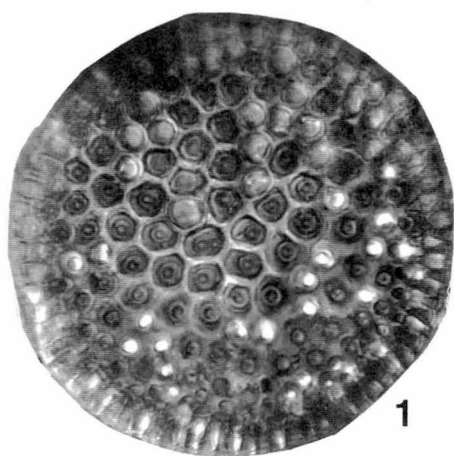
17



18

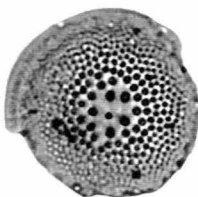
## Plate 16.

- |  |   |
|--|---|
| <b>1</b> <i>Coscinodiscus marginatus</i> ,                                     | (Bardin Bluffs Formation, Bardin bottom)      |
| <b>2</b> <i>Thalassiosira inura</i> ,<br>(fragment)                            | (Bardin Bluffs Formation, Bainmedart top)     |
| <b>3</b> <i>Stephanodiscus</i> sp.,<br>(fragment)                              | (Bardin Bluffs Formation, Pagodroma Gorge SE) |
| <b>4</b> <i>Fragilariopsis interfrigidaria</i> ,<br>(fragment)                 | (Bardin Bluffs Formation, Glossopteris top)   |
| <b>5</b> <i>Fragilariopsis curta</i> ,   | (Bardin Bluffs Formation, Glossopteris top)   |
| <b>6</b> <i>Actinocyclus octonarius</i> var. <i>asteriscus</i> ,<br>(fragment) | (Fisher Massif Formation PCM 90-11)           |
| <b>7</b> <i>Rouxia</i> sp.,  | (Bardin Bluffs Formation PCM 90-7)            |
| <b>8</b> <i>Rhizosolenia hebetata</i> ,<br>(fragment)                          | (Bardin Bluffs Formation PCM 90-7)            |
| <b>9</b> <i>Eucampia antarctica</i> var. <i>recta</i> ,                        | (Bardin Bluffs Formation PCM 90-7)            |
| <b>10</b> <i>Distephanus speculum</i> ,  | (Bardin Bluffs Formation PCM 90-7)            |
| <b>11</b> <i>Aulacoseira</i> sp. A,  | (Bardin Bluffs Formation, Bainmedart bottom)  |
| <b>12</b> Diatomaceous sediment aggregate,                                     | (Bardin Bluffs Formation PCM 90-2)            |



1

scale =  
10  $\mu$ m



2



3



4



5



6



7



8



10

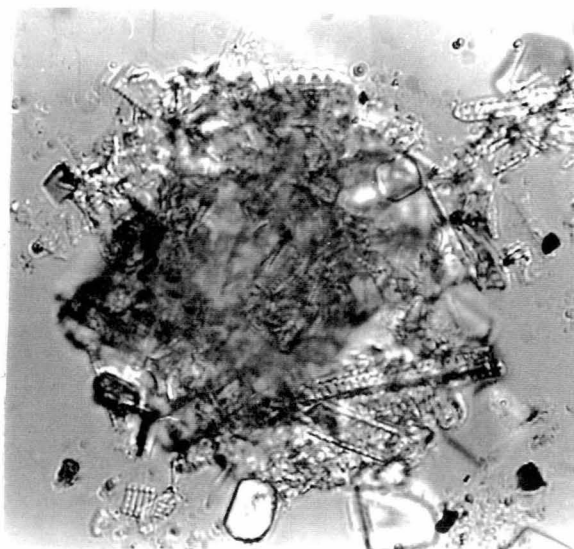


9



11

10  $\mu$ m



12

## Plate 17.

- |  |                                 |
|--|---------------------------------|
| 1 <i>Actinocyclus ingens</i> ,                           | (Fisher Bench Formation AM 015) |
| 2 <i>Actinocyclus ingens</i> var. <i>nodus</i> ,         | (Fisher Bench Formation AM 015) |
| 3 <i>Actinocyclus ingens</i> var. <i>nodus</i> ,         | (Fisher Bench Formation AM 015) |
| 4 <i>Isthmia</i> sp.,<br>(fragment)                      | (Fisher Bench Formation AM 015) |
| 5 <i>Coscinodiscus oculus-iridus</i> ,<br>(fragment)     | (Fisher Bench Formation AM 015) |
| 6 <i>Actinocyclus</i> aff. <i>ingens</i> ,<br>(fragment) | (Fisher Bench Formation AM 015) |
| 7 <i>Coscinodiscus radiatus</i> ,                        | (Fisher Bench Formation AM 015) |
| 8 <i>Coscinodiscus</i> sp. A,<br>(fragment)              | (Fisher Bench Formation AM 015) |
| 9 <i>Eucampia antarctica</i> var. <i>recta</i> ,         | (Fisher Bench Formation AM 015) |
| 10 <i>Denticulopsis simonsenii</i> ,                     | (Fisher Bench Formation AM 015) |

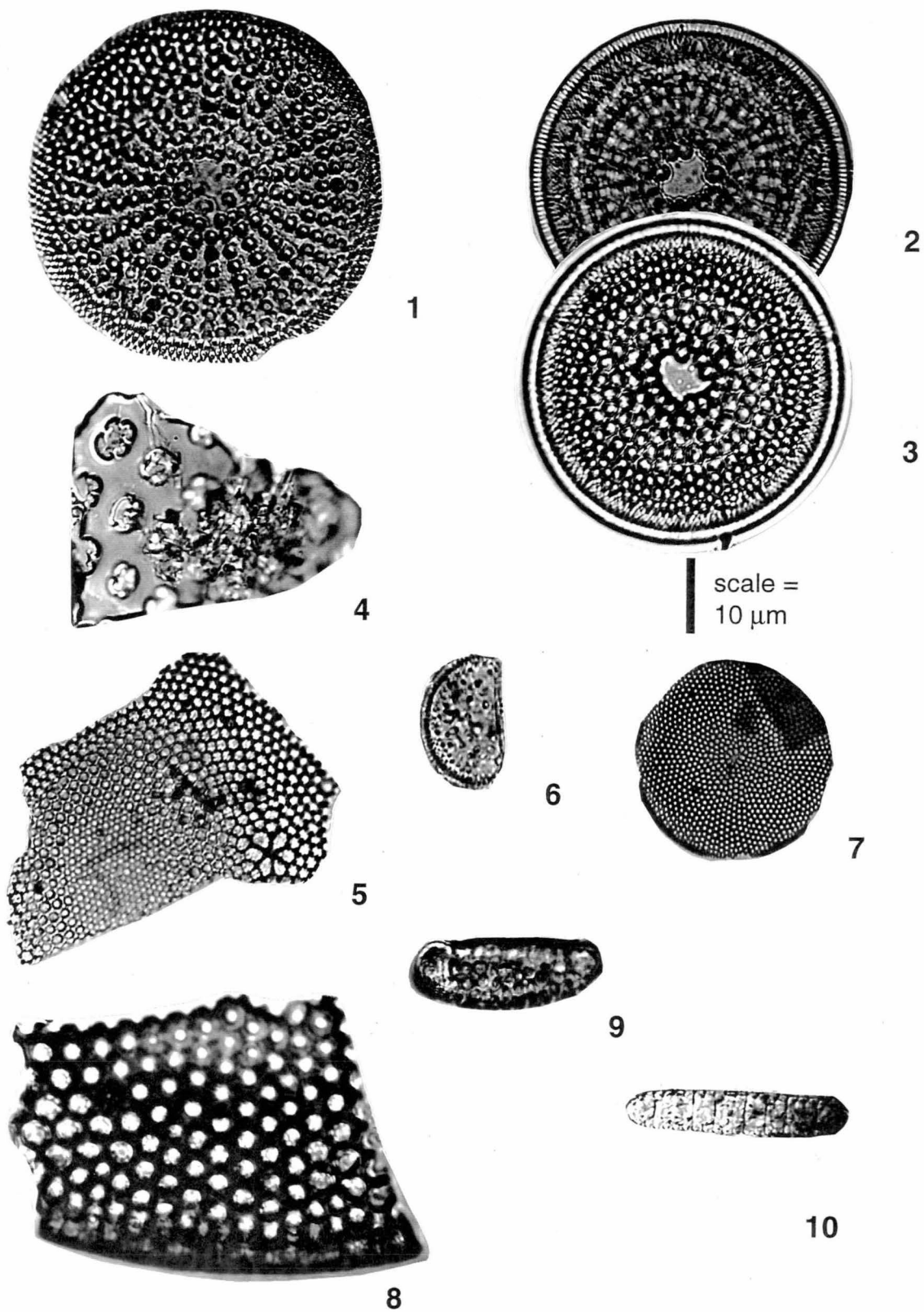
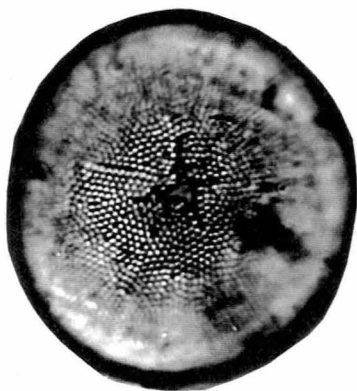


## Plate 18.

- |   |                                 |
|---|---------------------------------|
| <b>1</b> <i>Stellarima stellaris</i> ,<br>(fragment)          | (Fisher Bench Formation AM 015) |
| <b>2</b> <i>Stellarima microtrias</i> ,                       | (Fisher Bench Formation AM 015) |
| <b>3</b> <i>Rhabdonema japonica</i> ,<br>(fragment)           | (Fisher Bench Formation AM 015) |
| <b>4</b> <i>Pseudammodochium lingii</i> ,<br>(ebridian)       | (Fisher Bench Formation AM 015) |
| <b>5</b> Gen. <i>et</i> sp. indet. A,                         | (Fisher Bench Formation AM 015) |
| <b>6</b> <i>Trinacria excavata</i> ,                          | (Fisher Bench Formation AM 015) |
| <b>7</b> <i>Rhaphoneis</i> sp. A ,<br>(fragment)              | (Fisher Bench Formation AM 015) |
| <b>8</b> <i>Chaetoceros</i> sp.,<br>(spine)                   | (Fisher Bench Formation AM 015) |
| <b>9</b> <i>Proboscia barboi</i> ,<br>(fragment)              | (Fisher Bench Formation AM 015) |
| <b>10</b> <i>Distephanus speculum</i> ,<br>(silicoflagellate) | (Fisher Bench Formation AM 015) |



1

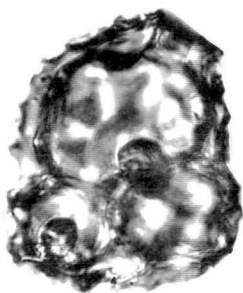


2



3

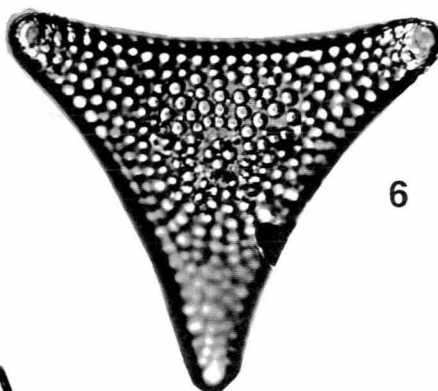
scale =  
10  $\mu$ m



4



5



6



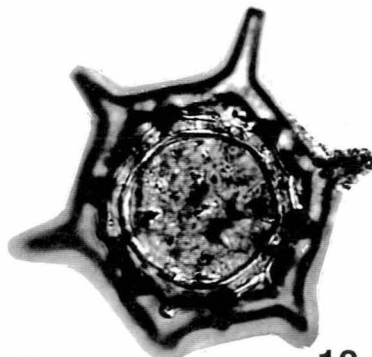
7



8



9



10